

THIRD EDITION

FRACTAL GEOMETRY

Mathematical Foundations and Applications

Kenneth Falconer

WILEY

Preface to the first edition

I am frequently asked questions such as ‘What are fractals?’, ‘What is fractal dimension?’, ‘How can one find the dimension of a fractal and what does it tell us anyway?’ or ‘How can mathematics be applied to fractals?’ This book endeavours to answer some of these questions.

The main aim of the book is to provide a treatment of the mathematics associated with fractals and dimensions at a level which is reasonably accessible to those who encounter fractals in mathematics or science. Although basically a mathematics book, it attempts to provide an intuitive as well as a mathematical insight into the subject.

The book falls naturally into two parts. Part I is concerned with the general theory of fractals and their geometry. Firstly, various notions of dimension and methods for their calculation are introduced. Then geometrical properties of fractals are investigated in much the same way as one might study the geometry of classical figures such as circles or ellipses: locally, a circle may be approximated by a line segment, the projection or ‘shadow’ of a circle is generally an ellipse, a circle typically intersects a straight line segment in two points (if at all) and so on. There are fractal analogues of such properties, usually with dimension playing a key role. Thus, we consider, for example, the local form of fractals and projections and intersections of fractals.

Part II of the book contains examples of fractals, to which the theory of the first part may be applied, drawn from a wide variety of areas of mathematics and physics. Topics include self-similar and self-affine sets, graphs of functions, examples from number theory and pure mathematics, dynamical systems, Julia sets, random fractals and some physical applications.

There are many diagrams in the text and frequent illustrative examples. Computer drawings of a variety of fractals are included, and it is hoped that enough information is provided to enable readers with a knowledge of programming to produce further drawings for themselves.

It is hoped that the book will be a useful reference for researchers, by providing an accessible development of the mathematics underlying fractals and showing how it may be applied in particular cases. The book covers a wide variety of mathematical ideas that may be related to fractals and, particularly in Part II, provides a flavour of what is available rather than exploring any one subject in too much detail. The selection of topics is to some extent at the author's whim—there are certainly some important applications that are not included. Some of the material dates back to early twentieth century, whilst some is very recent.

Notes and references are provided at the end of each chapter. The references are by no means exhaustive; indeed, complete references on the variety of topics covered would fill a large volume. However, it is hoped that enough information is included to enable those who wish to do so to pursue any topic further.

It would be possible to use the book as a basis for a course on the mathematics of fractals, at postgraduate or, perhaps, final-year undergraduate level, and exercises are included at the end of each chapter to facilitate this. Harder sections and proofs are marked with an asterisk and may be omitted without interrupting the development.

An effort has been made to keep the mathematics to a level that can be understood by a mathematics or physics graduate and, for the most part, by a diligent final-year undergraduate. In particular, measure theoretic ideas have been kept to a minimum, and the reader is encouraged to think of measures as ‘mass distributions’ on sets. Provided that it is accepted that measures with certain (intuitively almost obvious) properties exist, there is little need for technical measure theory in our development.

Results are always stated precisely to avoid the confusion which would otherwise result. Our approach is generally rigorous, but some of the harder or more technical proofs are either just sketched or omitted altogether. (However, a few harder proofs that are not available in that form elsewhere have been included, in particular those on sets with large intersection and on random fractals.) Suitable diagrams can be a help in understanding the proofs, many of which are of a geometric nature. Some diagrams are included in the book; the reader may find it helpful to draw others.

Chapter 1 begins with a rapid survey of some basic mathematical concepts and notation, for example, from the theory of sets and functions, which are used throughout the book. It also includes an introductory section on measure theory and mass distributions which, it is hoped, will be found adequate. The section on probability theory may be helpful for the chapters on random fractals and Brownian motion.

With the wide variety of topics covered, it is impossible to be entirely consistent in the use of notation, and inevitably, sometimes, there has to be a compromise between consistency within the book and standard usage.

In the past few years, fractals have become enormously popular as an art form, with the advent of computer graphics, and as a model of a wide variety of physical phenomena. Whilst it is possible in some ways to appreciate fractals with little or no knowledge of their mathematics, an understanding of the mathematics that can be applied to such a diversity of objects certainly enhances one's appreciation. The phrase 'the beauty of fractals' is often heard—it is the author's belief that much of their beauty is to be found in their mathematics.

It is a pleasure to acknowledge those who have assisted in the preparation of this book. Philip Drazin and Geoffrey Grimmett provided helpful comments on parts of the manuscript. Peter Shiarly gave valuable help with the computer drawings, and Aidan Foss produced some diagrams. I am indebted to Charlotte Farmer,

Jackie Cowling and Stuart Gale of John Wiley & Sons for overseeing the production of the book.

Special thanks are due to David Marsh—not only did he make many useful comments on the manuscript and produce many of the computer pictures but he also typed the entire manuscript in a most expert way.

Finally, I would like to thank my wife Isobel for her support and encouragement, which extended to reading various drafts of the book.

Kenneth J. Falconer

Bristol

April 1989

Preface to the second edition

It is 13 years since *Fractal Geometry—Mathematical Foundations and Applications* was first published. In the meantime, the mathematics and applications of fractals have advanced enormously, with an ever-widening interest in the subject at all levels. The book was originally written for those working in mathematics and science who wished to know more about fractal mathematics. Over the past few years, with changing interests and approaches to mathematics teaching, many universities have introduced undergraduate and postgraduate courses on fractal geometry and a considerable number have been based on parts of this book.

Thus, this edition has two main aims. Firstly, it indicates some recent developments in the subject, with updated notes and suggestions for further reading. Secondly, more attention is given to the needs of students using the book as a course text, with extra details to help understanding, along with the inclusion of further exercises.

Parts of the book have been rewritten. In particular, multifractal theory has advanced considerably since the first edition was published, so the chapter on ‘Multifractal Measures’ has been completely rewritten. The notes and references have been updated. Numerous minor changes, corrections and additions have been incorporated, and some of the notation and terminology has been changed to conform with what has become standard usage. Many of the diagrams have been replaced to take advantage of the more sophisticated computer technology now available. Where possible, the numbering of sections, equations and figures has been left as in the first edition, so that earlier references to the book remain valid.

Further exercises have been added at the end of the chapters. Solutions to these exercises and additional supplementary material

may be found on the World Wide Web at
<http://www.wileyeurope.com/fractal>.

In 1997, a sequel, *Techniques in Fractal Geometry*, was published, presenting a variety of techniques and ideas current in fractal research. Readers wishing to study fractal mathematics beyond the bounds of this book may find the sequel helpful.

I am most grateful to all who have made constructive suggestions on the text. In particular, I am indebted to Carmen Fernández, Gwyneth Stallard and Alex Cain for their help with this revision. I am also very grateful for the continuing support given to the book by the staff of John Wiley & Sons; and in particular, to Rob Calver and Lucy Bryan, for overseeing the production of this second edition and to John O'Connor and Louise Page for the cover design.

Kenneth J. Falconer

St Andrews

January 2003

Preface to the third edition

It is now 23 years since *Fractal Geometry—Mathematical Foundations and Applications* was first published and 10 years since the second edition. During those years, interest in the mathematics and applications of fractals has seen a phenomenal increase at all levels, with many mathematicians and scientists now involved in fractal-related topics. The book was originally written for researchers wanting to know more about fractals and their mathematics. However, many universities now present undergraduate and postgraduate courses on fractal geometry, often based on parts of this book, and the needs of students have been very much in mind during the revision. I am continually surprised by the number of researchers whom I meet who tell me that they first learnt about fractal geometry from this book.

This edition incorporates substantial changes from its predecessor with parts rewritten and new sections added. Student courses on fractal geometry usually present the simpler box-counting dimension before the more sophisticated Hausdorff dimension, so Chapters 2 and 3 have been reorganised in this way. The chapter on Brownian motion has been largely rewritten, and there are numerous minor changes and additions throughout the text. Some new sections have been added to give a glimpse of some of the recent ideas and directions, such as porosity and complex dimensions, that have evolved in fractal geometry.

When the first edition was written, the literature on fractals was comparatively limited and it was possible to include a reasonably comprehensive bibliography. In recent years, there has been an explosion in the number of research papers in the area and only a tiny proportion can be listed. Thus, the bibliography now focusses on papers that have a historical or innovative significance together with books and survey articles that provide overviews and many

further references. The notes at the end of each chapter are a pointer to where next to go to find out more about a topic.

Some exercises at the end of the chapters have been modified and some more have been added, and, as before, solutions and other supplementary material may be found on the website
<http://www.wiley.com/go/fractal>.

Those wishing to study fractals further may find helpful the sequel, *Techniques in Fractal Geometry* published in 1997, which is a natural continuation of this book and includes many ideas in use in current research.

Once again, I express my gratitude to the support given to the book by the staff of John Wiley & Sons and, in particular, to Richard Davies, Prachi Sinha-Sahay and Debbie Jupe for overseeing the production of this third edition. I am also very grateful to Ben Falconer for the new cover picture.

Kenneth J. Falconer
St Andrews
June 2013

Course suggestions

There is far too much material in this book for a standard length course on fractal geometry. Depending on the emphasis required, appropriate sections may be selected as a basis for an undergraduate or a postgraduate course.

A course for mathematics students could be based on the following sections.

a. Mathematical background

- 1.1** Basic set theory;
- 1.2** Functions and limits;
- 1.3** Measures and mass distributions.

b. Box-counting dimension

- 2.1** Box-counting dimensions;
- 2.2** Properties of box-counting dimensions.

c. Hausdorff measures and dimension

- 3.1** Hausdorff measure;
- 3.2** Hausdorff dimension;
- 3.3** Calculation of Hausdorff dimension;
- 4.1** Basic methods of calculating dimensions.

d. Iterated function systems

- 9.1** Iterated function systems;
- 9.2** Dimensions of self-similar sets;
- 9.3** Some variations;
- 10.2** Continued fraction examples.

e. Graphs of functions

11.1 Dimensions of graphs, the Weierstrass function and self-affine graphs.

f. Dynamical systems

13.1 Repellers and iterated function systems;

13.2 The logistic map.

g. Iteration of complex functions

14.1 Sketch of general theory of Julia sets;

14.2 The Mandelbrot set;

14.3 Julia sets of quadratic functions.

Introduction

In the past, mathematics has been concerned largely with sets and functions to which the methods of classical calculus can be applied. Sets or functions that are not sufficiently smooth or regular have tended to be ignored as ‘pathological’ and not worthy of study. Certainly, they were regarded as individual curiosities and only rarely were thought of as a class to which a general theory might be applicable.

In recent years, this attitude has changed. It has been realised that a great deal can be said, and is worth saying, about the mathematics of non-smooth objects. Moreover, irregular sets provide a much better representation of many natural phenomena than do the figures of classical geometry. Fractal geometry provides a general framework for the study of such irregular sets.

We begin by looking briefly at a number of simple examples of fractals, and note some of their features.

The middle third Cantor set is one of the best known and most easily constructed fractals; nevertheless, it displays many typical fractal characteristics. It is constructed from a unit interval by a sequence of deletion operations (see [Figure 0.1](#)). Let E_0 be the interval $[0, 1]$. (Recall that $[a, b]$ denotes the set of real numbers x such that $a \leq x \leq b$.) Let E_1 be the set obtained by deleting the middle third of E_0 , so that E_1 consists of the two intervals $[0, \frac{1}{3}]$ and $[\frac{2}{3}, 1]$.

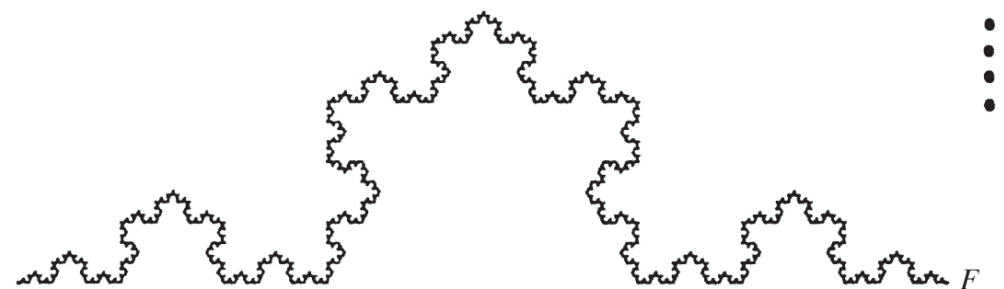
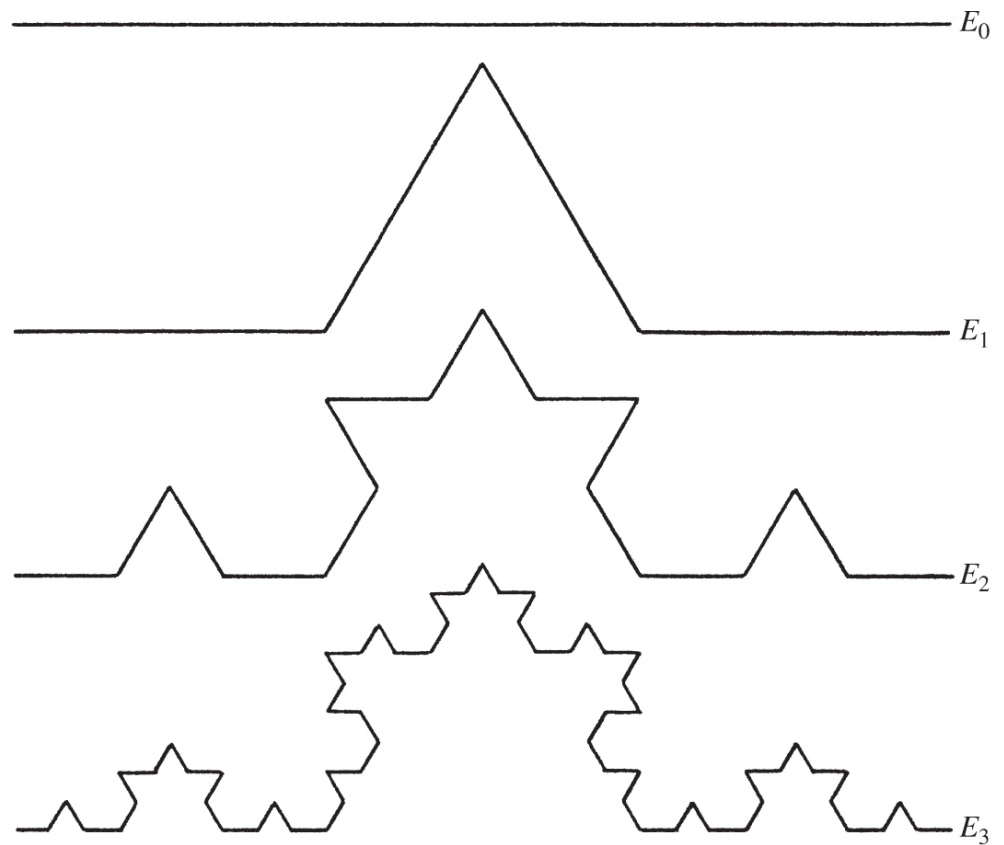
Deleting the middle thirds of these intervals gives E_2 ; thus, E_2 comprises the four intervals $[0, \frac{1}{9}], [\frac{2}{9}, \frac{1}{3}], [\frac{2}{3}, \frac{7}{9}]$ and $[\frac{8}{9}, 1]$. We continue in this way, with E_k obtained by deleting the middle third of each interval in E_{k-1} . Thus, E_k consists of 2^k intervals each of length 3^{-k} . The *middle third Cantor set* F consists of the numbers that are in E_k for all k ; mathematically, F is the intersection $\bigcap_{k=0}^{\infty} E_k$. The Cantor set F may be thought of as the limit of the sequence of sets E_k as k tends to infinity. It is obviously impossible to draw the set F itself,

with its infinitesimal detail, so ‘pictures of F ’ tend to be pictures of one of the E_k , which are a good approximation to F when k is reasonably large (see [Figure 0.1](#)).

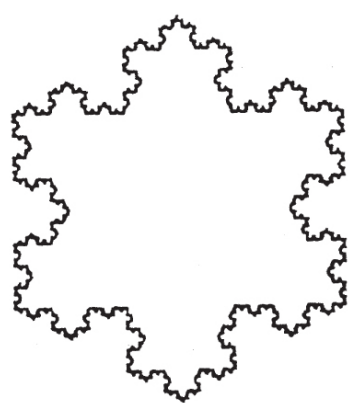


Figure 0.1 Construction of the middle third Cantor set F , by repeated removal of the middle third of intervals. Note that F_L and F_R , the left and right parts of F , are copies of F scaled by a factor $\frac{1}{3}$.

At first glance, it might appear that we have removed so much of the interval $[0, 1]$ during the construction of F , that nothing remains. In fact, F is an infinite (and indeed uncountable) set, which contains infinitely many numbers in every neighbourhood of each of its points. The middle third Cantor set F consists precisely of those numbers in $[0, 1]$ whose base-3 expansion does not contain the digit 1, that is, all numbers $a_1 3^{-1} + a_2 3^{-2} + a_3 3^{-3} + \dots$ with $a_i = 0$ or 2 for each i . To see this, note that to get E_1 from E_0 , we remove those numbers with $a_1 = 1$; to get E_2 from E_1 , we remove those numbers with $a_2 = 1$ and so on.



(a)



(b)

Figure 0.2 (a) Construction of the von Koch curve F . At each stage, the middle third of each interval is replaced by the other two sides of an equilateral triangle. (b) Three von Koch curves fitted together to form a snowflake curve.

We list some of the features of the middle third Cantor set F ; as we shall see, similar features are found in many fractals.

- i. F is self-similar. It is clear that the part of F in the interval $[0, \frac{1}{3}]$ and the part of F in $[\frac{2}{3}, 1]$ are both geometrically similar to F , scaled by a factor $\frac{1}{3}$. Again, the parts of F in each of the four intervals of E_2 are similar to F but scaled by a factor $\frac{1}{9}$, and so on. The Cantor set contains copies of itself at many different scales.
- ii. The set F has a ‘fine structure’; that is, it contains detail at arbitrarily small scales. The more we enlarge the picture of the Cantor set, the more gaps become apparent to the eye.
- iii. Although F has an intricately detailed structure, the actual definition of F is very straightforward.
- iv. F is obtained by a recursive procedure. Our construction consisted of repeatedly removing the middle thirds of intervals. Successive steps give increasingly good approximations E_k to the set F .
- v. The geometry of F is not easily described in classical terms: neither is it the locus of the points that satisfy some simple geometric condition nor is it the set of solutions of any simple equation.
- vi. It is awkward to describe the local geometry of F —near each of its points are a large number of other points, separated by gaps of varying lengths.
- vii. Although F is in some ways quite a large set (it is uncountably infinite), its size is not quantified by the usual measures such as length—by any reasonable definition F has length zero.

Our second example, the von Koch curve, will also be familiar to many readers (see [Figure 0.2](#)). We let E_0 be a line segment of unit length. The set E_1 consists of the four segments obtained by removing the middle third of E_0 and replacing it by the other two sides of the equilateral triangle based on the removed segment. We construct E_2 by applying the same procedure to each of the segments in E_1 and so on. Thus, E_k comes from replacing the middle third of each straight line segment of E_{k-1} by the other two sides of an equilateral triangle. When k is large, the curves E_{k-1} and E_k differ only in fine detail and as k tends to be infinity, the sequence of polygonal curves E_k approaches a limiting curve F , called the *von Koch curve*.

The von Koch curve has features in many ways similar to those listed for the middle third Cantor set. It is made up of four ‘quarters’ each similar to the whole, but scaled by a factor $\frac{1}{3}$. The fine structure is reflected in the irregularities at all scales; nevertheless, this intricate structure stems from a basically simple construction. Whilst it is reasonable to call F a curve, it is much too irregular to have tangents in the classical sense. A simple calculation shows that E_k is of length $(\frac{4}{3})^k$; letting k tend to infinity implies that F has infinite length. On the other hand, F occupies zero area in the plane, so neither length nor area provides a very useful description of the size of F .

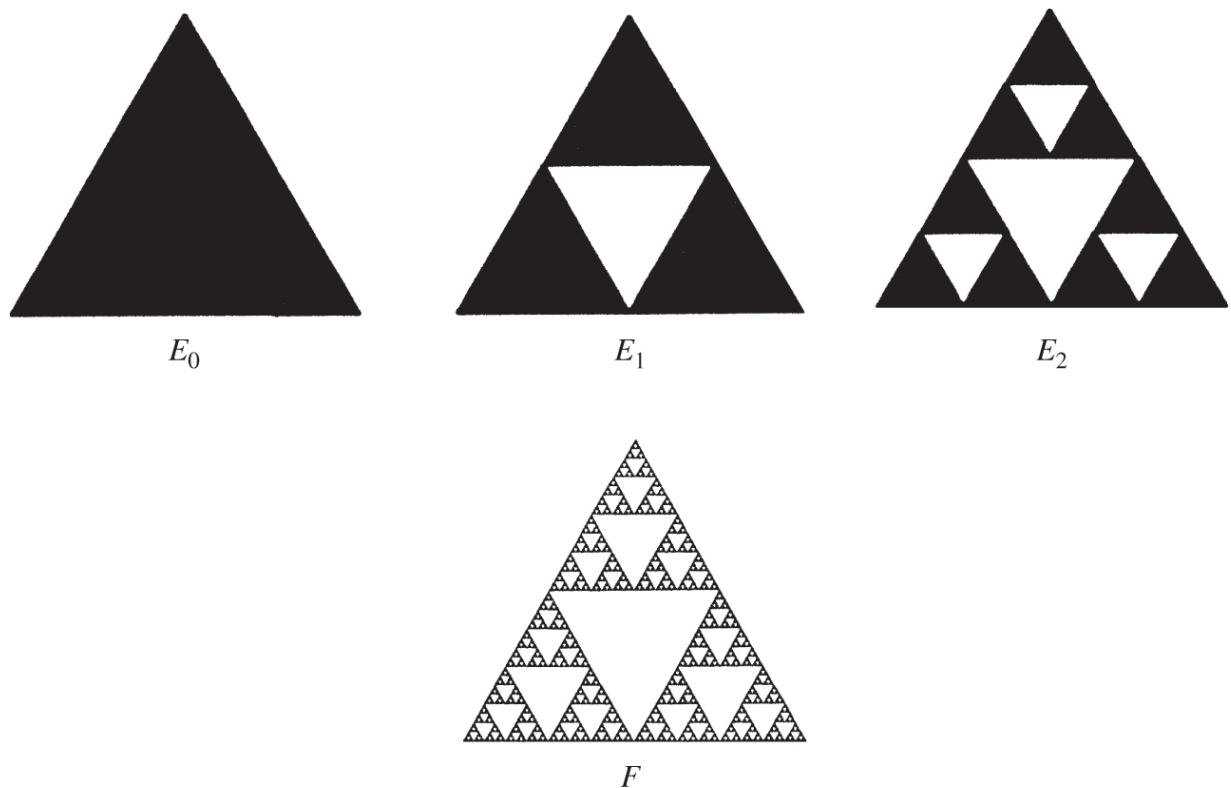


Figure 0.3 Construction of the Sierpiński triangle ($\dim_{\text{H}} F = \dim_{\text{B}} F = \log 3 / \log 2$).

Many other sets may be constructed using such recursive procedures. For example, the *Sierpiński triangle* or *gasket* is obtained by repeatedly removing (inverted) equilateral triangles from an initial equilateral triangle of unit side length (see [Figure 0.3](#)). (For many purposes, it is better to think of this procedure as repeatedly replacing an equilateral triangle by three triangles of half the height.) A plane analogue of the Cantor set, a ‘Cantor dust’, is illustrated in [Figure 0.4](#). At each stage, each remaining square is divided into 16 smaller squares of which four are kept and the rest discarded. (Of course, other arrangements or numbers of squares could be used to get different sets.) It should be clear that such examples have properties similar to those mentioned in connection with the Cantor set and the von Koch curve. The example depicted in [Figure 0.5](#) is constructed using two different similarity ratios.

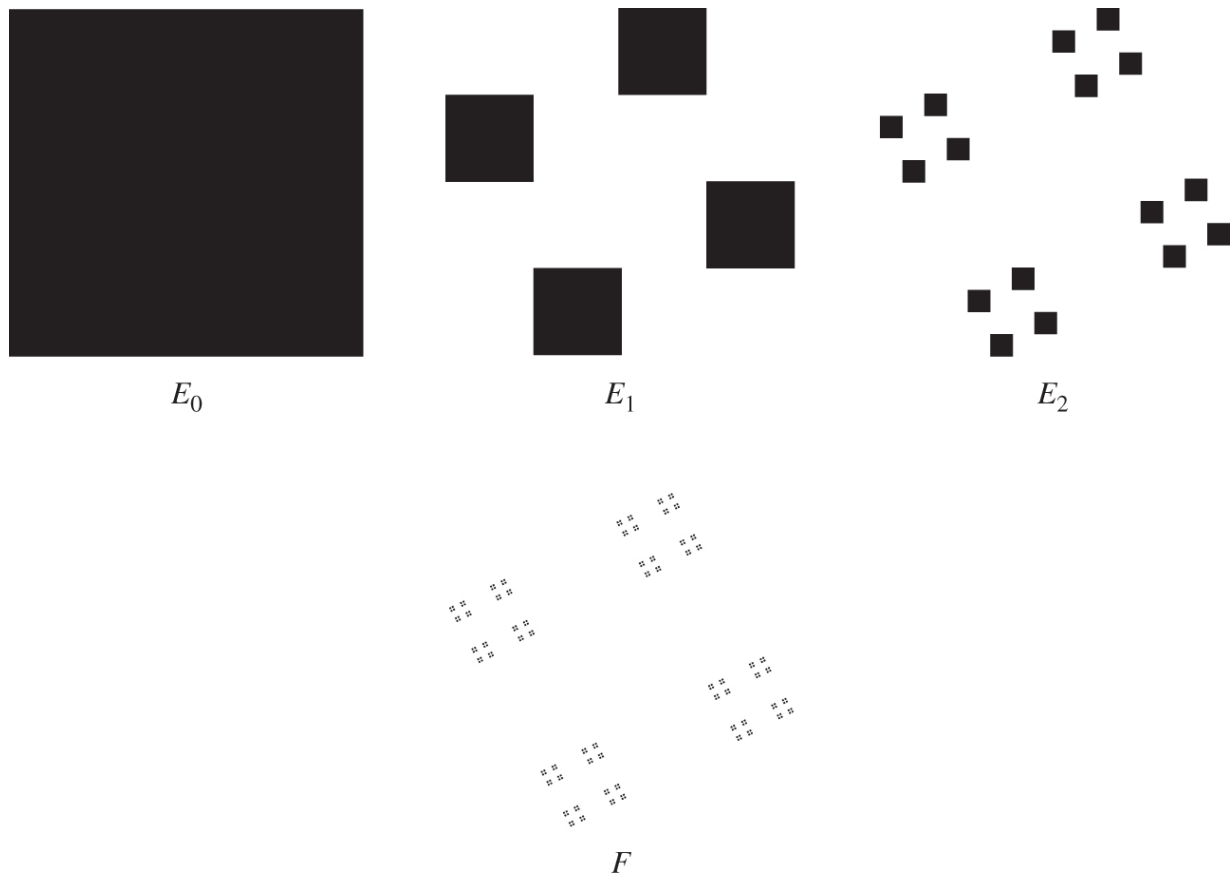


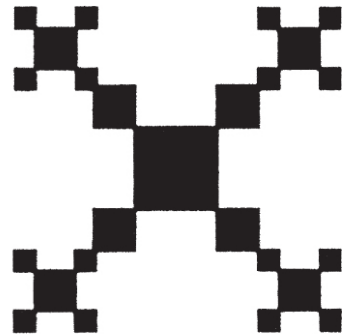
Figure 0.4 Construction of a ‘Cantor dust’ ($\dim_H F = \dim_B F = 1$).



E_0



E_1



E_2

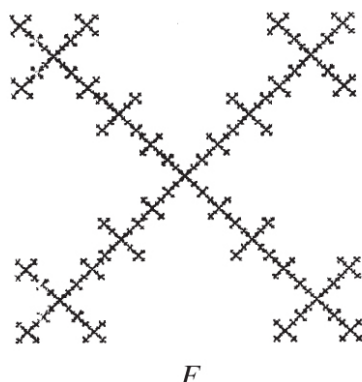


Figure 0.5 Construction of a self-similar fractal with two different similarity ratios.

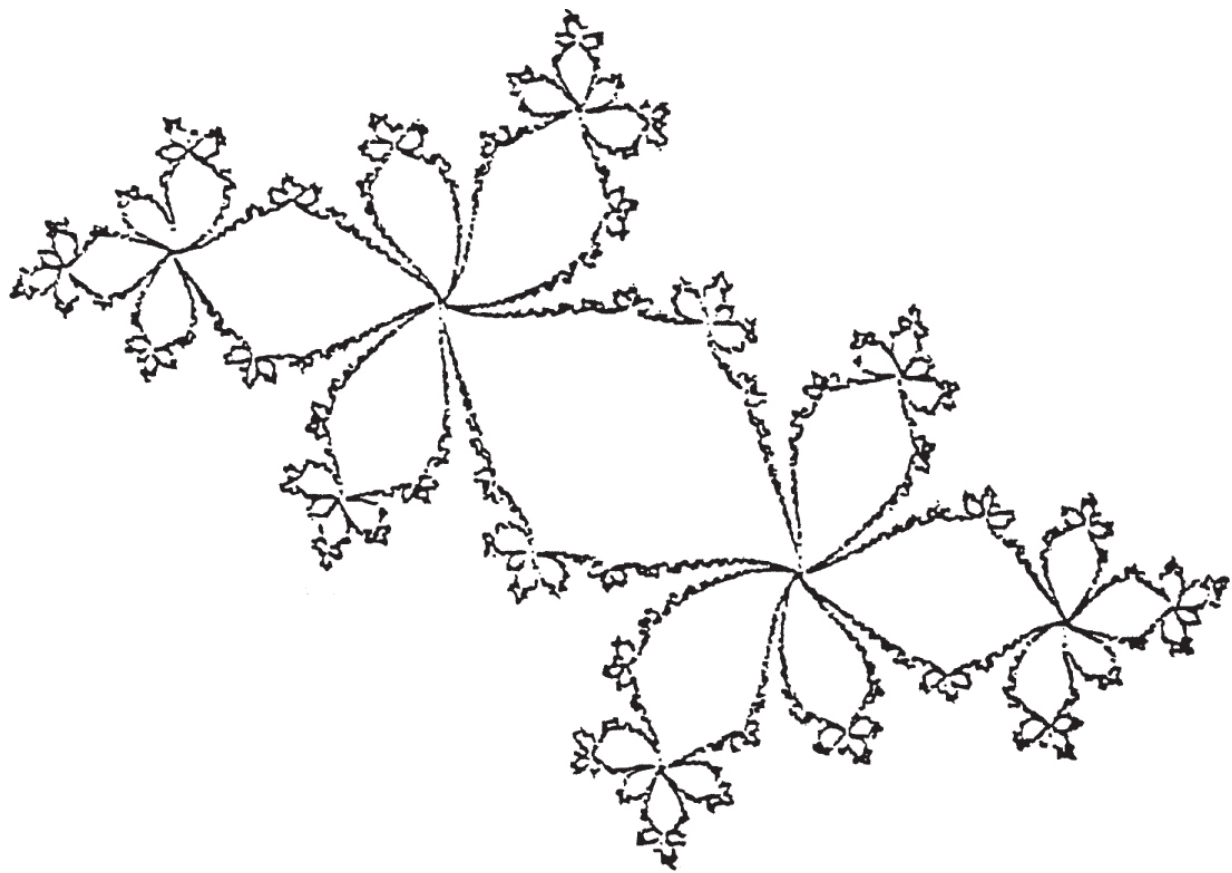
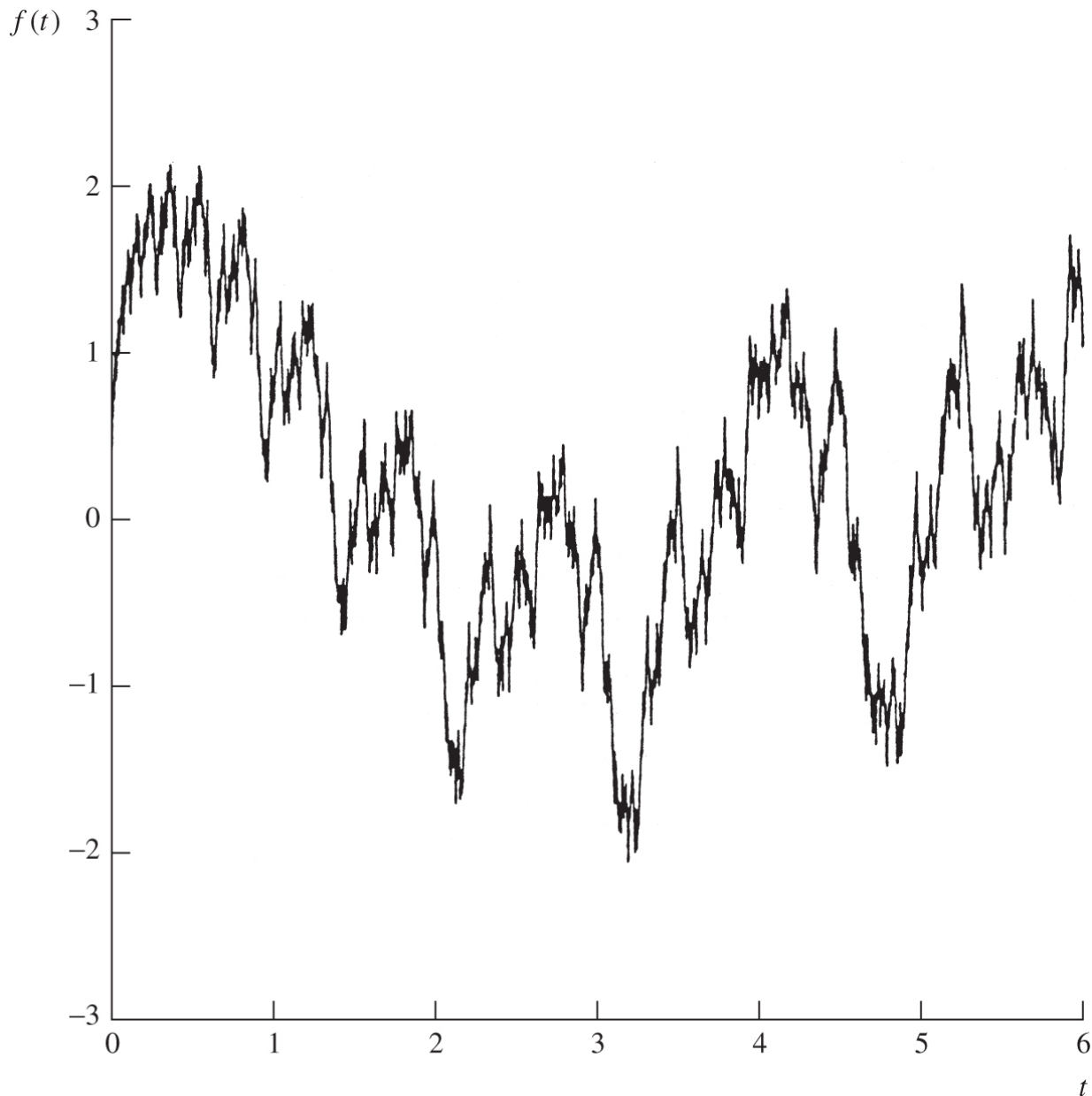


Figure 0.6 A Julia set.

There are many other types of construction, some of which will be discussed in detail later in the book, that also lead to sets with these sorts of properties. The highly intricate structure of the Julia set illustrated in [Figure 0.6](#) stems from the single quadratic function $f(z) = z^2 + c$ for a suitable constant c . Although the set is not strictly self-similar in the sense that the Cantor set and von Koch curve are, it is ‘quasi-self-similar’ in that arbitrarily small portions of the set can be magnified and then distorted smoothly to coincide with a large part of the set.

[Figure 0.7](#) shows the graph of the function $f(t) = \sum_{k=0}^{\infty} \left(\frac{3}{2}\right)^{-k/2} \sin\left(\left(\frac{3}{2}\right)^k t\right)$; the infinite summation leads to the graph having a fine structure, rather than being a smooth curve to which classical calculus is applicable.

Some of these constructions may be ‘randomised’. [Figure 0.8](#) shows a ‘random von Koch curve’—a coin was tossed at each step in the construction to determine on which side of the curve to place the new pair of line segments. This random curve certainly has a fine structure, but the strict self-similarity of the von Koch curve has been replaced by a ‘statistical self-similarity’.



[Figure 0.7](#) Graph of $f(t) = \sum_{k=0}^{\infty} \left(\frac{3}{2}\right)^{-k/2} \sin\left(\left(\frac{3}{2}\right)^k t\right)$.

These are all examples of sets that are commonly referred to as *fractals*. (The word ‘fractal’ was coined by Mandelbrot in his fundamental essay from the Latin *fractus*, meaning broken, to describe objects that were too irregular to fit into a traditional geometrical setting.) Properties such as those listed for the Cantor set are characteristic of fractals, and it is sets with such properties that we will have in mind throughout the book. Certainly, any fractal worthy of the name will have a fine structure, that is, detail at all scales. Many fractals have some degree of self-similarity—they are made up of parts that resemble the whole in some way. Sometimes, the resemblance may be weaker than strict geometrical similarity; for example, the similarity may be approximate or statistical.

Methods of classical geometry and calculus are unsuited to study fractals and we need alternative techniques. The main tool of fractal geometry is dimension in its many forms. We are familiar enough with the idea that a (smooth) curve is a 1-dimensional object and a surface is 2-dimensional. It is less clear that, for many purposes, the Cantor set should be regarded as having dimension

$\log 2/\log 3 = 0.631\dots$ and the von Koch curve as having dimension $\log 4/\log 3 = 1.262\dots$. This latter number is, at least, consistent with the von Koch curve being ‘larger than 1-dimensional’ (having infinite length) and ‘smaller than 2-dimensional’ (having zero area).

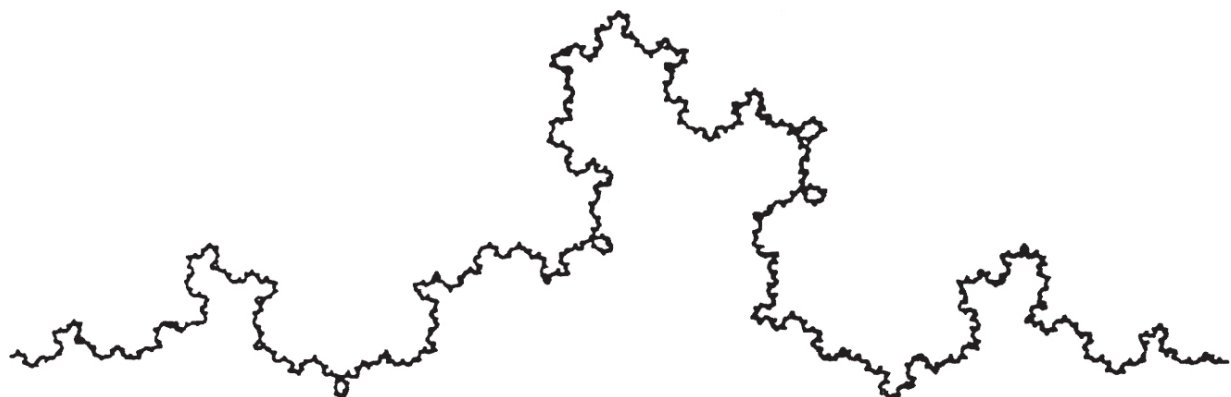


Figure 0.8 A random version of the von Koch curve.

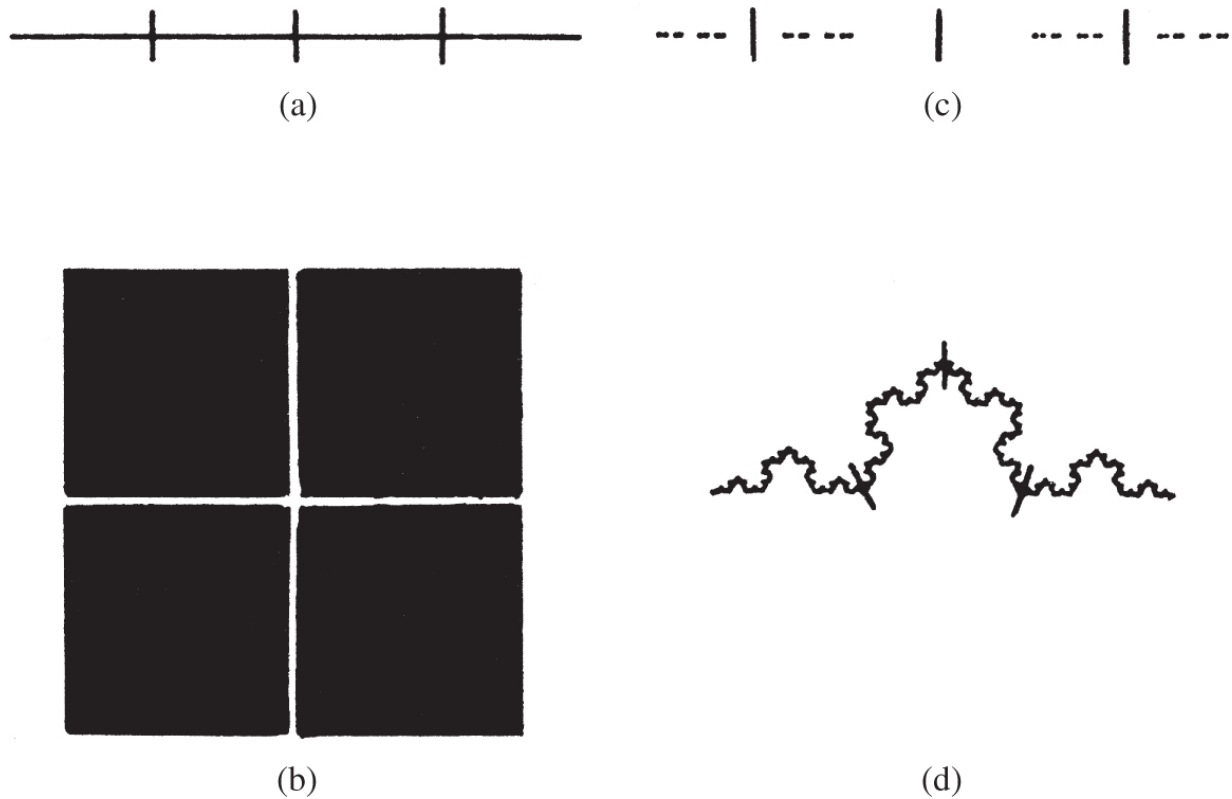


Figure 0.9 Division of certain sets into four parts. The parts are similar to the whole with ratios: (a) $\frac{1}{4}$ for line segment; (b) $\frac{1}{2}$ for square; (c) $\frac{1}{9}$ for middle third Cantor set; (d) $\frac{1}{3}$ for von Koch curve.

The following argument gives one (rather crude) interpretation of the meaning of these ‘dimensions’ indicating how they reflect scaling properties and self-similarity. As Figure 0.9 indicates, a line segment is made up of four copies of itself, scaled by a factor $\frac{1}{4}$. The segment has dimension $-\log 4/\log \frac{1}{4} = 1$. A square, however, is made up of four copies of itself scaled by a factor $\frac{1}{2}$ (i.e. with half the side length) and has dimension $-\log 4/\log \frac{1}{2} = 2$. In the same way, the von Koch curve is made up of four copies of itself scaled by a factor $\frac{1}{3}$, and has dimension $-\log 4/\log \frac{1}{3} = \log 4/\log 3$, and the Cantor set may be regarded as comprising four copies of itself scaled by a factor $\frac{1}{9}$ and having dimension $-\log 4/\log \frac{1}{9} = \log 2/\log 3$. In general, a set made up of m copies of itself scaled by a factor r might be thought of as

having dimension $-\log m/\log r$. The number obtained in this way is usually referred to as the *similarity dimension* of the set.

Unfortunately, similarity dimension is meaningful only for a relatively small class of strictly self-similar sets. Nevertheless, there are other definitions of dimension that are much more widely applicable. For example, Hausdorff dimension and the box-counting dimensions may be defined for any sets and, in these four examples, may be shown to equal the similarity dimension. The early chapters of the book are concerned with the definition and properties of Hausdorff and box dimensions, along with methods for their calculation. Very roughly, a dimension provides a description of how much space a set fills. It is a measure of the prominence of the irregularities of a set when viewed at very small scales. A dimension contains much information about the geometrical properties of a set.

A word of warning is appropriate at this point. It is possible to define the ‘dimension’ of a set in many ways, some satisfactory and others less so. It is important to realise that different definitions may give different values of dimension for the same set and may also have very different properties. Inconsistent usage has sometimes led to considerable confusion. In particular, warning lights flash in my mind (as in the minds of other mathematicians) whenever the term ‘fractal dimension’ is seen. Although some authors attach a precise meaning to this, I have known others interpret it inconsistently in a single piece of work. The reader should always be aware of the definition in use in any discussion.

In his original essay, Mandelbrot defined a fractal to be a set with Hausdorff dimension strictly greater than its topological dimension. (The *topological dimension* of a set is always an integer and is 0 if it is totally disconnected, 1 if each point has arbitrarily small neighbourhoods with boundary of dimension 0 and so on.) This definition proved to be unsatisfactory in that it excluded a number of sets that clearly ought to be regarded as fractals. Various other

definitions have been proposed, but they all seem to have this same drawback.

My personal feeling is that the definition of a ‘fractal’ should be regarded in the same way as a biologist regards the definition of ‘life’. There is no hard-and-fast definition but just a list of properties characteristic of a living thing, such as the ability to reproduce or to move or to exist to some extent independently of the environment. Most living things have most of the characteristics on the list, although there are living objects that are exceptions to each of them. In the same way, it seems best to regard a fractal as a set that has properties such as those listed below, rather than to look for a precise definition which will almost certainly exclude some interesting cases. From the mathematician’s point of view, this approach is no bad thing. It is difficult to avoid developing properties of dimension other than in a way that applies to ‘fractal’ and ‘non-fractal’ sets alike. For ‘non-fractals’, however, such properties are of little interest—they are generally almost obvious and could be obtained more easily by other methods.

Therefore, when we refer to a set F as a fractal, we will typically have the following in mind.

- i. F has a fine structure, that is, detail on arbitrarily small scales.
- ii. F is too irregular to be described in traditional geometrical language, both locally and globally.
- iii. Often F has some form of self-similarity, perhaps approximate or statistical.
- iv. Usually, the ‘fractal dimension’ of F (defined in some way) is greater than its topological dimension.
- v. In most cases of interest, F is defined in a very simple way, perhaps recursively.

What can we say about the geometry of as diverse a class of objects as fractals? Classical geometry gives us a clue. In Part I of this book,

we study certain analogues of familiar geometrical properties in the fractal situation. The orthogonal projection or ‘shadow’ of a circle in space onto a plane is, in general, an ellipse. The fractal projection theorems tell us about the ‘shadows’ of a fractal. For many purposes, a tangent provides a good local approximation to a circle. Although fractals tend not to have tangents in any sense, it is often possible to say a surprising amount about their local form. Two circles in the plane in ‘general position’ either intersect in two points or not at all (we regard the case of mutual tangents as ‘exceptional’). Using dimension, we can make similar statements about the intersection of fractals. Moving a circle perpendicular to its plane sweeps out a cylinder, with properties that are related to those of the original circle. Similar, and indeed more general, constructions are possible with fractals.

Although classical geometry is of considerable intrinsic interest, it is also called upon widely in other areas of mathematics. For example, circles or parabolae occur as the solution curves of certain differential equations, and a knowledge of the geometrical properties of such curves aids our understanding of the differential equations. In the same way, the general theory of fractal geometry can be applied to the many branches of mathematics in which fractals occur. Various examples of this are given in Part II of the book.

Historically, interest in geometry has been stimulated by its applications to nature. The ellipse assumed importance as the shape of planetary orbits, as did the sphere as the shape of the earth. The geometry of the ellipse and sphere can be applied to these physical situations. Of course, orbits are not quite elliptical, and the earth is not actually spherical, but for many purposes, such as the prediction of planetary motion or the study of the earth’s gravitational field, these approximations may be perfectly adequate.

A similar situation pertains to fractals. A glance at the recent physics literature shows the variety of natural objects that are described as fractals—cloud boundaries, topographical surfaces,

coastlines, turbulence in fluids and so on. None of these are actual fractals—their fractal features disappear if they are viewed at sufficiently small scales. Nevertheless, over certain ranges of scale, they appear very much like fractals, and at such scales may usefully be regarded as such. The distinction between ‘natural fractals’ and the mathematical ‘fractal sets’ that might be used to describe them was emphasised in Mandelbrot’s original essay, but this distinction seems to have become somewhat blurred. There are no true fractals in nature. (There are no true straight lines or circles either!)

If the mathematics of fractal geometry is to be really worthwhile, then it should be applicable to physical situations. Considerable progress is being made in this direction and some examples are given towards the end of this book. Although there are natural phenomena that have been explained in terms of fractal mathematics (Brownian motion is a good example), many applications tend to be descriptive rather than predictive. Much of the basic mathematics used in the study of fractals is not particularly new, although much recent mathematics has been specifically geared to address fractals. For further progress to be made, development and application of appropriate mathematics remain a high priority.

Notes and references

Unlike the rest of the book, which consists of fairly solid mathematics, this introduction contains some of the author’s opinions and prejudices, which may well not be shared by other workers on fractals. *Caveat emptor!*

The foundational treatise on fractals, which may be appreciated at many levels, is the scientific, philosophical and pictorial essay of Mandelbrot (1982) (developed from an earlier version, Mandelbrot (1977)), containing a great diversity of natural and mathematical examples. This essay has been the inspiration for much of the work that has been done on fractals.

Many books and papers have been written on diverse aspects of fractals, and appropriate references are cited at the end of each chapter. Here, we mention a selection of books with a broad coverage. There are short overviews by Falconer (2013) and Lesmoir-Gordon, Rood and Edney (2009) aimed at the non-specialist. Introductory mathematical treatments include those by Addison (1997) and Schroeder (2009). The books by Barnsley (2006, 2012); Edgar (1998, 2008) and Peitgen, Jürgens, and Saupe (2004) provide other mathematical treatments at a level that is similar to this. Falconer (1985a); Mattila (1999); Federer (1996) and Morgan (2008) go into more detail on the geometric measure theory side and Rogers (1998) addresses the general theory of Hausdorff measures. Books with a computational emphasis include Devaney and Keen (2006); Hoggar (1993); Baumann (2005); Peitgen and Saupe (2011) and Pickover (2012). The sequel to this book, Falconer (1997), contains more advanced mathematical techniques for studying fractals.

Whilst this book and much of the literature concentrates on fractals in Euclidean spaces, much of the mathematics may be developed in more general settings; see, for example, the books by David and Semmes (1997); Rogers (1998) and Semmes (2000).

A great deal of interesting and readable material may be found in proceedings of various conferences on fractal mathematics and its applications. The proceedings of the series of Fractals and Stochastics meetings, edited by Bandt, Graf and Zähle (1995, 2000); Bandt, Mosco and Zähle (2004) and Bandt, Mörters and Zähle (2009), contain many excellent surveys, as do those on Fractals and Related Fields edited by Barral and Seuret (2010, 2013) along with those edited by Grabner and Woess (2003). Volumes produced in honour of Benoit Mandelbrot include those edited by Evertsz, Peitgen and Voss (1995) and by Lapidus and van Frankenhuysen (2004). Essays collated by Frame and Mandelbrot (2002) address the role of fractals in mathematics and science education. Books and conference papers more concerned with applications of fractals are listed in section titled Notes and References of Chapter 18.

Mandelbrot's 'Selecta' (1997, 1999, 2002, 2004) include a wide range of papers with commentaries which, together with his memoirs, Mandelbrot (2012), provide a fascinating insight into the development of fractal mathematics and science. Edgar (1993) brings together a selection of landmark papers in the development of fractal mathematics from the past 140 years.

Countless papers relating to fractals have been published in a wide range of mathematics and science journals. There are two subject specific journals: the interdisciplinary *Fractals* covers a wide range of theory and applications, whilst *The Journal of Fractal Geometry* concentrates on mathematical research.

Part I

Foundations

Chapter 1

Mathematical background

This chapter reviews some of the basic mathematical ideas and notations that are used throughout the book. Section 1.1 on set theory and Section 1.2 on functions are rather concise; readers unfamiliar with this type of material are advised to consult a more detailed text on mathematical analysis. Measures and mass distributions play an important part in the theory of fractals and a treatment adequate for our needs is given in Section 1.3. By asking the reader to take on trust the existence of certain measures, we can avoid many of the technical difficulties usually associated with measure theory. Some notes on probability theory are given in Section 1.4; this is needed in Chapters 15 and 16.

1.1 Basic set theory

In this section, we recall some basic notions from set theory and point set topology.

We generally work in *n-dimensional Euclidean space*, \mathbb{R}^n , where $\mathbb{R}^1 = \mathbb{R}$ is just the set of real numbers or the ‘real line’, and \mathbb{R}^2 is the (Euclidean) plane. Points in \mathbb{R}^n will generally be denoted by lower case letters x , y , and so on, and we will occasionally use the coordinate form $x = (x_1, \dots, x_n)$, $y = (y_1, \dots, y_n)$. Addition and scalar multiplication are defined in the usual manner, so that

$x + y = (x_1 + y_1, \dots, x_n + y_n)$ and $\lambda x = (\lambda x_1, \dots, \lambda x_n)$, where λ is a real scalar. We use the usual *Euclidean distance* or *metric* on \mathbb{R}^n so if x and y are points of \mathbb{R}^n , the distance between them is $|x - y| = (\sum_{i=1}^n |x_i - y_i|^2)^{1/2}$. In particular, the triangle inequality $|x + y| \leq |x| + |y|$, the reverse triangle inequality $||x| - |y|| \leq |x - y|$ and the metric triangle inequality $|x - y| \leq |x - z| + |z - y|$ hold for all $x, y, z \in \mathbb{R}^n$.

Sets, which will generally be subsets of \mathbb{R}^n , are denoted by capital letters E , F , U , and so on. In the usual way, $x \in E$ means that the point x belongs to the set E , and $E \subset F$ means that E is a subset of the set F . We write $\{x : \text{condition}\}$ for the set of x for which ‘condition’ is true. Certain frequently occurring sets have a special notation. The empty set, which contains no elements, is written as \emptyset . The integers are denoted by \mathbb{Z} , and the rational numbers by \mathbb{Q} . We use a superscript $+$ to denote the positive elements of a set; thus, \mathbb{R}^+ are the positive real numbers, and \mathbb{Z}^+ are the positive integers. Sometimes we refer to the complex numbers \mathbb{C} , which for many purposes may be identified with the plane \mathbb{R}^2 , with $x_1 + ix_2$ corresponding to the point (x_1, x_2) .

The *closed ball* of centre x and radius r is defined by

$B(x, r) = \{y : |y - x| \leq r\}$. Similarly, the *open ball* is

$B^o(x, r) = \{y : |y - x| < r\}$. Thus, the closed ball contains its bounding sphere, but the open ball does not. Of course, in \mathbb{R}^2 , a ball is a disc and in \mathbb{R}^1 a ball is just an interval. If $a < b$, we write $[a, b]$ for the *closed interval* $\{x : a \leq x \leq b\}$ and (a, b) for the *open interval* $\{x : a < x < b\}$. Similarly, $[a, b)$ denotes the half-open interval $\{x : a \leq x < b\}$, and so on.

The *coordinate cube* of side $2r$ and centre $x = (x_1, \dots, x_n)$ is the set $\{y = (y_1, \dots, y_n) : |y_i - x_i| \leq r \text{ for all } i = 1, \dots, n\}$. (A cube in \mathbb{R}^2 is just a square and in \mathbb{R}^1 is an interval.)

From time to time we refer to the δ -neighbourhood or δ -parallel body, A_δ , of a set A , that is, the set of points within distance δ of A ; thus, $A_\delta = \{x : |x - y| \leq \delta \text{ for some } y \text{ in } A\}$ (see [Figure 1.1](#)).

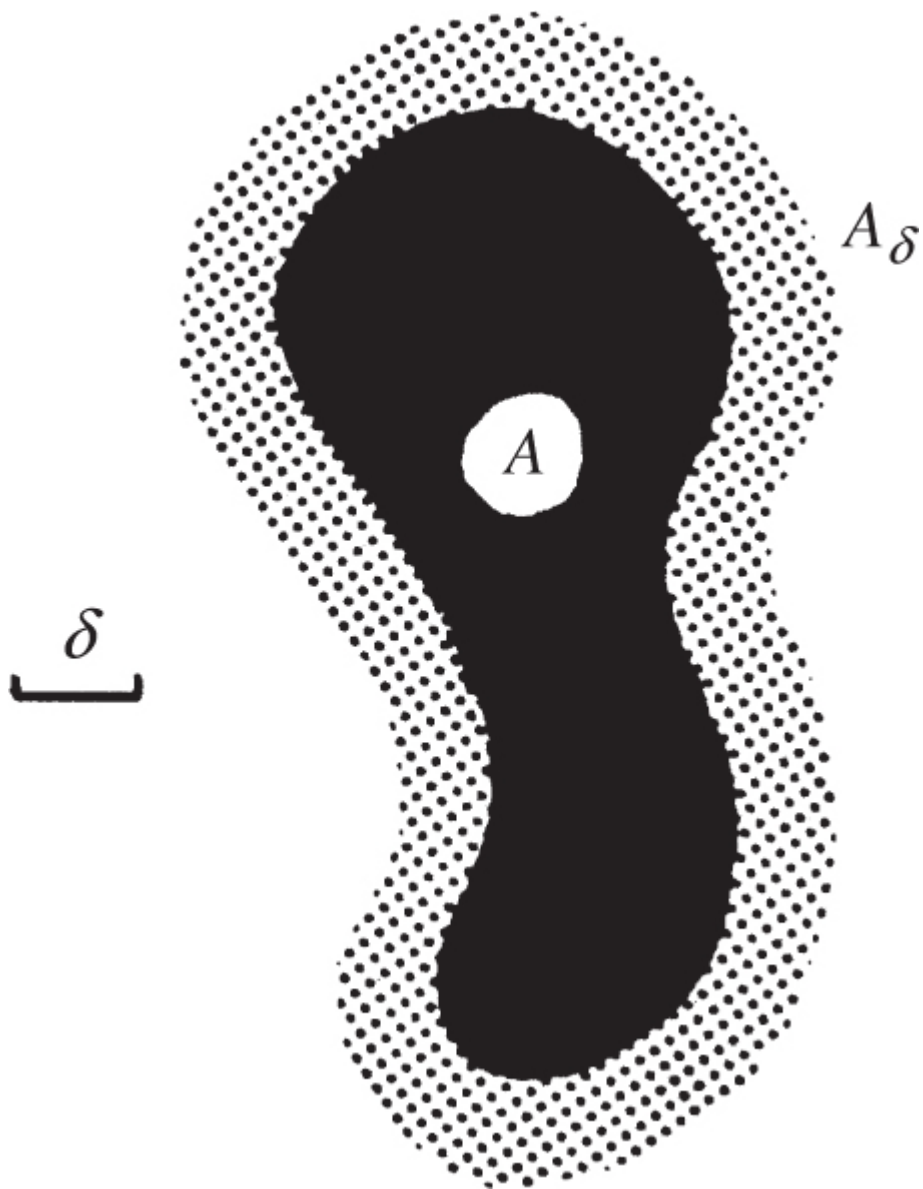


Figure 1.1 A set A and its δ -neighbourhood A_δ .

We write $A \cup B$ for the *union* of the sets A and B , that is, the set of points belonging to either A or B , or both. Similarly, we write $A \cap B$ for their *intersection*, the points in both A and B . More generally, $\bigcup_\alpha A_\alpha$ denotes the union of an arbitrary collection of sets $\{A_\alpha\}$, that is, those points in at least one of the sets A_α , and $\bigcap_\alpha A_\alpha$ denotes their intersection, consisting of the set of points common to all of the A_α . A collection of sets is *disjoint* if the intersection of any pair is the empty set. The *difference* $A \setminus B$ of A and B consists of the points in A but not B . The set $\mathbb{R}^n \setminus A$ is termed the *complement* of A .

The set of all ordered pairs $\{(a, b) : a \in A \text{ and } b \in B\}$ is called the (*Cartesian*) *product* of A and B and is denoted by $A \times B$. If $A \subset \mathbb{R}^n$ and $B \subset \mathbb{R}^m$, then $A \times B \subset \mathbb{R}^{n+m}$.

If A and B are subsets of \mathbb{R}^n and λ is a real number, we define the *vector sum* of the sets as $A + B = \{x + y : x \in A \text{ and } y \in B\}$ and we define the *scalar multiple* $\lambda A = \{\lambda x : x \in A\}$.

An infinite set A is *countable* if its elements can be listed in the form x_1, x_2, \dots with every element of A appearing at a specific place in the list; otherwise, the set is *uncountable*. The sets \mathbb{Z} and \mathbb{Q} are countable but \mathbb{R} is uncountable. Note that a countable union of countable sets is countable.

If A is any non-empty set of real numbers, then its *supremum* $\sup A$ is the least number m such that $x \leq m$ for every x in A or is ∞ if no such number exists. Similarly, the *infimum* $\inf A$ is the greatest number m such that $m \leq x$ for all x in A or is $-\infty$. Intuitively, the supremum and infimum are thought of as the maximum and minimum of the set, although it is important to realise that $\sup A$ and $\inf A$ need not be members of the set A itself. For example, $\sup(0, 1) = 1$, but $1 \notin (0, 1)$. We write $\sup_{x \in B}(\)$ for the supremum of the quantity in brackets, which may depend on x , as x ranges over the set B .

We define the *diameter* $|A|$ of a non-empty subset of \mathbb{R}^n as the greatest distance apart of pairs of points in A . Thus, $|A| = \sup\{|x - y| : x, y \in A\}$. In \mathbb{R}^n , a ball of radius r has diameter $2r$, and a cube of side length δ has diameter $\delta\sqrt{n}$. A set A is *bounded* if it has finite diameter or, equivalently, if A is contained in some (sufficiently large) ball.

Convergence of sequences is defined in the usual way. A sequence $\{x_k\}$ in \mathbb{R}^n *converges* to a point x of \mathbb{R}^n as $k \rightarrow \infty$ if, given $\varepsilon > 0$, there exists a number K such that $|x_k - x| < \varepsilon$ whenever $k > K$, that is, if $|x_k - x|$ converges to 0. The number x is called the *limit* of the sequence, and we write $x_k \rightarrow x$ or $\lim_{k \rightarrow \infty} x_k = x$.

The ideas of ‘open’ and ‘closed’ that have been mentioned in connection with balls apply to much more general sets. Intuitively, a set is closed if it contains its boundary and open if it contains none of its boundary points. More precisely, a subset A of \mathbb{R}^n is *open* if, for all points x in A , there is some ball $B(x, r)$, centred at x and is of positive radius that is contained in A . A set is *closed* if whenever $\{x_k\}$ is a sequence of points of A converging to a point x of \mathbb{R}^n , then x is in A (see [Figure 1.2](#)). The empty set \emptyset and \mathbb{R}^n are regarded as both open and closed.

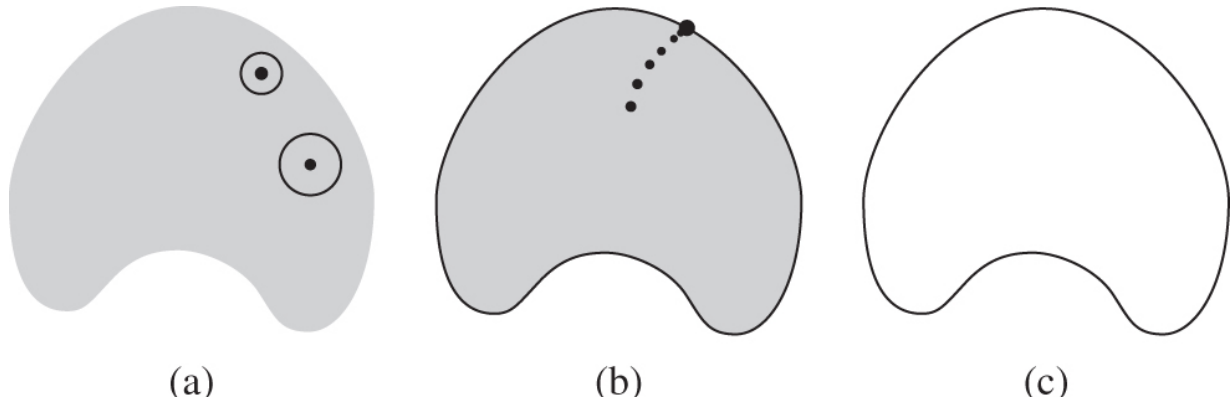


Figure 1.2 (a) An open set—there is a ball contained in the set centred at each point of the set. (b) A closed set—the limit of any convergent sequence of points from the set lies in the set. (c) The boundary of the set in (a) or (b).

It may be shown that a set is open if and only if its complement is closed. The union of any collection of open sets is open, as is the intersection of any finite number of open sets. The intersection of any collection of closed sets is closed, as is the union of any finite number of closed sets (see Exercise 1.6).

A set A is called a *neighbourhood* of a point x if there is some (small) ball $B(x, r)$ centred at x and contained in A .

The intersection of all the closed sets containing a set A is called the *closure* of A , written \bar{A} . The union of all the open sets contained in A is the *interior* $\text{int } A$ of A . The closure of A is thought of as the smallest closed set containing A , and the interior as the largest open set contained in A . The *boundary* ∂A of A is given by

$\partial A = \overline{A} \setminus \text{int } A$, thus $x \in \partial A$ if and only if the ball $B(x, r)$ intersects both A and its complement for all $r > 0$.

A set B is a *dense* in A if $A \subset \overline{B}$, that is, if there are points of B arbitrarily close to each point of A .

A set A is *compact* if any collection of open sets that covers A (i.e. with union containing A) has a finite subcollection which also covers A . Technically, compactness is an extremely useful property that enables infinite sets of conditions to be reduced to finitely many. However, as far as most of this book is concerned, it is enough to take the definition of a compact subset of \mathbb{R}^n as one that is both closed and bounded.

The intersection of any collection of compact sets is compact. It may be shown that if $A_1 \supset A_2 \supset \dots$ is a decreasing sequence of compact sets, then the intersection $\bigcap_{i=1}^{\infty} A_i$ is non-empty (see Exercise 1.7). Moreover, if $\bigcap_{i=1}^{\infty} A_i$ is contained in V for some open set V , then the finite intersection $\bigcap_{i=1}^k A_i$ is contained in V for some k .

A subset A of \mathbb{R}^n is *connected* if there do not exist open sets U and V such that $U \cup V$ contains A with $A \cap U$ and $A \cap V$ disjoint and non-empty. Intuitively, we think of a set A as connected if it consists of just one ‘piece’. The largest connected subset of A containing a point x is called the *connected component* of x . The set A is *totally disconnected* if the connected component of each point consists of just that point. This will certainly be so if for every pair of points x and y in A we can find disjoint open sets U and V such that $x \in U, y \in V$ and $A \subset U \cup V$.

There is one further class of set that must be mentioned, although its precise definition is indirect and should not concern the reader unduly. The class of *Borel sets* is the smallest collection of subsets of \mathbb{R}^n with the following properties:

1. Every open set and every closed set is a Borel set.
2. The union of every finite or countable collection of Borel sets is a Borel set, and the intersection of every finite or countable

collection of Borel sets is a Borel set.

Throughout this book, virtually all of the subsets of \mathbb{R}^n that will be of any interest to us will be Borel sets. Any set that can be constructed using a sequence of countable unions or intersections starting with the open sets or closed sets will certainly be Borel. The reader will not go far wrong with the material of the sort described in this book by assuming that all the sets encountered are Borel sets.

1.2 Functions and limits

Let X and Y be any sets. A *mapping*, *function* or *transformation* f from X to Y is a rule or formula that associates a point $f(x)$ of Y with each point x of X . We write $f : X \rightarrow Y$ to denote this situation; X is called the *domain* of f and Y is called the *codomain*. If A is any subset of X , we write $f(A)$ for the *image* of A , given by $\{f(x) : x \in A\}$. If B is a subset of Y , we write $f^{-1}(B)$ for the *inverse image* or *pre-image* of B , that is, the set $\{x \in X : f(x) \in B\}$; note that in this context, the inverse image of a single point can contain many points.

A function $f : X \rightarrow Y$ is called an *injection* or a *one-to-one* function if $f(x) \neq f(y)$ whenever $x \neq y$, that is, different elements of X are mapped to different elements of Y . The function is called a *surjection* or an *onto* function if, for every y in Y , there is an element x in X with $f(x) = y$, that is, every element of Y is the image of some point in X . A function that is both an injection and a surjection is called a *bijection* or *one-to-one correspondence* between X and Y . If $f : X \rightarrow Y$ is a bijection, then we may define the *inverse function* $f^{-1} : Y \rightarrow X$ by taking $f^{-1}(y)$ as the unique element of X such that $f(x) = y$. In this situation, $f^{-1}(f(x)) = x$ for all x in X and $f(f^{-1}(y)) = y$ for all y in Y .

The *composition* of the functions $f : X \rightarrow Y$ and $g : Y \rightarrow Z$ is the function $g \circ f : X \rightarrow Z$ given by $(g \circ f)(x) = g(f(x))$. This definition

extends to the composition of any finite number of functions in the obvious way.

Certain functions from \mathbb{R}^n to \mathbb{R}^n have a particular geometric significance; often, in this context, they are referred to as *transformations* and are denoted by capital letters. Their effects are shown in [Figure 1.3](#). The transformation $S : \mathbb{R}^n \rightarrow \mathbb{R}^n$ is called a *congruence* or *isometry* if it preserves distances, that is if $|S(x) - S(y)| = |x - y|$ for x, y in \mathbb{R}^n . Congruences also preserve angles and transform sets into geometrically congruent ones. Special cases include *translations*, which are of the form $S(x) = x + a$ and have the effect of shifting points parallel to the vector a , *rotations* which have a centre a such that $|S(x) - a| = |x - a|$ for all x (for convenience, we also regard the identity transformation given by $I(x) = x$ as a rotation) and *reflections*, which maps points to their mirror images in some $(n - 1)$ -dimensional plane. A congruence that may be achieved by a combination of a rotation and a translation, that is, does not involve reflection, is called a *rigid motion* or *direct congruence*. A transformation $S : \mathbb{R}^n \rightarrow \mathbb{R}^n$ is a *similarity* of *ratio* or *scale* $c > 0$ if $|S(x) - S(y)| = c|x - y|$ for all x, y in \mathbb{R}^n . A similarity transforms sets into geometrically similar ones with all lengths multiplied by the factor c .

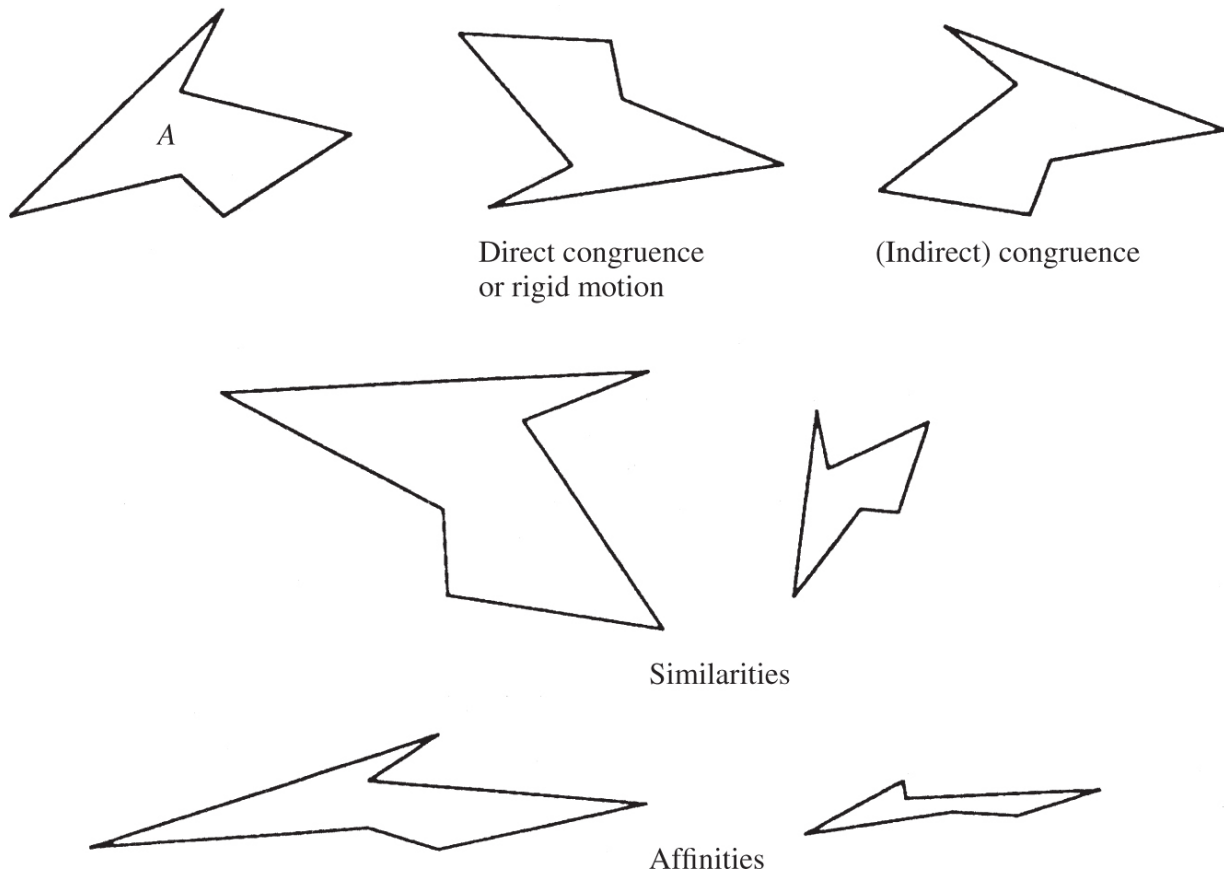


Figure 1.3 The effect of various transformations on a set A .

A transformation $T : \mathbb{R}^n \rightarrow \mathbb{R}^n$ is *linear* if $T(x + y) = T(x) + T(y)$ and $T(\lambda x) = \lambda T(x)$ for all $x, y \in \mathbb{R}^n$ and $\lambda \in \mathbb{R}$; linear transformations may be represented by matrices in the usual way. Such a linear transformation is *non-singular* if $T(x) = 0$ if and only if $x = 0$. If $S : \mathbb{R}^n \rightarrow \mathbb{R}^n$ is of the form $S(x) = T(x) + a$, where T is a non-singular linear transformation and a is a vector in \mathbb{R}^n , then S is called an *affine transformation* or an *affinity*. An affinity may be thought of as a shearing transformation; its contracting or expanding effect need not be the same in every direction. However, if T is orthonormal, then S is a congruence, and if T is a scalar multiple of an orthonormal transformation, then T is a similarity.

It is worth pointing out that such classes of transformation form groups under composition of mappings. For example, the composition of two translations is a translation, the identity transformation is trivially a translation, and the inverse of a

translation is a translation. Finally, the associative law $S \circ (T \circ U) = (S \circ T) \circ U$ holds for all translations S, T, U . Similar group properties hold for the congruences, the rigid motions, the similarities and the affinities.

A function $f : X \rightarrow Y$ is called a *Hölder function of exponent α* if

$$|f(x) - f(y)| \leq c|x - y|^\alpha \quad (x, y \in X)$$

for some constant $c \geq 0$. The function f is called *Lipschitz* if α may be taken to be equal to 1, that is if

$$|f(x) - f(y)| \leq c|x - y| \quad (x, y \in X)$$

and *bi-Lipschitz* if

$$c_1|x - y| \leq |f(x) - f(y)| \leq c_2|x - y| \quad (x, y \in X)$$

for $0 < c_1 \leq c_2 < \infty$, in which case both f and $f^{-1} : f(X) \rightarrow X$ are Lipschitz functions. Lipschitz and Hölder functions play an important role in fractal geometry.

We next remind readers of the basic ideas of limits and continuity of functions. Let X and Y be subsets of \mathbb{R}^n and \mathbb{R}^m , respectively, let $f : X \rightarrow Y$ be a function, and let a be a point of \bar{X} . We say that $f(x)$ has *limit y* (or *tends to y* , or *converges to y*) as x tends to a , if, given $\varepsilon > 0$, there exists $\delta > 0$ such that $|f(x) - y| < \varepsilon$ for all $x \in X$ with $|x - a| < \delta$. We denote this by writing $f(x) \rightarrow y$ as $x \rightarrow a$ or by $\lim_{x \rightarrow a} f(x) = y$. For a function $f : X \rightarrow \mathbb{R}$, we say that $f(x)$ *tends to infinity* (written $f(x) \rightarrow \infty$) as $x \rightarrow a$ if, given M , there exists $\delta > 0$ such that $f(x) > M$ whenever $|x - a| < \delta$. The definition of $f(x) \rightarrow -\infty$ is similar.

Suppose, now, that $f : \mathbb{R}^+ \rightarrow \mathbb{R}$. We shall frequently be interested in the values of such functions for small positive values of x . Note that if $f(x)$ is increasing as x decreases, then $\lim_{x \rightarrow 0} f(x)$ exists either as a finite limit or as ∞ , and if $f(x)$ is decreasing as x decreases, then $\lim_{x \rightarrow 0} f(x)$ exists and is finite or $-\infty$. Of course, $f(x)$ can fluctuate wildly for small x and $\lim_{x \rightarrow 0} f(x)$ need not exist at all. We use lower

and upper limits to describe such fluctuations. We define the *lower limit* as

$$\underline{\lim}_{x \rightarrow 0} f(x) \equiv \lim_{r \rightarrow 0} (\inf \{f(x) : 0 < x < r\}).$$

As $\inf \{f(x) : 0 < x < r\}$ is either $-\infty$ for all positive r or else increases as r decreases, $\underline{\lim}_{x \rightarrow 0} f(x)$ always exists. Similarly, the *upper limit* is defined as

$$\overline{\lim}_{x \rightarrow 0} f(x) \equiv \lim_{r \rightarrow 0} (\sup \{f(x) : 0 < x < r\}).$$

The lower and upper limits exist (as real numbers or $-\infty$ or ∞) for every function f and are indicative of the variation of f for x close to 0 (see [Figure 1.4](#)). Clearly, $\underline{\lim}_{x \rightarrow 0} f(x) \leq \overline{\lim}_{x \rightarrow 0} f(x)$; if the lower and upper limits are equal, then $\lim_{x \rightarrow 0} f(x)$ exists and equals this common value. Note that if $f(x) \leq g(x)$ for $x > 0$, then $\underline{\lim}_{x \rightarrow 0} f(x) \leq \underline{\lim}_{x \rightarrow 0} g(x)$ and $\overline{\lim}_{x \rightarrow 0} f(x) \leq \overline{\lim}_{x \rightarrow 0} g(x)$. In the same way, it is possible to define lower and upper limits as $x \rightarrow a$ for functions $f : X \rightarrow \mathbb{R}$ where X is a subset of \mathbb{R}^n with a in \bar{X} .

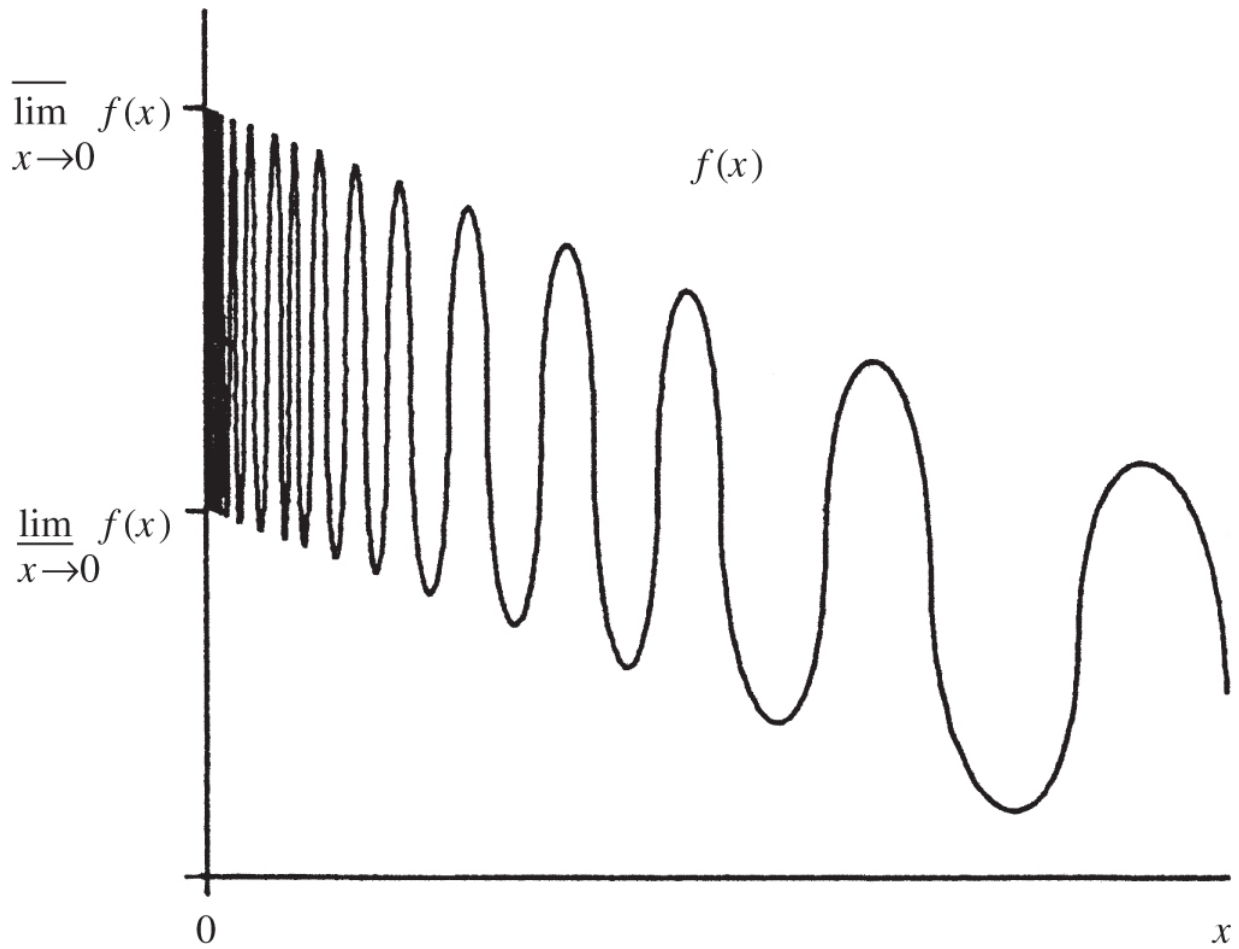


Figure 1.4. The upper and lower limits of a function.

We sometimes need to compare two functions $f, g : \mathbb{R}^+ \rightarrow \mathbb{R}$ for small values. We write $f(x) \sim g(x)$ to mean that $f(x)/g(x) \rightarrow 1$ as $x \rightarrow 0$. We will often have that $f(x) \sim x^s$; in other words, f obeys an approximate power law of exponent s when x is small. We use the notation $f(x) \simeq g(x)$ more loosely, to mean that $f(x)$ and $g(x)$ are approximately equal in some sense, to be specified in the particular circumstances.

Recall that a function $f : X \rightarrow Y$ is *continuous* at a point a of X if $f(x) \rightarrow f(a)$ as $x \rightarrow a$ and is *continuous on X* if it is continuous at all points of X . In particular, Lipschitz and Hölder mappings are continuous. If $f : X \rightarrow Y$ is a continuous bijection with continuous inverse $f^{-1} : Y \rightarrow X$, then f is called a *homeomorphism*, and X and Y are termed *homeomorphic sets*. Congruences, similarities and affine transformations on \mathbb{R}^n are examples of homeomorphisms.

The function $f : \mathbb{R} \rightarrow \mathbb{R}$ is *differentiable* at x with the number $f'(x)$ as *derivative* if

$$\lim_{h \rightarrow 0} \frac{f(x+h) - f(x)}{h} = f'(x).$$

A function f is termed *continuously differentiable* if $f'(x)$ is continuous in x . Very significant is the *mean value theorem* that states that, given $x < y$ and a real-valued function f that is differentiable over an interval containing x and y , there exists w with $x < w < y$ such that

$$\frac{f(y) - f(x)}{y - x} = f'(w)$$

(intuitively, any chord of the graph of f is parallel to the slope of f at some intermediate point). A consequence of the mean value theorem is that if $|f'(x)|$ is bounded over an interval, then f is Lipschitz over that interval.

More generally, if $f : \mathbb{R}^n \rightarrow \mathbb{R}^n$, we say that f is *differentiable* at x and has *derivative* given by the linear mapping $f'(x) : \mathbb{R}^n \rightarrow \mathbb{R}^n$ if

$$\lim_{h \rightarrow 0} \frac{|f(x+h) - f(x) - f'(x)h|}{|h|} = 0.$$

Occasionally, we shall be interested in the convergence of a sequence of functions $f_k : X \rightarrow Y$ where X and Y are subsets of Euclidean spaces. We say that functions f_k converge *pointwise* to a function $f : X \rightarrow Y$ if $f_k(x) \rightarrow f(x)$ as $k \rightarrow \infty$ for each x in X . We say that the convergence is *uniform* if $\sup_{x \in X} |f_k(x) - f(x)| \rightarrow 0$ as $k \rightarrow \infty$. Uniform convergence is a rather stronger property than pointwise convergence; the rate at which the limit is approached is uniform across X . If the functions f_k are continuous and converge uniformly to f , then f is continuous.

Finally, we remark that logarithms will always be to base e. Recall that, for $a, b > 0$, we have that $\log ab = \log a + \log b$ and that $\log a^c = c \log a$ for real numbers c . The identity $a^c = b^{c \log a / \log b}$ will often

be used. The logarithm is the inverse of the exponential function, so that $e^{\log x} = x$, for $x > 0$, and $\log e^y = y$ for $y \in \mathbb{R}$.

1.3 Measures and mass distributions

Anyone studying the mathematics of fractals will not get far before encountering measures in some form or other. Many people are put off by the seemingly technical nature of measure theory—often unnecessarily so, because for most fractal applications only a few basic ideas are needed. Moreover, these ideas are often already familiar in the guise of the mass or charge distributions encountered in basic physics.

We need only be concerned with measures on subsets of \mathbb{R}^n . Basically, a measure is just a way of ascribing a numerical ‘size’ to sets, such that if a set is decomposed into a finite or countable number of pieces in a reasonable way, then the size of the whole is the sum of the sizes of the pieces.

We call μ a *measure* on \mathbb{R}^n if μ assigns a non-negative number, possibly ∞ , to each subset of \mathbb{R}^n such that

$$(a) \mu(\emptyset) = 0; \quad \mathbf{1.1}$$

$$(b) \mu(A) \leq \mu(B) \quad \text{if } A \subset B; \quad \mathbf{1.2}$$

(c) if A_1, A_2, \dots is a countable (or finite) sequence of sets, then

$$\mu\left(\bigcup_{i=1}^{\infty} A_i\right) \leq \sum_{i=1}^{\infty} \mu(A_i) \quad \mathbf{1.3}$$

with equality in (1.3), that is

$$\mu\left(\bigcup_{i=1}^{\infty} A_i\right) = \sum_{i=1}^{\infty} \mu(A_i), \quad \mathbf{1.4}$$

if the A_i are disjoint Borel sets.

We call $\mu(A)$ the *measure* of the set A and think of $\mu(A)$ as the size of A measured in some way. Condition (a) says that the empty set has zero measure, condition (b) says ‘the larger the set, the larger the measure’ and condition (c) says that if a set is a union of a countable number of pieces (which may overlap), then the sum of the measure of the pieces is at least equal to the measure of the whole. If a set is decomposed into a countable number of disjoint Borel sets, then the total measure of the pieces equals the measure of the whole.

Technical note

For the measures that we shall encounter, (1.4) generally holds for a much wider class of sets than just the Borel sets, in particular for all images of Borel sets under continuous functions. However, for reasons that need not concern us here, we cannot in general require that (1.4) holds for every countable collection of disjoint sets A_i . The reader who is familiar with measure theory will realise that our definition of a measure on \mathbb{R}^n is the definition of what would normally be termed ‘an outer measure on \mathbb{R}^n for which the Borel sets are measurable’.

However, to save frequent referral to ‘measurable sets’, it is convenient to have $\mu(A)$ defined for every set A , and because we are usually interested in measures of Borel sets, it is enough to have (1.4) holding for Borel sets rather than for a larger class. If μ is defined and satisfies (1.1)–(1.4) for the Borel sets, the definition of μ may be extended to an outer measure on all sets in such a way that (1.1)–(1.3) hold, so our definition is consistent with the usual one.

If $A \supseteq B$, then A may be expressed as a disjoint union $A = B \cup (A \setminus B)$, so it is immediate from (1.4) that, if A and B are Borel sets with $\mu(B)$ finite,

$$\mu(A \setminus B) = \mu(A) - \mu(B).$$

1.5

Similarly, if $A_1 \subset A_2 \subset \dots$ is an increasing sequence of Borel sets, then

$$\mu\left(\bigcup_{i=1}^{\infty} A_i\right) = \lim_{i \rightarrow \infty} \mu(A_i). \quad \text{1.6}$$

To see this, note that $\bigcup_{i=1}^{\infty} A_i = A_1 \cup (A_2 \setminus A_1) \cup (A_3 \setminus A_2) \cup \dots$, with this union disjoint, so that

$$\begin{aligned} \mu\left(\bigcup_{i=1}^{\infty} A_i\right) &= \mu(A_1) + \sum_{i=1}^{\infty} (\mu(A_{i+1}) - \mu(A_i)) \\ &= \mu(A_1) + \lim_{k \rightarrow \infty} \sum_{i=1}^k (\mu(A_{i+1}) - \mu(A_i)) \\ &= \lim_{k \rightarrow \infty} \mu(A_k). \end{aligned}$$

A simple extension of this is that if, for $\delta > 0$, A_δ are Borel sets that are increasing as δ decreases, that is, $A_{\delta'} \subset A_\delta$ for $0 < \delta < \delta'$, then

$$\mu\left(\bigcup_{\delta>0} A_\delta\right) = \lim_{\delta \rightarrow 0} \mu(A_\delta). \quad \text{1.7}$$

We think of the support of a measure as the set on which the measure is concentrated. Formally, the *support* of μ , written $\text{spt } \mu$, is the smallest closed set X such that $\mu(\mathbb{R}^n \setminus X) = 0$. Thus, x is in the support if and only if $\mu(B(x, r)) > 0$ for all positive radii r . We say that μ is a measure *on* a set A if A contains the support of μ .

A measure on a bounded subset of \mathbb{R}^n for which $0 < \mu(\mathbb{R}^n) < \infty$ will be called a *mass distribution*, and we think of $\mu(A)$ as the mass of the set A . We often think of this intuitively: we take a finite mass and spread it in some way across a set X to get a mass distribution on X ; the conditions for a measure will then be satisfied.

We give some examples of measures and mass distributions. In general, we omit the proofs that measures with the stated properties exist. Much of technical measure theory concerns the existence of

such measures, but, as far as applications go, their existence is intuitively reasonable, and can be taken on trust.

Example 1.1 The counting measure

For each subset A of \mathbb{R}^n , let $\mu(A)$ be the number of points in A if A is finite and ∞ otherwise. Then μ is a measure on \mathbb{R}^n .

Example 1.2 Point mass

Let a be a point in \mathbb{R}^n and define $\mu(A)$ to be 1 if A contains a and 0 otherwise. Then μ is a mass distribution, thought of as a unit point mass concentrated at a .

Example 1.3 Lebesgue measure on \mathbb{R}

Lebesgue measure \mathcal{L}^1 extends the idea of ‘length’ to a large collection of subsets of \mathbb{R} that includes the Borel sets. For open and closed intervals, we take $\mathcal{L}^1(a, b) = \mathcal{L}^1[a, b] = b - a$. If $A = \bigcup_i [a_i, b_i]$ is a finite or countable union of disjoint intervals, we let

$\mathcal{L}^1(A) = \sum (b_i - a_i)$ be the length of A , thought of as the sum of the length of the intervals. This leads us to the definition of the *Lebesgue measure* $\mathcal{L}^1(A)$ of an arbitrary set A . We define

$$\mathcal{L}^1(A) = \inf \left\{ \sum_{i=1}^{\infty} (b_i - a_i) : A \subset \bigcup_{i=1}^{\infty} [a_i, b_i] \right\},$$

that is, we look at all coverings of A by countable collections of intervals and take the smallest total interval length possible. It is not hard to see that (1.1)–(1.3) hold; it is rather harder to show that (1.4) holds for disjoint Borel sets A_i , and we avoid this question here. (In fact, (1.4) holds for a much larger class of sets than the Borel sets, ‘the Lebesgue measurable sets’, but not for all subsets of \mathbb{R} .) Lebesgue measure on \mathbb{R} is generally thought of as ‘length’, and we often write $\text{length}(A)$ for $\mathcal{L}^1(A)$ when we wish to emphasise this intuitive meaning.

Example 1.4 Lebesgue measure on \mathbb{R}^n

We call a set of the form $A = \{(x_1, \dots, x_n) \in \mathbb{R}^n : a_i \leq x_i \leq b_i\}$ a *coordinate parallelepiped* in \mathbb{R}^n , its n -dimensional volume of A is given by

$$\text{vol}^n(A) = (b_1 - a_1)(b_2 - a_2) \cdots (b_n - a_n).$$

(Of course, if $n = 1$, a coordinate parallelepiped is just an interval with vol^1 as length, as in Example 1.3; if $n = 2$, it is a rectangle with vol^2 as area, and if $n = 3$, it is a cuboid with vol^3 the usual 3-dimensional volume.) Then n -dimensional Lebesgue measure \mathcal{L}^n may be thought of as the extension of n -dimensional volume to a large class of sets. Just as in Example 1.3, we obtain a measure on \mathbb{R}^n by defining

$$\mathcal{L}^n(A) = \inf \left\{ \sum_{i=1}^{\infty} \text{vol}^n(A_i) : A \subset \bigcup_{i=1}^{\infty} A_i \right\}$$

where the infimum is taken over all coverings of A by coordinate parallelepipeds A_i . We get that $\mathcal{L}^n(A) = \text{vol}^n(A)$ if A is a coordinate parallelepiped or, indeed, any set for which the volume can be determined by the usual rules of mensuration. Again, to aid intuition, we sometimes write $\text{area}(A)$ in place of $\mathcal{L}^2(A)$, $\text{vol}(A)$ for $\mathcal{L}^3(A)$ and $\text{vol}^n(A)$ for $\mathcal{L}^n(A)$.

Sometimes, we need to define ‘ k -dimensional’ volume on a k -dimensional plane X in \mathbb{R}^n ; this may be done by identifying X with \mathbb{R}^k and using \mathcal{L}^k on subsets of X in the obvious way.

Example 1.5 Uniform mass distribution on a line segment

Let L be a line segment of unit length in the plane. For $A \subset \mathbb{R}^2$ define $\mu(A) = \mathcal{L}^1(L \cap A)$, that is, the ‘length’ of intersection of A with L . Then μ is a mass distribution with support L , because $\mu(A) = 0$ if $A \cap L = \emptyset$. We may think of μ as unit mass spread evenly along the line segment L .

Example 1.6 Restriction of a measure

Let μ be a measure on \mathbb{R}^n and E a Borel subset of \mathbb{R}^n . We may define a measure ν on \mathbb{R}^n , called the *restriction of μ to E* , by $\nu(A) = \mu(E \cap A)$ for every set A . Then ν is a measure on \mathbb{R}^n with support contained in \overline{E} .

As far as this book is concerned, the most important measures we shall meet are the s -dimensional Hausdorff measures \mathcal{H}^s on subsets of \mathbb{R}^n , where $0 \leq s \leq n$. These measures, which are introduced in Section 3.1, are a generalisation of Lebesgue measures to dimensions that are not necessarily integral.

The following method is often used to construct a mass distribution on a subset of \mathbb{R}^n . It involves repeated subdivision of a mass between parts of a bounded Borel set E . Let \mathcal{E}_0 consist of the single set E . For $k = 1, 2, \dots$, we let \mathcal{E}_k be a collection of disjoint Borel subsets of E such that each set U in \mathcal{E}_k is contained in one of the sets of \mathcal{E}_{k-1} and contains a finite number of the sets in \mathcal{E}_{k+1} . We assume that the maximum diameter of the sets in \mathcal{E}_k tends to 0 as $k \rightarrow \infty$. We define a mass distribution on E by repeated subdivision (see [Figure 1.5](#)). We let $\mu(E)$ satisfy $0 < \mu(E) < \infty$, and we split this mass between the sets U_1, \dots, U_m in \mathcal{E}_1 by defining $\mu(U_i)$ in such a way that $\sum_{i=1}^m \mu(U_i) = \mu(E)$. Similarly, we assign masses to the sets of

\mathcal{E}_2 so that if U_1, \dots, U_m are the sets of \mathcal{E}_2 contained in a set U of \mathcal{E}_1 , then $\sum_{i=1}^m \mu(U_i) = \mu(U)$. In general, we assign masses so that

$$\sum_i \mu(U_i) = \mu(U) \quad \mathbf{1.8}$$

for each set U of \mathcal{E}_k , where the $\{U_i\}$ are the disjoint sets in \mathcal{E}_{k+1} contained in U . For each k , we let E_k be the union of the sets in \mathcal{E}_k , and we define $\mu(A) = 0$ for all A with $A \cap E_k = \emptyset$.

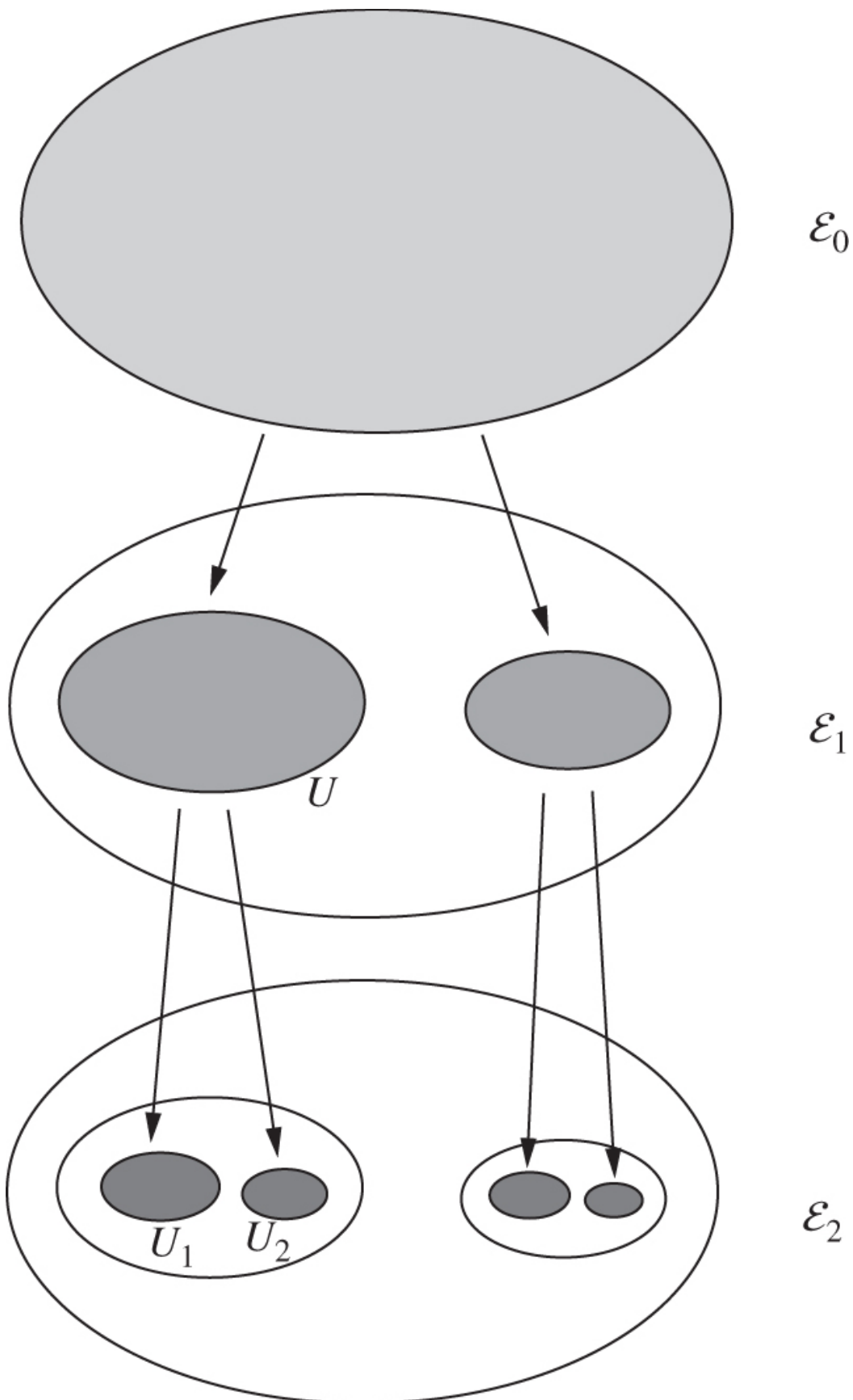


Figure 1.5 Steps in the construction of a mass distribution μ by repeated subdivision. The mass on the sets of \mathcal{E}_k is divided between the sets of \mathcal{E}_{k+1} , so for example, $\mu(U) = \mu(U_1) + \mu(U_2)$.

Let \mathcal{E} denote the collection of sets that belong to \mathcal{E}_k for some k together with the subsets of the $\mathbb{R}^n \setminus E_k$. The above procedure defines the mass $\mu(A)$ of every set A in \mathcal{E} , and it should seem reasonable that, by building up sets from the sets in \mathcal{E} , it specifies enough about the distribution of the mass μ across \mathcal{E} to determine $\mu(A)$ for any (Borel) set A . This is indeed the case, as the following proposition states.

Proposition 1.7

Let μ be defined on a collection of sets \mathcal{E} as above. Then the definition of μ may be extended to all subsets of \mathbb{R}^n so that μ becomes a measure. The value of $\mu(A)$ is uniquely determined if A is a Borel set. The support of μ is contained in $E_\infty = \bigcap_{k=1}^{\infty} \overline{E}_k$.

Note on Proof

If A is any subset of \mathbb{R}^n , let

$$\mu(A) = \inf \left\{ \sum_{i=1}^{\infty} \mu(U_i) : A \cap E_{\infty} \subset \bigcup_{i=1}^{\infty} U_i \text{ and } U_i \in \mathcal{E} \right\}. \quad 1.9$$

(Thus, we take the smallest value we can of $\sum_{i=1}^{\infty} \mu(U_i)$ where the sets U_i are in \mathcal{E} and cover $A \cap E_{\infty}$; we have already defined $\mu(U_i)$ for such U_i .) It is not difficult to see that if A is one of the sets in \mathcal{E} , then (1.9) reduces to the mass $\mu(A)$ specified in the construction. The complete proof that μ satisfies all the conditions of a measure and that its values on the sets of \mathcal{E} determine its values on the Borel sets is quite involved, and need not concern us here. As $\mu(\mathbb{R}^n \setminus E_k) = 0$, we have $\mu(A) = 0$ if A is an open set that does not intersect E_k for some k , so the support of μ is in \overline{E}_k for all k .

Example 1.8 Lebesgue measure by repeated subdivision

Let \mathcal{E}_k denote the collection of ‘binary intervals’ of length 2^{-k} , that is of the form $[r2^{-k}, (r+1)2^{-k}]$ where $0 \leq r \leq 2^k - 1$. If we take $\mu[r2^{-k}, (r+1)2^{-k}] = 2^{-k}$ in the above construction, we get that μ is Lebesgue measure on $[0, 1]$.

To see this, note that if I is an interval in \mathcal{E}_k of length 2^{-k} and I_1, I_2 are the two subintervals of I in \mathcal{E}_{k+1} of length 2^{-k-1} , we have $\mu(I) = \mu(I_1) + \mu(I_2)$ which is (1.8). By Proposition 1.7, μ extends to a mass distribution on $[0, 1]$. We have $\mu(I) = \text{length}(I)$ for I in \mathcal{E} , and it may be shown that this implies that μ coincides with Lebesgue measure on any set.

We say that a property holds for *almost all* x , or *almost everywhere* (with respect to a measure μ) if the set for which the property fails has μ -measure zero. For example, we might say that almost all real numbers are irrational with respect to Lebesgue measure. The rational numbers \mathbb{Q} are countable; they may be listed as x_1, x_2, \dots , say, so that $\mathcal{L}^1(\mathbb{Q}) = \sum_{i=1}^{\infty} \mathcal{L}^1\{x_i\} = 0$.

Although we shall usually be interested in measures in their own right, we shall sometimes need to integrate functions with respect to measures. There are technical difficulties concerning which functions can be integrated. We may get around these difficulties by assuming that for $f : D \rightarrow \mathbb{R}$ a function defined on a Borel subset D of \mathbb{R}^n , the set $f^{-1}(-\infty, a] = \{x \in D : f(x) \leq a\}$ is a Borel set for all real numbers a . A very large class of functions satisfies this condition, including all continuous functions (for which $f^{-1}(-\infty, a]$ is closed and therefore a Borel set). We make the assumption throughout this book that all functions to be integrated satisfy this condition; this is true of functions that are likely to be encountered in this area of mathematics.

To define integration we first suppose that $f : D \rightarrow \mathbb{R}$ is a **simple function**, that is, one that takes only finitely many values a_1, \dots, a_k . We define the *integral with respect to the measure μ* of a non-negative simple function f as

$$\int f d\mu = \sum_{i=1}^k a_i \mu\{x : f(x) = a_i\}.$$

The integral of more general functions is defined using **approximation by simple functions**. If $f : D \rightarrow \mathbb{R}$ is a non-negative function, we define its integral as

$$\int f d\mu = \sup \left\{ \int g d\mu : g \text{ is simple, } 0 \leq g \leq f \right\}.$$

To complete the definition, if f takes both positive and negative values, we let $f_+(x) = \max\{f(x), 0\}$ and $f_-(x) = \max\{-f(x), 0\}$, so that $f = f_+ - f_-$, and define

$$\int f d\mu = \int f_+ d\mu - \int f_- d\mu$$

provided that both $\int f_+ d\mu$ and $\int f_- d\mu$ are finite.

All the usual properties hold for integrals, for example,

$$\int (f + g) d\mu = \int f d\mu + \int g d\mu$$

and

$$\int \lambda f d\mu = \lambda \int f d\mu$$

if λ is a scalar. Very useful is the monotone convergence theorem, that is, if $f_k : D \rightarrow \mathbb{R}$ is an increasing sequence of non-negative functions converging (pointwise) to f , then

$$\lim_{k \rightarrow \infty} \int f_k d\mu = \int f d\mu.$$

If A is a Borel subset of D , we define integration over the set A by

$$\int_A f d\mu = \int f \chi_A d\mu$$

where $\chi_A : \mathbb{R}^n \rightarrow \mathbb{R}$ is the ‘indicator function’ of A , defined by $\chi_A(x) = 1$ if x is in A and $\chi_A(x) = 0$ otherwise.

Note that if $f(x) \geq 0$ and $\int f d\mu = 0$, then $f(x) = 0$ for μ -almost all x .

As usual, integration is denoted in various ways, such as $\int f d\mu$, $\int f$ or $\int f(x) d\mu(x)$, depending on the emphasis required. When μ is n -dimensional Lebesgue measure \mathcal{L}^n , we usually write $\int f dx$ or $\int f(x) dx$ in place of $\int f d\mathcal{L}^n$.

On a couple of occasions we shall need to use Egoroff’s theorem. Let D be a Borel subset of \mathbb{R}^n and μ a measure with $\mu(D) < \infty$. Let f_1, f_2, \dots and f be functions from D to \mathbb{R} such that $f_k(x) \rightarrow f(x)$ for each x in D . Egoroff’s theorem states that for any $\delta > 0$, there is a Borel

subset E of D such that $\mu(D \setminus E) < \delta$ and such that the sequence $\{f_k\}$ converges uniformly to f on E , that is, with $\sup_{x \in E} |f_k(x) - f(x)| \rightarrow 0$ as $k \rightarrow \infty$. For the measures that we shall be concerned with, it may be shown that we can always take the set E to be compact.

1.4 Notes on probability theory

Understanding some of the later chapters of the book requires a basic knowledge of probability theory. We provide a very brief overview of the concepts needed.

Probability theory starts with the idea of an *experiment* or *trial*; that is, an action whose outcome is, for all practical purposes, not predetermined. Mathematically, such an experiment is described by a probability space, which has three components: the set of all possible outcomes of the experiment, the list of all the events that may occur as consequences of the experiment and an assessment of likelihood of these events. For example, if a die is thrown, the possible outcomes are $\{1, 2, 3, 4, 5, 6\}$, the list of events includes ‘a 3 is thrown’, ‘an even number is thrown’ and ‘at least a 4 is thrown’. For a ‘fair die’, it may be reasonable to assess the six possible outcomes as equally likely.

The set of all possible outcomes of an experiment is called the *sample space*, denoted by Ω . Questions of interest concerning the outcome of an experiment can always be phrased in terms of subsets of Ω ; in the above example, ‘is an odd number thrown?’ asks ‘is the outcome in the subset $\{1, 3, 5\}$?’ Associating events dependent on the outcome of the experiment with subsets of Ω in this way, it is natural to think of the union $A \cup B$ as ‘either A or B occurs’, the intersection $A \cap B$ as ‘both A and B occur’, and the complement $\Omega \setminus A$ as the event ‘ A does not occur’, for any events A and B . In general, there is a collection \mathcal{F} of subsets of Ω that particularly interest us, which we call *events*. In the example of the die, \mathcal{F} would normally be the collection of all subsets of Ω , but in more complicated situations, a relatively small collection of subsets might be relevant. Usually, \mathcal{F} satisfies certain conditions; for example, if the occurrence of an event interests us, then so does its non-occurrence, so if A is in \mathcal{F} , we would expect the complement $\Omega \setminus A$ also to be in \mathcal{F} .

We call a (non-empty) collection \mathcal{F} of subsets of the sample space Ω an *event space* if

$$\Omega \setminus A \in \mathcal{F} \quad \text{whenever } A \in \mathcal{F} \quad \mathbf{1.10}$$

and

$$\bigcup_{i=1}^{\infty} A_i \in \mathcal{F} \quad \text{whenever } A_i \in \mathcal{F} \quad (1 \leq i < \infty). \quad \mathbf{1.11}$$

It follows from these conditions that \emptyset and Ω are in \mathcal{F} and that $A \setminus B$ and $\bigcap_{i=1}^{\infty} A_i$ are in \mathcal{F} whenever A, B and A_i are in \mathcal{F} . As far as our applications are concerned, we do not, in general, specify \mathcal{F} precisely —this avoids technical difficulties connected with the existence of suitable event spaces.

Next, we associate probabilities with the events of \mathcal{F} , with $P(A)$ thought of as the probability, or likelihood, that the event A occurs. We call P a *probability* or *probability measure* if P assigns a number $P(A)$ to each A in \mathcal{F} , such that the following conditions hold:

$$0 \leq P(A) \leq 1 \quad \text{for all } A \in \mathcal{F} \quad \mathbf{1.12}$$

$$P(\emptyset) = 0 \quad \text{and} \quad P(\Omega) = 1 \quad \mathbf{1.13}$$

and if A_1, A_2, \dots are disjoint events in \mathcal{F} ,

$$P\left(\bigcup_{i=1}^{\infty} A_i\right) = \sum_{i=1}^{\infty} P(A_i). \quad \mathbf{1.14}$$

It should seem natural for any definition of probability to satisfy these conditions.

We call a triple (Ω, \mathcal{F}, P) a *probability space* if \mathcal{F} is an event space of subsets of Ω and P is a probability measure defined on the sets of \mathcal{F} .

For the die-throwing experiment, we might have $\Omega = \{1, 2, 3, 4, 5, 6\}$ with the event space consisting of all subsets of Ω , and with

$P(A) = \frac{1}{6} \times \text{number of elements in } A$. This describes the ‘fair die’ situation with each outcome equally likely.

Often, Ω is an infinite set. For example, we might have $\Omega = [0, 1]$ and think of a random number drawn from $[0, 1]$ with the probability of the number in a set A as $P(A) = \text{length}(A)$. Here, the event space might be the Borel subsets of $[0, 1]$.

The resemblance of the definition of probability to the definition of a measure in (1.1)–(1.4) and the use of the term probability measure is no coincidence. Probabilities and measures may be put into the same context, with Ω corresponding to \mathbb{R}^n and with the event space in some ways analogous to the Borel sets.

In our applications later on in the book, we shall be particularly interested in events (on rather large sample spaces such as spaces of continuous functions) that are virtually certain to occur. We say that an event A occurs *with probability 1* or *almost surely* if $P(A) = 1$.

Sometimes, we may possess partial information about the outcome of an experiment; for example, we might be told that the number showing on the die is even. This leads us to reassess the probabilities of the various events. If A and B are in \mathcal{F} with $P(B) > 0$, the *conditional probability of A given B*, denoted by $P(A|B)$, is defined by

$$P(A|B) = \frac{P(A \cap B)}{P(B)}. \quad \mathbf{1.15}$$

This is thought of as the probability of A given that the event B is known to occur; as would be expected $P(B|B) = 1$. It is easy to show that $(\Omega, \mathcal{F}, P')$ is a probability space, where $P'(A) = P(A|B)$. We also have the partition formula: if B_1, B_2, \dots are disjoint events with $\bigcup_i B_i = \Omega$ and $P(B_i) > 0$ for all i , then for an event A ,

$$P(A) = \sum_i P(A|B_i)P(B_i). \quad \mathbf{1.16}$$

In the case of the ‘fair die’ experiment, if B_1 is the event ‘an even number is thrown’, B_2 is ‘an odd number is thrown’ and A is ‘at least 4 is thrown’, then

$$P(A|B_1) = P(4 \text{ or } 6 \text{ is thrown})/P(2, 4 \text{ or } 6 \text{ is thrown}) = \frac{2}{6}/\frac{3}{6} = \frac{2}{3}.$$

$$P(A|B_2) = P(5 \text{ is thrown})/P(1, 3 \text{ or } 5 \text{ is thrown}) = \frac{1}{6}/\frac{3}{6} = \frac{1}{3}$$

from which (1.16) is easily verified.

We think of two events as independent if the occurrence of one does not affect the probability that the other occurs, that is, if $P(A|B) = P(A)$ and $P(B|A) = P(B)$. Using (1.15), we are led to make the definition that two events A and B in a probability space are *independent* if

$$P(A \cap B) = P(A)P(B). \quad \mathbf{1.17}$$

More generally, an arbitrary collection of events is independent if for every finite subcollection $\{A_k : k \in J\}$ we have

$$P\left(\bigcap_{k \in J} A_k\right) = \prod_{k \in J} P(A_k). \quad \mathbf{1.18}$$

In the die example, it is easy to see that ‘a throw of at least 5’ and ‘an even number is thrown’ are independent events, but ‘a throw of at least 4’ and ‘an even number is thrown’ are not.

The idea of a random variable and its expectation (or average or mean) is fundamental to probability theory. Essentially, a random variable X is a real-valued function on a sample space. In the die example, X might represent the score on the die. Alternatively, it might represent the reward for throwing a particular number, for example, $X(\omega) = 0$ if $\omega = 1, 2, 3$, or 4, $X(5) = 1$ and $X(6) = 2$. The outcome of an experiment determines a value of the random variable. The expectation of the random variable is the average of these values weighted according to the likelihood of each outcome.

The precise definition of a random variable requires a little care. We say that X is a *random variable* on a probability space (Ω, \mathcal{F}, P) if $X : \Omega \rightarrow \mathbb{R}$ is a function such that $X^{-1}((-\infty, a])$ is an event in \mathcal{F} for each real number a ; in other words, the set of ω in Ω with $X(\omega) \leq a$ is in the event space. This condition is equivalent to saying that $X^{-1}(E)$ is in \mathcal{F} for any Borel set E . In particular, for any such E , the probability that the random variable X takes a value in E , that is, $P(\{\omega : X(\omega) \in E\})$, is defined. It may be shown that $P(\{\omega : X(\omega) \in E\})$ is determined for all Borel sets E from a knowledge of $P(\{\omega : X(\omega) \leq a\})$ for each real number a . Note that it is usual to abbreviate expressions such as $P(\{\omega : X(\omega) \in E\})$ to $P(X \in E)$.

It is not difficult to show that if X and Y are random variables on (Ω, \mathcal{F}, P) and λ is a real number, then $X + Y, X - Y, XY$ and λX are all random variables (these are defined in the obvious way, e.g. $(X + Y)(\omega) = X(\omega) + Y(\omega)$ for each $\omega \in \Omega$). Moreover, if X_1, X_2, \dots is a sequence of random variables with $X_k(\omega)$ increasing and bounded for each ω , then $\lim_{k \rightarrow \infty} X_k$ is a random variable.

A collection of random variables $\{X_k\}$ is *independent* if, for any Borel sets E_k , the events $\{(X_k \in E_k)\}$ are independent in the sense of (1.18); that is, if, for every finite set of indices J ,

$$P(X_k \in E_k \text{ for all } k \in J) = \prod_{k \in J} P(X_k \in E_k).$$

Intuitively, X and Y are independent if the probability of Y taking any particular value is unaffected by a knowledge of the value of X . Consider the probability space representing two successive throws of a die, with sample space $\{(x, y) : x, y = 1, 2, \dots, 6\}$ and probability measure P defined by $P\{(x, y)\} = \frac{1}{36}$ for each pair (x, y) . If X and Y are the random variables given by the scores on successive throws, then X and Y are independent, modelling the assumption that one throw does not affect the other. However, X and $X + Y$ are not independent —this reflects that the bigger the score for the first throw, the greater the chance of a high total score.

The formal definition of the expectation of a random variable is analogous to the definition of the integral of a function; indeed, expectation is really the integral of the random variable with respect to the probability measure. Let X be a random variable on a probability space (Ω, \mathcal{F}, P) . First suppose that $X(\omega) \geq 0$ for all ω in Ω and that X takes only finitely many values x_1, \dots, x_k ; we call such a random variable *simple*. We define the *expectation, mean or average* $E(X)$ of X as

$$E(X) = \sum_{i=1}^k x_i P(X = x_i). \quad \mathbf{1.19}$$

The expectation of an arbitrary random variable is defined using approximation by simple random variables. Thus for a non-negative random variable X

$$E(X) = \sup\{E(Y) : Y \text{ is a simple random variable with } 0 \leq Y(\omega) \leq X(\omega) \text{ for all } \omega \in \Omega\}.$$

Lastly, if X takes both positive and negative values, we let $X_+ = \max\{X, 0\}$ and $X_- = \max\{-X, 0\}$, so that $X = X_+ - X_-$, and define

$$E(X) = E(X_+) - E(X_-)$$

provided that $E(X_+) < \infty$ and $E(X_-) < \infty$.

The random variable X representing the score of a fair die is a simple random variable, because $X(\omega)$ takes just the values $1, \dots, 6$. Thus

$$E(X) = \sum_{i=1}^6 \left(i \times \frac{1}{6}\right) = 3\frac{1}{2}.$$

Expectation satisfies certain basic properties, analogous to those for the integral. If X_1, X_2, \dots are random variables, then

$$E(X_1 + X_2) = E(X_1) + E(X_2)$$

and, more generally,

$$\mathbb{E}\left(\sum_{i=1}^k X_i\right) = \sum_{i=1}^k \mathbb{E}(X_i).$$

If λ is a constant,

$$\mathbb{E}(\lambda X) = \lambda \mathbb{E}(X)$$

and if the sequence of non-negative random variables X_1, X_2, \dots is increasing with $X = \lim_{k \rightarrow \infty} X_k$ a (finite) random variable, then

$$\lim_{k \rightarrow \infty} \mathbb{E}(X_k) = \mathbb{E}(X).$$

Provided that X_1 and X_2 are independent, we also have

$$\mathbb{E}(X_1 X_2) = \mathbb{E}(X_1) \mathbb{E}(X_2).$$

Thus, if X_i represents that k th throw of a fair die in a sequence of throws, the expectation of the sum of the first k throws is

$$\mathbb{E}(X_1 + \dots + X_k) = \mathbb{E}(X_1) + \dots + \mathbb{E}(X_k) = 3\frac{1}{2} \times k.$$

We define the *conditional expectation* $\mathbb{E}(X|B)$ of X given an event B with $\mathbb{P}(B) > 0$ in a similar way but starting with

$$\mathbb{E}(X|B) = \sum_{i=1}^k x_i \mathbb{P}(X = x_i|B) \quad \text{1.20}$$

in place of (1.19). We get a partition formula resembling (1.16)

$$\mathbb{E}(X) = \sum_i \mathbb{E}(X|B_i) \mathbb{P}(B_i), \quad \text{1.21}$$

where B_1, B_2, \dots are disjoint events with $\bigcup_i B_i = \Omega$ and $\mathbb{P}(B_i) > 0$.

It is often useful to have an indication of the fluctuation of a random variable across a sample space. Thus we introduce the *variance* of the random variable X as

$$\begin{aligned}\text{var}(X) &= \mathbb{E}((X - \mathbb{E}(X))^2) \\ &= \mathbb{E}(X^2) - \mathbb{E}(X)^2\end{aligned}$$

by a simple calculation. Using the properties of expectation, we get

$$\text{var}(\lambda X) = \lambda^2 \text{var}(X),$$

for any real number λ , and

$$\text{var}(X + Y) = \text{var}(X) + \text{var}(Y)$$

provided that X and Y are independent.

If the probability distribution of a random variable is given by an integral, that is,

$$\mathbb{P}(X \leq x) = \int_{-\infty}^x f(u) du, \quad \mathbf{1.22}$$

the function f is called the *probability density function* for X . It may be shown from the definition of expectation that

$$\mathbb{E}(X) = \int_{-\infty}^{\infty} u f(u) du$$

and

$$\mathbb{E}(X^2) = \int_{-\infty}^{\infty} u^2 f(u) du$$

which allows $\text{var}(X) = \mathbb{E}(X^2) - \mathbb{E}(X)^2$ to be calculated.

Note that the density function tells us about the distribution of the random variable X without reference to the underlying probability space, which, for many purposes, is irrelevant. We may express the probability that X belongs to any Borel set E in terms of the density function as

$$\mathbb{P}(X \in E) = \int_E f(u) du.$$

We say that a random variable X has *uniform distribution* on the interval $[a, b]$ if

$$P(X \leq x) = \frac{1}{b-a} \int_a^x du \quad (a \leq x \leq b). \quad \mathbf{1.23}$$

Thus, the probability of X lying in a subinterval of $[a, b]$ is proportional to the length of the interval. In this case, we get that $E(X) = \frac{1}{2}(a+b)$ and $\text{var}(X) = \frac{1}{12}(b-a)^2$.

A random variable X has *normal* or *Gaussian distribution* of mean m and variance σ^2 if

$$P(X \leq x) = \frac{1}{\sigma\sqrt{2\pi}} \int_{-\infty}^x \exp\left(\frac{-(u-m)^2}{2\sigma^2}\right) du. \quad \mathbf{1.24}$$

It may be verified by integration that $E(X) = m$ and $\text{var}(X) = \sigma^2$. If X_1 and X_2 are independent normally distributed random variables of means m_1 and m_2 and variances σ_1^2 and σ_2^2 , respectively, then $X_1 + X_2$ is normal with mean $m_1 + m_2$ and variance $\sigma_1^2 + \sigma_2^2$, and λX_1 is normal with mean λm_1 and variance $\lambda^2 \sigma_1^2$, for any real number λ .

If we throw a fair die a large number of times, we might expect the average score thrown to be very close to $3\frac{1}{2}$, the expectation or mean outcome of each throw. Moreover, the larger the number of throws, the closer the average should be to the mean. This ‘law of averages’ is made precise as the strong law of large numbers.

Let (Ω, \mathcal{F}, P) be a probability space. Let X_1, X_2, \dots be random variables that are independent and that have identical distribution (i.e. for every set E , $P(X_i \in E)$ is the same for all i), with expectation m and variance σ^2 , both assumed finite. For each k , we may form the random variable $S_k = X_1 + \dots + X_k$, so that the random variable S_k/k is the average of the first k trials. The *strong law of large numbers* states that, with probability 1, this average approaches the mean, that is,

$$\lim_{k \rightarrow \infty} \frac{1}{k} S_k = m.$$

1.25

We can also say a surprising amount about the distribution of the random variable S_k when k is large. It may be shown that S_k has approximately the normal distribution with mean km and variance $k\sigma^2$. This is the content of the *central limit theorem*, which states that for every real number x ,

$$P\left(\frac{S_k - km}{\sigma\sqrt{k}} \leq x\right) \rightarrow \int_{-\infty}^x \frac{1}{\sqrt{2\pi}} \exp\left(-\frac{1}{2}u^2\right) du \quad \text{as } k \rightarrow \infty, \quad \text{1.26}$$

that is, $(S_k - km)/(\sigma\sqrt{k})$ converges (in some sense) to a normal distribution. This is one reason why the normal distribution is so important—it is the form of distribution approached by sums of a large number of independent identically distributed random variables.

We may apply these remarks to the experiment consisting of an infinite sequence of die throws. Let Ω be the set of all infinite sequences $\{\omega = (\omega_1, \omega_2, \dots) : \omega_i = 1, 2, \dots, 6\}$ (we think of ω_i as the outcome of the k th throw). It is possible to define an event space \mathcal{F} and probability measure P in such a way that for any given k and sequence $\omega_1, \dots, \omega_k$ ($\omega_i = 1, 2, \dots, 6$), the event ‘the first k throws are $\omega_1, \dots, \omega_k$ ’ is in \mathcal{F} and has probability $(\frac{1}{6})^k$. Let X_k be the random variable given by the outcome of the k th throw, so that $X_k(\omega) = \omega_k$. It is easy to see that the X_k are independent and identically distributed, with mean $m = 3\frac{1}{2}$ and variance $2\frac{11}{12}$. The strong law of large numbers tells us that, with probability 1, the average of the first k throws, S_k/k converges to $3\frac{1}{2}$ as k tends to infinity, and the central limit theorem tells us that when k is large, the sum S_k is approximately normally distributed, with mean $3\frac{1}{2} \times k$ and variance $2\frac{11}{12} \times k$. Thus, if we repeat the experiment of throwing k dice a large number of times, the sum of the k throws will have a distribution close to the normal distribution, in the sense of (1.26).

1.5 Notes and references

The material outlined in this chapter is covered at various levels of sophistication in numerous undergraduate and graduate mathematical texts. Any of the many books on mathematical analysis, for example, the classics by Apostol (1974); Rudin (1976) or Howie (2001), contain the basic theory of sets and functions. For thorough treatments of measure theory see, for example, Taylor (1973a); Edgar (1998); Capinski and Kopp (2007) or Tao (2011). For probability theory, Grimmett and Stirzaker (2001) or Billingsley (2012) may be helpful.

Exercises

The following exercises do no more than emphasise some of the many facts that have been mentioned in this chapter.

1.1 Verify that for $x, y, z \in \mathbb{R}^n$, (i) $|x + y| \leq |x| + |y|$, (ii) $|x - y| \geq ||x| - |y||$ and (iii) $|x - y| \leq |x - z| + |z - y|$.

1.2 Show from the definition of δ -neighbourhood that $A_{\delta+\delta'} = (A_\delta)_{\delta'}$.

1.3 Show that a (non-empty) set is bounded if and only if it is contained in some ball $B(o, r)$ with centre the origin.

1.4 Determine which of the following subsets of \mathbb{R} are open and which are closed. In each case, determine the interior and closure of the set. (i) A non-empty finite set A , (ii) the interval $(0, 1)$, (iii) the interval $[0, 1]$, (iv) the interval $[0, 1)$, (v) the set $\{0, 1, \frac{1}{2}, \frac{1}{3}, \frac{1}{4}, \dots\}$.

1.5 Show that the middle third Cantor set, [Figure 0.1](#), is compact and totally disconnected. What is its interior, closure and boundary?

1.6 Show that the union of any collection of open subsets of \mathbb{R}^n is open and that the intersection of any finite collection of open sets is open. Show that a subset of \mathbb{R}^n is closed if and only if its complement is open and hence deduce the corresponding result for unions and intersections of closed sets.

1.7 Show that if $A_1 \supset A_2 \supset \dots$ is a decreasing sequence of non-empty compact subsets of \mathbb{R}^n then $\bigcap_{k=1}^{\infty} A_k$ is a non-empty compact set.

1.8 Show that the half-open interval $[0, 1] = \{x \in \mathbb{R} : 0 \leq x < 1\}$ is a Borel subset of \mathbb{R} .

1.9 Let F be the set of numbers in $[0, 1]$ whose decimal expansions contain the digit 5 infinitely many times. Show that F is a Borel set.

1.10 Show that the coordinate transformation of the plane

$$\begin{pmatrix} x_1 \\ x_2 \end{pmatrix} \mapsto \begin{pmatrix} c \cos \theta & -c \sin \theta \\ c \sin \theta & c \cos \theta \end{pmatrix} \begin{pmatrix} x_1 \\ x_2 \end{pmatrix} + \begin{pmatrix} a_1 \\ a_2 \end{pmatrix}$$

is a similarity of ratio c , and describe the transformation geometrically.

1.11 Find $\underline{\lim}_{x \rightarrow 0} f(x)$ and $\overline{\lim}_{x \rightarrow 0} f(x)$ where $f : \mathbb{R}^+ \rightarrow \mathbb{R}$ is given by (i) $\sin x$; (ii) $\sin(1/x)$ and (iii) $x^2 + (3+x)\sin(1/x)$.

1.12 Let $f, g : [0, 1] \rightarrow \mathbb{R}$ be Lipschitz functions. Show that the functions defined on $[0, 1]$ by $f(x) + g(x)$ and $f(x)g(x)$ are also Lipschitz.

1.13 Let $f : \mathbb{R} \rightarrow \mathbb{R}$ be differentiable with $|f'(x)| \leq c$ for all x . Show, using the mean value theorem, that f is a Lipschitz function.

1.14 Show that every Lipschitz function $f : \mathbb{R} \rightarrow \mathbb{R}$ is continuous.

1.15 Let $f : \mathbb{R} \rightarrow \mathbb{R}$ be given by $f(x) = x^2 + x$. Find (i) $f^{-1}(2)$, (ii) $f^{-1}(-2)$ and (iii) $f^{-1}([2, 6])$.

1.16 Show that $f(x) = x^2$ is Lipschitz on $[0, 2]$, bi-Lipschitz on $[1, 2]$ and not Lipschitz on \mathbb{R} .

1.17 Show that if E is a compact subset of \mathbb{R}^n and $f : E \rightarrow \mathbb{R}^n$ is continuous, then $f(E)$ is compact.

1.18 Let A_1, A_2, \dots be a decreasing sequence of Borel subsets of \mathbb{R}^n and let $A = \bigcap_{k=1}^{\infty} A_k$. If μ is a measure on \mathbb{R}^n with $\mu(A_1) < \infty$, show using (1.6) that $\mu(A_k) \rightarrow \mu(A)$ as $k \rightarrow \infty$.

1.19 Show that the point mass concentrated at a (see Example 1.2) is a measure.

1.20 Show how to define a mass distribution on the middle third Cantor set, [Figure 0.1](#), in as uniform a way as possible.

1.21 Verify that Lebesgue measure satisfies (1.1)–(1.3).

1.22 Let $f : [0, 1] \rightarrow \mathbb{R}$ be a continuous function. For A a subset of \mathbb{R}^2 define $\mu(A) = \mathcal{L}\{(x, f(x)) \in A\}$, where \mathcal{L} is Lebesgue measure. Show that μ is a mass distribution on \mathbb{R}^2 supported by the graph of f .

1.23 Let D be a Borel subset of \mathbb{R}^n and let μ be a measure on D with $\mu(D) < \infty$. Let $f_k : D \rightarrow \mathbb{R}$ be a sequence of functions such that $f_k(x) \rightarrow f(x)$ for all x in D . Prove Egoroff's theorem: that given $\varepsilon > 0$, there exists a Borel subset A of D with $\mu(D \setminus A) < \varepsilon$ such that $f_k(x)$ converges to $f(x)$ uniformly for x in A .

1.24 Prove that if μ is a measure on D and $f : D \rightarrow \mathbb{R}$ satisfies $f(x) \geq 0$ for all x in D and $\int_D f \, d\mu = 0$ then $f(x) = 0$ for μ -almost all x .

1.25 If X is a random variable show that $E((X - E(X))^2) = E(X^2) - E(X)^2$ (these numbers equalling the variance of X).

1.26 Verify that if X has the uniform distribution on $[a, b]$ (see (1.23)), then $E(X) = \frac{1}{2}(a + b)$ and $\text{var}(X) = (b - a)^2 / 12$.

1.27 Let A_1, A_2, \dots be a sequence of independent events in some probability space such that $P(A_k) = p$ for all k , where $0 < p < 1$. Let N_k be the random variable defined by taking N_k to equal the number of i with $1 \leq i \leq k$ for which A_i occurs. Use the strong law of large numbers to show that, with probability 1, $N_k/k \rightarrow p$ as $k \rightarrow \infty$. Deduce that the proportion of successes in a sequence of independent trials converges to the probability of success of each trial.

1.28 A fair die is thrown 6000 times. Use the central limit theorem to estimate the probability that at least 1050 sixes are thrown. (A numerical method will be needed if the integral obtained is to be evaluated.)

Chapter 2

Box-counting dimension

The notion of dimension is central to fractal geometry. Fractal dimensions extend, to wide classes of sets, the familiar notion that a straight line or smooth curve is 1-dimensional, a surface is 2-dimensional and so on. Roughly, a dimension indicates, in some way, how much space a set occupies near to each of its points. Fundamental to most definitions of dimension is the idea of ‘measurement of a set at scale δ ’. For each δ , we measure a set in a way that detects irregularities of size delta δ , and we see how these measurements behave as $\delta \rightarrow 0$.

2.1 Box-counting dimensions

This chapter mainly concerns box-counting dimension, which has a simple intuitive formulation and is one of the most widely used dimensions. The definition goes back at least to the 1930s, and its popularity is largely due to its relative ease of mathematical calculation and empirical estimation.

Given a subset F of the plane, for each $\delta > 0$, we find the smallest number of sets of diameter at most δ that can cover the set F and we call this number $N_\delta(F)$, indicating the number of ‘clumps’ of size about δ into which F may be divided. The dimension of F reflects the way in which $N_\delta(F)$ grows as $\delta \rightarrow 0$. If $N_\delta(F)$ obeys, at least approximately, a power law

$$N_\delta(F) \simeq c\delta^{-s}$$

for positive constants c and s , we say that F has box dimension s . (The reason for this name will soon become apparent.) To solve for s , we take logarithms

$$\log N_\delta(F) \simeq \log c - s \log \delta,$$

2.1

so

$$s \simeq \frac{\log N_\delta(F)}{-\log \delta} + \frac{\log c}{\log \delta}.$$

and we might hope to obtain s as

$$s = \lim_{\delta \rightarrow 0} \frac{\log N_\delta(F)}{-\log \delta},$$

with the second term disappearing in the limit.

This motivates the formal definition of box-counting dimension.

Recall that if U is any non-empty subset of n -dimensional Euclidean space, \mathbb{R}^n , the *diameter* of U is defined as

$|U| = \sup\{|x - y| : x, y \in U\}$, that is, the greatest distance apart of any pair of points in U . If $\{U_i\}$ is a countable or finite collection of sets of diameter at most δ that cover F , that is, $F \subset \bigcup_{i=1}^{\infty} U_i$ and $0 < |U_i| \leq \delta$ for each i , we say that $\{U_i\}$ is a δ -cover of F . Let F be any non-empty bounded subset of \mathbb{R}^n and let $N_\delta(F)$ be the least number of sets of diameter at most δ which can cover F , that is, the least number of sets in any δ -cover of F . The *lower* and *upper box-counting dimensions* of F , respectively, are defined as

$$\underline{\dim}_B F = \lim_{\delta \rightarrow 0} \frac{\log N_\delta(F)}{-\log \delta} \quad \text{2.2}$$

$$\overline{\dim}_B F = \lim_{\delta \rightarrow 0} \frac{\log N_\delta(F)}{-\log \delta}. \quad \text{2.3}$$

Of course, $\underline{\dim}_B F \leq \overline{\dim}_B F$, and if these are equal, we refer to the common value as the *box-counting dimension* or *box dimension* of F .

$$\dim_B F = \lim_{\delta \rightarrow 0} \frac{\log N_\delta(F)}{-\log \delta}. \quad \text{2.4}$$

Here, and throughout the book, we assume that $\delta > 0$ is sufficiently small to ensure that $-\log \delta$ and similar quantities are strictly positive. To avoid problems with ‘ $\log 0$ ’ or ‘ $\log \infty$ ’, we generally consider box dimension only for non-empty bounded sets and we make this assumption in developing the general theory of box dimensions.

Roughly speaking, (2.4) says that $N_\delta(F) \simeq c\delta^{-s}$ for small δ , where $s = \dim_B F$, or, more precisely, that

$$N_\delta(F)\delta^s \rightarrow \infty \quad \text{if } s < \dim_B F$$

and

$$N_\delta(F)\delta^s \rightarrow 0 \quad \text{if } s > \dim_B F.$$

There are several equivalent definitions of box dimension that are sometimes more convenient to use. We get exactly the same values if in (2.2)-(2.4) we take $N_\delta(F)$ to be the smallest number of balls of radius δ , or the smallest number of cubes of side r that cover F , or even the *largest* number of *disjoint* balls of radius r with centres in F . Furthermore, there is the ‘box-counting’ approach itself. The family of cubes of the form

$$[m_1\delta, (m_1 + 1)\delta] \times \cdots \times [m_n\delta, (m_n + 1)\delta],$$

where m_1, \dots, m_n are integers, is called the δ -*mesh* or δ -*grid* of \mathbb{R}^n . (Recall that a ‘cube’ is an interval in \mathbb{R}^1 and a square in \mathbb{R}^2 .) Then taking $N_\delta(F)$ to be the ‘ δ -box count’ that is the number of δ -mesh cubes that intersect F , again gives the same values of dimension.

These equivalent definitions are summarised in the following statement (see [Figure 2.1](#)).

Equivalent definitions 2.1

The lower and upper box-counting dimensions of a subset F of \mathbb{R}^n are given by

$$\dim_B F = \lim_{\delta \rightarrow 0} \frac{\log N_\delta(F)}{-\log \delta} \quad \underline{2.5}$$

$$\overline{\dim}_B F = \lim_{\delta \rightarrow 0} \frac{\log N_\delta(F)}{-\log \delta} \quad \underline{2.6}$$

and the box-counting dimension of F by

$$\dim_B F = \lim_{\delta \rightarrow 0} \frac{\log N_\delta(F)}{-\log \delta} \quad \underline{2.7}$$

(if this limit exists), where $N_\delta(F)$ is any of the following:

- i. the smallest number of sets of diameter at most δ that cover F ;
- ii. the smallest number of closed balls of radius δ that cover F ;
- iii. the smallest number of cubes of side δ that cover F ;
- iv. the number of δ -mesh cubes that intersect F ;
- v. the largest number of disjoint balls of radius δ with centres in F .

Proof of equivalence

We give some sample proofs of the equivalence of pairs of these definitions. The others are very similar.

(i) \Leftrightarrow (iv) Write $N_\delta(F)$ for the smallest number of sets of diameter δ that can cover F . Let $N'_\delta(F)$ be the number of δ -mesh cubes that intersect F ; since these cubes obviously provide a collection of $N'_\delta(F)$ sets of diameter $\delta\sqrt{n}$ that cover F ,

$$N_{\delta\sqrt{n}}(F) \leq N'_\delta(F).$$

On the other hand, any set of diameter at most δ is contained in 3^n mesh cubes of side δ (by choosing a cube containing some point of the set together with its neighbouring cubes), so

$$N'_\delta(F) \leq 3^n N_\delta(F).$$

Combining these inequalities and dividing by $-\log \delta$,

$$\frac{\log N_{\delta\sqrt{n}}(F)}{-\log(\delta\sqrt{n}) + \log \sqrt{n}} \leq \frac{\log N'_\delta(F)}{-\log \delta} \leq \frac{\log 3^n + \log N_\delta(F)}{-\log \delta}, \quad \text{2.8}$$

so taking lower limits as $\delta \rightarrow 0$,

$$\lim_{\delta \rightarrow 0} \frac{\log N_\delta(F)}{-\log \delta} \leq \lim_{\delta \rightarrow 0} \frac{\log N'_\delta(F)}{-\log \delta} \leq \lim_{\delta \rightarrow 0} \frac{\log N_\delta(F)}{-\log \delta}, \quad \text{2.9}$$

with the other terms disappearing in the limit. Thus, the definition of lower box dimension (2.5) is the same working with either $N_\delta(F)$ or $N'_\delta(F)$. Taking upper limits in (2.8), we get a similar conclusion for upper box dimension.

(i) \Leftrightarrow (v) As before let $N_\delta(F)$ be the smallest number of sets of diameter δ that can cover F . Let $N''_\delta(F)$ be the largest possible number of disjoint balls of radius δ with centres in F and let $B_1, \dots, B_{N''_\delta(F)}$ be such a collection of balls. If x belongs to F , then

x must be within distance δ of one of the B_i , otherwise the ball of centre x and radius δ can be added to form a larger collection of disjoint balls. Thus, the $N''_\delta(F)$ balls concentric with the B_i but of radius 2δ (and diameter 4δ) cover F , giving

$$N_{4\delta}(F) \leq N''_\delta(F).$$

Suppose now that $B_1, \dots, B_{N''_\delta(F)}$ are disjoint balls of radii δ with centres in F . Let U_1, \dots, U_k be any collection of sets of diameter at most δ which cover F . Since the U_j must cover the centres of the B_i , each B_i must contain at least one of the U_j . As the B_i are disjoint, there are at least as many U_j as B_i . Hence,

$$N''_\delta(F) \leq N_\delta(F).$$

Just as in (2.8)-(2.9), on taking logarithms of these inequalities, dividing by $-\log \delta$ and taking the limit, we see that the values of (2.5)-(2.7) are unaltered if $N_\delta(F)$ is replaced by this $N''_\delta(F)$.

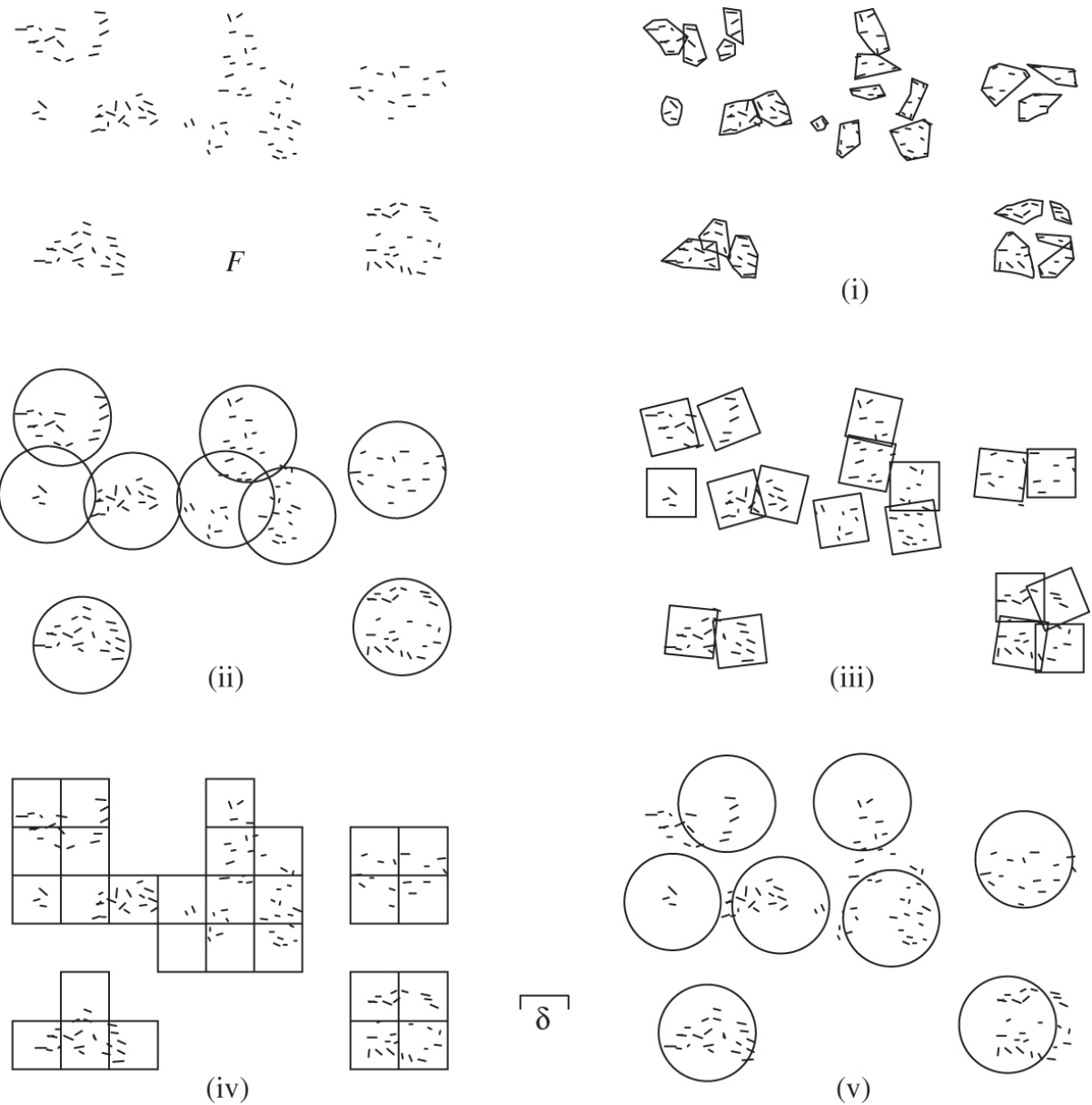


Figure 2.1 Five ways of finding the box dimension of F ; see Equivalent definitions 2.1. The number $N_\delta(F)$ is taken to be (i) the least number of sets of diameter at most δ that cover F ; (ii) the least number of closed balls of radius δ that cover F ; (iii) the least number of cubes of side δ that cover F ; (iv) the number of δ -mesh cubes that intersect F ; (v) the greatest number of disjoint balls of radius δ with centres in F .

Note that one consequence of the equivalence of definitions (i) and (iv) is that the box-counting formulation (iv) is independent of the origin and orientation chosen for the δ -mesh.

This list of equivalent definitions could be extended further; in practice one adopts the definition most convenient for a particular application. Box dimension has been variously termed *Kolmogorov entropy*, *entropy dimension*, *capacity dimension* (a term best avoided in view of potential theoretic associations), *metric dimension*, *logarithmic density* and *information dimension*.

The box-counting formulation (iv) is widely used empirically. To find the box dimension of a plane set F , we draw a mesh of squares or boxes of side δ and count the number $N_\delta(F)$ that overlap the set for a range of values of δ . Assuming a relationship such as (2.1), the dimension s is given by the gradient of the graph of $\log N_\delta(F)$ against $-\log \delta$. ‘Real’ fractals, such as coastlines or ferns, only display fractality over a limited range of scales, but box-counting can nevertheless give a ‘dimension’ that is meaningful across this range.

It is worth noting that in (2.5)-(2.7), it is enough to consider limits as δ tends to 0 through any decreasing sequence δ_k such that $\delta_{k+1} \geq c\delta_k$ for some constant $0 < c < 1$, in particular for $\delta_k = c^k$. To see this, note that if $\delta_{k+1} \leq \delta < \delta_k$, then, with $N_\delta(F)$ the least number of sets in a δ -cover of F ,

$$\frac{\log N_\delta(F)}{-\log \delta} \leq \frac{\log N_{\delta_{k+1}}(F)}{-\log \delta_k} = \frac{\log N_{\delta_{k+1}}(F)}{-\log \delta_{k+1} + \log(\delta_{k+1}/\delta_k)} \leq \frac{\log N_{\delta_{k+1}}(F)}{-\log \delta_{k+1} + \log c}$$

and so

$$\overline{\lim}_{\delta \rightarrow 0} \frac{\log N_\delta(F)}{-\log \delta} \leq \lim_{k \rightarrow \infty} \frac{\log N_{\delta_k}(F)}{-\log \delta_k}. \quad \text{2.10}$$

The opposite inequality is trivial; the case of lower limits may be dealt with in the same way.

We now give some basic examples of box-dimension calculations. Typically, they involve finding a lower bound and an upper bound

separately, each bound depending on a geometric observation followed by an analytic stage involving taking logarithms and passing to the limit. This is typical of fractal geometry arguments that often have geometric and analytic components.

Example 2.2

Let F be the middle third Cantor set (Figure 0.1). Then

$$\underline{\dim}_B F = \overline{\dim}_B F = \log 2 / \log 3.$$

Calculation

If $3^{-k} < \delta \leq 3^{-k+1}$, then the 2^k level- k intervals of E_k of length 3^{-k} provide a δ -cover of F , so that $N_\delta(F) \leq 2^k$, where $N_\delta(F)$ is the least number of sets in a δ -cover of F . From (2.3)

$$\overline{\dim}_B F = \lim_{\delta \rightarrow 0} \frac{\log N_\delta(F)}{-\log \delta} \leq \lim_{k \rightarrow \infty} \frac{\log 2^k}{-\log 3^{-k+1}} = \lim_{k \rightarrow \infty} \frac{k \log 2}{(k-1) \log 3} = \frac{\log 2}{\log 3}.$$

On the other hand, any interval of length δ with $3^{-k-1} \leq \delta < 3^{-k}$ intersects at most one of the level- k intervals of length 3^{-k} used in the construction of F (the gap between the level- k intervals is at least 3^{-k}). There are 2^k such intervals, all containing points of F , so at least 2^k intervals of length δ are required to cover F . Hence, $N_\delta(F) \geq 2^k$ so

$$\underline{\dim}_B F = \lim_{\delta \rightarrow 0} \frac{\log N_\delta(F)}{-\log \delta} \geq \lim_{k \rightarrow \infty} \frac{\log 2^k}{-\log 3^{-k-1}} = \lim_{k \rightarrow \infty} \frac{k \log 2^k}{(k+1) \log 3} = \frac{\log 2}{\log 3}. \quad \square$$

The form of this Cantor set calculation is typical of the dimension calculation for many fractals. Here is an example in the plane.

Example 2.3

Let F be the Sierpiński triangle (Figure 0.3) with side length 1. Then $\underline{\dim}_B F = \overline{\dim}_B F = \log 3 / \log 2$.

Calculation

The basic geometric observation here is that in construction of F shown in Figure 0.3, the k th stage of the construction consists of 3^k equilateral triangles of side length and diameter 2^{-k} . Thus, if $2^{-k} < \delta \leq 2^{-k+1}$, the 3^k triangles of E_k give a δ cover of F , so $N_\delta(F) \leq 3^k$. Then

$$\overline{\dim}_B F = \overline{\lim}_{\delta \rightarrow 0} \frac{\log N_\delta(F)}{-\log \delta} \leq \overline{\lim}_{k \rightarrow \infty} \frac{\log 3^k}{-\log 2^{-k+1}} = \frac{\log 2}{\log 3}.$$

On the other hand, any plane set of diameter δ , where $2^{-k-1} \leq \delta < 2^{-k}$, can intersect at most three of the triangles of E_k (such a set cannot intersect two triangles distance 2^{-k} or more apart). There are 3^k triangles in E_k , all containing points of F , so at least $3^k/3$ sets of diameter δ or less are required to cover F . Hence, $N_\delta(F) \geq 3^{k-1}$, so

$$\underline{\dim}_B F = \underline{\lim}_{\delta \rightarrow 0} \frac{\log N_\delta(F)}{-\log \delta} \geq \underline{\lim}_{k \rightarrow \infty} \frac{\log 3^{k-1}}{-\log 2^{-k-1}} = \frac{\log 2}{\log 3}.$$

More generally a set F made up of m similar disjoint copies of itself at scale r has $\dim_B F = \log m / -\log r$.

There is an equivalent definition of box dimension of a rather different form that is often useful. Recall that the δ -neighbourhood F_δ of a subset F of \mathbb{R}^n is

$$F_\delta = \{x \in \mathbb{R}^n : |x - y| \leq \delta \text{ for some } y \in F\},$$

2.11

that is, the set of points within distance δ of F . We consider the rate at which the n -dimensional volume, that is, n -dimensional Lebesgue measure \mathcal{L}^n , of F_δ shrinks as $\delta \rightarrow 0$. In \mathbb{R}^3 , if F is a segment of length l , then F_δ is ‘sausage-like’ with $\mathcal{L}^3(F_\delta) \sim \pi l \delta^2$; if F is a flat set of area a , then F_δ is essentially a thickening of F with $\mathcal{L}^3(F_\delta) \sim 2a\delta$ and if F is a solid sphere of volume v , then F_δ is a slightly enlarged ball with $\mathcal{L}^3(F_\delta) \sim v$. In each case, $\mathcal{L}^3(F_\delta) \sim c\delta^{3-s}$ where the integer s is the dimension of F , so that exponent of δ is indicative of the dimension. The coefficient c of δ^{3-s} is a measure of the length, area or volume of F as appropriate.

This idea extends to fractional dimensions. If F is a subset of \mathbb{R}^n and $\lim_{\delta \rightarrow 0} (\mathcal{L}^n(F_\delta)/\delta^{n-s}) = c$ for some $s > 0$ and $0 < c < \infty$, it makes sense to regard F as s -dimensional, and it turns out that s is just the box-counting dimension. The number c is called the *s-dimensional Minkowski content* of F — a quantity that is useful in some concepts but has the disadvantages that it does not exist for many standard fractals and that it is not necessarily additive on disjoint subsets, that is, is not a measure. Even if this limit does not exist, we can take lower and upper limits, and these are related to the box dimensions.

Proposition 2.4

If F is a subset of \mathbb{R}^n , then

$$\underline{\dim}_B F = n - \overline{\lim}_{\delta \rightarrow 0} \frac{\log \mathcal{L}^n(F_\delta)}{\log \delta}$$

$$\overline{\dim}_B F = n - \underline{\lim}_{\delta \rightarrow 0} \frac{\log \mathcal{L}^n(F_\delta)}{\log \delta},$$

where F_δ is the δ -neighbourhood of F .

Proof

If F can be covered by $N_\delta(F)$ balls of radius $\delta < 1$, then F_δ can be covered by the concentric balls of radius 2δ . Hence,

$$\mathcal{L}^n(F_\delta) \leq N_\delta(F)c_n(2\delta)^n,$$

where c_n is the volume of the unit ball in \mathbb{R}^n . Taking logarithms,

$$\frac{\log \mathcal{L}^n(F_\delta)}{-\log \delta} \leq \frac{\log 2^n c_n + n \log \delta + \log N_\delta(F)}{-\log \delta},$$

so

$$\lim_{\delta \rightarrow 0} \frac{\log \mathcal{L}^n(F_\delta)}{-\log \delta} \leq -n + \underline{\dim}_B F \quad \text{2.12}$$

with a similar inequality for the upper limits. On the other hand, if there are $N_\delta(F)$ disjoint balls of radius δ with centres in F , then by adding their volumes,

$$N_\delta(F)c_n\delta^n \leq \mathcal{L}^n(F_\delta).$$

Taking logarithms and letting $\delta \rightarrow 0$ gives the opposite inequality to (2.12), using Equivalent definition 2.1(v).

In the context of Proposition 2.4, box dimension is sometimes referred to as *Minkowski dimension* or *Minkowski–Bouligand dimension*.

Rather surprisingly, the box dimension of a compact subset of \mathbb{R} depends only on the lengths of its complementary intervals and not on their relative positions. Indeed, if F is a compact subset of \mathbb{R} with $\mathcal{L}(F) = 0$, so that, apart from the two unbounded intervals at each end, the complement of F consists of a countable sequence of open intervals of lengths $l_1 \geq l_2 \geq l_3 \geq \dots$, then

$$\dim_B F = -1 \left/ \lim_{j \rightarrow \infty} \frac{\log l_j}{\log j} \right. \quad \underline{2.13}$$

provided this limit exists. This will be proved later in Proposition 9.16.

For example, for the middle third Cantor set, $l_j = 3^{-k}$ when $2^{k-1} \leq j \leq 2^k - 1$, so

$$\frac{\log 3^{-k}}{\log 2^k} \leq \frac{\log l_j}{\log j} \leq \frac{\log 3^{-k}}{\log 2^{k-1}}$$

so $\log l_j / \log j \rightarrow -\log 3 / \log 2$, as would be expected.

2.2 Properties and problems of box-counting dimension

We list a number of basic properties that box dimension satisfies.

Monotonicity. If $E \subset F$, then $\underline{\dim}_B E \leq \underline{\dim}_B F$ and $\overline{\dim}_B E \leq \overline{\dim}_B F$. This follows from the definitions of the dimensions noting that $N_\delta(E) \leq N_\delta(F)$ for all δ .

Range of values. For F a non-empty bounded subset of \mathbb{R}^n ,

$$0 \leq \underline{\dim}_B F \leq \overline{\dim}_B F \leq n.$$

The first two inequalities are obvious; for the third, F may be enclosed in a large cube C so by counting δ -mesh squares $N_\delta(F) \leq N_\delta(C) \leq c\delta^{-n}$ for some constant c .

Finite stability. $\overline{\dim}_B$ is finitely stable, that is,

$$\overline{\dim}_B(E \cup F) = \max \{\overline{\dim}_B E, \overline{\dim}_B F\}.$$

To see this note that $N_\delta(E \cup F) \leq N_\delta(E) + N_\delta(F)$ so dividing by $-\log \delta$ and taking upper limits gives $\overline{\dim}_B(E \cup F) \leq \max \{\overline{\dim}_B E, \overline{\dim}_B F\}$. The opposite inequality follows since $E, F \subset E \cup F$. Note that the corresponding

identity does *not* hold for $\underline{\dim}_B$ nor is it true for infinite unions of sets.

Open sets. If $F \subset \mathbb{R}^n$ is open, then $\dim_B F = n$. Since F contains a cube C , $N_\delta(F) \geq N_\delta(C) \geq c\delta^{-n}$ where c is independent of δ .

Finite sets. If F is non-empty and finite, then $\dim_B F = 0$, since if F comprises m distinct points, then $N_\delta(F) = m$ for all sufficiently small δ .

Smooth sets. If F is a smooth (i.e. continuously differentiable) bounded m -dimensional submanifold (i.e. m -dimensional surface) of \mathbb{R}^n , then $\dim_H F = m$. In particular, smooth curves have dimension 1 and smooth surfaces have dimension 2. We will verify this for curves shortly.

Lipschitz mappings play an important role in fractal geometry, in particular the image of a set under the Lipschitz mapping has dimension no more than that of the original set. This basic property is the content of the following proposition.

Proposition 2.5

a. If $F \subset \mathbb{R}^n$ and $f : F \rightarrow \mathbb{R}^m$ is a Lipschitz transformation, that is,

$$|f(x) - f(y)| \leq c|x - y| \quad (x, y \in F), \quad \text{2.14}$$

then $\underline{\dim}_B f(F) \leq \underline{\dim}_B F$ and $\overline{\dim}_B f(F) \leq \overline{\dim}_B F$.

b. If $F \subset \mathbb{R}^n$ and $f : F \rightarrow \mathbb{R}^m$ is a bi-Lipschitz transformation, that is,

$$c_1|x - y| \leq |f(x) - f(y)| \leq c|x - y| \quad (x, y \in F), \quad \text{2.15}$$

where $0 < c_1 \leq c < \infty$, then $\underline{\dim}_B f(F) = \underline{\dim}_B F$ and $\overline{\dim}_B f(F) = \overline{\dim}_B F$.

Proof

(a) Note that if $\{U_i\}$ is a δ -cover of F , then so is $\{U_i \cap F\}$. Taking images of these sets under f , we see that $\{f(U_i \cap F)\}$ is a $c\delta$ -cover of $f(F)$, since by (2.14) $|f(U_i \cap F)| \leq c|U_i \cap F| \leq c|U_i| \leq c\delta$. Thus, $N_{c\delta}(f(F)) \leq N_\delta(F)$ for all $\delta > 0$, so

$$\frac{\log N_{c\delta}(f(F))}{-\log(c\delta) + \log c} \leq \frac{\log N_\delta(F)}{-\log \delta},$$

and taking lower and upper limits as $\delta \rightarrow 0$ gives the conclusions.

(b) If f is bi-Lipschitz, then $f : F \rightarrow f(F)$ is a bijection with inverse $f^{-1} : f(F) \rightarrow F$. For $u, v \in f(F)$ set $x = f^{-1}(u), y = f^{-1}(v)$ in the left-hand inequality of (2.15). Then

$$c_1 |f^{-1}(u) - f^{-1}(v)| \leq |f(f^{-1}(u)) - f(f^{-1}(v))| = |u - v|,$$

so f^{-1} is Lipschitz. Applying part (a) to f^{-1} gives

$\underline{\dim}_B F = \underline{\dim}_B f^{-1}(f(F)) \leq \underline{\dim}_B f(F)$ and $\overline{\dim}_B F = \overline{\dim}_B f^{-1}(f(F)) \leq \overline{\dim}_B f(F)$, with the reverse inequalities already obtained in part (a).

Several further properties of box dimensions follow from Proposition 2.5.

Geometric invariance. Let $f : F \rightarrow \mathbb{R}^m$ be a congruence, similarity or affine transformation. Since all such transformations are bi-Lipschitz, $\underline{\dim}_B f(F) = \underline{\dim}_B F$ and $\overline{\dim}_B f(F) = \overline{\dim}_B F$.

Smooth curves. Let $g : [0, 1] \rightarrow \mathbb{R}$ be Lipschitz. Then $\dim_B \text{graph}(g) = 1$ where $\text{graph}(g) = \{(x, g(x)) : x \in [0, 1]\}$ is the graph of the function g . In particular, this is the case if g is differentiable with $|g'(x)| \leq c$ for all $x \in [0, 1]$ for some constant c .

To see this, note that the function $f : [0, 1] \rightarrow \text{graph}(g)$ given by $f(x) = (x, g(x))$ is bi-Lipschitz, since for $x, y \in [0, 1]$,

$$\begin{aligned}|x - y| &\leq |f(x) - f(y)| = |(x, g(x)) - (y, g(y))| = (|x - y|^2 + |g(x) - g(y)|^2)^{1/2} \quad \mathbf{2.16} \\ &\leq (|x - y|^2 + c^2|x - y|^2)^{1/2} = (1 + c^2)^{1/2}|x - y|.\end{aligned}$$

By Proposition 2.5(b), $\dim_B \text{graph}(g) = \dim_B [0, 1] = 1$. The differentiable case follows since such functions g are Lipschitz, using the mean value theorem.

Another consequence, which we will meet in more detail in Chapter 7, concerns orthogonal projections, or ‘shadows’ of sets. Here, we just consider projections of plane sets onto lines.

Projections. Let proj denote orthogonal projection from \mathbb{R}^2 onto some given line through the origin. Then for $F \subset \mathbb{R}^2$, $\underline{\dim}_B \text{proj } F \leq \min\{1, \underline{\dim}_B F\}$, with a similar inequality for $\overline{\dim}_B$. This follows since, as is easily checked, orthogonal projection does not increase distances, that is

$$|\text{proj } x - \text{proj } y| \leq |x - y| \quad (x, y \in \mathbb{R}^2),$$

so proj is the Lipschitz mapping.

We now begin to encounter the disadvantages of box-counting dimension. The next proposition is at first appealing but has undesirable consequences.

Proposition 2.6

Let \overline{F} denote the closure of F (i.e. the smallest closed subset of \mathbb{R}^n containing F). Then

$$\underline{\dim}_B \overline{F} = \underline{\dim}_B F$$

and

$$\overline{\dim}_B \overline{F} = \overline{\dim}_B F.$$

Proof

Let B_1, \dots, B_k be a finite collection of closed balls of radii δ . The closed set $\bigcup_{i=1}^k B_i$ contains F if and only if it also contains \overline{F} . Hence, the smallest number of closed balls of radius δ that cover F equals the smallest number required to cover the larger set \overline{F} . The result follows.

An immediate consequence of this is that if F is a dense subset of an open region of \mathbb{R}^n , then $\underline{\dim}_B F = \overline{\dim}_B F = n$. For example, let F be the (countable) set of rational numbers between 0 and 1. Then \overline{F} is the entire interval $[0, 1]$, so that $\underline{\dim}_B F = \overline{\dim}_B F = 1$. Thus, countable sets, which are very small compared to the real numbers, can have non-zero box dimension. Moreover, the box-counting dimension of each rational number regarded as a one-point set is clearly zero, but the countable union of these singleton sets has dimension 1.

Consequently, it is not generally true that $\dim_B \bigcup_{i=1}^{\infty} F_i = \sup_i \{\dim_B F_i\}$.

This severely limits the usefulness of box dimension—introducing a small, that is, countable, set of points can play havoc with the dimension. We might hope to salvage something by restricting attention to closed sets, but difficulties still remain, as the following example of a ‘sparse’ set with non-zero dimension shows.

Example 2.7

$F = \{0, 1, \frac{1}{2}, \frac{1}{3}, \dots\}$ is a compact subset of \mathbb{R} with $\dim_B F = \frac{1}{2}$.

Calculation

Let $0 < \delta < \frac{1}{2}$ and let k be the integer satisfying

$1/(k-1)k > \delta \geq 1/k(k+1)$. If $|U| \leq \delta$, then U can cover at most one of the points $\{1, \frac{1}{2}, \dots, 1/k\}$ since the distance between any pair of these points is at least $1/(k-1) - 1/k = 1/(k-1)k > \delta$. Thus, at least k sets of diameter δ are required to cover F , so $N_\delta(F) \geq k$ giving

$$\frac{\log N_\delta(F)}{-\log \delta} \geq \frac{\log k}{\log k(k+1)} = \frac{\log k}{2 \log k \log(1 + 1/k)} \rightarrow \frac{1}{2}$$

as $k \rightarrow \infty$ corresponding to $\delta \rightarrow 0$, so $\underline{\dim}_B F \geq \frac{1}{2}$.

On the other hand, if $0 < \delta < \frac{1}{2}$, take k such that

$1/(k-1)k > \delta \geq 1/k(k+1)$. Then $(k+1)$ intervals of length δ cover $[0, 1/k]$, leaving $k-1$ points of F which can be covered by another $k-1$ intervals. Thus, $N_\delta(F) \leq 2k$, so

$$\frac{\log N_\delta(F)}{-\log \delta} \leq \frac{\log(2k)}{\log k(k-1)} = \frac{\log 2 + \log k}{2 \log k + \log(1 - 1/k)} \rightarrow \frac{1}{2}$$

on taking the limit, giving $\overline{\dim}_B F \leq \frac{1}{2}$.

Few would think of this set, with all but one of its points isolated, as a fractal, yet it has large box dimension.

Despite these drawbacks, box-counting dimensions have many advantages. They are often much easier to calculate than other forms of dimension, and the box-counting version of the definition is convenient for empirical estimation. Moreover, as we will see later, the interplay between box dimensions and other definitions of dimension can be used to powerful effect.

*2.3 Modified box-counting dimensions

One way of overcoming the difficulties of box dimensions outlined at the end of Section 2.1 is to modify the definition. This may at first seem unappealing since direct calculation may become much harder. Nevertheless, these modified dimensions turn out to be closely related to the important packing dimension which we shall meet in the next chapter.

For F a subset of \mathbb{R}^n , we can try to decompose F into a countable number of pieces F_1, F_2, \dots in such a way that the largest piece has as small a dimension as possible. This idea leads to the following *lower and upper modified box-counting dimensions*:

$$\underline{\dim}_{\text{MB}} F = \inf \left\{ \sup_i \underline{\dim}_B F_i : F \subset \bigcup_{i=1}^{\infty} F_i \right\} \quad \text{2.17}$$

$$\overline{\dim}_{\text{MB}} F = \inf \left\{ \sup_i \overline{\dim}_B F_i : F \subset \bigcup_{i=1}^{\infty} F_i \right\}. \quad \text{2.18}$$

(In both the cases, the infimum is over all possible finite or countable covers $\{F_i\}$ of F , with the F_i non-empty and bounded.) Clearly, $\underline{\dim}_{\text{MB}} F \leq \underline{\dim}_B F$ and $\overline{\dim}_{\text{MB}} F \leq \overline{\dim}_B F$. However, we now have that $\underline{\dim}_{\text{MB}} F = \overline{\dim}_{\text{MB}} F = 0$ if F is countable—just take the F_i to be one-point sets. Moreover, for any subset F of \mathbb{R}^n ,

$$0 \leq \underline{\dim}_{\text{MB}} F \leq \overline{\dim}_{\text{MB}} F \leq \overline{\dim}_B F \leq n. \quad \text{2.19}$$

It is easy to see from the definitions that $\underline{\dim}_{\text{MB}}$ and $\overline{\dim}_{\text{MB}}$ inherit all the properties listed for box-counting dimensions, including the Lipschitz function property. Moreover, they are also *countably stable*, that is,

$$\underline{\dim}_{\text{MB}} \left(\bigcup_{i=1}^{\infty} F_i \right) = \sup_i \{\underline{\dim}_{\text{MB}} F_i\}$$

for any finite or countable sequence of sets $\{F_i\}$, with a similar identity for the upper modified box dimension.

We have seen that the modified box dimensions of a set can be smaller than the box dimensions, but there is a useful test for equality. It applies to compact sets that might be described as ‘dimensionally homogeneous’.

Proposition 2.8

Let $F \subset \mathbb{R}^n$ be compact. Suppose that

$$\overline{\dim}_B(F \cap V) = \overline{\dim}_B F \quad \mathbf{2.20}$$

for all open sets V that intersect F . Then $\overline{\dim}_B F = \overline{\dim}_{MB} F$. The corresponding result holds for lower box-counting dimensions.

Proof

Let $F \subset \bigcup_{i=1}^{\infty} F_i$ with each F_i closed. A version of Baire's category theorem (which may be found in any text on basic general topology) states that if a closed subset of \mathbb{R}^n is covered by such a countable union of closed sets, there is an index i and an open set $V \subset \mathbb{R}^n$ such that $\emptyset \neq F \cap V \subset F_i$. For this i ,

$\overline{\dim}_B F_i \geq \overline{\dim}_B(F_i \cap V) = \overline{\dim}_B F$. Using (2.18) and Proposition 2.6,

$$\begin{aligned} \overline{\dim}_{MB} F &= \inf \left\{ \sup \overline{\dim}_B F_i : F \subset \bigcup_{i=1}^{\infty} F_i \text{ where the } F_i \text{ are closed sets} \right\} \\ &\geq \overline{\dim}_B F. \end{aligned}$$

The opposite inequality is part of (2.19). A similar argument deals with the lower dimensions.

For an example, let F be a compact set with a high degree of self-similarity such as the middle third Cantor set or the von Koch curve. If V is any open set that intersects F , then $F \cap V$ contains a

geometrically similar copy of F that must have box dimensions equal to those of F , so by Proposition 2.8, the box and modified box dimensions are equal.

There is another property involving the notion of Baire category that is also useful. We say that a set $F \subset \mathbb{R}^n$ is of *second category* in \mathbb{R}^n if it cannot be expressed as a countable union of nowhere dense sets, in other words, given a countable covering of F , say $F \subset \bigcup_{i=1}^{\infty} F_i$, there is some F_i and a non-empty open set V such that $V \subset \overline{F \cap F_i}$. In particular, Baire's category theorem implies that if F is a G_δ set that is dense in some open region of \mathbb{R}^n then F is of second category. (A G_δ set is one that may be expressed as the intersection of a countable collection of open sets.)

Proposition 2.9

Let $F \subset \mathbb{R}^n$ be of second category. Then $\underline{\dim}_{\text{MB}} F = \overline{\dim}_{\text{MB}} F = n$.

Proof

Let $F \subset \bigcup_{i=1}^{\infty} F_i$ with each F_i closed. From the definition of second category, there is a non-empty open set V such that $V \subset \overline{F \cap F_i}$ for one of the F_i , so

$$n = \underline{\dim}_B V \leq \underline{\dim}_B \overline{F \cap F_i} = \underline{\dim}_B F \cap F_i \leq \underline{\dim}_B F_i \leq \overline{\dim}_B F_i \leq n.$$

The conclusion follows from the definitions of modified box dimensions.

2.4 Some other definitions of dimension

Many other definitions of dimension have been proposed, all of which depend on some sort of measurement of sets at fine scales.

Two of the most important definitions, Hausdorff and packing dimensions will be introduced in Chapter 3. Some definitions only apply to restricted classes of sets such as curves, others have been introduced because they are convenient to apply in specific contexts. There are no hard-and-fast rules for deciding whether a quantity may reasonably be regarded as a dimension. The factors that determine the acceptability of a definition of a fractal dimension are recognised largely by experience and intuition. A word of warning: apparently similar definitions of dimension can have widely differing properties. It should not be assumed that different definitions give the same value of dimension, even for ‘nice’ sets. Such assumptions have led to considerable misconceptions and confusion. It is necessary to derive the properties of any ‘dimension’ from its definition.

What are the desirable properties of a ‘dimension’? We have encountered the following possibilities in connection with box or modified box dimensions.

Monotonicity. If $E \subset F$, then $\dim E \leq \dim F$.

Range of values. If $F \subset \mathbb{R}^n$, then $0 \leq \dim F \leq n$.

Stability. $\dim(E \cup F) = \max(\dim E, \dim F)$.

Countable stability. $\dim(\bigcup_{i=1}^{\infty} F_i) = \sup_i \dim F_i$.

Lipschitz invariance. $\dim f(F) = \dim F$ if f is a bi-Lipschitz transformation.

Geometric invariance. $\dim f(F) = \dim F$ if f is a transformation of \mathbb{R}^n such as a translation, rotation, similarity or affinity.

Countable sets. $\dim F = 0$ if F is finite or countable.

Open sets. If F is an open subset of \mathbb{R}^n , then $\dim F = n$.

Smooth manifolds. $\dim F = m$ if F is a smooth m -dimensional manifold (curve, surface, etc.).

All definitions of dimension are monotonic, most are stable, but some common definitions fail to exhibit countable stability and may

have countable sets of positive dimension. All the usual dimensions are the Lipschitz invariant and, therefore, geometrically invariant. The ‘open sets’ and ‘smooth manifolds’ properties ensure that the dimension is an extension of the classical definition.

There are several definitions of dimension that apply specifically to curves, notably ‘divider dimension’. We define a *curve* or *Jordan curve* C to be the image of an interval $[a, b]$ under a continuous injection $f : [a, b] \rightarrow \mathbb{R}^n$. (Thus, we restrict attention to curves that are non-self-intersecting.) If C is a curve and $\delta > 0$, we define $M_\delta(C)$ to be the maximum number of points x_0, x_1, \dots, x_m , on the curve C , in that order, such that $|x_k - x_{k-1}| = \delta$ for $k = 1, 2, \dots, m$. Thus, $(M_\delta(C) - 1)\delta$ may be thought of as the ‘length’ of the curve C measured using a pair of dividers with points set at a distance δ apart. The *divider dimension* is defined as

$$\lim_{\delta \rightarrow 0} \frac{\log M_\delta(C)}{-\log \delta} \quad \underline{2.21}$$

assuming the limit exists (otherwise we may define upper and lower divider dimensions using upper and lower limits). It is easy to see that the divider dimension of a curve is at least equal to the box dimension (assuming that they both exist) and for simple self-similar curves, such as the von Koch curve, they are equal. The assertion that the coastline of Britain has dimension 1.2 is usually made with the divider dimension in mind—this empirical value comes from estimating the ratio in (2.21) on maps with values of δ between about 20 m and 200 km.

Sometimes, we are interested in the dimension of a fractal F that is the boundary of a set A . We can define the box dimension of F in the usual way, but it may be useful to distinguish between A and its complement. Thus, the following variation of the Minkowski definition of box dimension, but taking the volume of the set of points within distance δ of F that lie in A , is sometimes used. The *one-sided dimension* of the boundary F of a set A in \mathbb{R}^n is defined as

$$n - \lim_{\delta \rightarrow 0} \frac{\log \mathcal{L}^n(F_\delta \cap A)}{\log \delta},$$

where F_δ is the δ -neighbourhood of F (compare Proposition 2.4). This definition has applications to the surface physics of solids where it is the volume very close to the surface that is important and also to partial differential equations in domains with fractal boundaries.

2.5 Notes and references

The origin of box dimension seems hard to trace—it seems certain that it would have been considered by the pioneers of the Hausdorff measure and dimension and was probably rejected as being less satisfactory from a mathematical viewpoint. Bouligand (1928) adapted the Minkowski content to non-integral dimensions, and the more usual definition of box dimension was given by Pontrjagin and Schnirelman (1932). Most of the general texts on fractals include some treatment of box dimensions. The relationship between box dimension and lengths of complementary intervals (2.13) was first investigated by Besicovitch and Taylor (1954) and fuller treatments are given in Falconer (1997) and Lapidus and van Frankenhuysen (2012).

Exercises

2.1 Verify directly from the definitions that Equivalent definitions 2.1(ii) and (iv) give the same values for box dimension.

2.2 Generalise Proposition 2.5 by showing that if $f : F \rightarrow \mathbb{R}^n$ satisfies the Hölder condition $|f(x) - f(y)| \leq c|x - y|^\alpha$ where $c > 0$ and $0 < \alpha \leq 1$, then $\underline{\dim}_B f(F) \leq (1/\alpha)\underline{\dim}_B F$ and $\overline{\dim}_B f(F) \leq (1/\alpha)\overline{\dim}_B F$.

2.3 Let F consist of those numbers in $[0, 1]$ whose decimal expansions do not contain the digit 5. Find $\dim_B F$, showing that this box dimension exists.

2.4 Verify that the Cantor dust depicted in [Figure 0.4](#) has box dimension 1 (take E_0 to have side length 1).

2.5 Use Equivalent definition 2.1(i) to check that the upper box dimension of the von Koch curve is at most $\log 4 / \log 3$ and 2.1(v) to check that the lower box dimension is at least this value.

2.6 Use convenient parts of Equivalent definition 2.1 to find the box dimension of the Sierpiński triangle in [Figure 0.3](#).

2.7 Let F be the middle third Cantor set. For $0 < \delta < 1$, find the length of the δ -neighbourhood F_δ of F , and hence, find the box dimension of F using Proposition 2.4.

2.8 Construct a set F for which $\underline{\dim}_B F < \overline{\dim}_B F$. (Hint: let $k_n = 10^n$, and adapt the Cantor set construction by deleting, at the k th stage, the middle $\frac{1}{3}$ of intervals if $k_{2n} < k \leq k_{2n+1}$, but the middle $\frac{3}{5}$ of intervals if $k_{2n-1} < k \leq k_{2n}$.)

2.9 Find subsets E and F of \mathbb{R} such that $\underline{\dim}_B(E \cup F) > \max\{\underline{\dim}_B E, \underline{\dim}_B F\}$. (Hint: consider two sets of the form indicated in Exercise 2.8.)

2.10 What are the Hausdorff and box dimensions of the set $\{0, 1, \frac{1}{4}, \frac{1}{9}, \frac{1}{16}, \dots\}$?

2.11 What is the modified box dimension of the von Koch curve?

2.12 Find the divider dimension ([2.21](#)) of the von Koch curve.

2.13 Show that the divider dimension ([2.21](#)) of a curve is greater than or equal to its box dimension, assuming that they both exist.

2.14 Let $0 < \lambda < 1$ and let F be the ‘middle- λ Cantor set’ obtained by repeated removal of the middle proportion λ from intervals. Show that the dimension of F defined by ([2.13](#)) in terms of removed intervals equals the box dimension of F .

Chapter 3

Hausdorff and packing measures and dimensions

Of the wide variety of ‘fractal dimensions’, Hausdorff dimension, based on a construction of Carathéodory, is the oldest and probably the most important. It has the advantage of being defined for any set and is based on the measures that are mathematically convenient to work with. A disadvantage is that it is often hard to calculate or to estimate by computational methods. However, for a proper understanding of the mathematics of fractals, familiarity with Hausdorff measure and dimension is essential. Hausdorff dimension depends on covering a set by small sets and a ‘dual’ definition was introduced much later, based on packings of disjoint small discs with centres in the set. Whilst many sets have equal Hausdorff and packing dimensions, there are plenty of interesting cases where the values differ, and nowadays problems are often analysed from both points of view.

3.1 Hausdorff measure

Recall that a δ -cover of a set F is a countable (or finite) collection of sets $\{U_i\}$ with diameters $0 < |U_i| \leq \delta$ that cover F . Suppose that F is a subset of \mathbb{R}^n and $s \geq 0$. For each $\delta > 0$, we define

$$\mathcal{H}_\delta^s(F) = \inf \left\{ \sum_{i=1}^{\infty} |U_i|^s : \{U_i\} \text{ is a } \delta\text{-cover of } F \right\}. \quad 3.1$$

Thus, we look at all covers of F by sets of diameter at most δ and seek to minimise the sum of the s th powers of the diameters ([Figure 3.1](#)). As δ decreases, the class of permissible covers of F in [\(3.1\)](#) is reduced. Therefore, the infimum $\mathcal{H}_\delta^s(F)$ increases, or at least does not increase, as $\delta \rightarrow 0$ and so approaches a limit. We write

$$\mathcal{H}^s(F) = \lim_{\delta \rightarrow 0} \mathcal{H}_\delta^s(F).$$

3.2

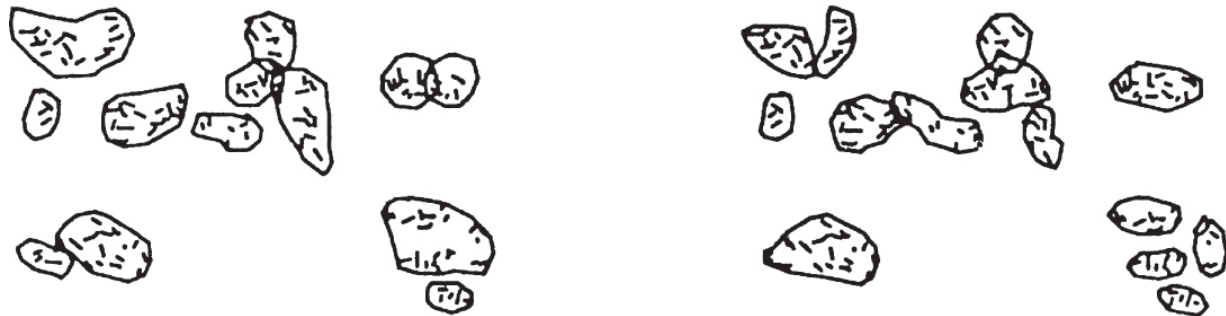
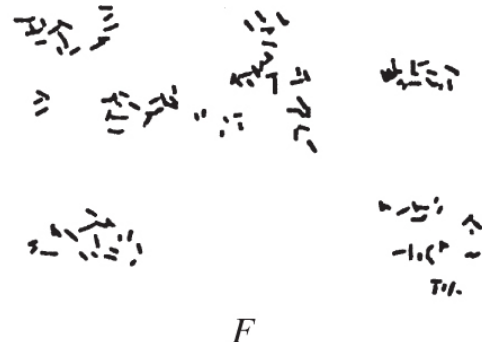


Figure 3.1 A set F and two possible δ -covers for F . The infimum of $\sum |U_i|^s$ over all such δ -covers $\{U_i\}$ gives $\mathcal{H}_\delta^s(F)$.

This limit exists for any subset F of \mathbb{R}^n , although the limiting value can be (and usually is) 0 or ∞ . We call $\mathcal{H}^s(F)$ the *s-dimensional Hausdorff measure* of F .

With a certain amount of effort, \mathcal{H}^s may be shown to be a measure (see Section 1.31.3). It is straightforward to show that $\mathcal{H}^s(\emptyset) = 0$, that if E is contained in F , then $\mathcal{H}^s(E) \leq \mathcal{H}^s(F)$, and that if $\{F_i\}$ is any countable collection of sets, then

$$\mathcal{H}^s \left(\bigcup_{i=1}^{\infty} F_i \right) \leq \sum_{i=1}^{\infty} \mathcal{H}^s(F_i).$$

3.3

It is rather harder to show that there is equality in (3.3) if the $\{F_i\}$ are disjoint Borel sets.

Hausdorff measures generalise the familiar ideas of length, area, volume, and so on. It may be shown that for subsets of \mathbb{R}^n , n -dimensional Hausdorff measure is, to within a constant multiple, just n -dimensional Lebesgue measure, that is, the usual n -dimensional volume. More precisely, if F is a Borel subset of \mathbb{R}^n , then

$$\mathcal{H}^n(F) = c_n^{-1} \text{vol}^n(F), \quad \text{3.4}$$

where c_n is the volume of an n -dimensional ball of diameter 1, so that $c_n = \pi^{n/2}/2^n(n/2)!$ if n is even and $c_n = \pi^{(n-1)/2}((n-1)/2)!/n!$ if n is odd. Similarly, for ‘nice’ lower-dimensional subsets of \mathbb{R}^n , we have that $\mathcal{H}^0(F)$ is the number of points in F ; $\mathcal{H}^1(F)$ gives the length of a smooth curve F ; $\mathcal{H}^2(F) = (4/\pi) \times \text{area}(F)$ if F is a smooth surface; $\mathcal{H}^3(F) = (6/\pi) \times \text{vol}(F)$; and $\mathcal{H}^m(F) = c_m^{-1} \times \text{vol}^m(F)$ if F is a smooth m -dimensional submanifold of \mathbb{R}^n (i.e. an m -dimensional surface in the classical sense).

As with box-counting dimensions, Hausdorff measures behave well under Lipschitz mappings and, more generally, under Hölder mappings, that is mappings that satisfy (3.5), termed a *Hölder condition of exponent α* .

Proposition 3.1

Let $F \subset \mathbb{R}^n$ and $f : F \rightarrow \mathbb{R}^m$ be a mapping such that

$$|f(x) - f(y)| \leq c|x - y|^\alpha \quad (x, y \in F) \quad 3.5$$

for constants $\alpha > 0$ and $c > 0$. Then for each s

$$\mathcal{H}^{s/\alpha}(f(F)) \leq c^{s/\alpha} \mathcal{H}^s(F). \quad 3.6$$

In particular, if f is a Lipschitz mapping, that is, if $\alpha = 1$, then

$$\mathcal{H}^s(f(F)) \leq c^s \mathcal{H}^s(F). \quad 3.7$$

Proof

If $\{U_i\}$ is a δ -cover of F , then since $|f(F \cap U_i)| \leq c|F \cap U_i|^\alpha \leq c|U_i|^\alpha$, it follows that $\{f(F \cap U_i)\}$ is a $c\delta^\alpha$ -cover of $f(F)$. Thus, $\sum_i |f(F \cap U_i)|^{s/\alpha} \leq c^{s/\alpha} \sum_i |U_i|^s$, so that $\mathcal{H}_{c\delta^\alpha}^{s/\alpha}(f(F)) \leq c^{s/\alpha} \mathcal{H}_\delta^s(F)$. Letting $\delta \rightarrow 0$ gives (3.6).

The result for the Lipschitz case is immediate on setting $\alpha = 1$.

The scaling properties of length, area and volume are well known. On enlargement by a factor λ , the length of a curve is multiplied by λ , the area of a plane region is multiplied by λ^2 and the volume of a 3-dimensional object is multiplied by λ^3 . As might be anticipated, s -dimensional Hausdorff measure scales with a factor λ^s ([Figure 3.2](#)). This scaling property, which is an immediate corollary to Proposition 3.1, is a fundamental property of Hausdorff measures.

Scaling property 3.2

Let $f : \mathbb{R}^n \rightarrow \mathbb{R}^n$ be a similarity transformation of scale factor $\lambda > 0$. If $F \subset \mathbb{R}^n$, then

$$\mathcal{H}^s(f(F)) = \lambda^s \mathcal{H}^s(F).$$

3.8

Proof

Since

$$|f(x) - f(y)| = \lambda|x - y| \text{ and so } |f^{-1}(x) - f^{-1}(y)| = \lambda^{-1}|x - y| \quad (x, y \in F),$$

applying Proposition 3.1 to f and to f^{-1} gives (3.8).

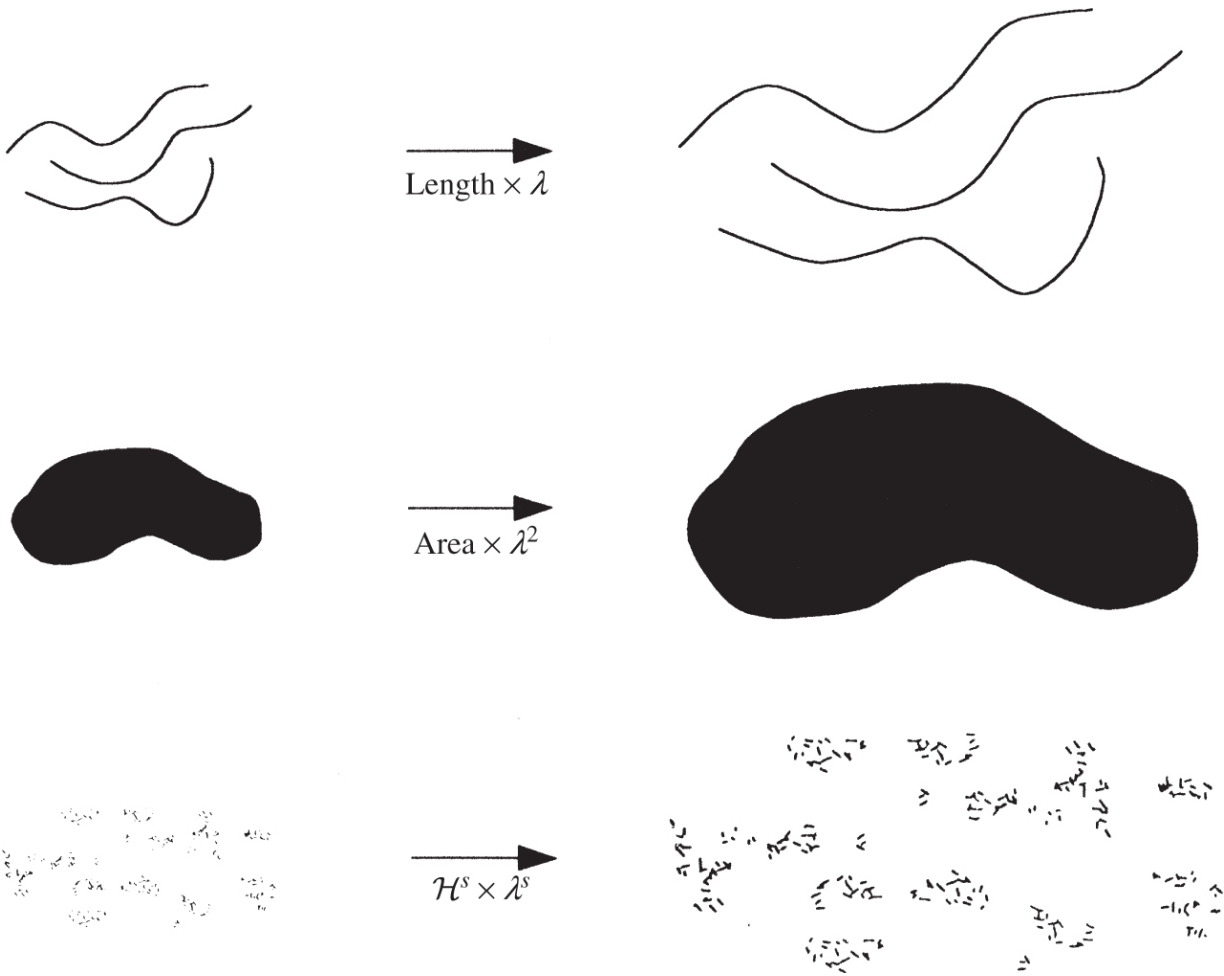


Figure 3.2 Scaling sets by a factor λ increases length by a factor λ , area by a factor λ^2 and s -dimensional Hausdorff measure by a factor λ^s .

In particular, if f is a congruence or isometry, that is, $|f(x) - f(y)| = |x - y|$ for all $x, y \in \mathbb{R}^n$, then $\mathcal{H}^s(f(F)) = \mathcal{H}^s(F)$. Thus, Hausdorff measures are translation invariant (i.e. $\mathcal{H}^s(F + z) = \mathcal{H}^s(F)$, where $F + z = \{x + z : x \in F\}$), and rotation invariant, as would certainly be expected.

3.2 Hausdorff dimension

Returning to definition (3.1), it is clear that for any given set $F \subset \mathbb{R}^n$ and $\delta < 1$, $\mathcal{H}_\delta^s(F)$ is non-increasing with s , so by (3.2), $\mathcal{H}^s(F)$ is also

non-increasing. In fact, rather more is true: if $t > s$ and $\{U_i\}$ is a δ -cover of F , then

$$\sum_i |U_i|^t \leq \sum_i |U_i|^{t-s} |U_i|^s \leq \delta^{t-s} \sum_i |U_i|^s \quad \text{3.9}$$

so, taking infima over all δ -covers,

$$\mathcal{H}_\delta^t(F) \leq \delta^{t-s} \mathcal{H}_\delta^s(F).$$

Letting $\delta \rightarrow 0$, we see that if $\mathcal{H}^s(F) < \infty$, then $\mathcal{H}^t(F) = 0$ for $t > s$. Thus, a graph of $\mathcal{H}^s(F)$ against s (Figure 3.3) shows that there is a critical value of s at which $\mathcal{H}^s(F)$ ‘jumps’ from ∞ to 0. This critical value is called the *Hausdorff dimension* of F , written as $\dim_H F$; it is defined for any set $F \subset \mathbb{R}^n$. (Note that some authors refer to the *Hausdorff–Besicovitch dimension*.) Formally,

$$\dim_H F = \inf \{s \geq 0 : \mathcal{H}^s(F) = 0\} = \sup \{s : \mathcal{H}^s(F) = \infty\} \quad \text{3.10}$$

(taking the supremum of the empty set to be 0), so that

$$\mathcal{H}^s(F) = \begin{cases} \infty & \text{if } 0 \leq s < \dim_H F \\ 0 & \text{if } s > \dim_H F \end{cases}. \quad \text{3.11}$$

If $s = \dim_H F$, then $\mathcal{H}^s(F)$ may be zero or infinite or may satisfy

$$0 < \mathcal{H}^s(F) < \infty.$$

A Borel set satisfying this last condition is called an *s-set*.

Mathematically, s -sets are by far the most convenient sets to study, and fortunately, they occur surprisingly often.

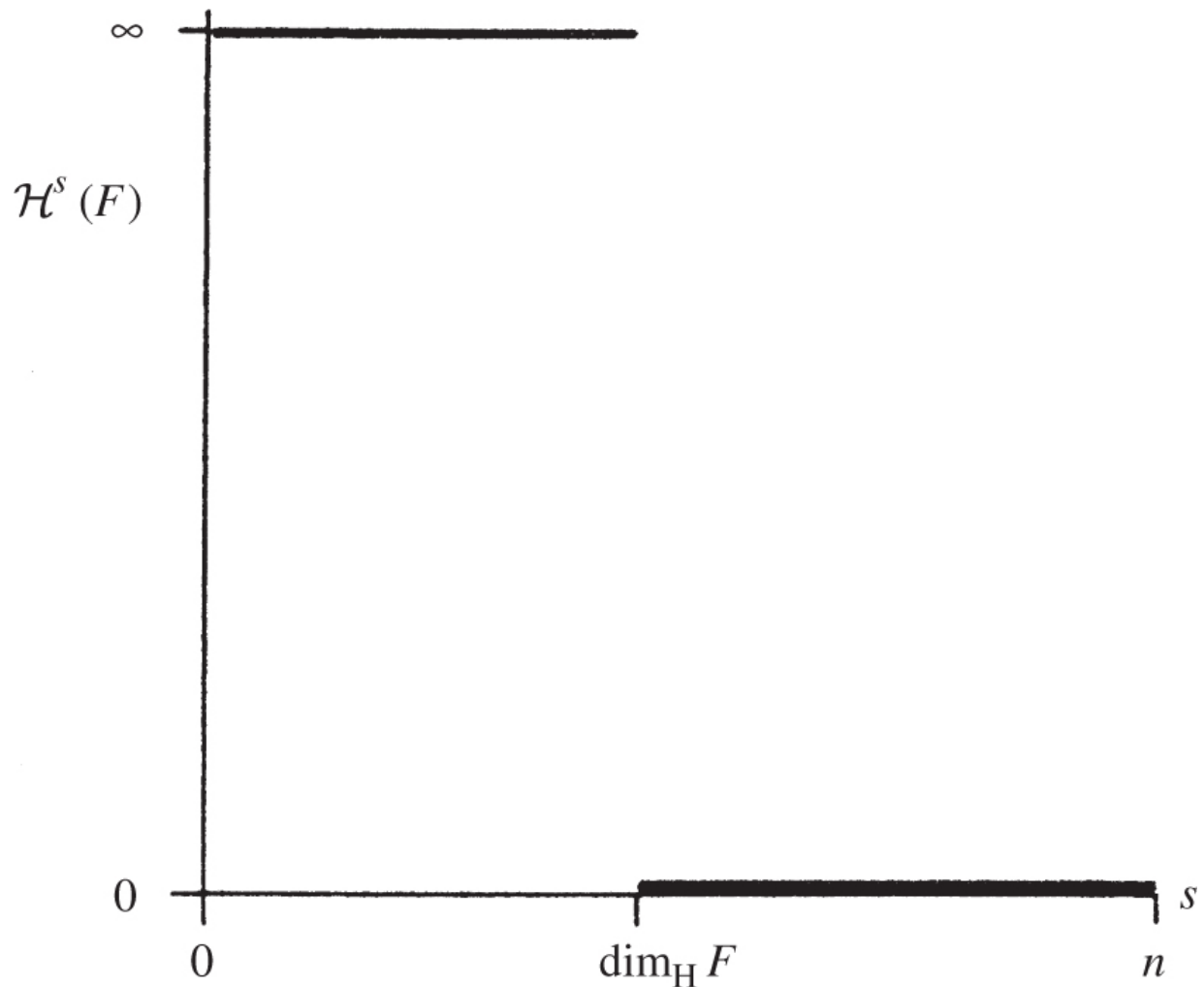


Figure 3.3 Graph of $\mathcal{H}^s(F)$ against s for a set F . The Hausdorff dimension is the value of s at which the ‘jump’ from ∞ to 0 occurs.

For a very simple example, let F be a flat disc of unit radius in \mathbb{R}^3 .

From familiar properties of length, area and volume,

$$\mathcal{H}^1(F) = \text{length}(F) = \infty, \quad 0 < \mathcal{H}^2(F) = (4/\pi) \times \text{area}(F) = 4 < \infty \text{ and}$$

$$\mathcal{H}^3(F) = (6/\pi) \times \text{vol}(F) = 0. \text{ Thus, } \dim_H F = 2, \text{ with } \mathcal{H}^s(F) = \infty \text{ if } s < 2 \text{ and} \\ \mathcal{H}^s(F) = 0 \text{ if } s > 2.$$

Most of the basic properties of Hausdorff dimension follow easily from those of Hausdorff measures.

Monotonicity. If $E \subset F$, then $\dim_H E \leq \dim_H F$. This is immediate from the measure property that $\mathcal{H}^s(E) \leq \mathcal{H}^s(F)$ for each s .

Range of values. If $F \subset \mathbb{R}^n$, then $0 \leq \dim_H F \leq n$. Clearly, Hausdorff dimensions are non-negative. By considering coverings by δ -mesh cubes, if F is bounded and $s > n$, then $\mathcal{H}^s(F) = 0$. Since every subset of \mathbb{R}^n is a countable union of bounded sets, $\mathcal{H}^s(F) = 0$ if $s > n$ for all $F \subset \mathbb{R}^n$ by countable additivity of Hausdorff measures, so $\dim_H F \leq n$.

Countable stability. If F_1, F_2, \dots is a (countable) sequence of sets, then $\dim_H \bigcup_{i=1}^{\infty} F_i = \sup_{1 \leq i < \infty} \{\dim_H F_i\}$. Certainly, $\dim_H \bigcup_{i=1}^{\infty} F_i \geq \dim_H F_j$ for each j by monotonicity. On the other hand, if $s > \dim_H F_i$ for all i , then $\mathcal{H}^s(F_i) = 0$, so that $\mathcal{H}^s(\bigcup_{i=1}^{\infty} F_i) \leq \sum_{i=1}^{\infty} \mathcal{H}^s(F_i) = 0$, giving the opposite inequality.

Countable sets. If F is countable, then $\dim_H F = 0$. For if F_i is a single point, $\mathcal{H}^0(F_i) = 1$ and $\dim_H F_i = 0$, so by countable stability, $\dim_H \bigcup_{i=1}^{\infty} F_i = 0$.

Open sets. If $F \subset \mathbb{R}^n$ is open, then $\dim_H F = n$. Since F contains a ball of positive n -dimensional volume, $\dim_H F \geq n$.

As with box dimension, Hausdorff dimension behaves well under Lipschitz mappings.

Proposition 3.3

- a. Let $F \subset \mathbb{R}^n$ and suppose that $f : F \rightarrow \mathbb{R}^m$ satisfies the Hölder condition

$$|f(x) - f(y)| \leq c|x - y|^{\alpha} \quad (x, y \in F).$$

Then $\dim_H f(F) \leq (1/\alpha)\dim_H F$. In particular, if f is a Lipschitz mapping, that is, if $\alpha = 1$, then $\dim_H f(F) \leq \dim_H F$.

- b. If $f : F \rightarrow \mathbb{R}^m$ is a bi-Lipschitz transformation, that is,

$$c_1|x - y| \leq |f(x) - f(y)| \leq c|x - y| \quad (x, y \in F), \quad \text{3.12}$$

where $0 < c_1 \leq c < \infty$, then $\dim_H f(F) = \dim_H F$.

Proof

- (a) If $s > \dim_H F$, then by Proposition 3.1 $\mathcal{H}^{s/\alpha}(f(F)) \leq c^{s/\alpha} \mathcal{H}^s(F) = 0$, implying that $\dim_H f(F) \leq s/\alpha$ for all $s > \dim_H F$. The conclusion for Lipschitz mappings is immediate on taking $\alpha = 1$.
- (b) For the bi-Lipschitz case, just as in Proposition 2.5 for box dimension, applying the Lipschitz result to $f^{-1} : f(F) \rightarrow F$ yields the reverse inequality $\dim_H F \leq \dim_H f(F)$.

The next few properties follow because the associated transformations are Lipschitz or bi-Lipschitz, just as for box dimensions.

Geometric invariance. Let f be a congruence, similarity or affine transformation on \mathbb{R}^n . Then $\dim_H f(F) = \dim_H F$.

Smooth sets. If F is a smooth m -dimensional manifold (curve, surface, etc.), then $\dim_H F = m$.

Projections. With proj denoting orthogonal project from \mathbb{R}^2 onto some given line through the origin, $\dim_H \text{proj } F \leq \min\{1, \dim_H F\}$.

It is natural to wonder about the relationship between Hausdorff dimension and the box-counting dimensions, and this is summarised in the following proposition.

Proposition 3.4

For every non-empty bounded $F \subset \mathbb{R}^n$,

$$\dim_H F \leq \underline{\dim}_B F \leq \overline{\dim}_B F.$$

3.13

Proof

Suppose that $1 < \mathcal{H}^s(F) = \lim_{\delta \rightarrow 0} \mathcal{H}_\delta^s(F)$ for some $s \geq 0$. Then, for all sufficiently small δ ,

$$1 < \mathcal{H}_\delta^s(F) \leq N_\delta(F)\delta^s,$$

where $N_\delta(F)$ is the least number of sets of diameter δ that can cover F , using (3.1). Taking logarithms, $0 < \log N_\delta(F) + s \log \delta$, and it follows that $s \leq \underline{\lim}_{\delta \rightarrow 0} \log N_\delta(F) / -\log \delta$.

We do *not* in general get equality here. Although Hausdorff and box dimensions are equal for many ‘reasonably regular’ sets, there are plenty of examples where there is strict inequality in (3.13).

We have seen in Propositions 2.5 and 3.3 that the Hausdorff dimensions of a set and its image under a bi-Lipschitz mapping are equal, and as are the box dimensions. This is a fundamental property of dimension: *Hausdorff dimension, lower box dimension and upper box dimension are all invariant under bi-Lipschitz transformations*. Thus, if two sets have different dimensions, there cannot be a bi-Lipschitz mapping from one onto the other. This is reminiscent of the situation in topology where various ‘invariants’ (such as homotopy or homology groups) are set up to distinguish between sets that are not homeomorphic: if the topological invariants of two sets differ, then there cannot be a homeomorphism (continuous one-to-one mapping with continuous inverse) between the two sets.

In topology, two sets are regarded as equivalent if there is a homeomorphism between them. One approach to fractal geometry is to regard two sets as equivalent if there is a bi-Lipschitz mapping between them. Just as topological invariants are used to distinguish between non-homeomorphic sets, we may seek parameters, including dimension, to distinguish between sets that are not bi-

Lipschitz equivalent. Since bi-Lipschitz transformations (3.12) are necessarily homeomorphisms, topological parameters provide a start in this direction, and Hausdorff dimension (and other definitions of dimension) provide further distinguishing characteristics between fractals.

In general, the dimension of a set alone tells us little about its topological properties. However, any set of dimension less than 1 is necessarily so sparse as to be totally disconnected; that is, no two of its points lie in the same connected component.

Proposition 3.5

Every set $F \subset \mathbb{R}^n$ with $\dim_H F < 1$ is totally disconnected.

Proof

Let x and y be distinct points of F . Define a mapping $f : \mathbb{R}^n \rightarrow [0, \infty]$ by $f(z) = |z - x|$. Using the reverse triangle inequality,

$$|f(z) - f(w)| = ||z - x| - |w - x|| \leq |(z - x) - (w - x)| = |z - w|,$$

so f is Lipschitz, and by Proposition 3.3(a), $\dim_H f(F) \leq \dim_H F < 1$. Thus, $f(F)$ is a subset of \mathbb{R} of \mathcal{H}^1 -measure (or length) zero and so has a dense complement. Choosing r with $r \notin f(F)$ and $0 < r < f(y)$, it follows that

$$F = \{z \in F : |z - x| < r\} \cup \{z \in F : |z - x| > r\}.$$

Thus, F is contained in two disjoint open sets with x in one set and y in the other, so that x and y lie in different connected components of F .

To end this section, we remark that it is possible to define Hausdorff dimension without directly using Hausdorff measures. For $F \subset \mathbb{R}^n$, let

$$\mathcal{H}_\infty^s(F) = \inf \left\{ \sum_{i=1}^{\infty} |U_i|^s : \{U_i\} \text{ is a countable cover of } F \right\}.$$

Then the Hausdorff dimension of F is given by

$$\dim_H F = \inf \{s \geq 0 : \mathcal{H}_\infty^s(F) = 0\}.$$

To see this, note that if $s > \dim_H F$, then for all $\delta > 0$ we have $0 = \mathcal{H}_\delta^s(F) \geq \mathcal{H}_\infty^s(F)$. On the other hand, if $\mathcal{H}_\infty^s(F) = 0$, then for all $\delta > 0$ we may find a cover $\{U_i\}$ of F with $\sum_{i=1}^{\infty} |U_i|^s \leq \delta^s$, so $\{U_i\}$ is necessarily a δ -cover. Thus, $\mathcal{H}_\delta^s(F) \leq \delta^s \rightarrow 0$ giving $\mathcal{H}^s(F) = 0$ and $s \geq \dim_H F$.

3.3 Calculation of Hausdorff dimension—simple examples

Here, we show how to find the Hausdorff dimension of some simple fractals including some of those mentioned in Introduction. Other methods will be encountered throughout the book. Most dimension calculations involve an upper estimate and a lower estimate, which hopefully will give the same values. Each of these estimates usually involves a geometric observation followed by a calculation.

Example 3.6

Let F be the Cantor dust constructed from the unit square as in Figure 0.4. (At each stage of the construction, the squares are divided into 16 squares with a quarter of the side length, from which the same pattern of four squares is retained.) Then

$$1 \leq \mathcal{H}^1(F) \leq \sqrt{2}, \text{ so } \dim_H F = 1.$$

Calculation

Observe that E_k , the k th stage of the construction, consists of 4^k squares of side 4^{-k} and thus of diameter $4^{-k}\sqrt{2}$. Taking the squares of E_k as a δ -cover of F where $\delta = 4^{-k}\sqrt{2}$, we get an estimate $\mathcal{H}_\delta^1(F) \leq 4^k 4^{-k}\sqrt{2} = \sqrt{2}$ for the infimum in (3.1). This is true for arbitrarily small δ so $\mathcal{H}^1(F) \leq \sqrt{2}$.

For the lower estimate, let proj denote orthogonal projection onto the x -axis. As noted before, $|\text{proj } x - \text{proj } y| \leq |x - y|$ if $x, y \in \mathbb{R}^2$, so proj is a Lipschitz mapping. By virtue of the construction of F , the projection or ‘shadow’ of F on the x -axis, $\text{proj } F$, is the unit interval $[0, 1]$. Using Proposition 3.1,

$$1 = \text{length } [0, 1] = \mathcal{H}^1([0, 1]) = \mathcal{H}^1(\text{proj } F) \leq \mathcal{H}^1(F).$$

Note that the same argument and result hold for a set obtained by repeated division of squares into m^2 squares of side length $1/m$ of which one square in each column is retained.

This trick of using orthogonal projection to get a lower estimate of Hausdorff measure only works in special circumstances and is not the basis of a more general method. Usually, we need to work rather harder. The following calculation for the middle third Cantor set is more typical; first we give a heuristic argument and then a rigorous one.

Example 3.7

Let F be the middle third Cantor set (see Figure 0.1). Then $\dim_H F = \log 2 / \log 3 = 0.6309\dots$ with $\frac{1}{2} \leq \mathcal{H}^s(F) \leq 1$ where $s = \log 2 / \log 3$.

Heuristic calculation

The Cantor set F splits into a left part $F_L = F \cap [0, \frac{1}{3}]$ and a right part $F_R = F \cap [\frac{2}{3}, 1]$. Clearly, both parts are geometrically similar to F but scaled by a ratio $\frac{1}{3}$, and $F = F_L \cup F_R$ with this union disjoint. Thus, for any s ,

$$\mathcal{H}^s(F) = \mathcal{H}^s(F_L) + \mathcal{H}^s(F_R) = \left(\frac{1}{3}\right)^s \mathcal{H}^s(F) + \left(\frac{1}{3}\right)^s \mathcal{H}^s(F)$$

by the Scaling property 3.2 of Hausdorff measures. *Assuming that at the critical value $s = \dim_H F$ we have $0 < \mathcal{H}^s(F) < \infty$* (a big assumption, but one that can be justified), we may divide by $\mathcal{H}^s(F)$ to get $1 = 2\left(\frac{1}{3}\right)^s$ or $s = \log 2 / \log 3$.

Rigorous calculation

We call the intervals that make up the sets E_k in the construction of F level- k intervals. Thus, E_k consists of 2^k level- k intervals each of length 3^{-k} . Taking the intervals of E_k as a 3^{-k} -cover of F gives that $\mathcal{H}_{3^{-k}}^s(F) \leq 2^k 3^{-ks} = 1$ if $s = \log 2 / \log 3$. Letting $k \rightarrow \infty$ gives $\mathcal{H}^s(F) \leq 1$.

To prove that $\mathcal{H}^s(F) \geq \frac{1}{2}$, we show that

$$\sum |U_i|^s \geq \frac{1}{2} = 3^{-s} \quad 3.14$$

for any cover $\{U_i\}$ of F . Clearly, it is enough to assume that the $\{U_i\}$ are intervals, and by expanding them slightly and using the compactness of F , we need only to verify (3.14) if $\{U_i\}$ is a finite collection of closed subintervals of $[0, 1]$. For each U_i , let k be the integer such that

$$3^{-(k+1)} \leq |U_i| < 3^{-k}. \quad 3.15$$

Then U_i can intersect at most one level- k interval since the separation of these level- k intervals is at least 3^{-k} . If $j \geq k$, then, by construction, U_i intersects at most $2^{j-k} = 2^j 3^{-sk} \leq 2^j 3^s |U_i|^s$ level- j intervals of E_j , using (3.15). If we choose j large enough so that $3^{-(j+1)} \leq |U_i|$ for all U_i , then since the $\{U_i\}$ intersect all 2^j basic intervals of length 3^{-j} , counting intervals gives $2^j \leq \sum_i 2^j 3^s |U_i|^s$, which reduces to (3.14).

With extra effort, the above calculation can be adapted to show that $\mathcal{H}^s(F) = 1$.

It is already becoming apparent that calculation of Hausdorff measures and dimensions can be a little involved, even for fairly basic fractals. For the upper estimate, there are often natural coverings that can be used. Usually, it is the lower estimate that is more awkward since, according to the definition of Hausdorff measure, we have to consider all possible δ -covers to obtain the infimum value. As we shall see, there are techniques that can simplify this process.

The ‘heuristic’ method of calculation used in Example 3.7 gives the right answer for the dimension of many self-similar sets. For example, the von Koch curve is made up of four copies of itself scaled by a factor $\frac{1}{3}$ and by a similar argument has dimension $\log 4 / \log 3$. More generally, if $F = \bigcup_{i=1}^m F_i$, where each F_i is geometrically similar to F but scaled by a factor r_i , then provided that the F_i do not overlap ‘too much’, the heuristic argument gives $\dim_H F$ as the number s satisfying $\sum_{i=1}^m r_i^s = 1$. The validity of this formula is discussed in detail in Chapter 9.

3.4 Equivalent definitions of Hausdorff dimension

Whilst the definition of Hausdorff measures involved coverings by arbitrary sets of diameter at most δ , it is sometimes useful to use restricted classes of covering set that define measures leading to the same values of Hausdorff dimension. For example, we could use coverings by spherical balls: letting

$$B_\delta^s(F) = \inf \left\{ \sum_i |B_i|^s : \{B_i\} \text{ is a } \delta\text{-cover of } F \text{ by balls} \right\}, \quad 3.16$$

we obtain a measure $B^s(F) = \lim_{\delta \rightarrow 0} B_\delta^s(F)$ and a ‘dimension’ at which $B^s(F)$ jumps from ∞ to 0. Clearly, $H_\delta^s(F) \leq B_\delta^s(F)$ since any δ -cover of F by balls is a permissible covering in the definition of H_δ^s . On the other hand, if $\{U_i\}$ is a δ -cover of F , then $\{B_i\}$ is a 2δ -cover, where,

for each i , B_i is chosen to be some ball containing U_i and of radius $|U_i| \leq \delta$. Thus $\Sigma |B_i|^s \leq \Sigma (2|U_i|)^s = 2^s \Sigma |U_i|^s$, and taking infima gives $\mathcal{B}_{2\delta}^s(F) \leq 2^s \mathcal{H}_\delta^s(F)$. Letting $\delta \rightarrow 0$, it follows that $\mathcal{H}^s(F) \leq \mathcal{B}^s(F) \leq 2^s \mathcal{H}^s(F)$. In particular, this implies that the values of s at which \mathcal{H}^s and \mathcal{B}^s jump from ∞ to 0 are the same, so that the dimensions defined by the two measures are equal.

It is easy to check that we get the same values for Hausdorff measure and dimension if in (3.1) we use δ -covers of just open sets or just closed sets. Moreover, if F is compact, then by expanding the covering sets slightly to open sets, and taking a finite subcover, we get the same value of $\mathcal{H}^s(F)$ if we merely consider δ -covers by finite collections of sets.

Net measures are another useful variant. For the sake of simplicity, let F be a subset of the interval $[0, 1]$. A *binary interval* is an interval that is of the form $[r2^{-k}, (r+1)2^{-k}]$ where $k = 0, 1, 2, \dots$ and $r = 0, 1, \dots, 2^k - 1$. We define

$$\mathcal{M}_\delta^s(F) = \inf \{ \Sigma |U_i|^s : \{U_i\} \text{ is a } \delta\text{-cover of } F \text{ by binary intervals} \} \quad 3.17$$

leading to the *net measures*

$$\mathcal{M}^s(F) = \lim_{\delta \rightarrow 0} \mathcal{M}_\delta^s(F). \quad 3.18$$

Since any interval $U \subset [0, 1]$ is contained in two consecutive binary intervals each of length at most $2|U|$, we see, in just the same way as for the measure \mathcal{B}^s , that

$$\mathcal{H}^s(F) \leq \mathcal{M}^s(F) \leq 2^{s+1} \mathcal{H}^s(F). \quad 3.19$$

It follows that the value of s at which $\mathcal{M}^s(F)$ jumps from ∞ to 0 equals the Hausdorff dimension of F , that is, both the definitions of measure give the same dimension.

For certain purposes, net measures are much more convenient than Hausdorff measures. This is because two binary intervals are either disjoint or one of them is contained in the other, allowing any cover

of a set by binary intervals to be reduced to a cover by *disjoint* binary intervals. We will use net measures in Section 1.2.

*3.5 Packing measure and dimensions

Hausdorff dimension is defined in terms of measures, and this can be a great advantage in developing mathematical theory. This is not the case for box dimensions, but nevertheless, there is a natural measure construction, namely, packing measure, that is in a sense ‘dual’ to Hausdorff measure, which leads to modified upper box-counting dimension. Recall that Hausdorff dimension may be defined using economical coverings by small balls (3.16). Coverings and packings play a dual role in many areas of mathematics, and it is natural to try to look for a dimension that is defined in terms of ‘packings’ by large collections of disjoint balls of small radii with centres in the set under consideration.

We try to follow the pattern of definition of Hausdorff measure and dimension. For $s \geq 0$ and $\delta > 0$, let

$$\mathcal{P}_\delta^s(F) = \sup \left\{ \sum_{i=1}^{\infty} |B_i|^s : \{B_i\} \text{ is a collection of disjoint balls of radii at most } \delta \text{ with centres in } F \right\}. \quad \text{3.20}$$

Since $\mathcal{P}_\delta^s(F)$ decreases with δ , the limit

$$\mathcal{P}_0^s(F) = \lim_{\delta \rightarrow 0} \mathcal{P}_\delta^s(F) \quad \text{3.21}$$

exists, possibly 0 or ∞ . At this point, we meet problems similar to those encountered with box-counting dimensions: by considering countable dense sets, it is easy to see that $\mathcal{P}_0^s(F)$ is not a measure. Hence, we modify the definition by decomposing F into a countable collection of sets and define

$$\mathcal{P}^s(F) = \inf \left\{ \sum_{i=1}^{\infty} \mathcal{P}_0^s(F_i) : F \subset \bigcup_{i=1}^{\infty} F_i \right\}. \quad \text{3.22}$$

It may be shown that $\mathcal{P}^s(F)$ is a measure on \mathbb{R}^n , known as *s-dimensional packing measure*.

We define the *packing dimension* in the natural way as the ‘jump value’ of s :

$$\dim_p F = \sup\{s \geq 0 : \mathcal{P}^s(F) = \infty\} = \inf\{s : \mathcal{P}^s(F) = 0\}. \quad \text{3.23}$$

The underlying measure structure immediately implies monotonicity: that $\dim_p E \leq \dim_p F$ if $E \subset F$. Moreover, for a countable collection of sets $\{F_i\}$,

$$\dim_p \left(\bigcup_{i=1}^{\infty} F_i \right) = \sup_i \dim_p F_i, \quad \text{3.24}$$

since if $s > \dim_p F_i$ for all i , then $\mathcal{P}^s(\bigcup_i F_i) \leq \sum_i \mathcal{P}^s(F_i) = 0$ implying $\dim_p(\bigcup_i F_i) \leq s$, with the opposite inequality following from monotonicity.

We now investigate the relationship of packing dimension with other definitions of dimension and verify the surprising fact that packing dimension is just the same as the modified upper box dimension.

Lemma 3.8

For F a non-empty bounded subset of \mathbb{R}^n ,

$$\dim_p F \leq \overline{\dim}_B F. \quad \text{3.25}$$

Proof

If $\dim_P F = 0$, the result is obvious. Otherwise choose any t and s with $0 < t < s < \dim_P F$. Then $\mathcal{P}^s(F) = \infty$, so $\mathcal{P}_0^s(F) = \infty$. Thus, given $0 < \delta \leq 1$, there are disjoint balls $\{B_i\}$, of radii at most δ with centres in F , such that $1 < \sum_{i=1}^{\infty} |B_i|^s$. Suppose that for each k , exactly n_k of these balls satisfy $2^{-k-1} < |B_i| \leq 2^{-k}$; then

$$1 < \sum_{k=0}^{\infty} n_k 2^{-ks}. \quad 3.26$$

There must be some k with $n_k > 2^{kt}(1 - 2^{t-s})$, otherwise the sum in (3.26) would be at most $\sum_{k=0}^{\infty} 2^{kt-ks}(1 - 2^{t-s}) = 1$, by summing the geometric series. These n_k balls all contain balls of radii $2^{-k-2} \leq \delta$ centred in F . Hence, if $N_{\delta}(F)$ denotes the greatest number of disjoint balls of radius δ with centres in F , then

$$N_{2^{-k-2}}(F)(2^{-k-2})^t \geq n_k (2^{-k-2})^t > 2^{-2t}(1 - 2^{t-s}),$$

where $2^{-k-2} \leq \delta$. Since we can obtain this for δ arbitrarily small, $\lim_{\delta \rightarrow 0} N_{\delta}(F)\delta^t > 0$, so that $\overline{\dim}_B F \geq t$ using Equivalent definition 2.1(v). This is true for any $0 < t < \dim_P F$ so (3.25) follows.

Proposition 3.9

If $F \subset \mathbb{R}^n$ then $\dim_P F = \overline{\dim}_{MB} F$.

Proof

If $F \subset \bigcup_{i=1}^{\infty} F_i$ where the F_i are non-empty and bounded, then by (3.24) and (3.25),

$$\dim_p F \leq \sup_i \dim_p F_i \leq \sup_i \overline{\dim}_B F_i.$$

Definition (2.18) now gives that $\dim_p F \leq \overline{\dim}_{MB} F$.

Conversely, if $s > \dim_p F$, then $\mathcal{P}^s(F) = 0$, so that $F \subset \bigcup_i F_i$ for a collection of sets F_i with $\mathcal{P}_0^s(F_i) < \infty$ for each i , by (3.22). Hence, for each i , if δ is small enough, then $\mathcal{P}_\delta^s(F_i) < \infty$, so by (3.20), $N_\delta(F_i)\delta^s$ is bounded as $\delta \rightarrow 0$, where $N_\delta(F_i)$ is the largest number of disjoint balls of radius δ with centres in F_i . By Equivalent definition 2.1(v), $\overline{\dim}_B F_i \leq s$ for each i , giving that $\overline{\dim}_{MB} F \leq s$ by (2.18), as required.

We have established the following relations:

$$\dim_H F \leq \underline{\dim}_{MB} F \leq \overline{\dim}_{MB} F = \dim_p F \leq \overline{\dim}_B F \quad \text{3.27}$$

(where the left-hand inequality follows from (3.13) and the countable stability of Hausdorff dimension). Suitable examples show that all of these inequalities may be strict.

As with Hausdorff dimension, packing dimension permits the use of powerful measure theoretic techniques in its study. The introduction of packing measures (remarkably some 60 years after Hausdorff measures) has led to a much greater understanding of the geometric measure theory of fractals, with packing measures behaving in a way that is dual to Hausdorff measures in many respects. Indeed, corresponding results for Hausdorff and packing measures are often presented side by side. Nevertheless, one cannot pretend that packing measures and dimensions are easy to work

with or to calculate; the extra step (3.22) in their definition makes them more awkward to use than the Hausdorff analogues.

This situation is improved slightly by the equality of packing dimension and the modified upper box dimension. The following corollary expresses the category results for modified box dimensions in terms of packing dimension. In particular the packing and upper box dimensions are equal for ‘dimensionally homogeneous’ compact sets—a situation that occurs frequently in practice, in particular in sets with some kind of self-similarity or self-affinity.

Corollary 3.10

a. Let $F \subset \mathbb{R}^n$ be compact and such that

$$\overline{\dim}_B(F \cap V) = \overline{\dim}_B F \quad 3.28$$

for all open sets V that intersect F . Then $\dim_P F = \overline{\dim}_B F$.

b. Let $F \subset \mathbb{R}^n$ be of second category. Then $\dim_P F = n$. In particular, this is the case if F is, or contains, a dense G_δ set.

Proof

This is immediate by applying Proposition 3.9 to Propositions 2.8 and 2.9.

The nicest case, of course, is of fractals with equal Hausdorff and upper box dimensions, in which case equality holds throughout (3.27)—we shall see many such examples later on. However, even the much weaker condition $\dim_H F = \dim_P F$, although sometimes hard to prove, eases analysis of F .

*3.6 Finer definitions of dimension

It is sometimes desirable to have a sharper indication of dimension than just a number. To achieve this, let $h : \mathbb{R}^+ \rightarrow \mathbb{R}^+$ be a function that is increasing and continuous, which we call a *dimension function* or *gauge function*. Analogously to (3.1), we define

$$\mathcal{H}_\delta^h(F) = \inf \left\{ \sum_i h(|U_i|) : \{U_i\} \text{ is a } \delta\text{-cover of } F \right\} \quad 3.29$$

for each subset F of \mathbb{R}^n . This leads to a measure, taking

$\mathcal{H}^h(F) = \lim_{\delta \rightarrow 0} \mathcal{H}_\delta^h(F)$. Setting $h(t) = t^s$ just gives the usual definition of s -dimensional Hausdorff measure. If h and g are dimension functions such that $h(t)/g(t) \rightarrow 0$ as $t \rightarrow 0$, then by an argument similar to (3.9), we get that $\mathcal{H}^h(F) = 0$ whenever $\mathcal{H}^g(F) < \infty$. Thus, partitioning the dimension functions into those for which \mathcal{H}^h is finite and those for which it is infinite gives a more precise indication of the ‘dimension’ of F than just the number $\dim_H F$.

An important example of this is Brownian motion in \mathbb{R}^3 (see Chapter 16 for further details). It may be shown that with probability 1, a Brownian path has Hausdorff dimension 2 but with \mathcal{H}^2 -measure equal to 0. More refined calculations show that such a path has positive and finite \mathcal{H}^h -measure, where $h(t) = t^2 \log \log(1/t)$. Although Brownian paths have dimension 2, the dimension is, in a sense, logarithmically smaller than 2.

In the same way, packing measure and dimension can be defined using a more delicate dimension function. This requires replacing $\sum_i |B_i|^s$ by $\sum_i h(|B_i|)$ in (3.20) to define $\mathcal{P}_\delta^h(F)$, leading to $\mathcal{P}_0^h(F)$ and $\mathcal{P}^h(F)$ as before.

*3.7 Dimension prints

Dimension prints provide an interesting variation on Hausdorff dimension of a rather different nature. Dimension prints may be thought of as a sort of ‘fingerprint’ that enables sets with differing

characteristics to be distinguished, even though they may have the same Hausdorff dimension. In particular they reflect non-isotropic features of a set.

We restrict attention to subsets of the plane, in which case the dimension print will also be planar. The definition of dimension prints is very similar to that of Hausdorff dimension but coverings by rectangles are used with side lengths replacing diameters. Let U be a rectangle (the sides need not be parallel to the coordinate axes) and let $a(U) \geq b(U)$ be the lengths of the sides of U . Let s, t be non-negative numbers. For F a subset of \mathbb{R}^2 , let

$$\mathcal{H}_\delta^{s,t}(F) = \inf \left\{ \sum_i a(U_i)^s b(U_i)^t : \{U_i\} \text{ is a } \delta\text{-cover of } F \text{ by rectangles} \right\}.$$

In the usual way, we get measures of ‘Hausdorff type’, $\mathcal{H}^{s,t}$, by letting $\delta \rightarrow 0$:

$$\mathcal{H}^{s,t}(F) = \lim_{\delta \rightarrow 0} \mathcal{H}_\delta^{s,t}(F).$$

(Note that $\mathcal{H}^{s,0}$ is just an equivalent variant of s -dimensional Hausdorff measure where only rectangles are allowed in the δ -covers.) The *dimension print*, print F , of F is defined to be the set of non-negative pairs (s, t) for which $\mathcal{H}^{s,t}(F) > 0$.

Using standard properties of measures, it is easy to see that we have monotonicity

$$\text{print } F_1 \subset \text{print } F_2 \text{ if } F_1 \subset F_2 \quad \text{3.3Q}$$

and countable stability

$$\text{print} \left(\bigcup_{i=1}^{\infty} F_i \right) = \bigcup_{i=1}^{\infty} \text{print } F_i. \quad \text{3.31}$$

Moreover, if (s, t) is a point in $\text{print } F$ and (s', t') satisfies

$$s' + t' \leq s + t$$

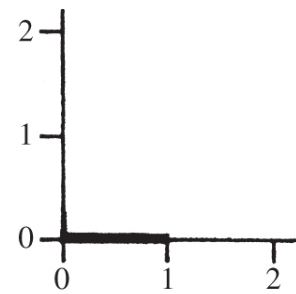
$$t' \leq t,$$

3.32

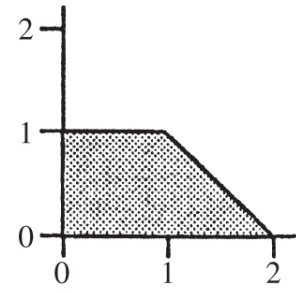
then (s', t') is also in print F .

Unfortunately, dimension prints are not particularly easy to calculate. We display a few known examples in [Figure 3.4](#). Notice that the Hausdorff dimension of a set is given by the point where the edge of its print intersects the x -axis.

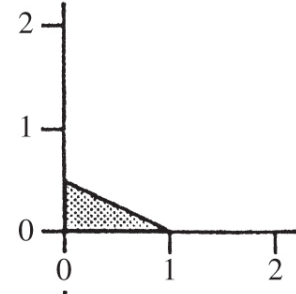
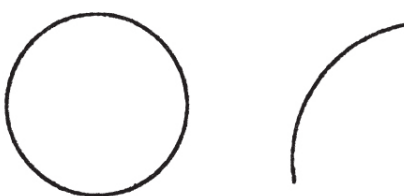
Straight line segment



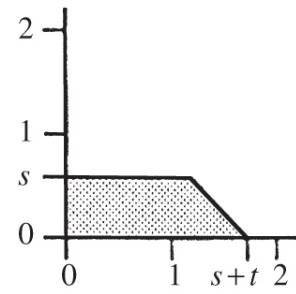
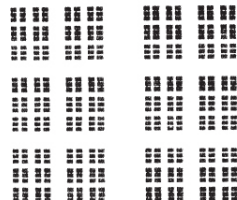
Solid square



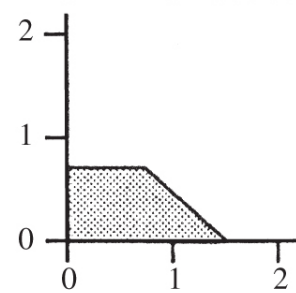
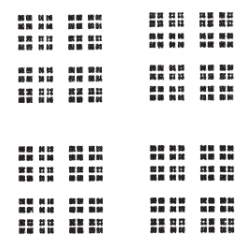
Perimeter of circle or circular arc



Product of uniform Cantor sets of Hausdorff dimensions s and t , $s \leq t$ (see Corollary 7.4)



'Dust-like' set of Hausdorff dimension $1\frac{1}{2}$, formed by the product of two uniform Cantor sets of dimensions $\frac{3}{4}$



'Stratified' set of Hausdorff dimension $1\frac{1}{2}$, formed by the product of a uniform Cantor set of dimension $\frac{1}{2}$ and a line segment

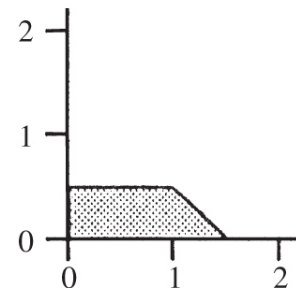
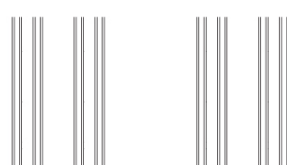


Figure 3.4 A selection of dimension prints of plane sets.

Dimension prints are a useful and appealing extension of the idea of Hausdorff dimension. Notice how the prints in the last two cases distinguish between two sets of Hausdorff (or box) dimension $1\frac{1}{2}$, one of which is dust-like and the other stratified.

One disadvantage of dimension prints defined in this way is that they are *not* Lipschitz invariants. The straight line segment and smooth convex curve are bi-Lipschitz equivalent, but their prints are different. In the latter case, the dimension print takes into account the curvature. It would be possible to avoid this difficulty by redefining print F as the set of (s, t) such that $\mathcal{H}^{s,t}(F') > 0$ for all bi-Lipschitz images F' of F . This would restore Lipschitz invariance of the prints, but would add further complications to their calculation.

Of course, it would be possible to define dimension prints by analogy with box dimensions rather than Hausdorff dimensions, using covers by equal rectangles. Calculations still seem awkward.

*3.8 Porosity

Whilst dimension in its various forms is a useful and fundamental quantity to associate with fractals, a single number cannot hope to capture all the features of such a wide class of objects. For example, fractals of the same dimension can have a variety of topological structures: a fractal of dimension $\log 4 / \log 3$ might be a curve, it might be totally disconnected or dust-like, it might be striated, that is, consist of parallel curves with a fractal spacing, or it might be multiply connected with many holes. For example, the Sierpiński triangle contains holes at arbitrarily fine scales; such sets are often referred to as having high ‘porosity’ (from the Greek *poros* meaning passage) or ‘lacunarity’ (from the Latin *lacuna* meaning hole). Of the ways that have been proposed for quantifying the size and abundance of holes in a fractal, porosity is most commonly encountered. Let $F \subset \mathbb{R}^n$. For all $x \in \mathbb{R}^n$ and $r > 0$, let

$$\text{por}(F, x, r) = \sup \{ \alpha \geq 0 : B(y, \alpha r) \subset B(x, r) \setminus F \text{ for some } y \in \mathbb{R}^n \},$$

3.33

see [Figure 3.5](#) The *porosity* of F at x is defined by

$$\text{por}(F, x) = \lim_{r \rightarrow 0} \text{por}(F, x, r); \quad \text{3.34}$$

Thus, $\text{por}(F, x)$ indicates the relative size of holes of F within small balls centred on x . The *porosity* of the set F itself is then given by

$$\text{por}(F) = \inf_{x \in F} \text{por}(F, x). \quad \text{3.35}$$

We also refer to a set F as α -uniformly porous if there is a number $r_0 > 0$ such that

$$\text{por}(F, x, r) \geq \alpha \text{ for all } x \in F \text{ and } 0 < r \leq r_0. \quad \text{3.36}$$

From (3.33), if $x \in F$, then $0 \leq \text{por}(F, x, r) \leq \frac{1}{2}$, so $0 \leq \text{por}(F, x) \leq \frac{1}{2}$ and $0 \leq \text{por}(F) \leq \frac{1}{2}$. If $\text{por}(F)$ is close to 0, then parts of F have few large pores or gaps, whereas if $\text{por}(F)$ is near $\frac{1}{2}$, then there is plenty of space near each point of F . The porosity of a set depends on the ambient space, for example, a line segment in \mathbb{R} has porosity 0, whereas a line segment F in the plane is uniformly porous with porosity $\frac{1}{2}$ since every disc of radius r with centre in F contains a disc of radius $\frac{1}{2}r$ with interior disjoint from F .

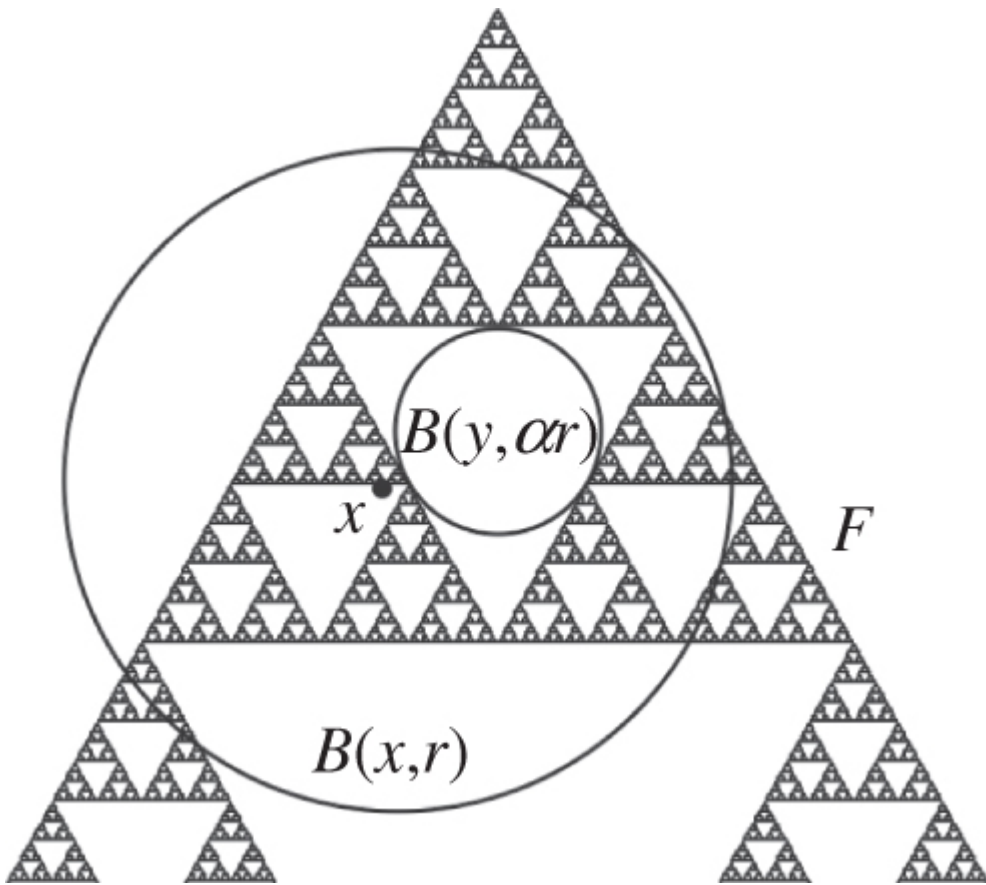


Figure 3.5 Finding the porosity of the Sierpiński triangle: $B(y, \alpha r)$ is the largest disc in $B(x, r) \setminus F$.

The porosity of certain regular fractals, such as Cantor-like sets which have an abundance of gaps, may be found explicitly.

Example 3.11

Let $F \subset \mathbb{R}$ be the middle third Cantor set (see Figure 0.1). Then F is uniformly porous with $\text{por}(F) = \frac{1}{4}$.

Calculation

Let $x \in F$, let $0 < r < 1$ and let

$$2 \cdot 3^{-k} < r \leq 2 \cdot 3^{-k+1}$$

3.37

for some positive integer k . Considering the position of x relative to the intervals of E_k , which are all of length 3^{-k} (see [Figure 0.1](#)), the interval $B(x, r)$ overlaps one of the intervals in the complement of E_{k-1} by at least

$$\min\{r - 3^{-k}, 3^{-(k-1)}\} \geq \frac{1}{2}r,$$

using the two inequalities of (3.37). Thus, for some y ,
 $B(x, r/4) \subset B(x, r) \setminus E_{k-1} \subset B(x, r) \setminus F$ so that $\text{por}(F, x, r) \geq \frac{1}{4}$.

If x is an inner end point of one of the pairs of the intervals in E_k , then $B(x, 2 \cdot 3^{-k}) \setminus F$ contains two intervals of length 3^{-k} and no larger intervals, so $\text{por}(F, x, 2 \cdot 3^{-k}) = \frac{1}{4}$. Thus, if $x \in F$ is chosen so that for a sequence y_k of inner end points of pairs of intervals of E_k , $\lim_{k \rightarrow \infty} |x - y_k| / 3^{-k} = 0$, then $\text{por}(F, x) = \frac{1}{4}$, giving $\text{por}(F) = \frac{1}{4}$.

In a similar way, the ‘middle- λ ’ Cantor set, constructed by removing a proportion λ from the middle of intervals at each stage, is uniformly porous with porosity $\lambda/(\lambda + 1)$, where $0 < \lambda < 1$.

If a set F has high porosity, there must be a lot of space close to each point of F so one might expect that the dimension of F is not too large. The following proposition expresses this quantitatively, with part (a) giving reasonable bounds for the dimension of F when $\text{por}(F)$ is close to 0 and part (b) when it is close to $\frac{1}{2}$.

Proposition 3.12

There are constants $c_1, c_2 > 0$ depending only on n such that for all $F \subset \mathbb{R}^n$, if $\text{por}(F) \geq \alpha$, then

a.

$$\dim_H F \leq \dim_P F \leq n - c_1 \alpha^n$$

b.

$$\dim_H F \leq \dim_P F \leq n - 1 + \frac{c_2}{\log(1/(1 - 2\alpha))}.$$

Partial proof

Here, we will derive a slightly weaker version of part (a) with α^n replaced by $\alpha^n / \log(1/\alpha)$.

First assume that F is uniformly porous with porosity α , satisfying (3.36) for some $r_0 > 0$. Let m be the least positive odd integer such that $m > 2\sqrt{n}/\alpha$. We claim that if a cube of side δ is divided into a mesh of subcubes of side δ/m in the natural way, then at least one of these subcubes does not intersect F . Either the central subcube C contains no point of F or, for some $x \in C \cap F$, the ball centre x and radius $\delta/2$ contains a ball $B(y, \alpha\delta/2)$ that is disjoint from F . Since $\alpha\delta/2 > \delta\sqrt{n}/m$, this ball must contain one of the subcubes, establishing the claim.

Thus, with $N_\delta(F)$ denoting the number of δ -mesh cubes that intersect F ,

$$N_{\delta/m}(F) \leq (m^n - 1)N_\delta(F)$$

provided that $\delta \leq r_0$. Iterating this,

$$N_{m^{-k}r_0}(F) \leq (m^n - 1)^k N_{r_0}(F).$$

It follows from Equivalent definition 2.1(iv) of box-counting dimension, noting the remark before (2.10), that

$$\overline{\dim}_B F = \lim_{\delta \rightarrow 0} \frac{-\log N_\delta(F)}{-\log \delta} \leq \lim_{k \rightarrow \infty} \frac{-\log((m^n - 1)^k N_{r_0}(F))}{-\log(m^{-k}r_0)} \leq \frac{\log(m^n - 1)}{\log m}$$

$$= \frac{n \log m + \log(1 - 1/m^n)}{\log m} \leq n - \frac{1/m^n}{\log m} \leq n - \frac{c_1 \alpha^n}{\log(1/\alpha)}.$$

This will be valid for sufficiently small α for any $c_1 < 2^{-n}n^{-n/2}$.

If F is now any set with $\text{por}(F) \geq \alpha$, we may express $F = \bigcup_{i=1}^{\infty} F_i$ as a countable union of sets where each F_i is uniformly porous

satisfying (3.36) for $r_0 = 1/i$. Using the characterisation of packing dimension in terms of modified box dimension, Proposition 3.9,

$$\dim_H F \leq \dim_P F \leq \sup_i \overline{\dim}_B F_i \leq n - \frac{c_1 \alpha^n}{\log(1/\alpha)}$$

on applying the earlier conclusion to each F_i .

Although, as the previous proposition shows, porosity and dimension are not entirely unrelated, they reflect rather different features of fractals and behave in different ways. For example, dimension of fractals is preserved by bi-Lipschitz mappings, but this is not the case for porosity, although it is preserved by smooth conformal mappings defined on a neighbourhood of the set.

3.9 Notes and references

The idea of defining measures using covers by small sets was introduced by Carathéodory (1914). Hausdorff (1919) used this method to define the measures that now bear his name and showed that the middle third Cantor set has positive and finite measure of dimension $\log 2 / \log 3$ as well as finding the dimensions of other Cantor-like sets. Properties of Hausdorff measures and estimates of Hausdorff dimensions and measures of many classes of sets have been developed ever since, not least by Besicovitch and his students. Technical aspects of Hausdorff measures and dimensions are discussed in rather more detail in Falconer (1985a) and Mattila (1999) and in greater generality in the books of Federer (1996) and Rogers (1998).

Packing measures and dimensions are much more recent, introduced by Tricot (1982). Used alongside Hausdorff measures and dimensions they have provided many new insights. Packing measures and box and packing dimensions are discussed in Edgar (1998) and Mattila (1999).

Many other definitions of ‘fractal dimension’ have been proposed, some are equivalent, others not, some generally applicable, some only pertinent for certain classes of sets. For example, curves and their dimensions are considered by Tricot (2011).

Dimension prints are an innovation of Rogers (1988, 1998).

Surveys of porosity and lacunarity are provided by Mandelbrot (1995); Järvenpää (2010) and Shmerkin (2011). Relationships between porosity and dimension were established by Mattila (1988) and Salli (1991), and Järvenpää, Järvenpää and Mauldin (2002) consider the porosity of self-similar and other sets.

Exercises

3.1 Verify that the value of $\mathcal{H}^s(F)$ is unaltered if, in (3.1), we only consider δ -covers by sets $\{U_i\}$ that are all closed.

3.2 Show that $\mathcal{H}^0(F)$ equals the number of points in the set F .

3.3 Verify from the definition that $\mathcal{H}^s(\emptyset) = 0$, that $\mathcal{H}^s(E) \subset \mathcal{H}^s(F)$ if $E \subset F$ and that $\mathcal{H}^s(\bigcup_{i=1}^{\infty} F_i) \leq \sum_{i=1}^{\infty} \mathcal{H}^s(F_i)$.

3.4 Let F be the closed interval $[0, 1]$. Show that $\mathcal{H}^s(F) = \infty$ if $0 \leq s < 1$, that $\mathcal{H}^s(F) = 0$ if $s > 1$ and that $0 < \mathcal{H}^1(F) < \infty$.

3.5 Let $f : \mathbb{R} \rightarrow \mathbb{R}$ be a differentiable function with continuous derivative. Show that $\dim_H f(F) \leq \dim_H F$ for any set F . (Consider the case of F bounded first and show that f is Lipschitz on F .)

3.6 Let $f : \mathbb{R} \rightarrow \mathbb{R}$ be the function $f(x) = x^2$, and let F be any subset of \mathbb{R} . Show that $\dim_H f(F) = \dim_H F$.

3.7 Let $f : [0, 1] \rightarrow \mathbb{R}$ be a Lipschitz function. Writing $\text{graph } f = \{(x, f(x)) : 0 \leq x \leq 1\}$, show that $\dim_H \text{graph } f = 1$. Note, in particular, that this is true if f is continuously differentiable, see Exercise 1.13.

3.8 What is the Hausdorff dimension of the sets of real numbers $\{0, 1, 2, 3, \dots\}$ and $\{0, 1, \frac{1}{2}, \frac{1}{3}, \frac{1}{4}, \dots\}$?

3.9 Let F be the set consisting of the numbers between 0 and 1 whose decimal expansions do not contain the digit 5. Use a ‘heuristic’ argument to show that $\dim_H F = \log 9 / \log 10$. Can you prove this by a rigorous argument? Generalise this result.

3.10 Let F consist of the points $(x, y) \in \mathbb{R}^2$ such that the decimal expansions of neither x nor y contain the digit 5. Use a ‘heuristic’ argument to show that $\dim_H F = 2 \log 9 / \log 10$.

3.11 Use a ‘heuristic’ argument to show that the Hausdorff dimension of the set depicted in Figure 0.5 is given by the solution of the equation $4\left(\frac{1}{4}\right)^s + \left(\frac{1}{2}\right)^s = 1$. By solving a quadratic equation in $\left(\frac{1}{2}\right)^s$, find an explicit expression for s .

3.12 Let F be the set of real numbers that have a base-3 expansion $b_m b_{m-1} \cdots b_1 \cdot a_1 a_2 \cdots$ with none of the digits b_i or a_i equal to 1. (Thus, F is constructed by a Cantor-like process extending outwards as well as inwards.) What is the Hausdorff dimension of F ?

3.13 What is the Hausdorff dimension of the set of numbers x with base-3 expansion $0 \cdot a_1 a_2 \cdots$ for which there is a positive integer k (which may depend on x) such that $a_i \neq 1$ for all $i \geq k$?

3.14 Let F be the middle- λ Cantor set (obtained by removing a proportion $0 < \lambda < 1$ from the middle of intervals). Use a ‘heuristic argument’ to show that $\dim_H F = \log 2 / \log(2/(1-\lambda))$. Now let $E = F \times F \subset \mathbb{R}^2$. Show in the same way that $\dim_H E = 2 \log 2 / \log(2/(1-\lambda))$.

3.15 Show that there is a totally disconnected subset of the plane of Hausdorff dimension s for every $0 \leq s \leq 2$. (Modify the construction of the Cantor dust in [Figure 0.4](#).)

3.16 Let S be the unit circle in the plane, with points on S parametrised by the angle θ subtended at the centre with a fixed axis, so that θ_1 and θ_2 represent the same point if and only if θ_1 and θ_2 differ by a multiple of 2π , in the usual way. Let $F = \{\theta \in S : 0 \leq 3^k \theta \leq \pi \pmod{2\pi} \text{ for all } k = 1, 2, \dots\}$. Show that $\dim_H F = \log 2 / \log 3$.

3.17 Find two disjoint Borel subsets E and F of \mathbb{R} such that $\mathcal{P}_0^s(E \cup F) \neq \mathcal{P}_0^s(E) + \mathcal{P}_0^s(F)$.

3.18 Show that if h and g are dimension functions such that $h(t)/g(t) \rightarrow 0$ as $t \rightarrow 0$, then $\mathcal{H}^h(F) = 0$ whenever $\mathcal{H}^g(F) < \infty$.

3.19 Verify properties (3.30)-(3.32) of dimension prints. Given an example of a set with a non-convex dimension print.

3.20 Show that the Sierpiński triangle (Figure 0.3) is $\frac{1}{9}$ -uniformly porous.

Chapter 4

Techniques for calculating dimensions

A direct attempt at calculating the dimensions, in particular the Hausdorff dimension, of almost any set will convince the reader of the practical limitations of working from the definitions. Rigorous dimension calculations can involve pages of complicated manipulations and estimates that provide little intuitive enlightenment.

In this chapter, we bring together some of the basic techniques that are available for dimension calculations. Other methods that are applicable in more specific cases may be found throughout the book.

4.1 Basic methods

As a general rule, we get upper bounds for the Hausdorff measures and dimensions by finding effective coverings by small sets and lower bounds by putting measures or mass distributions on the set. For most fractals, ‘obvious’ upper estimates of dimension may be obtained using coverings by sets that occur naturally in the construction of the fractals.

Proposition 4.1

Suppose F can be covered by n_k sets of diameter at most δ_k with $\delta_k \rightarrow 0$ as $k \rightarrow \infty$. Then

$$\dim_H F \leq \underline{\dim}_B F \leq \lim_{k \rightarrow \infty} \frac{\log n_k}{-\log \delta_k}.$$

Moreover, if $n_k \delta_k^s$ remains bounded as $k \rightarrow \infty$, then $\mathcal{H}^s(F) < \infty$. If $\delta_k \rightarrow 0$ but $\delta_{k+1} \geq c\delta_k$ for some $0 < c < 1$, then

$$\overline{\dim}_B F \leq \lim_{k \rightarrow \infty} \frac{\log n_k}{-\log \delta_k}.$$

Proof

The inequalities for the box-counting dimension are immediate from the definitions and the remark at (2.10). That $\dim_H F \leq \underline{\dim}_B F$ is in (3.13), and if $n_k \delta_k^s$ is bounded, then $\mathcal{H}_{\delta_k}^s(F) \leq n_k \delta_k^s$, so $\mathcal{H}_{\delta_k}^s(F)$ tends to a finite limit $\mathcal{H}^s(F)$ as $k \rightarrow \infty$.

Thus, as we have seen already (Example 3.7), in the case of the middle third Cantor set, the natural coverings by 2^k intervals of length 3^{-k} give $\dim_H F \leq \underline{\dim}_B F \leq \overline{\dim}_B F \leq \log 2 / \log 3$.

Surprisingly often, the ‘obvious’ upper bound for the Hausdorff dimension of a set turns out to be the actual value. However, demonstrating this can be difficult. To obtain an upper bound, it is enough to evaluate sums of the form $\sum |U_i|^s$ for specific coverings $\{U_i\}$ of F , whereas for a lower bound we must show that $\sum |U_i|^s$ is greater than some positive constant for all δ -coverings of F . Clearly, an enormous number of such coverings are available. In particular, when working with Hausdorff dimension as opposed to box dimension, consideration must be given to covers where some of the U_i are very small and others have relatively large diameters—

this prohibits sweeping estimates for $\sum |U_i|^s$ such as those available for upper bounds. Even if there is a natural construction of the fractal, such as for the middle third Cantor set and its variants, to get good lower bounds not only is the size of the components important but also their spacing must be taken into account, as was done in the rigorous calculation of Example 3.7.

One way of getting around these difficulties in finding lower bounds is to show that no *individual* set U can cover too much of F compared with its size measured as $|U|^s$. Then if $\{U_i\}$ covers the whole of F , the sum $\sum |U_i|^s$ cannot be too small. A standard way to do this is to concentrate a suitable mass distribution μ on F and compare the mass $\mu(U)$ with $|U|^s$ for each set U . (Recall that a mass distribution on F is a measure with support contained in F such that $0 < \mu(F) < \infty$, see Section 1.3.)

Mass distribution principle 4.2

Let μ be a mass distribution on F and suppose that for some $s > 0$, there are numbers $c > 0$ and $\varepsilon > 0$ such that

$$\mu(U) \leq c|U|^s$$

4.1

for all sets U with $|U| \leq \varepsilon$. Then $\mathcal{H}^s(F) \geq \mu(F)/c$ and

$$s \leq \dim_H F \leq \underline{\dim}_B F \leq \overline{\dim}_B F.$$

Proof

If $\{U_i\}$ is any cover of F , so $F \subset \bigcup_i U_i$, then

$$0 < \mu(F) \leq \mu\left(\bigcup_i U_i\right) \leq \sum_i \mu(U_i) \leq c \sum_i |U_i|^s, \quad \text{4.2}$$

using measure properties and (4.1).

Taking infima, $\mathcal{H}_\delta^s(F) \geq \mu(F)/c$ if δ is small enough, so

$\mathcal{H}^s(F) \geq \mu(F)/c$. In particular, since $\mu(F) > 0$, we get $\dim_H F \geq s$.

Notice that the conclusion $\mathcal{H}^s(F) \geq \mu(F)/c$ remains true if μ is a mass distribution on \mathbb{R}^n and $F \subset \mathbb{R}^n$ is any subset.

The Mass distribution principle 4.2 gives a quick lower estimate for the Hausdorff dimension of the middle third Cantor set F (Figure 0.1). Let μ be the natural mass distribution on F , so that each of the 2^k k th level intervals of length 3^{-k} in E_k in the construction of F carry a mass 2^{-k} . (We imagine that we start with unit mass on E_0 and repeatedly divide the mass on each interval of E_k equally between its two subintervals in E_{k+1} ; see Proposition 1.7.) Let U be a set with $|U| < 1$ and let k be the integer such that $3^{-(k+1)} \leq |U| < 3^{-k}$. Then U can intersect at most one of the intervals of E_k , so

$$\mu(U) \leq 2^{-k} = (3^{\log 2 / \log 3})^{-k} = (3^{-k})^{\log 2 / \log 3} \leq (3|U|)^{\log 2 / \log 3}$$

and hence $\mathcal{H}^{\log 2 / \log 3}(F) \geq 3^{-\log 2 / \log 3} = \frac{1}{2}$ by the mass distribution principle, and in particular, $\dim_H F \geq \log 2 / \log 3$, which of course is the actual value of the Hausdorff and box dimensions.

Example 4.3

Let $F_1 = F \times [0, 1] \subset \mathbb{R}^2$ be the product of the middle third Cantor set F and the unit interval. Then, setting $s = 1 + \log 2 / \log 3$, we have $\dim_B F_1 = \dim_H F_1 = s$, with $0 < \mathcal{H}^s(F_1) < \infty$.

Calculation

For each k , there is a covering of F by 2^k intervals of length 3^{-k} . A column of 3^k squares of side 3^{-k} (diameter $3^{-k}\sqrt{2}$) covers the part of F_1 above each such interval, so taking these all together, F_1 may be covered by $2^k 3^k$ squares of side 3^{-k} . Thus,
$$\mathcal{H}_{3^{-k}\sqrt{2}}^s(F_1) \leq 3^k 2^k (3^{-k}\sqrt{2})^s = (3 \cdot 2 \cdot 3^{-1-\log 2 / \log 3})^k 2^{s/2} = 2^{s/2}$$
, so $\mathcal{H}^s(F_1) \leq 2^{s/2}$
and $\dim_H F_1 \leq \underline{\dim}_B F_1 \leq \overline{\dim}_B F_1 \leq s$.

For a lower estimate, we define a mass distribution μ on F_1 by taking the natural mass distribution on F described above (each k th level interval of F of side 3^{-k} having mass 2^{-k}) and ‘spreading it’ uniformly along the intervals above F . Thus, if U is a rectangle, with sides parallel to the coordinate axes, of height $h \leq 1$, above a k th level interval of F , then $\mu(U) = h2^{-k}$. Any set U is contained in a square of side $|U|$ with sides parallel to the coordinate axes. If $3^{-(k+1)} \leq |U| < 3^{-k}$, then U lies above at most one k th level interval of F of side 3^{-k} , so

$$\begin{aligned}\mu(U) &\leq |U|2^{-k} \leq |U|3^{-k \log 2 / \log 3} \leq |U|(3|U|)^{\log 2 / \log 3} \\ &= 3^{\log 2 / \log 3} |U|^s = 2|U|^s.\end{aligned}$$

By the Mass distribution principle 4.2, $\mathcal{H}^s(F_1) > \frac{1}{2}$.

Notice that in this example, the dimension of the product of two sets equals the sum of the dimensions of the sets. We study this in greater depth in Chapter 7.

The procedure used for finding dimensions in the above example, by taking a natural covering to get an upper bound and using the mass distribution principle for the lower bound, is the basis of many dimension calculations. We will apply it to a wide class of self-similar fractals in Theorem 9.3. For now we consider a *general construction* of fractal subsets of \mathbb{R} which may be thought of as generalisation of the middle third Cantor set. Let

$[0, 1] = E_0 \supset E_1 \supset E_2 \supset \dots$ be a decreasing sequence of sets, with each E_k a union of a finite number of disjoint closed intervals called k th *level basic intervals*, with each interval of E_k containing at least two intervals of E_{k+1} , and the maximum length of k th level intervals tending to 0 as $k \rightarrow \infty$. Then the set

$$F = \bigcap_{k=0}^{\infty} E_k \quad \text{4.3}$$

is a totally disconnected subset of $[0, 1]$ which is generally a fractal ([Figure 4.1](#)).

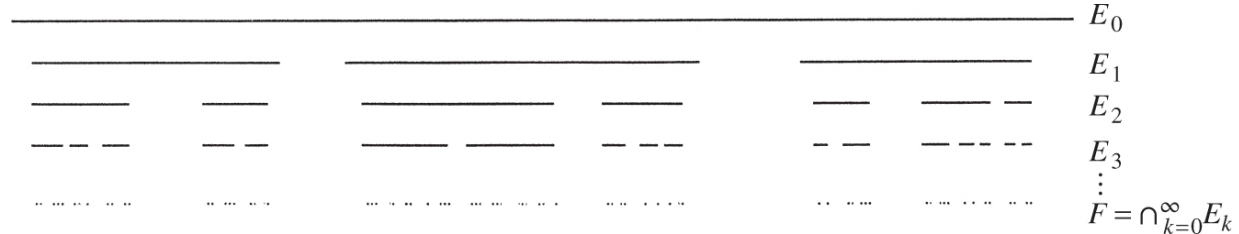


[**Figure 4.1**](#) An example of the general construction of a subset of \mathbb{R} .

Obvious upper bounds for the dimension of F are available by taking the intervals of each E_k as covering intervals but, as usual, it is harder to find lower bounds that equal the upper bounds. Note that in the following examples, the upper estimates for $\dim_H F$ depend on the number and size of the basic intervals, whilst the lower estimates depend on their spacing. For these to be equal, the $(k+1)$ th level intervals must be ‘nearly uniformly distributed’ inside the k th level intervals.

Example 4.4

Let s be a number with $0 < s < 1$. Assume that in the general construction (4.3), for each k th level interval I , the $(k+1)$ th level intervals I_1, \dots, I_m ($m \geq 2$) contained in I are of equal length and equally spaced, the lengths being given by

$$|I_i|^s = \frac{1}{m} |I|^s \quad (1 \leq i \leq m) \quad \text{4.4}$$

with the left-hand ends of I_1 and I coinciding, and the right-hand ends of I_m and I coinciding. Then $\dim_H F = s$ and $0 < \mathcal{H}^s(F) < \infty$. (We allow m to be different for different intervals I in the construction, so that the k th level intervals may have widely differing lengths.)

Calculation

With I, I_i , as above,

$$|I|^s = \sum_{i=1}^m |I_i|^s. \quad 4.5$$

Applying this inductively to the k th level intervals for successive k and recalling that E_0 comprises a single interval of length 1, we have, for each k , that $1 = \sum_{I_i \in E_k} |I_i|^s$, where the sum is over all the k th level intervals I_i . The k th level intervals cover F ; since the maximum length of k th level intervals tends to 0 as $k \rightarrow \infty$, it follows that $\mathcal{H}_\delta^s(F) \leq 1$ for sufficiently small δ , giving $\mathcal{H}^s(F) \leq 1$.

Now distribute a mass μ on F in such a way that $\mu(I) = |I|^s$ whenever I is any level k interval. Thus, starting with unit mass on $[0, 1]$, we divide this equally between each level 1 interval, the mass on each of these intervals being divided equally between each level 2 subinterval and so on; see Proposition 1.7. Equation (4.5) ensures that we get a mass distribution on F with $\mu(I) = |I|^s$ for every basic interval. We estimate $\mu(U)$ for an interval U with end points in F . Let I be the smallest basic interval that contains U ; suppose that I is a k th level interval, and let I_1, \dots, I_m be the $(k+1)$ th level intervals, all of length $m^{-1/s}|I|$, contained in I . Then U intersects a number $j \geq 2$ of the I_i , otherwise U would be contained in a smaller basic interval. The spacing between consecutive I_i is

$$\begin{aligned} (|I| - m|I_i|)/(m-1) &= \frac{|I|(1 - m|I_i|/|I|)}{(m-1)} \\ &= \frac{|I|(1 - m^{1-1/s})}{(m-1)} \\ &\geq c_s |I|/m, \end{aligned}$$

where $c_s = (1 - 2^{1-1/s})$, using that $m \geq 2$ and $0 < s < 1$. Thus

$$|U| \geq (j-1) \frac{c_s |I|}{m} \geq \frac{j c_s}{2m} |I|.$$

By (4.4),

$$\begin{aligned}\mu(U) &\leq j\mu(I_i) = j|I_i|^s = \frac{j}{m}|I|^s \\ &\leq 2^s c_s^{-s} \left(\frac{j}{m}\right)^{1-s} |U|^s \leq 2^s c_s^{-s} |U|^s.\end{aligned}\tag{4.6}$$

This is true for any interval U with end points in F , and so for any set U on applying (4.6) to the smallest interval containing $U \cap F$. By the Mass distribution principle 4.2, $\mathcal{H}^s(F) > 0$.

A more careful estimate of $\mu(U)$ in Example 4.4 leads to $\mathcal{H}^s(F) = 1$.

We call the sets obtained when m is kept constant throughout the construction of Example 4.4 *uniform Cantor sets* (see [Figure 4.2](#)). These provide a natural generalisation of the middle third Cantor set.

Example 4.5 Uniform Cantor sets

Let $m \geq 2$ be an integer and $0 < r < 1/m$. Let F be the set obtained by the construction in which each basic interval I is replaced by m equally spaced subintervals of lengths $r|I|$, the ends of I coinciding with the ends of the extreme subintervals. Then $\dim_H F = \dim_B F = \log m / -\log r$, and $0 < \mathcal{H}^{\log m / -\log r}(F) < \infty$.

Calculation

The set F is obtained on taking m constant and $s = \log m / (-\log r)$ in Example 4.4. Equation (4.4) becomes $(r|I|)^s = (1/m)|I|^s$, which is satisfied identically, so $\dim_H F = s$. For the box dimension, note that F is covered by the m^k k th level intervals of length r^{-k} for each k , leading to $\overline{\dim}_B F \leq \log m / -\log r$ in the usual way.

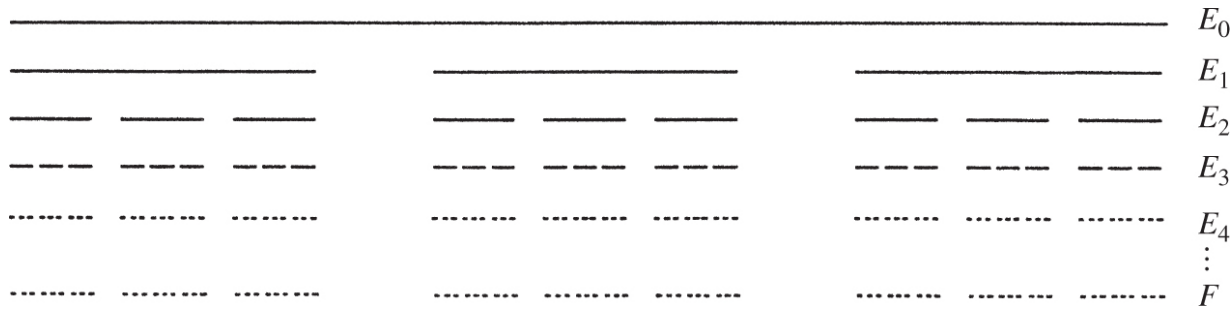


Figure 4.2 A uniform Cantor set (Example 4.5) with $m = 3$ and $r = \frac{4}{15}$, so $\dim_H F = \dim_B F = \log 3 / -\log \frac{4}{15} = 0.831\dots$

The *middle- λ Cantor set* is obtained by repeatedly removing a proportion $0 < \lambda < 1$ from the middle of intervals, starting with the unit interval. This is a special case of a uniform Cantor set, having $m = 2$ and $r = \frac{1}{2}(1 - \lambda)$ and thus Hausdorff and box dimensions $\log 2 / \log(2/(1 - \lambda))$.

The next example is another case of the general construction.

Example 4.6

(a) Suppose in the general construction (4.3) each $(k - 1)$ th level interval contains at least $m_k \geq 2$ k th level intervals ($k = 1, 2, \dots$) which are separated by gaps of at least ε_k , where $0 < \varepsilon_{k+1} < \varepsilon_k$ for each k . Then

$$\dim_H F \geq \varliminf_{k \rightarrow \infty} \frac{\log(m_1 \cdots m_{k-1})}{-\log(m_k \varepsilon_k)}. \quad 4.7$$

(b) Suppose that in addition the k th level intervals are all of length δ_k and that each $(k - 1)$ th level interval contains exactly m_k k th level intervals, which are ‘roughly equally spaced’ in the sense that $m_k \varepsilon_k \geq c \delta_{k-1}$, where $c > 0$ is a constant. Then

$$\dim_H F = \varlimsup_{k \rightarrow \infty} \frac{\log(m_1 \cdots m_{k-1})}{-\log \delta_{k-1}} = \varlimsup_{k \rightarrow \infty} \frac{\log(m_1 \cdots m_{k-1})}{-\log(m_k \varepsilon_k)}.$$

Calculation

(a) We may assume that each $(k-1)$ th level interval contains exactly m_k k th level intervals; if not we may throw out excess intervals to get smaller sets E_k and F for which this is so. Then we may define a mass distribution μ on F by assigning a mass of $(m_1 \cdots m_k)^{-1}$ to each of the $m_1 \cdots m_k$ k th level intervals.

Let U be an interval with $0 < |U| < \varepsilon_1$; we estimate $\mu(U)$. Let k be the integer such that $\varepsilon_k \leq |U| < \varepsilon_{k-1}$. The number of k th level intervals that intersect U is

- i. at most m_k since U intersects at most one $(k-1)$ th level interval
- ii. at most $(|U|/\varepsilon_k) + 1 \leq 2|U|/\varepsilon_k$ since the k th level intervals have gaps of at least ε_k between them.

Each k th level interval supports mass $(m_1 \cdots m_k)^{-1}$ so that

$$\begin{aligned}\mu(U) &\leq (m_1 \cdots m_k)^{-1} \min\{2|U|/\varepsilon_k, m_k\} \\ &\leq (m_1 \cdots m_k)^{-1} (2|U|/\varepsilon_k)^s m_k^{1-s}\end{aligned}$$

for every $0 \leq s \leq 1$. Hence

$$\frac{\mu(U)}{|U|^s} \leq \frac{2^s}{(m_1 \cdots m_{k-1}) m_k^s \varepsilon_k^s}.$$

If

$$s < \lim_{k \rightarrow \infty} \frac{\log(m_1 \cdots m_{k-1})}{-\log(m_k \varepsilon_k)}$$

then $(m_1 \cdots m_{k-1}) m_k^s \varepsilon_k^s > 1$ for all sufficiently large k , so $\mu(U) \leq 2^s |U|^s$ if $|U|$ is small enough, and $\dim_H F \geq s$ by the Mass distribution principle 4.2, giving (4.7).

(b) With the additional conditions, (4.7) becomes

$$\dim_H F \geq \lim_{k \rightarrow \infty} \frac{\log(m_1 \cdots m_{k-1})}{-\log c - \log \delta_{k-1}} = \lim_{k \rightarrow \infty} \frac{\log(m_1 \cdots m_{k-1})}{-\log \delta_{k-1}}.$$

But E_{k-1} comprises $m_1 \cdots m_{k-1}$ intervals of length δ_{k-1} , so this expression equals the upper bound for $\dim_H F$ given by Proposition 4.1. Thus, in the situation where the intervals are well spaced, we get equality in (4.7).

Sets of the following form occur in number theory, see Section 10.3. We find their dimension using Example 4.6.

Example 4.7

Fix $0 < s < 1$ and let n_0, n_1, n_2, \dots be a rapidly increasing sequence of integers, say $n_{k+1} \geq \max\{n_k^k, 4n_k^{1/s}\}$ for each k . For each k , let $H_k \subset \mathbb{R}$ consist of equally spaced equal intervals of lengths $n_k^{-1/s}$ with the midpoints of consecutive intervals distance n_k^{-1} apart. Let $F = \bigcap_{k=1}^{\infty} H_k$, then $\dim_H F = s$.

Calculation

Since $F \subset H_k$ for each k , the set $F \cap [0, 1]$ is contained in at most $n_k + 1$ intervals of length $n_k^{-1/s}$, so Proposition 4.1 gives

$$\dim_H(F \cap [0, 1]) \leq \lim_{k \rightarrow \infty} \frac{\log(n_k + 1)}{-\log n_k^{-1/s}} = s.$$

Similarly, $\dim_H(F \cap [n, n+1]) \leq s$ for all $n \in \mathbb{Z}$, so $\dim_H F \leq s$ as a countable union of such sets.

Now let $E_0 = [0, 1]$ and, for $k \geq 1$, let E_k consist of the intervals of H_k that are completely contained in E_{k-1} . Then each interval I of E_{k-1} contains at least $n_k |I| - 2 \geq n_k n_{k-1}^{-1/s} - 2 \geq 2$ intervals of E_k , which are separated by gaps of at least $n_k^{-1} - n_k^{-1/s} \geq \frac{1}{2} n_k^{-1}$ if k is large enough. Using Example 4.6, and noting that setting $m_k = n_k n_{k-1}^{-1/s}$ rather than $m_k = n_k n_{k-1}^{-1/s} - 2$ does not affect the limit,

$$\begin{aligned} \dim_H(F \cap [0, 1]) &\geq \dim_H \bigcap_{k=1}^{\infty} E_k \geq \lim_{k \rightarrow \infty} \frac{\log(n_0^{-1/s} (n_1 \cdots n_{k-2})^{1-1/s} n_{k-1})}{-\log(n_k n_{k-1}^{-1/s} \frac{1}{2} n_k^{-1})} \\ &= \lim_{k \rightarrow \infty} \frac{\log(n_0^{-1/s} (n_1 \cdots n_{k-2})^{1-1/s}) + \log n_{k-1}}{\log 2 + (\log n_{k-1})/s}. \end{aligned}$$

Provided that n_k is sufficiently rapidly increasing, the terms in $\log n_{k-1}$ in the numerator and denominator of this expression are dominant, so we conclude $\dim_H F \geq \dim_H(F \cap [0, 1]) \geq s$, as required.

It should be remembered that these calculations can be used in conjunction with the basic properties of dimensions discussed in Chapters 2 and 3. For example, since $f(x) = x^2$ is Lipschitz on $[0, 1]$ and bi-Lipschitz on $[\frac{2}{3}, 1]$, then $\dim_H \{x^2 : x \in C\} = \dim_H f(C) = \log 2 / \log 3$, where C is the middle third Cantor set.

Although the Mass distribution principle 4.2 is based on a simple idea, we have seen that it can be very useful in finding Hausdorff dimensions. We end this section with some variants that will be needed later. It is enough for condition (4.1) to hold just for sufficiently small balls centred at each point of F . This is expressed in Proposition 4.9(a). Although mass distribution methods for upper bounds are required far less frequently, we include part (b) because it is, in a sense, dual to (a). Note that density expressions, such as $\lim_{r \rightarrow 0} \mu(B(x, r)) / r^s$, where $B(x, r)$ is the closed ball of centre x and radius r , play a major role in the study of local properties of fractals (see Chapter 5).

We require the following covering lemma in the proof of Proposition 4.9(b).

Covering lemma 4.8

Let C be a family of balls contained in some bounded region of \mathbb{R}^n . Then there is a (finite or countable) disjoint subcollection $\{B_i\}$ such that

$$\bigcup_{B \in C} B \subset \bigcup_i \tilde{B}_i, \quad 4.8$$

where \tilde{B}_i is the closed ball concentric with B_i and of four times the radius.

Proof

For simplicity, we give the proof when \mathcal{C} is a finite family; the basic idea is the same in the general case. We select the $\{B_i\}$ inductively. Let B_1 be a ball in \mathcal{C} of maximum radius. Suppose that B_1, \dots, B_{k-1} have been chosen. We take B_k to be the largest ball in \mathcal{C} (or one of the largest) that does not intersect B_1, \dots, B_{k-1} . The process terminates when no such ball remains. Clearly, the balls selected are disjoint; we must check that (4.8) holds. If $B \in \mathcal{C}$, then either $B = B_i$, for some i , or B intersects one of the B_i with $|B_i| \geq |B|$; if this were not the case, then B would have been chosen instead of the first ball B_k with $|B_k| < |B|$. Either way, $B \subset \tilde{B}_i$, so we have (4.8). (It is easy to see that the result remains true taking \tilde{B}_i as the ball concentric with B_i and of $3 + \varepsilon$ times the radius, for any $\varepsilon > 0$; if \mathcal{C} is finite, we may take $\varepsilon = 0$.)

Proposition 4.9

Let μ be a mass distribution on \mathbb{R}^n , let $F \subset \mathbb{R}^n$ be a Borel set and let $0 < c < \infty$ be a constant.

- If $\overline{\lim}_{r \rightarrow 0} \mu(B(x, r))/r^s < c$ for all $x \in F$, then $\mathcal{H}^s(F) \geq \mu(F)/c$.
- If $\overline{\lim}_{r \rightarrow 0} \mu(B(x, r))/r^s > c$ for all $x \in F$, then $\mathcal{H}^s(F) \leq 2^s \mu(\mathbb{R}^n)/c$.

Proof

a. For each $\delta > 0$, let

$$F_\delta = \{x \in F : \mu(B(x, r)) < cr^s \text{ for all } 0 < r \leq \delta\}.$$

Let $\{U_i\}$ be a δ -cover of F and thus of F_δ . For each U_i containing a point x of F_δ , the ball B with centre x and radius $|U_i|$ certainly contains U_i . By definition of F_δ ,

$$\mu(U_i) \leq \mu(B) < c|U_i|^s$$

so that

$$\mu(F_\delta) \leq \sum_i \{\mu(U_i) : U_i \text{ intersects } F_\delta\} \leq c \sum_i |U_i|^s.$$

Since this is valid for any δ -cover $\{U_i\}$ of F , it follows that $\mu(F_\delta) \leq c\mathcal{H}_\delta^s(F) \leq c\mathcal{H}^s(F)$. But F_δ increases to F as δ decreases to 0, so $\mu(F) \leq c\mathcal{H}^s(F)$ by (1.7).

b. For simplicity, we prove a weaker version of (b) with 2^s replaced by 8^s , but the basic idea is similar. Suppose first that F is bounded. Fix $\delta > 0$ and let C be the collection of balls

$$\{B(x, r) : x \in F, 0 < r \leq \delta \text{ and } \mu(B(x, r)) > cr^s\}.$$

Then by the hypothesis of (b) $F \subset \bigcup_{B \in C} B$. Applying the Covering lemma 4.8 to the collection C , there is a sequence of disjoint balls $B_i \in C$ such that $\bigcup_{B \in C} B \subset \bigcup_i \tilde{B}_i$ where \tilde{B}_i is the ball concentric with B_i but of four times the radius. Thus, $\{\tilde{B}_i\}$ is an 8δ -cover of F , so

$$\begin{aligned} \mathcal{H}_{8\delta}^s(F) &\leq \sum_i |\tilde{B}_i|^s \leq 4^s \sum_i |B_i|^s \\ &\leq 8^s c^{-1} \sum_i \mu(B_i) \leq 8^s c^{-1} \mu(\mathbb{R}^n), \end{aligned}$$

since the B_i are disjoint. Letting $\delta \rightarrow 0$, we get

$\mathcal{H}^s(F) \leq 8^s c^{-1} \mu(\mathbb{R}^n) < \infty$. Finally, if F is unbounded and

$\mathcal{H}^s(F) > 8^s c^{-1} \mu(\mathbb{R}^n)$, the \mathcal{H}^s -measure of some bounded subset of F will also exceed this value, contrary to the above.

Note that it is immediate from Proposition 4.9 that if $\underline{\lim}_{r \rightarrow 0} \log \mu(B(x, r)) / \log r = s$ for all $x \in F$, then $\dim_H F = s$. However, we omit the details; related arguments give the dual result, that if $\overline{\lim}_{r \rightarrow 0} \log \mu(B(x, r)) / \log r = s$ for all $x \in F$, then $\dim_P F = s$. We omit the details, but related arguments give the dual result that if...

4.2 Subsets of finite measure

This section may seem out of place in a chapter about finding dimensions. However, Theorem 4.10 is required for the important potential theoretic methods developed in the following section. Sets of infinite measure can be awkward to work with, and reducing them to sets of positive finite measure can provide a very useful simplification.

Theorem 4.10 guarantees that any (Borel) set F with $\mathcal{H}^s(F) = \infty$ contains a subset E with $0 < \mathcal{H}^s(E) < \infty$ (i.e. with E an s -set). At first, this might seem obvious—just shave pieces off F until what remains has positive finite measure. Unfortunately, it is not quite this simple—it is possible to jump from infinite measure to zero measure without passing through any intermediate value. Stating this in mathematical terms, it is possible to have a decreasing sequence of sets $E_1 \supset E_2 \supset \dots$ with $\mathcal{H}^s(E_k) = \infty$ for all k , but with $\mathcal{H}^s(\bigcap_{k=1}^{\infty} E_k) = 0$. (For a simple example, take $E_k = [0, 1/k] \subset \mathbb{R}$ and $0 < s < 1$.) To prove the theorem, we need to look rather more closely at the structure of Hausdorff measures. Readers mainly concerned with techniques for finding dimensions may prefer to omit the proof.

Theorem 4.10

Let F be a Borel subset of \mathbb{R}^n with $0 < \mathcal{H}^s(F) \leq \infty$. Then there is a compact set $E \subset F$ such that $0 < \mathcal{H}^s(E) < \infty$.

*Sketch of proof

The complete proof of this is complicated. We indicate the ideas involved in the case where F is a compact subset of $[0, 1] \subset \mathbb{R}$ and $0 < s < 1$.

We work with the net measures \mathcal{M}^s , which are defined in (3.17)–(3.18) using the binary intervals $[r2^{-k}, (r+1)2^{-k}]$ and are related to Hausdorff measure by (3.19). We define inductively a decreasing sequence $E_0 \supset E_1 \supset E_2 \supset \dots$ of compact subsets of F . Let $E_0 = F$. For $k \geq 0$, we define E_{k+1} by specifying its intersection with each binary interval I of length 2^{-k} . If $\mathcal{M}_{2^{-(k+1)}}^s(E_k \cap I) \leq 2^{-sk}$, we let $E_{k+1} \cap I = E_k \cap I$. Then

$$\mathcal{M}_{2^{-(k+1)}}^s(E_{k+1} \cap I) = \mathcal{M}_{2^{-k}}^s(E_k \cap I) \quad 4.9$$

since using I itself as a covering interval in calculating $\mathcal{M}_{2^{-k}}^s$ gives an estimate at least as large as would be obtained using shorter binary intervals. On the other hand, if $\mathcal{M}_{2^{-(k+1)}}^s(E_{k+1} \cap I) > 2^{-sk}$, we take $E_{k+1} \cap I$ to be a compact subset of $E_k \cap I$ with $\mathcal{M}_{2^{-(k+1)}}^s(E_{k+1} \cap I) = 2^{-sk}$. Such a subset exists since $\mathcal{M}_{2^{-(k+1)}}^s(E_k \cap I \cap [0, u])$ is finite and continuous in u . (This is why we need to work with the \mathcal{M}_δ^s rather than \mathcal{M}^s .) Since $\mathcal{M}_{2^{-k}}^s(E_k \cap I) = 2^{-sk}$, (4.9) again holds. Summing (4.9) over all binary intervals of length 2^{-k} , we get

$$\mathcal{M}_{2^{-(k+1)}}^s(E_{k+1}) = \mathcal{M}_{2^{-k}}^s(E_k). \quad 4.10$$

Repeated application of (4.10) gives $\mathcal{M}_{2^{-k}}^s(E_k) = \mathcal{M}_1^s(E_0)$ for all k . Let E be the compact set $\bigcap_{k=0}^{\infty} E_k$. Taking the limit as $k \rightarrow \infty$ gives $\mathcal{M}^s(E) = \mathcal{M}_1^s(E_0)$ (this step needs some justification). The covering of $E_0 = F$ by the single interval $[0, 1]$ gives $\mathcal{M}^s(E) = \mathcal{M}_1^s(E_0) \leq 1$. Since $\mathcal{M}^s(E_0) \geq \mathcal{H}^s(E_0) > 0$, we have $\mathcal{M}_{2^{-k}}^s(E_0) > 0$ if k is large enough. For such a k , either $\mathcal{M}^s(E) = \mathcal{M}_1^s(E_0) \geq 2^{-ks}$ or $\mathcal{M}_1^s(E_0) < 2^{-ks}$ in which

case $\mathcal{M}^s(E) = \mathcal{M}_1^s(E_0) = \mathcal{M}_{2^{-k}}^s(E_0) > 0$. Thus, $0 < \mathcal{M}^s(E) < \infty$, and the theorem follows from (3.19).

A number of results, for example, those in Chapter 5, apply only to s -sets, that is, sets with $0 < \mathcal{H}^s(F) < \infty$. One way of approaching s -dimensional sets with $\mathcal{H}^s(F) = \infty$ is to use Theorem 4.10 to extract a subset of positive finite measure, to study its properties as an s -set and then to interpret these properties in the context of the larger set F . Similarly, if $0 < s < t$, any set F of Hausdorff dimension t has $\mathcal{H}^s(F) = \infty$ and so contains an s -set.

The following proposition and its corollary guarantee subsets of finite measure with control of the measure of small balls.

Proposition 4.11

Let F be a Borel set satisfying $0 < \mathcal{H}^s(F) < \infty$. There is a constant b and a compact set $E \subset F$ with $\mathcal{H}^s(E) > 0$ such that

$$\mathcal{H}^s(E \cap B(x, r)) \leq br^s$$

4.11

for all $x \in \mathbb{R}^n$ and $r > 0$.

Proof

In Proposition 4.9(b), take μ as the restriction of \mathcal{H}^s to F , that is, $\mu(A) = \mathcal{H}^s(F \cap A)$. Then, if

$$F_1 = \left\{ x \in \mathbb{R}^n : \overline{\lim}_{r \rightarrow 0} \mathcal{H}^s(F \cap B(x, r)) / r^s > 2^{1+s} \right\}$$

it follows that $\mathcal{H}^s(F_1) \leq 2^s 2^{-(1+s)} \mu(F) = \frac{1}{2} \mathcal{H}^s(F)$. Thus,

$\mathcal{H}^s(F \setminus F_1) \geq \frac{1}{2} \mathcal{H}^s(F) > 0$, so if $E_1 = F \setminus F_1$, then $\mathcal{H}^s(E_1) > 0$ and $\overline{\lim}_{r \rightarrow 0} \mathcal{H}^s(F \cap B(x, r)) / r^s \leq 2^{1+s}$ for $x \in E_1$. By Egoroff's theorem (see Section 1.3), it follows that there is a compact set $E \subset E_1$ with $\mathcal{H}^s(E) > 0$ and a number $r_0 > 0$ such that $\mathcal{H}^s(F \cap B(x, r)) / r^s \leq 2^{2+s}$ for all $x \in E$ and all $0 < r \leq r_0$. However, we have that $\mathcal{H}^s(F \cap B(x, r)) / r^s \leq \mathcal{H}^s(F) / r_0^s$ if $r \geq r_0$ so (4.11) holds for all $r > 0$ for suitable b .

Corollary 4.12

Let F be a Borel subset of \mathbb{R}^n with $0 < \mathcal{H}^s(F) \leq \infty$. Then there is a compact set $E \subset F$ such that $0 < \mathcal{H}^s(E) < \infty$ and a constant b such that

$$\mathcal{H}^s(E \cap B(x, r)) \leq b r^s$$

for all $x \in \mathbb{R}^n$ and $r > 0$.

Proof

Theorem 4.10 provides us with a compact subset F_1 of F of positive finite measure, and applying Proposition 4.11 to F_1 gives the result.

Corollary 4.12, which may be regarded as a converse of the Mass distribution principle 4.2, is often called ‘Frostman’s lemma’.

4.3 Potential theoretic methods

In this section, we introduce a technique for calculating the Hausdorff dimensions that is widely used both in theory and in practice. This replaces the need for estimating the mass of a large number of small sets, as in the mass distribution principle, by a single check for the convergence of a certain integral.

The ideas of potential and energy will be familiar to readers with a knowledge of gravitation or electrostatics. For $s \geq 0$, the s -potential at a point x of \mathbb{R}^n resulting from the mass distribution μ on \mathbb{R}^n is defined as

$$\phi_s(x) = \int \frac{d\mu(y)}{|x - y|^s}. \quad \text{4.12}$$

(If we are working in \mathbb{R}^3 and $s = 1$, then this is essentially the familiar Newtonian gravitational potential.) The s -energy of μ is

$$I_s(\mu) = \int \phi_s(x)d\mu(x) = \int \frac{d\mu(x)d\mu(y)}{|x - y|^s}. \quad \text{4.13}$$

The following theorem relates Hausdorff dimension to seemingly unconnected potential theoretic ideas. Particularly useful is part (a): if there is a mass distribution on a set F which has finite s -energy, then F has dimension at least s .

Theorem 4.13

Let F be a subset of \mathbb{R}^n .

- a. If there is a mass distribution μ on F with $I_s(\mu) < \infty$, then $\mathcal{H}^s(F) = \infty$ and $\dim_H F \geq s$.
- b. If F is a Borel set with $0 < \mathcal{H}^s(F) < \infty$, then for all $0 < t < s$, there exists a mass distribution μ on F with $I_t(\mu) < \infty$.

Proof

- a. Suppose that $I_s(\mu) < \infty$ for some mass distribution μ with support contained in F . Define

$$F_1 = \{x \in F : \overline{\lim}_{r \rightarrow 0} \mu(B(x, r))/r^s > 0\}.$$

If $x \in F_1$, we may find $\varepsilon > 0$ and a sequence of numbers $r_1 > r_2 > \dots$ decreasing to 0 such that $\mu(B(x, r_i)) \geq \varepsilon r_i^s$. Since $\mu(\{x\}) = 0$ (otherwise $I_s(\mu) = \infty$), it follows from the continuity of μ that, by taking $q_i (0 < q_i < r_i)$ small enough, we get $\mu(A_i) \geq \frac{1}{4}\varepsilon r_i^s (i = 1, 2, \dots)$, where A_i is the annulus $B(x, r_i) \setminus B(x, q_i)$. Taking subsequences if necessary, we may assume that $r_{i+1} < q_i$ for all i , so that the A_i are disjoint annuli centred on x . Hence, for all $x \in F_1$,

$$\begin{aligned} \phi_s(x) &= \int \frac{d\mu(y)}{|x - y|^s} \geq \sum_{i=1}^{\infty} \int_{A_i} \frac{d\mu(y)}{|x - y|^s} \\ &\geq \sum_{i=1}^{\infty} \frac{1}{4}\varepsilon r_i^s r_i^{-s} = \infty \end{aligned}$$

since $|x - y|^{-s} \geq r_i^{-s}$ on A_i . But $I_s(\mu) = \int \phi_s(x)d\mu(x) < \infty$, so $\phi_s(x) < \infty$ for μ -almost all x . We conclude that $\mu(F_1) = 0$. Since $\overline{\lim}_{r \rightarrow 0} \mu(B(x, r))/r^s = 0$ if $x \in F \setminus F_1$, Proposition 4.9(a) tells us that for all $c > 0$, we have

$$\mathcal{H}^s(F) \geq \mathcal{H}^s(F \setminus F_1) \geq \mu(F \setminus F_1)/c \geq (\mu(F) - \mu(F_1))/c = \mu(F)/c.$$

Hence, $\mathcal{H}^s(F) = \infty$.

- b. Suppose that $0 < \mathcal{H}^s(F) < \infty$. Starting with \mathcal{H}^s , we construct a mass distribution μ on F with $I_s(\mu) < \infty$. By Corollary 4.12, there exist a compact set $E \subset F$ with $0 < \mathcal{H}^s(E) < \infty$ and a constant b such that

$$\mathcal{H}^s(E \cap B(x, r)) \leq br^s$$

for all $x \in \mathbb{R}^n$ and $r > 0$. Let μ be the restriction of \mathcal{H}^s to E , so that $\mu(A) = \mathcal{H}^s(E \cap A)$; then μ is a mass distribution on F . Fix $x \in \mathbb{R}^n$ and write

$$m(r) = \mu(B(x, r)) = \mathcal{H}^s(E \cap B(x, r)) \leq br^s.$$

4.14.

Then, if $0 < t < s$

$$\begin{aligned}\phi_t(x) &= \int_{|x-y|\leq 1} \frac{d\mu(y)}{|x-y|^t} + \int_{|x-y|>1} \frac{d\mu(y)}{|x-y|^t} \\ &\leq \int_0^1 r^{-t} dm(r) + \mu(\mathbb{R}^n) \\ &= [r^{-t} m(r)]_{0^+}^1 + t \int_0^1 r^{-(t+1)} m(r) dr + \mu(\mathbb{R}^n) \\ &\leq b + bt \int_0^1 r^{s-t-1} dr + \mu(\mathbb{R}^n) \\ &= b \left(1 + \frac{t}{s-t}\right) + \mathcal{H}^s(F) = c,\end{aligned}$$

say, after integrating by parts and using (4.14). Thus, $\phi_t(x) \leq c$ for all $x \in \mathbb{R}^n$, so that $I_t(\mu) = \int \phi_t(x) d\mu(x) \leq c\mu(\mathbb{R}^n) < \infty$.

Important applications of Theorem 4.13 will be given later in the book, for example, in the proof of the projection theorems in Chapter 6 and in the determination of the dimension of Brownian paths in Chapter 16. The theorem is often used to find the dimension of fractals F_θ which depend on a parameter θ . There may be a natural way to define a mass distribution μ_θ on F_θ for each θ . If we can show that for some s ,

$$\int I_s(\mu_\theta) d\theta = \iiint \frac{d\mu_\theta(x) d\mu_\theta(y) d\theta}{|x-y|^s} < \infty,$$

then $I_s(\mu_\theta) < \infty$ for almost all θ , so that $\dim_H F_\theta \geq s$ for almost all θ .

Readers familiar with potential theory may have encountered the definition of the *s*-capacity of a set F :

$$C_s(F) = \sup_{\mu} \{1/I_s(\mu) : \mu \text{ is a mass distribution on } F \text{ with } \mu(F) = 1\}$$

(with the convention that $1/\infty = 0$). Thus, another way of expressing Theorem 4.13 is

$$\dim_H F = \inf \{s \geq 0 : C_s(F) = 0\} = \sup \{s \geq 0 : C_s(F) > 0\}.$$

Whilst this is reminiscent of the definition (3.10) of the Hausdorff dimension in terms of Hausdorff measures, it should be noted that capacities behave very differently from measures. In particular, they are not generally additive.

*4.4 Fourier transform methods

In this section, we do no more than indicate that Fourier transforms can be a powerful tool for analysing dimensions.

The n -dimensional Fourier transforms of an integrable function f and a mass distribution μ on \mathbb{R}^n are defined by

$$\hat{f}(u) = \int_{\mathbb{R}^n} f(x) \exp(ix \cdot u) dx \quad (u \in \mathbb{R}^n) \quad \mathbf{4.15}$$

$$\hat{\mu}(u) = \int_{\mathbb{R}^n} \exp(ix \cdot u) d\mu(x) \quad (u \in \mathbb{R}^n) \quad \mathbf{4.16}$$

where $x \cdot u$ represents the usual scalar product. (Fourier transformation may be extended to a much wider class of function using the theory of distributions.)

The s -potential (4.12) of a mass distribution μ is just the convolution

$$\phi_s(x) = (|\cdot|^{-s} * \mu)(x) \equiv \int |x - y|^{-s} d\mu(y).$$

Formally, the transform of $|x|^{-s}$ may be shown to be $c|u|^{s-n}$, where c depends on n and s , so the convolution theorem, which states that the transform of the convolution of two functions equals the product of the transforms of the functions, gives

$$\hat{\phi}_s(u) = c|u|^{s-n}\hat{\mu}(u).$$

Parseval's theorem tells us that

$$\int \phi_s(x)d\mu(x) = (2\pi)^n \int \hat{\phi}_s(u)\overline{\hat{\mu}(u)}du$$

where the bar denotes complex conjugation, so

$$I_s(\mu) = (2\pi)^n c \int |u|^{s-n} |\hat{\mu}(u)|^2 du. \quad \text{4.17}$$

This expression for $I_s(\mu)$, which may be established rather more rigorously, is sometimes a convenient way of expressing the energy (4.13) required in Theorem 4.13. Thus, if there is a mass distribution μ on a set F for which the integral (4.16) is finite, then $\dim_H F \geq s$. In particular, if

$$|\hat{\mu}(u)| \leq b|u|^{-t/2} \quad \text{4.18}$$

for some constant b , then, noting that, by (4.16), $|\hat{\mu}(u)| \leq \mu(\mathbb{R}^n)$ for all u , we have from (4.16) that for some constants c_1 and c_2 ,

$$I_s(\mu) \leq c_1 \int_{|u| \leq 1} |u|^{s-n} du + c_2 \int_{|u| > 1} |u|^{s-n} |u|^{-t} du$$

which is finite if $0 < s < t$. Thus, if (4.17) holds, any set F which supports μ has Hausdorff dimension at least t . The greatest value of t for which there is a mass distribution μ on F satisfying (4.17) is sometimes called the *Fourier dimension* of F , which never exceeds the Hausdorff dimension.

4.5 Notes and references

Many papers are devoted to calculating dimensions of various classes of fractal, for example, the papers of Eggleston (1952); Beardon (1965) and Peyrière (1977) discuss fairly general constructions.

The potential theoretic approach was essentially due to Frostman (1935); see Taylor (1961); Hayman and Kennedy (1976) and Carleson (1998). The book by Kahane (1993) includes many applications to dimensions. For an introduction to Fourier transforms, see Vretblad (2005).

The work on subsets of finite measure originates from Besicovitch (1952) and a very general treatment is given in Rogers (1998). Subsets of finite positive packing measure are investigated by Joyce and Preiss (1995). For extensions of Proposition 4.9, including to packing dimension, see Cutler (1995). Complete proofs of Theorem 4.10 may be found in Falconer (1985a) and Mattila (1999).

Exercises

4.1 What is the Hausdorff dimension of the ‘Cantor tartan’ which is given by $\{(x, y) \in \mathbb{R}^2 : \text{either } x \in F \text{ or } y \in F\}$, where F is the middle third Cantor set?

4.2 Use the mass distribution principle and a natural upper bound to show that the set of numbers in $[0, 1]$ containing only even digits has the Hausdorff dimension $\log 5 / \log 10$.

4.3 Use the mass distribution method to show that the ‘Cantor dust’ depicted in [Figure 4.2](#) has the Hausdorff dimension 1. (Hint: note that taking the square E_0 to have side 1, any two squares in the set E_k of the construction are separated by a distance of at least 4^{-k} .)

4.4 Fix $0 < \lambda \leq \frac{1}{2}$, and let F be the set of real numbers

$$F = \left\{ \sum_{k=1}^{\infty} a_k \lambda^k : a_k = 0 \text{ or } 1 \text{ for } k = 1, 2, \dots \right\}.$$

Find the Hausdorff and box dimensions of F .

4.5 What is the Hausdorff dimension of $F \times F \subset \mathbb{R}^2$, where F is the middle third Cantor set?

4.6 Let F be the middle third Cantor set. What is the Hausdorff dimension of the plane set given by $\{(x, y) \in \mathbb{R}^2 : x \in F \text{ and } 0 \leq y \leq x^2\}$?

4.7 Use a mass distribution method to obtain the result of Example 4.5 directly rather than via Example 4.4.

4.8 Show that every number $x \geq 0$ may be expressed in the form

$$x = m + \frac{a_2}{2!} + \frac{a_3}{3!} + \dots,$$

where $m \geq 0$ is an integer and a_k is an integer with $0 \leq a_k \leq k - 1$ for each k . Let $F = \{x \geq 0 : m = 0 \text{ and } a_k \text{ is even for } k = 2, 3, \dots\}$. Find $\dim_H F$.

4.9 Show that there is a compact subset F of $[0, 1]$ of Hausdorff dimension 1 but with $\mathcal{H}^1(F) = 0$. (Hint: try a ‘Cantor set’ construction, but reduce the proportion of intervals removed at each stage.)

4.10 Deduce from Theorem 4.10 that if F is a Borel subset of \mathbb{R}^n with $\mathcal{H}^s(F) = \infty$ and c is a positive number, then there is a Borel subset E of F with $\mathcal{H}^s(E) = c$.

4.11 Let μ be the natural mass distribution on the middle third Cantor set F (see after Principle 4.2). Estimate the s -energy of μ for $s < \log 2 / \log 3$ and deduce from Theorem 4.13 that $\dim_H F \geq \log 2 / \log 3$.

Chapter 5

Local structure of fractals

Classical calculus involves finding local approximations to curves and surfaces by tangent lines and planes. Viewed at a fine scale, the neighbourhood of a point on a smooth curve appears close to a line segment. Can we say anything about the local structure of as diverse a class of objects as fractals? Surprisingly, the answer in many cases is yes. We can go some way to establishing the form of fractals in a neighbourhood of a general point. In particular, we can study the concentration of fractals about typical points, in other words, their local densities and the directional distribution of fractals around points including the question of whether tangents exist. A knowledge of the local form of a fractal is useful both in developing theory and in applications.

In order to realise the power of Hausdorff measures, it is necessary to restrict attention to s -sets, that is, Borel sets of Hausdorff dimension s with positive finite s -dimensional Hausdorff measure. (More generally, it is possible to work with s -sets of positive finite \mathcal{H}^h -measure for some dimension function h ; see Section 3.7—we do not consider this generalisation here.) This is not so restrictive as it first appears. Many fractals encountered in practice are s -sets, but even if $\mathcal{H}^s(F) = \infty$, then by Theorem 4.10, F has subsets that are s -sets to which this theory can be applied. Alternatively, it sometimes happens that a set F of dimension s is a countable union of s -sets, and the properties of these component sets can often be transferred to F .

The material outlined in this chapter lies at the heart of geometric measure theory, a subject where rigorous proofs are often intricate and difficult. We omit the harder proofs; it is hoped that those included will be found instructive and will give the flavour to the subject. We generally restrict attention to subsets of the plane—the

higher-dimensional analogues, although valid, are often considerably harder.

5.1 Densities

Let F be a subset of the plane. The *density* of F at x is

$$\lim_{r \rightarrow 0} \frac{\text{area}(F \cap B(x, r))}{\text{area}(B(x, r))} = \lim_{r \rightarrow 0} \frac{\text{area}(F \cap B(x, r))}{\pi r^2}, \quad 5.1$$

where $B(x, r)$ is the closed disc of radius r and centre x . The classical Lebesgue density theorem tells us that for a Borel set F , this limit exists and equals 1 when $x \in F$ and 0 when $x \notin F$, except for a set of x of area 0. In other words, for a typical point x of F , small discs centred at x are almost entirely filled by F , but if x is outside F then small discs centred at x generally contain very little of F (see [Figure 5.1](#)).



Figure 5.1 The Lebesgue density theorem. The point x is in F , and $\text{area}(F \cap B(x, r))/\text{area}(B(x, r))$ is close to 1 if r is small. The point y is outside F , and $\text{area}(F \cap B(y, r))/\text{area}(B(y, r))$ is close to 0 if r is small

Similarly, if F is a smooth curve in the plane and x is a point of F (other than an end point), then $F \cap B(x, r)$ is close to a diameter of

$B(x, r)$ for small r and

$$\lim_{r \rightarrow 0} \frac{\text{length}(F \cap B(x, r))}{2r} = 1.$$

If $x \notin F$, then this limit is clearly 0.

Density theorems such as these tell us how much of the set F , in the sense of area or length, is concentrated near x . In the same way, it is natural to investigate densities of fractals—if F has dimension s , how does the s -dimensional Hausdorff measure of $F \cap B(x, r)$ behave as $r \rightarrow 0$? We look at this question when F is an s -set in \mathbb{R}^2 with $0 < s < 2$ (0-sets are just finite sets of points, and there is little to say, and \mathcal{H}^2 is essentially area, so if $s = 2$, we are in the Lebesgue density situation (5.1)).

We define the *lower* and *upper densities* of an s -set F at a point $x \in \mathbb{R}^n$ as

$$\underline{D}^s(F, x) = \lim_{r \rightarrow 0} \frac{\mathcal{H}^s(F \cap B(x, r))}{(2r)^s} \quad 5.2$$

and

$$\overline{D}^s(F, x) = \lim_{r \rightarrow 0} \frac{\mathcal{H}^s(F \cap B(x, r))}{(2r)^s}, \quad 5.3$$

respectively (note that $|B(x, r)| = 2r$). If $\underline{D}^s(F, x) = \overline{D}^s(F, x)$, we say that the *density* of F at x exists and we write $D^s(F, x)$ for the common value.

A point x at which $\underline{D}^s(F, x) = \overline{D}^s(F, x) = 1$ is called a *regular* point of F , otherwise x is an *irregular* point. An s -set is termed *regular* if \mathcal{H}^s -almost all of its points (i.e. all of its points except for a set of \mathcal{H}^s -measure 0) are regular and *irregular* if \mathcal{H}^s -almost all of its points are irregular. (Note that for sets, ‘irregular’ does *not* mean ‘not regular’!) As we shall see, a fundamental result is that an s -set F must be irregular unless s is an integer. However, if s is integral an s -set decomposes into a regular part and an irregular part. Roughly speaking, a regular 1-set consists of portions of rectifiable curves of

finite length, whereas an irregular 1-set is totally disconnected and dust-like and typically of fractal form.

By definition, a regular set is one for which the direct analogue of the Lebesgue density theorem holds. However, even the densities of irregular sets cannot behave too erratically.

Proposition 5.1

Let F be an s -set in \mathbb{R}^n . Then

- a. $\underline{D}^s(F, x) = \overline{D}^s(F, x) = 0$ for \mathcal{H}^s -almost all $x \notin F$
- b. $2^{-s} \leq \overline{D}^s(F, x) \leq 1$ for \mathcal{H}^s -almost all $x \in F$.

Partial proof

- a. If F is closed and $x \notin F$, then $B(x, r) \cap F = \emptyset$ if r is small enough. Hence, $\lim_{r \rightarrow 0} \mathcal{H}^s(F \cap B(x, r)) / (2r)^s = 0$. If F is not closed, the proof is a little more involved and we omit it here.
- b. This follows quickly from Proposition 4.9(a) by taking μ as the restriction of \mathcal{H}^s to F , that is, $\mu(A) = \mathcal{H}^s(F \cap A)$: if

$$F_1 = \left\{ x \in F : \overline{D}^s(F, x) = \overline{\lim}_{r \rightarrow 0} \frac{\mathcal{H}^s(F \cap B(x, r))}{(2r)^s} < 2^{-s}c \right\},$$

then $\mathcal{H}^s(F_1) \geq \mathcal{H}^s(F)/c \geq \mathcal{H}^s(F_1)/c$. If $0 < c < 1$, this is only possible if $\mathcal{H}^s(F_1) = 0$; thus, for almost all $x \in F$, we have $\overline{D}^s(F, x) \geq 2^{-s}$. The upper bound follows in essentially the same way using Proposition 4.9(b).

Note that an immediate consequence of Proposition 5.1(b) is that an irregular set has a lower density which is strictly less than 1 almost

everywhere.

We will sometimes need to relate the densities of a set to those of certain subsets. Let F be an s -set and let E be a Borel subset of F . Then

$$\frac{\mathcal{H}^s(F \cap B(x, r))}{(2r)^s} = \frac{\mathcal{H}^s(E \cap B(x, r))}{(2r)^s} + \frac{\mathcal{H}^s((F \setminus E) \cap B(x, r))}{(2r)^s}.$$

For almost all x in E , we have

$$\frac{\mathcal{H}^s((F \setminus E) \cap B(x, r))}{(2r)^s} \rightarrow 0 \quad \text{as } r \rightarrow 0$$

by Proposition 5.1(a), so letting $r \rightarrow 0$ gives

$$\underline{D}^s(F, x) = \underline{D}^s(E, x); \quad \overline{D}^s(F, x) = \overline{D}^s(E, x) \quad \text{5.4}$$

for \mathcal{H}^s -almost all x in E . Thus, from the definitions of regularity, if E is a subset of an s -set F with $\mathcal{H}^s(E) > 0$, then E is regular if F is regular and E is irregular if F is irregular. In particular, the intersection of a regular and an irregular set, being a subset of both, has \mathcal{H}^s -measure zero.

Estimates for lower densities are altogether harder to obtain, and we do not pursue them here.

In general, it is quite involved to show that s -sets of non-integral dimension are irregular, but in the case $0 < s < 1$, the following ‘annulus’ proof is appealing.

Theorem 5.2

Let F be an s -set in \mathbb{R}^2 . Then F is irregular unless s is an integer.

Partial Proof

We show that F is irregular if $0 < s < 1$ by showing that the density $D^s(F, x)$ fails to exist almost everywhere in F . Suppose to the contrary: then there is a set $F_1 \subset F$ of positive measure where the density exists and, therefore, where $\frac{1}{2} < 2^{-s} \leq D^s(F, x)$, by Proposition 5.1(b). By Egoroff's theorem (see Section 1.3), we may find $r_0 > 0$ and a Borel set $E \subset F_1 \subset F$ with $\mathcal{H}^s(E) > 0$ such that

$$\mathcal{H}^s(F \cap B(x, r)) > \frac{1}{2}(2r)^s \quad 5.5$$

for all $x \in E$ and $r < r_0$. Let $y \in E$ be a cluster point of E (i.e. a point y with other points of E arbitrarily close). Let η be a number with $0 < \eta < 1$, and let $A_{r,\eta}$ be the annulus $B(y, r(1 + \eta)) \setminus B(y, r(1 - \eta))$ (see [Figure 5.2](#)). Then

$$\begin{aligned} (2r)^{-s} \mathcal{H}^s(F \cap A_{r,\eta}) &= (2r)^{-s} \mathcal{H}^s(F \cap B(y, r(1 + \eta))) \\ &\quad - (2r)^{-s} \mathcal{H}^s(F \cap B(y, r(1 - \eta))) \\ &\rightarrow D^s(F, y)((1 + \eta)^s - (1 - \eta)^s) \end{aligned} \quad 5.6$$

as $r \rightarrow 0$. For a sequence of values of r tending to 0, we may find $x \in E$ with $|x - y| = r$. Then $B(x, r\eta/2) \subset A_{r,\eta}$ so by (5.5)

$$\frac{1}{2}r^s\eta^s < \mathcal{H}^s(F \cap B(x, r\eta/2)) \leq \mathcal{H}^s(F \cap A_{r,\eta}).$$

Combining with (5.6), this implies that

$$\begin{aligned} 2^{-s-1}\eta^s &\leq D^s(F, y)((1 + \eta)^s - (1 - \eta)^s) \\ &= D^s(F, y)(2s\eta + \text{terms in } \eta^2 \text{ or higher}). \end{aligned}$$

Letting $\eta \rightarrow 0$, we see that this is impossible when $0 < s < 1$ and the result follows by contradiction.

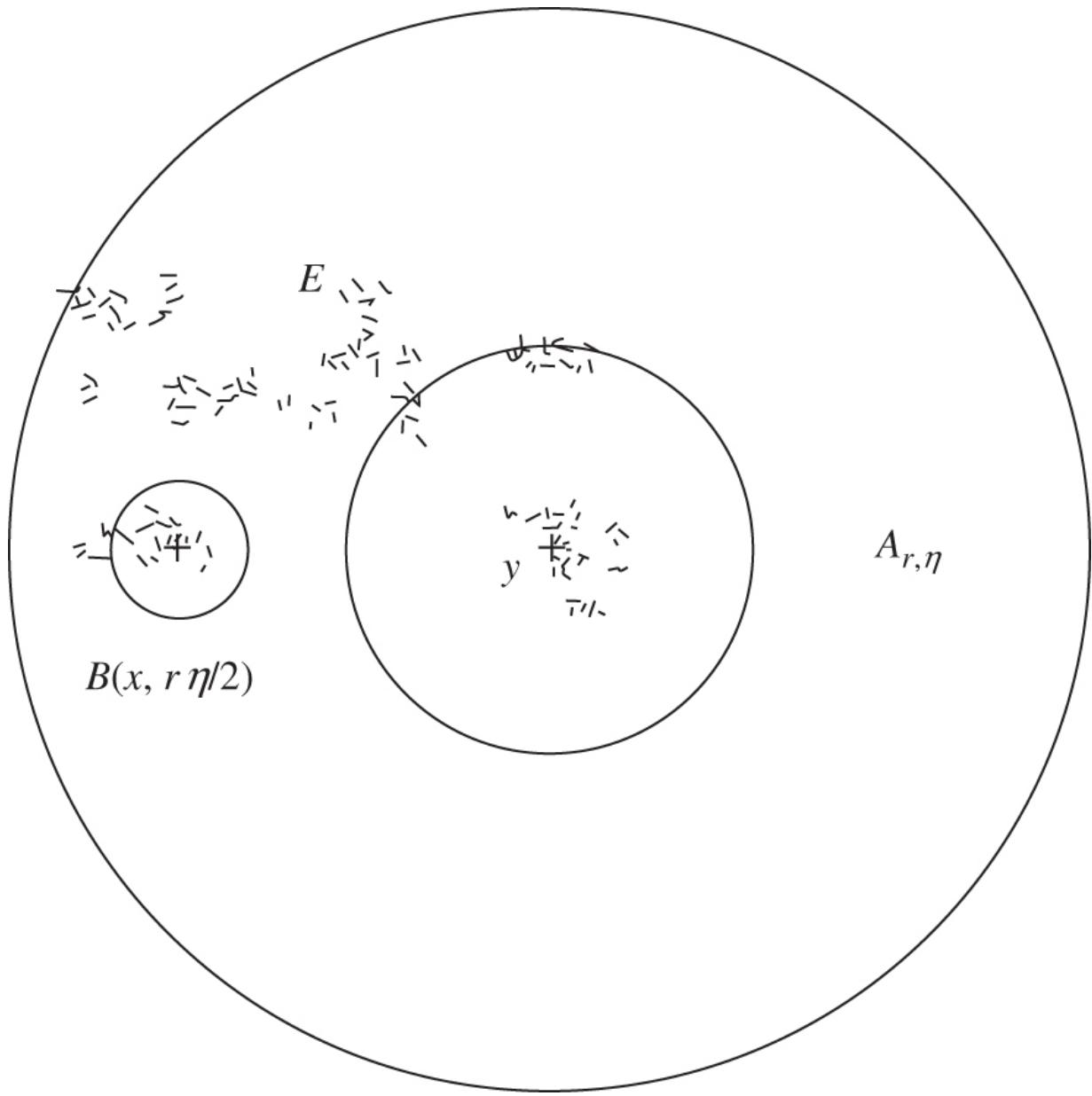


Figure 5.2 The ‘annulus’ proof of Theorem 5.2.

5.2 Structure of 1-sets

As pointed out in Section 5.1, sets of non-integral dimension must be irregular. The situation for sets of integral dimension is more complicated. The following decomposition theorem, indicated in [Figure 5.3](#), enables us to split a 1-set into a regular and an irregular

part, so that we can analyse each separately and recombine them without affecting density properties.

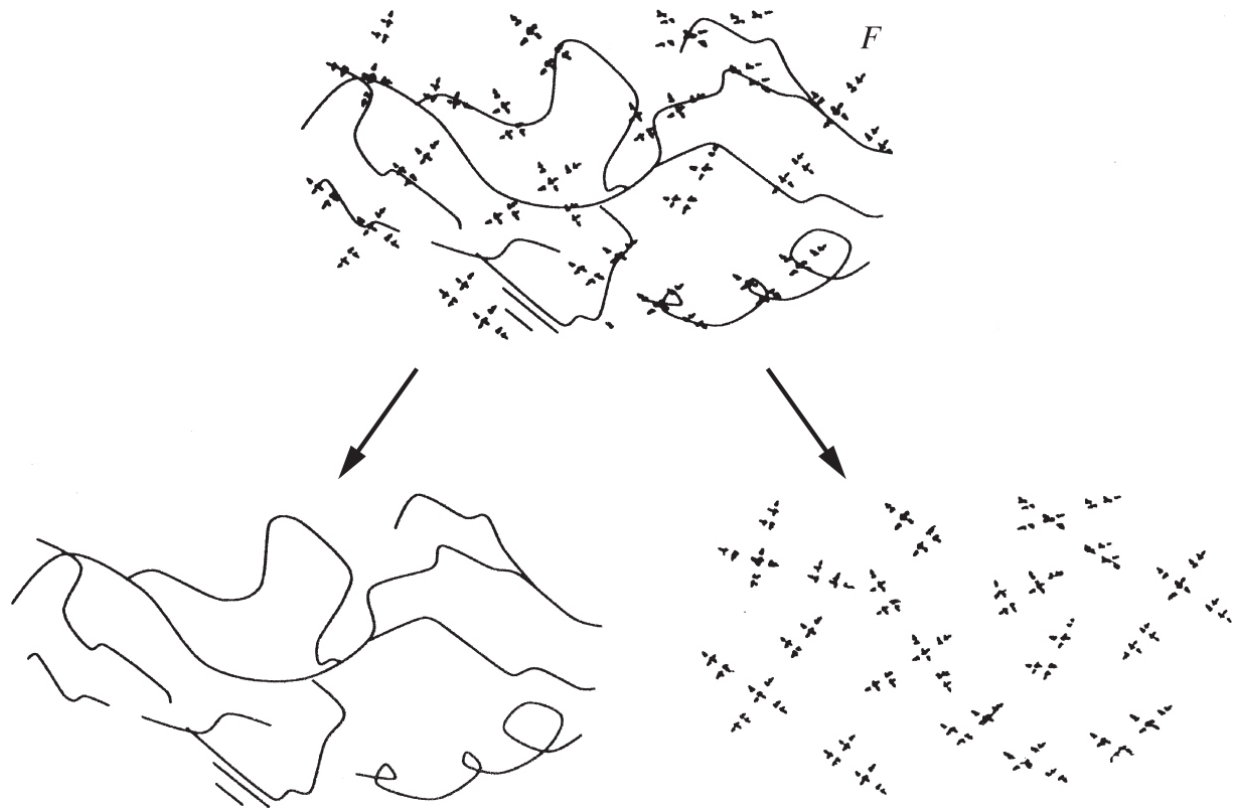


Figure 5.3 Decomposition of a 1-set into a regular ‘curve-like’ part and an irregular ‘curve-free’ part.

Decomposition theorem 5.3

Let F be a 1-set. The set of regular points of F forms a regular set, the set of irregular points forms an irregular set.

Proof

This is immediate from (5.4), taking E as the set of regular and irregular points.

Examples of regular and irregular 1-sets abound. Smooth curves are regular and provide us with the shapes of classical geometry such as the perimeters of circles or ellipses. On the other hand, the iterated construction of [Figure 0.4](#) gives an irregular 1-set which is a totally disconnected fractal. This is typical—as we shall see, regular 1-sets are made up from pieces of curve, whereas irregular 1-sets are dust-like and ‘curve-free’, that is, intersect any (finite length) curve in length zero.

To study 1-sets, we need a few facts about curves. For our purposes, a *curve* or *Jordan curve* C is the image of a continuous injection (one-to-one function) $\psi : [a, b] \rightarrow \mathbb{R}^2$, where $[a, b] \subset \mathbb{R}$ is a proper closed interval. According to our definition, curves are not self-intersecting, have two ends and are compact connected subsets of the plane. The length $\mathcal{L}(C)$ of the curve C is given by polygonal approximation:

$$\mathcal{L}(C) = \sup \sum_{i=1}^m |x_i - x_{i-1}|,$$

where the supremum is taken over all dissections of C by points x_0, x_1, \dots, x_m in that order along the curve. If the length $\mathcal{L}(C)$ is positive and finite, we call C a *rectifiable curve*.

As one might expect, the length of a curve equals its 1-dimensional Hausdorff measure.

Lemma 5.4

If C is a rectifiable curve, then $\mathcal{H}^1(C) = \mathcal{L}(C)$.

Proof

For $x, y \in C$, let $C_{x,y}$ denote that part of C between x and y . As orthogonal projection onto the line through x and y does not increase distances, (3.7) gives $\mathcal{H}^1(C_{x,y}) \geq \mathcal{H}^1[x, y] = |x - y|$, where $[x, y]$ is the straight-line segment joining x to y . Hence, for any dissection x_0, x_1, \dots, x_m of C ,

$$\sum_{i=1}^m |x_i - x_{i-1}| \leq \sum_{i=1}^m \mathcal{H}^1(C_{x_i, x_{i-1}}) \leq \mathcal{H}^1(C)$$

so taking the supremum over all dissections gives $\mathcal{L}(C) \leq \mathcal{H}^1(C)$. On the other hand, let $f : [0, \mathcal{L}(C)] \rightarrow C$ be the mapping that takes t to the point on C at distance t along the curve from one of its ends. Clearly, $|f(t) - f(u)| \leq |t - u|$ for $0 \leq t, u \leq \mathcal{L}(C)$, that is, f is Lipschitz with $\mathcal{H}^1(C) \leq \mathcal{H}^1[0, \mathcal{L}(C)] = \mathcal{L}(C)$ by (3.7) as required.

It is straightforward to show that rectifiable curves are regular.

Lemma 5.5

A rectifiable curve is a regular 1-set.

Proof

As C is rectifiable $\mathcal{L}(C) < \infty$, and because C has distinct end points p and q , it is clear that $\mathcal{L}(C) \geq |p - q| > 0$. By Lemma 5.4, $0 < \mathcal{H}^1(C) < \infty$, so C is a 1-set.

A point x of C that is not an end point divides C into two parts $C_{p,x}$ and $C_{x,q}$. If r is sufficiently small, then moving away from x along the curve $C_{x,q}$, we reach a first point y on C with $|x - y| = r$. Then $C_{x,y} \subset B(x, r)$ and

$$r = |x - y| \leq \mathcal{L}(C_{x,y}) = \mathcal{H}^1(C_{x,y}) \leq \mathcal{H}^1(C_{x,q} \cap B(x, r)).$$

Similarly, $r \leq \mathcal{H}^1(C_{p,x} \cap B(x, r))$, so, adding, $2r \leq \mathcal{H}^1(C \cap B(x, r))$, if r is small enough. Thus

$$\underline{D}^1(C, x) = \lim_{r \rightarrow 0} \frac{\mathcal{H}^1(C \cap B(x, r))}{2r} \geq 1.$$

By Proposition 5.1(b), $\underline{D}^1(C, x) \leq \overline{D}^1(C, x) \leq 1$ for \mathcal{H}^1 -almost all x , so $D^1(C, x)$ exists and equals 1 for almost all $x \in C$, so C is regular.

Other regular sets are easily constructed. By (5.4), subsets of regular sets and unions of regular sets should also be regular. With this in mind, we define a 1-set to be *curve-like* if it is contained in a countable union of rectifiable curves.

Proposition 5.6

A curve-like 1-set is a regular 1-set.

Proof

If F is a curve-like 1-set, then $F \subset \bigcup_{i=1}^{\infty} C_i$ where the C_i are rectifiable curves. For each i and \mathcal{H}^1 -almost all $x \in F \cap C_i$, we have, using Lemma 5.5 and (5.4),

$$1 = \underline{D}^1(C_i, x) = \underline{D}^1(F \cap C_i, x) \leq \underline{D}^1(F, x)$$

and, hence, $1 \leq \underline{D}^1(F, x)$ for almost all $x \in F$. But for almost all $x \in F$, we have $\underline{D}^1(F, x) \leq \overline{D}^1(F, x) \leq 1$ by Proposition 5.1, so $D^1(F, x) = 1$ almost everywhere, and F is regular.

It is natural to introduce a complementary definition: a 1-set is called *curve-free* if its intersection with every rectifiable curve has \mathcal{H}^1 -measure zero.

Proposition 5.7

An irregular 1-set is curve-free.

Proof

If F is irregular and C is a rectifiable curve, then $F \cap C$ is a subset of both a regular and an irregular set so has zero \mathcal{H}^1 -measure.

These two propositions begin to suggest that regular and irregular sets might be characterised as curve-like and curve-free, respectively. This is indeed the case, but it is far from easy to prove. The crux of the matter is the following lower-density estimate, which depends on an intricate investigation of the properties of

curves and connected sets and some ingenious geometrical arguments.

Proposition 5.8

Let F be a curve-free 1-set in \mathbb{R}^2 . Then $\underline{D}^1(F, x) \leq \frac{3}{4}$ at almost all $x \in F$.

Proof

Omitted.

Assuming this proposition, a complete characterisation of regular and irregular sets is relatively easy.

Theorem 5.9

- a. A 1-set in \mathbb{R}^2 is irregular if and only if it is curve-free.
- b. A 1-set in \mathbb{R}^2 is regular if and only if it is the union of a curve-like set and a set of \mathcal{H}^1 -measure zero.

Proof

- a. A curve-free set must be irregular by Proposition 5.8.
 Proposition 5.7 provides the converse implication.

By Proposition 5.6, a curve-like set is regular, and adding in a set of measure zero does not affect densities or, therefore, regularity.

If F is regular, then any Borel subset E of positive measure is regular with $D^1(E, x) = 1$ for almost all $x \in E$. By Proposition 5.8, the set E cannot be curve-free, so some rectifiable curve intersects E in a set of positive length. We use this fact to define inductively a sequence of rectifiable curves $\{C_i\}$. We choose C_1 to cover a reasonably large part of F say

$$\mathcal{H}^1(F \cap C_1) \geq \frac{1}{2} \sup \{\mathcal{H}^1(F \cap C) : C \text{ is rectifiable}\} > 0.$$

If C_1, \dots, C_k have been selected and the regular set $F_k = F \setminus \bigcup_{i=1}^k C_i$ has positive measure, let C_{k+1} be a rectifiable curve for which

$$\mathcal{H}^1(F_k \cap C_{k+1}) \geq \frac{1}{2} \sup \{\mathcal{H}^1(F_k \cap C) : C \text{ is rectifiable}\} > 0. \quad 5.7$$

If the process terminates, then for some k , the curves C_1, \dots, C_k cover almost all of F and F is curve-like.
 Otherwise,

$$\sum_{k=1}^{\infty} \mathcal{H}^1(F_k \cap C_{k+1}) \leq \mathcal{H}^1(F) < \infty$$

because the $F_k \cap C_{k+1}$ are disjoint, so that $\mathcal{H}^1(F_k \cap C_{k+1}) \rightarrow 0$ as $k \rightarrow \infty$. If $\mathcal{H}^1(F \setminus \bigcup_{i=1}^{\infty} C_i) > 0$, there is a rectifiable curve C such that $\mathcal{H}^1((F \setminus \bigcup_{i=1}^{\infty} C_i) \cap C) = d$ for some $d > 0$. But $\mathcal{H}^1(F_k \cap C_{k+1}) < \frac{1}{2}d$ for some k , so according to (5.7), C would have been selected in preference to C_{k+1} . Hence,

$\mathcal{H}^1(F \setminus \bigcup_{i=1}^{\infty} C_i) = 0$, and F consists of the curve-like set $F \cap \bigcup_{i=1}^{\infty} C_i$ together with $F \setminus \bigcup_{i=1}^{\infty} C_i$, which is of measure zero.

Thus, regular 1-sets are essentially unions of subsets of rectifiable curves, but irregular 1-sets contain no pieces of rectifiable curves at all. This dichotomy is remarkable in that the definition of regularity is purely in terms of densities and makes no reference to curves.

Propositions 5.6 and 5.8 provide a further contrast. Almost everywhere, a regular set has lower density 1, whereas an irregular set has lower density at most $\frac{3}{4}$. Thus, in any 1-set F , the set of points for which $\frac{3}{4} < \underline{D}^1(F, x) < 1$ has \mathcal{H}^1 -measure zero.

Regular 1-sets may be connected but, similar to sets of dimension less than 1, irregular 1-sets must be totally disconnected. We know at least that distinct points cannot be joined by a rectifiable curve in an irregular set, and further investigation shows that no two points can lie in the same connected component.

Further differences between regular and irregular sets include the existence of tangents (see Section 5.3) and projection properties (see Chapter 6). In all these ways, the classes of regular and irregular 1-sets are set apart from each other. For the special case of 1-sets, it would make sense mathematically to define fractals to be those sets which are irregular.

5.3 Tangents to s -sets

Suppose that a smooth curve C has a tangent (in the classical sense) at x . This means that close to x , the set C is concentrated in two diametrically opposite directions. What can be said about the directional distribution of an s -set about a typical point? Is there a meaningful definition of a tangent to an s -set, and when do such tangents exist?

Any generalisation of the definition of tangents should reflect the local directional distribution of sets of positive measure—for sets of

the complexity that we have in mind, there is no hope of a definition involving *all* nearby points; we must be content with a condition on *almost all* points. We say that an s -set F in \mathbb{R}^n has a *tangent at x in direction θ* , where θ is a unit vector, if

$$\overline{D}^s(F, x) > 0 \quad \text{5.8}$$

and for every angle $\varphi > 0$,

$$\lim_{r \rightarrow 0} r^{-s} \mathcal{H}^s(F \cap (B(x, r) \setminus S(x, \theta, \varphi))) = 0, \quad \text{5.9}$$

where $S(x, \theta, \varphi)$ is the *double sector* with vertex x , consisting of those y such that the line segment $[x, y]$ makes an angle at most φ with θ or $-\theta$ (see [Figure 5.4](#)). Thus, for a tangent in direction θ , (5.8) requires that a significant part of F lies near x , of which, by (5.9), a negligible amount close to x lies outside any double sector $S(x, \theta, \varphi)$ (see [Figure 5.5](#)).

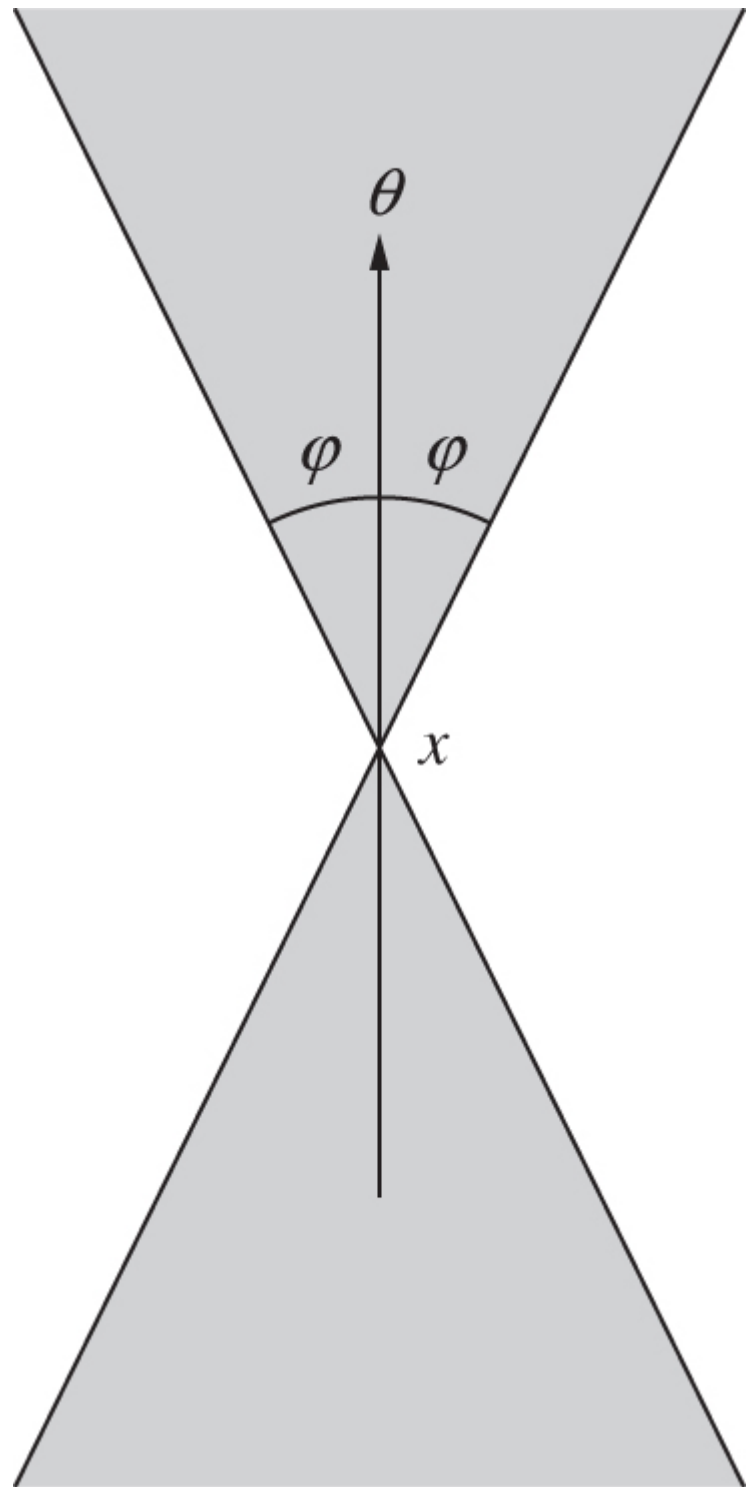


Figure 5.4. The double sector $S(x, \theta, \varphi)$.

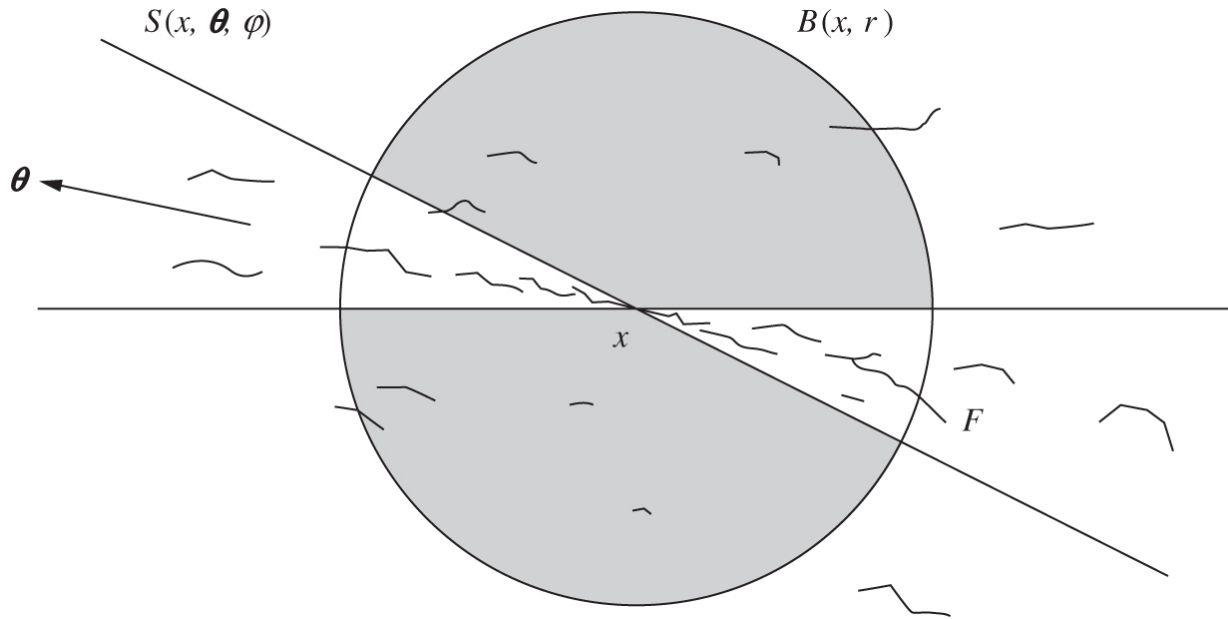


Figure 5.5 For F to have a tangent in direction θ at x , there must be a negligible part of F in $B(x, r) \setminus S(x, \theta, \varphi)$ (shaded) for small r .

We first discuss tangents to regular 1-sets in the plane, a situation not far removed from the classical calculus of curves.

Proposition 5.10

A rectifiable curve C has a tangent at almost all of its points.

Proof

By Lemma 5.5, the upper density $\overline{D}^1(C, x) = 1 > 0$ for almost all $x \in C$.

We may re-parametrise the defining function of the curve C by arc length, so that $\psi : [0, \mathcal{L}(C)] \rightarrow \mathbb{R}^2$ gives $\psi(t)$ as the point distance t along C from the end point $\psi(0)$. To say that $\mathcal{L}(C) < \infty$ simply means that ψ has bounded variation; in other words, $\sup \sum_{i=1}^m |\psi(t_i) - \psi(t_{i-1})| < \infty$ where the supremum is over dissections $0 = t_0 < t_1 < \dots < t_m = \mathcal{L}(C)$. We quote a standard result from the theory of functions that functions of bounded variation are differentiable almost everywhere, so $\psi'(t)$ exists as a vector for almost all t . Because of the arc-length parametrisation, $|\psi'(t)| = 1$ for such t . Hence, at almost all points $\psi(t)$ on C , there exists a unit vector θ such that $\lim_{u \rightarrow t} (\psi(u) - \psi(t))/(u - t) = \theta$. Thus, given $\varphi > 0$, there is a number $\varepsilon > 0$ such that $\psi(u) \in S(\psi(t), \theta, \varphi)$ whenever $|u - t| < \varepsilon$. As C has no double points, we may find r such that $\psi(u) \notin B(\psi(t), r)$ if $|u - t| \geq \varepsilon$, so $C \cap (B(\psi(t), r) \setminus S(\psi(t), \theta, \varphi))$ is empty. By the definitions (5.8) and (5.9), the curve C has a tangent at $\psi(t)$. Such points account for almost all points on C .

Just as with densities, we can transfer tangency properties from curves to curve-like sets.

Proposition 5.11

A regular 1-set F in \mathbb{R}^2 has a tangent at almost all of its points.

Proof

By definition of regularity, $\overline{D}^1(F, x) = 1 > 0$ at almost all $x \in F$.

If C is any rectifiable curve, then for almost all x in C , there exists θ such that if $\varphi > 0$

$$\begin{aligned}\lim_{r \rightarrow 0} r^{-1} \mathcal{H}^1((F \cap C) \cap (B(x, r) \setminus S(x, \theta, \varphi))) \\ \leq \lim_{r \rightarrow 0} r^{-1} \mathcal{H}^1(C \cap (B(x, r) \setminus S(x, \theta, \varphi))) = 0\end{aligned}$$

by Proposition 5.10. Moreover,

$$\begin{aligned}\lim_{r \rightarrow 0} r^{-1} \mathcal{H}^1((F \setminus C) \cap (B(x, r) \setminus S(x, \theta, \varphi))) \\ \leq \lim_{r \rightarrow 0} r^{-1} \mathcal{H}^1((F \setminus C) \cap B(x, r)) = 0\end{aligned}$$

for almost all $x \in C$ by Proposition 5.1(a). Adding these inequalities

$$\lim_{r \rightarrow 0} r^{-1} \mathcal{H}^1(F \cap (B(x, r) \setminus S(x, \theta, \varphi))) = 0$$

for almost all $x \in C$ and so for almost all $x \in F \cap C$. As a countable collection of such curves covers almost all of F , the result follows.

In contrast to regular sets, irregular 1-sets do not generally support tangents.

Proposition 5.12

At almost all points of an irregular 1-set, no tangent exists.

Proof

The proof, which depends on the characterisation of irregular sets as curve-free sets, is too involved to include here.

We turn now to s -sets in \mathbb{R}^2 for non-integral s , which, as we have seen, are necessarily irregular. For $0 < s < 1$, tangency questions are not particularly interesting, because any set contained in a smooth curve will automatically satisfy (5.9) with θ the direction of the tangent to the curve at x . For example, the middle third Cantor set F regarded as a subset of the plane is a $(\log 2 / \log 3)$ -set that satisfies (5.8) and (5.9) for all x in F and $\varphi > 0$, where θ is a vector pointing along the set. On the other hand, if F , say, is a Cartesian product of two uniform Cantor sets, each formed by repeated removal of a proportion $\alpha > \frac{1}{2}$ from the centre of intervals, then a little calculation (see Chapter 7) shows that F is an s -set with $s = 2 \log 2 / \log(2/(1 - \alpha)) < 1$ with no tangents at any of its points.

It is at least plausible that s -sets in \mathbb{R}^2 with $1 < s < 2$ do not have tangents—such sets are so large that they radiate in many directions from a typical point, so that (5.9) cannot hold. This is made precise in the following proposition.

Proposition 5.13

If F is an s -set in \mathbb{R}^2 with $1 < s < 2$, then at almost all points of F no tangent exists.

Proof

For $r_0 > 0$, let

$$E = \{y \in F : \mathcal{H}^s(F \cap B(y, r)) < 2(2r)^s \text{ for all } r < r_0\}. \quad \text{5.10}$$

For each $x \in E$, each unit vector θ , and each angle φ with $0 < \varphi < \frac{1}{2}\pi$, we estimate how much of E lies in $B(x, r) \cap S(x, \theta, \varphi)$. For $r < r_0/20$ and $i = 1, 2, \dots$, let A_i be the intersection of the annulus and the double sector given by

$$A_i = (B(x, ir\varphi) \setminus B(x, (i-1)r\varphi)) \cap S(x, \theta, \varphi).$$

Then $B(x, r) \cap S(x, \theta, \varphi) \subset \bigcup_{i=1}^m A_i \cup \{x\}$ for some integer $m < 2/\varphi$. Each A_i comprises two parts, both of diameter at most $10r\varphi < r_0$, so applying (5.10) to the parts that contain points of E , and summing,

$$\mathcal{H}^s(E \cap B(x, r) \cap S(x, \theta, \varphi)) \leq 2m2(20r\varphi)^s \leq (4\varphi^{-1})2(20r\varphi)^s$$

so that

$$(2r)^{-s} \mathcal{H}^s(E \cap B(x, r) \cap S(x, \theta, \varphi)) \leq 8.10^s \varphi^{s-1} \quad \text{5.11}$$

if $r < r_0/20$.

Now, almost all $x \in E$ satisfy $\overline{D}^s(F \setminus E, x) = 0$ by Proposition 5.1(a). Decomposing $F \cap B(x, r)$ into three parts, we get

$$\begin{aligned} \mathcal{H}^s(F \cap B(x, r)) &= \mathcal{H}^s((F \setminus E) \cap B(x, r)) + \mathcal{H}^s(E \cap B(x, r) \cap S(x, \theta, \varphi)) \\ &\quad + \mathcal{H}^s(E \cap (B(x, r) \setminus S(x, \theta, \varphi))). \end{aligned}$$

Dividing by $(2r)^s$ and taking upper limits as $r \rightarrow 0$,

$$\overline{D}^s(F, x) \leq 0 + 8.10^s \varphi^{s-1} + \limsup_{r \rightarrow 0} (2r)^{-s} \mathcal{H}^s(E \cap (B(x, r) \setminus S(x, \theta, \varphi)))$$

for almost all $x \in E$, using (5.11). Choosing φ sufficiently small, it follows that for all θ , both (5.8) and (5.9) cannot hold, so no tangent exists at such x . To complete the proof, we note that almost all $x \in F$ belong to the set E defined in (5.10) for some $r_0 > 0$, by Proposition 5.1(b).

The results of this chapter begin to provide a local picture of fractals that are s -sets. By taking these methods rather further, it is possible to obtain much more precise estimates of densities and also of the directional distributions of s -sets about typical points. For example, it may be shown that if $s > 1$, almost every line through \mathcal{H}^s -almost every point of an s -set F intersects F in a set of dimension $s - 1$.

Recently, packing measures (see Section 3.5) have been employed in the study of local properties, and it has been shown that regularity of a set corresponds closely to the equality of its packing measure and (slightly modified) Hausdorff measure.

These ideas extend, albeit with considerable effort, to higher dimensions. Regular s -sets in \mathbb{R}^n may be defined using densities and, again, s -sets can only be regular if s is an integer. Regular s -sets have tangents almost everywhere and are ‘ s -dimensional-surface-like’ in the sense that, except for a subset of \mathcal{H}^s -measure zero, they may be covered by a countable collection of Lipschitz images of subsets of \mathbb{R}^s .

5.4 Notes and references

This chapter touches the surface of a deep area of mathematics known as *geometric measure theory*. It has its origins in the fundamental papers of Besicovitch (1928, 1938), which contain a remarkably complete analysis of 1-sets in the plane. Higher-dimensional analogues are obtained by Mattila (1975a). The results on s -sets in the plane for non-integral s are due to Marstrand (1954a). A succession of writers have extended this work to subsets of higher-dimensional space, culminating in the paper of Preiss

(1987), which solved many of the outstanding problems. More detailed discussions of regular and irregular sets may be found in Falconer (1985a); Federer (1996) and Mattila (1999). Modern approaches use *tangent measures*, introduced by Preiss (1987), which are described in Falconer (1997) and Mattila (1999). It is widely believed that the ' $\frac{3}{4}$ ' in Proposition 5.8 can be replaced by ' $\frac{1}{2}$ '. Farag (2002) has shown this in many cases, and Preiss and Tiser (1992) obtain $(2 + \sqrt{46})/12 = 0.732\dots$ in general.

Exercises

5.1 By applying Proposition 5.1 with $s = n = 2$, deduce the Lebesgue density theorem (5.1).

5.2 Let $f : \mathbb{R} \rightarrow \mathbb{R}$ be a continuously differentiable function such that $0 < c_1 \leq f'(x) \leq c_2$ for all x . Show that if F is an s -set in \mathbb{R} , then $\underline{D}^s(f(F), f(x)) = \underline{D}^s(F, x)$ for all x in \mathbb{R} , with a similar result for upper densities.

5.3 Let F be the middle third Cantor set. Show that $\underline{D}^s(F, x) \leq 2^{-s}$ for all x , where $s = \log 2 / \log 3$. Deduce that F is irregular.

5.4 The Cantor dust depicted in [Figure 0.4](#) is a 1-set. Estimate the upper and lower densities at points of the Cantor dust and show that it is irregular.

5.5 Adapt the proof of Theorem 5.2 to show that if F is an s -set with $0 < s < 1$, then $\underline{D}^s(F, x) \leq (1 + 2^{s/(s-1)})^{s-1}$ for almost all x .

5.6 Construct a regular 1-set that is totally disconnected. (Hint: start with an interval.)

5.7 Let E and F be s -sets in \mathbb{R}^2 such that for every disc $B(x, r)$, we have that $\mathcal{H}^s(B(x, r) \cap E) \leq \mathcal{H}^s(B(x, r) \cap F)$. Show that $\mathcal{H}^s(E \setminus F) = 0$. Does this imply $E \subset F$?

5.8 Let F_1, F_2, \dots be 1-sets in the plane such that $F = \bigcup_{k=1}^{\infty} F_k$ is a 1-set. Show that if F_k is regular for all k , then F is regular, and if F_k is irregular for all k , then F is irregular.

5.9 Show that if E is a regular 1-set and F an irregular 1-set, then $\mathcal{H}^1(E \cap F) = 0$.

Chapter 6

Projections of fractals

In this chapter, we consider the orthogonal projection or ‘shadow’ of fractals in \mathbb{R}^n onto lower-dimensional subspaces. A smooth (1-dimensional) curve in \mathbb{R}^3 generally has a (1-dimensional) curve as its shadow on a plane, but a (2-dimensional) surface or (3-dimensional) solid object generally has a 2-dimensional shadow, as in [Figure 6.1a](#). We examine analogues of this for fractals. Intuitively, one would expect a set F in \mathbb{R}^3 to have plane projections of dimension 2 if $\dim_H F > 2$ and of dimension $\dim_H F$ if $\dim_H F < 2$, as in [Figure 6.1b](#). Roughly speaking this is correct, but a precise formulation of the projection properties requires some care.

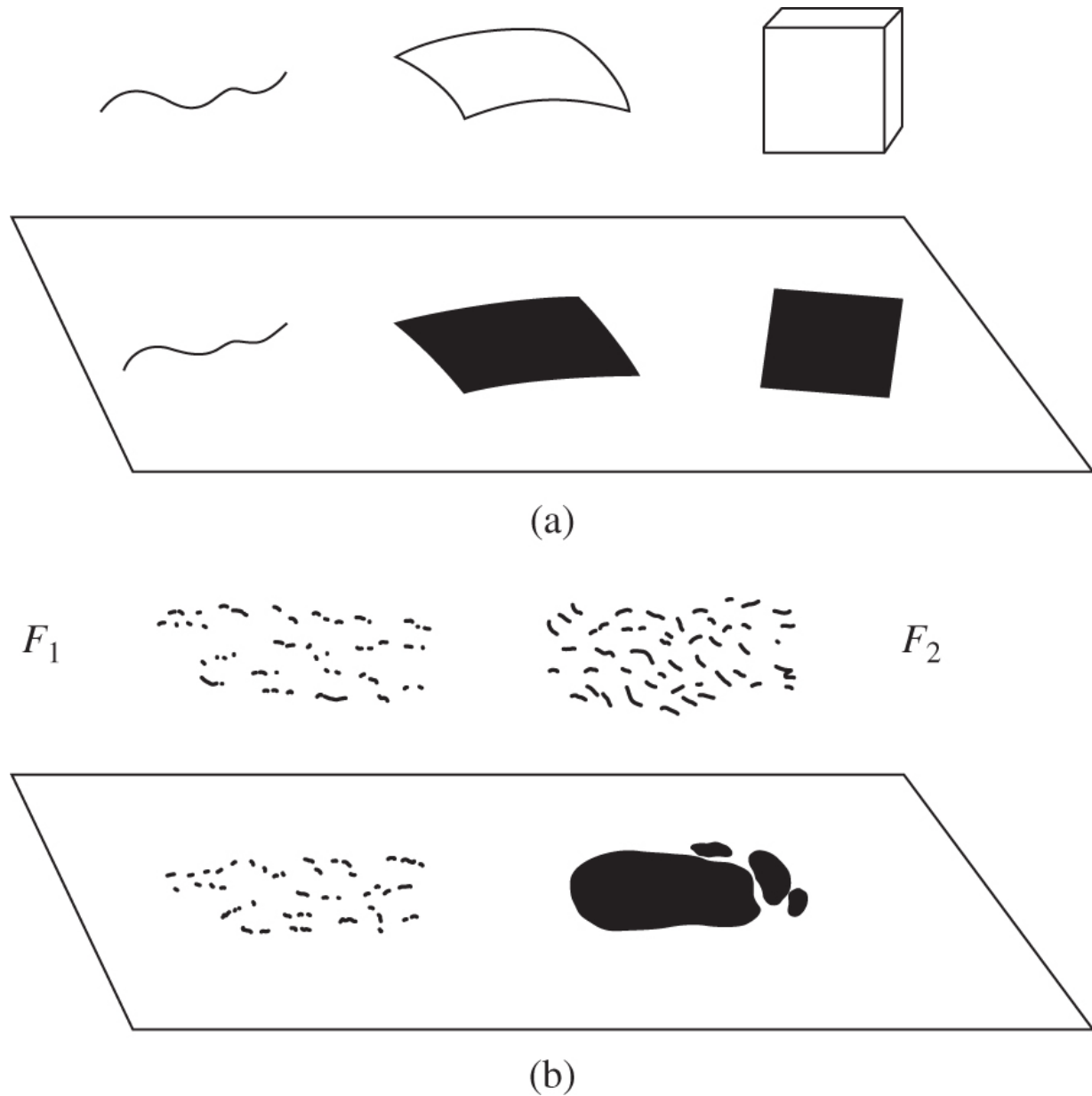


Figure 6.1 (a) Projections of classical sets onto a plane—a curve ‘typically’ has projection of dimension 1, but the surface and cube have projections of dimension 2 and of positive area. (b) Projections of fractal sets onto a plane. If $\dim_H F_1 < 1$ and $\dim_H F_2 > 1$, then ‘typically’, the projection of F_1 has dimension equal to $\dim_H F_1$ (and zero area) and the projection of F_2 has dimension 2 and positive area.

We prove the projection theorems in the simplest case, for projection of subsets of the plane onto lines, and then state the

higher-dimensional analogues.

6.1 Projections of arbitrary sets

Let L_θ be the line through the origin of \mathbb{R}^2 that makes an angle θ with the horizontal axis. We denote orthogonal projection onto L_θ by proj_θ , so that if F is a subset of \mathbb{R}^2 , then $\text{proj}_\theta F$ denotes the projection of F onto L_θ (see [Figure 6.2](#)). Clearly, $|\text{proj}_\theta x - \text{proj}_\theta y| \leq |x - y|$ if $x, y \in \mathbb{R}^2$, that is, proj_θ is a Lipschitz mapping. Thus

$$\dim_H(\text{proj}_\theta F) \leq \min \{\dim_H F, 1\} \quad \text{6.1}$$

for any F and θ , by Proposition 3.3(a). (As $\text{proj}_\theta F$ is a subset of the line L_θ , its dimension cannot be more than 1.) The interesting question is whether the opposite inequality is valid. The projection theorems tell us that this is so for almost all $\theta \in [0, \pi)$; that is, the exceptional values of θ for which inequality (6.1) is strict form a set of zero length, that is, zero 1-dimensional Lebesgue measure.

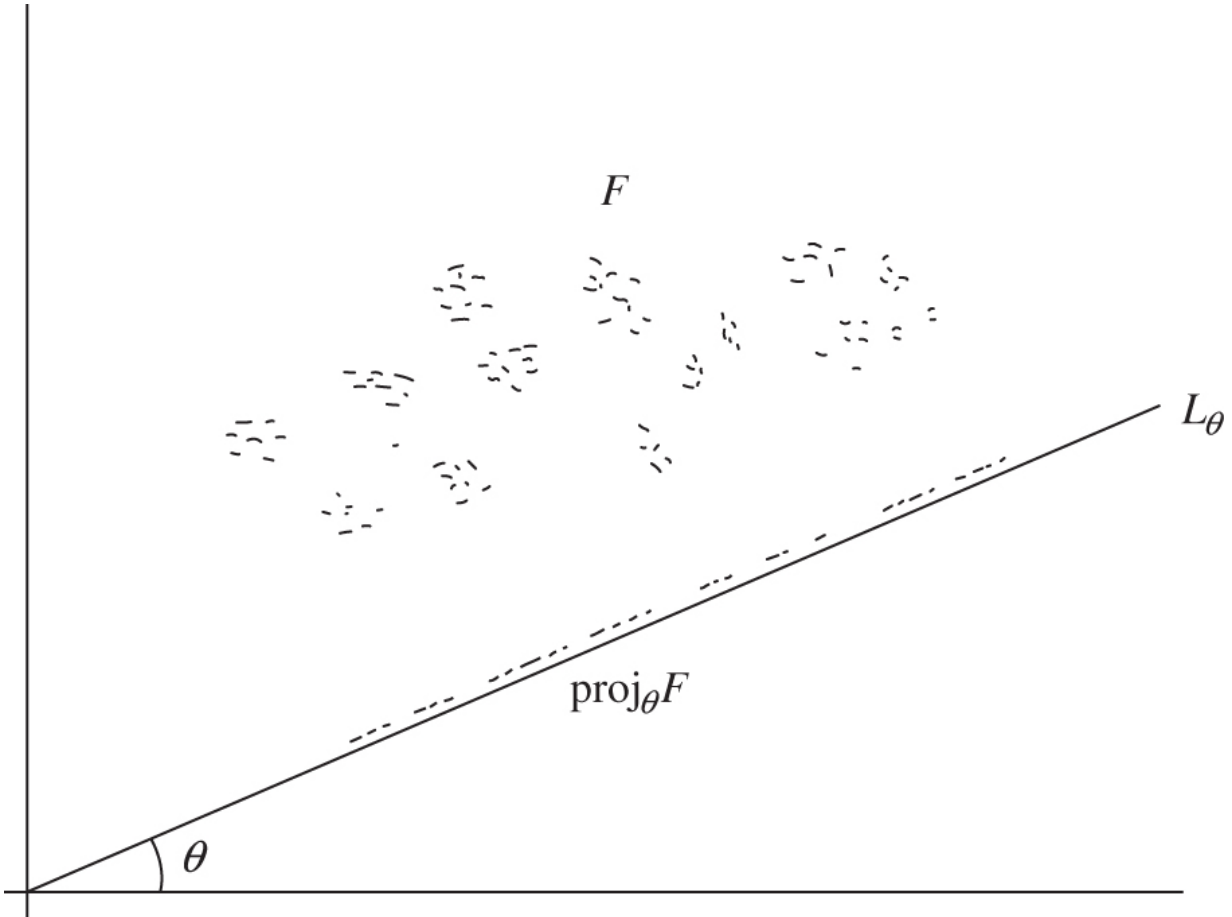


Figure 6.2 Projection of a set F onto a line L_θ .

Projection theorem 6.1

Let $F \subset \mathbb{R}^2$ be a Borel set.

- a. If $\dim_H F \leq 1$, then $\dim_H(\text{proj}_\theta F) = \dim_H F$ for almost all $\theta \in [0, \pi]$,
- b. If $\dim_H F > 1$, then $\text{proj}_\theta F$ has positive length (as a subset of L_θ), and thus has dimension 1, for almost all $\theta \in [0, \pi]$.

Proof

We give a proof that uses the potential theoretic characterisation of Hausdorff dimension in a very effective way. If $s < \dim_H F \leq 1$, then by Theorem 4.13(b), there exists a mass distribution μ on (a compact subset of) F with $0 < \mu(F) < \infty$ and

$$\int_F \int_F \frac{d\mu(x)d\mu(y)}{|x - y|^s} < \infty. \quad \underline{6.2}$$

For each θ , we project the mass distribution μ onto the line L_θ to get a mass distribution μ_θ on $\text{proj}_\theta F$. Thus, μ_θ is defined by the requirement that

$$\mu_\theta(A) = \mu\{x \in \mathbb{R}^2 : \text{proj}_\theta x \in A\}$$

for each interval $A \subset L_\theta$, or equivalently,

$$\int_{-\infty}^{\infty} f(t)d\mu_\theta(t) = \int_F f(x \cdot \theta)d\mu(x)$$

for each non-negative function f , where we identify L_θ with \mathbb{R} in the obvious way. (Here, θ is the unit vector in the direction θ , with x identified with its position vector and $x \cdot \theta$ the usual scalar product.) Then

$$\begin{aligned} \int_0^\pi \left[\int_{-\infty}^{\infty} \int_{-\infty}^{\infty} \frac{d\mu_\theta(u)d\mu_\theta(v)}{|u - v|^s} \right] d\theta &= \int_0^\pi \left[\int_F \int_F \frac{d\mu(x)d\mu(y)}{|x \cdot \theta - y \cdot \theta|^s} \right] d\theta \\ &= \int_0^\pi \left[\int_F \int_F \frac{d\mu(x)d\mu(y)}{|(x - y) \cdot \theta|^s} \right] d\theta \\ &= \int_F \int_F \int_0^\pi \frac{d\theta}{|\tau_{x-y} \cdot \theta|^s} \frac{d\mu(x)d\mu(y)}{|x - y|^s} \\ &= \int_F \int_F C_s \frac{d\mu(x)d\mu(y)}{|x - y|^s} < \infty, \end{aligned} \quad \underline{6.3}$$

where τ_{x-y} is the unit vector in the direction of $x - y$ and

$$c_s \equiv \int_0^\pi \frac{d\theta}{|\tau_{x-y} \cdot \theta|^s} = \int_0^\pi \frac{d\theta}{|\cos(\tau - \theta)|^s} < \infty$$

as $s < 1$, this integral being independent of τ_{x-y} . Then (6.3) is finite by virtue of (6.2). Hence,

$$\int_{-\infty}^{\infty} \int_{-\infty}^{\infty} \frac{d\mu_\theta(u)d\mu_\theta(v)}{|u-v|^s} < \infty$$

for almost all $\theta \in [0, \pi]$. By Theorem 4.13(a), the existence of such a mass distribution μ_θ on $\text{proj}_\theta F$ implies that $\dim_H(\text{proj}_\theta F) \geq s$. This is true for all $s < \dim_H F$, so part (a) of the result follows.

For (b), the same argument as in (a) gives that $\dim_H \text{proj}_\theta F = 1$ for almost all θ ; the proof that the projections have positive length follows similar lines, although Fourier transforms need to be introduced.

These projection theorems generalise to higher dimensions in the natural way. Let $G_{n,k}$ be the set of k -dimensional subspaces or ‘ k -planes through the origin’ in \mathbb{R}^n . These subspaces are naturally parametrised by $k(n-k)$ coordinates (‘generalised direction cosines’) so that we may refer to ‘almost all’ subspaces in a consistent way in terms of $k(n-k)$ -dimensional Lebesgue measure. We write proj_Π for orthogonal projection onto the k -plane Π .

Theorem 6.2 Higher-dimensional projection theorem

Let $F \subset \mathbb{R}^n$ be a Borel set.

- a. If $\dim_H F \leq k$, then $\dim_H(\text{proj}_\Pi F) = \dim_H F$ for almost all $\Pi \in G_{n,k}$.
- b. If $\dim_H F > k$, then $\text{proj}_\Pi F$ has positive k -dimensional measure, and so has dimension k , for almost all $\Pi \in G_{n,k}$.

Proof

The proof of Theorem 6.1 extends to higher dimensions without difficulty.

Thus, if F is a subset of \mathbb{R}^3 , the plane projections of F are, in general, of dimension $\min\{2, \dim_H F\}$. This result has important practical implications. We can estimate the dimension of an object in space by estimating the dimension of a photograph taken from a random direction. Provided this is less than 2, it is reasonable to assume that it equals the dimension of the object. Such a reduction can make dimension estimates of spatial objects tractable—box-counting methods are difficult to apply in three dimensions but can be applied with reasonable success in the plane.

6.2 Projections of s-sets of integral dimension

If a subset F of \mathbb{R}^2 has Hausdorff dimension exactly 1, then Theorem 6.1 tells us that the projections of F onto almost every L_θ have dimension 1. However, in this critical case, no information is given as to whether these projections have zero or positive length. In the special case, where F is a 1-set, that is, with $0 < \mathcal{H}^s(F) < \infty$, an analysis is possible. Recall from Theorem 5.3 that a 1-set may be decomposed into a regular curve-like part and an irregular dust-like part. The following two theorems provide another sharp contrast between these types of set.

Theorem 6.3

Let F be a regular 1-set in \mathbb{R}^2 . Then $\text{proj}_\theta F$ has positive length except for at most one $\theta \in [0, \pi)$.

Sketch of proof

By Theorem 5.9(b), it is enough to prove the result if F is a subset of positive length of a rectifiable curve C . Using the Lebesgue density theorem to approximate to such an F by short continuous subcurves of C , essentially, all we need to consider is the case when F is itself a rectifiable curve C_1 . But clearly, the projection onto L_θ of such a curve is of positive length for all θ , except in the case where C_1 is a straight line segment in which case there is a single exceptional direction θ perpendicular to the segment.

In general, for a regular 1-set F , $\text{proj}_\theta F$ will have positive length for *all* θ , unless, to within a set of \mathcal{H}^1 -measure 0, F is contained in a set of parallel line segments, in which case there is a single direction in which the projection has length 0.

Theorem 6.4

Let F be an irregular 1-set in \mathbb{R}^2 . Then $\text{proj}_\theta F$ has length zero for almost all $\theta \in [0, \pi)$.

Proof

We omit the complicated proof, which depends on the intricate density and angular density structure of irregular 1-sets.

These theorems may be combined in several ways.

Corollary 6.5

Let F be a 1-set in \mathbb{R}^2 . If the regular part of F has \mathcal{H}^1 -measure zero, then $\text{proj}_\theta F$ has length zero for almost all θ ; otherwise it has positive length for all but at most one value of θ .

The following characterisation of irregular sets is also useful.

Corollary 6.6

A 1-set in \mathbb{R}^2 is irregular if and only if it has projections of zero length in at least two directions.

Example 6.7

The Cantor dust F of Figure 0.4 is an irregular 1-set.

Calculation

In Example 3.6, we showed that F is a 1-set. The projections of F onto the lines L_θ where $\tan \theta = \frac{1}{2}$ and $\tan \theta = -2$ are just copies of the middle third Cantor set and have length 0, so F is irregular by Corollary 6.6.

The results of this section have been stated for sets for which $0 < \mathcal{H}^1(F) < \infty$, which is quite a strong property for 1-dimensional sets, although one which occurs surprisingly often. However, the theorems can be applied rather more widely. If F is any set that intersects some rectifiable curve in a set of positive length, so that F contains a regular subset, then $\text{proj}_\theta F$ has positive length for

almost all θ . Again, if F is a σ -finite irregular set, that is, one which may be expressed as a countable union of irregular 1-sets each of finite measure, then $\text{proj}_\theta F$ has zero length for almost all θ ; this follows by taking countable unions of the projections of these component 1-sets.

For the record, we state the higher-dimensional analogue of Theorems 6.3 and 6.4, although the proofs are even more complicated than in the plane case.

Theorem 6.8

Let F be a k -set in \mathbb{R}^n , where k is an integer.

- a. If F is regular, then $\text{proj}_\Pi F$ has positive k -dimensional measure for almost all $\Pi \in G_{n,k}$.
- b. If F is irregular, then $\text{proj}_\Pi F$ has zero k -dimensional measure for almost all $\Pi \in G_{n,k}$.

6.3 Projections of arbitrary sets of integral dimension

The theorems of Section 6.2, although mathematically elegant and sophisticated, do not provide a complete answer to the question of whether projections of plane sets onto lines have zero or positive length. A subset F of \mathbb{R}^2 of Hausdorff dimension 1 need not be a 1-set or even be of σ -finite \mathcal{H}^1 -measure (i.e. a countable union of sets of finite \mathcal{H}^1 -measure). Moreover, there need not be any dimension function h (see Section 1.7) for which $0 < \mathcal{H}^h(F) < \infty$, in which case mathematical analysis is extremely difficult. What can be said about the projections of such sets? The surprising answer is that by working in this rather delicate zone of sets of Hausdorff dimension 1 but of non- σ -finite \mathcal{H}^1 -measure, we can construct sets with

projections more or less what we please. For example, there is a set F in \mathbb{R}^2 such that $\text{proj}_\theta F$ contains an interval of length 1 for almost all θ with $0 \leq \theta < \frac{1}{2}\pi$ but with $\text{proj}_\theta F$ of length zero for $\frac{1}{2}\pi \leq \theta < \pi$.

More generally, we have the following result which says that there exist sets for which the projections in almost all directions are, to within length zero, anything that we care to prescribe. The measurability condition in square brackets is included for completeness but should not distract from the rest of the statement.

Theorem 6.9

Let G_θ be a subset of L_θ for each $\theta \in [0, \pi)$ [such that the set $\bigcup_{0 \leq \theta < \pi} G_\theta$ is plane Lebesgue measurable]. Then there exists a Borel set $F \subset \mathbb{R}^2$ such that

- a. $\text{proj}_\theta F \supset G_\theta$ for all θ ,
- b. $\text{length } (\text{proj}_\theta F \setminus G_\theta) = 0$ for almost all θ .

In particular, for almost all θ , the sets G_θ and $\text{proj}_\theta F$ differ by zero length.

Idea of proof

Without going into much detail, we indicate the basic building block for such sets, which has been termed the ‘iterated Venetian blind’ construction. This is shown in [Figure 6.3](#). Let E be a line segment of length λ . Let ε be a small angle and k a large number. We replace E by k line segments of lengths roughly λ/k , each at an angle ε to E and with end points equally spaced along E to form a new set, E_1 . We repeat this process with each segment of E_1 to form a set E_2 consisting of k^2 line segments all of lengths about λ/k^2 and at angle 2ε to E . We continue in this way, to get E_r , a set of k^r segments all of lengths about λ/k^r and at angle $r\varepsilon$ to E . We stop when r is such that $r\varepsilon$ is, say, about $\frac{1}{4}\pi$. Comparing the projections of E_r with that of the original line segment E , we see that if $0 \leq \theta < \frac{1}{2}\pi$, then $\text{proj}_\theta E$ and $\text{proj}_\theta E_r$ are nearly the same (since lines perpendicular to L_θ that cut E also cut E_r). However, if $-\frac{1}{4}\pi < \theta < 0$, then $\text{proj}_\theta E_r$ will have very small length, since most lines perpendicular to L_θ will pass straight between appropriately angled ‘slats’ of the construction. Thus, the projections of E_r are very similar to those of E in certain directions but are almost negligible in other directions. This idea may be adapted to obtain sets with projections very close to G_θ in a narrow band of directions but with almost null projections in other directions. Taking unions of such sets for various small bands of directions gives a set with approximately the required property. Taking a limit of a sequence of sets that give increasingly accurate approximations leads to a set with the properties stated.

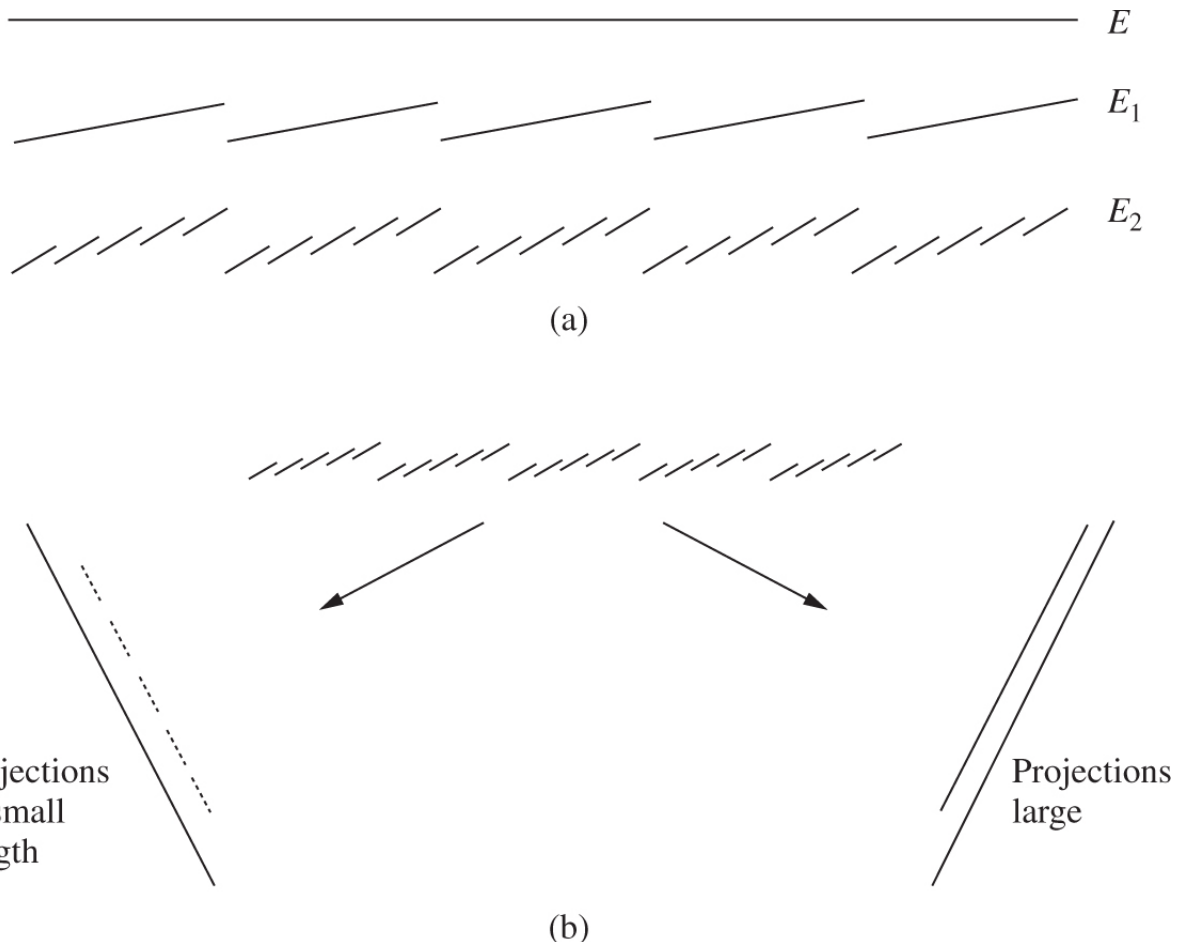


Figure 6.3 (a) The ‘iterated Venetian blind’ construction. (b) Projections in certain bands of directions have large lengths, whilst projections in other bands of directions have very small lengths.

This construction may be extended to higher dimensions: there exists a set F in \mathbb{R}^n such that almost all projections of F onto k -dimensional subspaces differ from prescribed sets by zero k -dimensional measure. In particular, there exists a set of Hausdorff dimension 2 in 3-dimensional space with almost all of its plane shadows anything we care to prescribe to within zero area. By specifying the shadows to be the thickened digits of the time when the sun is shining from a perpendicular direction, we obtain, at least in theory, a digital sundial (see [Figure 6.4](#)). As the sun moves across the sky, we get different projections of the set. The notion of a digital sundial was introduced to provide an intuitive view of this result, rather than as a feasible method of chronography, but,

amazingly, working digital sundials have recently been manufactured, albeit depending on a different principle!

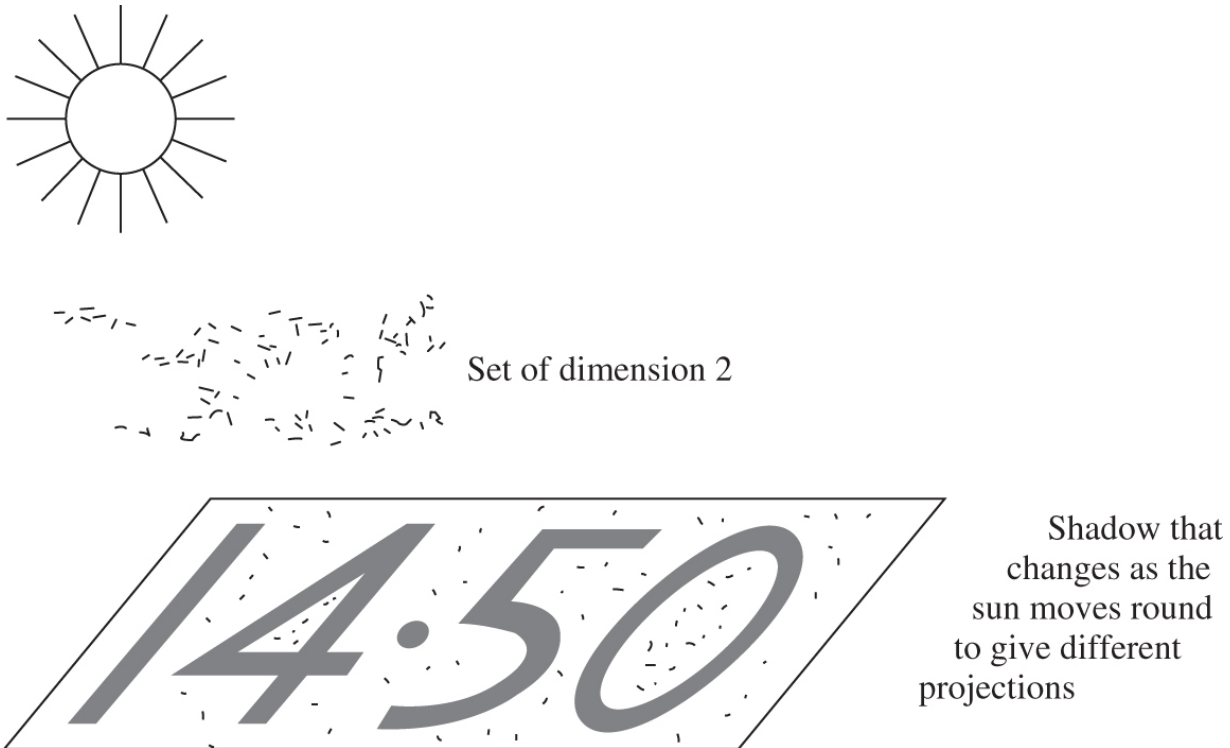


Figure 6.4 A digital sundial.

6.4 Notes and references

A geometric proof of the projection theorems for arbitrary subsets of the plane was given by Marstrand (1954a); the potential theoretic proof was due to Kaufman (1968). Mattila (1975b) obtained various generalisations including extensions to higher dimensions. The projection results for regular and irregular 1-sets in the plane are, surprisingly, rather older, dating back to Besicovitch (1939), with the analogous results for s -sets in \mathbb{R}^n in the mammoth paper of Federer (1947). More detailed accounts of the projection theorems are in Falconer (1985a) and Mattila (1999). Projection results for box and packing dimensions are more subtle, see Falconer and Howroyd (1997) and Howroyd (2001). A dual version of Theorem 6.9 was given by Davies (1952) and a direct proof, with the higher-dimensional generalisations, by Falconer (1986a).

The exceptional set of θ or Π for which the conclusions of Theorems 6.1 and 6.2 fail cannot be too large, and Kaufman (1968); Mattila (1975b) and Falconer (1982) have obtained bounds for the Hausdorff dimension of these exceptional sets. Peres and Schlag (2000) have extended these results on projections to the dimensions of images of sets under very general families of functions that satisfy a ‘transversality’ condition. Recently, dimensions of *all* projections of certain types of set, such as self-similar sets (see Chapter 9) have been analysed using sophisticated methods from ergodic theory, see Furstenberg (2008) and Hochman and Shmerkin (2012).

Exercises

6.1 Let $E = F \times F \subset \mathbb{R}^2$ where F is the middle λ Cantor set. (E has Hausdorff dimension $2\log 2/\log(2/(1-\lambda))$, see Examples 4.5 and 7.6.) What is $\dim_H \text{proj}_\theta E$ (a) for a typical θ and (b) for $\theta = 0$ and $\theta = \pi/2$?

6.2 Let E be the ‘circular Cantor set’ given in complex number form by $E = \{e^{2\pi i\varphi} : \varphi \in F\}$ where F is the middle third Cantor set. What is $\dim_H \text{proj}_\theta E$ for each θ ?

6.3 For each $0 < s < 1$, give an example of an s -set F in \mathbb{R}^2 such that $\text{proj}_\theta F$ is an s -set for all θ .

6.4 Let E and F be subsets of \mathbb{R} with Hausdorff dimensions strictly between 0 and 1. You are given that the subset $E \times F$ of \mathbb{R}^2 has Hausdorff dimension at least $\dim_H E + \dim_H F$ (see Chapter 9). Show that the projections of $E \times F$ onto the coordinate axes are always ‘exceptional’ as far Projection theorem 6.1 is concerned.

6.5 Show that $\dim_H \text{proj}_\theta F \geq \dim_H F - 1$ for all $F \subset \mathbb{R}^2$ and all θ .

6.6 Let F be an irregular 1-set in the plane. Deduce from Theorem 6.4 that F is totally disconnected.

6.7 Let F be a connected subset of \mathbb{R}^2 containing more than one point. Show that $\text{proj}_\theta F$ has positive length for all except possibly

one value of θ . (Thus the projection theorems in the plane are only really of interest for sets that are not connected.)

6.8 Let E and F be subsets of \mathbb{R} . Show that for almost all real numbers λ , $\dim_H(E + \lambda F) = \min\{1, \dim_H(E \times F)\}$, where $E + \lambda F$ denotes the set of real numbers $\{x + \lambda y : x \in E, y \in F\}$.

6.9 Show that the conclusion of Theorem 6.4 remains true if F is a countable union of irregular 1-sets.

6.10 Let E and F be any subsets of \mathbb{R} of length (1-dimensional Lebesgue measure) 0. Show that any rectifiable curve in \mathbb{R}^2 intersects the product $E \times F$ in a set of length 0.

6.11 If F is a set and x is a point in \mathbb{R}^2 , the projection of F at x , denoted by $\text{proj}_x F$, is defined as the set of θ in $[0, 2\pi)$ such that the half-line emanating from x in direction θ intersects F . Let L be a line. Show that if $\dim_H F \leq 1$, then $\dim_H \text{proj}_x F = \dim_H F$ for almost all x on L (in the sense of Lebesgue measure) and if $\dim_H F > 1$ then $\text{proj}_x F$ has positive length for almost all x on L . (Hint: consider a sphere tangential to the plane and a transformation that maps a point x on the plane to the point on the sphere intersected by the line joining x to the centre of the sphere.)

6.12 Let $F \subset \mathbb{R}^2$. Show that for all θ , $\underline{\dim}_B \text{proj}_\theta F \leq \underline{\dim}_B F$, $\overline{\dim}_B \text{proj}_\theta F \leq \overline{\dim}_B F$ and $\dim_P \text{proj}_\theta F \leq \dim_P F$. Show that $\dim_P \text{proj}_\theta F = \dim_P F$ for almost all θ if $\dim_P F = \dim_H F$.

Chapter 7

Products of fractals

One way of constructing ‘new fractals from old’ is by forming Cartesian products. Indeed, many fractals that occur in practice, for example, as attractors of certain dynamical systems, are products or, at least, locally product-like. In this chapter, we develop dimension formulae for products.

7.1 Product formulae

Recall that if E is a subset of \mathbb{R}^n and F is a subset of \mathbb{R}^m , the *Cartesian product*, or just *product*, $E \times F$ is defined as the set of points with first coordinate in E and second coordinate in F , that is,

$$E \times F = \{(x, y) \in \mathbb{R}^{n+m} : x \in E, y \in F\}. \quad 7.1$$

Thus, if E is a unit interval in \mathbb{R} , and F is a unit interval in \mathbb{R}^2 , then $E \times F$ is a unit square in \mathbb{R}^3 ([Figure 7.1](#)). Again, if F is the middle third Cantor set, then $F \times F$ is the ‘Cantor product’ ([Figure 7.2](#)) consisting of those points in the plane with both coordinates in F .

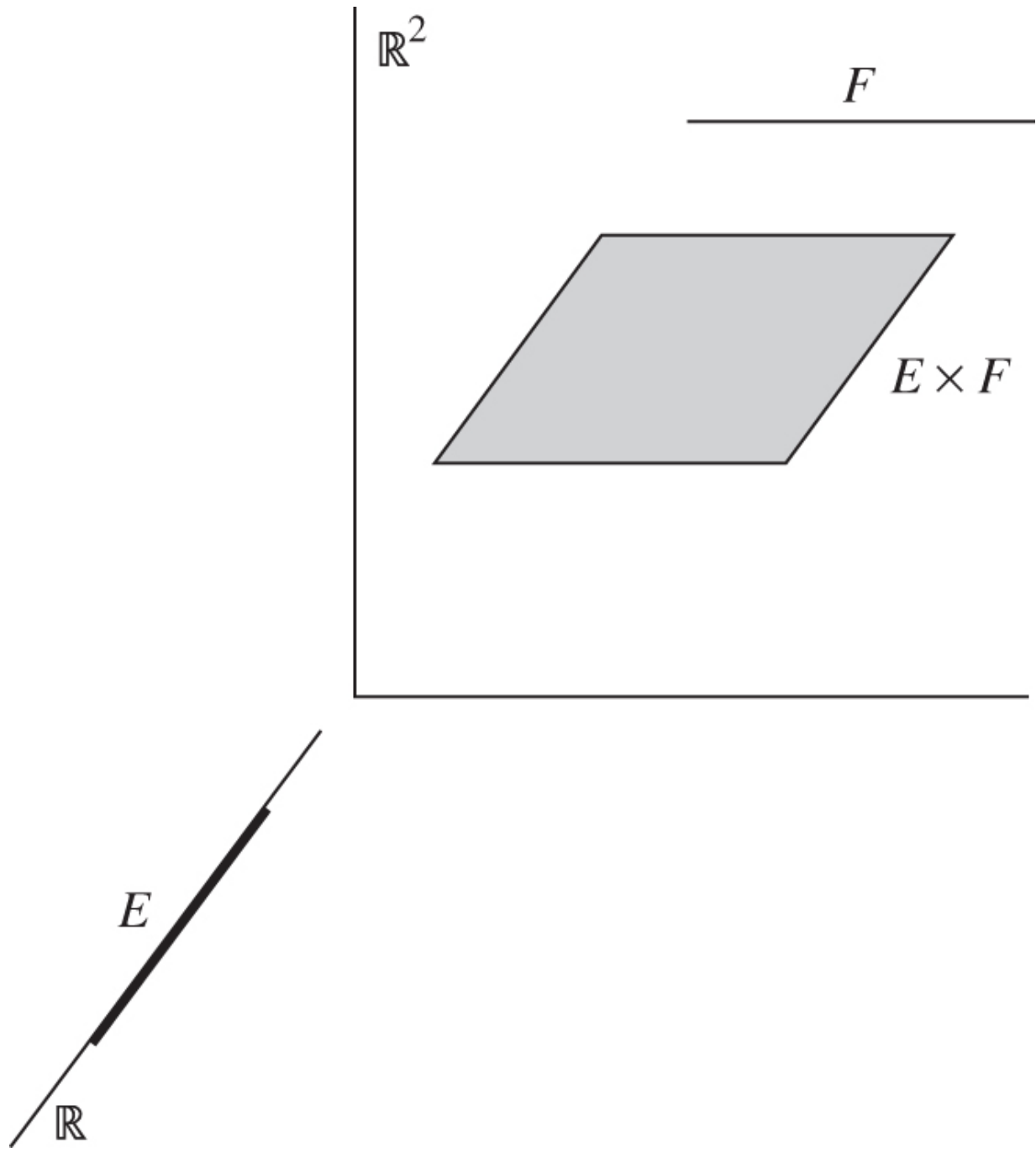


Figure 7.1 The Cartesian product of a unit interval in \mathbb{R} and a unit interval in \mathbb{R}^2 .

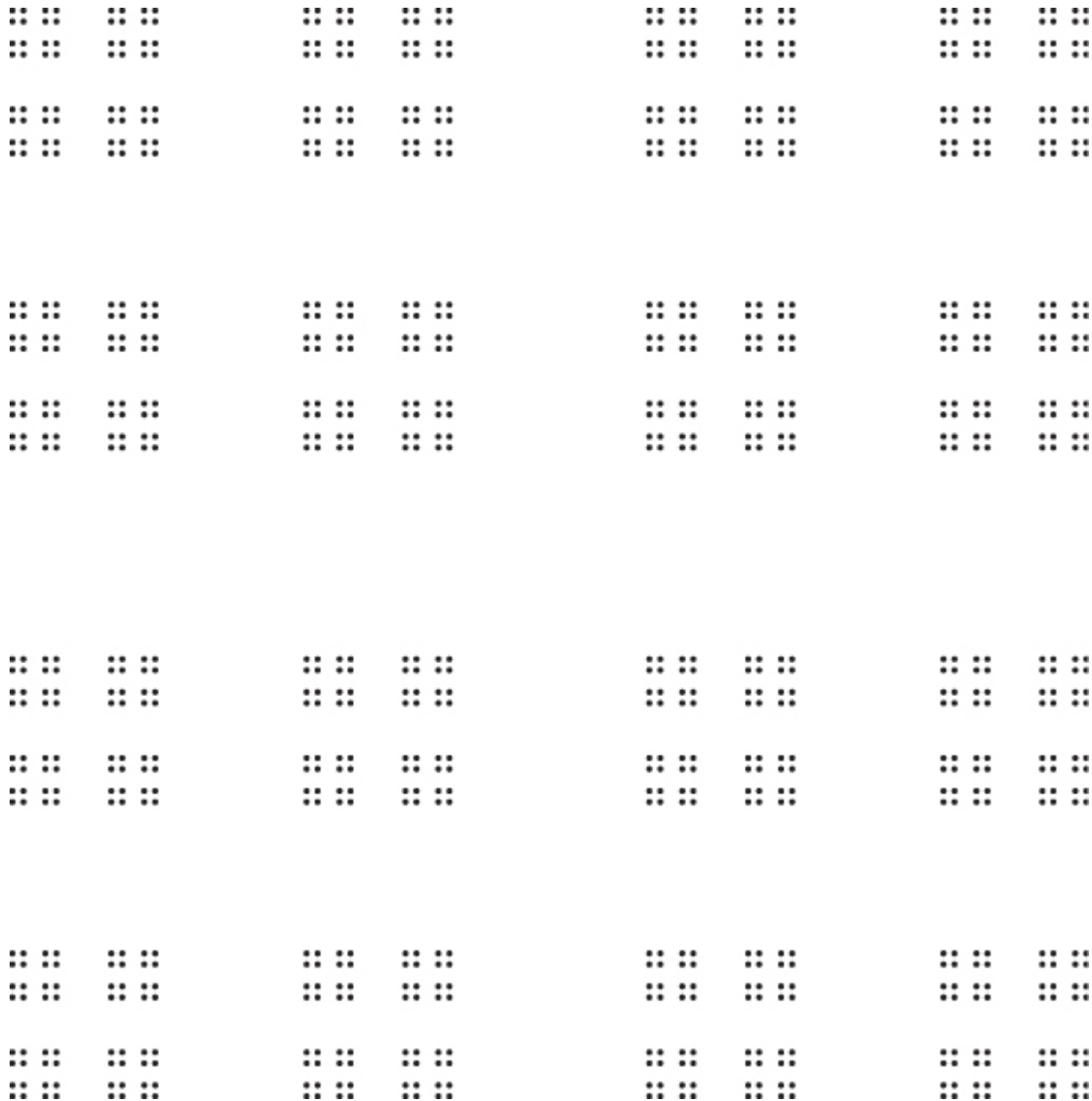


Figure 7.2 The product $F \times F$, where F is the middle third Cantor set. In this case, $\dim_H F \times F = 2 \dim_H F = 2 \log 2 / \log 3$.

In the first above-mentioned example, it is obvious that

$$\dim(E \times F) = \dim E + \dim F$$

using the classical definition of dimension. This holds more generally, in the ‘smooth’ situation, where E and F are smooth curves, surfaces or higher-dimensional manifolds. Unfortunately, this equation is not always valid for ‘fractal’ dimensions. For Hausdorff dimensions, the best general result possible is an

inequality $\dim_H(E \times F) \geq \dim_H E + \dim_H F$. Nevertheless, as we shall see in many situations equality does hold.

The proof of the product rule uses the Hausdorff measures on E and F to define a mass distribution μ on $E \times F$. Density bounds on E and F lead to estimates for μ suitable for a mass distribution method.

Proposition 7.1

If $E \subset \mathbb{R}^n, F \subset \mathbb{R}^m$ are Borel sets with $\mathcal{H}^s(E), \mathcal{H}^t(F) < \infty$, then

$$\mathcal{H}^{s+t}(E \times F) \geq c \mathcal{H}^s(E) \mathcal{H}^t(F), \quad 7.2$$

where $c > 0$ depends only on s and t .

Proof

For simplicity, we assume that $E, F \subset \mathbb{R}$, so that $E \times F \subset \mathbb{R}^2$; the general proof is almost identical. If either $\mathcal{H}^s(E)$ or $\mathcal{H}^t(F)$ is zero, then (7.2) is trivial, so suppose that E is an s -set and F is a t -set, that is, $0 < \mathcal{H}^s(E), \mathcal{H}^t(F) < \infty$. We may define a mass distribution μ on $E \times F$ by utilising the ‘product measure’ of \mathcal{H}^s and \mathcal{H}^t . Thus, if $I, J \subset \mathbb{R}$, we define μ on the ‘rectangle’ $I \times J$ by

$$\mu(I \times J) = \mathcal{H}^s(E \cap I)\mathcal{H}^t(F \cap J). \quad 7.3$$

It may be shown that this defines a mass distribution μ on $E \times F$ with $\mu(\mathbb{R}^2) = \mathcal{H}^s(E)\mathcal{H}^t(F)$.

By the density estimate Proposition 5.1(b), we have that

$$\overline{\lim}_{r \rightarrow 0} \mathcal{H}^s(E \cap B(x, r))(2r)^{-s} \leq 1 \quad 7.4$$

for \mathcal{H}^s -almost all $x \in E$ and

$$\overline{\lim}_{r \rightarrow 0} \mathcal{H}^t(F \cap B(y, r))(2r)^{-t} \leq 1 \quad 7.5$$

for \mathcal{H}^t -almost all $y \in F$. (Of course, since we are concerned with subsets of \mathbb{R} , the ‘ball’ $B(x, r)$ is just the interval of length $2r$ with midpoint x .) From the definition of μ , both (7.4) and (7.5) hold for μ -almost all (x, y) in $E \times F$. Since the disc $B((x, y), r)$ is contained in the square $B(x, r) \times B(y, r)$, we have that

$$\mu(B((x, y), r)) \leq \mu(B(x, r) \times B(y, r)) = \mathcal{H}^s(E \cap B(x, r))\mathcal{H}^t(F \cap B(y, r))$$

so

$$\frac{\mu(B((x, y), r))}{(2r)^{s+t}} \leq \frac{\mathcal{H}^s(E \cap B(x, r))}{(2r)^s} \frac{\mathcal{H}^t(F \cap B(y, r))}{(2r)^t}.$$

It follows, using (7.4) and (7.5), that $\overline{\lim}_{r \rightarrow 0} \mu(B((x, y), r))(2r)^{-(s+t)} \leq 1$ for μ -almost all $(x, y) \in E \times F$. By Proposition 4.9(a),

$$\mathcal{H}^s(E \times F) \geq 2^{-(s+t)} \mu(E \times F) = 2^{-(s+t)} \mathcal{H}^s(E) \mathcal{H}^t(F).$$

Product formula 7.2

If $E \subset \mathbb{R}^n, F \subset \mathbb{R}^m$ are Borel sets, then

$$\dim_H(E \times F) \geq \dim_H E + \dim_H F.$$

[7.6](#)

Proof

If s, t are any numbers with $s < \dim_H E$ and $t < \dim_H F$, then

$\mathcal{H}^s(E) = \mathcal{H}^t(F) = \infty$. Theorem 4.10 implies that there are Borel sets $E_0 \subset E$ and $F_0 \subset F$ with $0 < \mathcal{H}^s(E_0), \mathcal{H}^t(F_0) < \infty$. By Proposition 7.1, $\mathcal{H}^{s+t}(E \times F) \geq \mathcal{H}^{s+t}(E_0 \times F_0) \geq c \mathcal{H}^s(E_0) \mathcal{H}^t(F_0) > 0$. Hence, $\dim_H(E \times F) \geq s + t$. By choosing s and t arbitrarily close to $\dim_H E$ and $\dim_H F$, (7.6) follows.

Proposition 7.1 and Formula 7.3 are in fact valid for arbitrary (non-Borel) sets.

It follows immediately from (7.6) that the ‘Cantor product’ $F \times F$, where F is the middle third Cantor set, has Hausdorff dimension at least $2 \log 2 / \log 3$ (see [Figure 7.2](#)).

In general, inequality (7.6) cannot be reversed; see Example 7.8. However, if, as often happens, either E or F is ‘reasonably regular’ in the sense of having equal Hausdorff and upper box dimensions, then we do get equality.

Product formula 7.3

For any sets $E \subset \mathbb{R}^n$ and $F \subset \mathbb{R}^m$

$$\dim_H(E \times F) \leq \dim_H E + \overline{\dim}_B F.$$

7.7

Proof

Again for simplicity, take $E \subset \mathbb{R}$ and $F \subset \mathbb{R}$. Choose numbers $s > \dim_H E$ and $t > \overline{\dim}_B F$. Then there is a number $\delta_0 > 0$ such that F may be covered by $N_\delta(F) \leq \delta^{-t}$ intervals of length δ for all $\delta \leq \delta_0$. For such δ , let $\{U_i\}$ be any δ -cover of E by intervals with $\sum_i |U_i|^s < 1$. For each i , let $\{U_{i,j}\}$ be a cover of F by $N_{|U_i|}(F)$ intervals of length $|U_i|$. Then $U_i \times F$ is covered by $N_{|U_i|}(F)$ squares $\{U_i \times U_{i,j}\}$ of side $|U_i|$. Thus, $E \times F \subset \bigcup_i \bigcup_j (U_i \times U_{i,j})$, so that

$$\begin{aligned} \mathcal{H}_{\delta/2}^{s+t}(E \times F) &\leq \sum_i \sum_j |U_i \times U_{i,j}|^{s+t} \leq \sum_i N_{|U_i|}(F) 2^{(s+t)/2} |U_i|^{s+t} \\ &\leq 2^{(s+t)/2} \sum_i |U_i|^{-t} |U_i|^{s+t} < 2^{(s+t)/2}. \end{aligned}$$

Letting $\delta \rightarrow 0$ gives $\mathcal{H}^{s+t}(E \times F) < \infty$ whenever $s > \dim_H E$ and $t > \overline{\dim}_B F$, so $\dim_H(E \times F) \leq s + t$.

Corollary 7.4

If $\dim_H F = \overline{\dim}_B F$ then

$$\dim_H(E \times F) = \dim_H E + \dim_H F.$$

Proof

Combining Product formulae 7.2 and 7.3 gives

$$\dim_H E + \dim_H F \leq \dim_H(E \times F) \leq \dim_H E + \overline{\dim}_B F. \quad 7.8$$

It is worth noting that the basic product inequality for upper box dimensions is opposite to that for Hausdorff dimensions.

Product formula 7.5

For any sets $E \subset \mathbb{R}^n$ and $F \subset \mathbb{R}^m$,

$$\overline{\dim}_B(E \times F) \leq \overline{\dim}_B E + \overline{\dim}_B F. \quad 7.9$$

Proof

This is left as Exercise 7.5. The idea is just as in Formula 7.3—note that if E and F can be covered by $N_\delta(E)$ and $N_\delta(F)$ intervals of side δ respectively, then $E \times F$ is covered by the $N_\delta(E)N_\delta(F)$ squares formed by products of these intervals.

Example 7.6 Product with uniform Cantor sets

Let E, F be subsets of \mathbb{R} with F a uniform Cantor set (see Example 4.5). Then $\dim_H(E \times F) = \dim_H E + \dim_H F$.

Calculation

Example 4.5 shows that uniform Cantor sets have equal Hausdorff and upper box dimensions, so the result follows from Corollary 7.4.

Thus, the ‘Cantor product’ of the middle third Cantor set with itself has Hausdorff and box dimensions exactly $2 \log 2 / \log 3$. Similarly, if E is a subset of \mathbb{R} and F is a straight line segment, then $\dim_H(E \times F) = \dim_H E + 1$.

Many fractals encountered in practice are not actually products but are locally product-like. For example, the Hénon attractor (see (13.5)) looks locally like a product of a line segment and a Cantor-like set F . More precisely, there are smooth bijections from $[0, 1] \times F$ to small neighbourhoods of the attractor. Such sets may be analysed as the image of a product under a suitable Lipschitz transformation.

Example 7.7

The ‘Cantor target’ is the plane set given in polar coordinates by $F' = \{(r, \theta) : r \in F, 0 \leq \theta \leq 2\pi\}$ where F is the middle third Cantor set (see Figure 7.3). Then $\dim_H F' = 1 + \log 2 / \log 3$.

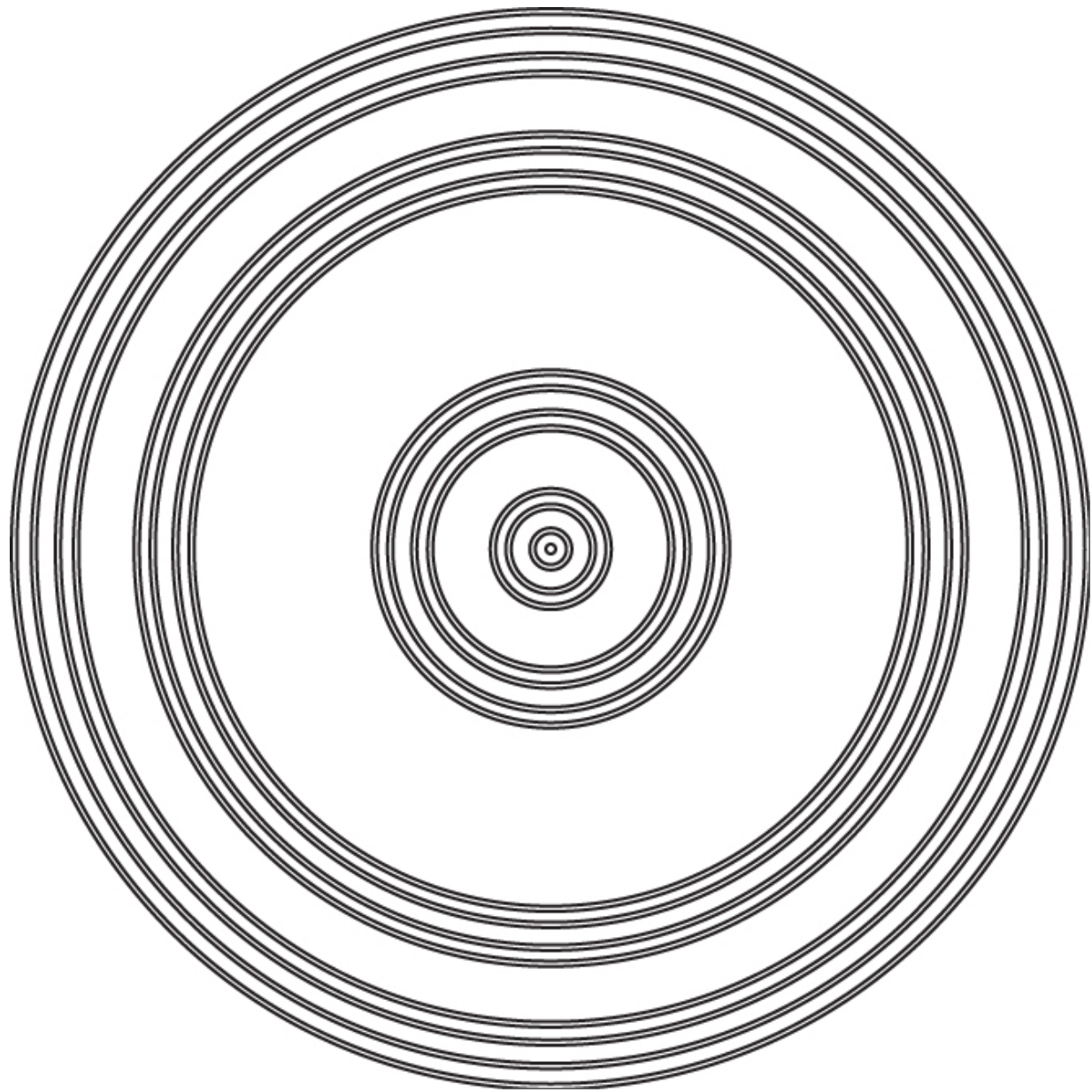


Figure 7.3 The ‘Cantor target’—the set swept out by rotating the middle third Cantor set about an end point.

Calculation

Let $f : \mathbb{R}^2 \rightarrow \mathbb{R}^2$ be given by $f(x, y) = (x \cos y, x \sin y)$. It is easy to see that f is a Lipschitz mapping and $F' = f(F \times [0, 2\pi])$. Thus,

$$\begin{aligned}\dim_H F' &= \dim_H f(F \times [0, 2\pi]) \leq \dim_H(F \times [0, 2\pi]) \\ &= \dim_H F + \dim_H[0, 2\pi] = (\log 2 / \log 3) + 1\end{aligned}$$

by Proposition 3.3(a) and Example 7.6. To obtain the opposite inequality, if we restrict f to $[\frac{2}{3}, 1] \times [0, \pi]$, then f is a bi-Lipschitz function on this domain. Since $F' \supset f((F \cap [\frac{2}{3}, 1]) \times [0, \pi])$, we have

$$\begin{aligned}\dim_H F' &\geq \dim_H f((F \cap [\frac{2}{3}, 1]) \times [0, \pi]) \\ &= \dim_H((F \cap [\frac{2}{3}, 1]) \times [0, \pi]) \\ &= \dim_H(F \cap [\frac{2}{3}, 1]) + \dim_H[0, \pi] \\ &= (\log 2 / \log 3) + 1\end{aligned}$$

by Proposition 3.3(b) and Example 7.6. This argument requires only minor modification to show that F' is an s -set for

$$s = 1 + \log 2 / \log 3.$$

The following example demonstrates that we do not in general get equality in the product formula (7.6) for Hausdorff measures.

Example 7.8

There exist sets $E, F \subset \mathbb{R}$ with $\dim_H E = \dim_H F = 0$ and $\dim_H(E \times F) \geq 1$.

Calculation

Let $0 = m_0 < m_1 < \dots$ be a rapidly increasing sequence of integers satisfying a condition to be specified below. Let E consist of those numbers in $[0, 1]$ with a zero in the r th decimal place whenever $m_k + 1 \leq r \leq m_{k+1}$ and k is even, and let F consist of those numbers with zero in the r th decimal place if $m_k + 1 \leq r \leq m_{k+1}$ and k is odd. Looking at the first m_{k+1} decimal places for even k , there is an obvious cover of E by 10^{j_k} intervals of length $10^{-m_{k+1}}$, where $j_k = (m_2 - m_1) + (m_4 - m_3) + \dots + (m_k - m_{k-1})$. Then $\log 10^{j_k} / -\log 10^{-m_{k+1}} = j_k/m_{k+1}$ which tends to 0 as $k \rightarrow \infty$, provided that the m_k are chosen to increase sufficiently rapidly. By Proposition 4.1, $\dim_H E \leq \underline{\dim}_B E = 0$. Similarly, $\dim_H F = 0$.

If $0 < w < 1$, then we can write $w = x + y$ where $x \in E$ and $y \in F$; just take the r th decimal digit of w from E if $m_k + 1 \leq r \leq m_{k+1}$ and k is odd and from F if k is even. The mapping $f : \mathbb{R}^2 \rightarrow \mathbb{R}$ given by $f(x, y) = x + y$ is easily seen to be Lipschitz, so

$$\dim_H(E \times F) \geq \dim_H f(E \times F) \geq \dim_H(0, 1) = 1$$

by Proposition 3.3(a).

A useful generalisation of the product formula relates the dimension of a set to the dimensions of parallel sections. We work in the (x, y) -plane and let L_x denote the line parallel to the y -axis through the point $(x, 0)$.

Proposition 7.9

Let F be a Borel subset of \mathbb{R}^2 . If $1 \leq s \leq 2$, then

$$\int_{-\infty}^{\infty} \mathcal{H}^{s-1}(F \cap L_x) dx \leq \mathcal{H}^s(F).$$

[7.10](#)

Proof

Given $\varepsilon > 0$, let $\{U_i\}$ be a δ -cover of F such that

$$\sum_i |U_i|^s \leq \mathcal{H}_\delta^s(F) + \varepsilon.$$

Each U_i is contained in a square S_i of side $|U_i|$ with sides parallel to the coordinate axes. Let χ_i be the indicator function of S_i (i.e. $\chi_i(x, y) = 1$ if $(x, y) \in S_i$ and $\chi_i(x, y) = 0$ if $(x, y) \notin S_i$). For each x , the sets $\{S_i \cap L_x\}$ form a δ -cover of $F \cap L_x$, so

$$\begin{aligned} \mathcal{H}_\delta^{s-1}(F \cap L_x) &\leq \sum_i |S_i \cap L_x|^{s-1} \\ &= \sum_i |U_i|^{s-2} |S_i \cap L_x| \\ &= \sum_i |U_i|^{s-2} \int_{-\infty}^{\infty} \chi_i(x, y) dy. \end{aligned}$$

Hence,

$$\begin{aligned} \int_{-\infty}^{\infty} \mathcal{H}_\delta^{s-1}(F \cap L_x) dx &\leq \sum_i |U_i|^{s-2} \iint \chi_i(x, y) dx dy \\ &= \sum_i |U_i|^s \\ &\leq \mathcal{H}_\delta^s(F) + \varepsilon. \end{aligned}$$

Since $\varepsilon > 0$ is arbitrary, $\int_{-\infty}^{\infty} \mathcal{H}_\delta^{s-1}(F \cap L_x) dx \leq \mathcal{H}_\delta^s(F)$. Letting $\delta \rightarrow 0$ and using the monotone convergence theorem gives (7.10).

Corollary 7.10

Let F be a Borel subset of \mathbb{R}^2 . Then, for almost all x (in the sense of 1-dimensional Lebesgue measure),

$$\dim_H(F \cap L_x) \leq \max\{0, \dim_H F - 1\}.$$

Proof

Take $s > \dim_H F$, so that $\mathcal{H}^s(F) = 0$. If $s > 1$, formula (7.10) gives that $\mathcal{H}^{s-1}(F \cap L_x) = 0$ and so $\dim_H(F \cap L_x) \leq s - 1$, for almost all x .

We state, without proof, a further useful generalisation.

Proposition 7.11

Let F be any subset of \mathbb{R}^2 , and let E be any subset of the x -axis. Suppose that there is a constant c such that $\mathcal{H}^t(F \cap L_x) \geq c$ for all $x \in E$. Then

$$\mathcal{H}^{s+t}(F) \geq bc\mathcal{H}^s(E)$$

7.11

where $b > 0$ depends only on s and t .

This result may be phrased in terms of dimensions.

Corollary 7.12

Let F be any subset of \mathbb{R}^2 , and let E be a subset of the x -axis. If $\dim_H(F \cap L_x) \geq t$ for all $x \in E$, then $\dim_H F \geq t + \dim_H E$.

The obvious higher-dimensional analogues of these results are all valid.

The following illustration of Proposition 7.9 is an example of a self-affine set, a class of sets which is discussed in more detail in Section 1.4.

Example 7.13 A self-affine set

Let F be the set with iterated construction indicated in Figure 7.4. (At the k th stage, each rectangle of E_k is replaced with an affine copy of the rectangles in E_1 . Thus, the contraction is greater in the ' y '-direction than in the ' x '-direction, with the width to height ratio of the rectangles in E_k tending to infinity as $k \rightarrow \infty$.) Then $\dim_H F = \dim_B F = 1\frac{1}{2}$.

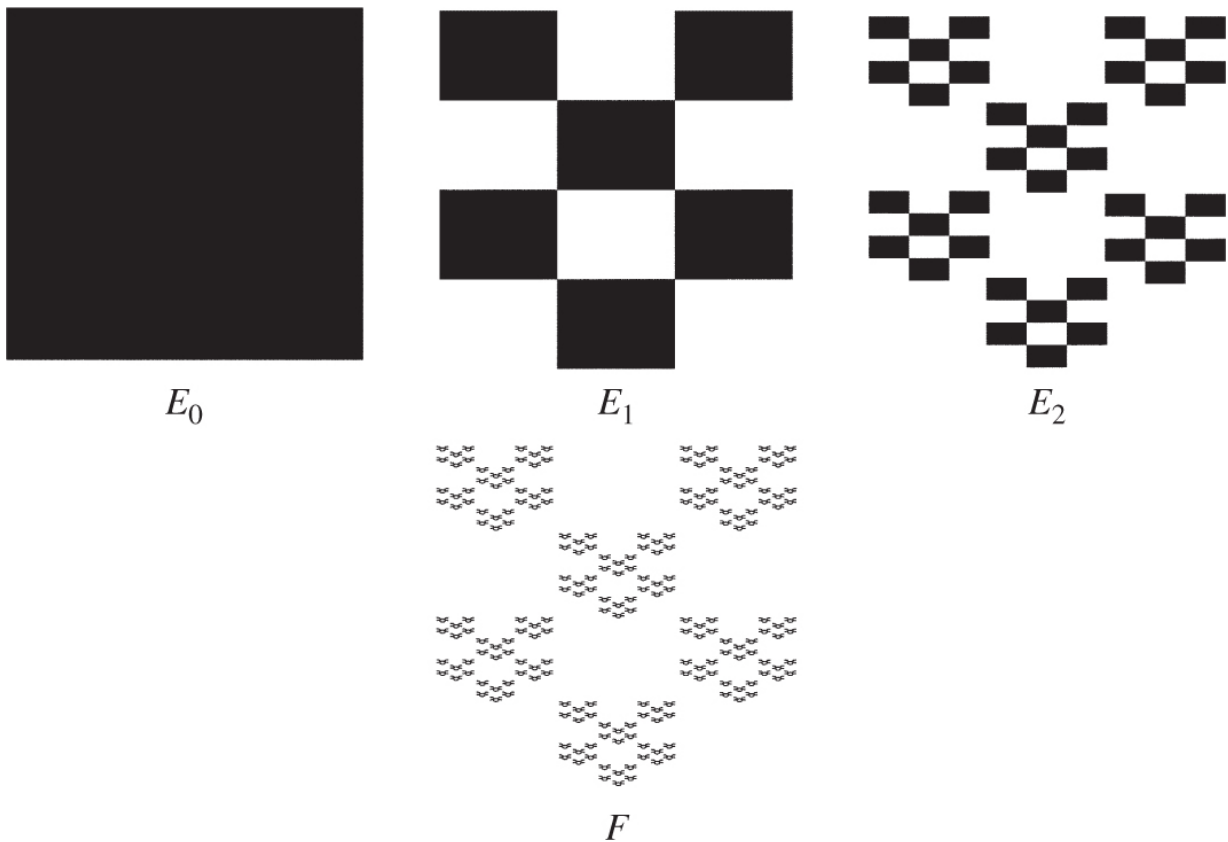


Figure 7.4. Construction of a self-affine set, $\dim_H F = 1\frac{1}{2}$.

Calculation

E_k consists of 6^k rectangles of size $3^{-k} \times 4^{-k}$. Each of these rectangles may be covered by at most $(4/3)^k + 1$ squares of side 4^{-k} , by dividing the rectangles using a series of vertical cuts. Hence, E_k may be covered by $6^k \times 2 \times 4^k \times 3^{-k} = 2 \times 8^k$ squares of diameter $4^{-k}\sqrt{2}$. In the usual way, this gives $\dim_H F \leq \dim_B F \leq \log 8 / \log 4 = 1\frac{1}{2}$.

On the other hand, except for x of the form $j3^{-k}$ where j and k are integers, we have that $E_k \cap L_x$ consists of 2^k intervals of length 4^{-k} . A standard application of the mass distribution method shows that $\mathcal{H}^{1/2}(F \cap L_x) \geq \frac{1}{2}$ for each such x . By Proposition 7.9, $\mathcal{H}^{3/2}(F) \geq \frac{1}{2}$. Hence, $\dim_H F = \dim_B F = 1\frac{1}{2}$.

7.2 Notes and references

Versions of the basic product formula date from Besicovitch and Moran (1945). A very general result, which includes Proposition 7.11, was proved by Marstrand (1954b) using net measures. For packing dimensions of products, see Tricot (1982) and Howroyd (1996).

Exercises

7.1 Show that for every set $F \subset [0, 1]$, we have

$$\dim_H(F \times [0, 1]) = 1 + \dim_H F.$$

7.2 Let F_λ denote the middle- λ Cantor set (see Example 4.5). What are the box and Hausdorff dimensions of $F_\lambda \times F_\mu$ for $0 < \lambda, \mu < 1$?

7.3 Let F be any subset of $[0, \infty)$ and let F' be the ‘target’ in \mathbb{R}^2 given in polar coordinates by $\{(r, \theta) : r \in F, 0 \leq \theta < 2\pi\}$. Show that $\dim_H F' = 1 + \dim_H F$.

7.4 Show that there is a subset F of \mathbb{R}^2 of Hausdorff dimension 2 with projections onto both coordinate axes of length 0. (Hint: see Exercise 4.9.) Show that any 1-set contained in such a set F is irregular and that any rectifiable curve intersects F in a set of length 0.

7.5 Derive Product formula 7.5.

7.6 What are the Hausdorff and box dimensions of the plane set $\{(x, y) \in \mathbb{R}^2 : x + y \in F \text{ and } x - y \in F\}$, where F is the middle third Cantor set?

7.7 Let $F \subset \mathbb{R}$ have equal Hausdorff and upper box dimensions. Let D be the set $\{x - y : x, y \in F\}$, known as the *difference set* of F . Show that $\dim_H D \leq \min \{1, 2\dim_H F\}$. (Hint: consider the set $F \times F$.)

7.8 Sketch the plane set $\{(x, y) : y - x^2 \in F\}$ where F is the middle third Cantor set, and find its Hausdorff and box dimensions.

7.9 Let L_x be as in Proposition 7.9. Let F be a subset of \mathbb{R}^2 and let $E_s = \{x \in \mathbb{R} : \dim_H(F \cap L_x) \geq s\}$ for all $0 \leq s \leq 1$. Show that $\dim_H F \geq \sup_{0 \leq s \leq 1} \{s + \dim_H E_s\}$.

7.10 Divide the unit square E_0 into a three column, five row array of rectangles of sides $\frac{1}{3}$ and $\frac{1}{5}$, and let E_1 be a set obtained by choosing some four of the five rectangles from each column. Let F be the self-affine set formed by repeatedly replacing rectangles by affine copies of E_1 (compare Example 7.13). Adapt the method of Example 7.13 to show that $\dim_H F = 1 + \log 4 / \log 5$.

7.11 Modify the construction of the previous exercise so that E_1 contains four rectangles from each of the first and third columns but none from the middle column. Show that

$$\dim_H F = \log 2 / \log 3 + \log 4 / \log 5.$$

Chapter 8

Intersections of fractals

The intersection of two fractals is often a fractal; it is natural to try to relate the dimension of this intersection to that of the original sets. It is immediately apparent that we can say almost nothing in the general case. For if F is bounded, there is a congruent copy F_1 of F such that $\dim_H(F \cap F_1) = \dim_H F$ (taking $F_1 = F$) and another congruent copy with $\dim_H(F \cap F_1) = \emptyset$ (taking F and F_1 disjoint). However, we can say rather more provided we consider the intersection of F and a congruent copy in a ‘typical’ relative position.

To illustrate this, let F and F_1 be unit line segments in the plane. Then $F \cap F_1$ can be a line segment, but only in the exceptional situation when F and F_1 are collinear. If F and F_1 cross at an angle, then $F \cap F_1$ is a single point, but now $F \cap F_1$ remains a single point if F_1 is replaced by a nearby congruent copy. Thus, whilst ‘in general’ $F \cap F_1$ contains at most one point, this situation occurs ‘frequently’.

We can make this rather more precise. Recall that a direct congruence transformation or rigid motion or σ of the plane transforms any set E to a congruent copy $\sigma(E)$ without reflection. The rigid motions may be parametrised by three coordinates (x, y, θ) where the origin is transformed to (x, y) and θ is the angle of rotation. Such a parametrisation provides a natural measure on the space of rigid motions, with the measure of a set A of rigid motions given by the 3-dimensional Lebesgue measure of the (x, y, θ) parametrising the motions in A . For example, the set of all rigid motions which map the origin to a point of the rectangle $[1, 2] \times [0, 3]$ has measure $1 \times 3 \times 2\pi$.

In the example with F a unit line segment, the set of transformations σ for which $F \cap \sigma(F)$ is a line segment has measure 0. However, $F \cap \sigma(F)$ is a single point for a set of transformations of positive measure, in fact a set of measure 4.

Similar ideas hold in higher dimensions. In \mathbb{R}^3 , ‘typically’, two surfaces intersect in a curve, a surface and a curve intersect in a point, and two curves are disjoint. In \mathbb{R}^n , if smooth manifolds E and F intersect at all, then ‘in general’ they intersect in a sub-manifold of dimension $\dim E + \dim F - n$ unless this number is negative in which case they typically do not intersect. More precisely, if $\dim E + \dim F - n \geq 0$, then $\dim(E \cap \sigma(F)) = \dim E + \dim F - n$ for a set of rigid motions σ of positive measure and is 0 for almost all other σ . (Of course, σ is now measured using the $\frac{1}{2}n(n+1)$ parameters required to specify a rigid transformation of \mathbb{R}^n .)

8.1 Intersection formulae for fractals

Are there analogues of these formulae if E and F are fractals and we use Hausdorff dimension? In particular, is it true that ‘in general’

$$\dim_H(E \cap \sigma(F)) \leq \max\{0, \dim_H E + \dim_H F - n\} \quad \underline{\text{8.1}}$$

and ‘often’

$$\dim_H(E \cap \sigma(F)) \geq \dim_H E + \dim_H F - n \quad \underline{\text{8.2}}$$

as σ ranges over a group G of transformations, such as the group of translations, congruences or similarities (see [Figure 8.1](#))? Of course ‘in general’ means ‘for almost all σ ’ and ‘often’ means ‘for a set of σ of positive measure’ with respect to a natural measure on the transformations in G . Generally, G can be parametrised by m coordinates in a straightforward way for some integer m and we can use m -dimensional Lebesgue measure on a parameter space which is a subset of \mathbb{R}^m .

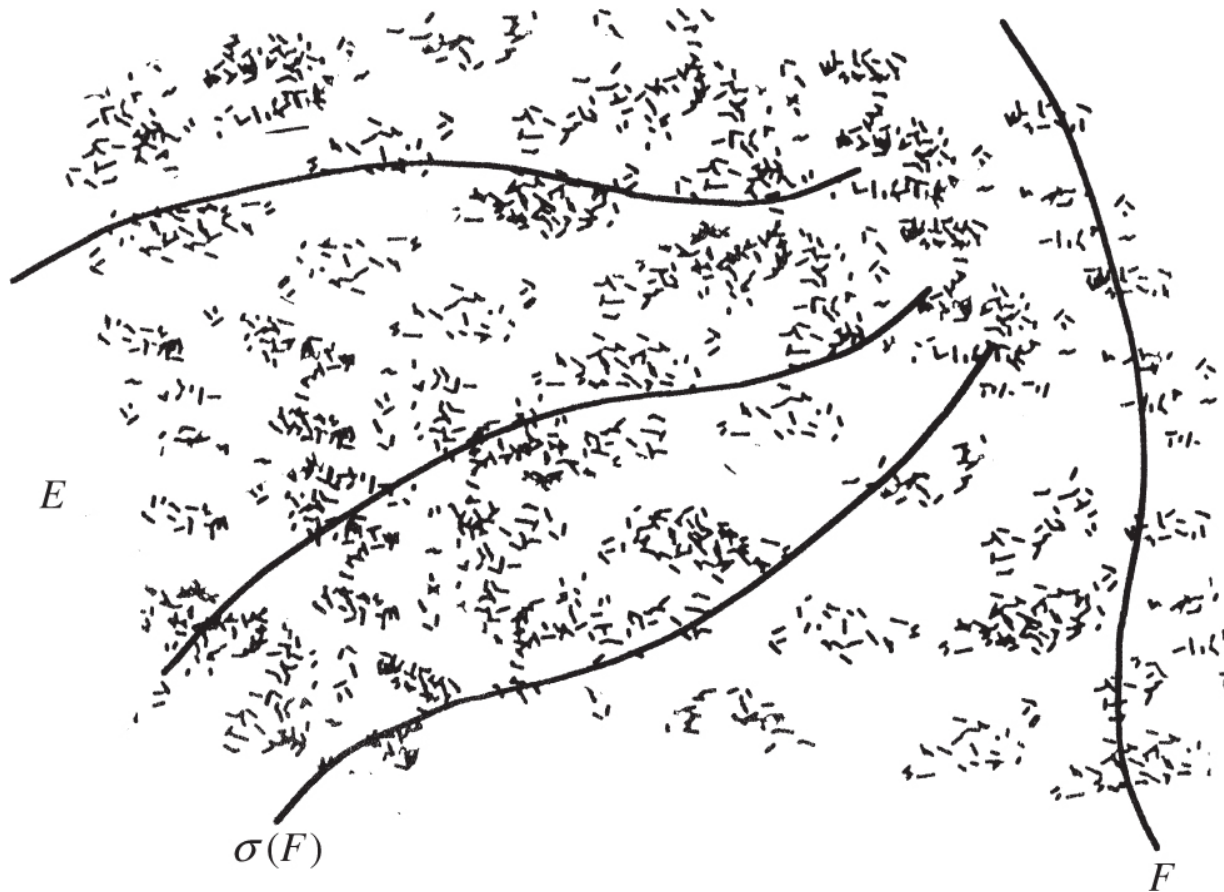


Figure 8.1 The intersection of a ‘dust-like’ set E with various congruent copies $\sigma(F)$ of a curve F . We are interested in the dimension of $E \cap \sigma(F)$ for ‘typical’ σ .

We may obtain upper bounds for $\dim_H(E \cap \sigma(F))$ when G is the group of translations; these bounds hold automatically for the larger groups of congruences and similarities. We have already proved (8.1) in the special case in the plane where one of the sets is a straight line; this is essentially Corollary 7.10. The general result is easily deduced from this special case. Recall that $F+x = \{x+y : y \in F\}$ denotes the set F translated by the vector x .

Theorem 8.1

If E, F are Borel subsets of \mathbb{R}^n , then

$$\dim_H(E \cap (F + x)) \leq \max\{0, \dim_H(E \times F) - n\}$$

[8.3](#)

for almost all $x \in \mathbb{R}^n$.

Proof

We prove this when $n = 1$; the proof for $n > 1$ is similar, using a higher-dimensional analogue of Corollary 7.10. Let L_c be the line in the (x, y) -plane with equation $x = y + c$. Assuming that $\dim_H(E \times F) > 1$, it follows from Corollary 7.10 (rotating the lines through 45° and changing notation slightly) that

$$\dim_H((E \times F) \cap L_c) \leq \dim_H(E \times F) - 1$$

[8.4](#)

for almost all $c \in \mathbb{R}$. But a point $(x, x - c)$ belongs to $(E \times F) \cap L_c$ if and only if $x \in E \cap (F + c)$. Thus, for each c , the projection onto the x -axis of $(E \times F) \cap L_c$ is the set $E \cap (F + c)$. In particular, $\dim_H(E \cap (F + c)) = \dim_H((E \times F) \cap L_c)$, so the conclusion follows from [\(8.4\)](#).

Corollary 8.2

Let E, F be Borel subsets of \mathbb{R}^n . Let G be the group of translations, the group of direct congruences or the group of similarities on \mathbb{R}^n . Then, for almost all $\sigma \in G$,

$$\dim_H(E \cap \sigma(F)) \leq \max\{0, \dim_H(E \times F) - n\}. \quad \underline{8.5}$$

In particular, if either $\dim_H E = \overline{\dim}_B E$ or $\dim_H F = \overline{\dim}_B F$, then

$$\dim_H(E \cap \sigma(F)) \leq \max\{0, \dim_H E + \dim_H F - n\}. \quad \underline{8.6}$$

Proof

We may parameterise the direct congruence transformations by a rotation together with a translation. Then by (8.3), inequality (8.5) holds for almost all translations for all rotations, that is, for almost all congruence transformations. In the same way, for similarities, we use a parameterisation by a rotation, scaling and translation.

Inequality (8.6) is immediate from (8.5) using Corollary 7.4.

Examples show that in general (8.5) cannot be improved to (8.6) without some additional condition on E or F .

Lower bounds for $\dim_H(E \cap \sigma(F))$ of the form (8.2) are rather harder to obtain. The main known results are contained in the following theorem.

Theorem 8.3

Let $E, F \subset \mathbb{R}^n$ be Borel sets, and let G be a group of transformations on \mathbb{R}^n . Then

$$\dim_H(E \cap \sigma(F)) \geq \dim_H E + \dim_H F - n$$

8.7

for a set of transformations $\sigma \in G$ of positive measure in the following cases:

- a. G is the group of similarities and E and F are arbitrary sets,
- b. G is the group of congruences, E is arbitrary and F is a rectifiable curve, surface or manifold,
- c. G is the group of congruences and E and F are arbitrary, with either $\dim_H E > \frac{1}{2}(n+1)$ or $\dim_H F > \frac{1}{2}(n+1)$.

*Outline of proof

The proof uses the potential theoretic methods of Section 1.3. In many ways, the argument resembles that of Projection theorem 6.1, but various technical difficulties make it much more complicated.

Briefly, if $s < \dim_H E$ and $t < \dim_H F$, there are mass distributions μ on E and ν on F with the energies $I_s(\mu)$ and $I_t(\nu)$ both finite. If ν happened to be absolutely continuous with respect to n -dimensional Lebesgue measure, that is, if there were a function f such that $\nu(A) = \int_A f(x)dx$ for each set A , then it would be natural to define a mass distribution η_σ on $E \cap \sigma(F)$ by
$$\frac{\eta_\sigma(A)}{d\mu(x)} = \int_A f(\sigma^{-1}(x))$$

If we could show that $I_{s+t-n}(\eta_\sigma) < \infty$ for almost all σ , Theorem 4.13(a) would imply that $\dim_H(E \cap \sigma(F)) \geq s + t - n$ if $\eta_\sigma(\mathbb{R}^n) > 0$. Unfortunately, when F is a fractal, ν is supported by a set of zero n -dimensional volume, so is anything but absolutely continuous. To get around this difficulty, we can approximate ν by absolutely continuous mass distributions ν_δ supported by the δ -neighbourhood of F . Then, if $\nu_\delta(A) = \int_A f_\delta(x)dx$ and

$$\frac{\eta_{\sigma,\delta}}{d\mu(x)} = \int_A f_\delta(\sigma^{-1}(x))$$
, we can estimate $I_{s+t-n}(\eta_{\sigma,\delta})$ and take the limit as $\delta \rightarrow 0$. Simplifying the integral $\int I_{s+t-n}(\eta_{\sigma,\delta})d\sigma$ isolates a term

$$\varphi_\delta(w) = \int_{G_0} \int_{\mathbb{R}^n} \nu_\delta(y) \nu_\delta(y + \sigma(w)) dy d\sigma$$

where integration with respect to σ is now over the subgroup G_0 of F which fixes the origin. Provided that

$$\varphi_\delta(w) \leq \text{constant } |w|^{t-n} \quad \underline{8.8}$$

for all w and δ , it may be shown that $\int I_{s+t-n}(\eta_{\sigma,\delta})d\sigma < c < \infty$, where c is independent of δ . Letting $\delta \rightarrow 0$, the measures $\eta_{\sigma,\delta}$ ‘converge’ to measures η_σ on $E \cap \sigma(F)$, where $\int I_{s+t-n}(\eta_\sigma)d\sigma < c$. Thus

$I_{s+t-n}(\eta_\sigma) < \infty$ for almost all σ , so, by Theorem 4.13(a), $\dim_H(E \cap \sigma(F)) \geq s + t - n$ whenever $\eta_\sigma(E \cap \sigma(F)) > 0$, which happens on a set of positive measure.

It may be shown that (8.8) holds if $I_t(v) < \infty$ in the cases (a), (b) and (c) listed. This is relatively easy to show for (a) and (b). Case (c) is more awkward, requiring a Fourier transform method.

The condition that $\dim_H E$ or $\dim_H F > \frac{1}{2}(n+1)$ in case (c) is a curious consequence of the use of Fourier transforms. It is not known whether the theorem remains valid for the group of congruences if $n \geq 2$ and $\frac{1}{2}n < \dim_H E, \dim_H F \leq \frac{1}{2}(n+1)$.

Example 8.4

Let $F \subset \mathbb{R}$ be the middle third Cantor set. For $\lambda, x \in \mathbb{R}$ write $\lambda F + x = \{\lambda y + x : y \in F\}$. Then $\dim_H(F \cap (F + x)) \leq 2(\log 2 / \log 3) - 1$ for almost all $x \in \mathbb{R}$, and $\dim_H(F \cap (\lambda F + x)) = 2(\log 2 / \log 3) - 1$ for a set of $(x, \lambda) \in \mathbb{R}^2$ of positive plane Lebesgue measure.

Calculation

Since $\dim_H F = \overline{\dim}_B F = \log 2 / \log 3$, the stated Hausdorff dimensions of the intersections follow from Corollary 8.2 and Theorem 8.3(a).

The box and packing dimensions of intersections of sets can behave very irregularly, with the dimensions of intersections often being ‘unexpectedly small’ (see Exercise 8.7).

8.2 Sets with large intersection

We have seen that (8.1) need not always hold; in this section, we examine a family of sets for which it fails dramatically. For each $0 < s < 1$, we construct a large class \mathcal{C}^s of subsets of \mathbb{R} of Hausdorff dimension at least s with the property that the intersection of any countable collection of sets in \mathcal{C}^s still has dimension at least s . Sets of this type occur naturally in number theory (see Section 1.3).

The class \mathcal{C}^s is defined in terms of sums similar to those in the definition of Hausdorff measures (3.1). For F a subset of \mathbb{R} , we let

$$\mathcal{H}_\infty^s(F) = \inf \left\{ \sum_{i=1}^{\infty} |U_i|^s : \bigcup_{i=1}^{\infty} U_i \text{ is any cover of } F \right\}.$$

Thus, $\mathcal{H}_\infty^s(F)$ is defined using covers of F without any diameter restriction. This ensures that $\mathcal{H}_\infty^s(I)$ is finite if I is a bounded interval, which would not be the case if we used \mathcal{H}^s . It is easy to see that $\mathcal{H}_\infty^s(F_1 \cup F_2) \leq \mathcal{H}_\infty^s(F_1) + \mathcal{H}_\infty^s(F_2)$ and that $\mathcal{H}_\infty^s(F_1) \leq \mathcal{H}_\infty^s(F_2)$ if $F_1 \subset F_2$.

Recall that $\overline{\lim}_{k \rightarrow \infty} E_k = \bigcap_{i=1}^{\infty} \bigcup_{k=i}^{\infty} E_k$ is the set of points that belong to infinitely many E_k ; such sets are termed *lim sup sets*. Let $0 < s < 1$ and let $[a, b] \subset \mathbb{R}$ be a proper closed interval. We say that a subset F of $[a, b]$ is a *member of the class $\mathcal{C}^s[a, b]$* if

$$\overline{\lim}_{k \rightarrow \infty} E_k \subset F, \quad \mathbf{8.9}$$

where $\{E_k\}$ is a sequence of subsets of $[a, b]$ such that

- a. each E_k is a finite union of disjoint closed intervals, and
- b. for every bounded closed interval I

$$\lim_{k \rightarrow \infty} \mathcal{H}_\infty^s(I \cap E_k) = |I|^s. \quad \mathbf{8.10}$$

(Of course, we always have $\mathcal{H}_\infty^s(I \cap E_k) \leq |I|^s$.) We define $\mathcal{C}^s(-\infty, \infty)$ by saying that $F \in \mathcal{C}^s(-\infty, \infty)$ if $F \cap I \in \mathcal{C}^s[a, b]$ for every bounded interval $[a, b]$. The results below extend easily from $\mathcal{C}^s[a, b]$ to $\mathcal{C}^s(-\infty, \infty)$.

As an example of the sets we have in mind, we might take

$$E_k = \{x : |x - p/k| < k^{-3} \text{ for some integer } p\},$$

so that $F = \overline{\lim}_{k \rightarrow \infty} E_k$ consists of those numbers which satisfy the inequality $|x - p/k| < k^{-3}$ for some p for infinitely many positive integers k . As we shall see, $F \in C^{1/3}(-\infty, \infty)$.

Any set in $C^s[a, b]$ must be dense in $[a, b]$; for if F is in $C^s[a, b]$ and I is a closed interval, then $I \cap E_{k_1}$ contains a closed interval I_1 if k_1 is large enough, by (8.10). Similarly, $I_1 \cap E_{k_2}$ contains a closed interval I_2 for some $k_2 > k_1$. Proceeding in this way, we get a sequence of closed intervals $I \supset I_1 \supset I_2 \supset \dots$ with $I_r \subset E_{k_r}$ for each r . Thus, the non-empty set $\bigcap_{r=1}^{\infty} I_r$ is contained in infinitely many E_k , so is contained in $F \cap I$. By a similar argument, writing $\text{int } E_k$ for the interior of E_k , $\bigcap_{i=1}^{\infty} \bigcup_{k=i}^{\infty} \text{int } E_k$ is dense in $[a, b]$ and is a G_{δ} set as a countable intersection of open sets. Thus, every $F \in C^s[a, b]$ is of second category, so by Proposition 3.10 has packing dimension 1.

By Proposition 2.6, any set in $C^s[a, b]$ has box-counting dimension 1. We now show that these sets have Hausdorff dimension at least s . We will also show that the intersection of any countable collection of sets in $C^s[a, b]$ is also in $C^s[a, b]$ and so has dimension at least s . Furthermore $f(F)$ is in $C^s[f(a), f(b)]$ if F is in $C^s[a, b]$, for a large class of functions f . The proofs, given below, are somewhat technical and might well be omitted on a first reading. The following lemma which extends (8.10) to unions of closed intervals is the key to these properties.

Lemma 8.5

Let $\{E_k\}$ be a sequence of closed subsets of \mathbb{R} such that

$$\lim_{k \rightarrow \infty} \mathcal{H}_\infty^s(I \cap E_k) = |I|^s \quad \text{8.11}$$

for every bounded closed interval I . Then, if A is a bounded set made up of a finite union of closed intervals,

$$\lim_{k \rightarrow \infty} \mathcal{H}_\infty^s(A \cap E_k) = \mathcal{H}_\infty^s(A). \quad \text{8.12}$$

Proof

Suppose that A consists of m disjoint intervals with minimum separation $d > 0$. Given $\varepsilon > 0$, we may, using (8.11), choose k_ε such that if $k \geq k_\varepsilon$

$$\mathcal{H}_\infty^s(I \cap E_k) > (1 - \varepsilon)|I|^s \quad 8.13$$

whenever $|I| \geq \varepsilon d$ and $I \subset A$. (Since $\mathcal{H}_\infty^s(E_k \cap I)$ varies continuously with I in the obvious sense, we may find a k_ε such that (8.13) holds simultaneously for all such I .) To estimate $\mathcal{H}_\infty^s(A \cap E_k)$, let $\{U_i\}$ be a cover of $A \cap E_k$. We may assume that this cover is finite, since $A \cap E_k$ is compact (see Section 1.4) and also that the U_i are closed intervals with endpoints in A , which are disjoint except possibly at endpoints. We divide the sets U_i into two batches according to whether $|U_i| \geq d$ or $|U_i| < d$. The set $A \setminus \bigcup_{|U_i| \geq d} U_i$ consists of disjoint intervals V_1, \dots, V_r where $r \leq m$, and

$$A \subset \bigcup_{|U_i| \geq d} U_i \cup \bigcup_j \bar{V}_j. \quad 8.14$$

Observe that any U_i with $|U_i| < d$ is contained in an interval of A , and so in one of the \bar{V}_j . For each j , the sets U_i contained in \bar{V}_j cover $\bar{V}_j \cap E_k$, so

$$\sum_{\{i: U_i \subset \bar{V}_j\}} |U_i|^s \geq \mathcal{H}_\infty^s(\bar{V}_j \cap E_k) > (1 - \varepsilon)|V_j|^s$$

if $|V_j| \geq \varepsilon d$, by (8.13). Hence,

$$\begin{aligned} \sum_i |U_i|^s &\geq \sum_{|U_i| \geq d} |U_i|^s + \sum_{|V_j| \geq \varepsilon d} \sum_{U_i \subset \bar{V}_j} |U_i|^s \\ &\geq \sum_{|U_i| \geq d} |U_i|^s + \sum_{|V_j| \geq \varepsilon d} (1 - \varepsilon)|V_j|^s. \end{aligned} \quad 8.15$$

From (8.14),

$$\begin{aligned}\mathcal{H}_\infty^s(A) &\leq \sum_{|U_i| \geq d} |U_i|^s + \sum_{|V_j| \geq \varepsilon d} |V_j|^s + \sum_{|V_j| < \varepsilon d} |V_j|^s \\ &\leq \sum_{|U_i| \geq d} |U_i|^s + \sum_{|V_j| \geq \varepsilon d} |V_j|^s + (\varepsilon d)^s m.\end{aligned}$$

Combining with (8.15), we see that

$$\mathcal{H}_\infty^s(A) \leq (1 - \varepsilon)^{-1} \sum_i |U_i|^s + (\varepsilon d)^s m$$

for any cover $\{U_i\}$ of $A \cap E_k$. Thus,

$$\mathcal{H}_\infty^s(A) \leq (1 - \varepsilon)^{-1} \mathcal{H}_\infty^s(A \cap E_k) + (\varepsilon d)^s m$$

if $k \geq k_\varepsilon$, which implies (8.12).

Repeated application of this Lemma now gives the dimension estimate we require.

Proposition 8.6

If $F \in \mathcal{C}^s[a, b]$ then $\mathcal{H}^s(F) > 0$, and in particular $\dim_H F \geq s$. Moreover, $\dim_P F = 1$.

Proof

For simplicity of notation, assume that $[a, b] = [0, 1]$. Suppose $\overline{\lim}_{k \rightarrow \infty} E_k \subset F \subset \bigcup_i U_i$ where the U_i are open sets. Taking $I = [0, 1]$ in (8.10), we may find a number k_1 such that $\mathcal{H}_\infty^s(E_{k_1}) > \frac{1}{2}$. Since E_{k_1} is a finite union of closed intervals, Lemma 8.5 implies that there is a number $k_2 > k_1$ such that $\mathcal{H}_\infty^s(E_{k_1} \cap E_{k_2}) > \frac{1}{2}$. Proceeding in this way, we get a sequence $k_1 < k_2 < \dots$ with $\mathcal{H}_\infty^s(E_{k_1} \cap \dots \cap E_{k_r}) > \frac{1}{2}$ for all r . We have $\bigcap_{i=1}^{\infty} E_{k_i} \subset F \subset \bigcup_i U_i$; since $E_{k_1} \cap \dots \cap E_{k_r}$ is a decreasing sequence of compact (i.e. closed and bounded) sets and $\bigcup_i U_i$ is open, there is an integer r such that $E_{k_1} \cap \dots \cap E_{k_r} \subset \bigcup_i U_i$. Thus we conclude that $\sum_i |U_i|^s \geq \mathcal{H}_\infty^s(E_{k_1} \cap \dots \cap E_{k_r}) > \frac{1}{2}$ for every cover of F by open sets, so $\mathcal{H}^s(F) \geq \frac{1}{2}$.

As noted above, F is of second category, so $\dim_p F = 1$ by Proposition 3.10.

Proposition 8.7

Let $F_j \in C^s[a, b]$ for $j = 1, 2, \dots$. Then $\bigcap_{j=1}^{\infty} F_j \in C^s[a, b]$.

Proof

For each j , there is a sequence of sets $E_{j,k}$, each a finite union of closed intervals, such that $F_j \supset \overline{\lim}_{k \rightarrow \infty} E_{j,k}$, where $\lim_{k \rightarrow \infty} \mathcal{H}_\infty^s(I \cap E_{j,k}) = \mathcal{H}_\infty^s(I)$ for every interval I . By Lemma 8.5,

$$\lim_{k \rightarrow \infty} \mathcal{H}_\infty^s(A \cap E_{j,k}) = \mathcal{H}_\infty^s(A) \quad \text{8.16}$$

for any finite union of closed intervals A . There are countably many intervals $[c, d] \subset [a, b]$ with c and d both rational: let I_1, I_2, \dots be an enumeration of all such intervals.

For each integer r , we define a set G_r as follows. Using (8.16), we may choose $k_1 \geq r$ large enough to make

$$\mathcal{H}_\infty^s(I_m \cap E_{1,k_1}) > \mathcal{H}_\infty^s(I_m) - 1/r$$

simultaneously for $m = 1, \dots, r$. Using (8.16) again, taking $A = I_m \cap E_{1,k_1}$, we may find $k_2 \geq r$ such that

$$\mathcal{H}_\infty^s(I_m \cap E_{1,k_1} \cap E_{2,k_2}) > \mathcal{H}_\infty^s(I_m) - 1/r$$

for $m = 1, \dots, r$. Continuing in this way, we get $k_1, \dots, k_r \geq r$ such that

$$\mathcal{H}_\infty^s\left(I_m \cap \bigcap_{j=1}^r E_{j,k_j}\right) > \mathcal{H}_\infty^s(I_m) - 1/r \quad \text{8.17}$$

for all $m = 1, \dots, r$. For each r , let G_r be the finite union of closed intervals

$$G_r = \bigcap_{j=1}^r E_{j,k_j}. \quad \text{8.18}$$

Let $I \subset [a, b]$ be any closed interval. Given $\varepsilon > 0$, there is an interval $I_m \subset I$ such that $\mathcal{H}_\infty^s(I_m) > \mathcal{H}_\infty^s(I) - \varepsilon/2$. If $r \geq m$ and $r > 2/\varepsilon$,

(8.17) gives that

$$\mathcal{H}_\infty^s(I \cap G_r) \geq \mathcal{H}_\infty^s(I_m \cap G_r) > \mathcal{H}_\infty^s(I_m) - 1/r > \mathcal{H}_\infty^s(I) - \varepsilon,$$

so

$$\lim_{r \rightarrow \infty} \mathcal{H}_\infty^s(I \cap G_r) = \mathcal{H}_\infty^s(I).$$

Let j be any positive integer. If $r > j$ and $x \in G_r$, then $x \in E_{j,k_j}$, by (8.18). Thus, if $x \in \overline{\lim}_{r \rightarrow \infty} G_r$, then $x \in E_{j,k_j}$ for infinitely many k_j , so $x \in \overline{\lim}_{i \rightarrow \infty} E_{j,i} \subset F_j$. Hence, $\overline{\lim}_{r \rightarrow \infty} G_r \subset F_j$ for each j , so $\bigcap_{i=1}^{\infty} F_i \in \mathcal{C}^s[a, b]$.

Corollary 8.8

Let $F_j \in \mathcal{C}^s[a, b]$ for all $j = 1, 2, \dots$. Then $\dim_H \bigcap_{j=1}^{\infty} F_j \geq s$.

Proof

This is immediate from Propositions 8.6 and 8.7.

Clearly, if F is in $\mathcal{C}^s(-\infty, \infty)$, then so is the translate $F + x$. Hence, given a set F in $\mathcal{C}^s(-\infty, \infty)$ and a sequence of numbers x_1, x_2, \dots , then $\bigcap_{i=1}^{\infty} (F + x_i) \in \mathcal{C}^s(-\infty, \infty)$, so that this intersection has dimension at least s . The same idea may be applied with more general transformations of F .

Proposition 8.9

Let $f : [a, b] \rightarrow \mathbb{R}$ be a mapping with a continuous derivative such that $|f'(x)| > c$ for some constant $c > 0$. If $F \in \mathcal{C}^s[a, b]$, then $f(F) \in \mathcal{C}^s[f(a), f(b)]$.

Proof

This may be proved in the same way as for Proposition 8.5. We omit the (rather tedious) details.

In a typical \mathcal{C}^s set, the E_k are made up of intervals which have lengths and spacings tending to 0 as $k \rightarrow \infty$ as is the case for the set F in the next example.

Example 8.10

Fix $\alpha > 2$. Let $E_k = \{x : |x - p/k| \leq k^{-\alpha} \text{ for some integer } p\}$, so that E_k is a union of equally spaced intervals of length $2k^{-\alpha}$. Then $F = \overline{\lim}_{k \rightarrow \infty} E_k \in \mathcal{C}^s(-\infty, \infty)$ for all $s < 1/\alpha$. In particular, $\dim_H F \geq 1/\alpha$.

Proof

Take $0 < s < 1/\alpha$ and a bounded closed interval I . We must show that

$$\lim_{k \rightarrow \infty} \mathcal{H}_\infty^s(I \cap E_k) = |I|^s.$$

[8.19](#)

The interval I contains m complete intervals of E_k , each of length $2k^{-\alpha}$, where $m \geq k|I| - 2$. Let μ be the mass distribution on $I \cap E_k$ obtained by distributing a mass $1/m$ uniformly across each complete interval of E_k contained in I . To estimate $\mathcal{H}_\infty^s(I \cap E_k)$, let U be a set in a covering of $I \cap E_k$; we may assume that U is a closed interval and that the ends of U are points of $I \cap E_k$. Then U intersects at most $k|U| + 2$ intervals of $I \cap E_k$. If $1/2k \leq |U| \leq |I|$, then

$$\begin{aligned} \mu(U) &\leq (k|U| + 2)/m \leq (k|U| + 2)/(k|I| - 2) = (|U| + 2k^{-1})/(|I| - 2k^{-1}) \\ &= |U|^s (|U|^{1-s} + 2k^{-1}|U|^{-s})/(|I| - 2k^{-1}) \\ &\leq |U|^s (|U|^{1-s} + 2^{s+1}k^{s-1})/(|I| - 2k^{-1}) \\ &= \frac{|U|^s}{|I|^s} \frac{(|U|^{1-s}|I|^{s-1} + 2^{s+1}k^{s-1}|I|^{s-1})}{(1 - 2k^{-1}|I|^{-1})} \\ &\leq \frac{|U|^s}{|I|^s} \frac{(1 + 2^{s+1}k^{s-1}|I|^{s-1})}{(1 - 2k^{-1}|I|^{-1})}. \end{aligned} \quad \text{8.20}$$

On the other hand, if k is large enough and $|U| < 1/2k$, then U can intersect just one interval of E_k so $|U| \leq 2k^{-\alpha}$, since the end points of U are in E_k . A mass of $1/m$ is distributed evenly across this interval of length $2k^{-\alpha}$, so

[8.21](#)

$$\begin{aligned} \mu(U) &\leq |U|/(2k^{-\alpha}m) = |U|^s |U|^{1-s}/(2k^{-\alpha}m) \leq |U|^s (2k^{-\alpha})^{1-s}/(2k^{-\alpha}(k|I| - 2)) \\ &\leq |U|^s 2^{-s} k^{s\alpha-1}/(|I| - 2k^{-1}). \end{aligned}$$

With I and $\epsilon > 0$ given, provided k is sufficiently large,

$$\mu(U) \leq (1 + \varepsilon)|U|^s / |I|^s$$

for all covering intervals U , using (8.20) and (8.21). Hence, if $I \cap E_k \subset \bigcup_i U_i$, then

$$1 = \mu(I \cap E_k) \leq \sum_i \mu(U_i) \leq (1 + \varepsilon)|I|^{-s} \sum_i |U_i|^s$$

so $\mathcal{H}_\infty^s(I \cap E_k) \geq |I|^s / (1 + \varepsilon)$, from which (8.19) follows.

That $\dim_H F \geq 1/\alpha$ follows from Proposition 8.6.

With F as in this example, it is clear that the translate $F+x$ is in $C^s(-\infty, \infty)$ for any real number x , so by Proposition 8.7, $\bigcap_{i=1}^\infty (F+x_i)$ belongs to $C^s(-\infty, \infty)$ for any countable sequence x_1, x_2, \dots , implying that $\dim_H \bigcap_{i=1}^\infty (F+x_i) \geq 1/\alpha$. More generally, $f(F)$ is in $C^s(-\infty, \infty)$ for all ‘reasonable’ functions f by Proposition 8.7, and this generates a large stock of C^s sets, countable intersections of which also have dimension at least $1/\alpha$.

In Section 1.3, we shall indicate how Example 8.10 may be improved to give F in $C^s(-\infty, \infty)$ for all $s < 2/\alpha$, with corresponding consequences for dimensions.

*8.3 Notes and references

The study of intersections of sets as they are moved relative to one another is part of a subject known as integral geometry. A full account in the classical setting is given by Santaló (2004). The main references for the fractal intersection formula of Section 8.1 are Kahane (1986) and Mattila (1984, 1985, 1999).

For the strange properties of packing dimension of intersections of sets, see Falconer, Järvenpää and Mattila (1999) and Csörnyei (2001).

There are several definitions of classes of sets with large intersections, such as those given by Baker and Schmidt (1970) and Falconer (1985b). An important class of ‘ubiquitous’ systems of sets

was introduced by Dodson, Rynne and Vickers (1990), see also Bernik and Dodson (2000), and their ‘Ubiquity theorem’ provides a powerful technique for finding dimensions of \limsup sets. Rynne (1992) compares different definitions of large intersection classes. Falconer (1994) presents a general theory of large intersection sets.

Exercises

8.1 Let E and F be rectifiable curves in \mathbb{R}^2 and let σ be a congruence transformation. Prove Poincaré's formula of classical integral geometry

$$4 \times \text{length}(E) \text{ length}(F) = \int (\text{number of points in } (E \cap \sigma(F))) d\sigma,$$

where integration is with respect to the natural measure on the set of congruences. (Hint: show this first when E and F are line segments, then for polygons, and obtain the general result by approximation.)

8.2 Show that if a curve C bounds a (compact) convex set in the plane, then the length of C is given by

$$\frac{1}{2} \int_{\theta=0}^{2\pi} \text{length}(\text{proj}_\theta C) d\theta.$$

(Hint: take E as C and F as a long line segment in the result of Exercise 8.1.)

8.3 In the plane, let E be the product of two middle third Cantor sets and let F be (i) a circle, (ii) the von Koch curve and (iii) a congruent copy of E . In each case, what can be said about the Hausdorff dimension of $E \cap \sigma(F)$ for congruence transformations σ ?

8.4 Show that the conclusion of Theorem 8.1 may be extended to give that $E \cap (F + x)$ is empty for almost all x if $\dim_H(E \times F) < n$.

8.5 By taking E as a suitable set dense in a region of \mathbb{R}^2 and F as a unit line segment, show that (8.7) fails if Hausdorff dimension is

replaced by box dimensions, even for the group of similarities.

8.6 Let $1 < s < 2$. Construct a plane s -set F in the unit disc B such that if E is any straight line segment of length 2 that intersects the interior of B , then $E \cap F$ is an $(s - 1)$ -set.

8.7 Let E be the set of parallel line segments

$$E = \{(0, 0)\} \cup \bigcup_{n=1}^{\infty} \{(x, n^{-1/2}) : 0 \leq x \leq n^{-1/2}\}.$$

Show that $\underline{\dim}_B E \geq 4/3$ but that $\dim_B(L \cap E) = 0$ for all lines L that do not pass through the origin. (Hint: see Example 2.7.)

8.8 Let E_k be the set of real numbers with base-3 expansion $m \cdot a_1 a_2 \dots$ such that $a_k = 0$ or 2. Show that $F = \overline{\lim}_{k \rightarrow \infty} E_k$ is in class $C^s(-\infty, \infty)$ for all $0 < s < 1$. (Note that F is the set of numbers with infinitely many base-3 digits different from 1.) Deduce that $\dim_H F = 1$ and that $\dim_H(\bigcap_{i=1}^{\infty}(F + x_i)) = 1$ for any countable sequence x_1, x_2, \dots

Part II

Applications and Examples

Chapter 9

Iterated function systems—self-similar and self-affine sets

9.1 Iterated function systems

Many fractals are made up of parts that are, in some way, similar to the whole. For example, the middle third Cantor set is the union of two similar copies of itself, and the von Koch curve is made up of four similar copies. These self-similarities are not only the properties of the fractals: they can actually be used to define them. Iterated function systems do this in a unified way and, moreover, often lead to a simple way of finding dimensions of fractals.

Let D be a closed subset of \mathbb{R}^n , often D is \mathbb{R}^n itself. A mapping $S : D \rightarrow D$ is called a *contraction* on D if there exists a number r with $0 < r < 1$ such that $|S(x) - S(y)| \leq r|x - y|$ for all $x, y \in D$. Clearly, any contraction is continuous. If equality holds, that is, if $|S(x) - S(y)| = r|x - y|$, then S transforms sets into geometrically similar sets, so S is a *contracting similarity*.

A finite family of contractions $\{S_1, S_2, \dots, S_m\}$, with $m \geq 2$, is called an *iterated function system* or IFS. We call a non-empty compact subset F of D an *attractor* (or *invariant set*) for the IFS if

$$F = \bigcup_{i=1}^m S_i(F),$$

that is, if it is made up of its images under the S_i . The fundamental property of an IFS is that it (essentially) determines a unique attractor, which is usually a fractal. For a simple example, take F to be the middle third Cantor set. Let $S_1, S_2 : \mathbb{R} \rightarrow \mathbb{R}$ be given by

$$S_1(x) = \frac{1}{3}x; \quad S_2(x) = \frac{1}{3}x + \frac{2}{3}.$$

9.1

Then $S_1(F)$ and $S_2(F)$ are just the left and right ‘halves’ of F , so $F = S_1(F) \cup S_2(F)$; thus F is an attractor of the IFS consisting of the contractions $\{S_1, S_2\}$, the two mappings which represent the basic self-similarities of the Cantor set.

We shall prove the fundamental property that an IFS has a unique non-empty compact (i.e. closed and bounded) attractor. This means, for example, that the middle third Cantor set is completely specified as the attractor of the mappings $\{S_1, S_2\}$ mentioned earlier.

To this end, we define a metric or distance d between subsets of D . Let \mathcal{S} denote the class of all non-empty compact subsets of D . Recall that the δ -neighbourhood of a set A is the set of points within distance δ of A , that is,

$$A_\delta = \{x \in D : |x - a| \leq \delta \text{ for some } a \in A\}.$$

We make \mathcal{S} into a metric space by defining the distance between two sets A and B to be the least δ such that the δ -neighbourhood of B contains A and vice versa:

$$d(A, B) = \inf \{\delta : A \subset B_\delta \text{ and } B \subset A_\delta\},$$

see [Figure 9.1](#). A simple check shows that d is a metric or distance function, that is, satisfies the three requirements (i) $d(A, B) \geq 0$ with equality if and only if $A = B$, (ii) $d(A, B) = d(B, A)$ and (iii) $d(A, B) \leq d(A, C) + d(C, B)$ for all $A, B, C \in \mathcal{S}$. The metric d is known as the *Hausdorff metric* on \mathcal{S} . In particular, if $d(A, B)$ is small, then A and B are close to each other as sets.

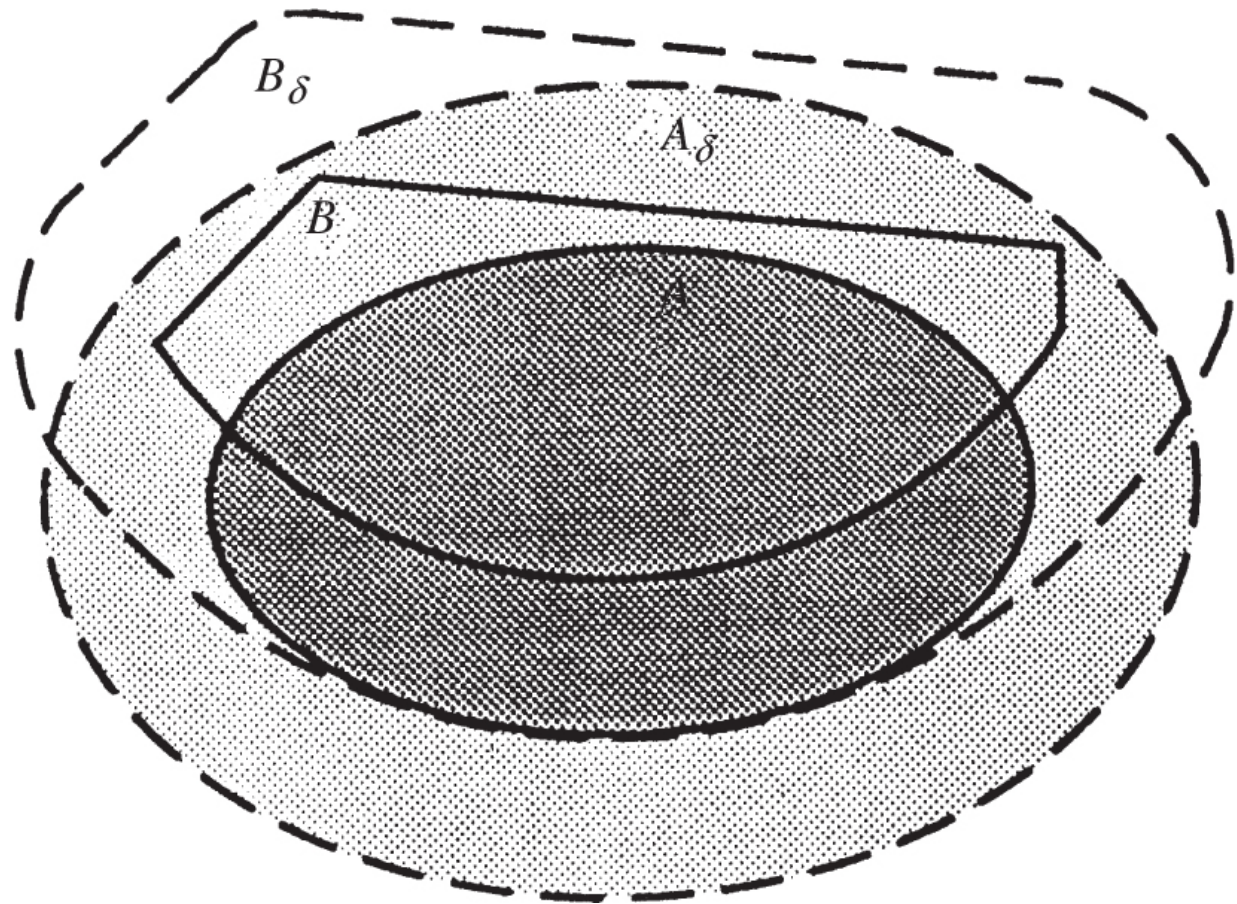


Figure 9.1 The Hausdorff distance between the sets A and B is the least $\delta > 0$ such that the δ -neighbourhood A_δ of A contains B and the δ -neighbourhood B_δ of B contains A .

We give two proofs of the fundamental result on IFSs. The first depends on Banach's contraction mapping theorem, and the second is direct and elementary. Both proofs use the transformation $S : \mathcal{S} \rightarrow \mathcal{S}$ on the non-empty compact sets given by

$$S(E) = \bigcup_{i=1}^m S_i(E) \quad \text{9.2}$$

for $E \in \mathcal{S}$. We write S^k for the k th iterate of S , so for $E \in \mathcal{S}$, $S^0(E) = E$ and $S^k(E) = S(S^{k-1}(E))$ for each integer $k \geq 1$.

Theorem 9.1

Let $\{S_1, \dots, S_m\}$ be an IFS of contractions on a closed set $D \subset \mathbb{R}^n$, so that

$$|S_i(x) - S_i(y)| \leq r_i |x - y| \quad (x, y \in D) \quad 9.3$$

with $r_i < 1$ for each i . Then the system has a unique attractor F , that is, a unique non-empty compact set such that

$$F = \bigcup_{i=1}^m S_i(F). \quad 9.4$$

Moreover,

$$F = \bigcap_{k=0}^{\infty} S^k(E) \quad 9.5$$

for every non-empty compact set $E \in \mathcal{S}$ such that $S_i(E) \subset E$ for all i .

First proof

If $A, B \in S$, then

$$d(S(A), S(B)) = d\left(\bigcup_{i=1}^m S_i(A), \bigcup_{i=1}^m S_i(B)\right) \leq \max_{1 \leq i \leq m} d(S_i(A), S_i(B))$$

using the definition of the metric d and noting that if the δ -neighbourhood $(S_i(A))_\delta$ contains $S_i(B)$ for all i , then $(\bigcup_{i=1}^m S_i(A))_\delta$ contains $\bigcup_{i=1}^m S_i(B)$, and vice versa. By (9.3),

$$d(S(A), S(B)) \leq (\max_{1 \leq i \leq m} r_i) d(A, B). \quad 9.6$$

It may be shown that d is a *complete* metric on S , that is, every Cauchy sequence of sets in S is convergent to a set in S . Since $0 < \max_{1 \leq i \leq m} r_i < 1$, (9.6) means that S is a contraction on the complete metric space (S, d) . By Banach's contraction mapping theorem, S has a unique fixed point, that is, there is a unique set $F \in S$ such that $S(F) = F$, satisfying (9.4), and moreover that $d(S^k(E), F) \rightarrow 0$ as $k \rightarrow \infty$. In particular, if $S_i(E) \subset E$ for all i , then $S(E) \subset E$, so that $S^k(E)$ is a decreasing sequence of non-empty compact sets containing F with intersection $\bigcap_{k=0}^{\infty} S^k(E)$ which must equal F .

Second proof

Let E be any set in S such that $S_i(E) \subset E$ for all i ; for example, $E = D \cap B(0, r)$ will do provided r is sufficiently large. Then $S^{k+1}(E) \subset S^k(E)$ for all positive integers k , so that $S^k(E)$ is a decreasing sequence of non-empty compact sets, which necessarily have non-empty compact intersection $F = \bigcap_{k=0}^{\infty} S^k(E)$. Since $S^k(E)$ is a decreasing sequence of sets, it follows that

$$S(F) = S\left(\bigcap_{k=0}^{\infty} S^k(E)\right) = \bigcap_{k=0}^{\infty} S(S^k(E)) = \bigcap_{k=1}^{\infty} S^k(E) = F$$

(that the third expression is contained in the second uses the compactness of E), so F satisfies (9.4) and is an attractor of the IFS.

To see that the attractor is unique, we derive (9.6) exactly as in the first proof. Then if A and B are both attractors $S(A) = A$ and $S(B) = B$, so (9.6) with $0 < \max_{1 \leq i \leq m} r_i < 1$ implies that $d(A, B) = 0$, so $A = B$.

Two main problems arise in connection with IFSs. The first problem is, given a set, to represent or ‘code’ it as the attractor of some IFS, and the second, given an IFS, to ‘decode’ it by displaying its attractor. In both cases, we may wish to go on to analyse the structure and dimensions of the attractor, and an IFS representation can be a great aid in doing this.

Finding an IFS that has a given F as its unique attractor can often be done by inspection, at least if F is self-similar or self-affine. For example, the Cantor dust (Figure 0.4) is easily seen to be the attractor of the four similarities on \mathbb{R}^2 which give the basic self-similarities of the set:

$$S_1(x, y) = \left(\frac{1}{4}x, \frac{1}{4}y + \frac{1}{2} \right), \quad S_2(x, y) = \left(\frac{1}{4}x + \frac{1}{4}, \frac{1}{4}y \right),$$

$$S_3(x, y) = \left(\frac{1}{4}x + \frac{1}{2}, \frac{1}{4}y + \frac{3}{4} \right), \quad S_4(x, y) = \left(\frac{1}{4}x + \frac{3}{4}, \frac{1}{4}y + \frac{1}{4} \right).$$

In general, it may not be possible to find an IFS with a given set as attractor, but we can normally find one with an attractor that is a close approximation to the required set. This question of representing general objects by IFSs is considered in Section 9.5.

The transformation S introduced in (9.2) is the key to computing the attractor of an IFS; indeed, (9.5) already provides a method for doing so. In fact, the sequence of iterates $S^k(E)$ converges to the attractor F in the Hausdorff metric for any initial set $E \in \mathcal{S}$, that is, $d(S^k(E), F) \rightarrow 0$. This follows since (9.6) implies that $d(S(E), F) = d(S(E), S(F)) \leq c d(E, F)$, so that $d(S^k(E), F) \leq c^k d(E, F)$, where $c = \max_{1 \leq i \leq m} r_i < 1$. Thus, the $S^k(E)$ provide increasingly good approximations to F . If F is a fractal, these approximations are sometimes called *pre-fractals* for F .

For each k ,

$$S^k(E) = \bigcup_{I_k} S_{i_1} \circ \cdots \circ S_{i_k}(E) = \bigcup_{I_k} S_{i_1}(S_{i_2}(\cdots(S_{i_k}(E))\cdots)), \quad 9.7$$

where the union is over the set I_k of all k -term sequences (i_1, \dots, i_k) with $1 \leq i_j \leq m$ (see [Figure 9.2](#)). (Recall that $S_{i_1} \circ \cdots \circ S_{i_k}$ denotes the composition of mappings, so that $(S_{i_1} \circ \cdots \circ S_{i_k})(x) = S_{i_1}(S_{i_2}(\cdots(S_{i_k}(x))\cdots))$.) If $S_i(E)$ is contained in E for each i and x is a point of F , it follows from (9.5) and (9.7) that there is a (not necessarily unique) sequence (i_1, i_2, \dots) such that $x \in S_{i_1} \circ \cdots \circ S_{i_k}(E)$ for all k . This sequence provides a natural coding for x , with

$$x = x_{i_1, i_2, \dots} = \bigcap_{k=1}^{\infty} S_{i_1} \circ \cdots \circ S_{i_k}(E), \quad 9.8$$

so that $F = \bigcup \{x_{i_1, i_2, \dots}\}$. This expression for $x_{i_1, i_2, \dots}$ is independent of E provided that $S_i(E)$ is contained in E for all i . Coding points of fractals in this way underlies many arguments in fractal geometry.

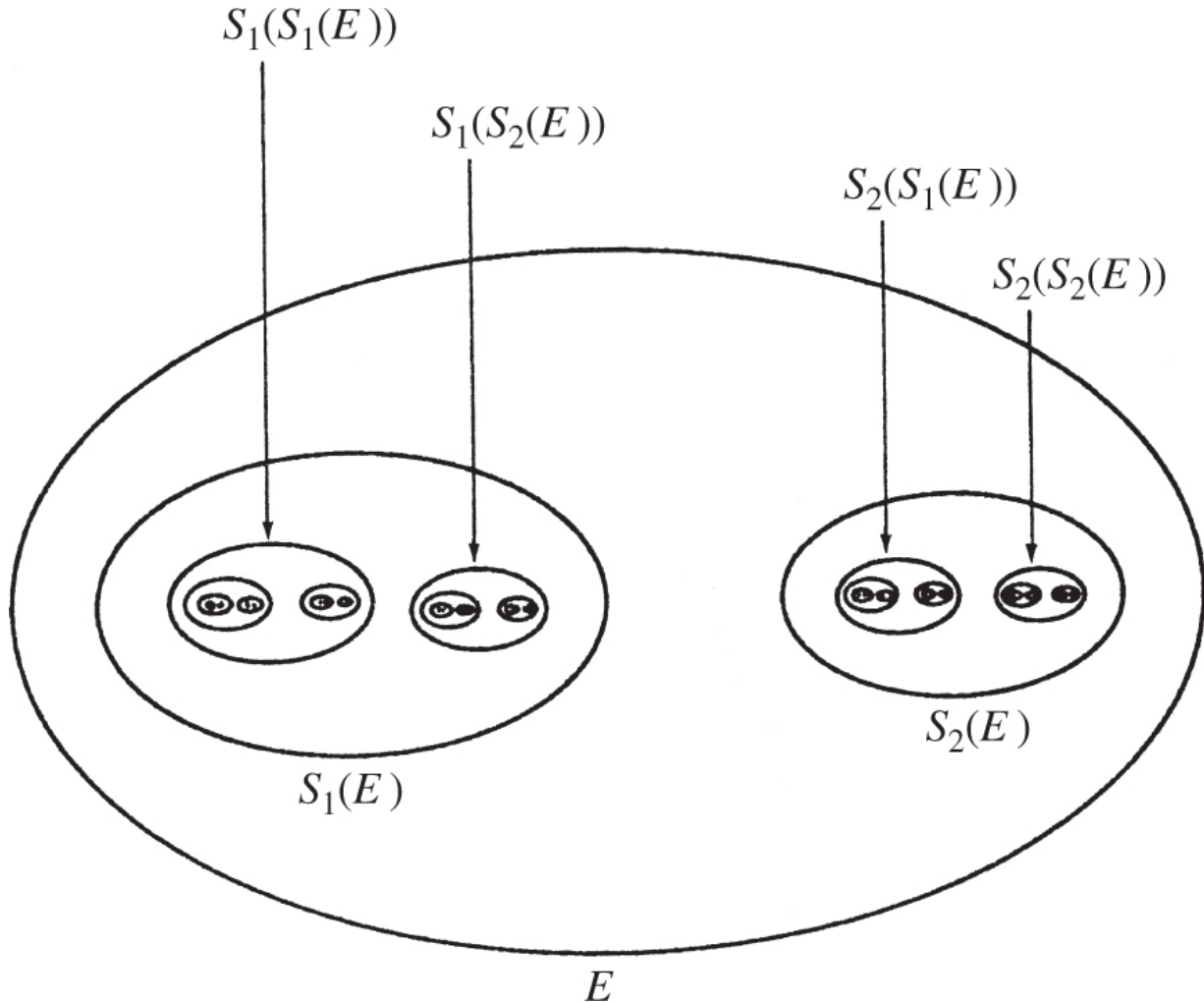


Figure 9.2 Construction of the attractor F for contractions S_1 and S_2 which map the large ellipse E onto the ellipses $S_1(E)$ and $S_2(E)$. The sets $S^k(E) = \bigcup_{i_1=1,2} S_{i_1} \circ \cdots \circ S_{i_k}(E)$ give increasingly good approximations to F .

Notice that if the union in (9.4) is disjoint, then F must be totally disconnected (provided the S_i are injections), since if $x_{i_1, i_2, \dots} \neq x_{i'_1, i'_2, \dots}$, we may find k such that $(i_1, \dots, i_k) \neq (i'_1, \dots, i'_k)$ so that the disjoint closed sets $S_{i_1} \circ \cdots \circ S_{i_k}(F)$ and $S_{i'_1} \circ \cdots \circ S_{i'_k}(F)$ disconnect the two points.

Again this may be illustrated by $S_1(x) = \frac{1}{3}x$, $S_2(x) = \frac{1}{3}x + \frac{2}{3}$ and F the Cantor set. If $E = [0, 1]$, then $S^k(E) = E_k$, the set of 2^k basic intervals of length 3^{-k} obtained at the k th stage of the usual Cantor set

construction (see [Figure 0.1](#)). Moreover, $x_{i_1, i_2, \dots}$ is the point of the Cantor set with base-3 expansion $0 \cdot a_1 a_2 \dots$, where $a_k = 0$ if $i_k = 1$ and $a_k = 2$ if $i_k = 2$. The pre-fractals $S^k(E)$ provide the usual construction of many fractals for a suitably chosen initial set E ; the $S_{i_1} \circ \dots \circ S_{i_k}(E)$ are called the *level-k sets* of the construction.

This theory provides us with two methods for computer drawing of IFS attractors in the plane, as indicated in [Figure 9.3](#). For the first method, take any initial set E (such as a square) and draw the k th approximation $S^k(E)$ to F given by (9.7) for a suitable value of k . The set $S^k(E)$ is made up of m^k small sets—either these can be drawn in full, or a representative point of each can be plotted. If E can be chosen as a line segment in such a way that $S_1(E), \dots, S_m(E)$ join up to form a polygonal curve with end points the same as those of E , then the sequence of polygonal curves $S^k(E)$ provides increasingly good approximations to the fractal curve F . Taking E as the initial interval in the von Koch curve construction is an example of this, with $S^k(E)$ just the k th step of the construction (E_k in [Figure 0.2](#)). Careful recursive programming is helpful when using this method.

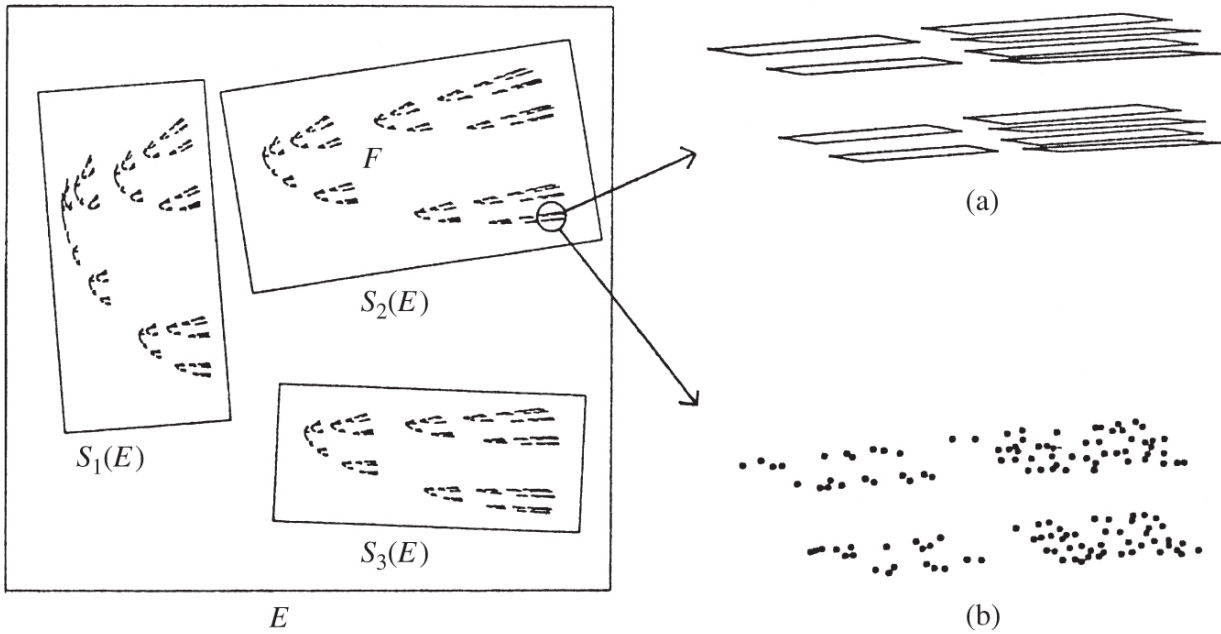


Figure 9.3 Two ways of computer drawing the attractor F of the IFS consisting of the three affine transformations S_1, S_2 and S_3 which map the square onto the rectangles. In method (a), the 3^k parallelograms $S_{i_1}(S_{i_2}(\cdots(S_{i_k}(E))\cdots))$ for $i_j = 1, 2, 3$ are drawn ($k = 6$ here). In method (b), the sequence of points x_k is plotted by choosing S_{i_k} at random from S_1, S_2 and S_3 for successive k and letting $x_k = S_{i_k}(x_{k-1})$.

The second method is known as the *chaos game*. Take x_0 as any initial point, select a contraction S_{i_1} from S_1, \dots, S_m at random (with equal probability, say) and let $x_1 = S_{i_1}(x_0)$. Continue in this way, choosing S_{i_k} from S_1, \dots, S_m at random and letting $x_k = S_{i_k}(x_{k-1})$ for $k = 1, 2, \dots$. For large enough k , the points x_k will be indistinguishably close to F , with x_k close to $S_{i_k} \circ \cdots \circ S_{i_1}(F)$, so the sequence $\{x_k\}$ will appear randomly distributed across F . A plot of the sequence $\{x_k\}$ from, say, the hundredth term onwards may give a good impression of F . (It is a consequence of a theorem in ergodic theory that, with probability 1, this sequence of points will fill F , in a manner that approximates a certain measure on F .)

An extension of these ideas allows IFSs to specify not only a set but also a ‘shading’ of the set. Without going into details (however, see Section 17.3), associating a probability p_i with each of the

contractions S_i , where $0 < p_i < 1$ and $\sum_{i=1}^m p_i = 1$, defines a mass distribution μ on the attractor F such that $\mu(A) = \sum_{i=1}^m p_i \mu(S_i^{-1}(A))$ for each set A . The local intensity of μ may then be regarded as the ‘grey level’ of the shading. In particular, if in the chaos game we choose each S_{i_k} from S_1, \dots, S_m so that the probability of choosing S_i is p_i , then plotting the sequence $\{x_k\}$ gives a rendering of the attractor F with the intensity of the points $\{x_k\}$ across F varying according to the measure μ .

9.2 Dimensions of self-similar sets

One of the advantages of an IFS representation is that the dimension of the attractor is often relatively easy to calculate or estimate in terms of the defining contractions. In this section, we discuss the case where $S_1, \dots, S_m : \mathbb{R}^n \rightarrow \mathbb{R}^n$ are *similarities*, that is, with

$$|S_i(x) - S_i(y)| = r_i|x - y| \quad (x, y \in \mathbb{R}^n), \quad \text{9.9}$$

where $0 < r_i < 1$ (r_i is called the *ratio* of S_i). Thus, each S_i transforms subsets of \mathbb{R}^n into geometrically similar sets. The attractor of such a collection of similarities is called a *self-similar set*, being a union of a number of smaller similar copies of itself. Standard examples include the middle third Cantor set, the Sierpiński triangle and the von Koch curve (see Figures 0.1–0.5). We show that, under fairly general conditions, a self-similar set F has Hausdorff and box dimensions given by its *similarity dimension*, that is, the number s that satisfies

$$\sum_{i=1}^m r_i^s = 1, \quad \text{9.10}$$

and further that F has positive and finite \mathcal{H}^s -measure. A ‘heuristic calculation’ similar to that of Example 3.7 indicates that the value given by (9.10) is at least plausible. If $F = \bigcup_{i=1}^m S_i(F)$ with the union ‘nearly disjoint’, we have that

$$\mathcal{H}^s(F) = \sum_{i=1}^m \mathcal{H}^s(S_i(F)) = \sum_{i=1}^m r_i^s \mathcal{H}^s(F) \quad \text{9.11}$$

using (9.9) and Scaling property 3.2. On the assumption that $0 < \mathcal{H}^s(F) < \infty$ at the ‘jump’ value $s = \dim_H F$, we may cancel the $\mathcal{H}^s(F)$ to get that s satisfies (9.10).

For this argument to give the right answer, we require a condition that ensures that the components $S_i(F)$ of F do no overlap ‘too much’. We say that the S_i satisfy the *open set condition* if there exists a non-empty bounded open set V such that

$$V \supset \bigcup_{i=1}^m S_i(V) \quad \text{9.12}$$

with this union disjoint. (For the middle third Cantor set example (9.1), the open set condition holds for $\{S_1, S_2\}$ taking V as the open interval $(0, 1)$.) In particular, the open set condition holds if the images of the attractor $S_1(F), \dots, S_m(F)$ are disjoint. We show that provided that the similarities S_i satisfy the open set condition, the Hausdorff dimension of the attractor is indeed given by (9.10).

We require the following geometrical estimate.

Lemma 9.2

Let $\{V_i\}$ be a collection of disjoint open subsets of \mathbb{R}^n such that each V_i contains a ball of radius $a_1 r$ and is contained in a ball of radius $a_2 r$. Then any ball B of radius r intersects at most $(1 + 2a_2)^n a_1^{-n}$ of the closures \overline{V}_i .

Proof

If \bar{V}_i meets B , then \bar{V}_i is contained in the ball concentric with B of radius $(1 + 2a_2)r$. Suppose that q of the sets \bar{V}_i intersect B . Summing the volumes of the corresponding interior balls of radii a_1r , it follows that $q(a_1r)^n \leq (1 + 2a_2)^n r^n$, giving the stated bound for q .

The derivation of the lower bound in the following theorem is a little awkward. The reader may find it helpful to follow through the proof with the middle third Cantor set in mind, or by referring to the ‘general example’ of [Figure 9.2](#). Alternatively, the proof of Proposition 9.7 covers the case when the sets $S_1(F), \dots, S_m(F)$ are disjoint and is rather simpler.

Theorem 9.3

Suppose that the open set condition (9.12) holds for the similarities S_i on \mathbb{R}^n with ratios $0 < r_i < 1$ for $1 \leq i \leq m$. If F is the attractor of the IFS $\{S_1, \dots, S_m\}$, that is,

$$F = \bigcup_{i=1}^m S_i(F), \tag{9.13}$$

then $\dim_H F = \dim_B F = s$, where s is given by

$$\sum_{i=1}^m r_i^s = 1. \tag{9.14}$$

Moreover, for this value of s , $0 < \mathcal{H}^s(F) < \infty$.

Proof

Let s satisfy (9.14). Let \mathcal{I}_k denote the set of all k -term sequences (i_1, \dots, i_k) with $1 \leq i_j \leq m$. For any set A and $(i_1, \dots, i_k) \in \mathcal{I}_k$, we write $A_{i_1, \dots, i_k} = S_{i_1} \circ \dots \circ S_{i_k}(A)$. It follows, by using (9.13) repeatedly, that

$$F = \bigcup_{\mathcal{I}_k} F_{i_1, \dots, i_k}.$$

We check that these covers of F provide a suitable upper estimate for the Hausdorff measure. Since the mapping $S_{i_1} \circ \dots \circ S_{i_k}$ is a similarity of ratio $r_{i_1} \cdots r_{i_k}$,

$$\sum_{\mathcal{I}_k} |F_{i_1, \dots, i_k}|^s = \sum_{\mathcal{I}_k} (r_{i_1} \cdots r_{i_k})^s |F|^s = \left(\sum_{i_1} r_{i_1}^s \right) \cdots \left(\sum_{i_k} r_{i_k}^s \right) |F|^s = |F|^s \quad 9.15$$

by (9.14). For each $\delta > 0$, we may choose k such that $|F_{i_1, \dots, i_k}| \leq (\max_i r_i)^k |F| \leq \delta$, so $\mathcal{H}_{\delta}^s(F) \leq |F|^s$ and hence $\mathcal{H}^s(F) \leq |F|^s$ and $\dim_H F \leq s$.

The lower bound is more awkward. Let \mathcal{I} be the set of all infinite sequences $\mathcal{I} = \{(i_1, i_2, \dots) : 1 \leq i_j \leq m\}$, and let

$I_{i_1, \dots, i_k} = \{(i_1, \dots, i_k, q_{k+1}, \dots) : 1 \leq q_j \leq m\}$ be the ‘cylinder’ consisting of those sequences in \mathcal{I} with initial terms (i_1, \dots, i_k) .

We may put a mass distribution μ on \mathcal{I} such that

$\mu(I_{i_1, \dots, i_k}) = (r_{i_1} \cdots r_{i_k})^s$. Since $(r_{i_1} \cdots r_{i_k})^s = \sum_{i=1}^m (r_{i_1} \cdots r_{i_k} r_i)^s$, that is,

$\mu(I_{i_1, \dots, i_k}) = \sum_{i=1}^m \mu(I_{i_1, \dots, i_k, i})$, it follows that μ is indeed a mass distribution on subsets of \mathcal{I} with $\mu(\mathcal{I}) = 1$. We may transfer μ to a mass distribution $\tilde{\mu}$ on F in a natural way by defining

$\tilde{\mu}(A) = \mu\{(i_1, i_2, \dots) : x_{i_1, i_2, \dots} \in A\}$ for subsets A of F . (Recall that $x_{i_1, i_2, \dots} = \bigcap_{k=1}^{\infty} F_{i_1, \dots, i_k}$.) Thus, the $\tilde{\mu}$ -mass of a set is the μ -mass of the corresponding sequences. It is easily checked that $\tilde{\mu}(F) = 1$.

We show that $\tilde{\mu}$ satisfies the conditions of the Mass distribution principle 4.2. Let V be an open set satisfying (9.12). Since

$\overline{V} \supset S(\overline{V}) = \bigcup_{i=1}^m S_i(\overline{V})$, the decreasing sequence of iterates $S^k(\overline{V})$ converges to F (see (9.5)). In particular, $\overline{V} \supset F$ and $\overline{V}_{i_1, \dots, i_k} \supset F_{i_1, \dots, i_k}$ for each finite sequence (i_1, \dots, i_k) . Let B be any ball of radius $r < 1$. We estimate $\tilde{\mu}(B)$ by considering the sets V_{i_1, \dots, i_k} with diameters comparable with that of B and with closures intersecting $F \cap B$.

We curtail each infinite sequence $(i_1, i_2, \dots) \in \mathcal{I}$ after the first term i_k for which

$$\left(\min_{1 \leq i \leq m} r_i \right) r \leq r_{i_1} r_{i_2} \cdots r_{i_k} \leq r \quad .9.16$$

and let \mathcal{Q} denote the finite set of all (finite) sequences obtained in this way. Then for every infinite sequence $(i_1, i_2, \dots) \in \mathcal{I}$, there is exactly one value of k with $(i_1, \dots, i_k) \in \mathcal{Q}$. Since V_1, \dots, V_m are disjoint, so are $V_{i_1, \dots, i_k, 1}, \dots, V_{i_1, \dots, i_k, m}$ for each (i_1, \dots, i_k) . Using this in a nested manner, it follows that the collection of open sets $\{V_{i_1, \dots, i_k} : (i_1, \dots, i_k) \in \mathcal{Q}\}$ is disjoint. Moreover,

$$F \subset \bigcup_{\mathcal{Q}} F_{i_1, \dots, i_k} \subset \bigcup_{\mathcal{Q}} \overline{V}_{i_1, \dots, i_k}.$$

We choose a_1 and a_2 so that V contains a ball of radius a_1 and is contained in a ball of radius a_2 . Then, for all $(i_1, \dots, i_k) \in \mathcal{Q}$, the set V_{i_1, \dots, i_k} contains a ball of radius $r_{i_1} \cdots r_{i_k} a_1$ and therefore one of radius $(\min_i r_i) a_1 r$ and is contained in a ball of radius $r_{i_1} \cdots r_{i_k} a_2$ and hence in a ball of radius $a_2 r$. Let \mathcal{Q}_1 denote those sequences (i_1, \dots, i_k) in \mathcal{Q} such that B intersects $\overline{V}_{i_1, \dots, i_k}$. By Lemma 9.2, there are at most $q = (1 + 2a_2)^n a_1^{-n} (\min_i r_i)^{-n}$ sequences in \mathcal{Q}_1 . Then

$$\tilde{\mu}(B) = \tilde{\mu}(F \cap B) = \mu\{(i_1, i_2, \dots) : x_{i_1, i_2, \dots} \in F \cap B\} \leq \mu \left\{ \bigcup_{\mathcal{Q}_1} I_{j_1, \dots, j_k} \right\}$$

since if $x_{i_1, i_2, \dots} \in F \cap B \subset \bigcup_{\mathcal{Q}_1} \overline{V}_{j_1, \dots, j_k}$, there is an integer k such that $(i_1, \dots, i_k) \in \mathcal{Q}_1$. Thus,

$$\tilde{\mu}(B) \leq \sum_{\mathcal{Q}_1} \mu(I_{i_1, \dots, i_k}) = \sum_{\mathcal{Q}_1} (r_{i_1} \cdots r_{i_k})^s \leq \sum_{\mathcal{Q}_1} r^s \leq r^s q$$

using (9.16). Since any set U is contained in a ball of radius $|U|$, we have $\tilde{\mu}(U) \leq |U|^s q$, so the Mass distribution principle 4.2 gives that $\mathcal{H}^s(F) \geq q^{-1} > 0$ and $\dim_H F \geq s$.

Finally, for box dimensions, given $r < 1$ let \mathcal{Q} be chosen as in (9.16). It follows inductively from (9.14) that $\sum_{\mathcal{Q}} (r_{i_1} r_{i_2} \cdots r_{i_k})^s = 1$, so \mathcal{Q} contains at most $(\min_i r_i)^{-s} r^{-s}$ sequences. For each

$(i_1, \dots, i_k) \in \mathcal{Q}$, we have $\frac{|\bar{V}_{i_1, \dots, i_k}|}{r_{i_1} \cdots r_{i_k} |\bar{V}|} = \frac{|\bar{V}_{i_1, \dots, i_k}|}{|\bar{V}|} \leq r |\bar{V}|$, so $\bigcup_{\mathcal{Q}} \bar{V}_{i_1, \dots, i_k}$ is a cover of F by at most $(\min_i r_i)^{-s} r^{-s}$ sets of diameter $r |\bar{V}|$. It follows from Equivalent definition 2.1(i) that $\overline{\dim}_B F \leq s$. Noting the standard relations $\dim_H F \leq \underline{\dim}_B F \leq \overline{\dim}_B F$, using (3.17), completes the proof.

If the open set condition is not assumed in Theorem 9.3, it may be shown that we still have $\dim_H F = \dim_B F$, although this value may be less than s .

The technique of curtailing the infinite sequences in \mathcal{I} to get a collection \mathcal{Q} of finite sequences for which the corresponding ratios are all comparable, as in (9.16), is frequently used in fractal geometry.

Theorem 9.3 enables us to find the dimension of many self-similar fractals with ease. Notice that if $\{S_1, \dots, S_m\}$ is an IFS of similarities all with ratio $r_i = r$, then (9.14) reduces to $s = \log m / -\log r$.

Example 9.4 Sierpiński triangle

The Sierpiński triangle or gasket F is constructed from an equilateral triangle by repeatedly removing inverted equilateral triangles (see Figure 0.3). Then $\dim_H F = \dim_B F = \log 3 / \log 2$.

Calculation

The set F is the attractor of the three obvious similarities of ratios $\frac{1}{2}$, which map the triangle E_0 onto the triangles of E_1 . The open set condition holds, taking V as the interior of E_0 . Thus, by Theorem 9.3, $\dim_H F = \dim_B F = \log 3 / \log 2$, which is the solution of $3\left(\frac{1}{2}\right)^s = \sum_1^3 \left(\frac{1}{2}\right)^s = 1$.

The next example involves similarity transformations of more than one ratio.

Example 9.5 Modified von Koch curve

Fix $0 < a \leq \frac{1}{3}$ and construct a curve F by repeatedly replacing the middle proportion a of each interval by the other two sides of an equilateral triangle (see Figure 9.4). Then $\dim_H F = \dim_B F$ is the solution of $2a^s + 2\left(\frac{1}{2}(1-a)\right)^s = 1$.

Calculation

The curve F is the attractor of the similarities that map the unit interval onto each of the four intervals in E_1 . The open set condition holds, taking V as the interior of the isosceles triangle of base length 1 and height $\frac{1}{2}a\sqrt{3}$, so Theorem 9.3 gives the dimension stated.

There is a convenient method of specifying certain self-similar sets diagrammatically, in particular self-similar curves such as Example 9.5. A *generator* consists of a number of straight line segments and two points specially identified. We associate with each line segment the similarity that maps the two special points onto the end points

of the segment. A sequence of sets approximating to the self-similar attractor may be built up by iterating the process of replacing each line segment by a similar copy of the generator; see [Figures 9.4–9.7](#) for some examples. Note that the similarities are defined by the generator only to within reflection and 180° rotation but the orientation may be specified by displaying the first step of the construction.

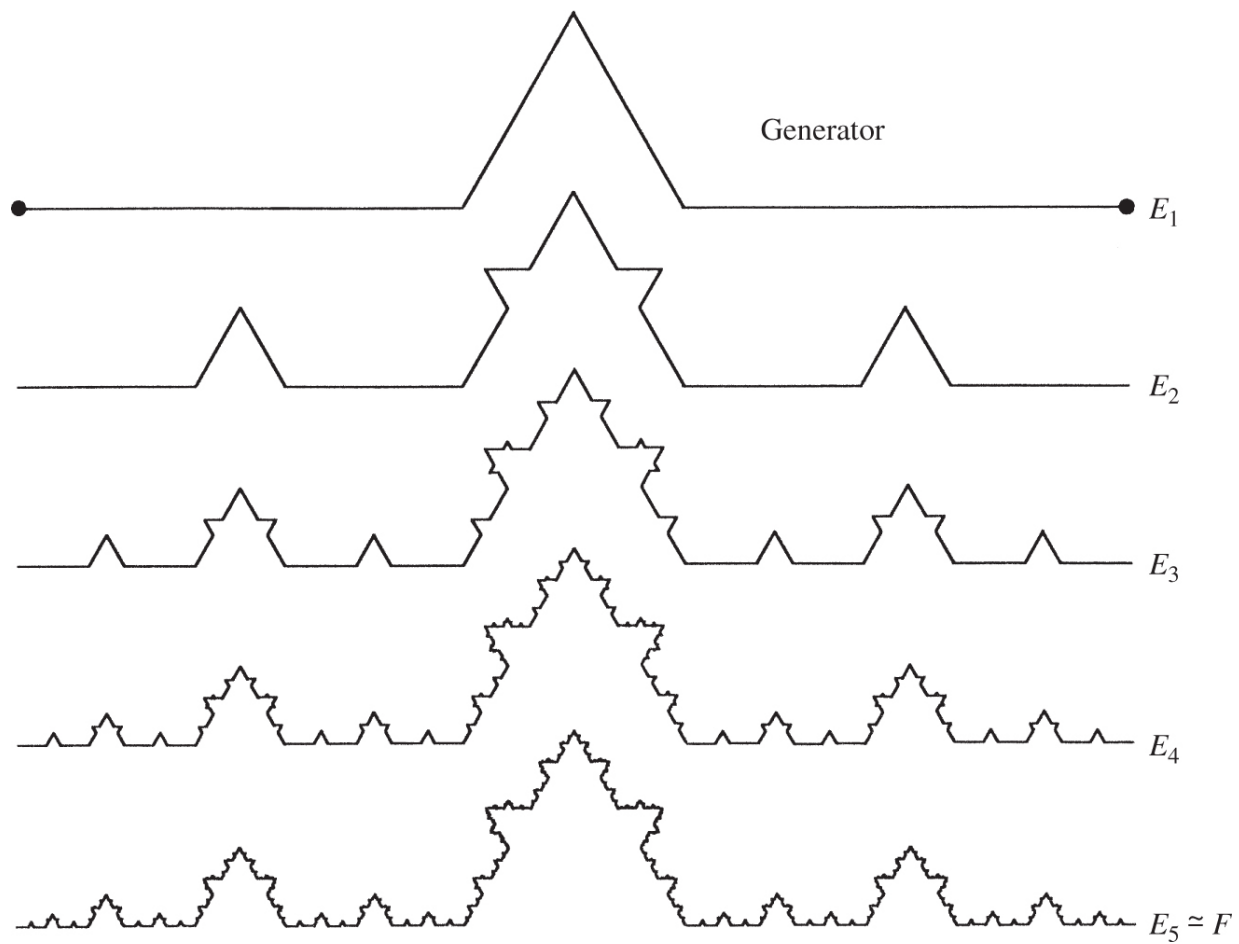


Figure 9.4. Construction of a modified von Koch curve—see Example 9.5.

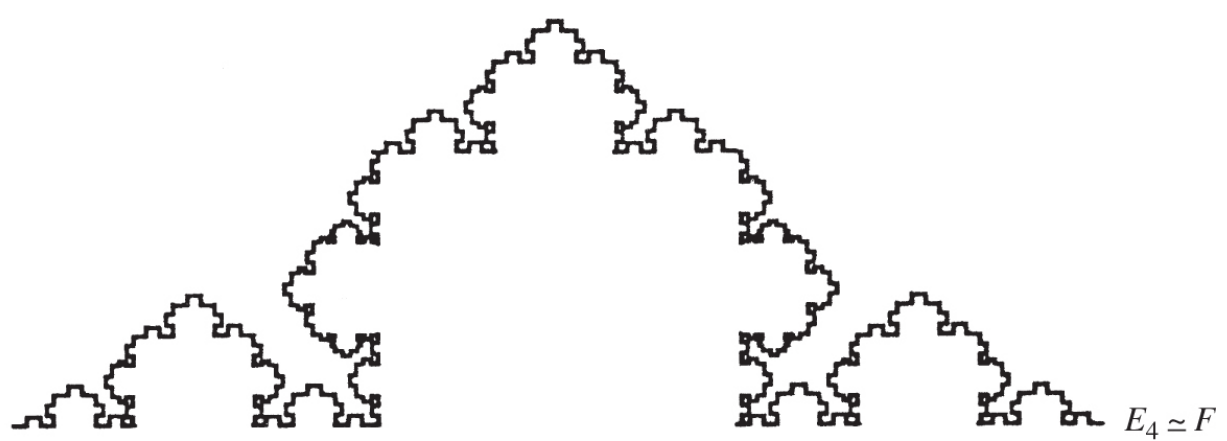
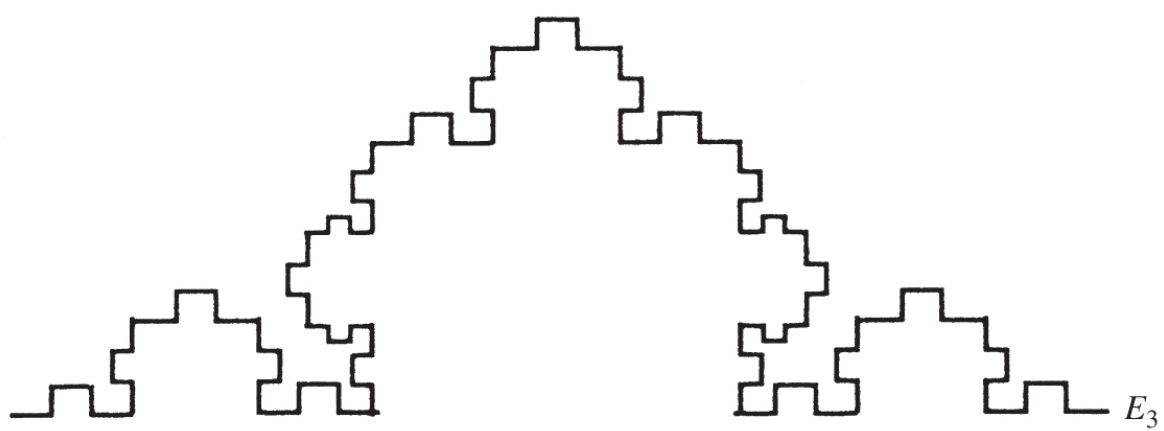
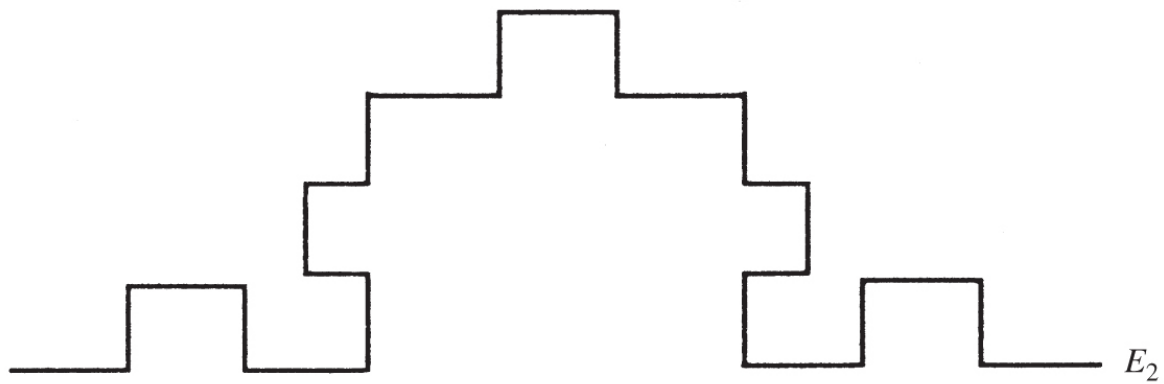
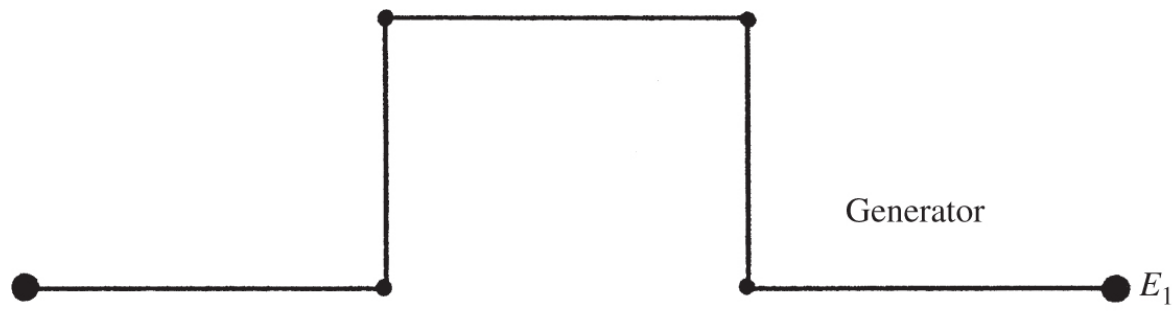


Figure 9.5 Stages in the construction of a fractal curve from a generator. The lengths of the segments in the generator are $\frac{1}{3}, \frac{1}{4}, \frac{1}{3}, \frac{1}{4}, \frac{1}{3}$, and the Hausdorff and box dimensions of F are given by $3\left(\frac{1}{3}\right)^s + 2\left(\frac{1}{4}\right)^s = 1$ or $s = 1.34\dots$

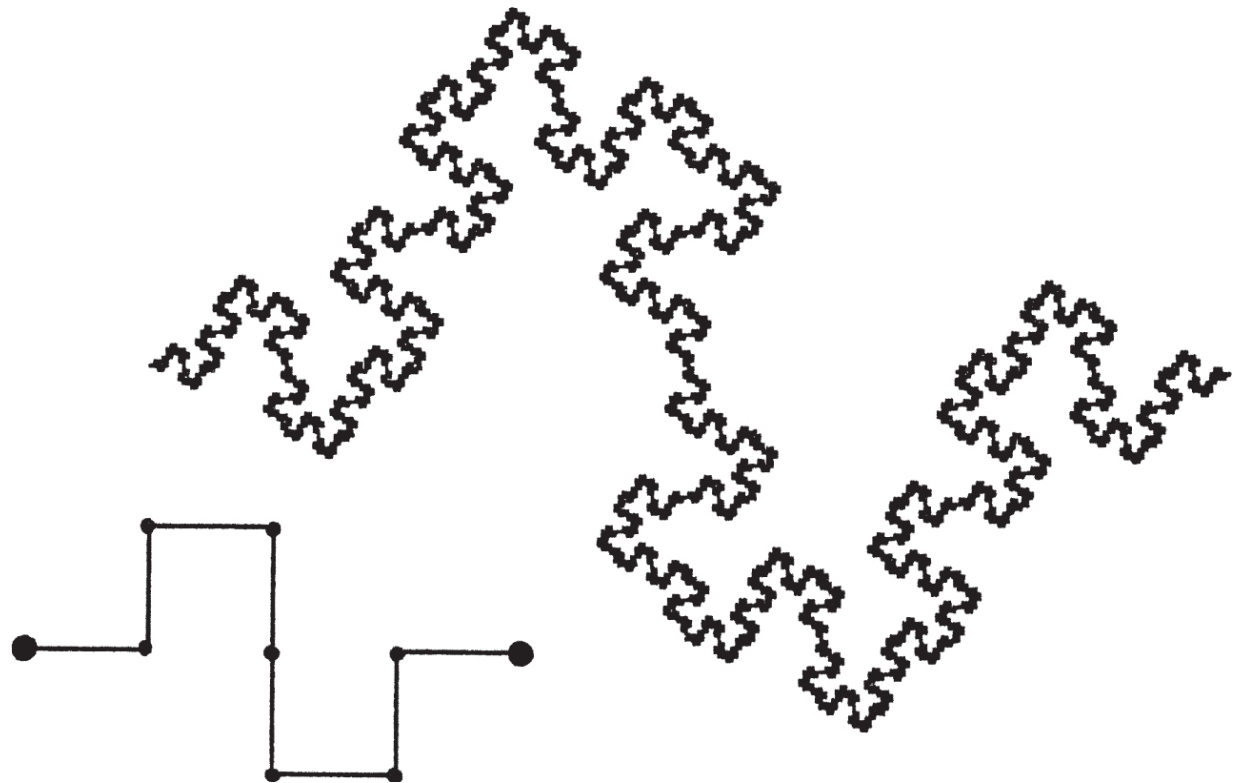


Figure 9.6 A fractal curve and its generator. The Hausdorff and box dimensions of the curve are equal to $\log 8 / \log 4 = 1\frac{1}{2}$.

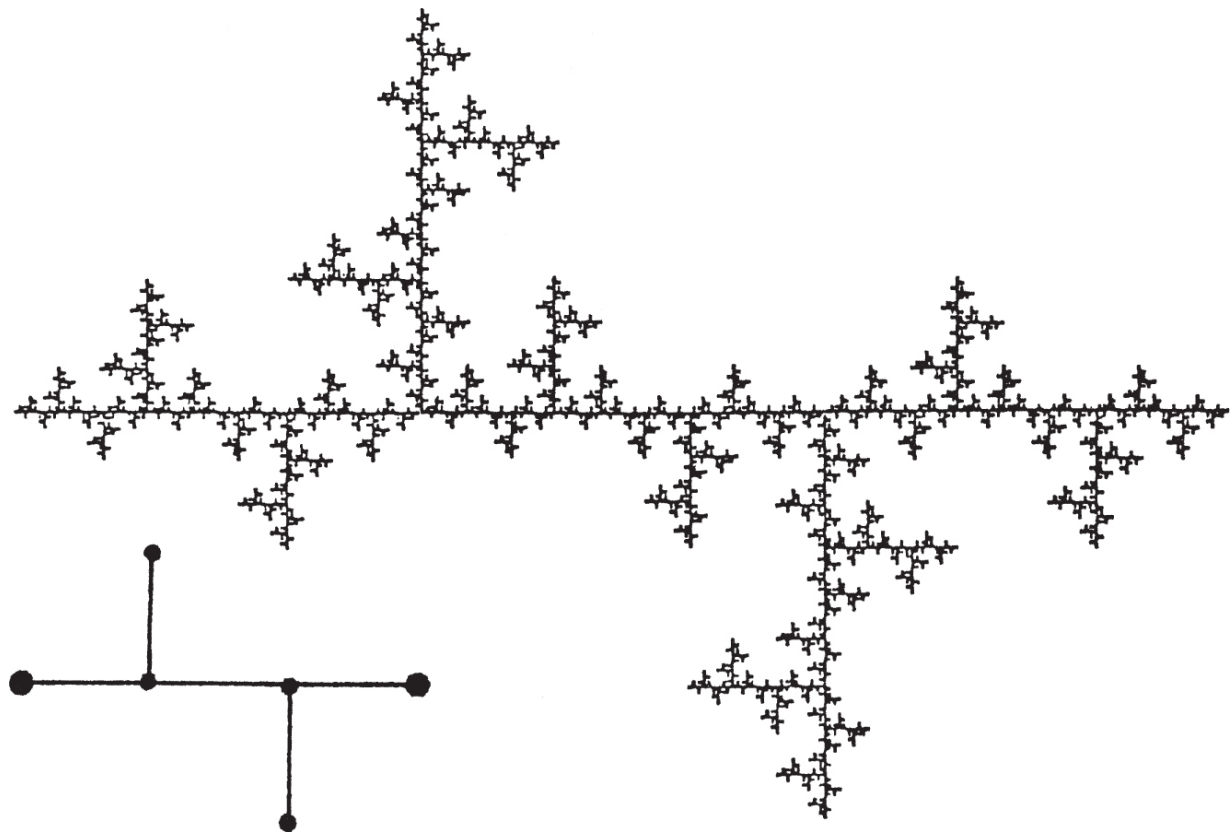


Figure 9.7 A tree-like fractal and its generator. The Hausdorff and box dimensions are equal to $\log 5 / \log 3 = 1.465 \dots$

9.3 Some variations

The calculations underlying Theorem 9.3 may be adapted to estimate the dimension of the attractor F of an IFS consisting of contractions that are not similarities.

Proposition 9.6

Let F be the attractor of an IFS consisting of contractions $\{S_1, \dots, S_m\}$ on a closed subset D of \mathbb{R}^n such that

$$|S_i(x) - S_i(y)| \leq r_i |x - y| \quad (x, y \in D)$$

with $0 < r_i < 1$ for each i . Then $\dim_H F \leq s$ and $\overline{\dim}_B F \leq s$, where $\sum_{i=1}^m r_i^s = 1$.

Proof

These estimates are essentially those of the first and last paragraphs of the proof of Theorem 9.3, noting that we have the inequality $|A_{i_1, \dots, i_k}| \leq r_{i_1} \cdots r_{i_k} |A|$ for each set A , rather than equality.

We next obtain a lower bound for dimension in the case where the components $S_i(F)$ of F are disjoint. Note that this will certainly be the case if there is *some* non-empty compact set E with $S_i(E) \subset E$ for all i and with the $S_i(E)$ disjoint.

Proposition 9.7

Consider the IFS consisting of contractions $\{S_1, \dots, S_m\}$ on a closed subset D of \mathbb{R}^n such that

$$b_i|x - y| \leq |S_i(x) - S_i(y)| \quad (x, y \in D) \quad \mathbf{9.17}$$

with $0 < b_i < 1$ for each i . Assume that the (non-empty compact) attractor F satisfies

$$F = \bigcup_{i=1}^m S_i(F), \quad \mathbf{9.18}$$

with this union disjoint. Then F is totally disconnected and $\dim_H F \geq s$ where

$$\sum_{i=1}^m b_i^s = 1. \quad \mathbf{9.19}$$

Proof

Let $d > 0$ be the minimum distance between any pair of the disjoint compact sets $S_1(F), \dots, S_m(F)$, that is,

$d = \min_{i \neq j} \inf \{ |x - y| : x \in S_i(F), y \in S_j(F) \}$. Let $F_{i_1, \dots, i_k} = S_{i_1} \circ \dots \circ S_{i_k}(F)$ and define μ by $\mu(F_{i_1, \dots, i_k}) = (b_{i_1} \cdots b_{i_k})^s$. Since

$$\begin{aligned}\sum_{i=1}^m \mu(F_{i_1, \dots, i_k, i}) &= \sum_{i=1}^m (b_{i_1} \cdots b_{i_k} b_i)^s = (b_{i_1} \cdots b_{i_k})^s = \mu(F_{i_1, \dots, i_k}) \\ &= \mu\left(\bigcup_{i=1}^k F_{i_1, \dots, i_k, i}\right)\end{aligned}$$

it follows that μ defines a mass distribution on F with $\mu(F) = 1$.

If $x \in F$, there is a unique infinite sequence i_1, i_2, \dots such that $x \in F_{i_1, \dots, i_k}$ for each k . For $0 < r < d$, let k be the least integer such that

$$b_{i_1} \cdots b_{i_k} d \leq r < b_{i_1} \cdots b_{i_{k-1}} d.$$

If i'_1, \dots, i'_k is distinct from i_1, \dots, i_k , the sets F_{i_1, \dots, i_k} and $F_{i'_1, \dots, i'_k}$ are disjoint and separated by a gap of at least $b_{i_1} \cdots b_{i_{k-1}} d > r$. (To see this, note that if j is the least integer such that $i_j \neq i'_j$, then $F_{i_j, \dots, i_k} \subset F_{i_j}$ and $F_{i'_j, \dots, i'_k} \subset F_{i'_j}$ are separated by d , so F_{i_1, \dots, i_k} and $F_{i'_1, \dots, i'_k}$ are separated by at least $b_{i_1} \cdots b_{i_{k-1}} d$.) It follows that $F \cap B(x, r) \subset F_{i_1, \dots, i_k}$ so

$$\mu(F \cap B(x, r)) \leq \mu(F_{i_1, \dots, i_k}) = (b_{i_1} \cdots b_{i_k})^s \leq d^{-s} r^s.$$

If U intersects F , then $U \subset B(x, r)$ for some $x \in F$ with $r = |U|$. Thus, $\mu(U) \leq d^{-s} |U|^s$, so by the Mass distribution principle 4.2, $\mathcal{H}^s(F) > 0$ and $\dim_H F \geq s$.

The separation between the components F_{i_1, \dots, i_k} indicated above implies that F is totally disconnected.

Example 9.8 ‘Non-linear’ Cantor set

Let $D = [\frac{1}{2}(1 + \sqrt{3}), (1 + \sqrt{3})]$ and let $S_1, S_2 : D \rightarrow D$ be given by

$S_1(x) = 1 + 1/x, S_2(x) = 2 + 1/x$. Then

$0.44 < \dim_H F \leq \underline{\dim}_B F \leq \overline{\dim}_B F < 0.66$ where F is the attractor of $\{S_1, S_2\}$. (This example arises in connection with number theory; see Section 10.2.)

Calculation

We note that $S_1(D) = [\frac{1}{2}(1 + \sqrt{3}), \sqrt{3}]$ and $S_2(D) = [\frac{1}{2}(3 + \sqrt{3}), 1 + \sqrt{3}]$, so

we can use Propositions 9.6 and 9.7 to estimate $\dim_H F$. By the mean-value theorem (see Section 1.2), if $x, y \in D$ are distinct points, then $(S_i(x) - S_i(y))/(x - y) = S'_i(z_i)$ for some $z_i \in D$. Thus, for $i = 1, 2$,

$$\inf_{x \in D} |S'_i(x)| \leq \frac{|S_i(x) - S_i(y)|}{|x - y|} \leq \sup_{x \in D} |S'_i(x)|.$$

Since $S'_1(x) = S'_2(x) = -1/x^2$, it follows that

$$\frac{1}{2}(2 - \sqrt{3}) = (1 + \sqrt{3})^{-2} \leq \frac{|S_i(x) - S_i(y)|}{|x - y|} \leq \left(\frac{1}{2}(1 + \sqrt{3})\right)^{-2} = 2(2 - \sqrt{3})$$

for both $i = 1$ and $i = 2$. According to Propositions 9.6 and 9.7, lower and upper bounds for the dimensions are given by the solutions of $2(\frac{1}{2}(2 - \sqrt{3}))^s = 1$ and $2(2(2 - \sqrt{3}))^s = 1$ which are $s = \log 2 / \log(2(2 - \sqrt{3})) = 0.34$ and $\log 2 / \log(\frac{1}{2}(2 + \sqrt{3})) = 1.11$, respectively.

For a subset of the real line, an upper bound greater than 1 is not of much interest. One way of getting better estimates is to note that F is also the attractor of the four mappings on $[0, 1]$

$$S_i \circ S_j = i + 1/(j + 1/x) = i + x/(jx + 1) \quad (i, j = 1, 2).$$

By calculating derivatives and using the mean-value theorem as before, we get that

$$(S_i \circ S_j)'(x) = (jx + 1)^{-2}$$

so

$$\left(j(1 + \sqrt{3}) + 1\right)^{-2} |x - y| \leq |S_i \circ S_j(x) - S_i \circ S_j(y)| \leq \left(\frac{1}{2}j(1 + \sqrt{3}) + 1\right)^{-2} |x - y|.$$

Lower and upper bounds for the dimensions are given by the solutions of $2(2 + \sqrt{3})^{-2s} + 2(3 + 2\sqrt{3})^{-2s} = 1$ and $2\left(\frac{1}{2}(3 + \sqrt{3})\right)^{-2s} + 2(2 + \sqrt{3})^{-2s} = 1$, giving $0.44 < \dim_H F < 0.66$, a considerable improvement on the previous estimates. In fact, $\dim_H F = 0.531$, a value that may be obtained by looking at yet higher-order iterates of the S_i .

*The rest of this subsection may be omitted.

The technique used in Example 9.8 to improve the dimension estimates is often useful for attractors of transformations that are not strict similarities. If F is the attractor for the IFS $\{S_1, \dots, S_m\}$ on D , then F is also the attractor for the IFS consisting of the m^k transformations $\{S_{i_1} \circ \dots \circ S_{i_k}\}$ for each k . If the S_i are, say, twice differentiable on an open set containing F , it may be shown that when k is large, the contractions $S_{i_1} \circ \dots \circ S_{i_k}$ are, in a sense, close to similarities on D . In particular, for transformations on a subset D of \mathbb{R} , if $b = \inf_{x \in D} |(S_{i_1} \circ \dots \circ S_{i_k})'(x)|$ and $c = \sup_{x \in D} |(S_{i_1} \circ \dots \circ S_{i_k})'(x)|$, then

$$b|x - y| \leq |S_{i_1} \circ \dots \circ S_{i_k}(x) - S_{i_1} \circ \dots \circ S_{i_k}(y)| \leq c|x - y| \quad (x, y \in D),$$

If k is large, then b/c will be close to 1, and applying Propositions 9.6 and 9.7 to the m^k transformations $S_{i_1} \circ \dots \circ S_{i_k}$ gives good upper and lower estimates for the dimensions of F .

We may take this further. If the S_i are twice differentiable on a subset D of \mathbb{R} ,

$$\frac{|S_{i_1} \circ \dots \circ S_{i_k}(x) - S_{i_1} \circ \dots \circ S_{i_k}(y)|}{|x - y|} \sim |(S_{i_1} \circ \dots \circ S_{i_k})'(w)|$$

for large k , where x, y and w are any points of D . The composition of mappings $S_{i_1} \circ \dots \circ S_{i_k}$ is close to a similarity on D , so by comparison with Theorem 9.3, we would expect the dimension of the attractor F to be close to the value of s for which

$$\sum_{\mathcal{I}_k} |(S_{i_1} \circ \cdots \circ S_{i_k})'(w)|^s = 1,$$

9.20

where the sum is over the set \mathcal{I}_k of all k -term sequences. This expectation motivates the following theorem.

Theorem 9.9

Let $V \subset \mathbb{R}$ be an open interval. Let S_1, \dots, S_m be contractions on \bar{V} that are twice differentiable on V with $a \leq |S_i'(w)| \leq c$ for all $1 \leq i \leq m$ and $w \in V$, where $0 < a \leq c < 1$ are constants. Suppose that the S_i satisfy the open set condition (9.12) with open set V . Then the limit

$$\lim_{k \rightarrow \infty} \left[\sum_{\mathcal{I}_k} |(S_{i_1} \circ \cdots \circ S_{i_k})'(w)|^s \right]^{1/k} = \varphi(s) \quad .9.21$$

exists for each $s > 0$, is independent of $w \in V$ and is strictly decreasing in s . If F is the attractor of $\{S_1, \dots, S_m\}$, then $\dim_H F = \dim_B F$ is the solution of $\varphi(s) = 1$, and F is an s -set, that is, $0 < \mathcal{H}^s(F) < \infty$ for this value of s .

Note on Proof

The main difficulty is to show that the limit (9.21) exists—this depends on the differentiability condition on the S_i . Given this, the argument outlined above may be used to show that the value of s satisfying (9.20) is a good approximation to the dimension when k is large; letting $k \rightarrow \infty$ then gives the result.

Similar ideas, but involving the rate of convergence to the limit in (9.21), are needed to show that $0 < \mathcal{H}^s(F) < \infty$.

There are higher-dimensional analogues of Theorem 9.9. Suppose that the contractions S_1, \dots, S_m on a domain D in the complex plane

are complex analytic mappings. Then the S_i are conformal, or in other words are locally like similarity transformations, contracting at the same rate in every direction. We have

$$S_i(z) = S_i(z_0) + S'_i(z_0)(z - z_0) + \text{terms in } (z - z_0)^2 \text{ and higher powers}$$

so that if $z - z_0$ is small,

$$S_i(z) \sim S_i(z_0) + S'_i(z_0)(z - z_0), \quad \text{9.22}$$

where $S'_i(z_0)$ is a complex number with $|S'_i(z_0)| < 1$. But the right-hand side of (9.22) is just a similarity expressed in complex notation. In this setting, Theorem 9.9 holds, by the same sort of argument as in the 1-dimensional case.

Results such as these are part of the ‘thermodynamic formalism’, a body of theory that leads to dimension formulae for attractors of IFSs and invariant sets of dynamical systems in a wide range of settings.

9.4 Self-affine sets

Self-affine sets form an important class of sets, which include self-similar sets as a particular case. An *affine transformation* $S : \mathbb{R}^n \rightarrow \mathbb{R}^n$ is a transformation of the form

$$S(x) = T(x) + b,$$

where T is a linear transformation on \mathbb{R}^n (representable by an $n \times n$ matrix) and b is a vector in \mathbb{R}^n . Thus, an affine transformation S is a combination of a translation, rotation, dilation and, perhaps, a reflection. In particular, S maps spheres to ellipsoids, squares to parallelograms, and so on. Unlike similarities, affine transformations contract with differing ratios in different directions.

If an IFS consists of affine contractions $\{S_1, \dots, S_m\}$ on \mathbb{R}^n , the attractor F guaranteed by Theorem 9.1 is termed a *self-affine set*. An example is given in [Figure 9.8](#): S_1, S_2 and S_3 are the transformations that map the square E onto the three rectangles in the obvious way. The attractor F is made up of the three affine copies of itself: $S_1(F), S_2(F)$ and $S_3(F)$.

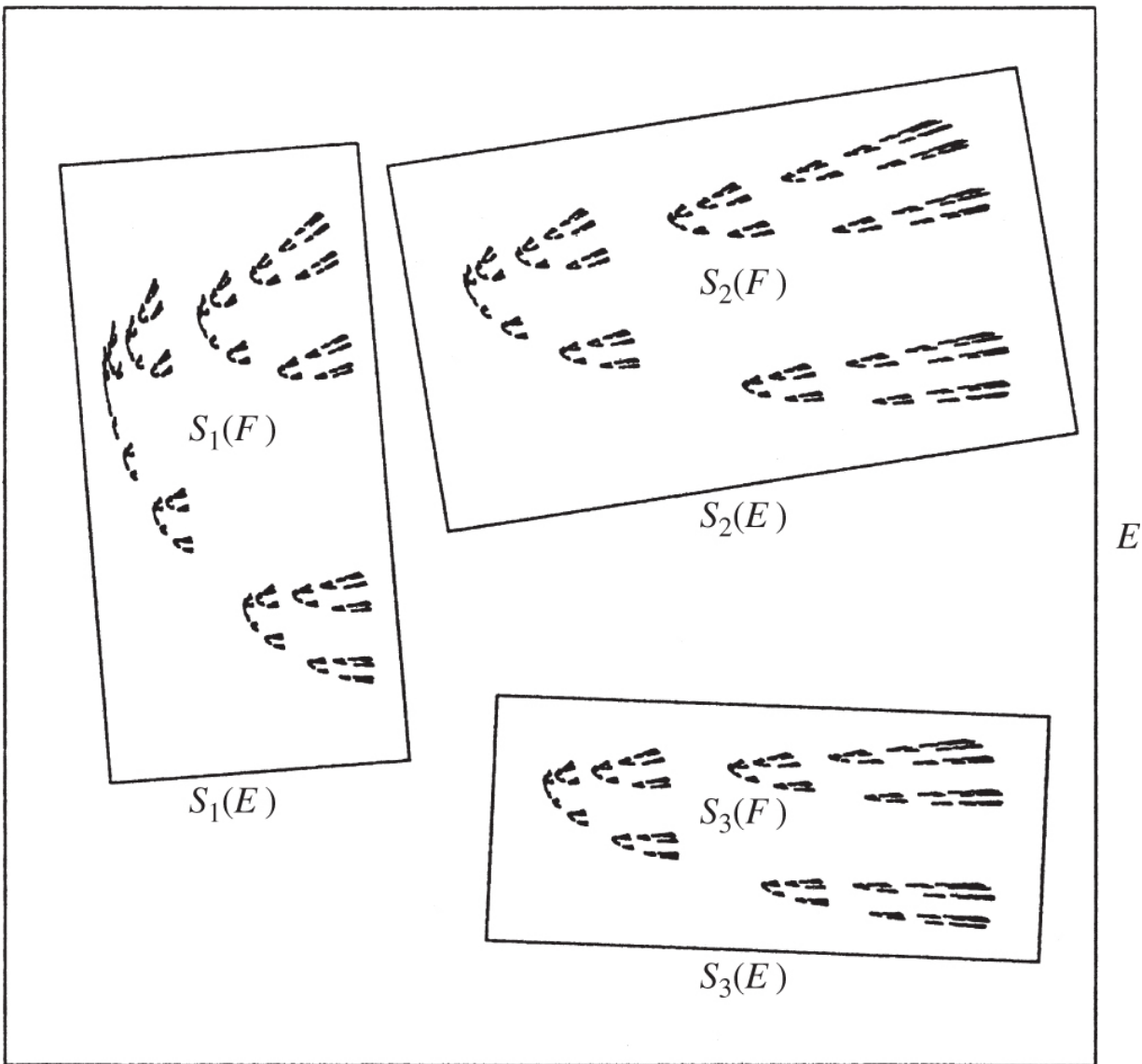


Figure 9.8 A self-affine set which is the attractor of the affine transformations that map the square E onto the rectangles is shown.

It is natural to look for a formula for the dimension of self-affine sets that generalises formula (9.14) for self-similar sets. We might hope that the dimension depends on the affine transformations in a reasonably simple way, easily expressible in terms of the matrices and vectors that represent the affine transformation. Unfortunately, the situation is much more complicated than this—the following example shows that if the affine transformations are varied in a

continuous way, the dimension of the self-affine set need not change continuously.

Example 9.10

Let S_1, S_2 be the affine contractions on \mathbb{R}^2 that map the unit square onto the rectangles R_1 and R_2 of sides $\frac{1}{2}$ and ε where $0 < \varepsilon < \frac{1}{2}$, as in Figure 9.9. The rectangle R_1 abuts the y -axis, but the end of R_2 is distance $0 \leq \lambda \leq \frac{1}{2}$ from the y -axis. If F is the attractor of the contractions $\{S_1, S_2\}$, we have $\dim_H F \geq 1$ when $\lambda > 0$, but $\dim_H F = \log 2 / -\log \varepsilon < 1$ when $\lambda = 0$.

Calculation

Suppose $\lambda > 0$ (Figure 9.9a). Then the k th stage of the construction $E_k = \bigcup S_{i_1} \circ \cdots \circ S_{i_k}(E)$ consists of 2^k rectangles of sides $2^{-k} \times \varepsilon^k$ with the projection of E_k onto the x -axis, $\text{proj } E_k$, containing the interval $[0, 2\lambda]$. Since $F = \bigcap_{i=1}^{\infty} E_k$, it follows that $\text{proj } F$ contains the interval $[0, 2\lambda]$. (Another way of seeing this is by noting that $\text{proj } F$ is the attractor of the contractions $\tilde{S}_1, \tilde{S}_2 : \mathbb{R} \rightarrow \mathbb{R}$ given by $\tilde{S}_1(x) = \frac{1}{2}x$, $\tilde{S}_2(x) = \frac{1}{2}x + \lambda$, which has as attractor the interval $[0, 2\lambda]$.) Thus, $\dim_H F \geq \dim_H \text{proj } F = \dim_H [0, 2\lambda] = 1$.

If $\lambda = 0$, the situation changes (Figure 9.9b). E_k consists of 2^k rectangles of sides 2^{-k} and ε^k which all have their left-hand ends abutting the y -axis, with E_k contained in the strip $\{(x, y) : 0 \leq x \leq 2^{-k}\}$. Letting $k \rightarrow \infty$, we see that F is a uniform Cantor set contained in the y -axis, which may be obtained by repeatedly removing a proportion $1 - 2\varepsilon$ from the centre of each interval. Thus, $\dim_H F = \log 2 / -\log \varepsilon < 1$ (see Example 4.5).

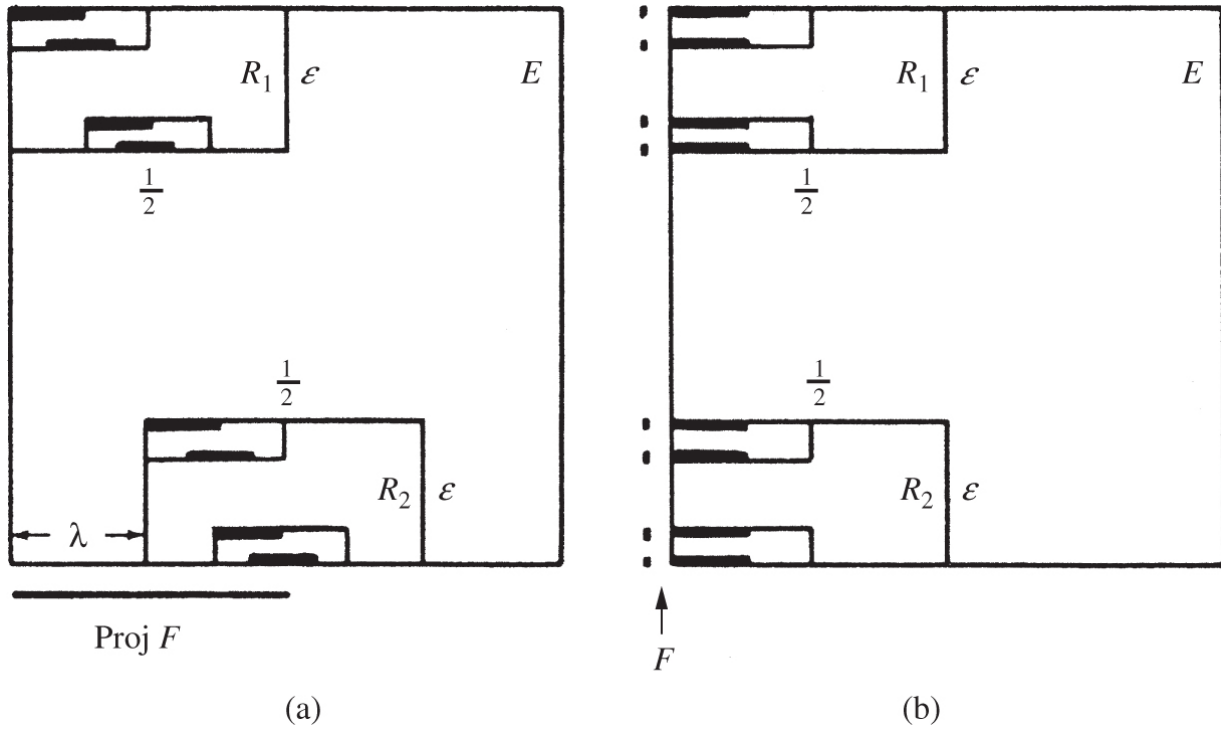


Figure 9.9. Discontinuity of the dimension of self-affine sets. The affine mappings S_1 and S_2 map the unit square E onto R_1 and R_2 . In (a), $\lambda > 0$ and $\dim_H F \geq \dim_H \text{proj } F = 1$, but in (b), $\lambda = 0$, and $\dim_H F = \log 2 / -\log \varepsilon < 1$.

With such discontinuous behaviour, which becomes even worse for more involved sets of affine transformations, one cannot expect a simple formula for the dimension of self-affine sets. However, one situation which has been completely analysed is the self-affine set obtained by the following recursive construction; a specific case is illustrated in [Figures 9.11](#) and [9.10](#).

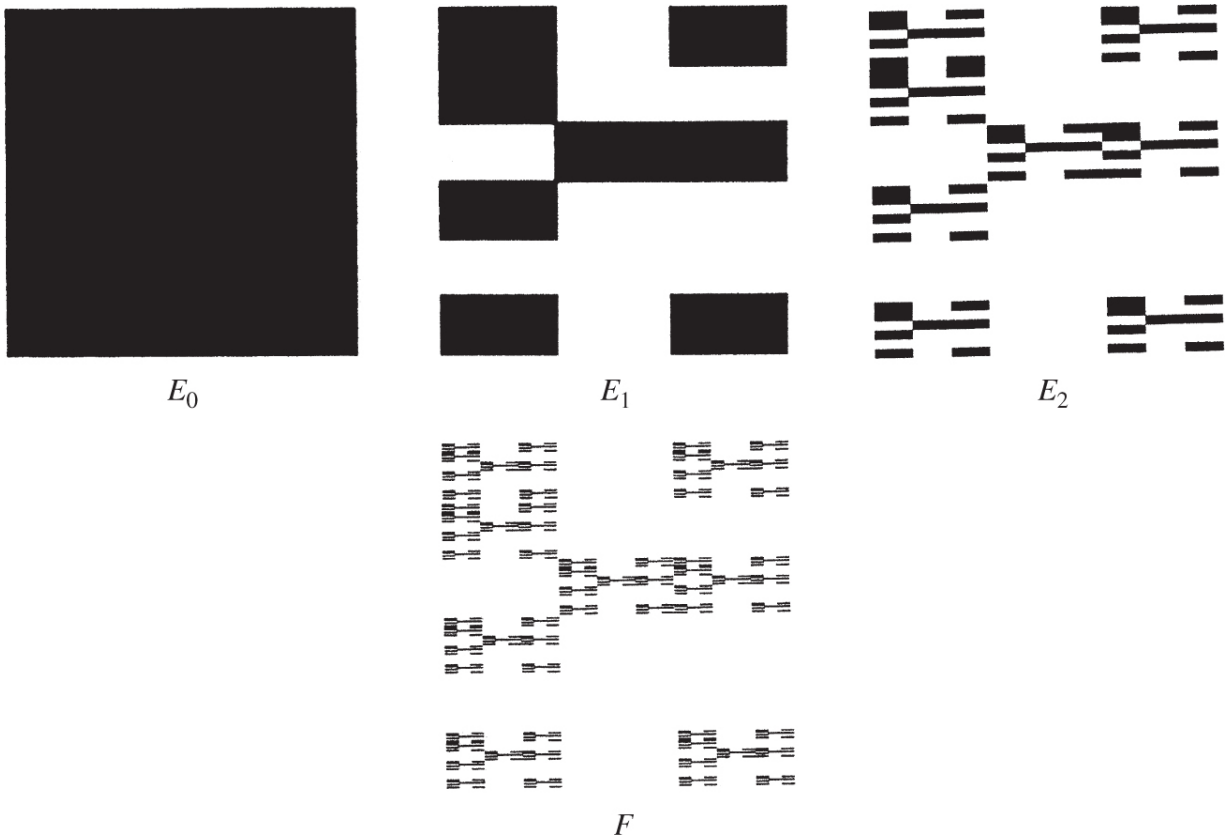


Figure 9.10 Construction of a self-affine set of the type considered in Example 9.11. Such sets may have different Hausdorff and box dimensions.

Example 9.11

Let the unit square E_0 be divided into a $p \times q$ array of rectangles of sides $1/p$ and $1/q$ where p and q are positive integers with $p < q$. Select a subcollection of these rectangles to form E_1 , and let N_j denote the number of rectangles selected from the j th column for $1 \leq j \leq p$ (see Figure 9.11). Iterate this construction in the usual way, with each rectangle replaced by an affine copy of E_1 , and let F be the limiting set obtained. Then

$$\dim_H F = \log \left(\sum_{j=1}^p N_j^{\log p / \log q} \right) \frac{1}{\log p}$$

and

$$\dim_B F = \frac{\log p_1}{\log p} + \log \left(\frac{1}{p_1} \sum_{j=1}^p N_j \right) \frac{1}{\log q},$$

where p_1 is the number of columns containing at least one rectangle of E_1 .

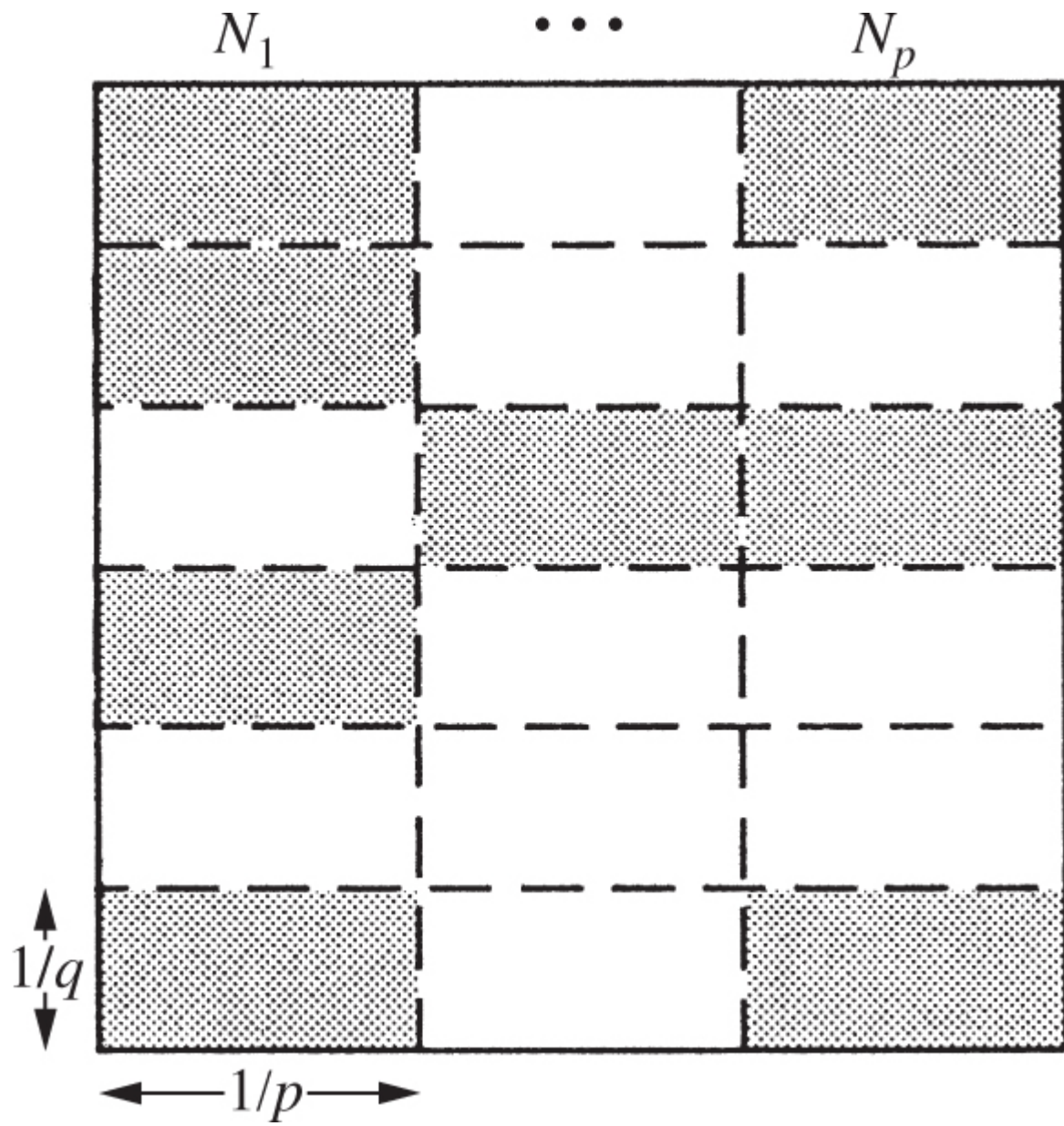


Figure 9.11 Data for the self-affine set of Example 9.11. The affine transformations map the square onto selected $1/p \times 1/q$ rectangles from the $p \times q$ array.

Calculation

This requires delicate estimates of numbers of covering sets and is omitted here.

Notice in this example that the dimension depends not only on the number of rectangles selected at each stage but also on their relative positions. Moreover, $\dim_H F$ and $\dim_B F$ are not, in general, equal.

**The rest of this subsection may be omitted.*

The above example is rather specific in that the affine transformations are all translates of each other. Obtaining a dimension formula valid for all self-affine sets is an intractable problem. We briefly outline an approach that leads to an expression for the dimension of the attractor of the affine contractions

$S_i(x) = T_i(x) + b_i$ ($1 \leq i \leq m$) for *almost all* sequences of vectors b_1, \dots, b_m

Let $T : \mathbb{R}^n \rightarrow \mathbb{R}^n$ be a linear mapping that is contracting and non-singular. The *singular values* $1 > \alpha_1 \geq \alpha_2 \geq \dots \geq \alpha_n > 0$ of T may be defined in two equivalent ways: they are the lengths of the principal semi-axes of the ellipsoid $T(B)$, where B is the unit ball in \mathbb{R}^n , and they are the positive square roots of the eigenvalues of T^*T , where T^* is the adjoint of T . Thus, the singular values reflect the contractive effect of T in different directions. For $0 \leq s \leq n$, we define the *singular value function*

$$\varphi^s(T) = \alpha_1 \alpha_2 \cdots \alpha_{r-1} \alpha_r^{s-r+1}, \quad \text{9.23}$$

where r is the integer for which $r-1 < s \leq r$. Then $\varphi^s(T)$ is continuous and strictly decreasing in s . Moreover, for fixed s , φ^s may be shown to be submultiplicative, that is,

$$\varphi^s(TU) \leq \varphi^s(T)\varphi^s(U) \quad \text{9.24}$$

for any linear mappings T and U . We introduce the k th level sums

$$\Sigma_k^s \equiv \sum_{\mathcal{I}_k} \varphi^s(T_{i_1} \circ \cdots \circ T_{i_k}),$$

where \mathcal{I}_k denotes the set of all k -term sequences (i_1, \dots, i_k) with $1 \leq i_j \leq m$. Using (9.24), for fixed s

$$\begin{aligned}
\Sigma_{k+q}^s &= \sum_{I_{k+q}} \varphi^s(T_{i_1} \circ \cdots \circ T_{i_{k+q}}) \\
&\leq \sum_{I_{k+q}} \varphi^s(T_{i_1} \circ \cdots \circ T_{i_k}) \varphi^s(T_{i_{k+1}} \circ \cdots \circ T_{i_{k+q}}) \\
&= \left(\sum_{I_k} \varphi^s(T_{i_1} \circ \cdots \circ T_{i_k}) \right) \left(\sum_{I_q} \varphi^s(T_{i_1} \circ \cdots \circ T_{i_q}) \right) = \Sigma_k^s \Sigma_q^s,
\end{aligned}$$

that is, the sequence of real numbers Σ_k^s is submultiplicative in k . By a standard property of submultiplicative sequences, $(\Sigma_k^s)^{1/k}$ converges to a number Σ_∞^s as $k \rightarrow \infty$. Since φ^s is decreasing in s , so is Σ_∞^s . Provided that $\Sigma_\infty^n \leq 1$, there is a unique s , which we denote by

$d(T_1, \dots, T_m)$, such that $1 = \Sigma_\infty^s = \lim_{k \rightarrow \infty} \left(\sum_{I_k} \varphi^s(T_{i_1} \circ \cdots \circ T_{i_k}) \right)^{1/k}$. Equivalently,

$$d(T_1, \dots, T_m) = \inf \left\{ s : \sum_{k=1}^{\infty} \sum_{I_k} \varphi^s(T_{i_1} \circ \cdots \circ T_{i_k}) < \infty \right\}. \quad \text{9.25}$$

Theorem 9.12

Let T_1, \dots, T_m be linear contractions and let $y_1, \dots, y_m \in \mathbb{R}^n$ be vectors. If F is the self-affine set satisfying

$$F = \bigcup_{i=1}^m (T_i(F) + y_i),$$

then $\dim_H F \leq \dim_B F \leq d(T_1, \dots, T_m)$. If $|T_i(x) - T_i(y)| \leq c|x - y|$ for all i where $0 < c < \frac{1}{2}$, then equality holds for almost all

$(y_1, \dots, y_m) \in \mathbb{R}^{nm}$ in the sense of nm -dimensional Lebesgue measure.

Partial proof

We show that $\dim_H F \leq d(T_1, \dots, T_m)$ for all y_1, \dots, y_m . Write S_i for the contracting affine transformation $S_i(x) = T_i(x) + y_i$. Let B be a large enough closed ball to ensure that $S_i(B) \subset B$ for all i . Given $\delta > 0$, we may choose k large enough to get $|S_{i_1} \circ \dots \circ S_{i_k}(B)| < \delta$ for every k -term sequence $(i_1, \dots, i_k) \in \mathcal{I}_k$. By (9.7), $F \subset \bigcup_{\mathcal{I}_k} S_{i_1} \circ \dots \circ S_{i_k}(B)$. But $S_{i_1} \circ \dots \circ S_{i_k}(B)$ is a translate of the ellipsoid $T_{i_1} \circ \dots \circ T_{i_k}(B)$ which has principal axes of lengths $\alpha_1|B|, \dots, \alpha_n|B|$, where $\alpha_1, \dots, \alpha_n$ are the singular values of $T_{i_1} \circ \dots \circ T_{i_k}$. Thus, $S_{i_1} \circ \dots \circ S_{i_k}(B)$ is contained in a rectangular parallelepiped P of side lengths $\alpha_1|B|, \dots, \alpha_n|B|$. If $0 \leq s \leq n$ and r is the least integer greater than or equal to s , we may cover P by at most

$$\left(\frac{2\alpha_1}{\alpha_r}\right)\left(\frac{2\alpha_2}{\alpha_r}\right)\dots\left(\frac{2\alpha_{r-1}}{\alpha_r}\right) \leq 2^n \alpha_1 \dots \alpha_{r-1} \alpha_r^{1-r}$$

cubes of side $\alpha_r|B| < \delta$. Hence, $S_{i_1} \circ \dots \circ S_{i_k}(B)$ may be covered by a collection of cubes U_i with $|U_i| < \delta \sqrt{n}$ such that

$$\begin{aligned} \sum_i |U_i|^s &\leq 2^n \alpha_1 \dots \alpha_{r-1} \alpha_r^{1-r} \alpha_r^s |B|^s \\ &\leq 2^n |B|^s \varphi^s(T_{i_1} \circ \dots \circ T_{i_k}). \end{aligned}$$

Taking such a cover of $S_{i_1} \circ \dots \circ S_{i_k}(B)$ for each $(i_1, \dots, i_k) \in \mathcal{I}_k$, it follows that

$$\mathcal{H}_{\delta \sqrt{n}}^s(F) \leq 2^n |B|^s \sum_{\mathcal{I}_k} \varphi^s(T_{i_1} \circ \dots \circ T_{i_k}).$$

But $k \rightarrow \infty$ as $\delta \rightarrow 0$, so by (9.25), $\mathcal{H}^s(F) = 0$ if $s > d(T_1, \dots, T_m)$. Thus, $\dim_H F \leq d(T_1, \dots, T_m)$.

The lower estimate for $\dim_H F$ may be obtained using the potential theoretic techniques of Section 1.3. We omit the

somewhat involved details.

One consequence of this theorem is that, unless we have been unfortunate enough to hit on an exceptional set of parameters, the fractals in [Figure 9.12](#) all have the same dimension, estimated at about 1.42.

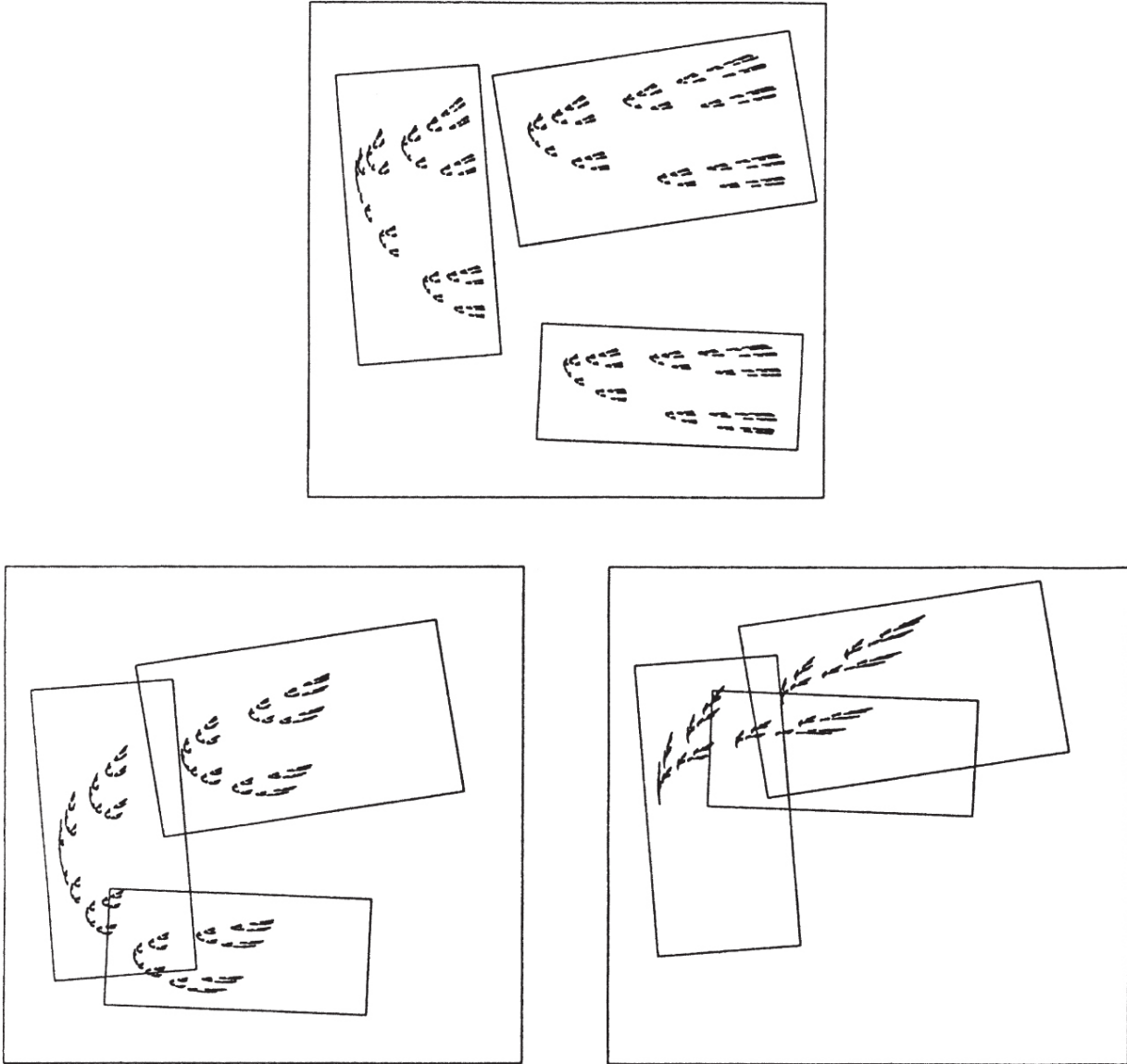


Figure 9.12 Each of the fractals depicted above is the attractor of the set of transformations that map the square onto the three rectangles. The affine transformations for each fractal differ only by translations, so by Theorem 9.12, the three fractals all have the same dimension (unless we have been very unlucky in our positioning!). A computation gives this common value of Hausdorff and box dimension as about 1.42.

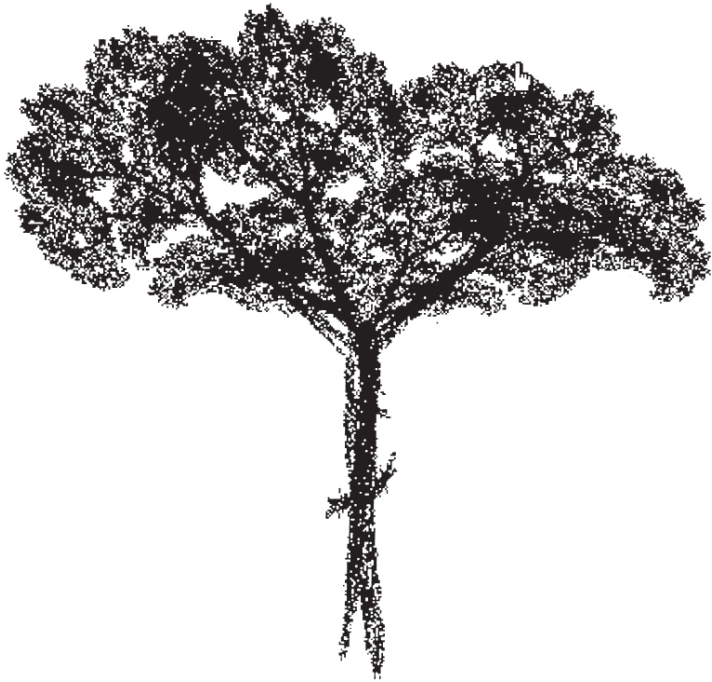
9.5 Applications to encoding images

The idea of image compression is to code pictures by a relatively small amount of information that is nevertheless enough to permit an accurate reconstruction of the pictures. Efficient image compression is essential for sending pictures across the internet rapidly. Sending images pixel by pixel would be very slow, although if the 2 million or so pixels on a computer screen were individually coloured (or set to black or white) at random, little compression would be possible. In practice, there is high correlation between colouring of pixels, with regions of a picture varying slowly in shade and texture, for example, an area of sky may have almost constant colour. Moreover, there may be repetition, for example, the individual daffodils in a flower bed may all be very similar. Image compression capitalises on such repetition and redundancy to obtain an efficient coding which decodes to something very close to the original image.

In this chapter, we have seen that IFSs can represent self-similar or self-affine fractals very efficiently. A little experimentation with drawing self-affine sets on a computer (see end of Section 9.1) can produce surprisingly good pictures of naturally occurring objects such as ferns, grasses, trees or clouds. The fern and tree in [Figure 9.13](#) are the attractors of just four and six affine transformations, respectively. The self-similarity and self-affinity of such objects enables them to be coded very efficiently in a way that enables easy reproduction.



(a)



(b)

Figure 9.13 The fern (a) and tree (b) are the attractors of just four and six affine transformations, respectively.

The next theorem, sometimes known as the *collage theorem*, gives an idea of how close an approximation the attractor of an IFS is to a given set. The corollary that follows shows that, in principle, any sets can be represented arbitrarily closely by an IFS attractor.

Theorem 9.13

Let $\{S_1, \dots, S_m\}$ be an IFS on $D \subset \mathbb{R}^n$ and suppose that $|S_i(x) - S_i(y)| \leq c|x - y|$ for all $x, y \in \mathbb{R}^n$ and all i , where $c < 1$. Let $E \subset D$ be any non-empty compact set. Then

$$d(E, F) \leq \frac{1}{(1-c)} d\left(E, \bigcup_{i=1}^m S_i(E)\right), \quad 9.26$$

where F is the attractor for the IFS and d is the Hausdorff metric.

Proof

Using the triangle inequality for the Hausdorff metric followed by the definition (9.4) of the attractor,

$$\begin{aligned} d(E, F) &\leq d\left(E, \bigcup_{i=1}^m S_i(E)\right) + d\left(\bigcup_{i=1}^m S_i(E), F\right) \\ &= d\left(E, \bigcup_{i=1}^m S_i(E)\right) + d\left(\bigcup_{i=1}^m S_i(E), \bigcup_{i=1}^m S_i(F)\right) \\ &\leq d\left(E, \bigcup_{i=1}^m S_i(E)\right) + cd(E, F) \end{aligned}$$

by (9.6), from which (9.26) follows.

Corollary 9.14

Let E be a non-empty compact subset of \mathbb{R}^n . Given $\delta > 0$, there exist IFSs of similarities $\{S_1, \dots, S_m\}$ with attractor F satisfying $d(E, F) < \delta$.

Proof

Let B_1, \dots, B_m be a collection of balls that cover E and which have centres in E and radii at most $\frac{1}{4}\delta$. Then $E \subset \bigcup_{i=1}^m B_i \subset E_{\delta/4}$, where $E_{\delta/4}$ is the $\frac{1}{4}\delta$ -neighbourhood of E . For each i , let S_i be any contracting similarity of ratio less than $\frac{1}{2}$ that maps E into B_i . Then $S_i(E) \subset B_i \subset (S_i(E))_{\delta/2}$, so $(\bigcup_{i=1}^m S_i(E)) \subset E_{\delta/4}$ and $E \subset \bigcup_{i=1}^m (S_i(E))_{\delta/2}$. By definition of the Hausdorff metric, $d(E, \bigcup_{i=1}^m S_i(E)) \leq \frac{1}{2}\delta$. It follows from (9.26) that $d(E, F) < \delta$ where F is the attractor.

The IFSs obtained in the above corollary is rather crude—the proof provides a very large number of contractions taking no account of any self-similar or self-affine features of E . One practical method which can give good results with a small number of transformations is to draw a rough outline of the object and then cover it, as closely as possible, by a number of smaller similar (or affine) copies. The similarities (or affinities) thus determined may be used to compute an attractor which may be compared with the object being modelled. Theorem 9.13 guarantees that the attractor will be a good approximation if the union of the smaller copies is close to the object. A trial-and-error process allows modification and improvements to the picture.

Ideally, one would like a ‘camera’ or ‘scanner’ which, for any picture, outputs an IFS with a fairly small number of affine transformations but whose attractor is a good approximation to the

original. A great deal of research was done in the 1990s to develop such a process by seeking out approximate self-similarities within the picture. One approach involves partitioning the picture into squares and, for each block of 2×2 squares, scanning the single squares to find the one in which the picture is closest to a scale $\frac{1}{2}$ image of that in the block. This identifies a similarity transformation from each block of squares to an individual square which together form a type of IFS with attractor hopefully not unlike the original picture.

As indicated at the end of Section 9.1, by adjoining probabilities to IFSs, these ideas may be extended to enable IFSs to represent pictures in grey scale rather than just in black and white. Indeed, with suitable modification, colour images may be coded by IFSs, and very effective pictures have been produced in this way using relatively few transformations.

Representing images using IFSs has various ‘pros and cons’. By utilising the self-similarity and repetition of nature and real-life phenomena, the method can enable objects or scenes to be described by a small number of contractions and probabilities in an effective manner, giving significant data compression. A corresponding disadvantage is that there is a high correlation between different parts of the picture—the method is excellent for giving an overall picture of a particular species of tree but is no use if the exact arrangement of the leaves on different branches is important. Given a set of affine contractions, reproduction of the image is computationally straightforward, is well-suited to parallel computation and is stable—small changes in the contractions lead to small changes in the attractor. The contractions define the image at arbitrarily small scales, and it is easy to produce a close-up of a small region. The main disadvantage of the method remains the difficulty of finding a set of contractions to represent a given object or picture.

*9.6 Zeta functions and complex dimensions

All definitions of dimension encountered so far have naturally been non-negative real numbers; nevertheless, it is possible to interpret complex numbers as dimensions in a meaningful and useful manner and we give a brief indication of this approach.

Let F be a compact subset of \mathbb{R} of length (Lebesgue measure) 0; we will assume for convenience that $F \subset [0, 1]$ with $0, 1 \in F$. Then the complement of F consists of a countable number of open intervals. These sets are often termed *fractal strings*: a string stretched across a Cantor-like set and fixed at points of the set might be plucked in any of the gaps to produce notes of various frequencies. Apart from the two unbounded intervals at each end of F , the lengths of these complementary intervals will always be listed in decreasing order as $l_1 \geq l_2 \geq l_3 \geq \dots$. For each $\delta > 0$, let $M(\delta)$ denote the number of i such that $l_i \geq \delta$.

We showed in Proposition 2.4 that the box-counting dimensions of a set could be obtained by in terms of the limiting behaviour of the Lebesgue measure of the δ -neighbourhood F_δ of F . For fractal strings, F_δ consists of all the complementary intervals of lengths less than 2δ , two intervals of length δ inside every complementary interval of length greater than 2δ and an interval of length δ at either end. Summing the lengths of these portions, with \mathcal{L} denoting Lebesgue measure,

$$\mathcal{L}(F_\delta) = \sum_{j: l_j < 2\delta}^{\infty} l_j + 2\delta M(2\delta) + 2\delta. \quad \underline{\text{9.27}}$$

The following Lemma relates the asymptotic behaviour of $\mathcal{L}(F_\delta)$, $M(\delta)$ and the l_j . Recall that we write $f(x) = O(g(x))$ to mean that there is a constant c such that $|f(x)| \leq c g(x)$ for appropriate values of x .

Lemma 9.15

Let $0 < s \leq 1$. The following statements are equivalent:

- i. $l_j = O(j^{-1/s})$ as $j \rightarrow \infty$;
- ii. $M(\delta) = O(\delta^{-s})$ as $\delta \rightarrow 0$;
- iii. $\mathcal{L}(F_\delta) = O(\delta^{1-s})$ as $\delta \rightarrow 0$.

Proof

(i) \Rightarrow (ii): Assuming (i), there is a constant c such that $l_j \leq cj^{-1/s}$ for all j , so if $\delta > 0$, then $l_j < \delta$ whenever $cj^{-1/s} < \delta$, that is, whenever $j > c^s\delta^{-s}$. Thus, $M(\delta) \leq c^s\delta^{-s}$.

(ii) \Rightarrow (i): If $M(\delta) \leq c\delta^{-s}$, then in particular $M(l_j) \leq cl_j^{-s}$ for each j , so $j \leq cl_j^{-s}$ or $l_j \leq c^{1/s}j^{-1/s}$.

(iii) \Rightarrow (ii): If $\mathcal{L}(F_\delta) \leq c\delta^{1-s}$ for all small δ , then $2\delta M(2\delta) \leq c\delta^{1-s}$ by (9.27), so $M(\delta') \leq c2^{s-1}\delta'^{-s}$ for sufficiently small $\delta' = 2\delta$.

(i) & (ii) \Rightarrow (iii): From (i), $l_j \leq cj^{-1/s}$ for some c . For small δ , we split the sum of complementary lengths in (9.27) according to $j < \delta^{-s}$ or $j \geq \delta^{-s}$:

$$\begin{aligned} \sum_{j: l_j < 2\delta}^{\infty} l_j &\leq \sum_{\substack{j < \delta^{-s} \\ l_j < 2\delta}}^{\infty} l_j + \sum_{j \geq \delta^{-s}}^{\infty} l_j \\ &\leq \delta^{-s}2\delta + \sum_{j \geq \delta^{-s}}^{\infty} cj^{-1/s} \\ &\leq 2\delta^{1-s} + c \int_{\delta^{-s}}^{\infty} t^{-1/s} dt \\ &\leq 2\delta^{1-s} + c_1\delta^{1-s}, \end{aligned}$$

where c_1 is independent of δ , using an integral test estimate. Using this together with (ii) in (9.27), we conclude that $\mathcal{L}(F_\delta) = O(\delta^{1-s})$.

We can now obtain the box dimension of a compact subset of \mathbb{R} purely in terms of the lengths of the complementary intervals.

Proposition 9.16

With notation as above

$$\overline{\dim}_B F = -1 \sqrt{\lim_{j \rightarrow \infty} \frac{\log l_j}{\log j}} \quad \text{9.28}$$

and

$$\underline{\dim}_B F \geq -1 \sqrt{\lim_{j \rightarrow \infty} \frac{\log l_j}{\log j}}, \quad \text{9.29}$$

so in particular

$$\dim_B F = -1 \sqrt{\lim_{j \rightarrow \infty} \frac{\log l_j}{\log j}}$$

whenever the limit exists.

Proof

Identity (9.28) follows directly from Proposition 2.4 using the equivalence of (i) and (iii) in Lemma 9.15.

If $\underline{\lim}_{j \rightarrow \infty} \log l_j / \log j > -1/s$, then $l_j \geq c j^{-1/s}$ for all j for some $c > 0$. From (9.27),

$$\mathcal{L}(F_\delta) \geq \sum_{j: l_j < 2\delta} l_j \geq \sum_{j \geq c^s(2\delta)^{-s}} c j^{-1/s} \geq c \int_{c^s(2\delta)^{-s}+1}^{\infty} t^{-1/s} dt \geq c_1 \delta^{1-s},$$

approximating the sum by an integral. From Proposition 2.4 $\underline{\dim}_B F \geq s$, giving (9.29).

Note that this characterisation of $\dim_B F$ depends only on the lengths of the complementary intervals not on their position or

arrangement. Thus, permuting the complementary intervals of a fractal subset of \mathbb{R} does not change its box dimensions. There are more delicate variants of Proposition 9.16 that relate the lengths of these intervals to the Minkowski content of F .

Next we introduce a *zeta function* given in terms of the complementary interval lengths by

$$\zeta(s) = \sum_{j=1}^{\infty} l_j^s. \quad \text{9.30}$$

Since $\sum_{j=1}^{\infty} l_j = 1$, the series (9.30) converges absolutely for complex numbers s with real part $\operatorname{Re}(s) \geq 1$. The infimum of the real numbers s for which the series converges is called the *abscissa of convergence* σ ; it turns out this equals the upper box dimension of F .

Proposition 9.17

With notation as above,

$$\sigma = \inf \left\{ s \in \mathbb{R} : \sum_{j=1}^{\infty} l_j^s \text{ converges} \right\} = \overline{\dim}_{\text{B}} F$$

Moreover, the series (9.30) converges absolutely if $s \in \mathbb{C}$ and $\operatorname{Re}(s) > \sigma$.

Proof

If $\sum_{j=1}^{\infty} l_j^s \leq a < \infty$, then by considering the j th partial sum of the series, $\sum_{j=1}^k l_j^s \leq a$ so $l_j \leq a^{1/s} j^{-1/s}$ giving $\overline{\dim}_B F \leq s$ by (9.28).

On the other hand, if $\overline{\dim}_B F < s$, then $l_j \leq c j^{-1/t}$ for some $t < s$ and $c > 0$ by (9.28). Then $\sum_{j=1}^{\infty} l_j^s \leq c^s \sum_{j=1}^{\infty} j^{-s/t} < \infty$. If $z \in \mathbb{C}$ and $s = \operatorname{Re}(z) > \sigma$, then $\sum_{j=1}^{\infty} |l_j^z| = \sum_{j=1}^{\infty} l_j^s < \infty$, so $\sum_{j=1}^{\infty} l_j^z$ is absolutely convergent.

The zeta function (9.30) can often be extended by analytic continuation to a meromorphic function. Recall that a function f is *meromorphic* on \mathbb{C} if it is analytic except at a set of isolated singularities which are poles. The point $\omega \in \mathbb{C}$ is a *pole of order* $p \in \mathbb{Z}^+$ if, in a neighbourhood U of ω ,

$$f(s) = \frac{g(s)}{(s - \omega)^p} \quad (s \in U),$$

where g is analytic on U and $g(\omega) \neq 0$. If $p = 1$ the pole is *simple* and $g(\omega)$ is the *residue* of f at ω written $\operatorname{Res}(f, \omega)$.

The behaviour of a zeta function in the complex plane often provides an insight into the asymptotics of sequences or functions, the classic example being the Riemann zeta function $\sum_{j=1}^{\infty} n^{-s}$ which is intimately connected to the prime numbers. Much of what is known about the distribution of the primes results from studying the Riemann zeta function, and related techniques can be used to investigate fractal strings.

Assuming that the zeta function (9.30) has a meromorphic extension to \mathbb{C} , the set

$$\mathcal{D} = \{a \in \mathbb{C} : \zeta \text{ has a pole at } a\}$$

is called the set of *complex dimensions* of the fractal string F .

For the simplest example, let $F \subset \mathbb{R}$ be the middle third Cantor set (see [Figure 0.1](#)). Then the complement of F contains 2^{k-1} gaps of length 3^{-k} for each $k \geq 1$. Thus,

$$\zeta(s) = \sum_{k=1}^{\infty} 2^{k-1} 3^{-ks} = \frac{3^{-s}}{1 - 2 \cdot 3^{-s}} \quad \text{9.31}$$

on summing the geometric series which is convergent if $\operatorname{Re}(s) > \log 2 / \log 3$, the dimension of F . But this closed form gives the analytic continuation of $\zeta(s)$ to \mathbb{C} . It is a meromorphic function with poles at those s for which $1 - 2 \cdot 3^{-s} = 0$, which is just the equation ([9.10](#)) for the similarity dimension of F . The set of poles is

$$\mathcal{D} = \left\{ \frac{\log 2}{\log 3} + i \frac{2\pi}{\log 3} k : k \in \mathbb{Z} \right\}$$

which all lie on the line $\operatorname{Re}(s) = \log 2 / \log 3$; it is no coincidence that this is the dimension of the Cantor set F .

More generally, let $F \subset [0, 1]$ be the self-similar attractor of an IFS of similarities S_1, \dots, S_m with ratios r_1, \dots, r_m , with $0, 1 \in F$ and with $F = \bigcup_{i=1}^m S_i(F)$ a disjoint union. If the gaps at the first level of the construction, that is, the bounded gaps between the intervals $S_i([0, 1])$, have lengths b_1, \dots, b_{m-1} , then the gaps that appear at the k th stage of the construction of F , that is, the gaps that first appear in $S^k([0, 1]) = \bigcup_{I_k} S_{i_1} \circ \dots \circ S_{i_k}([0, 1])$, are of lengths $r_{i_1} \cdots r_{i_{k-1}} b_j$ for $i_1, \dots, i_{k-1} \in I_{k-1}$ and $b_j = 1, \dots, m-1$. Thus,

$$\zeta(s) = \sum_{k=1}^{\infty} \sum_{i_1, \dots, i_{k-1} \in I_{k-1}} \sum_{j=1}^{m-1} r_{i_1}^s \cdots r_{i_{k-1}}^s b_j^s \quad \text{9.32}$$

$$= \frac{\sum_{j=1}^{m-1} b_j^s}{1 - \sum_{i=1}^m r_i^s}, \quad \text{9.33}$$

on summing the geometric series which converges absolutely provided that $s \in \mathbb{C}$ is such that $\left| \sum_{i=1}^m r_i^s \right| < 1$. Noting that $|x^s| = |x|^{\operatorname{Re}(s)}$ if $x \in \mathbb{R}$ and $s \in \mathbb{C}$,

$$\left| \sum_{i=1}^m r_i^s \right| \leq \sum_{i=1}^m |r_i^s| \leq \sum_{i=1}^m r_i^{\operatorname{Re}(s)} < 1,$$

so the series (9.32) converges if $\operatorname{Re}(s) > s_+$, where $\sum_{i=1}^m r_i^{s_+} = 1$. When $s = s_+$ the series diverges, so the abscissa of convergence is $\sigma = s_+$, which by Proposition 9.17 equals $\dim_B F = \dim_H F$.

The function (9.33) is meromorphic and so provides the analytic continuation of ζ to \mathbb{C} . The following proposition summarises some of the main properties of the poles and residues of (9.33) which are key to the behaviour of the zeta function.

Proposition 9.18

The singularities of the zeta function (9.33) of a self-similar fractal string $F \subset [0, 1]$ are all poles or removable singularities located at those $s \in \mathbb{C}$ such that

$$\sum_{i=1}^m r_i^s = 1. \quad \text{9.34}$$

All the singularites lie in the strip

$$\{s \in \mathbb{C} : s_- \leq \operatorname{Re}(s) \leq s_+\}, \quad \text{9.35}$$

where s_+ and s_- are the unique real numbers satisfying

$$\sum_{i=1}^m r_i^{s_+} = 1 \quad \text{and} \quad 1 + \sum_{i=1}^{m-p} r_i^{s_-} = p r_m^{s_-},$$

where the least contraction ratio r_m of the IFS defining F occurs p times amongst the r_i . If $\omega \in \mathbb{C}$ satisfies (9.34), then it is a simple pole of ζ with residue

$$\operatorname{Res}(\zeta, \omega) = \frac{-\sum_{j=1}^{m-1} b_j^\omega}{\sum_{i=1}^m r_i^\omega \log r_i}, \quad \text{9.36}$$

provided that both numerator and denominator of this quotient are non-zero. This is always the case for the unique real solution of (9.34), namely, $s_+ = \sigma = \dim_B F$, and also when $m = 2$, the ‘single gap’ case.

Proof

Singularities of (9.33) require the denominator to be 0, that is, they must satisfy (9.34). We have seen that there are no solutions to this if $\operatorname{Re}(s) > s_+$. On the other hand, if s satisfies (9.34), then with p as the multiplicity of the smallest contraction ratio r_m ,

$$pr_m^{\operatorname{Re}(s)} = p|r_m^s| = \left| 1 - \sum_{i=1}^{m-p} r_i^s \right| \leq 1 + \sum_{i=1}^{m-p} |r_i^s| \leq 1 + \sum_{i=1}^{m-p} |r_i|^{\operatorname{Re}(s)}$$

and this inequality cannot be satisfied if $\operatorname{Re}(s) < s_-$.

An expression of the form $\sum_{j=1}^m c_j^s$ where the c_j are positive real numbers is analytic throughout \mathbb{C} and all its zeros have finite multiplicity (since its power series about any point has an initial term). Thus, if $\omega \in \mathbb{C}$ is a solution of (9.34), then ω is a pole of (9.33) of finite order or, if the numerator is 0 at ω , then perhaps a removable singularity. Writing $s = \omega + z$ for small z ,

$$1 - \sum_{i=1}^m r_i^s = 1 - \sum_{i=1}^m r_i^\omega r_i^z = 1 - \sum_{i=1}^m r_i^\omega \exp(z \log r_i)$$

$$\sim 1 - \sum_{i=1}^m r_i^\omega (1 + z \log r_i) = -z \sum_{i=1}^m r_i^\omega \log r_i.$$

Hence, from (9.33), for s close to ω ,

$$\zeta(s) = \zeta(\omega + z) \sim \frac{-\sum_{j=1}^{m-1} b_j^\omega}{\sum_{i=1}^m r_i^\omega \log r_i} \frac{1}{z} = \frac{-\sum_{j=1}^{m-1} b_j^\omega}{\sum_{i=1}^m r_i^\omega \log r_i} \frac{1}{(s - \omega)},$$

provided both numerator and denominator of this coefficient are non-zero, in which case ω is a simple pole with residue (9.36). This is certainly the case when ω is the real number s_+ and also when $m = 2$ and there is a single term in the numerator.

In a generic sense, all the complex solutions of (9.34) will be simple poles, since the set of ratios and gaps $(r_1, \dots, r_m, b_1, \dots, b_{m-1})$ for which both numerator and denominator of (9.33) have a common zero has Lebesgue measure 0 in the $2m - 2$ -dimensional parameter space (constrained by $\sum_{i=1}^m r_i + \sum_{j=1}^{m-1} b_j = 1$).

A great deal more can be said about the location of the poles of the zeta function of a self-similar set and the complex solutions of (9.34). For example, since the r_i and b_i are real, s is a pole of (9.33) if and only if its conjugate \bar{s} is a pole, so the set of poles has reflective symmetry about the real axis.

There are two fundamentally different cases. Given a self-similar subset of $[0, 1]$ with ratios r_1, \dots, r_m , the numbers

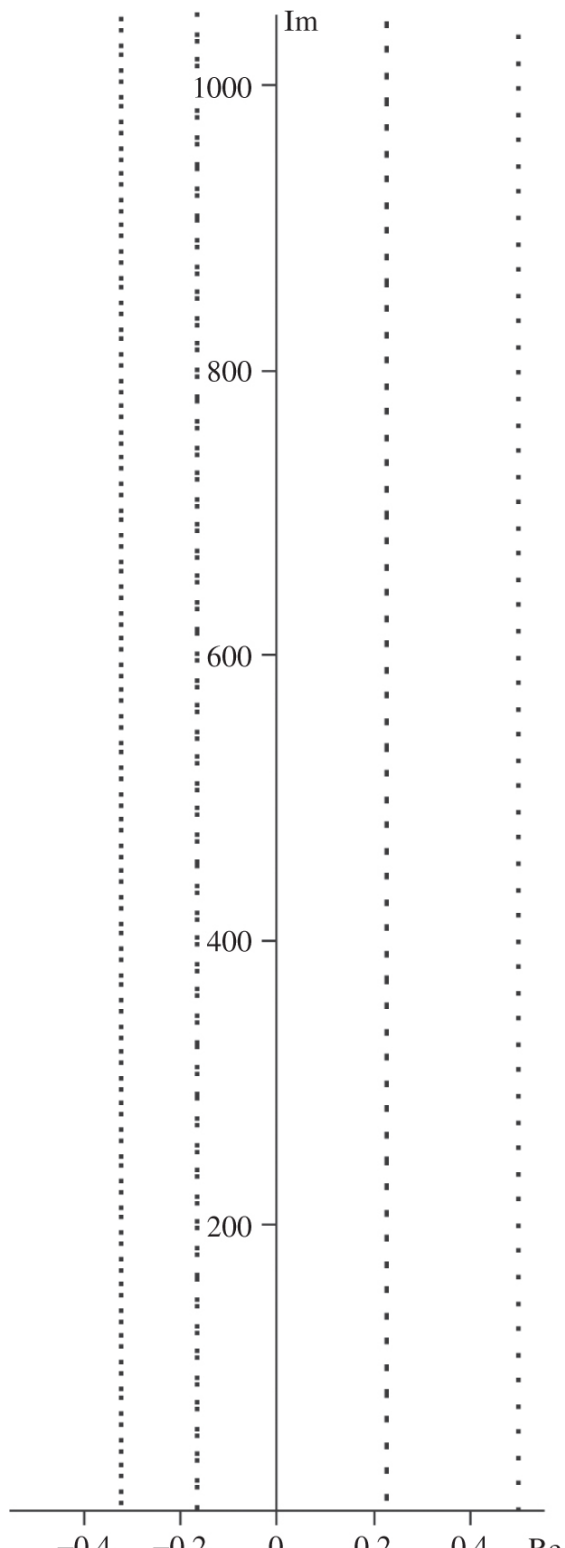
$$G = \left\{ r_1^{k_1} \cdots r_m^{k_m} : k_1, \dots, k_m \in \mathbb{Z} \right\}$$

forms a subgroup of \mathbb{R}^+ under multiplication. It may be shown that either G is a dense subset of \mathbb{R}^+ (i.e. contains points in every interval), termed the *non-lattice* case, or G is discrete and of the form $G = \{r^k : k \in \mathbb{Z}\}$ for some $r > 0$, the *lattice* case.

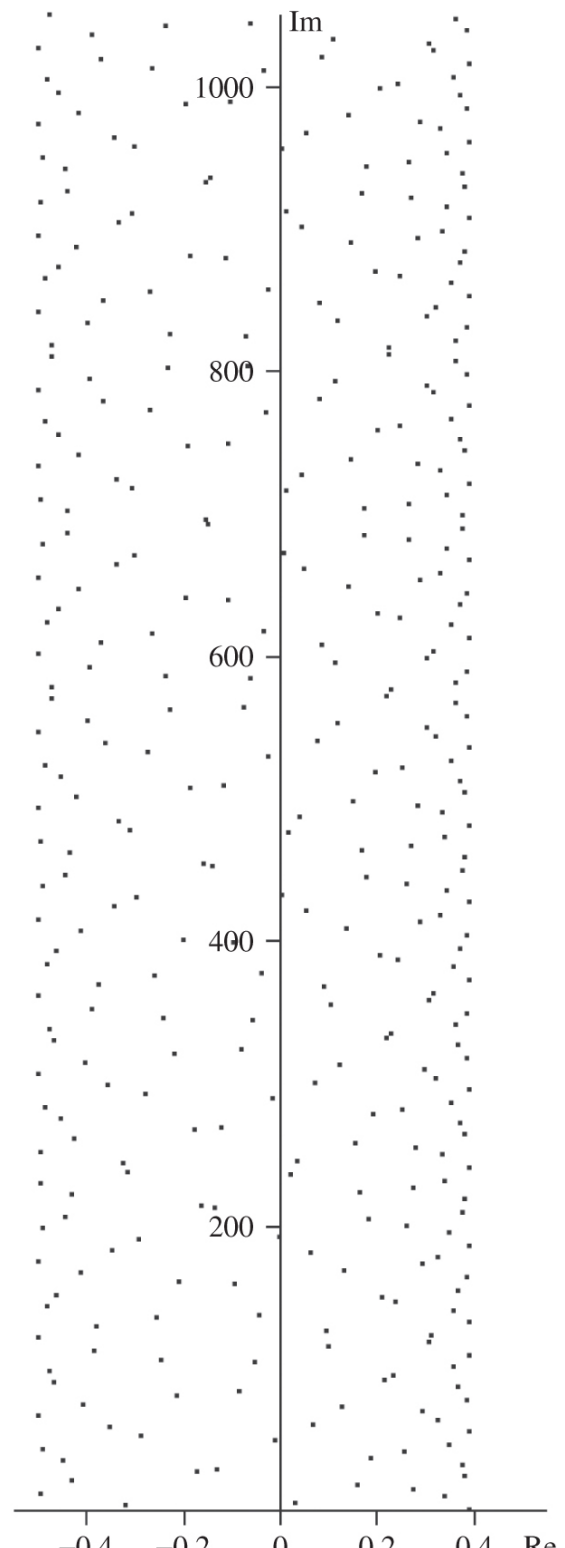
In the lattice case, the poles all lie on a finite number of vertical lines, with the poles on each of these lines (normally) appearing periodically with period $2\pi / -\log r$ (see [Figure 9.14a](#)). This follows since $r_j = r^{k_j}$ for some $k_j \in \mathbb{Z}$ for each j so

$$\sum_{j=1}^m r_j^{s+2\pi ik/\log r} = \sum_{j=1}^m r_j^s r^{k_j 2\pi ik/\log r} = \sum_{j=1}^m r_j^s e^{k_j 2\pi ik} = \sum_{j=1}^m r_j^s.$$

Thus, if s is a pole of ζ , then so is $s + 2\pi ik/\log r$ for each integer k , assuming that the numerator of (9.33) remains non-zero.



(a)



(b)

Figure 9.14 Complex dimensions of the IFSs (a)

$S_1(x) = 2^{-7/2}x, S_2(x) = \frac{1}{2}x + \frac{1}{2}$, the lattice case, (b) $S_1(x) = \frac{1}{9}x, S_2(x) = \frac{1}{4}x + \frac{3}{4}$, the non-lattice case.

In the non-lattice case, all poles apart from σ satisfy $\operatorname{Re}(\omega) < \sigma$, and at first sight, the poles seem haphazardly distributed within the strip (9.35) (Figure 9.14b). Nevertheless, there is a quasiperiodicity, in the sense that the poles can be approximated by the poles of a sequence of lattice self-similar fractals. Indeed, the poles appear to lie on certain natural curves in the complex plane, a consequence of number theoretic properties of the contraction ratios.

For a self-similar F , there are good estimates for the density of complex dimensions lying within the strip (9.35). Provided that the numerator and denominator of (9.33) are never simultaneously 0,

$$\{\text{number of poles } \omega \text{ of } \zeta \text{ with } |\operatorname{Im} \omega| \leq T\} = \frac{-\log r_m}{\pi} T + O(1),$$

where r_m is the smallest contraction ratio of the IFS defining F , with the poles counted according to multiplicity.

It is natural to ask why it is worth introducing a zeta function and considering complex dimensions as well as the usual (real) dimensions. Many of the quantities associated with fractal strings may be expressed in terms of the zeta function, for example,

$$\zeta(s) = s \int_0^\infty M(t)t^{s-1} dt, \quad 9.37$$

where, as before, $M(\delta)$ is the number of complementary interval lengths of at least δ . Moreover, studying the poles and residues of the zeta function can provide much more detailed information about the structure of fractals. The following instance illustrates what may be achieved.

Recall that if $F \subset \mathbb{R}$ is of box dimension s , its s -dimensional Minkowski content is given by

$$C(F) = \lim_{\delta \rightarrow 0} \frac{\mathcal{L}(F_\delta)}{\delta^{1-s}}$$

provided that this limit exists. Suppose F is a fractal string with a zeta function satisfying certain mild growth conditions (it is certainly enough for F to be self-similar). Then it may be shown that the Minkowski content of F exists if and only if the abscissa of convergence σ is a simple pole of ζ and is the only complex dimension of F with real part equal to σ . If this is the case, which occurs for self-similar F in the non-lattice case, then

$$C(F) = 2^{1-\sigma} \frac{\text{Res}(\zeta, \sigma)}{\sigma(1-\sigma)}. \quad \text{9.38}$$

Moreover, regardless of whether or not the Minkowski content exists, there is an expansion of the measure of the δ -neighbourhood of F in terms of the residues of ζ at its poles. Provided the poles are all simple and 0 is not a pole,

$$\mathcal{L}(F_\delta) = \sum_{\omega \text{ a pole of } \zeta} \text{Res}(\zeta, \omega) \frac{(2\delta)^{1-\omega}}{\omega(1-\omega)} + 2\delta\zeta(0). \quad \text{9.39}$$

(Formulae such as these are known as *tube formulae* since the δ -neighbourhood of a curve takes the form of a ‘tube’.) The expansion (9.39), which is derived using techniques from complex analysis, gives a great deal of information about $\mathcal{L}(F_\delta)$. Writing

$\delta^z = \delta^{\text{Re}(z)} \exp i(\text{Im}(z) \log \delta)$, the dominant terms of (9.39) are those in $\delta^{1-\sigma}$ corresponding to the poles with $\text{Re}(\omega) = \sigma$. If F is self-similar and non-lattice, this dominant contribution comes entirely from the real pole σ giving the Minkowski content (9.38). However, if F is self-similar and lattice, then there are infinitely many poles with $\text{Re}(\omega) = \sigma$ and the contributions from these are modulated by the oscillatory terms $\exp i(\text{Im}(1-\omega) \log \delta)$, so that as δ approaches 0 , $\mathcal{L}(F_\delta)/\delta^{1-s}$ does not approach a limit but oscillates in a manner that is precisely characterised by (9.39).

Zeta functions and complex dimensions relate to many other areas of fractal geometry and provide powerful methods of studying

fractal properties, for example, there are ways of introducing them for sets in higher-dimensional space.

9.7 Notes and references

The first systematic account of what are now known as iterated function systems (IFSs) is that of Hutchinson (1981). The derivation of the formula for the dimension of self-similar sets was given by Moran (1946) for the case with a disjoint union in (9.4). Computer pictures of self-similar sets and attractors of other IFSs are widespread, the works of Mandelbrot (1982); Peitgen, Jürgens and Saupe (2004) and Barnsley (2006 2012) contain many interesting and beautiful examples.

For details of the thermodynamic formalism and material relating to Theorem 9.9, see Ruelle (1982 1983); Falconer (1997); Pesin (1997) and Barreira (2011 2012).

Self-affine sets are surveyed in Peres and Solomyak (2000) and Falconer (2013). Full details of Example 9.11 are given by McMullen (1984) and of Theorem 9.12 by Falconer (1988) and Solomyak (1998).

The notion of IFSs has been extended in many directions: for IFSs with infinitely many transformations, see Mauldin and Urbański (1996 1999); for graph directed constructions, see Mauldin and Williams (1988) and for general classes of conformal IFSs, see Mauldin and Urbański (2003) and Przytycki and Urbański (2010). The book on superfractals by Barnsley (2006) presents many novel variants.

Applications to image compression and encoding are described by Barnsley and Hurd (1993) and Fisher (2011).

For much more on zeta functions and complex dimensions, see Lapidus and van Frankenhuyzen (2012) and the references therein.

Exercises

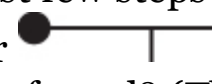
9.1 Verify that the Hausdorff metric satisfies the conditions for a metric.

9.2 Find a pair of similarity transformations on \mathbb{R} for which the interval $[0, 1]$ is the attractor. Now find infinitely many such pairs of transformations.

9.3 Find sets of (i) four and (ii) three similarity transformations on \mathbb{R} for which the middle third Cantor set is the attractor. Check that (9.14) has solution $\log 2 / \log 3$ in each case.

9.4 Write down (using matrix notation) the four basic similarity transformations that define the von Koch curve (Figure 0.2). Find an open set for which the open set condition holds and deduce from Theorem 9.3 that the von Koch curve does indeed have box and Hausdorff dimension of $\log 4 / \log 3$.

9.5 Find an IFS for the set depicted in Figure 0.5 and deduce that it has Hausdorff and box dimensions given by $4(\frac{1}{4})^s + (\frac{1}{2})^s = 1$.

9.6 Sketch the first few steps in the construction of a self-similar set with generator . What are the Hausdorff and box dimensions of this fractal? (The stem of the T is one quarter of the total length of the top.)

9.7 Let F be the set obtained by a Cantor-type construction in which each interval is replaced by two intervals, one of a quarter of the length at the left-hand end and one of half the length at the right-hand end. Thus, E_0 is the interval $[0, 1]$, E_1 consists of the intervals $[0, \frac{1}{4}]$ and $[\frac{1}{2}, 1]$, and so on. Find an IFS with attractor F , and thus find the Hausdorff and box dimensions of F .

9.8 Describe the attractors of the following IFSs on \mathbb{R} .

i. $S_1(x) = \frac{1}{4}x$, $S_2(x) = \frac{1}{4}x + \frac{3}{4}$;

ii. $S_1(x) = \frac{1}{2}x$, $S_2(x) = \frac{1}{2}x + \frac{1}{2}$;

iii. $S_1(x) = \frac{2}{3}x$, $S_2(x) = \frac{2}{3}x + \frac{1}{3}$.

9.9 Divide the unit square E_0 into p^2 squares of side $1/p$ in the obvious way and choose some m of these squares to form E_1 . Let $S_i (1 \leq i \leq m)$ be similarity transformations that map E_0 onto each of these squares. Show that the attractor F of the IFS so defined has $\dim_H F = \dim_B F = \log m / \log p$.

9.10 Let $S_1, S_2 : [0, 1] \rightarrow [0, 1]$ be given by $S_1(x) = x/(2+x)$, $S_2(x) = 2/(2+x)$. Show that the attractor F of this IFS satisfies $0.52 < \dim_H F < 0.81$.

9.11 Show that any self-similar set F satisfying the conditions of Theorem 9.3 has $c_1 \leq \underline{D}(F, x) \leq \overline{D}(F, x) \leq c_2$ for all $x \in F$, where c_1 and c_2 are positive constants. (See equations ((5.2)) and ((5.3)) for the definition of the densities.)

9.12 Let S_1, \dots, S_m be bi-Lipschitz contractions on a subset D of \mathbb{R}^n and let F be the attractor satisfying (9.4). Show that if V is any open set intersecting F , then F and $F \cap V$ have equal Hausdorff, equal upper box and equal lower box dimensions. Deduce from Corollary 3.10 that $\dim_p F = \overline{\dim}_B F$.

9.13 Verify the Hausdorff dimension formula in Example 9.11 in the cases (a) where $N_j = N$ for $1 \leq j \leq p$ and (b) where $N_j = N$ or 0 for $1 \leq j \leq p$, where N is an integer with $1 < N < q$. (Hint: see Example 7.13.)

9.14 Find the Hausdorff and box dimensions of the set in [Figure 9.10](#).

9.15 Write a computer programme to draw the attractor of a given collection of contractions of a plane region (see the end of Section 9.1). Examine the attractors of similarities, affinities and try some non-linear transformations.

9.16 Using the definition of the zeta function (9.30), obtain (9.37) for real $s > \sigma$, where $M(t)$ is the number of i for which the complementary interval lengths $l_i \geq t$. Deduce that this identity remains valid for all s with $\operatorname{Re}(s) > \sigma$ and thus by analytic continuation for all $s \in \mathbb{C}$.

Chapter 10

Examples from number theory

Number theory is the area of mathematics concerned with intrinsic properties of the integers, rational numbers and real numbers, including their distribution and representation. Fractals can often be defined in number theoretic terms, for instance, the middle third Cantor set consists of the real numbers between 0 and 1 which have a base-3 expansion containing only the digits 0 and 2. We examine three classes of fractals that occur in classical number theory—these examples serve to illustrate some of the ideas encountered earlier in the book.

10.1 Distribution of digits of numbers

We consider base- m expansions of real numbers, where $m \geq 2$ is a fixed integer. Let p_0, p_1, \dots, p_{m-1} be ‘proportions’ summing to 1, so that $0 < p_i < 1$ and $\sum_{i=0}^{m-1} p_i = 1$. Let $F(p_0, \dots, p_{m-1})$ be the set of numbers x in $[0, 1)$ with base- m expansions containing the digits $0, 1, \dots, m-1$ in proportions p_0, \dots, p_{m-1} , respectively. More precisely, if $n_j(x|_k)$ denotes the number of times the digit j occurs in the first k places of the base- m expansion of x , then

$$F(p_0, \dots, p_{m-1}) = \left\{ x \in [0, 1) : \lim_{k \rightarrow \infty} \frac{n_j(x|_k)}{k} = p_j \text{ for all } j = 0, \dots, m-1 \right\}. \quad \text{10.1}$$

Thus, we think of $F(\frac{1}{3}, \frac{2}{3})$ as the set of numbers with ‘two-thirds’ of their base-2 digits being 1 and ‘one-third’ of their digits 0.

It is well known that almost all numbers (in the sense of Lebesgue measure) are *normal* to all bases; that is, they have base- m expansions containing equal proportions of the digits $0, 1, \dots, m-1$ for all m . In our notation, $F(m^{-1}, \dots, m^{-1})$ has Lebesgue measure 1, and therefore dimension 1, for all m . Paradoxically, although almost

all numbers are normal to all bases, no specific example of such a number has ever been exhibited. We may use Hausdorff dimension to describe the size of the sets $F(p_0, \dots, p_{m-1})$ when the p_j are not all equal. (Such sets are dense in $[0, 1]$ so have box dimension 1.)

A mass distribution technique is used in the following proof—the mass distribution occurs naturally as a probability measure.

Proposition 10.1

With $F = F(p_0, \dots, p_{m-1})$ as above,

$$\dim_H F = -\frac{1}{\log m} \sum_{i=0}^{m-1} p_i \log p_i.$$

Proof

The proof is best thought of probabilistically. We imagine that base- m numbers $x = 0.i_1 i_2 \dots$ are selected at random in such a way that the k th digit i_k takes the value j with probability p_j , independently for each k . Thus, we take $[0, 1)$ as our sample space and define a probability measure P on subsets of $[0, 1)$ such that if I_{i_1, \dots, i_k} is the k th level basic interval containing the numbers with base- m expansion beginning $0.i_1 \dots i_k$, then the probability of a number being in this interval is

$$P(I_{i_1, \dots, i_k}) = p_{i_1} \cdots p_{i_k}. \quad \text{10.2}$$

Given j , the events ‘the k th digit of x is a j ’ are independent for $k = 1, 2, \dots$. A consequence of the strong law of large numbers (see Exercise 1.27) is that, with probability 1, the proportion of occurrences of an event in a number of repeated independent trials tends to the probability of the event occurring. Thus, with probability 1,

$$\frac{n_j(x|_k)}{k} = \frac{1}{k}(\text{number of occurrences of } j \text{ in the first } k \text{ digits}) \rightarrow p_j$$

as $k \rightarrow \infty$ for all j . Hence, $P(F) = 1$. We write $I_k(y) = I_{i_1, \dots, i_k}$ for the k th level interval (of length m^{-k}) to which y belongs. For a fixed y , the probability that $x \in I_k(y)$ is given by

$$\log P(I_k(y)) = n_0(y|_k) \log p_0 + \cdots + n_{m-1}(y|_k) \log p_{m-1}$$

by taking logarithms of (10.2). If $y \in F$, then $n_j(y|_k)/k \rightarrow p_j$ as $k \rightarrow \infty$ for each j , so

$$\begin{aligned}\frac{1}{k} \log \frac{\mathsf{P}(I_k(y))}{|I_k(y)|^s} &= \frac{1}{k} \log \mathsf{P}(I_k(y)) - \frac{1}{k} \log m^{-ks} \\ &\rightarrow \sum_{i=0}^{m-1} p_i \log p_i + s \log m.\end{aligned}$$

Hence, for all y in F , the ‘interval density’

$$\lim_{k \rightarrow \infty} \frac{\mathsf{P}(I_k(y))}{|I_k(y)|^s} = \begin{cases} 0 & \text{if } s < t \\ \infty & \text{if } s > t, \end{cases}$$

where

$$t = -\frac{1}{\log m} \sum_{i=0}^{m-1} p_i \log p_i.$$

We are now virtually in the situation of Proposition 4.9. The same results hold and may be proved in the same way if the ‘spherical densities’ $\lim_{r \rightarrow 0} \mu(B(x, r))/r^s$ are replaced by these interval densities. Thus, $\mathcal{H}^s(F) = \infty$ if $s < t$ and $\mathcal{H}^s(F) = 0$ if $s > t$, as required.

10.2 Continued fractions

Instead of defining sets of numbers in terms of base- m expansions, we may use continued fraction expansions. Any number x that is not an integer may be written as

$$x = a_0 + 1/x_1$$

where a_0 is an integer and $x_1 > 1$. Similarly, if x_1 is not an integer, then

$$x_1 = a_1 + 1/x_2$$

with $x_2 > 1$, so

$$x = a_0 + 1/(a_1 + 1/x_2).$$

Proceeding in this way,

$$x = a_0 + 1/(a_1 + 1/(a_2 + 1/(\cdots + 1/(a_{k-1} + 1/x_k))))$$

for each k , provided that at no stage is x_k an integer. We call the sequence of integers a_0, a_1, a_2, \dots the *partial quotients* of x and write

$$x = a_0 + \frac{1}{a_1 + \frac{1}{a_2 + \frac{1}{a_3 + \cdots}}}$$

for the *continued fraction expansion* of x . This expansion terminates if and only if x is rational, otherwise taking a finite number of terms,

$$a_0 + 1/(a_1 + 1/(a_2 + 1/(\cdots + 1/a_k)))$$

provides a sequence of rational approximations to x which converge to x as $k \rightarrow \infty$. (These approximations are in a sense the best possible and are closely allied to the theory of Diophantine approximation; see Section 10.3.)

Examples of continued fractions include

$$\begin{aligned}\sqrt{2} &= 1 + \frac{1}{2 + \frac{1}{2 + \frac{1}{2 + \cdots}}} \\ \sqrt{3} &= 1 + \frac{1}{1 + \frac{1}{2 + \frac{1}{1 + \frac{1}{2 + \cdots}}}}.\end{aligned}$$

More generally, any quadratic surd (i.e. root of a quadratic equation with integer coefficients) has eventually periodic partial quotients.

Sets of numbers defined by conditions on their partial quotients may be thought of as fractal attractors of certain iterated function systems (IFSs), as the following example illustrates.

Example 10.2

Let F be the set of positive real numbers x with non-terminating continued fraction expressions, which have all partial quotients equal to 1 or 2. Then F is the attractor of the IFS $\{S_1, S_2\}$ on $[1, 3]$ where $S_1(x) = 1 + 1/x$ and $S_2(x) = 2 + 1/x$, with $0.44 < \dim_H F < 0.66$.

Proof

It is easy to see that F is closed (since its complement is open) and bounded (since $F \subset [1, 3]$). Moreover, $x \in F$ precisely when $x = 1 + 1/y$ or $x = 2 + 1/y$ for some $y \in F$. With S_1 and S_2 as stated, it follows that $F = S_1(F) \cup S_2(F)$; in other words, F is the attractor of the IFS $\{S_1, S_2\}$ in the sense of (9.4). In fact F is just the set analysed in Example 9.8, which we showed to have Hausdorff dimension between 0.44 and 0.66.

Computational methods that enable dimensions of sets defined in terms of continued fraction expansions to be found very accurately have been developed. The set F of Example 10.2 has Hausdorff dimension 0.531 280 506

Obviously, varying the conditions on the partial quotients will lead to other fractals that are the attractors of certain transformations.

10.3 Diophantine approximation

How closely can a given irrational number x be approximated by a rational number p/q with denominator q no larger than q_0 ?

Diophantine approximation is the study of such problems, which can crop up in quite practical situations (see Section 13.6). A classical theorem of Dirichlet (see Exercise 10.8) states that for

every real number x , there are infinitely many positive integers q such that

$$\left| x - \frac{p}{q} \right| \leq \frac{1}{q^2}$$

for some integer p ; such p/q are ‘good’ rational approximations to x . Equivalently,

$$\|qx\| \leq q^{-1}$$

for infinitely many q , where $\|y\| = \min_{m \in \mathbb{Z}} |y - m|$ denotes the distance from y to the nearest integer.

There are variations on Dirichlet's result that apply to *almost all* numbers x . It may be shown that if $\psi(q)$ is a decreasing function of q with $0 < \psi(q)$, then

$$\|qx\| \leq \psi(q) \quad \text{10.3}$$

is satisfied by infinitely many q for almost all x or for almost no x (in the sense of 1-dimensional Lebesgue measure) according to whether the series $\sum_{q=1}^{\infty} \psi(q)$ diverges or converges. In the latter case, whilst the set of x for which (10.3) is satisfied by infinitely many q has Lebesgue measure 0, it is often a fractal of positive Hausdorff dimension.

We speak of a number x such that

$$\|qx\| \leq q^{1-\alpha} \quad \text{10.4}$$

for infinitely many positive integers q as being α -well-approximable. It is natural to ask how large this set of numbers is when $\alpha > 2$ and, indeed, whether such irrational numbers exist at all. We prove Jarník's theorem that the set of α -well-approximable numbers has Hausdorff dimension $2/\alpha$.

It is almost immediate from Example 4.7 (check!) that the set of α -well-approximable numbers has dimension at least $1/\alpha$. An extra

subtlety is required to obtain a value of $2/\alpha$. The idea is as follows. Let G_q be the set of $x \in [0, 1]$ satisfying (10.4). A factorisation argument shows that if n is large and p_1, p_2 are primes with $n < p_1, p_2 \leq 2n$, then G_{p_1} and G_{p_2} are disjoint (except for points very close to 0 or 1). Thus, the set

$$H_n = \bigcup_{\substack{p \text{ prime} \\ n < p \leq 2n}} G_p$$

consists of, roughly, $\sum_{n < p \leq 2n} p \simeq n^2 / \log n$ reasonably regularly spaced intervals of lengths at least $2(2n)^{-\alpha}$. We then show that if n_k is a rapidly increasing sequence, the intersection $\bigcap_{k=1}^{\infty} H_{n_k}$ has dimension at least $2/\alpha$, and note that any number in this intersection lies in infinitely many G_p and so is α -well approximable.

Jarník's theorem 10.3

Suppose $\alpha > 2$. Let F be the set of real numbers $x \in [0, 1]$ for which the inequality

$$\|qx\| \leq q^{1-\alpha} \quad \text{10.5}$$

is satisfied by infinitely many positive integers q . Then
 $\dim_H F = 2/\alpha$.

*Proof

For each q , let G_q denote the set of $x \in [0, 1]$ satisfying (10.5). Then G_q consists of $q - 1$ intervals of length $2q^{-\alpha}$ and two ‘end’ intervals of length $q^{-\alpha}$. Clearly, $F \subset \bigcup_{q=k}^{\infty} G_q$ for each k , so taking the intervals of G_q for $q \geq k$ as a cover of F gives that $\mathcal{H}_{\delta}^s(F) \leq \sum_{q=k}^{\infty} (q+1)(2q^{-\alpha})^s$ if $2k^{-\alpha} \leq \delta$. If $s > 2/\alpha$, the series $\sum_{q=1}^{\infty} (q+1)(2q^{-\alpha})^s$ converges, so $\lim_{k \rightarrow \infty} \sum_{q=k}^{\infty} (q+1)(2q^{-\alpha})^s = 0$ and $\mathcal{H}^s(F) = 0$. Hence, $\dim_H F \leq 2/\alpha$.

Let G'_q be the set of $x \in (q^{-\alpha}, 1 - q^{-\alpha})$ satisfying (10.5), so that G'_q is just G_q with the end intervals removed. Let n be a positive integer, and suppose p_1 and p_2 are prime numbers satisfying $n < p_1 < p_2 \leq 2n$. We show that G'_{p_1} and G'_{p_2} are disjoint and reasonably well separated. For if $1 \leq r_1 < p_1$ and $1 \leq r_2 < p_2$, then $p_1 r_2 \neq p_2 r_1$ since p_1 and p_2 are prime. Thus,

$$\left| \frac{r_1}{p_1} - \frac{r_2}{p_2} \right| = \frac{1}{p_1 p_2} |p_2 r_1 - p_1 r_2| \geq \frac{1}{p_1 p_2} \geq \frac{1}{4n^2},$$

that is, the distance between the centres of any interval from G'_{p_1} and any interval from G'_{p_2} is at least $1/4n^2$. Since these intervals have lengths at most $2n^{-\alpha}$, the distance between any point of G'_{p_1} and any point of G'_{p_2} is at least $\frac{1}{4}n^{-2} - 2n^{-\alpha} \geq \frac{1}{8}n^{-2}$ provided that $n \geq n_0$ for some sufficiently large n_0 . For such n , the set

$$H_n = \bigcup_{\substack{p \text{ prime} \\ n < p \leq 2n}} G'_p$$

is a disjoint union of the intervals in the G'_p for $n < p \leq 2n$, so H_n is made up of intervals of lengths at least $(2n)^{-\alpha}$ which are separated by gaps of lengths at least $\frac{1}{8}n^{-2}$. If $I \subset [0, 1]$ is any interval with $3/|I| < n < p \leq 2n$, then at least $p|I|/3 \geq n|I|/3$ of the intervals of G'_p are completely contained in I . A version of the prime number theorem states that the number of primes between 2 and n is

asymptotically $n/\log n$, so there are at least $n/(2\log n)$ primes in the range $(n, 2n]$ if $n \geq n_1$, for some large $n_1 \geq n_0$. Thus, at least

$$\frac{n^2|I|}{6\log n}$$

[10.6](#)

intervals of H_n are contained in I provided that $n \geq n_1$ and $|I| \geq 3/n$.

To complete the proof, we use Example 4.6. With n_1 as above, let $n_k = \max\{n_{k-1}^k, 3 \times 2^a n_{k-1}^a\}$, for $k = 2, 3, \dots$, where $a > \alpha$ is an integer. Let $E_0 = [0, 1]$, and for $k = 1, 2, \dots$, let E_k consist of those intervals of H_{n_k} that are completely contained in E_{k-1} . The intervals of E_k are of lengths at least $(2n_k)^{-\alpha}$ and are separated by gaps of at least $\varepsilon_k = \frac{1}{8}n_k^{-2}$. Using (10.6), each interval of E_{k-1} contains at least m_k intervals of E_k , where

$$m_k = \frac{n_k^2(2n_{k-1})^{-\alpha}}{6\log n_k} = \frac{cn_k^2n_{k-1}^{-\alpha}}{\log n_k}$$

if $k \geq 2$, where $c = 2^{-\alpha}/6$. (We take $m_1 = 1$.) By (4.7),

$$\begin{aligned} \dim_H \left(\bigcap_{k=1}^{\infty} E_k \right) &\geq \liminf_{k \rightarrow \infty} \frac{\log [c^{k-2}n_1^{-\alpha}(n_2 \cdots n_{k-2})^{2-\alpha}n_{k-1}^2(\log n_2)^{-1} \cdots (\log n_{k-1})^{-1}]}{-\log [cn_{k-1}^{-\alpha}(8\log n_k)^{-1}]} \\ &= \lim_{k \rightarrow \infty} \frac{\log [c^{k-2}n_1^{-\alpha}(n_2 \cdots n_{k-2})^{2-\alpha}(\log n_2)^{-1} \cdots (\log n_{k-1})^{-1}] + 2\log n_{k-1}}{-\log(c/8) + \log(k(\log n_{k-1})) + \alpha \log n_{k-1}} \\ &= 2/\alpha \end{aligned}$$

since the dominant terms in numerator and denominator are those in $\log n_{k-1}$. (Note that for k sufficiently large, $\log n_k = k \log n_{k-1}$ so $\log n_k = ck$!.) If $x \in E_k \subset H_{n_k}$ for all k , then x lies in infinitely many of the G'_p and so $x \in F$. Hence, $\dim_H F \geq 2/\alpha$.

*The rest of this section may be omitted.

Obviously, the set F of Jarník's theorem is dense in $[0, 1]$, with $\dim_H(F \cap I) = 2/\alpha$ for any interval I . However, considerably more than this is true, F is a ‘set of large intersection’ of the type discussed in Section 8.2, and this has some surprising consequences. For the definition of C^s , in the following proposition, see (8.9) and (8.10).

Proposition 10.4

Suppose $\alpha > 2$. If F is the set of positive numbers such that $\|qx\| \leq q^{1-\alpha}$ for infinitely many q , then $F \in C^s[0, \infty)$ for all $s < 2/\alpha$.

Note on proof

This follows the proof of Jarník's Theorem 10.3 up to the definition of H_n . Then a combination of the method of Example 8.10 and prime number theorem estimates is used to show that $\lim_{n \rightarrow \infty} \mathcal{H}_\infty^s(I \cap H_n) = \mathcal{H}_\infty^s(I)$. Slightly different methods are required to estimate the number of intervals of H_n that can intersect a covering interval U , depending on whether $|I| < 1/n$ or $|I| \geq 1/n$.

The first deduction from Proposition 10.4 is that $\dim_H F = 2/\alpha$, which we know already from Jarník's Theorem. However, Proposition 8.9 tells us that smooth bijective images of F are also in C^s . Thus, if $s < 2/\alpha$, then $f(F \cap [a, b])$ is in $C^s[f(a), f(b)]$ for any continuously differentiable function $f : [a, b] \rightarrow \mathbb{R}$ with $|f'(x)| > c > 0$. Taking the functions given by $f_m(x) = x^{1/m}$, we have that $f_m(F) \cap [1, 2]$ is in $C^s[1, 2]$ for $s < 2/\alpha$. It follows from Proposition 8.7 that $\bigcap_{m=1}^{\infty} f_m(F) \cap [1, 2]$ is in $C^s[1, 2]$, so

$$\dim_H \left(\bigcap_{m=1}^{\infty} f_m(F) \right) = 2/\alpha.$$

But

$$f_m(F) = \{x : \|qx^m\| \leq q^{1-\alpha} \text{ for infinitely many } q\}$$

so we have shown that the set of x for which all positive integral powers are α -well-approximable also has Hausdorff dimension $2/\alpha$.

Clearly, many variations are possible using different sequences of functions f_m .

10.4 Notes and references

There are many introductory books on general number theory; for example, the classic by Hardy and Wright (2008) and the recent text by Baker (2012).

The dimensional analysis of the distribution of base- m digits is given in Billingsley (1978). Continued fractions are discussed in most basic texts in number theory. Rogers (1998) discusses dimensional aspects, and Mauldin and Urbański (1999) consider them in the context of IFSs with infinitely many mappings. Hensley (1996) and Jenkinson and Pollicott (2001) have calculated the Hausdorff dimension of various sets of numbers defined by continued fractions to many decimal places.

A general account of Diophantine approximation may be found in the book by Schmidt (1980). Various proofs of Jarník's theorem have been given by Jarník (1931); Besicovitch (1934); Eggleston (1952) and Kaufman (1981). The books by Bernik and Dodson (2000) and Bugeaud (2012) and the surveys by Bugeaud, Dal'bo and Drutu (2009) and Bugeaud (2013) cover many aspects of the fast developing area of Diophantine approximation and dimension.

Some novel relations between fractals and number theory may be found in Lapidus and van Frankenhuyzen (2012).

Exercises

10.1 Find an IFS of similarities on \mathbb{R} with attractor F consisting of those numbers in $[0, 1]$ whose decimal expansions contain only even

digits. Show that $\dim_H F = \log 5 / \log 10$.

10.2 Show that the set $F(p_0, \dots, p_{m-1})$ in (10.1) satisfies (9.4) for a set of m similarity transformations. (It is not, of course, compact.)

10.3 Find the Hausdorff dimension of the set of numbers whose base-3 expansions have ‘twice as many 2’s as 1’s’ (i.e. those x such that $2\lim_{k \rightarrow \infty} n_1(x|_k)/k = \lim_{k \rightarrow \infty} n_2(x|_k)/k$ with both these limits existing).

10.4 Find the continued fraction representations of (i) $41/9$ and (ii) $\sqrt{5}$.

10.5 What number has continued fraction representation

$$1 + \frac{1}{1 + \frac{1}{1 + \frac{1}{1 + \dots}}}?$$

10.6 Use the continued fraction representation of $\sqrt{2}$ (with partial quotients $1, 2, 2, 2, \dots$) to obtain some good rational approximations to $\sqrt{2}$. (In fact, the number obtained by curtailing a partial fraction at the k th partial quotient gives the best rational approximation by any number with equal or smaller denominator.)

10.7 Find an IFS whose attractor is the set of positive numbers with infinite continued fraction expansions that have partial quotients containing only the digits 2 and 3. Thus estimate the Hausdorff and box dimensions of this set.

10.8 Let x be a real number and Q a positive integer. By considering the set of numbers $\{rx(\text{mod}1) : r = 0, 1, \dots, Q\}$, prove Dirichlet's theorem: that is, there is an integer q with $0 \leq q \leq Q$ such that $\|qx\| \leq Q^{-1}$. Deduce that there are infinitely many positive integers q such that $\|qx\| \leq q^{-1}$.

10.9 Let n and d be positive integers. Show that if the Diophantine equation $x^n - dy^n = 1$ has infinitely many solutions (x, y) with x and y positive integers, then $d^{1/n}$ must be n -well-approximable.

10.10 Fix $\alpha > 3$, let F be the set of (x, y) in \mathbb{R}^2 such that $\|qx\| \leq q^{1-\alpha}$ and $\|qy\| \leq q^{1-\alpha}$ are satisfied simultaneously for infinitely many positive integers q . Show, in a similar way to the first part of the

proof of Theorem 10.3, that $\dim_H F \leq 3/\alpha$. (In fact, it may be shown, using a generalisation of the remainder of the proof, that $\dim_H F = 3/\alpha$.)

10.11 Show that the set of real numbers x , such that $(x+m)^2$ is α -well-approximable for all integers m , has Hausdorff dimension $2/\alpha$.

Chapter 11

Graphs of functions

A variety of interesting fractals, both of theoretical and practical importance, occur as graphs of functions. Indeed, many real phenomena plotted as functions of time display fractal features. Examples include financial data such as stock market prices, wind speeds, reservoir levels and population data, particularly when recorded over fairly long time spans.

11.1 Dimensions of graphs

Under certain circumstances, the graph of a function $f : [a, b] \rightarrow \mathbb{R}$,

$$\text{graph } f = \{(t, f(t)) : a \leq t \leq b\},$$

regarded as a subset of the (t, x) -coordinate plane may be a fractal. (We work with coordinates (t, x) rather than (x, y) for consistency with the rest of the book, and because the independent variable is frequently time.) If f is a Lipschitz function or has a continuous derivative, then $\text{graph } f$ has dimension 1. The same is true if f is of bounded variation; that is, if $\sum_{i=0}^{m-1} |f(t_i) - f(t_{i+1})|$ is bounded for all dissections $0 = t_0 < t_1 < \dots < t_m = 1$. However, it is possible for a continuous function to be sufficiently irregular to have a graph of dimension strictly greater than 1. Perhaps the best known example is

$$f(t) = \sum_{k=1}^{\infty} \lambda^{(s-2)k} \sin(\lambda^k t)$$

where $1 < s < 2$ and $\lambda > 1$. This function, essentially Weierstrass's example of a continuous function that is nowhere differentiable, has box dimension s , and is believed to have Hausdorff dimension s .

.

We first derive some simple but widely applicable estimates for the box dimension of graphs. Given a function f and an interval $[t_1, t_2]$, we write R_f for the *maximum range* of f over an interval,

$$R_f[t_1, t_2] = \sup_{t_1 \leq t, u \leq t_2} |f(t) - f(u)|.$$

Proposition 11.1

Let $f : [0, 1] \rightarrow \mathbb{R}$ be continuous. Let $0 < \delta < 1$, and let m be the least integer greater than or equal to $1/\delta$. Then, if N_δ is the number of squares of the δ -mesh that intersect $\text{graph } f$,

$$\delta^{-1} \sum_{i=0}^{m-1} R_f[i\delta, (i+1)\delta] \leq N_\delta \leq 2m + \delta^{-1} \sum_{i=0}^{m-1} R_f[i\delta, (i+1)\delta]. \quad \text{11.1}$$

The right-hand inequality remains true even if f is not continuous.

Proof

The number of mesh squares of side δ in the column above the interval $[i\delta, (i+1)\delta]$ that intersect $\text{graph } f$ is at most $2 + R_f[i\delta, (i+1)\delta]/\delta$, and if f is continuous is at least $R_f[i\delta, (i+1)\delta]/\delta$. Summing over all such intervals gives (11.1). This is illustrated in [Figure 11.1](#).

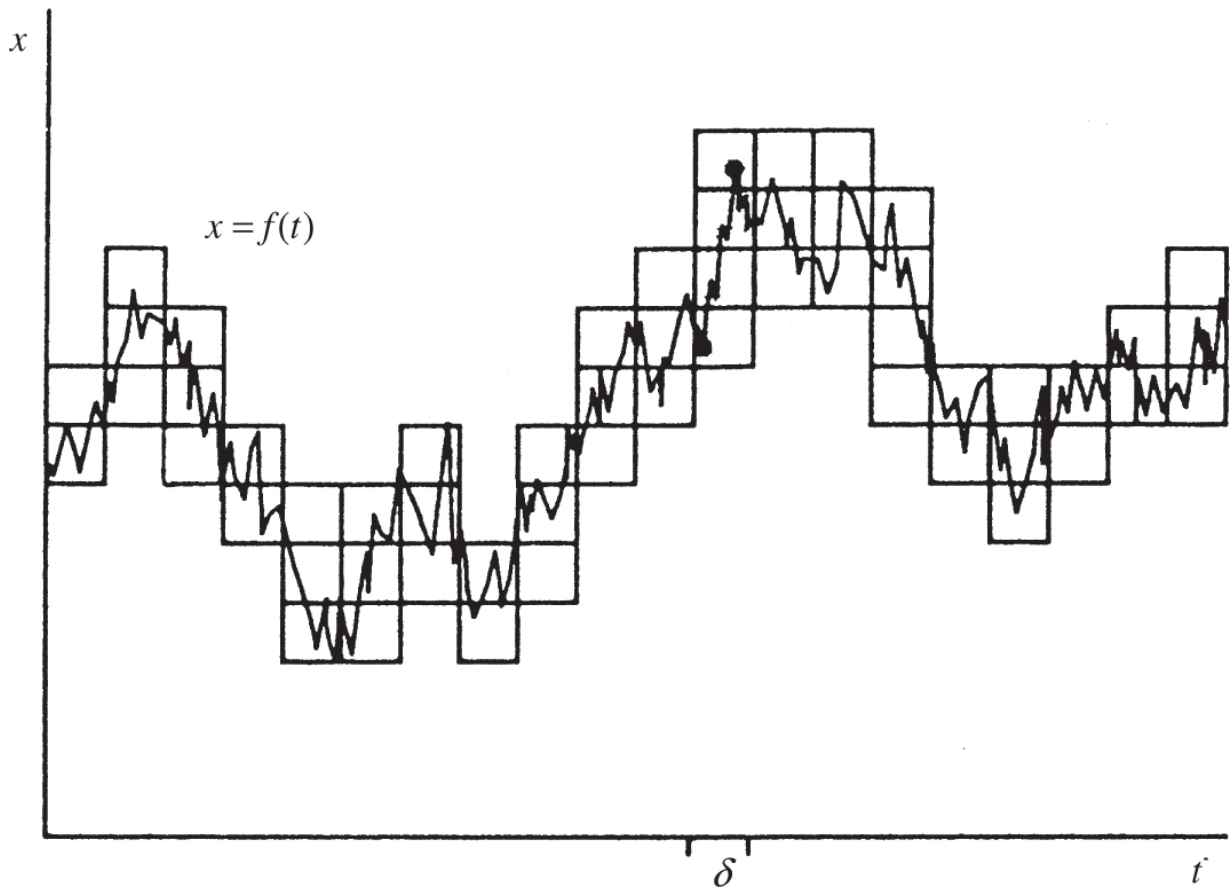


Figure 11.1 The number of δ -mesh squares in a column above an interval of width δ that intersect graph f is approximately the range of f over that interval divided by δ . Summing these numbers gives estimates for the box dimension of graph f .

This proposition may be applied immediately to functions satisfying a Hölder condition.

Corollary 11.2

Let $f : [0, 1] \rightarrow \mathbb{R}$ be a continuous function.

a. Suppose

$$|f(t) - f(u)| \leq c|t - u|^{2-s} \quad (0 \leq t, u \leq 1), \quad \text{11.2}$$

where $c > 0$ and $1 \leq s \leq 2$. Then, $\mathcal{H}^s(\text{graph } f) < \infty$ and $\dim_H \text{graph } f \leq \underline{\dim}_B \text{graph } f \leq \overline{\dim}_B \text{graph } f \leq s$. This remains true if, for some $\delta > 0$, (11.2) holds when $|t - u| < \delta$.

b. Suppose that there are numbers $c > 0$, $\delta_0 > 0$ and $1 \leq s < 2$ with the following property: for each $t \in [0, 1]$ and $0 < \delta \leq \delta_0$, there exists u such that $|t - u| \leq \delta$ and

$$|f(t) - f(u)| \geq c\delta^{2-s}. \quad \text{11.3}$$

Then, $s \leq \underline{\dim}_B \text{graph } f$.

Proof

- a. It is immediate from (11.2) that $R_f[t_1, t_2] \leq c|t_1 - t_2|^{2-s}$ for $0 \leq t_1, t_2 \leq 1$. With notation as in Proposition 11.1, $m < (1 + \delta^{-1})$, so by (11.1)

$$N_\delta \leq 2m + \delta^{-1}mc\delta^{2-s} \leq (1 + \delta^{-1})(2 + c\delta^{-1}\delta^{2-s}) \leq c_1\delta^{-s}$$

where c_1 is independent of δ . The conclusion follows from Proposition 4.1.

- b. In the same way, (11.3) implies that $R_f[t_1, t_2] \geq c|t_1 - t_2|^{2-s}$. Since $\delta^{-1} \leq m$, we have from (11.1) that

$$N_\delta \geq \delta^{-1}mc\delta^{2-s} \geq \delta^{-1}\delta^{-1}c\delta^{2-s} = c\delta^{-s}$$

So, Equivalent definition 3.1(iv) gives $s \leq \dim_B \text{graph } f$.

Unfortunately, lower bounds for the Hausdorff dimension of graphs are generally very much more awkward to find than box dimensions.

Example 11.3 The Weierstrass function

Fix $\lambda > 1$ and $1 < s < 2$. Define $f : [0, 1] \rightarrow \mathbb{R}$ by

$$f(t) = \sum_{k=1}^{\infty} \lambda^{(s-2)k} \sin(\lambda^k t). \quad 11.4$$

Then, provided λ is large enough, $\dim_B \text{graph } f = s$.

Calculation

Given $0 < h < \lambda^{-1}$, let N be the integer such that

$$\lambda^{-(N+1)} \leq h < \lambda^{-N}.$$

11.5

Then,

$$\begin{aligned} |f(t+h) - f(t)| &\leq \sum_{k=1}^N \lambda^{(s-2)k} |\sin(\lambda^k(t+h)) - \sin(\lambda^k t)| \\ &\quad + \sum_{k=N+1}^{\infty} \lambda^{(s-2)k} |\sin(\lambda^k(t+h)) - \sin(\lambda^k t)| \\ &\leq \sum_{k=1}^N \lambda^{(s-2)k} \lambda^k h + \sum_{k=N+1}^{\infty} 2\lambda^{(s-2)k} \end{aligned}$$

using that $|\sin u - \sin v| \leq |u - v|$ (a consequence of the mean-value theorem) on the first N terms of the sum, and that $|\sin u| \leq 1$ on the remaining terms. Summing these geometric series,

$$\begin{aligned} |f(t+h) - f(t)| &\leq \frac{h\lambda^{(s-1)N}}{1 - \lambda^{1-s}} + \frac{2\lambda^{(s-2)(N+1)}}{1 - \lambda^{s-2}} \\ &\leq ch^{2-s}, \end{aligned}$$

where c is independent of h , using (11.5). Corollary 11.2(a) now gives that $\overline{\dim}_B \text{graph } f \leq s$.

In the same way, but splitting the sum into three parts—the first $N-1$ terms, the N th term and the rest—we get that

$$\begin{aligned} &|f(t+h) - f(t) - \lambda^{(s-2)N} (\sin \lambda^N(t+h) - \sin \lambda^N t)| \\ &\leq \frac{\lambda^{(s-2)N-s+1}}{1 - \lambda^{1-s}} + \frac{2\lambda^{(s-2)(N+1)}}{1 - \lambda^{s-2}} \end{aligned} \tag{11.6}$$

if $\lambda^{-(N+1)} \leq h < \lambda^{-N}$.

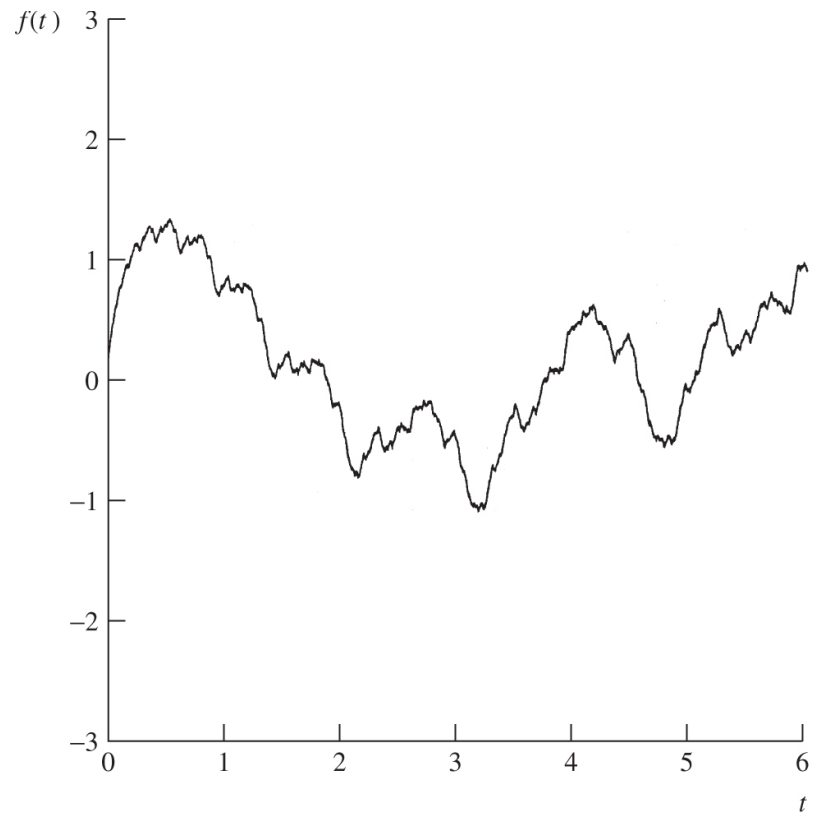
Let $\lambda > 2$ be large enough for the right-hand side of (11.6) to be less than $\frac{1}{20}\lambda^{(s-2)N}$ for all N . For $\delta < \lambda^{-1}$, take N such that

$\lambda^{-N} \leq \delta < \lambda^{-(N-1)}$. For each t , we may choose h with $h < \lambda^{-N} \leq \delta$ such that $|\sin \lambda^N(t+h) - \sin \lambda^N t| > \frac{1}{10}$, so by (11.6)

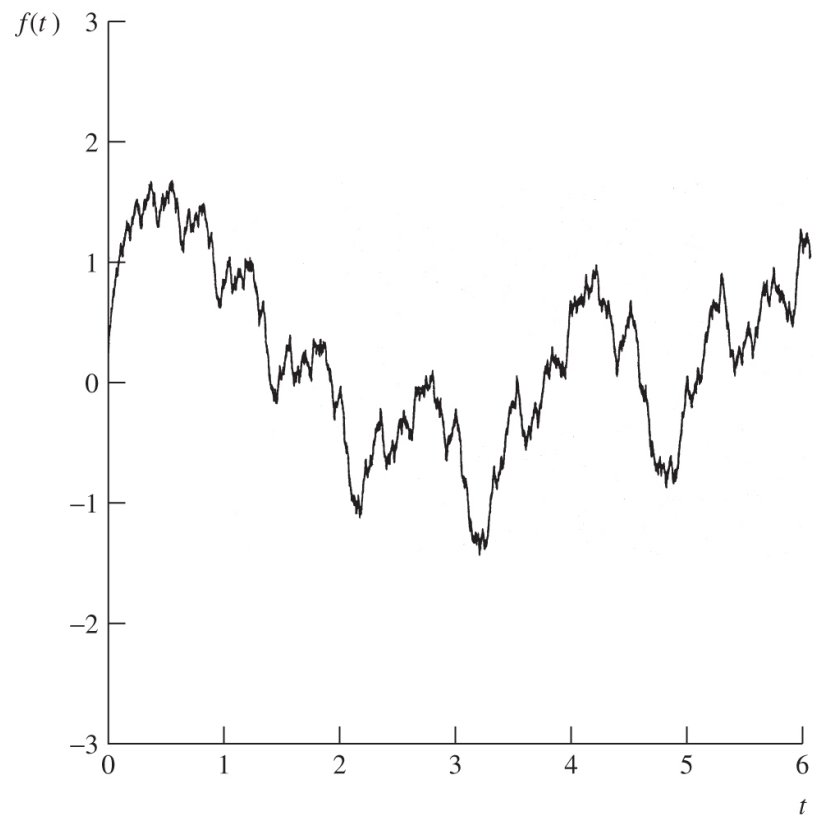
$$|f(t+h) - f(t)| \geq \frac{1}{10}\lambda^{(s-2)N} - \frac{1}{20}\lambda^{(s-2)N} = \frac{1}{20}\lambda^{(s-2)N} \geq \frac{1}{20}\lambda^{s-2}\delta^{2-s}.$$

It follows from Corollary 11.2(b) that $\dim_B \text{graph } f \geq s$.

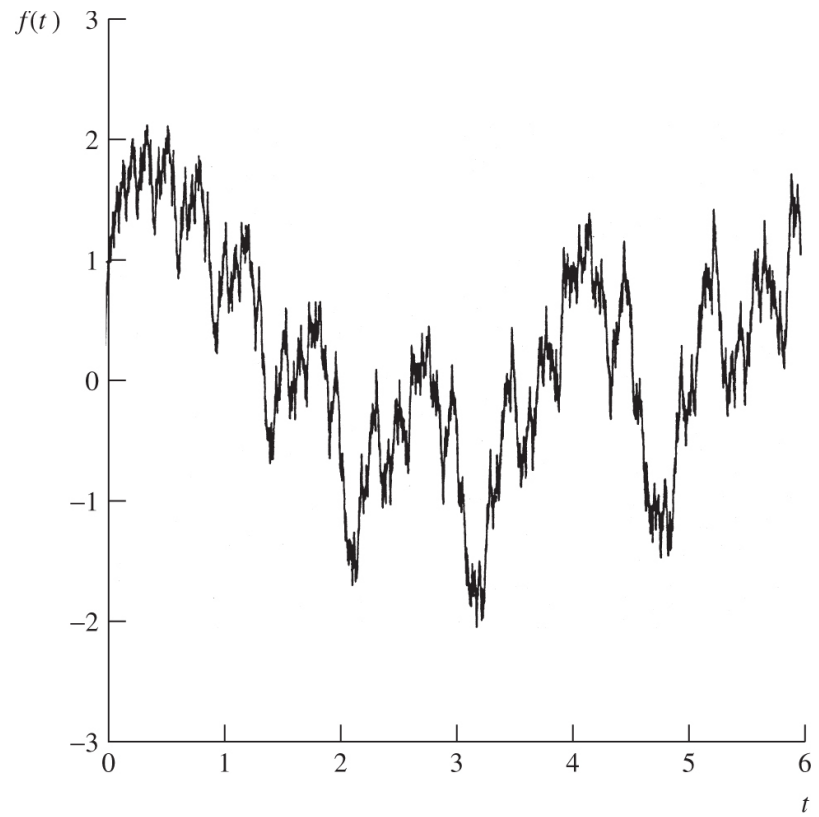
Various cases of the Weierstrass function are shown in [Figure 11.2](#).



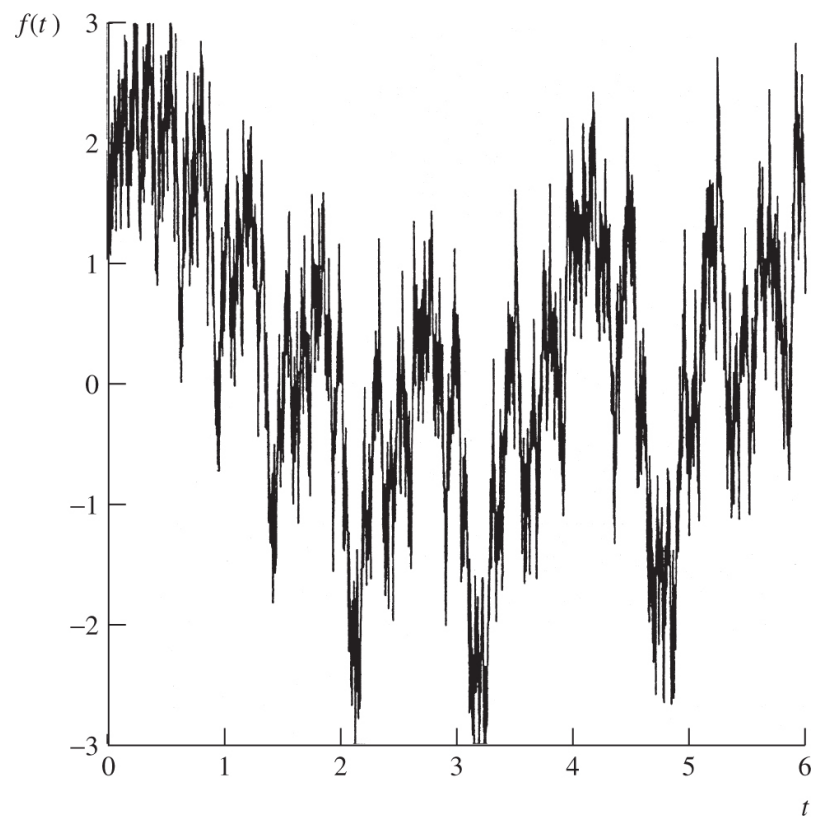
(a)



(b)



(c)



(d)

Figure 11.2 The Weierstrass function $f(t) = \sum_{k=0}^{\infty} \lambda^{(s-2)k} \sin(\lambda^k t)$ with $\lambda = 1.5$ and (a) $s = 1.1$, (b) $s = 1.3$, (c) $s = 1.5$ and (d) $s = 1.7$.

It is immediate from Example 11.3 that the Hausdorff dimension of the graph of the Weierstrass function (11.4) is at most s . It is widely believed that it equals s , at least for ‘most’ values of λ . The difficulty is that there could be coverings of the graph by sets of widely varying sizes that give a smaller value. Even to show that $\dim_H \text{graph } f > 1$ is not trivial. Lower bounds come from mass distribution methods depending on estimates for $\mathcal{L}\{(t, f(t)) \in B\}$, where B is a disc and \mathcal{L} is Lebesgue measure. The rapid small-scale oscillation of f ensures that the graph is inside B relatively rarely, so that this measure is small. In this way, it is possible to show that there is a constant c such that

$$s \geq \dim_H \text{graph } f \geq s - c/\log \lambda$$

so, when λ is large, the Hausdorff dimension cannot be much less than the conjectured value.

The Weierstrass function (11.4) is representative of a much wider class of functions to which these methods apply. If g is a suitable periodic function, a similar method can often show that

$$f(t) = \sum_{k=1}^{\infty} \lambda^{(s-2)k} g(\lambda^k t) \quad \text{11.7}$$

has $\dim_B \text{graph } f = s$. At first, such functions seem rather contrived, but their occurrence as repellers in certain dynamical systems (see Exercise 13.9) gives them a new significance.

In Section 1.4, we saw that self-affine sets defined by iterated function systems are often fractals; by a suitable choice of affine transformations, they can also be graphs of functions. Let $\{S_i, \dots, S_m\}$ be affine transformations represented in matrix notation with respect to (t, x) coordinates by

$$S_i \begin{bmatrix} t \\ x \end{bmatrix} = \begin{bmatrix} 1/m & 0 \\ a_i & r_i \end{bmatrix} \begin{bmatrix} t \\ x \end{bmatrix} + \begin{bmatrix} (i-1)/m \\ b_i \end{bmatrix}, \quad \underline{\textbf{11.8}}$$

that is,

$$S_i(t, x) = (t/m + (i-1)/m, a_i t + r_i x + b_i).$$

Thus, for each i , S_i transforms vertical lines to vertical lines, with the vertical strip $0 \leq t \leq 1$ mapped onto the strip $(i-1)/m \leq t \leq i/m$. We suppose that

$$1/m < r_i < 1, \quad \underline{\textbf{11.9}}$$

for each i , so that contractions in the t direction are stronger than in the x direction.

Let $p_1 = (0, b_1/(1 - r_1))$ and $p_m = (1, (a_m + b_m)/(1 - r_m))$ be the fixed points of S_1 and S_m . We assume that the matrix entries have been chosen so that

$$S_i(p_m) = S_{i+1}(p_1) \quad (1 \leq i \leq m-1) \quad \underline{\textbf{11.10}}$$

so that the segments $[S_i(p_1), S_i(p_m)]$ join up to form a polygonal curve E_1 . To avoid trivial cases, we also assume that the points $S_1(p_1), \dots, S_m(p_1), p_m$ are not all collinear. The attractor F of the iterated function system $\{S_1, \dots, S_m\}$ (see (9.4)) may be constructed by repeatedly replacing line segments by affine images of the ‘generator’ E_1 ; see [Figures 11.3](#) and [11.4](#). Condition (11.10) ensures that the segments join up with the result that F is the graph of some continuous function $f : [0, 1] \rightarrow \mathbb{R}$. Note that these conditions do not necessarily imply that the S_i are contractions with respect to Euclidean distance. However, it is possible to redefine distance in the (x, t) plane in such a way that the S_i become contractions, and in this context the IFS theory guarantees a unique attractor.

Example 10.4 Self-affine curves

Let $F = \text{graph } f$ be the self-affine curve described above. Then,
 $\dim_B F = 1 + \log(r_1 + \dots + r_m) / \log m$.

Calculation

Let T_i be the ‘linear part’ of S_i , represented by the matrix

$$\begin{bmatrix} 1/m & 0 \\ a_i & r_i \end{bmatrix}.$$

Let I_{i_1, \dots, i_k} be the interval of the t -axis consisting of those t with base- m expansion beginning $0.i'_1 \dots i'_k$, where $i'_j = i_j - 1$. Then, the part of F above I_{i_1, \dots, i_k} is the affine image $S_{i_1} \circ \dots \circ S_{i_k}(F)$, which is a translate of $T_{i_1} \circ \dots \circ T_{i_k}(F)$. The matrix representing $T_{i_1} \circ \dots \circ T_{i_k}$ is easily seen by induction to be

$$\begin{bmatrix} m^{-k} & 0 \\ m^{1-k}a_{i_1} + m^{2-k}r_{i_1}a_{i_2} + \dots + r_{i_1}r_{i_2} \dots r_{i_{k-1}}a_{i_k} & r_{i_1}r_{i_2} \dots r_{i_k} \end{bmatrix}.$$

This is a shear transformation, contracting vertical lines by a factor $r_{i_1}r_{i_2} \dots r_{i_k}$. Observe that the bottom left-hand entry is bounded by

$$\begin{aligned} & |m^{1-k}a + m^{2-k}r_{i_1}a + \dots + r_{i_1} \dots r_{i_{k-1}}a| \\ & \leq ((mc)^{1-k} + (mc)^{2-k} + \dots + 1)r_{i_1} \dots r_{i_{k-1}}r_{i_k}c^{-1}a \\ & \leq rr_{i_1} \dots r_{i_{k-1}}r_{i_k}, \end{aligned}$$

where $a = \max |a_i|$, $c = \min\{r_i\} > 1/m$ and $r = a/c(1 - (mc)^{-1})$ from summing the geometric series. Thus, the image $T_{i_1} \circ \dots \circ T_{i_k}(F)$ is contained in a rectangle of height $(r + h)r_{i_1} \dots r_{i_k}$, where h is the height of F . On the other hand, if q_1, q_2, q_3 are three non-collinear points chosen from $S_1(p_1), \dots, S_m(p_1), p_m$, then $T_{i_1} \circ \dots \circ T_{i_k}(F)$ contains the points $T_{i_1} \circ \dots \circ T_{i_k}(q_j)$ ($j = 1, 2, 3$). The height of the triangle with these vertices is at least $r_{i_1} \dots r_{i_k}d$, where d is the vertical distance from q_2 to the segment $[q_1, q_3]$. Thus, the range of the function f over the interval I_{i_1, \dots, i_k} satisfies

$$dr_{i_1} \dots r_{i_k} \leq R_f[I_{i_1, \dots, i_k}] \leq r_1r_{i_1} \dots r_{i_k},$$

where $r_1 = r + h$.

For fixed k , we sum this over all the m^k intervals I_{i_1, \dots, i_k} of lengths m^{-k} to get, using Proposition 11.1,

$$m^k d \sum r_{i_1} \cdots r_{i_k} \leq N_{m^{-k}}(F) \leq 2m^k + m^k r_1 \sum r_{i_1} \cdots r_{i_k},$$

where $N_{m^{-k}}(F)$ is the number of mesh squares of side m^{-k} that intersect F . For each j , the number r_{i_j} ranges through the values r_1, \dots, r_m , so that $\sum r_{i_1} \cdots r_{i_k} = (r_1 + \cdots + r_m)^k$. Thus,

$$dm^k(r_1 + \cdots + r_m)^k \leq N_{m^{-k}}(F) \leq 2m^k + r_1 m^k (r_1 + \cdots + r_m)^k.$$

Taking logarithms and using Equivalent definition 2.1(iv) of box dimension gives the value stated.

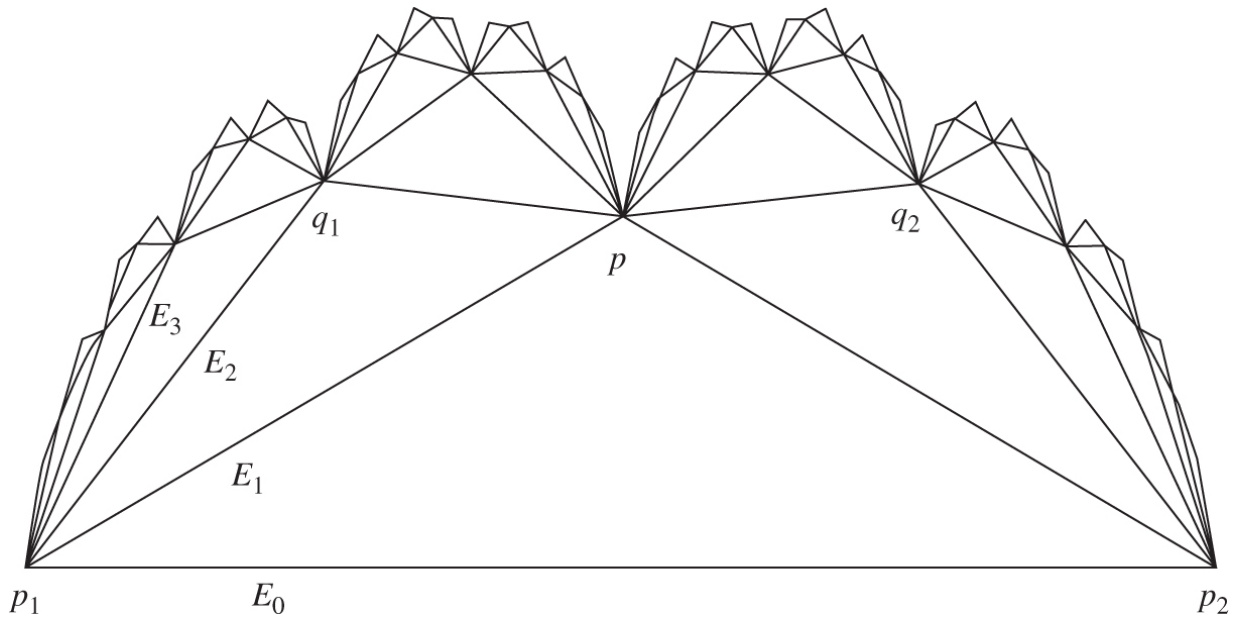
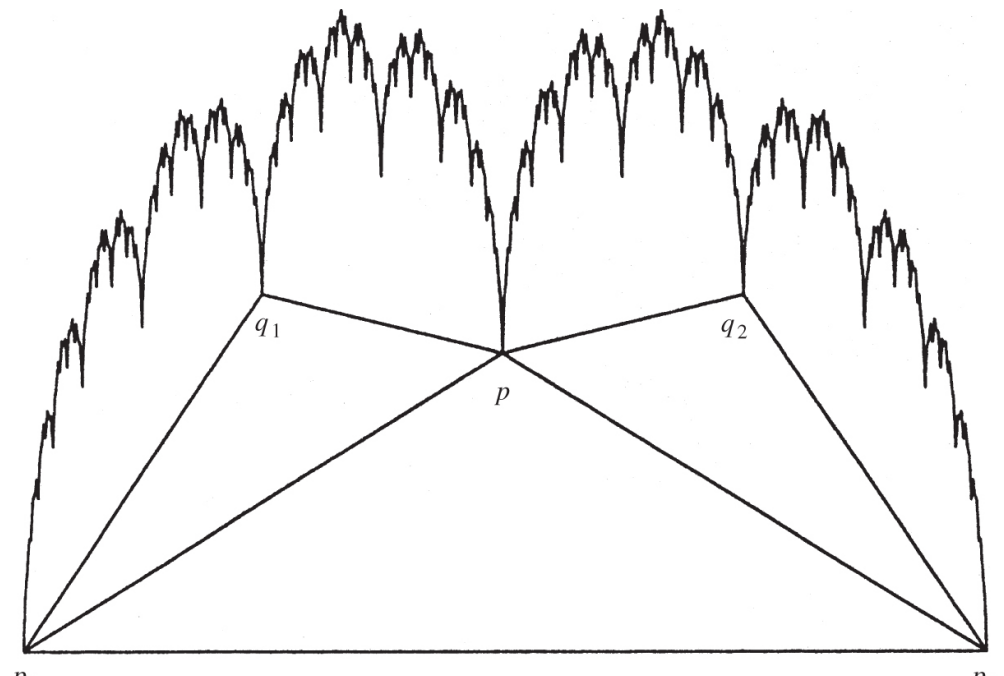
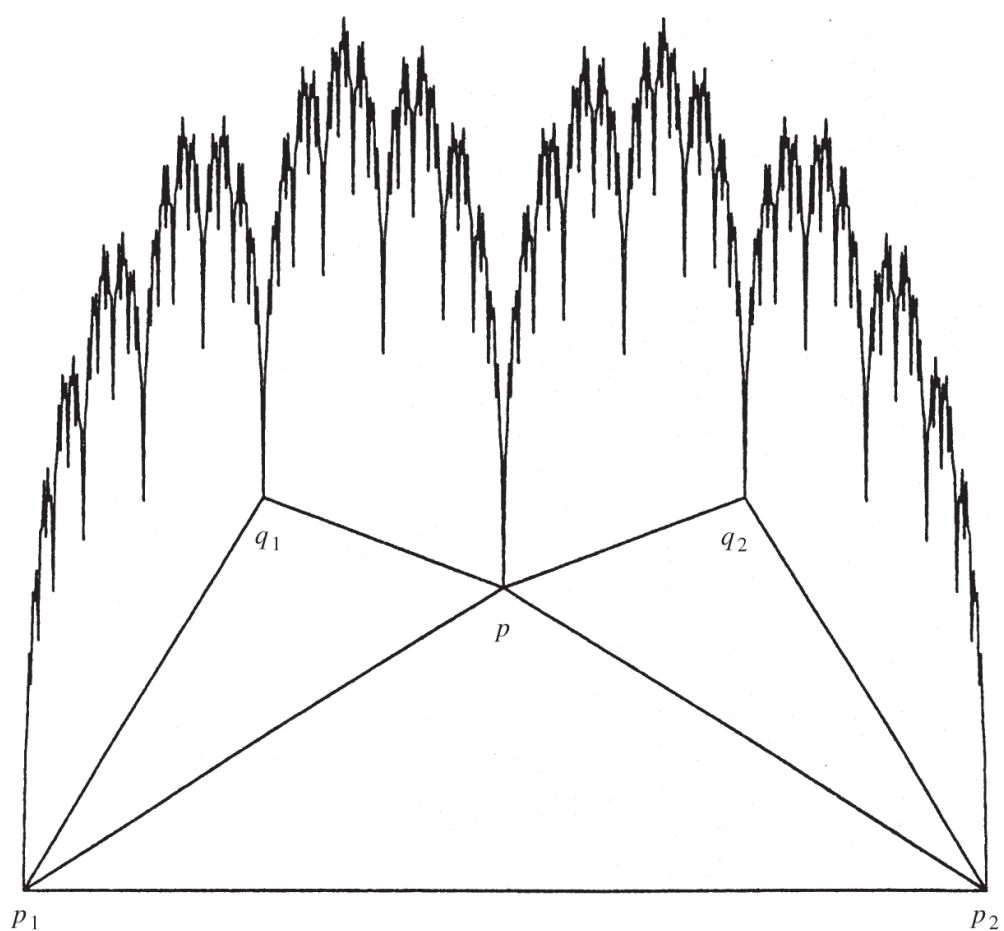


Figure 11.3 Stages in the construction of a self-affine curve F . The affine transformations S_1 and S_2 map the generating triangle p_1pp_2 onto the triangles p_1q_1p and pq_2p_2 , respectively, and transform vertical lines to vertical lines. The rising sequence of polygonal curves E_0, E_1, \dots are given by $E_{k+1} = S_1(E_k) \cup S_2(E_k)$ and provide increasingly good approximations to F (shown in [Figure 11.4a](#) for this case).



(a)



(b)

Figure 11.4 Self-affine curves defined by the two affine transformations that map the triangle p_1pp_2 onto p_1q_1p and pq_2p_2 , respectively. In (a), the vertical contraction of both transformations is 0.7, giving $\dim_B \text{graph } f = 1.49$, and in (b), the vertical contraction of both transformations is 0.8, giving $\dim_B \text{graph } f = 1.68$.

Self-affine functions are useful for *fractal interpolation*. Suppose we wish to find a fractal curve of a given dimension passing through the points with coordinates $(i/m, x_i)$ for $i = 0, 1, \dots, m$. By choosing transformations (11.8) in such a way that s_i maps the segment $[p_1, p_m]$ onto the segment $[(i-1)/m, x_{i-1}], (i/m, x_i)]$ for each i , the construction described above gives a self-affine function with graph passing through the given points. By adjusting the values of the matrix entries, we can ensure that the curve has the required box dimension; there is also some freedom to vary the appearance of the curve in other ways. Fractal interpolation has been used very effectively to picture mountain skylines.

Of course, self-affine functions can be generalised, so that the s_i do not all have the same contraction ratio in the t direction. This leads to fractal interpolation between points at unequally spaced intervals of t . The calculation of Example 11.4 may be extended to give the box dimension of such curves.

An example of fractal interpolation is illustrated in [Figure 11.5](#).

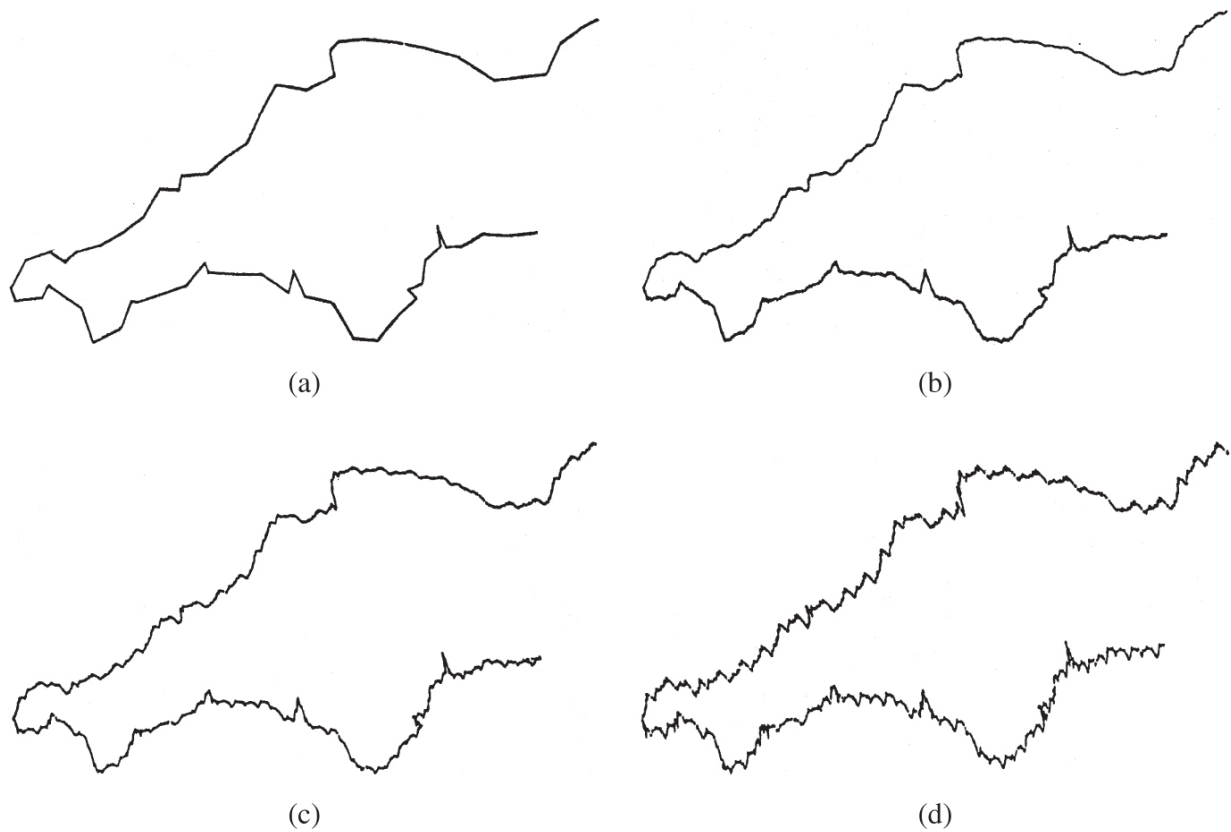


Figure 11.5 Fractal interpolation on the northern and southern halves of a map of South-West England, using the vertices of the polygon in figure (a) as data points. The dimensions of the self-affine curves fitted to these data points are (b) 1.1, (c) 1.2 and (d) 1.3.

*11.2 Autocorrelation of fractal functions

As we have remarked, quantities varying with time often turn out to have fractal graphs. One way in which their fractal nature is often manifested is by a power-law behaviour of the correlation between measurements separated by time h . In this section, we merely outline the ideas involved; we make no attempt to be rigorous. In particular, the limits used are all assumed to exist.

For convenience of analysis, we assume that $f : \mathbb{R} \rightarrow \mathbb{R}$ is a continuous bounded function and we consider the average behaviour of f over long periods $[-T, T]$. (Similar ideas hold if f is

just defined on $[0, \infty)$ or on a finite interval by extending f to \mathbb{R} in a periodic manner.) We write \bar{f} for the average value of f , that is,

$$\bar{f} = \lim_{T \rightarrow \infty} \frac{1}{2T} \int_{-T}^T f(t) dt.$$

A measure of the correlation between f at times separated by h is provided by the *autocorrelation function*

$$C(h) = \lim_{T \rightarrow \infty} \frac{1}{2T} \int_{-T}^T (f(t+h) - \bar{f})(f(t) - \bar{f}) dt \quad \text{11.11}$$

$$= \lim_{T \rightarrow \infty} \frac{1}{2T} \int_{-T}^T f(t+h)f(t) dt - (\bar{f})^2. \quad \text{11.12}$$

From (11.11), we see that $C(h)$ is positive if $f(t+h) - \bar{f}$ and $f(t) - \bar{f}$ tend to have the same sign, and is negative if they tend to have opposite signs. If there is no correlation, $C(h) = 0$. Since

$$\int (f(t+h) - f(t))^2 dt = \int f(t+h)^2 dt + \int f(t)^2 dt - 2 \int f(t+h)f(t) dt$$

we have

$$\begin{aligned} C(h) &= \bar{f}^2 - (\bar{f})^2 - \frac{1}{2} \lim_{T \rightarrow \infty} \frac{1}{2T} \int_{-T}^T (f(t+h) - f(t))^2 dt \\ &= C(0) - \frac{1}{2} \lim_{T \rightarrow \infty} \frac{1}{2T} \int_{-T}^T (f(t+h) - f(t))^2 dt \end{aligned} \quad \text{11.13}$$

where

$$\bar{f}^2 = \lim_{T \rightarrow \infty} \frac{1}{2T} \int_{-T}^T f(t)^2 dt$$

is the mean square of f , assumed to be positive and finite. With $C(h)$ in the form (11.13), we can infer a plausible relationship between the autocorrelation function of f and the dimension of $\text{graph } f$. The clue is in Corollary 11.2. Suppose that f is a function satisfying

(11.2) and also satisfying (11.3) in a ‘reasonably uniform way’. Then, there are constants c_1 and c_2 such that

$$c_1 h^{4-2s} \leq \frac{1}{2T} \int_{-T}^T (f(t+h) - f(t))^2 dt \leq c_2 h^{4-2s} \quad \text{11.14}$$

for small h . Obviously, this is not directly equivalent to (11.2) and (11.3), but in many reasonably ‘time-homogeneous’ situations, the conditions do correspond. Thus, if the autocorrelation function of f satisfies

$$C(0) - C(h) \simeq ch^{4-2s}$$

for small h , it is reasonable to expect the box dimension of $\text{graph } f$ to equal s .

The autocorrelation function is closely connected with the *power spectrum* of f , defined by

$$S(\omega) = \lim_{T \rightarrow \infty} \frac{1}{2T} \left| \int_{-T}^T f(t) e^{it\omega} dt \right|^2. \quad \text{11.15}$$

For functions with any degree of long-term regularity, $S(\omega)$ is likely to exist. The power spectrum reflects the strength of the frequency ω in the harmonic decomposition of f .

We show that the power spectrum is the Fourier transform of the autocorrelation function. By working with $f(t) - \bar{f}$, we may assume that f has zero mean. Let $f_T(t)$ be given by $f(t)$ if $|t| \leq T$ and be 0 otherwise, and define

$$\begin{aligned} C_T(h) &= \frac{1}{2T} \int_{-\infty}^{\infty} f_T(t+h) f_T(t) dt \\ &= \frac{1}{2T} f_T^- * f_T(-h), \end{aligned}$$

where $f_T^-(t) = f_T(-t)$ and $*$ denotes convolution. By the convolution theorem for Fourier transforms (see Section 1.4), this equation transforms to

$$\begin{aligned}\hat{C}_T(\omega) &= \frac{1}{2T} \hat{f}_T^-(\omega) \hat{f}_T(\omega) \\ &= \frac{1}{2T} |\hat{f}_T(\omega)|^2,\end{aligned}$$

where $\hat{C}_T(\omega) = \int_{-\infty}^{\infty} C_T(t) e^{it\omega} dt$ and $\hat{f}_T(\omega) = \int_{-\infty}^{\infty} f_T(t) e^{it\omega} dt$ are the usual Fourier transforms. (Note that we cannot work with the transform of f itself, since the integral would diverge.) Letting $T \rightarrow \infty$, we see that $C_T(h) \rightarrow C(h)$ for each h and $\hat{C}_T(\omega) \rightarrow S(\omega)$ for each ω . It may be shown that this implies that

$$\hat{C}(\omega) = S(\omega).$$

Clearly S and C are both real and even functions, so the transforms are cosine transforms. Thus,

$$S(\omega) = \int_{-\infty}^{\infty} C(t) e^{it\omega} dt = \int_{-\infty}^{\infty} C(t) \cos(\omega t) dt \quad \text{11.16}$$

and, by the inversion formula for Fourier transforms,

$$C(h) = \frac{1}{2\pi} \int_{-\infty}^{\infty} S(\omega) e^{-ih\omega} d\omega = \frac{1}{2\pi} \int_{-\infty}^{\infty} S(\omega) \cos(\omega h) d\omega. \quad \text{11.17}$$

In this analysis, we have not gone into questions of convergence of the integrals too carefully, but in most practical situations the argument can be justified.

Autocorrelations provide us with several methods of estimating the dimension of the graph of a function or ‘signal’ f . We may compute the autocorrelation function $C(h)$ or equivalently, the mean-square change in signal in time h over a long period, so from (11.13)

$$2[C(0) - C(h)] \simeq \frac{1}{2T} \int_{-T}^T (f(t+h) - f(t))^2 dt. \quad \text{11.18}$$

If the power-law behaviour

$$C(0) - C(h) \simeq ch^{4-2s} \quad \text{11.19}$$

is observed for small h , we might expect the box dimension of $\text{graph } f$ to be s . In other words,

$$\dim_B \text{graph } f = 2 - \lim_{h \rightarrow 0} \frac{\log(C(0) - C(h))}{2 \log h} \quad \mathbf{11.20}$$

if this limit exists. We might then seek functions with graphs known to have this dimension, such as those of Examples 11.3 and 11.4 or the fractional Brownian functions of Section 16.2 to provide simulations of signals with similar characteristics.

Alternatively, we can work from the power spectrum $S(\omega)$ and use (11.17) to find the autocorrelation function. We need to know about $C(0) - C(h)$ for small h ; typically this depends on the behaviour of its transform $S(\omega)$ when ω is large. The situation of greatest interest is when the power spectrum obeys a power law $S(\omega) \sim c/\omega^\alpha$ for large ω , in which case

$$C(0) - C(h) \sim bh^{\alpha-1} \quad \mathbf{11.21}$$

for small h , for some constant b . To see this formally, note that from (11.17)

$$\pi(C(0) - C(h)) = \int_0^\infty S(\omega)(1 - \cos(\omega h))d\omega = 2 \int_0^\infty S(\omega)\sin^2\left(\frac{1}{2}\omega h\right)d\omega$$

and taking $S(\omega) = \omega^{-\alpha}$ gives

$$\frac{1}{2}\pi(C(0) - C(h)) = \int_0^\infty \omega^{-\alpha}\sin^2\left(\frac{1}{2}\omega h\right)d\omega = h^{\alpha-1} \int_0^\infty u^{-\alpha}\sin^2\left(\frac{1}{2}u\right)du$$

having substituted $u = \omega h$. It may be shown that (11.21) also holds if S is any sufficiently smooth function such that $S(\omega) \sim c\omega^{-\alpha}$ as $\omega \rightarrow \infty$. Comparing (11.19) and (11.21) suggests that $\text{graph } f$ has box dimension s , where $4 - 2s = \alpha - 1$ or $s = \frac{1}{2}(5 - \alpha)$. Thus, it is reasonable to expect a signal with a $1/\omega^\alpha$ power spectrum to have a graph of dimension $\frac{1}{2}(5 - \alpha)$ for $1 < \alpha < 3$.

In practice, curves of dimension $\frac{1}{2}(5 - \alpha)$ often provide good simulations and display similar characteristics to signals observed to have $1/\omega^\alpha$ power spectra.

11.3 Notes and references

The dimension of fractal graphs was first studied by Besicovitch and Ursell (1937). For analysis of Weierstrass-type curves, see Berry and Lewis (1980); Mauldin and Williams (1986b) and Hunt (1998). Bedford (1989) and Urbanski (1990), respectively, find the box-counting and Hausdorff dimensions of self-affine graphs. Self-affine curves are treated thoroughly in the book by Massopust (1995), which, along with Massopust (2010), discusses fractal interpolation.

The theory of autocorrelation functions is described in most books on time series analysis, for example, Sprott (2003). For fractal methods in signal processing, see Al-Akaidi (2004) and Abry, Gonçlaves and Williams (2009).

Exercises

11.1 Verify that if $f : [0, 1] \rightarrow \mathbb{R}$ has a continuous derivative, then $\text{graph } f$ is a regular 1-set; see Section 1.1.

11.2 Let $f, g : [0, 1] \rightarrow \mathbb{R}$ be continuous functions and define the sum function $f + g$ by $(f + g)(t) = f(t) + g(t)$. Suppose that f is a Lipschitz function. By setting up a Lipschitz mapping between $\text{graph}(f + g)$ and $\text{graph } g$, show that $\dim_H \text{graph}(f + g) = \dim_H \text{graph } g$, with a similar result for box dimensions.

11.3 Let $f, g : [0, 1] \rightarrow \mathbb{R}$ be continuous functions such that the box dimension of their graphs exist. Use Proposition 11.1 to show that $\dim_B \text{graph}(f + g)$ equals the greater of $\dim_B \text{graph } f$ and $\dim_B \text{graph } g$, provided that these dimensions are unequal. Give an example to show that this proviso is necessary.

11.4 Show that any function satisfying the conditions of Corollary 11.2(b) with $1 < s \leq 2$ must be nowhere differentiable. Deduce that the Weierstrass function of Example 11.3 and the self-affine curves of Example 11.4 are nowhere differentiable.

11.5 For $\lambda > 1$ and $1 < s < 2$, let $f : [0, 1] \rightarrow \mathbb{R}$ be a Weierstrass function modified to include given ‘phases’ θ_k :

$$f(t) = \sum_{k=1}^{\infty} \lambda^{(s-2)k} \sin(\lambda^k t + \theta_k).$$

Show that $\dim_B \text{graph } f = s$, provided that λ is large enough.

11.6 Let $g : \mathbb{R} \rightarrow \mathbb{R}$ be the ‘zig-zag’ function of period 4 given by

$$g(4k+t) = \begin{cases} t & (0 \leq t < 1) \\ 2-t & (1 \leq t < 3) \\ t-4 & (3 \leq t < 4) \end{cases}$$

where k is an integer and $0 \leq t < 4$. Let $1 < s < 2$ and $\lambda > 1$ and define $f : \mathbb{R} \rightarrow \mathbb{R}$ by

$$f(t) = \sum_{k=1}^{\infty} \lambda^{(s-2)k} g(\lambda^k t).$$

Show that $\dim_B \text{graph } f = s$, provided that λ is sufficiently large.

11.7 Suppose that the function $f : [0, 1] \rightarrow \mathbb{R}$ satisfies the Hölder condition (11.2). Let F be a subset of $[0, 1]$. Obtain an estimate for $\dim_H f(F)$ in terms of $\dim_H F$.

11.8 Let $f : [0, 1] \rightarrow \mathbb{R}$ be a function. Suppose that

$$\int_0^1 \int_0^1 [|f(t) - f(u)|^2 + |t - u|^2]^{-s/2} dt du < \infty$$

for some s with $1 < s < 2$. Show, using Theorem 4.13, that $\dim_H \text{graph } f \geq s$.

11.9 Let D be the unit square $[0, 1] \times [0, 1]$ and let $f : D \rightarrow \mathbb{R}$ be a continuous function such that

$$|f(x) - f(y)| \leq c|x - y|^{3-s} \quad (x, y \in D).$$

Show that the surface $\{(x, f(x)) : x \in D\}$ has box dimension at most s . Similarly, find a surface analogue to part (b) of Corollary 11.2.

11.10 Consider the affine maps

$$S_1(t, x) = \left(\frac{1}{2}t, \frac{1}{4}t + \frac{5}{6}x\right), \quad S_2(t, x) = \left(\frac{1}{2}t + \frac{1}{2}, -\frac{1}{4}t + \frac{5}{6}x + \frac{1}{4}\right).$$

Show that the attractor of $\{S_1, S_2\}$ is the graph of a self-affine function on $[0, 1]$. Sketch the first three stages in the construction of the graph and find its box dimension.

11.11 Answer the same question as [11.10](#) with the three affine maps

$$S_1(t, x) = \left(\frac{1}{3}t, \frac{1}{3}t + \frac{1}{2}x\right), \quad S_2(t, x) = \left(\frac{1}{3}t + \frac{1}{3}, -\frac{2}{3}t + \frac{1}{2}x + \frac{1}{3}\right),$$

$$S_3(t, x) = \left(\frac{1}{3}t + \frac{2}{3}, \frac{1}{3}t + \frac{1}{2}x - \frac{1}{3}\right).$$

11.12 Estimate $C(0) - C(h)$, where $C(h)$ is the autocorrelation function of the Weierstrass function ([11.4](#)).

11.13 Investigate the graphs of Weierstrass-type functions ([11.7](#)) using a computer. Examine the effect of varying s and λ and experiment with various functions g .

11.14 Write a computer program to draw self-affine curves given by ([11.8](#)). Investigate the effect of varying the values of the r_i .

Chapter 12

Examples from pure mathematics

Fractal constructions have provided counterexamples, and, sometimes, solutions to a variety of problems where more regular constructions have failed. In this chapter, we look at several simple but elegant instances from differing areas of pure mathematics.

12.1 Duality and the Kakeya problem

The method of duality converts sets of points in the plane to sets of lines and may be used to create new fractals from old. The techniques can be applied to construct sets with particular properties, for example, to construct a plane set of zero area that contains a line running in every direction.

For each point (a, b) of \mathbb{R}^2 , let $L(a, b)$ denote the set of points on the line $y = a + bx$; see [Figure 12.1](#). If F is any subset of \mathbb{R}^2 , we define the *line set* $L(F)$ to be the union of the lines corresponding to the points of F , that is, $L(F) = \bigcup\{L(a, b) : (a, b) \in F\}$. Writing L_c for the vertical line $x = c$, we have

$$L(a, b) \cap L_c = (c, a + bc) = (c, (a, b) \cdot (1, c)),$$

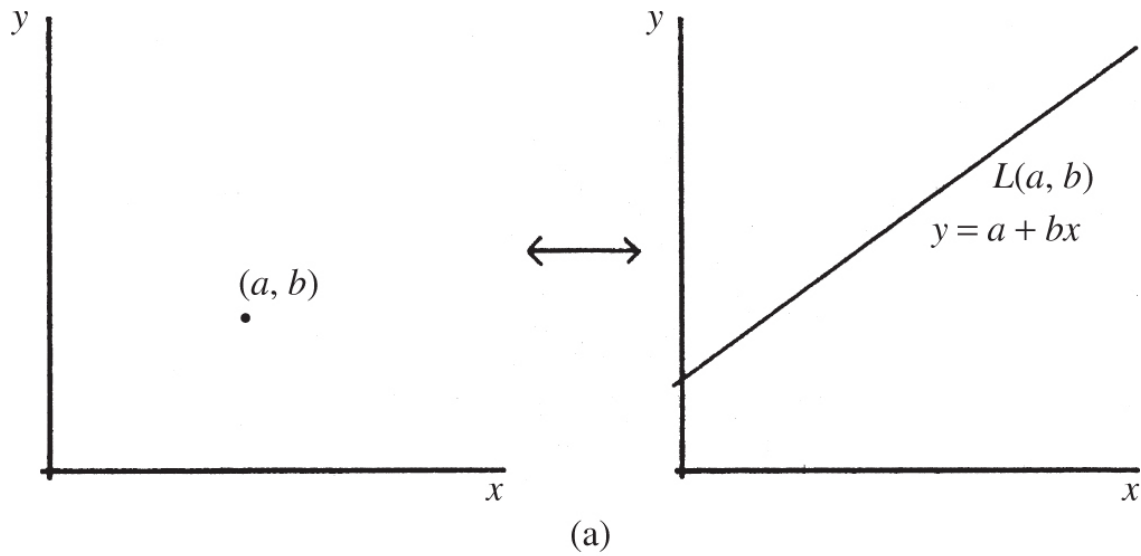
where ‘ \cdot ’ is the usual scalar product in \mathbb{R}^2 ; thus for a subset F of \mathbb{R}^2

$$L(F) \cap L_c = \{(c, (a, b) \cdot (1, c)) : (a, b) \in F\}.$$

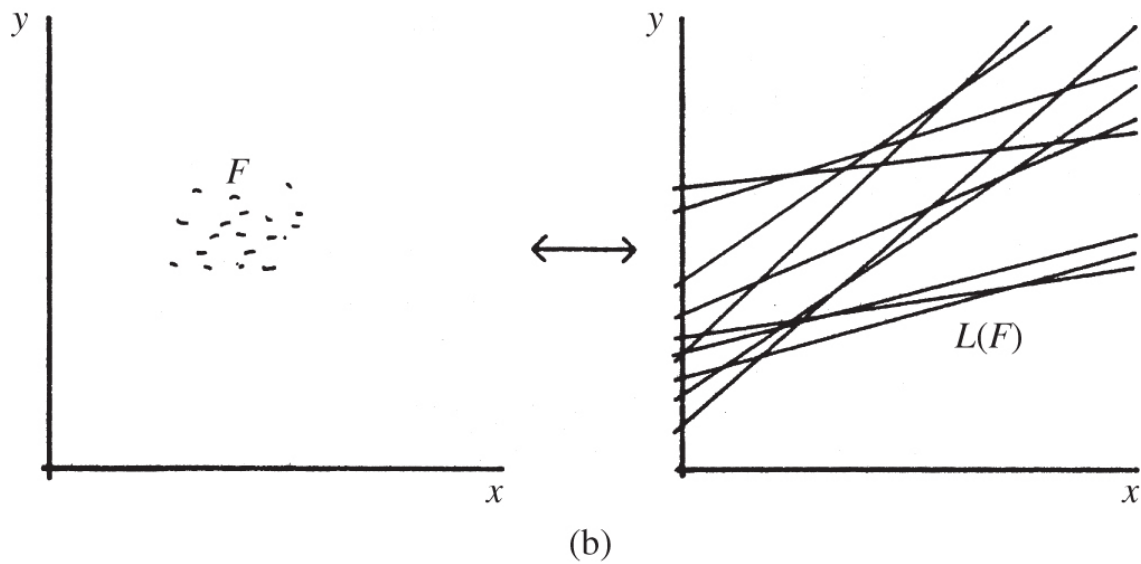
Taking a scalar product with the vector $(1, c)$ may be interpreted geometrically as projecting onto the line in the direction of $(1, c)$ and stretching by a factor $(1 + c^2)^{1/2}$. Thus, the set $L(F) \cap L_c$ is a similar copy of $\text{proj}_\theta F$ scaled by $(1 + c^2)^{1/2}$, where proj_θ denotes orthogonal projection onto the line through the origin at angle θ to the x -axis, where $c = \tan \theta$. In particular,

$$\dim_{\mathrm{H}}(L(F)\cap L_c)=\dim_{\mathrm{H}}(\mathrm{proj}_{\theta}F),$$

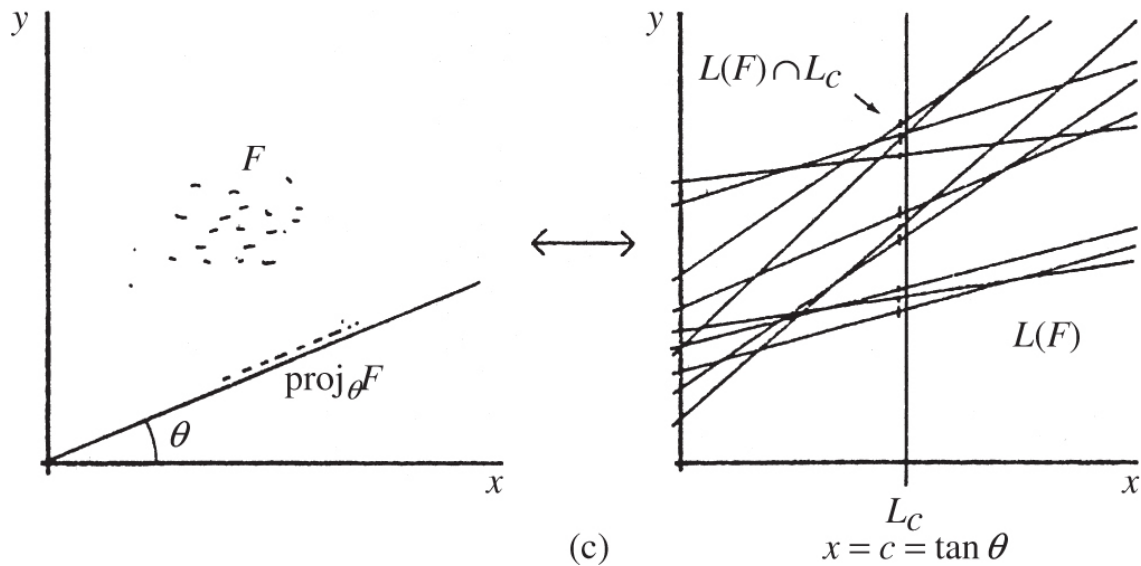
12.1



(a)



(b)



(c)

Figure 12.1 The duality principle: (a) the point (a, b) corresponds to the line $y = a + bx$; (b) the set F corresponds to the line set $L(F)$; (c) the projection $\text{proj}_\theta F$ is geometrically similar to $L(F) \cap L_c$, where $c = \tan \theta$.

and

$$\mathcal{L}(L(F) \cap L_c) = 0 \quad \text{if and only if} \quad \mathcal{L}(\text{proj}_\theta F) = 0, \quad \underline{\text{12.2}}$$

where \mathcal{L} denotes 1-dimensional Lebesgue measure, that is, length. In this way, duality relates the projections of F (for which we have the theory of Chapter 6) to the intersections of the line set $L(F)$ with vertical lines.

Projection onto the y -axis also has an interpretation. The gradient of the line $L(a, b)$ is just $b = \text{proj}_{\pi/2}(a, b)$, so, for any F , the set of gradients of the lines in the line set $L(F)$ is given by $\text{proj}_{\pi/2}F$.

If F is a fractal, its line set $L(F)$ often has a fractal structure, albeit a highly fibrous one. (In fact, $L(F)$ need not be a Borel set if F is Borel, though it will be if F is compact. We ignore the minor technical difficulties that this introduces.) We have the following dimensional relationship.

Proposition 12.1

Let $L(F)$ be the line set of a Borel set $F \subset \mathbb{R}^2$. Then

- a. $\dim_H L(F) \geq \min\{2, 1 + \dim_H F\}$, and
- b. if F is a 1-set then $\text{area}(L(F)) = 0$ if and only if F is irregular.

Proof

- a. By the Projection theorem 6.1, $\dim_H(\text{proj}_\theta F) = \min\{1, \dim_H F\}$ for almost all $\theta \in [0, \pi]$, so from (12.1) $\dim_H(L(F) \cap L_c) = \min\{1, \dim_H F\}$ for almost all $-\infty < c < \infty$. Part (a) now follows from Corollary 7.10.
- b. Let F be a 1-set. Corollary 6.5 tells us that if F is irregular, then $\mathcal{L}(\text{proj}_\theta F) = 0$ for almost all θ , otherwise $\mathcal{L}(\text{proj}_\theta F) > 0$ for almost all θ . Using (12.2), we get the dual statement that if F is irregular, then $\mathcal{L}(L(F) \cap L_c) = 0$ for almost all c , otherwise $\mathcal{L}(L(F) \cap L_c) > 0$ for almost all c . Since $\text{area}(L(F)) = \int_{-\infty}^{\infty} \mathcal{L}(L(F) \cap L_c) dc$, part (b) follows.

In 1917, Kakeya posed the problem of finding the plane set of least area inside which a unit line segment could be reversed, that is, manoeuvred continuously without leaving the set to reach its original position but rotated through 180° . Essentially, this problem reduces to that of finding the smallest region that contains a unit line segment in every direction; certainly any set in which a segment can be reversed must have this property. By 1928, Besicovitch had found a surprising construction of a set of arbitrarily small area inside which a unit segment could be reversed. Only many years later did he realise that the method of duality gave a short and elegant solution to the problem.

Proposition 12.2

There is a plane set of zero area, which contains a line in every direction. Any Borel set with this property must have Hausdorff dimension 2.

Proof

Let F be any irregular 1-set such that the projection of F onto the y -axis, $\text{proj}_{\pi/2}F$, contains the interval $[0, 1]$. (The set of [Figure 0.4](#), see Examples 2.6 and 6.7, certainly meets this requirement.) Since F is irregular, $L(F)$ has zero area, by Proposition 12.1(b). However, since $[0, 1] \subset \text{proj}_{\pi/2}F$, the set $L(F)$ contains lines that cut the x -axis at all angles between 0 and $\pi/4$. Taking $L(F)$, together with copies rotated through $\pi/4, \pi/2$ and $3\pi/4$, gives a set of area 0 containing a line in every direction.

For the second part, suppose that E contains a line in every direction. If

$$F = \{(a, b) : L(a, b) \subset E\}$$

then $\text{proj}_{\pi/2}F$ is the entire y -axis. Projection does not increase the dimension (see (6.1)), so $\dim_H F \geq 1$. By Proposition 12.1(a), $\dim_H L(F) = 2$; since $L(F) \subset E$, it follows that $\dim_H E = 2$.

A set in \mathbb{R}^n that contains a line segment in every direction is called a *Besicovitch set*. Proposition 12.2 shows that Besicovitch sets exist in \mathbb{R}^2 , and taking a product with \mathbb{R}^{n-2} gives a Besicovitch set in \mathbb{R}^n . Along-standing conjecture is that every Besicovitch set in \mathbb{R}^n has dimension n ; we have shown this if $n = 2$.

Sets of this type have important applications in functional analysis. For a simple example, let $g : \mathbb{R}^2 \rightarrow \mathbb{R}$ and write $G(\theta, t)$ for the integral of g along the line making angle θ with the x -axis and perpendicular distance t from the origin. Let F be a set of zero area containing a line in every direction, and let $g(x, y) = 1$ if (x, y) is a point of F and $g(x, y) = 0$ otherwise. It is clear that $G(\theta, t)$ is not continuous in t for any fixed value of θ . This example becomes significant when contrasted with the 3-dimensional situation. If $g : D \rightarrow \mathbb{R}$ is a bounded function on a bounded domain D in \mathbb{R}^3 , and $G(\theta, t)$ is the

integral of g over the plane perpendicular to the unit vector θ and perpendicular distance t from the origin, it may be shown that $G(\theta, t)$ must be continuous in t for almost all unit vectors θ .

The Besicovitch construction may be thought of as a packing of lines in all directions into a set of area zero. Similar problems may be considered for packings of other collections of curves. For example, there are sets of zero area that contain the circumference of a circle of every radius; see Exercises 12.1 and 12.2. However, every set that contains some circle circumference centred at each point in the plane necessarily has positive area.

12.2 Vitushkin's conjecture

A long-standing conjecture of Vitushkin in complex potential theory was disproved using a fractal construction. For geometrical purposes, we identify the complex plane \mathbb{C} with the Euclidean plane \mathbb{R}^2 .

Let F be a compact subset of \mathbb{C} . We say that F is a *removable* set if, given any bounded open domain V containing F and any bounded analytic (i.e. differentiable in the complex sense) function f on the complement $V \setminus F$, then f has an analytic extension to the whole of V . Thus, the functions that are bounded and analytic on V are essentially the same as those that are bounded and analytic on $V \setminus F$; removing F makes no difference.

The problem of providing a geometrical characterisation of removable sets dates back many years. The removability, or otherwise, of F has now been established in the following cases:

Removable	Not removable
$\dim_H F < 1$	$\dim_H F > 1$
$0 < \mathcal{H}^1(F) < \infty$ and F irregular	$0 < \mathcal{H}^1(F) < \infty$ and F not irregular

This table should remind the reader of the projection theorems of Chapter 6. According to Theorem 6.1 and Corollary 6.5, if $\dim_H F < 1$,

then the projection $\text{proj}_\theta F$ has length 0 for almost all θ , but if $\dim_H F > 1$ or if F is a 1-set that is not irregular, $\text{proj}_\theta F$ has positive length for almost all θ . This correspondence between removability and almost all projections having length 0, together with a considerable amount of further evidence makes Vitushkin's conjecture seem very natural: F is removable if and only if $\text{length}(\text{proj}_\theta F) = 0$ for almost all $\theta \in [0, \pi]$.

A fractal construction shows that Vitushkin's conjecture cannot be true. Let V be an open domain in \mathbb{C} and let $\phi : V \rightarrow \phi(V)$ be a conformal mapping (i.e. an analytic bijection) on V that is not linear, so that straight lines are typically mapped onto (non-straight) curves; V as the unit disc and $\phi(z) = (z + 2)^2$ would certainly be suitable. It is possible to construct a compact subset F of V such that $\text{proj}_\theta F$ has zero length for almost all θ , but $\text{proj}_\theta \phi(F)$ has positive length for almost all θ (see [Figure 12.2](#)). This may be achieved using a version of the ‘iterated Venetian blind’ construction, outlined in the proof of Theorem 6.9—it may be shown that the ‘slats’ can be arranged so that they generally miss straight lines in V , but tend to intersect the inverse images under ϕ of straight lines in $\phi(V)$. It follows that the property ‘ $\text{proj}_\theta F$ has zero length for almost all θ ’ is not invariant under conformal transformations since it can hold for F but not $\phi(F)$. However, removability is conformally invariant since the function $f(z)$ is analytic on $\phi(V)$ (respectively on $\phi(V \setminus F)$) if and only if $f(\phi(z))$ is analytic on V (respectively on $V \setminus F$). Therefore, the property of having almost all projections of zero length cannot be equivalent to removability.

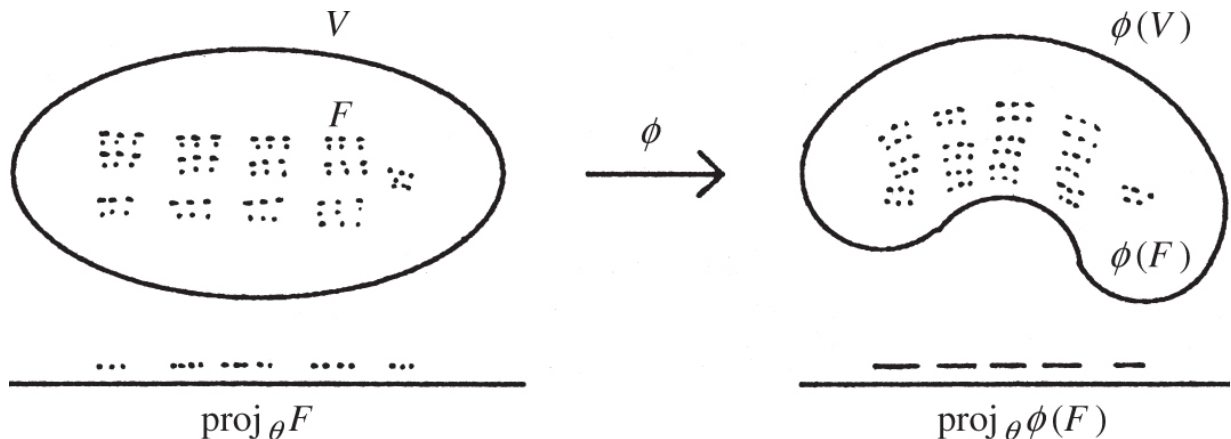


Figure 12.2 ϕ is an analytic mapping such that $\text{proj}_\theta F$ has zero length for almost all θ but $\text{proj}_\theta \phi(F)$ has positive length for almost all θ .

One of the curious features of this particular argument is that it leaves us none the wiser as to whether sets with almost all projections of zero length must be removable or vice versa. All we can deduce is that both cannot be true.

Subsequently, a non-removable set with almost all projections of zero length was obtained using an iterated construction.

12.3 Convex functions

This section illustrates a frequent use of dimension across mathematics: to bound the size of the set of points where some form of ‘bad behaviour’ can occur. A continuous function $f : \mathbb{R}^2 \rightarrow \mathbb{R}$ is *convex* if

$$f(\lambda x + (1 - \lambda)y) \leq f(x) + (1 - \lambda)f(y)$$

for all $x, y \in \mathbb{R}^2$ and $0 \leq \lambda \leq 1$. Geometrically, if $S = \{(x, f(x)) : x \in \mathbb{R}^2\}$ is the surface in \mathbb{R}^3 representing the graph of f , then f is convex if the line segment joining any two points of S lies in or above S .

A convex function f need not be particularly smooth—there may be points where f is not differentiable. However, convexity means that the set of such ‘singular’ points cannot be too big in the sense of

dimension. Note that if f is not differentiable at x , then the surface S supports more than one tangent plane at $(x, f(x))$. Also, notice that if P_1 and P_2 are distinct tangent planes at $(x, f(x))$, then there is a continuum of tangent planes through this point, namely, those planes ‘between P_1 and P_2 ’ that contain the line $P_1 \cap P_2$.

Theorem 12.3

Let $f : \mathbb{R}^2 \rightarrow \mathbb{R}$ be a convex function. Then, the set of points at which f is not differentiable is contained in a countable union of rectifiable curves, so, in particular, has Hausdorff dimension at most 1.

Proof

Without the loss of generality, we may assume that the minimum value of f is strictly positive. Let S be the surface given by the graph of f and let $g : \mathbb{R}^2 \rightarrow S$ be the ‘nearest point’ mapping, so that if $x \in \mathbb{R}^2$, then $g(x)$ is that point of S for which the distance $|g(x) - x|$ is least; see [Figure 12.3](#). Convexity of f guarantees that this point is unique. If $x, y \in \mathbb{R}^2$, then the angles of the (possibly skew) quadrilateral $x, g(x), g(y), y$ at $g(x)$ and $g(y)$ must both be at least $\pi/2$; otherwise the segment $(g(x), g(y))$ will contain a point on or above S that is nearer to x or y . It follows that g is distance decreasing, that is

$$|g(x) - g(y)| \leq |x - y| \quad (x, y \in \mathbb{R}^2).$$

[12.3](#)

If f fails to be differentiable at x , then S supports more than one tangent plane at $(x, f(x))$. Thus, $g^{-1}(x, f(x))$, the subset of the coordinate plane \mathbb{R}^2 mapped to this point by g is the intersection of \mathbb{R}^2 with the normals to the tangent planes to S at $(x, f(x))$ and so contains a straight line segment. Let $\{L_1, L_2, \dots\}$ be the countable collection of line segments in \mathbb{R}^2 with end points having rational coordinates. If f is not differentiable at x , then $g^{-1}(x, f(x))$ contains a segment which must cut at least one of the L_i . Thus, if $F = \{(x, f(x)) : f \text{ is not differentiable at } x\}$, then $\bigcup_{i=1}^{\infty} g(L_i) \supset F$. Using [\(12.3\)](#), it follows that $g(L_i)$ is either a point or a rectifiable curve with $\mathcal{H}^1(g(L_i)) \leq \text{length}(L_i) < \infty$; see [\(3.7\)](#). Then, $\bigcup_{i=1}^{\infty} g(L_i)$ is a countable union of rectifiable curves containing F , which, in particular, has Hausdorff dimension at most 1.

The set of points x at which f is non-differentiable is just the orthogonal projection of F onto the coordinate plane \mathbb{R}^2 , so has Hausdorff dimension at most 1 since orthogonal projection does not increase dimension; see [Section 3.2](#).

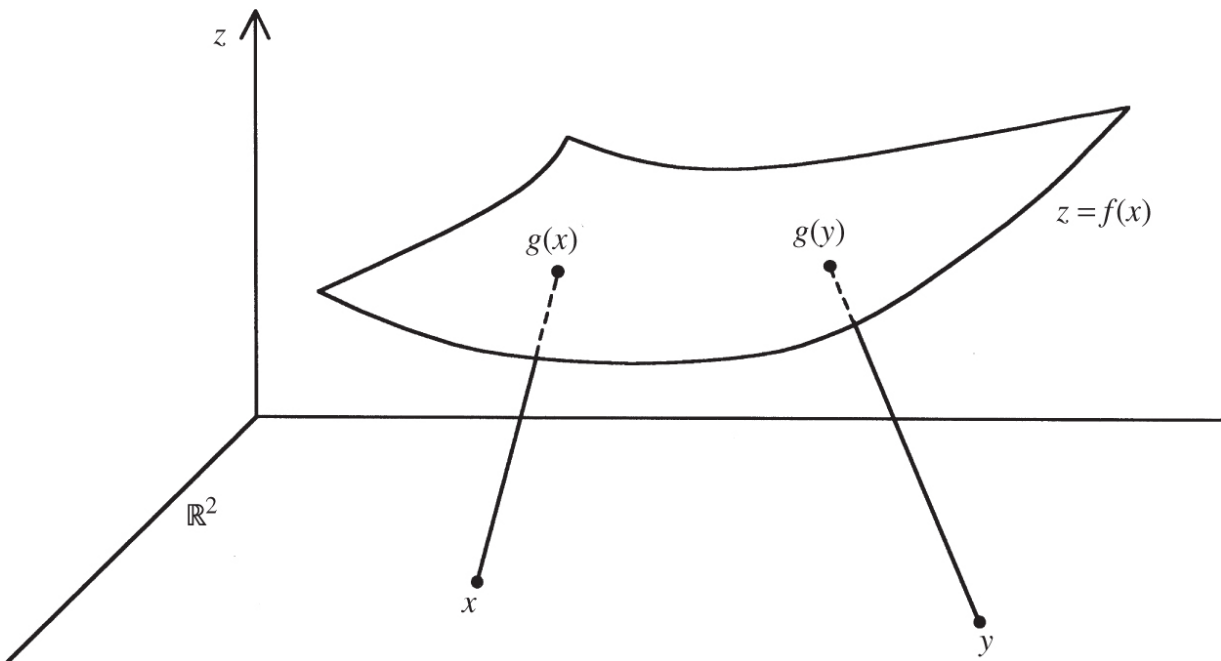


Figure 12.3 The ‘nearest point mapping’ g from \mathbb{R}^2 to the surface $z = f(x)$ of a convex function is distance decreasing.

Hausdorff dimension has been used in various other ways to quantify the irregularity of surfaces. For example, a convex surface may contain line segments; however, the set of directions of such line segments may be shown to have dimension at most 1.

12.4 Fractal groups and rings

A subset F of \mathbb{R} is a *subgroup* of the real numbers under the operation of addition if

- i. $0 \in F$,
- ii. $x + y \in F$ whenever $x \in F$ and $y \in F$, and
- iii. $-x \in F$ whenever $x \in F$.

The set F is a *subring* of \mathbb{R} under addition and multiplication if, also,

- iv. $xy \in F$ whenever $x \in F$ and $y \in F$.

There are many simple examples of such structures: the integers, the rationals and the set of numbers $\{r + s\sqrt{2} : r, s \in \mathbb{Z}\}$ are all subrings (and therefore subgroups) of \mathbb{R} . These examples are countable sets and therefore have Hausdorff dimension 0. Do there exist subgroups and subrings of \mathbb{R} of Hausdorff dimension s if $0 < s < 1$?

It is relatively easy to modify the earlier Example 4.7 to obtain a subgroup of any given dimension.

Example 12.4

Fix $0 < s < 1$. Let n_0, n_1, n_2, \dots be a rapidly increasing sequence of integers, say with $n_{k+1} \geq \max\{n_k^s, 4n_k^{1/s}\}$ for each k . For $r = 1, 2, \dots$, let

$$F_r = \{x \in \mathbb{R} : |x - p/n_k| \leq r n_k^{-1/s} \text{ for some integer } p, \text{ for all } k\}$$

and let $F = \bigcup_{r=1}^{\infty} F_r$. Then, $\dim_H F = s$, and F is a subgroup of \mathbb{R} under addition.

Calculation

F_r is essentially the set of Example 4.7, so $\dim_H F_r = s$ for all r (it is easy to see that the value of r does not affect the dimension). Taking a countable union, $\dim_H F = s$.

Clearly $0 \in F_1 \subset F$. If $x, y \in F$ then $x, y \in F_r$ for some r , noting that $F_{r'} \subset F_r$ if $r' \leq r$. Thus, for each k , there are integers p, q such that

$$|x - p/n_k| \leq rn_k^{-1/s} \quad |y - q/n_k| \leq rn_k^{-1/s}.$$

Adding,

$$|x + y - (p + q)/n_k| \leq 2rn_k^{-1/s},$$

so $x + y \in F_{2r} \subset F$. Clearly, if $x \in F_r$, then $-x \in F_r$, so F satisfies conditions (i)–(iii) above.

Subrings are rather harder to analyse. One geometrical approach depends on estimating the dimension of the set of distances realised by a plane set. If E is a subset of \mathbb{R}^2 , we define the *distance set* of E by

$$D(E) = \{|x - y| : x, y \in E\} \subset \mathbb{R}.$$

There is a great deal of interest in obtaining lower bounds for the Hausdorff dimension of $D(E)$ in terms of that of E . We give one known estimate (12.4), but it is unlikely that it is the best inequality possible.

Theorem 12.5

Let $E \subset \mathbb{R}^2$ be a Borel set. Then,

$$\dim_H D(E) \geq \min\{1, \dim_H E - \frac{1}{2}\}.$$

[12.4](#)

Note on proof

The potential theoretic proof of this theorem is a little complicated. Fourier transforms and the convolution theorem are used to examine the circles with centres in E that intersect E .

Assuming this theorem, it is not difficult to obtain a partial solution to the subrings problem.

Theorem 12.6

Let F be a subring of \mathbb{R} under addition and multiplication. If F is a Borel set, then either $\dim_H F = 0$ or $F = \mathbb{R}$.

Partial Proof

We use a geometrical method to show there are no subrings of dimension between $\frac{1}{2}$ and 1. Using (x, y) coordinates in \mathbb{R}^2 , if

$(x_1, y_1), (x_2, y_2) \in F \times F \subset \mathbb{R}^2$, then

$|x_1 - x_2|^2 = (x_1 - x_2)^2 + (y_1 - y_2)^2 \in F$, since F is a subring.

Thus, if $D^2(F \times F)$ denotes the set of squares of distances between points of $F \times F$, we have $D^2(F \times F) \subset F$. Since the mapping $t \rightarrow t^2$ preserves Hausdorff dimension (see Exercise 3.6),

$$\begin{aligned}\dim_H F &\geq \dim_H D^2(F \times F) = \dim_H D(F \times F) \\ &\geq \min \left\{ 1, \dim_H(F \times F) - \frac{1}{2} \right\} \\ &\geq \min \left\{ 1, 2\dim_H F - \frac{1}{2} \right\}\end{aligned}$$

using Theorem 12.5 and Product formula 7.2. This inequality is satisfied if and only if $\dim_H F = 1$ or $\dim_H F \leq \frac{1}{2}$.

We mention briefly another type of fractal group, which has major significance in infinite group theory. Very briefly, let T be the rooted infinite binary tree, that is, the graph with vertices given by all finite sequences $\{(i_1, \dots, i_k) : i_j = 1, 2 \text{ and } k \geq 0\}$ with edges joining each vertex (i_1, \dots, i_k) to its parent (i_1, \dots, i_{k-1}) and its children $(i_1, \dots, i_k, 1)$ and $(i_1, \dots, i_k, 2)$. The root is the empty sequence \emptyset . Let $\text{Aut}(T)$ be the group of all automorphisms of T , that is, the group of bijections between the vertices of T that map edges onto edges and leave the root fixed, with composition of automorphisms as the group operation. There is a natural way of defining a metric or distance between pairs of automorphisms, which permits Hausdorff dimension to be defined on subsets of $\text{Aut}(T)$ such that $\dim_H \text{Aut}(T) = 1$. It is possible to define subgroups of $\text{Aut}(T)$ in a ‘self-similar’ manner, such as the Grigorchuk group G which was the first infinite group to exhibit ‘intermediate growth’. Using a combination of group

theoretic and covering arguments, it may be shown that $\dim_H G = \frac{5}{8}$. Many other self-similar groups have since been investigated.

12.5 Notes and references

More detailed accounts of the Kakeya problem and its variants are given by Besicovitch (1963); Cunningham (1974) and Falconer (1985a); the dual approach was introduced by Besicovitch (1964). For more recent surveys, see Wolff (1999) and Katz and Tao (2000). Lately attention has turned to Kakeya problems over finite fields, see, for example, Ellenberg, Oberlin and Tao (2010). The book by Stein (1993) includes applications of Kakeya sets to functional and harmonic analysis.

The book by Dudziak (2010) provides a comprehensive account of Vitushkin's conjecture. The counter-example described here is due to Mattila (1986), and the non-removable set with projections of lengths zero was constructed by Jones and Murai (1988). David (1999) showed that irregular 1-sets are removable.

For general books on convex geometry, see Webster (1994) and Gruber (2007). The result given here is due to Anderson and Klee (1952). For other results involving Hausdorff dimension and convexity, see Dalla and Larman (1980) and the survey of Schneider (1993).

Examples of groups of fractional dimension were given by Erdös and Volkmann (1966) who raised the question of dimensions of rings. Falconer (1985c) used Fourier transform methods to show that Borel rings could not have dimension between $\frac{1}{2}$ and 1; see also Mattila (1999). The complete proof of Theorem 12.6 is due to Edgar and Miller (2003). There has been considerable interest recently in variants of Theorem 12.5, in particular, whether the Lebesgue measure of the distance set $\mathcal{L}(D(E)) > 0$ if $E \subset \mathbb{R}^2$ with $\dim_H E > 1$; see Falconer (1985c) and Erdoan (2006). For an account of self-similar fractal groups, see Bartholdi, Grigorchuk and Nekrashevych (2002).

Exercises

12.1 Construct a plane set of zero area that contains a line at every perpendicular distance from the origin between 0 and 1. (Hint: consider the image of the set F in Proposition 12.2 under the transformation $(a, b) \rightarrow (a(1 + b^2)^{1/2}, b)$.)

12.2 By transforming the set obtained in the previous exercise by the mapping given in polar coordinates by $(r, \theta) \rightarrow (1/r, \theta)$, show that there exists a plane set of zero area that contains a circle of radius r for all $r > 0$.

12.3 Show that there is a subset of the plane of area 0 that contains a different straight line through every point on the x -axis.

12.4 Let A be a (Borel) subset of $[0, \pi]$. Let F be a subset of the plane that contains a line running in direction θ for every $\theta \in A$. Show that $\dim_H F \geq 1 + \dim_H A$.

12.5 Dualise Theorem 6.9 to show that any Borel set of finite area a may be completely covered by a collection of straight lines of total area a .

12.6 Show that if a compact subset F of \mathbb{C} supports a mass distribution μ such that $f(z) = \int_F (z - w)^{-1} d\mu(w)$ is bounded, then F is not removable in the sense of Section 12.2. Show that this is the case if $1 < \dim_H F \leq 2$. (Hint: see the proof of Theorem 4.13(b).)

12.7 Show that every finite set is removable. Show that the unit circle is not removable.

12.8 Let $f : \mathbb{R} \rightarrow \mathbb{R}$ be a convex function. Show that the set of points at which f is not differentiable is finite or countable.

12.9 Find a convex $f : \mathbb{R}^2 \rightarrow \mathbb{R}$ such that the set of points of non-differentiability has Hausdorff dimension 1. Find a (non-convex) $f : \mathbb{R}^2 \rightarrow \mathbb{R}$ such that the set of points of non-differentiability has Hausdorff dimension 2.

12.10 Show that any subgroup of \mathbb{R} under addition has box dimension 0 or 1.

12.11 Show that, for all $0 < s < 2$, there is a subgroup of \mathbb{R}^2 under vector addition with Hausdorff dimension s . (Hint: consider a product of subgroups of \mathbb{R} .)

Chapter 13

Dynamical systems

Dynamical systems have a central place in mathematics and science. The theory continues to develop, and provides tools for the whole spectrum of mathematics. In recent years, new insights into the behaviour of systems have come from numerical simulations on powerful computers. Most importantly, dynamical systems have a vast range of applications across the whole spectrum of science, including in biology, medicine, geography, economics and social sciences as well as in the more traditional disciplines of physics and engineering. We make no attempt to provide a general account, which would require excursions into ergodic theory, bifurcation theory and many other areas, but we illustrate various ways in which fractals can occur in dynamical systems.

Let D be a subset of \mathbb{R}^n (often \mathbb{R}^n itself), and let $f : D \rightarrow D$ be a continuous mapping. As usual, f^k denotes the k th iterate of f , so that $f^0(x) = x$, $f^1(x) = f(x)$, $f^2(x) = f(f(x))$, and so on. Clearly, if x is a point of D , then $f^k(x)$ is in D for all k . Typically, $x, f(x), f^2(x), \dots$ are the values of some quantity at times $0, 1, 2, \dots$. Thus, the value at time $k+1$ is given in terms of the value at time k by the function f . For example, $f^k(x)$ might represent the size after k years of a biological population or the value of an investment subject to certain interest and tax conditions.

An iterative scheme $\{f^k\}$ is called a *discrete dynamical system*. We are interested in the behaviour of the sequence of *iterates*, or *orbits*, $\{f^k(x)\}_{k=1}^\infty$ for various initial points $x \in D$, and are often especially interested in what happens to the iterates when k is large.

Sometimes $f^k(x)$ may converge to a *fixed point* w , that is, a point of D with $f(w) = w$. For example, if $f(x) = \cos x$, the sequence $f^k(x)$ converges to the fixed point $0.739\dots$ as $k \rightarrow \infty$ for any initial x : try repeatedly pressing the cosine button on a calculator and see! More

generally, $f^k(x)$ may converge to an orbit of *period-p points* $\{w, f(w), \dots, f^{p-1}(w)\}$, where p is the least positive integer with $f^p(w) = w$, in the sense that $|f^k(x) - f^k(w)| \rightarrow 0$ as $k \rightarrow \infty$. Sometimes, however, $f^k(x)$ may appear to move about almost at random, but always remaining close to a certain set, which may be a fractal. In this chapter, we examine several ways in which such ‘fractal attractors’ or ‘strange attractors’ can occur.

Roughly speaking, an attractor is a set to which all nearby orbits converge. However, as frequently happens in dynamical systems theory, the precise definition varies between authors. We shall call a subset F of D an *attractor* for f if F is a closed set that is *invariant* under f (i.e. with $f(F) = F$) such that the distance from $f^k(x)$ to F converges to zero as k tends to infinity for all x in an open set V containing F . The largest such open set V is called the *basin of attraction* of F . It is usual to require that F is minimal in the sense that it has no proper subset satisfying these conditions. Similarly, a closed invariant set F from which all nearby points not in F are iterated away is called a *repeller*; this is roughly equivalent to F being an ‘attractor’ for the (perhaps multivalued) inverse f^{-1} . An attractor or repeller may just be a single point or a period- p orbit. However, even relatively simple maps f can have fractal attractors.

Since $f(D) \subset D$, repeatedly applying f gives that $f^k(D) \subset f^{k-1}(D) \subset \dots \subset f(D) \subset D$, so $\bigcap_{i=1}^k f^i(D) = f^k(D)$. Thus, the set $F = \bigcap_{k=1}^{\infty} f^k(D)$ is invariant under f . Since $f^k(x) \in \bigcap_{i=1}^k f^i(D)$ for all $x \in D$, the iterates $f^k(x)$ approach F as $k \rightarrow \infty$, and F is frequently an attractor of f .

If F is a fractal attractor or repeller of f , then if $x \in F$, the iterates $f^k(x)$ remain in F for all k and often exhibit ‘chaotic’ or apparently random behaviour around F . There are various definitions of chaos; f would certainly be regarded as *chaotic* on F if the following are all true:

- i. For some $x \in F$, the orbit $\{f^k(x)\}$ is dense in F .

- ii. The periodic points of f in F (points for which $f^p(x) = x$ for some positive integer p) are dense in F .
- iii. f has *sensitive dependence on initial conditions*; that is, there is a number $\delta > 0$ such that for every x in F , there are points y in F arbitrarily close to x such that $|f^k(x) - f^k(y)| \geq \delta$ for some k . Thus, points that are initially close to each other do not remain close under iterates of f .

Condition (i) implies that F cannot be decomposed into smaller closed invariant sets, (ii) suggests a skeleton of regularity in the structure of F and (iii) reflects the unpredictability of iterates of points on F . In particular, (iii) implies that accurate long-term numerical approximation to orbits of f is impossible since a tiny numerical error will be magnified under iteration. Often conditions that give rise to fractal attractors also lead to chaotic behaviour.

Dynamical systems are naturally suited to computer investigation. Roughly speaking, attractors are the sets that are seen when orbits are plotted on a computer. For some initial point x , one plots perhaps 10 000 iterates $f^k(x)$, starting at $k = 101$, say, to ensure that they are indistinguishable from any attractor. If an attractor appears fractal, a ‘box-counting’ method can be used to estimate its dimension. However, computer pictures can be misleading, in that the distribution of $f^k(x)$ across an attractor can be very uneven, with certain parts of the attractor visited very rarely.

13.1 Repellers and iterated function systems

Under certain circumstances, a repeller in a dynamical system coincides with the attractor of a related iterated function system (IFS). This is best seen by an example. The mapping $f : \mathbb{R} \rightarrow \mathbb{R}$ given by

$$f(x) = \frac{3}{2}(1 - |2x - 1|)$$

is called the *tent map* because of the form of its graph; see [Figure 13.1](#). Clearly, f maps \mathbb{R} in a two-to-one manner onto $(-\infty, \frac{3}{2})$.

Defining an IFS $S_1, S_2 : [0, 1] \rightarrow [0, 1]$ by the contractions,

$$S_1(x) = \frac{1}{3}x, \quad S_2(x) = 1 - \frac{1}{3}x$$

we see that

$$f(S_1(x)) = f(S_2(x)) = x \quad (0 \leq x \leq 1).$$

Thus, S_1 and S_2 are the two branches of f^{-1} . Theorem 9.1 implies that there is a unique non-empty compact attractor $F \subset [0, 1]$ satisfying

$$F = S_1(F) \cup S_2(F), \tag{13.1}$$

which is given by $F = \bigcap_{k=0}^{\infty} S^k([0, 1])$ (writing $S(E) = S_1(E) \cup S_2(E)$ for any set E). Clearly the attractor F is the middle third Cantor set, with Hausdorff and box dimensions $\log 2 / \log 3$.

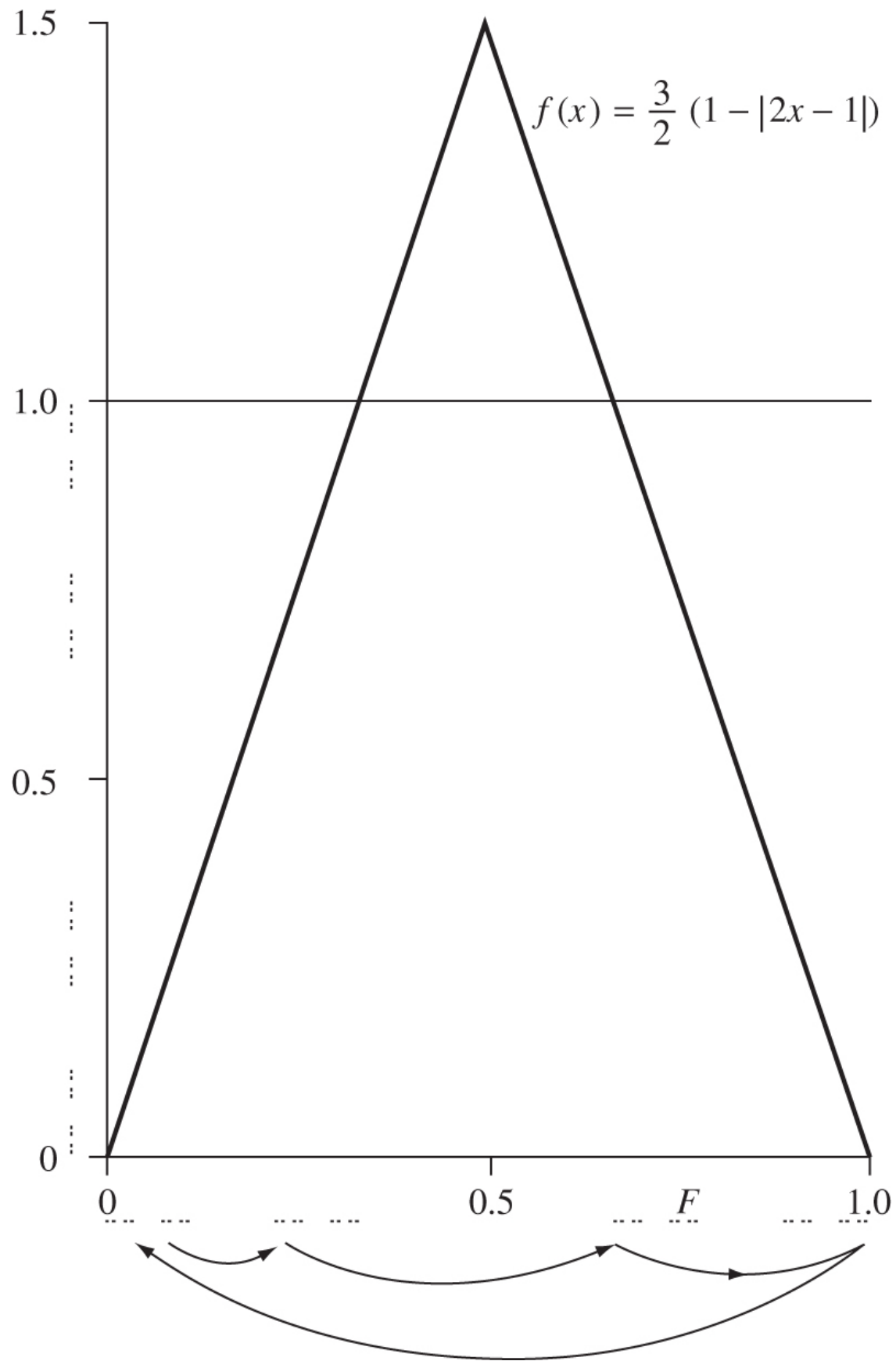


Figure 13.1 The tent map f . Notice that the middle third Cantor set F is mapped onto itself by f and is an invariant repeller. Notice, also, the chaotic nature of f on F : the iterates of a point are indicated by the arrows.

It follows from (13.1) that $f(F) = F$. To see that F is a repeller, observe that if $x < 0$, then $f(x) = 3x$, so $f^k(x) = 3^k x \rightarrow -\infty$ as $k \rightarrow \infty$. If $x > 1$, then $f(x) < 0$ and again $f^k(x) \rightarrow -\infty$. If $x \in [0, 1] \setminus F$, then for some k , we have $x \notin S^k[0, 1] = \cup\{S_{i_1} \circ \dots \circ S_{i_k}[0, 1] : i_j = 1, 2\}$, so $f^k(x) \notin [0, 1]$, and again $f^k(x) \rightarrow -\infty$ as $k \rightarrow \infty$. All points outside F are iterated to $-\infty$, so F is a repeller.

With the notation of Section 1.1, the chaotic nature of f on F is readily apparent. Denoting the points of F by $x_{i_1, i_2, \dots}$ with $i_j = 1, 2$, as in (9.8), $|x_{i_1, i_2, \dots} - x_{i'_1, i'_2, \dots}| \leq 3^{-k}$ if $i_1 = i'_1, \dots, i_k = i'_k$. Since

$x_{i_1, i_2, \dots} = S_{i_1}(x_{i_2, i_3, \dots})$, it follows that $f(x_{i_1, i_2, \dots}) = x_{i_2, i_3, \dots}$. Suppose that (i_1, i_2, \dots) is an infinite sequence with every finite sequence of 1s and 2s appearing as a consecutive block of terms; for example,

$$(1, 2, 1, 1, 1, 2, 2, 1, 2, 2, 1, 1, 1, 1, 1, 2, \dots),$$

where the spacing is just to indicate the form of the sequence. For each point $x_{i'_1, i'_2, \dots}$ in F and each integer q , we may find k such that $(i'_1, i'_2, \dots, i'_q) = (i_{k+1}, \dots, i_{k+q})$. Then, $|x_{i_{k+1}, i_{k+2}, \dots} - x_{i'_1, i'_2, \dots}| \leq 3^{-q}$, so the iterates $f^k(x_{i_1, i_2, \dots}) = x_{i_{k+1}, i_{k+2}, \dots}$ come arbitrarily close to each point of F for suitable large k , so that f has dense orbits in F . Similarly, since $x_{i_1, \dots, i_k, i_1, \dots, i_k, i_1, \dots}$ is a periodic point of period k , the periodic points of f are dense in F . The iterates have sensitive dependence on initial conditions since $f^k(x_{i_1, \dots, i_k, 1, \dots}) \in [0, \frac{1}{3}]$ but $f^k(x_{i_1, \dots, i_k, 2, \dots}) \in [\frac{2}{3}, 1]$. We conclude that F is a chaotic repeller for f . (The study of f by its effect on points of F represented by sequences (i_1, i_2, \dots) is known as *symbolic dynamics*.)

In exactly the same way, the attractors of general IFSs correspond to repellers of functions. If S_1, \dots, S_m is a set of bijective contractions on a domain D with attractor F such that $S_1(F), \dots, S_m(F)$ are disjoint, then F is a repeller for any mapping f such that $f(x) = S_i^{-1}(x)$

when x is near $S_i(F)$. Again, by examining the effect of f on the point $x_{i_1, i_2, \dots}$, it may be shown that f acts chaotically on F . Indeed, for many dynamical systems f , it is possible to decompose the domain D into parts (called a *Markov partition*) such that the branches of f^{-1} on each part look rather like an IFS. See Theorem 14.15 for an example in the complex plane.

13.2 The logistic map

The logistic map $f : \mathbb{R} \rightarrow \mathbb{R}$ is given by

$$f_\lambda(x) = \lambda x(1 - x), \quad \text{13.2}$$

where λ is a positive constant. This mapping was introduced to model the population development of certain species—if the (normalised) population is x at the end of a given year, it is assumed to be $f_\lambda(x)$ at the end of the following year. The logistic map has been studied intensively as an archetypal 1-dimensional dynamical system that undergoes bifurcations as the parameter λ increases. We content ourselves here with an analysis when λ is large, and a brief discussion when λ is small.

For $\lambda > 2 + \sqrt{5} = 4.236\dots$, we get a non-linear version of the tent map repeller of Section 13.1. Write $a = \frac{1}{2} - \sqrt{\frac{1}{4} - 1/\lambda}$ and $1 - a = \frac{1}{2} + \sqrt{\frac{1}{4} - 1/\lambda}$ for the roots of $f_\lambda(x) = 1$. Each of the intervals $[0, a]$ and $[1 - a, 1]$ is mapped bijectively onto $[0, 1]$ by f_λ . The mappings $S_1 : [0, 1] \rightarrow [0, a]$ and $S_2 : [0, 1] \rightarrow [1 - a, 1]$ given by

$$S_1(x) = \frac{1}{2} - \sqrt{\frac{1}{4} - x/\lambda} \quad S_2(x) = \frac{1}{2} + \sqrt{\frac{1}{4} - x/\lambda}$$

are the values of the inverse f_λ^{-1} in $[0, a]$ and $[1 - a, 1]$, with $f_\lambda(S_1(x)) = f_\lambda(S_2(x)) = x$ for each x in $[0, 1]$. For $i = 1, 2$, we have

$$|S'_i(x)| = \frac{1}{2\lambda} \left(\frac{1}{4} - x/\lambda \right)^{-1/2},$$

so

$$\frac{1}{\lambda} \leq |S'_i(x)| \leq \frac{1}{2\lambda} \left(\frac{1}{4} - 1/\lambda \right)^{-1/2} = \frac{1}{(\lambda^2 - 4\lambda)^{1/2}}$$

if $0 \leq x \leq 1$. By the mean-value theorem

$$\frac{1}{\lambda} |x - y| \leq |S_i(x) - S_i(y)| \leq \frac{1}{(\lambda^2 - 4\lambda)^{1/2}} |x - y| \quad (0 \leq x, y \leq 1). \quad \text{13.3}$$

Thus, if $\lambda > 2 + \sqrt{5}$, then $(\lambda^2 - 4\lambda)^{-1/2} < 1$, so the mappings S_1 and S_2 are contractions on $[0, 1]$, and by Theorem 9.1, the IFS $\{S_1, S_2\}$ has a unique (non-empty compact) attractor $F \subset [0, 1]$ satisfying

$$F = S_1(F) \cup S_2(F),$$

and it follows that $f_\lambda(F) = F$. Since this union is disjoint, F is totally disconnected. In exactly the same way as for the tent map, F is a repeller, with $f_\lambda^k(x) \rightarrow -\infty$ if $x \notin F$, and f is chaotic on F .

To estimate the dimension of F , we proceed as in Example 9.8. Using Propositions 9.6 and 9.7, it follows from (13.3) that

$$\frac{\log 2}{\log \lambda} \leq \dim_H F \leq \underline{\dim}_B F \leq \overline{\dim}_B F \leq \frac{\log 2}{\log(\lambda(1 - 4/\lambda)^{1/2})}.$$

Thus, if λ is large, the dimension of F is close to $\log 2 / \log \lambda$.

For smaller values of λ , the dynamics of the logistic map (13.2) are subtle. If $0 < \lambda \leq 4$, the function f_λ maps $[0, 1]$ into itself, and we can restrict attention to the interval $[0, 1]$. If x is a period- p point of f , that is, $f^p(x) = x$ and p is the least positive integer with this property, we say that x is *stable* or *unstable* according to whether $|f^{p-1}(x)| < 1$ or > 1 . Stable periodic points attract nearby orbits, and unstable periodic points repel them. If $0 < \lambda \leq 1$, then f_λ has a fixed point at 0 which is attractive, in the sense that $f_\lambda^k(x) \rightarrow 0$ for all $x \in [0, 1]$. For $1 < \lambda < 3$, the function f_λ has an unstable fixed point 0, and a stable fixed point $1 - 1/\lambda$, so $f_\lambda^k(x) \rightarrow 1 - 1/\lambda$ for all $x \in (0, 1)$. As λ increases through the value $\lambda_1 = 3$, the fixed point at $1 - 1/\lambda$ becomes unstable, splitting or ‘bifurcating’ into a stable orbit of period 2 to which all but countably many points of $(0, 1)$ are attracted (see Figure 13.2).

When λ reaches $\lambda_2 = 1 + \sqrt{6}$, the period-2 orbit becomes unstable and is replaced by a stable period-4 orbit. As λ is increased further, this period doubling continues with a stable orbit of period 2^q appearing at $\lambda = \lambda_q$; this orbit attracts all but countably many initial points in $(0, 1)$.

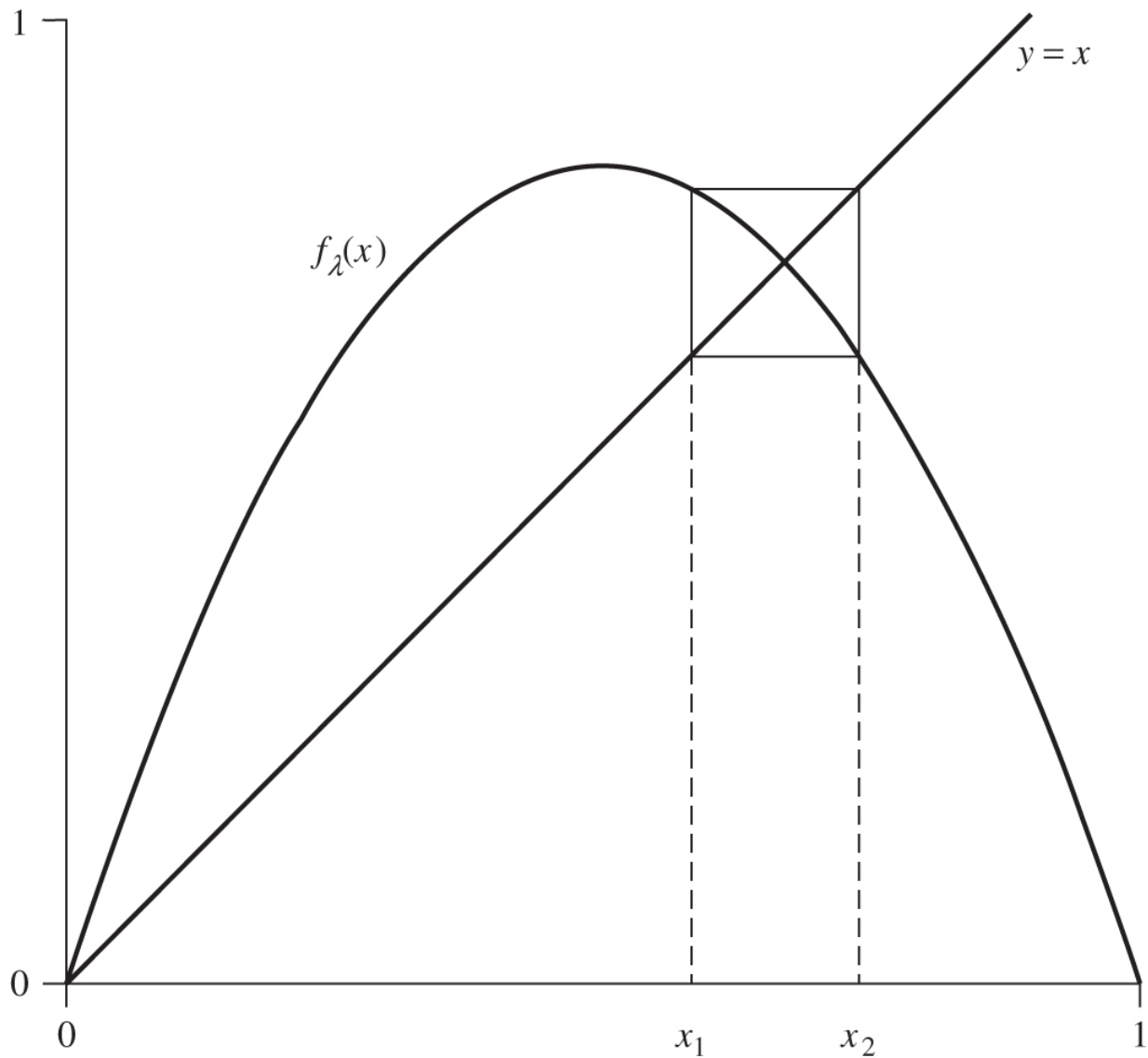
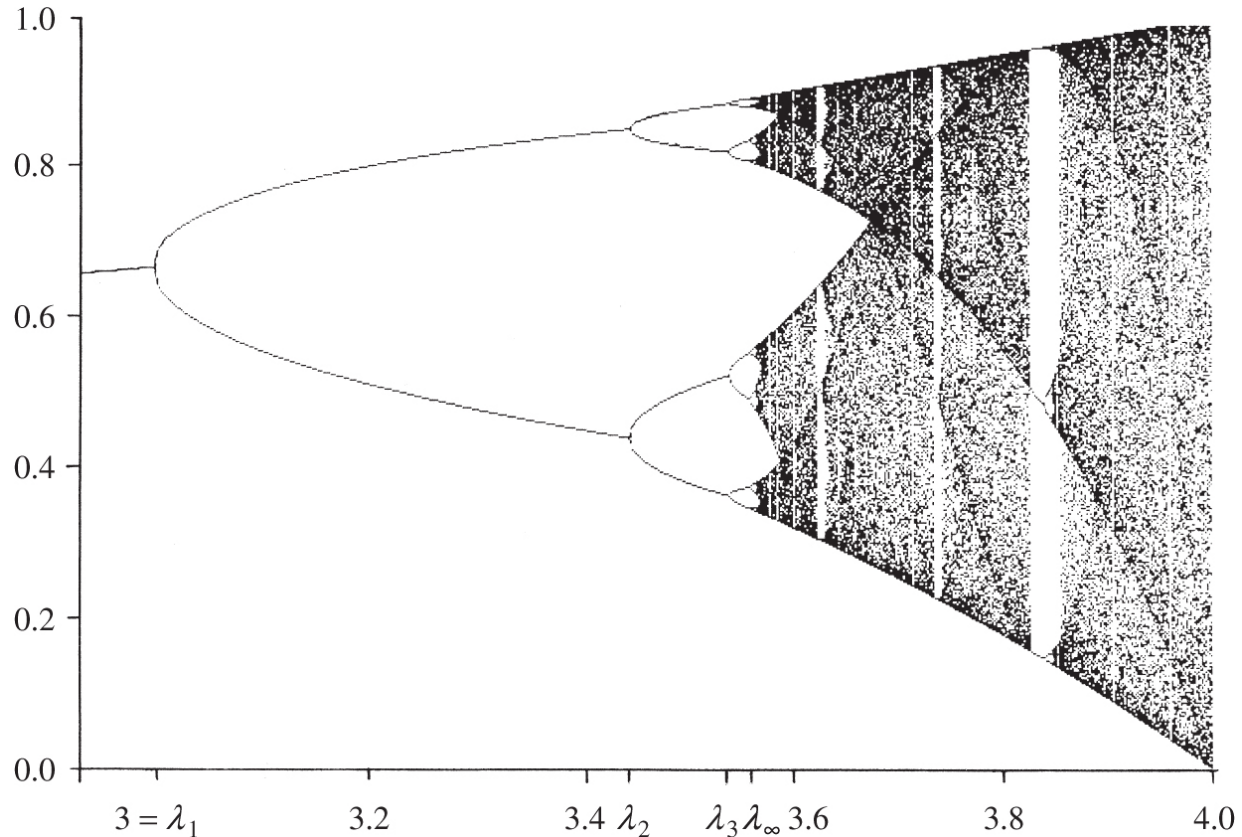


Figure 13.2 The logistic map $f_\lambda(x) = \lambda x(1 - x)$ for $\lambda = 3.38$. Note the period-2 orbit x_1, x_2 with $f_\lambda(x_1) = x_2$ and $f_\lambda(x_2) = x_1$.

One of the surprising features of this process is that the period doubling occurs more and more frequently as λ increases, and $q \rightarrow \infty$ as $\lambda \rightarrow \lambda_\infty$, where $\lambda_\infty \approx 3.570$. As λ approaches λ_∞ , the repeated

splitting of stable orbits of period 2^q into nearby stable orbits of period 2^{q+1} provides a sequence of attracting orbits that approximate to a Cantor set; see [Figure 13.3](#).



[Figure 13.3](#) For each λ , the iterates $f_\lambda^k(x)$ are plotted for k between 150 and 300, for a suitable initial x . The intersection of the plot with vertical lines shows the periodic attractors for $\lambda < \lambda_\infty$. As λ approaches λ_∞ , repeated splitting of the periodic orbits results in an attractor of Cantor set form at $\lambda = \lambda_\infty$.

When $\lambda = \lambda_\infty$, the attractor F actually is a set of Cantor type. Then, F is invariant under f_{λ_∞} with all except a countable number of points of $[0, 1]$ approaching F under iteration by f_{λ_∞} (the exceptional points are those that iterate onto the unstable periodic orbits). The effect of f_{λ_∞} on F can be analysed by extrapolating from the periodic orbits of f_{λ_q} when q is large. There are dense orbits but no sensitive dependence on initial conditions. It is possible to show that F is the attractor in the sense of (9.4) of a certain IFS, and, using the

method of Example 9.8, the Hausdorff dimension may be estimated as 0.538 A complete analysis of the structure of this fractal attractor is beyond the scope of this book.

For $\lambda_\infty < \lambda < 4$, several types of behaviour occur. There is a set of parameters K such that if $\lambda \in K$, then f_λ has a truly chaotic attractor of positive length. Moreover, K itself has positive Lebesgue measure. However, in the gaps or ‘windows’ of K , period doubling again occurs. For example, when $\lambda \approx 3.83$, there is a stable period-3 orbit; as λ increases, it splits first into a stable period-6 orbit, then into a stable period-12 orbit, and so on. When λ reaches about 3.855, the ‘limit’ of these stable orbits gives a Cantor-like attractor. Similarly, there are other windows where period doubling commences with a five-cycle, a seven-cycle, and so on.

One of the most fascinating features of this period doubling is its universality: the behaviour of the logistic map as λ increases is qualitatively the same as that of *any* family of transformations of an interval $f_\lambda(x) = \lambda f(x)$, provided that f is unimodal, that is, has a single maximum at c say, with $f''(c) < 0$. Although the values $\lambda_1, \lambda_2, \dots$ at which period doubling occurs depend on f , the rate at which these values approach λ_∞ is universal, that is, $\lambda_\infty - \lambda_k \approx c\delta^{-k}$, where $\delta = 4.6692 \dots$ is the *Feigenbaum constant* and c depends on f . Moreover, the Hausdorff dimension of the fractal attractor of f_{λ_∞} is 0.538 . . . ; the same value occurs for any differentiable and unimodal f .

Mappings that have been used to model biological populations and exhibit similar features include the following:

$$\begin{aligned}f_\lambda(x) &= \lambda \sin \pi x \\f_\lambda(x) &= x \exp \lambda(1-x) \\f_\lambda(x) &= x(1 + \lambda(1-x)) \\f_\lambda(x) &= \lambda x / (1 + ax)^5.\end{aligned}$$

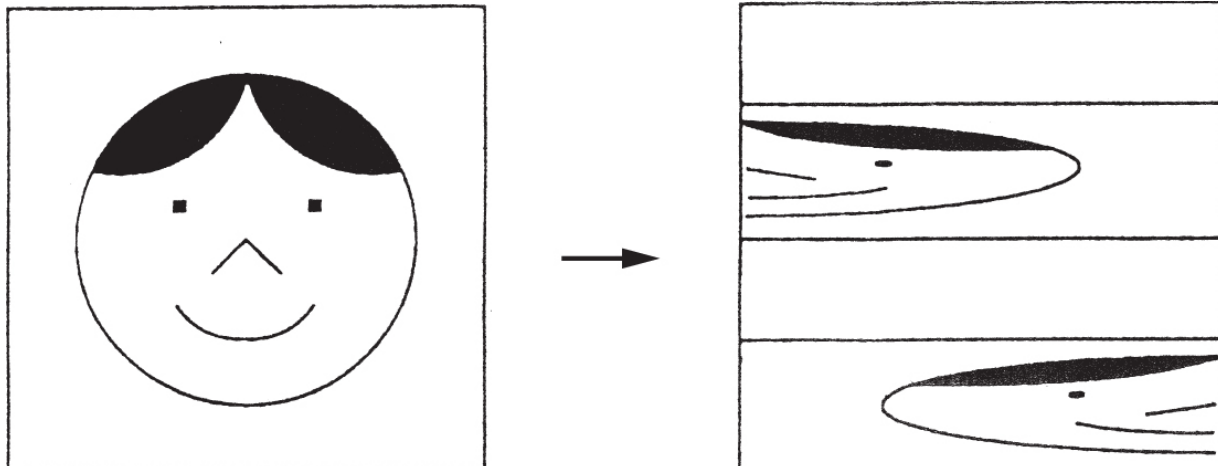
13.3 Stretching and folding transformations

One of the simplest planar dynamical systems with a fractal attractor is the ‘baker’s’ transformation, so-called because it resembles the process of repeatedly stretching a piece of dough and folding it in two. Let $E = [0, 1] \times [0, 1]$ be the unit square. For fixed $0 < \lambda < \frac{1}{2}$, we define the *baker’s transformation* $f : E \rightarrow E$ by

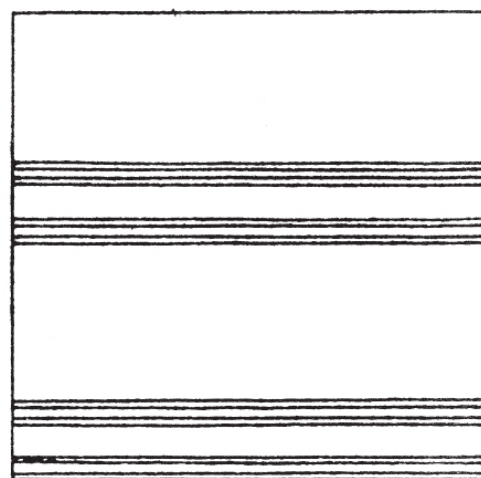
$$f(x, y) = \begin{cases} (2x, \lambda y) & (0 \leq x \leq \frac{1}{2}) \\ (2x - 1, \lambda y + \frac{1}{2}) & (\frac{1}{2} < x \leq 1) \end{cases} \quad \text{13.4}$$

This transformation may be thought of as stretching E into a $2 \times \lambda$ rectangle, cutting it into two $1 \times \lambda$ rectangles and placing these above each other with a gap of $\frac{1}{2} - \lambda$ in between; see [Figure 13.4](#).

Then, $E_k = f^k(E)$ is a decreasing sequence of sets, with E_k comprising 2^k horizontal strips of height λ^k separated by gaps of at least $(\frac{1}{2} - \lambda)\lambda^{k-1}$. Since $f(E_k) = E_{k+1}$, the compact limit set $F = \bigcap_{k=0}^{\infty} E_k$ satisfies $f(F) = F$. (Strictly speaking, $f(F)$ does not include part of F in the left edge of the square E , a consequence of f being discontinuous. However, this has little effect on the behaviour.) If $(x, y) \in E$, then $f^k(x, y) \in E_k$, so $f^k(x, y)$ lies within distance λ^k of F . Thus, all points of E are attracted to F under iteration by f .



(a)



(b)

Figure 13.4. The baker's transformation: (a) its effect on the unit square; (b) its attractor.

If the initial point (x, y) has $x = 0.a_1a_2\dots$ in base 2, and $x \neq \frac{1}{2}, 1$ then it is easily checked that

$$f^k(x, y) = (0.a_{k+1}a_{k+2}\dots, y_k)$$

where y_k is some point in the strip of E_k numbered $a_k a_{k-1} \dots a_1$ (base 2) counting from the bottom with the bottom strip numbered 0.

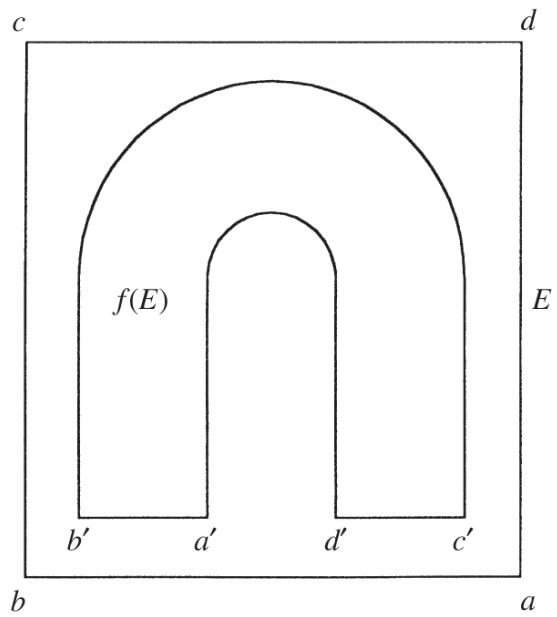
Thus, when k is large, the position of $f^k(x, y)$ depends largely on the base-2 digits a_i of x with i close to k . By choosing an x with base 2

expansion containing all finite sequences, we can arrange for $f^k(x, y)$ to be dense in F for certain initial (x, y) , just as in the case of the tent map.

Further analysis along these lines shows that f has sensitive dependence on initial conditions, and that the periodic points of f are dense in F , so that F is a chaotic attractor for f . Certainly, F is a fractal—it is essentially the product $[0, 1] \times F_1$, where F_1 is a Cantor set, that is the IFS attractor of $S_1(x) = \lambda x$, $S_2(x) = \frac{1}{2} + \lambda x$. Theorem 9.3 gives $\dim_H F_1 = \dim_B F_1 = \log 2 / -\log \lambda$, so $\dim_H F = 1 + \log 2 / -\log \lambda$, using Corollary 7.4.

The baker's transformation is rather artificial, being piecewise linear and discontinuous. However, it does serve to illustrate how the 'stretching and cutting' procedure leads to a fractal attractor.

The closely related process of 'stretching and folding' *can* occur for continuous functions on plane regions. Let $E = [0, 1] \times [0, 1]$ and suppose that f maps E in a continuous one-to-one manner onto a horseshoe-shaped region $f(E)$ contained in E . Then f may be thought of as stretching E into a long thin rectangle, which is then bent in the middle. This figure is repeatedly stretched and bent by f , so that $f^k(E)$ consists of an increasing number of side-by-side strips; see [Figure 13.5](#). We have $E \supset f(E) \supset f^2(E) \supset \dots$, and the compact set $F = \bigcap_{k=1}^{\infty} f^k(E)$ attracts all points of E . Locally, F looks like the product of a Cantor set and an interval.



(a)

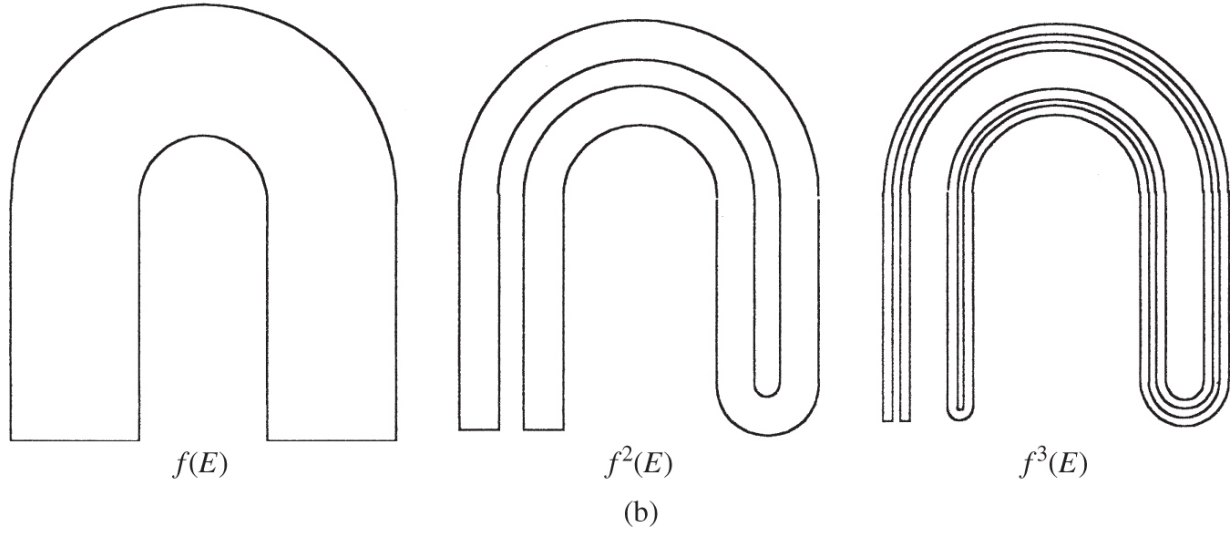
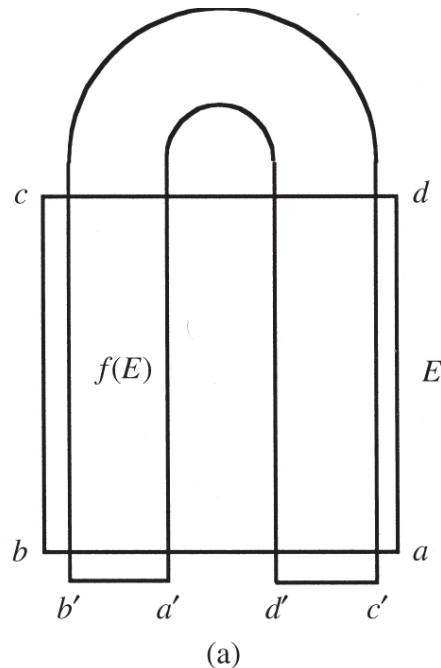


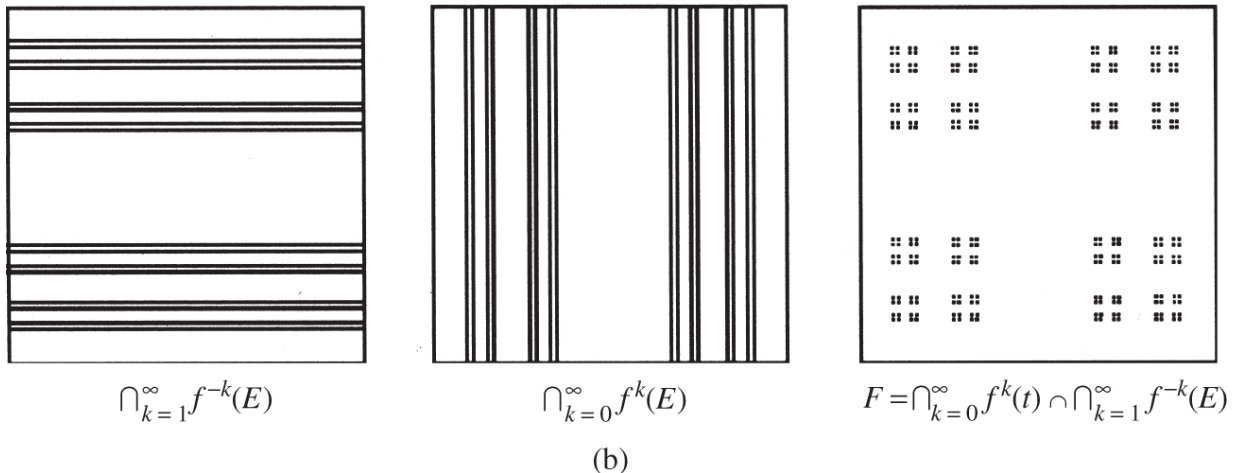
Figure 13.5 A horseshoe map. (a) The square E is transformed, by stretching and bending, to the horseshoe $f(E)$, with a, b, c, d mapped to a', b', c', d' , respectively. (b) The iterates of E under f form a set that is locally a product of a line segment and a Cantor set.

A variation of this construction gives a transformation with rather different characteristics; see [Figure 13.6](#). If D is a plane domain containing the unit square E and $f : D \rightarrow D$ is such that $f(E)$ is a horseshoe with ‘ends’ and ‘arch’ lying in a part of D outside E that is never iterated back into E , then almost all points of the square E

(in the sense of plane measure) are eventually iterated outside E by f . If $f^k(x, y) \in E$ for all positive k , then $(x, y) \in \bigcap_{k=1}^{\infty} f^{-k}(E)$. With f suitably defined, $f^{-1}(E)$ consists of two horizontal bars across E , so $\bigcap_{k=1}^{\infty} f^{-k}(E)$ is the product of $[0, 1]$ and a Cantor set. The set $F = \bigcap_{k=-\infty}^{\infty} f^k(E) = \bigcap_{k=0}^{\infty} f^k(E) \cap \bigcap_{k=1}^{\infty} f^{-k}(E)$ is compact and invariant for f , and is the product of two Cantor sets. However, F is not an attractor since points arbitrarily close to F are iterated outside E .



(a)



(b)

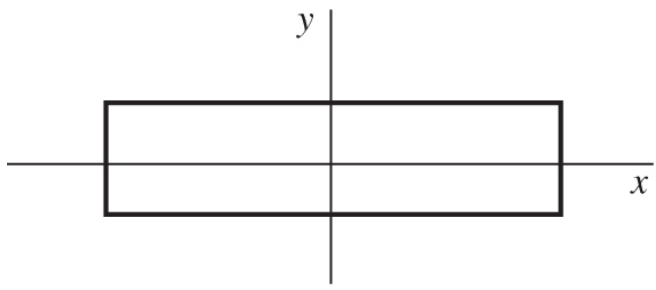
Figure 13.6 An alternative horseshoe map. (a) The square E is transformed, so that the ‘arch’ and ‘ends’ of $f(E)$ lie outside E . (b) The sets $\bigcap_{k=1}^{\infty} f^{-k}(E)$ and $\bigcap_{k=0}^{\infty} f^k(E)$ are both products of a Cantor set and a unit interval. Their intersection F is an unstable invariant set for f .

A specific example of a ‘stretching and folding’ transformation is the Hénon map $f : \mathbb{R}^2 \rightarrow \mathbb{R}^2$,

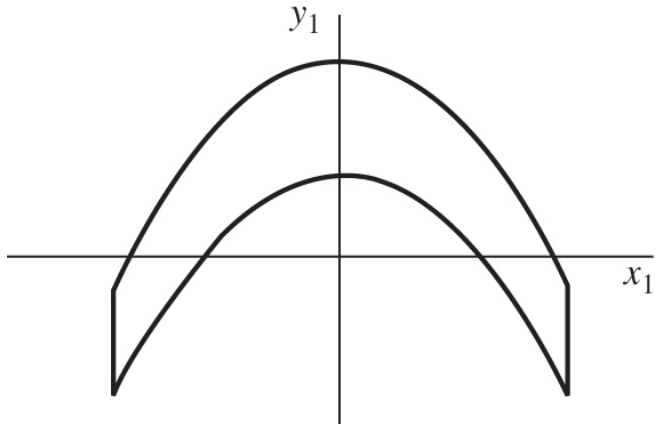
$$f(x, y) = (y + 1 - ax^2, bx),$$

13.5

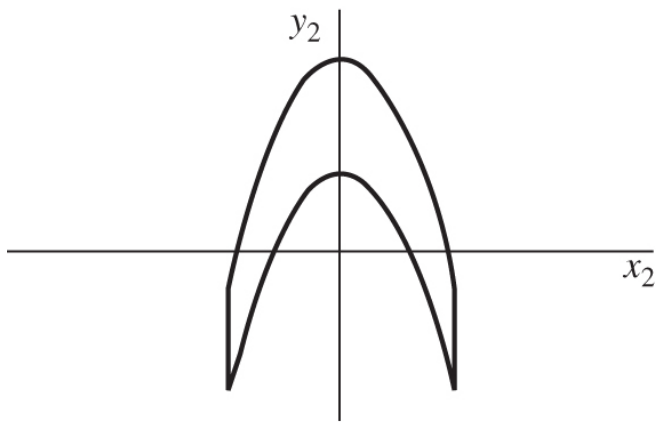
where a and b are constants. (The values $a = 1.4$ and $b = 0.3$ are usually chosen for study. For these values, there is a quadrilateral D for which $f(D) \subset D$ to which we can restrict attention.) This mapping has Jacobian $-b$ for all (x, y) , so it contracts area at a constant rate throughout \mathbb{R}^2 ; to within a linear change of coordinates, (13.5) is the most general quadratic mapping with this property. The transformation (13.5) may be decomposed into an (area-preserving) bend, a contraction and a reflection, the net effect being ‘horseshoe-like’; see [Figure 13.7](#). This leads us to expect f to have a fractal attractor, and this is borne out by computer pictures, [Figure 13.8](#). Detailed pictures show banding indicative of a set that is locally the product of a line segment and a Cantor-like set. Numerical estimates suggest that the attractor has box dimension of about 1.26 when $a = 1.4$ and $b = 0.3$.



Area-preserving bend
 $(x_1, y_1) = (x, 1 - ax^2 + y)$



Contraction in x -direction
 $(x_2, y_2) = (bx_1, y_1)$



Reflection in the line $y = x$
 $(x_3, y_3) = (y_2, x_2)$

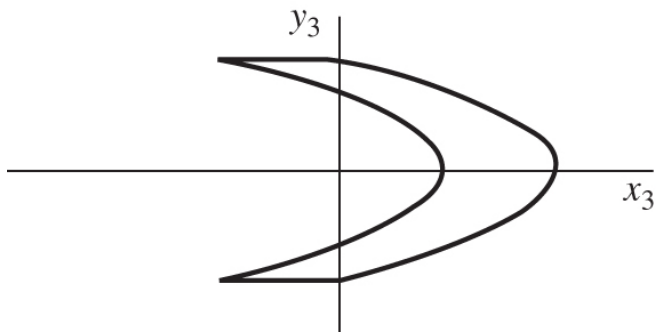


Figure 13.7 The Hénon map may be decomposed into an area-preserving bend, followed by a contraction, which is then followed by a reflection in the line $y = x$. The diagrams show the effect of these successive transformations on a rectangle.

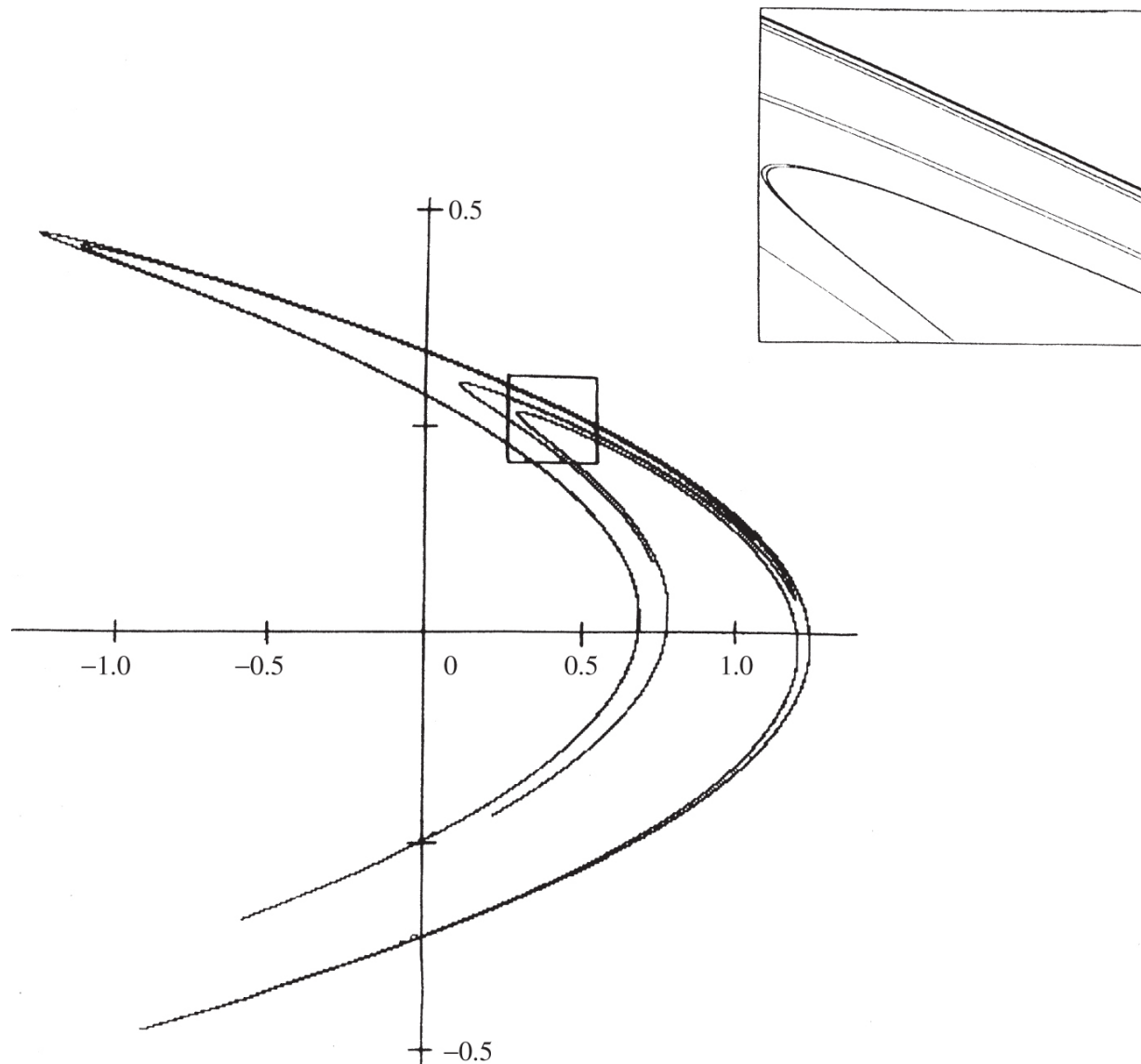


Figure 13.8 Iterates of a point under the Hénon map (13.5) showing the form of the attractor. Banding is apparent in the enlarged portion in the inset.

Detailed analysis of the dynamics of the Hénon map is complicated. In particular, the bifurcations, that is, qualitative changes in behaviour that occur as a and b vary, are highly intricate.

Many other types of ‘stretching and folding’ are possible. Transformations can fold several times or even be many-to-one; for example, the ends of a horseshoe might cross. Such transformations often have fractal attractors, but their analysis tends to be difficult.

13.4 The solenoid

Our next example is of a transformation of a 3-dimensional region—a solid torus. If a unit disc B is rotated through 360° about an axis L in the plane of, but not intersecting, B , a solid torus D is swept out. The torus D may be thought of as the product of the circle C , of radius $r > 1$, obtained by rotating the centre of B around L , and B . This gives a convenient parametrisation of D as

$$\{(\phi, w) \in C \times B : 0 \leq \phi < 2\pi, |w| \leq 1\},$$

where the angle ϕ specifies a point on C , and where w is a position vector relative to the centre of B ; see [Figure 13.9](#).

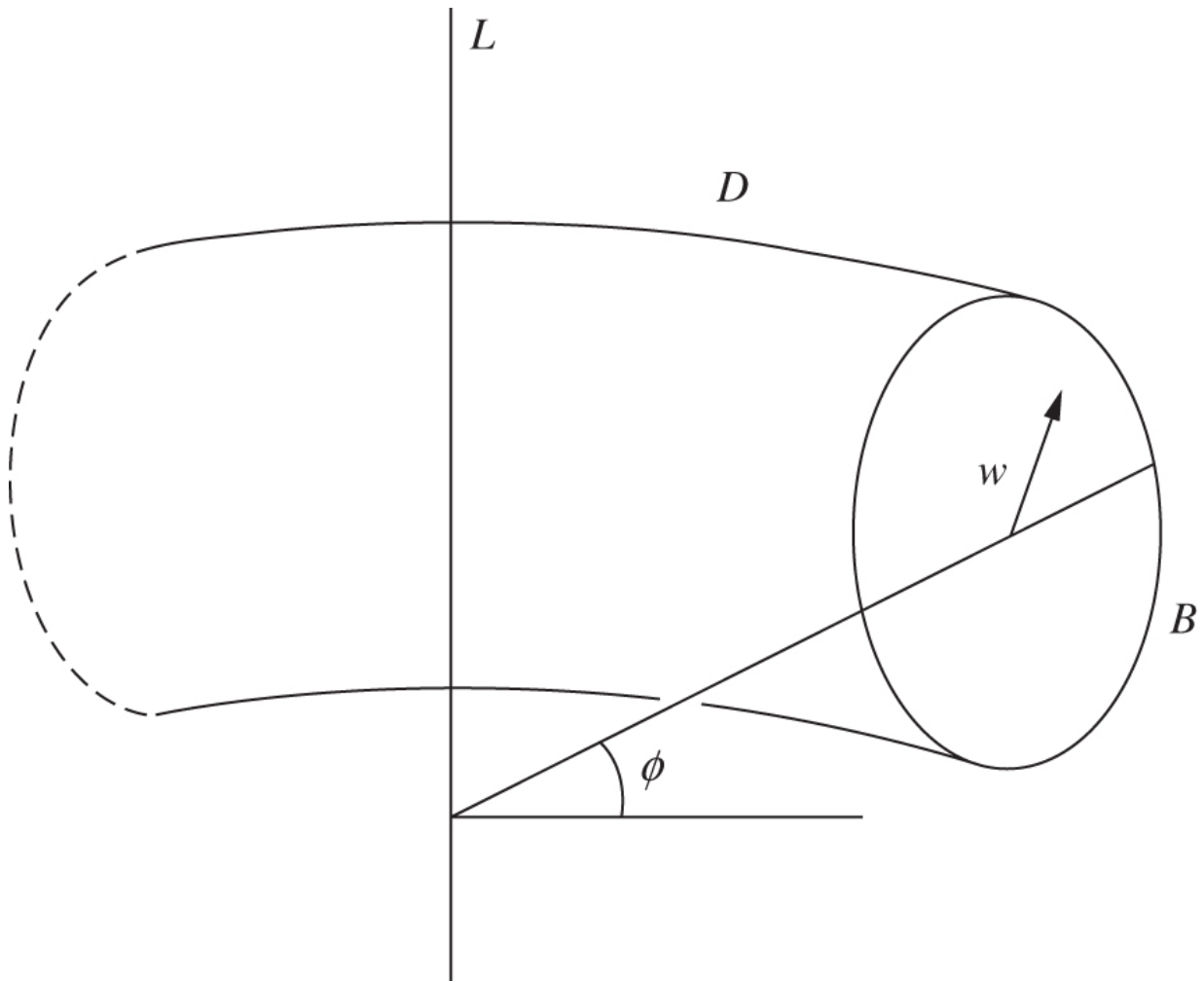


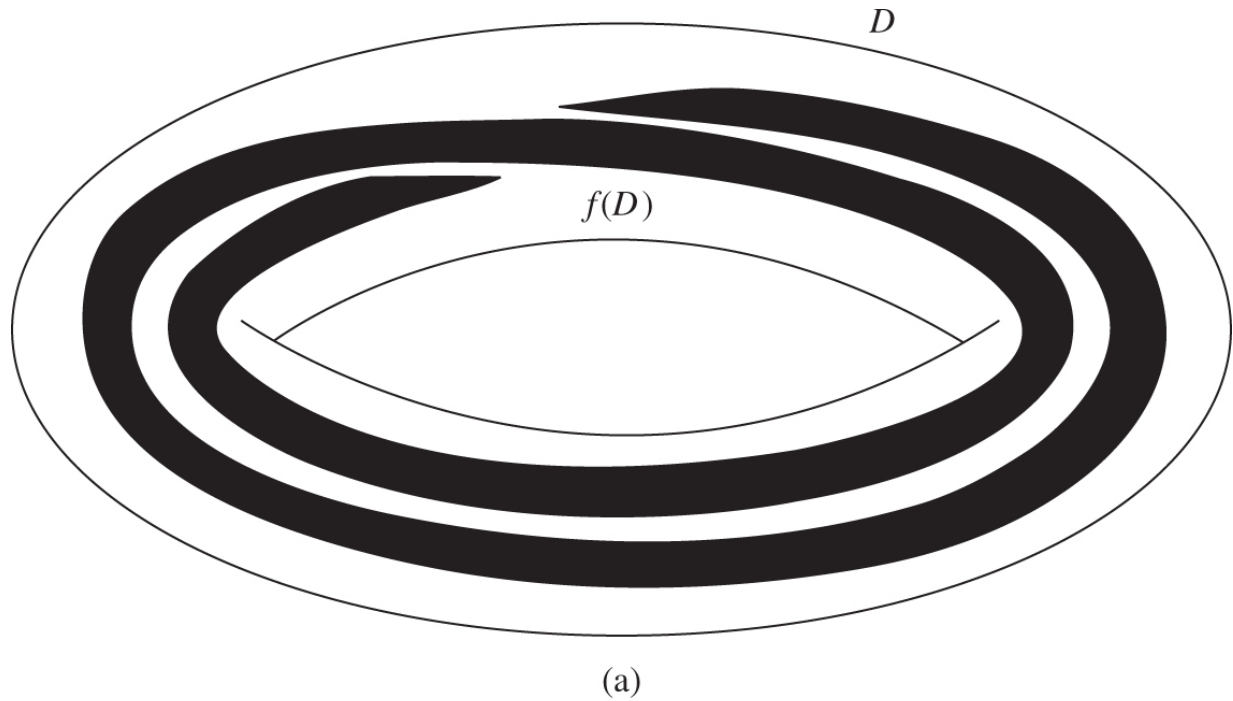
Figure 13.9. Parametrisation of the torus D .

Fix $0 < a < \frac{1}{4}$ and define $f : D \rightarrow D$ by

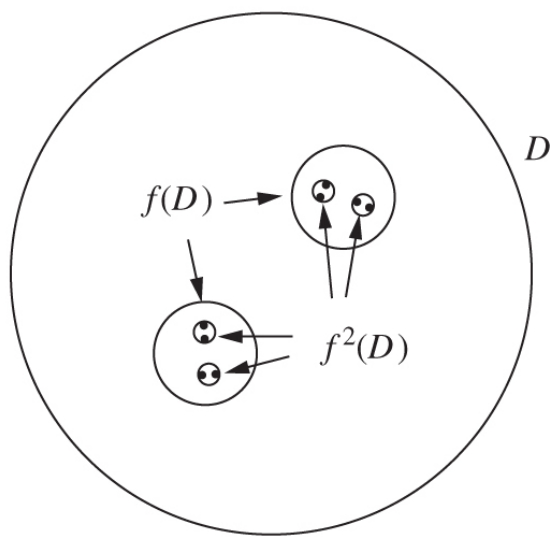
$$f(\phi, w) = \left(2\phi(\text{mod } 2\pi), aw + \frac{1}{2}\hat{\phi}\right), \quad 13.6$$

where $\hat{\phi}$ is the unit vector in B at angle ϕ to the outwards axis. Then f maps D onto a solid tube of radius a that traverses D twice; see [Figure 13.10](#). Note that (ϕ, w) and $(\phi + \pi, w)$ are mapped to points in the same ‘slice’ of D , that is, the same half-plane bounded by L . The second iterate $f^2(D)$ is a tube of radius a^2 going round $f(D)$ twice, so around D four times; $f^3(D)$ traverses D eight times, and so on. The intersection $F = \bigcap_{k=1}^{\infty} f^k(D)$ is highly fibrous—locally it looks like a bundle of line segments that cut any cross section of D in a

Cantor-like set. The set F , called a *solenoid*, is invariant under f , and attracts all points of D .



(a)



(b)

Figure 13.10 The solenoid. (a) The torus D and its image under f . (b) A plane section through D intersects F in a Cantor-like set.

We may find the dimension of F by routine methods. Let P_ϕ be the half-plane bounded by L and cutting C at ϕ . Observe that $f^k(C)$ is a smooth closed curve traversing the torus 2^k times, with total length at most $2^k c$, where c is independent of k ($f^k(C)$ cannot oscillate too wildly—the angle between every curve $f^k(C)$ and every half-plane P_ϕ has a positive lower bound). The set $f^k(D)$ is a ‘fattening’ of the curve $f^k(C)$ to a tube of radius a^k , so it may be covered by a collection of balls of radius $2a^k$ spaced at intervals of a^k along $f^k(C)$. Clearly, $2 \times 2^k c a^{-k}$ balls will suffice, so applying Proposition 4.1 in the usual way, we get $\dim_H F \leq \overline{\dim}_B F \leq s$ and $\mathcal{H}^s(F) < \infty$ for $s = 1 + \log 2 / -\log a$.

To get a lower estimate for the dimension, we examine the sections $F \cap P_\phi$ for each ϕ . The set $f(D) \cap P_\phi$ consists of two discs of radius a situated diametrically opposite to each other with centres $\frac{1}{2}$ apart inside $D \cap P_\phi$. Each of these discs contains two discs of $f^2(D) \cap P_\phi$ of radius a^2 and with centres $\frac{1}{2}a$ apart, and so on. We may place a mass distribution μ on $F \cap P_\phi$ in such a way that each of the 2^k discs of $f^k(D) \cap P_\phi$ has mass 2^{-k} . If $U \subset P_\phi$ satisfies

$$a^k \left(\frac{1}{2} - 2a \right) \leq |U| < a^{k-1} \left(\frac{1}{2} - 2a \right)$$

for some positive integer k , then U intersects at most one disc of $f^k(D) \cap P_\phi$, so

$$\mu(U) \leq 2^{-k} = a^{k(\log 2 / -\log a)} \leq c_1 |U|^{\log 2 / -\log a},$$

where c_1 is independent of $|U|$. It follows from the Mass distribution principle 4.2 that

$$\mathcal{H}^{\log 2 / -\log a}(F \cap P_\phi) \geq c_1^{-1}.$$

Since F is built up from sections $F \cap P_\phi$ ($0 \leq \phi < 2\pi$), a higher dimensional modification of Proposition 7.9 implies $\mathcal{H}^s(F) > 0$, where $s = 1 + \log 2 / -\log a$. We conclude that $\dim_H F = \dim_B F = s$, and that $0 < \mathcal{H}^s(F) < \infty$.

If $\phi/2\pi = 0 \cdot a_1 a_2 \dots$ to base 2, it follows from (13.6) that $f^k(\phi, w) = (\phi_k, v_k)$, where $\phi_k/2\pi = 0 \cdot a_{k+1} a_{k+2} \dots$ and where the integer with base-2 representation $a_k a_{k-1} \dots a_{k-d+1}$ determines which of the 2^d discs of $f^d(D) \cap P_{\phi_k}$ the point v_k belongs to for $d \leq k$. Just as in previous examples, suitable choice of the digits a_1, a_2, \dots leads to initial points (ϕ, w) with $f^k(\phi, w)$ dense in F , or alternatively to periodic orbits, so that f is chaotic on F .

13.5 Continuous dynamical systems

A discrete dynamical system may be thought of as a formula relating the value of a quantity at successive discrete time intervals. If the time interval is allowed to tend to 0, then the formula becomes a differential equation in the usual way. Thus, it is natural to regard an autonomous (i.e. time-independent) differential equation as a continuous dynamical system.

Let D be a domain in \mathbb{R}^n and let $f : D \rightarrow \mathbb{R}^n$ be a smooth function. The differential equation

$$\dot{x} = \frac{dx}{dt} = f(x) \quad 13.7$$

has a family of *solution curves* or *trajectories* that fill D . If an initial point $x(0)$ is given, the solution $x(t)$ moves along the unique trajectory that passes through $x(0)$ for all time t , with speed and direction when it is at x given by the vector $f(x)$; the behaviour of $x(t)$ as $t \rightarrow \pm\infty$ may be found by following the trajectory. Given reasonable conditions on f , no two trajectories cross; otherwise the equations (13.7) would not determine the motion of x . Moreover, the trajectories vary smoothly across D except at points where $\dot{x} = f(x) = 0$ and the trajectories are single points.

As in the discrete case, continuous dynamical systems give rise to attractors and repellers. A closed subset F of D might be termed an attractor with basin of attraction V containing F if, for all initial points $x(0)$ in the open set V , the trajectory $x(t)$ through $x(0)$

approaches F as t tends to infinity. Of course, we require F to be invariant, so that if $x(0)$ is a point of F , then $x(t)$ is in F for $-\infty < t < \infty$, implying that F is a union of trajectories. We also require F to be minimal, in the sense that there is some point $x(0)$ such that $x(t)$ is dense in F .

When D is a plane domain, the range of attractors for continuous systems is rather limited. The only attractors possible are isolated points (x for which $f(x) = 0$ in (13.7)) or closed loops. More complicated attractors cannot occur. To demonstrate this, suppose that $x(t)$ is a dense trajectory in an attractor and that for t near t_2 it runs close to, but distinct from, its path when t is near t_1 . Assuming that the trajectories vary smoothly, the directions of $x(t)$ at t_1 and t_2 are almost parallel (see Figure 13.11). Thus, for $t > t_2$, the trajectory $x(t)$ is ‘blocked’ from ever getting too close to $x(t_1)$, so that $x(t_1)$ cannot in fact be a point on an attractor. (The precise formulation of this fact is known as the Poincaré–Bendixson theorem.)

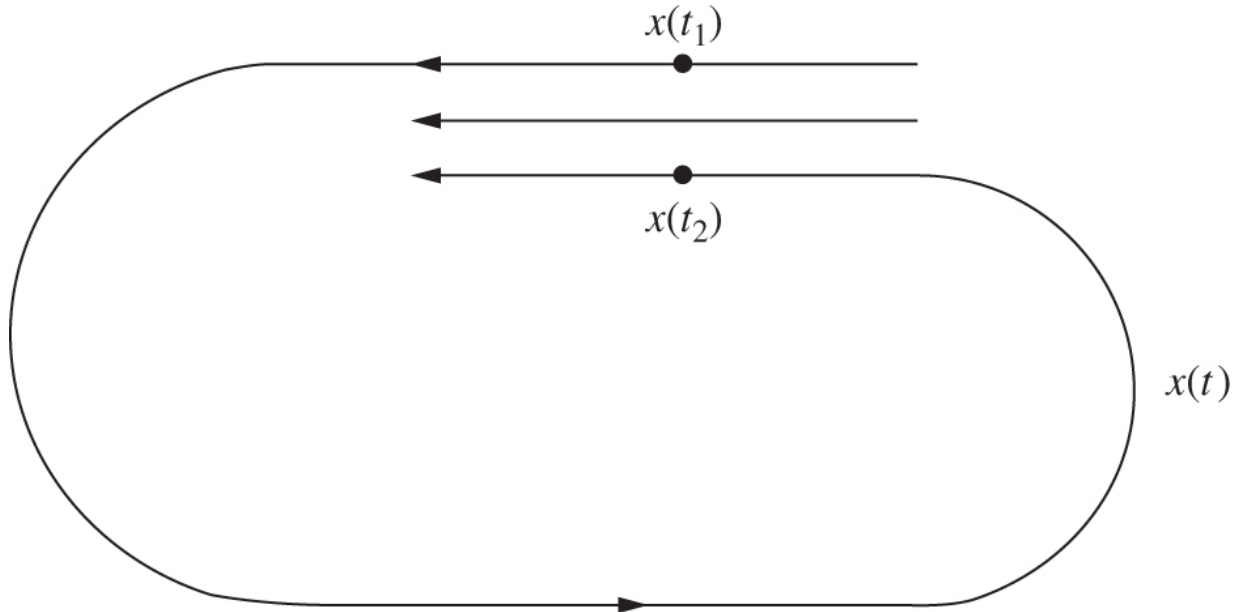


Figure 13.11 A trajectory of a continuous dynamical system in the plane. Assuming that the trajectories vary smoothly, the trajectory shown is ‘cut off’ from returning too close to $x(t_1)$ any time after t_2 .

Consequently, to find continuous dynamical systems with fractal attractors, we need to look at systems in three or more dimensions.

Linear differential equations (with $f(x)$ a linear function of x in (13.7)) can essentially be solved completely by classical methods, the solutions involving periodic or exponential terms. However, even simple non-linear terms can lead to trajectories of a highly intricate form. Non-linear differential equations, particularly in higher dimensions, are notoriously difficult to analyse, requiring a combination of qualitative mathematical analysis and numerical study. One standard approach is to reduce a 3-dimensional continuous system to a 2-dimensional discrete system by looking at plane cross sections or *Poincaré sections* as they are called. If P is a plane region transverse to the trajectories, we may define the *first return map* $g: P \rightarrow P$ by taking $g(x)$ as the point at which the trajectory through x next intersects P , see Figure 13.12. Then, g is a discrete dynamical system on P . If g has an attractor E in P , it follows that the union of trajectories through the points of E is an attractor F of f . Locally F looks like a product of E and a line segment, and typically $\dim_H F = 1 + \dim_H E$, by a variation on Corollary 7.4.

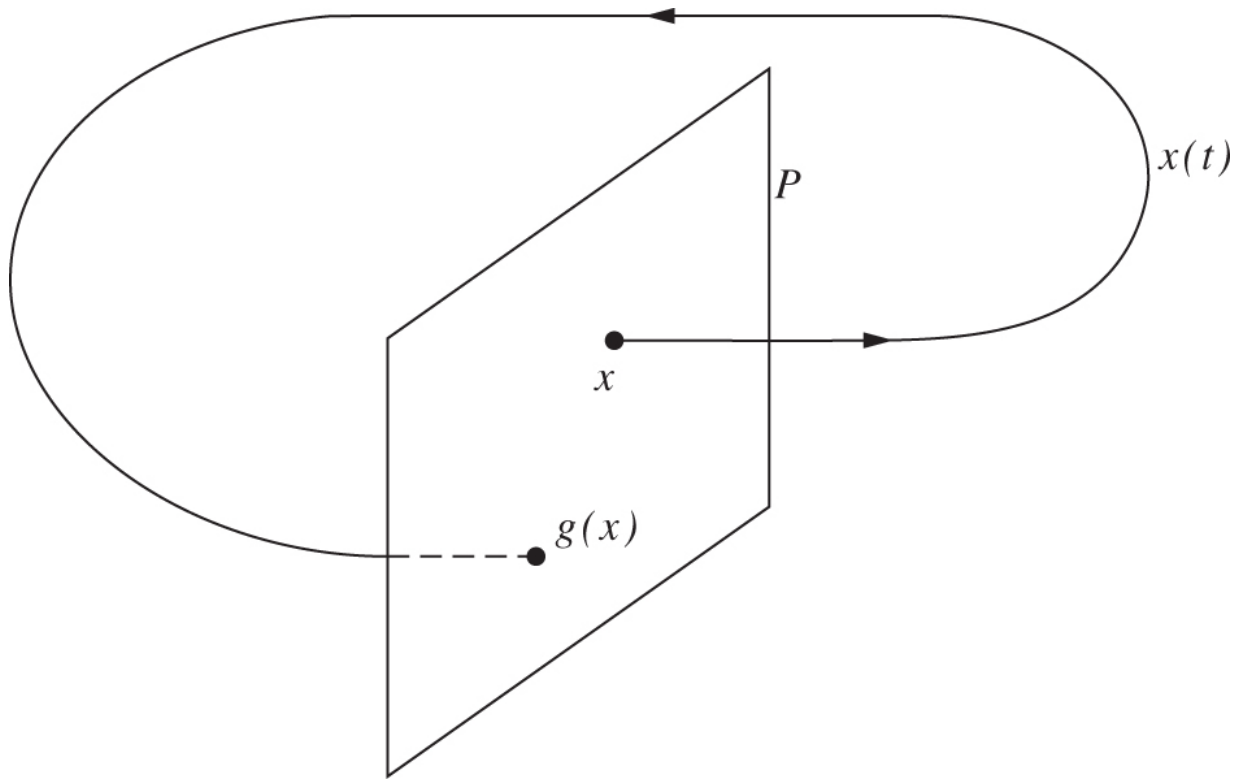


Figure 13.12 A continuous dynamical system in \mathbb{R}^3 induces a discrete dynamical system on the plane P by the ‘first return’ map g .

One of the best known examples of a continuous dynamical system with a fractal attractor is the Lorenz system of equations. Lorenz studied thermal convection of a horizontal layer of fluid heated from below: the warm fluid may rise owing to its buoyancy and circulate in cylindrical rolls. Under certain conditions, these cells are a series of parallel rotating cylindrical rolls; see [Figure 13.13](#). Lorenz used the continuity equation and Navier–Stokes equations from fluid dynamics, together with the heat conduction equation to describe the behaviour of one of these rolls. A series of approximations and simplifications lead to the *Lorenz equations*

$$\begin{aligned}\dot{x} &= \sigma(y - x) & 13.8 \\ \dot{y} &= rx - y - xz \\ \dot{z} &= xy - bz.\end{aligned}$$

The term x represents the rate of rotation of the cylinder, z represents the deviation from a linear vertical temperature gradient, and y corresponds to the difference in temperature at opposite sides of the cylinder. The constant σ is the Prandtl number of the air (the Prandtl number involves the viscosity and thermal conductivity), b depends on the width-to-height ratio of the layer and r is a control parameter representing the fixed temperature difference between the bottom and top of the system. The non-linearity in the second and third equations results from the non-linearity of the equations of flow.

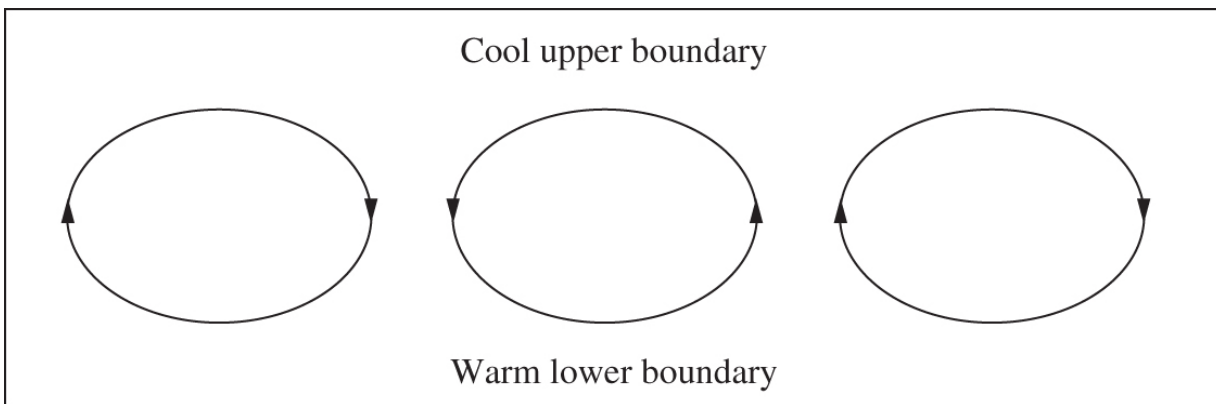


Figure 13.13 The Lorenz equations describe the behaviour of one of the rotating cylindrical rolls of heat-conducting viscous fluid.

Working in (x, y, z) -space, the first thing to notice is that the system (13.8) contracts volumes at a constant rate. The differences in velocity between pairs of opposite faces of a small coordinate box of side δ are approximately $\delta(\partial\dot{x}/\partial x), \delta(\partial\dot{y}/\partial y), \delta(\partial\dot{z}/\partial z)$, so the rate of change of volume of the box is

$$\delta^3 \left(\frac{\partial\dot{x}}{\partial x} + \frac{\partial\dot{y}}{\partial y} + \frac{\partial\dot{z}}{\partial z} \right) = -(\sigma + b + 1)\delta^3 < 0.$$

Nevertheless, with $\sigma = 10, b = \frac{8}{3}, r = 28$ (the values usually chosen for study), the trajectories are concentrated onto an attractor of a highly complex form. This *Lorenz attractor* consists of two ‘discs’ each made up of spiralling trajectories (Figure 13.14). Certain trajectories leave each of the discs almost perpendicularly and flow into the

other disc. If a trajectory $x(t)$ is computed, the following behaviour is typical. As t increases, $x(t)$ circles around one of the discs a number of times and then ‘flips’ over to the other disc. After a few loops round this second disc, it flips back to the original disc. This pattern continues, with an apparently random number of circuits before leaving each disc. The motion seems to be chaotic; in particular, points that are initially close together soon have completely different patterns of residence in the two discs of the attractor. One interpretation of this sensitive dependence on initial conditions is that, so far as the Lorenz equations model a very specific feature of the weather, long-term weather prediction is impossible.

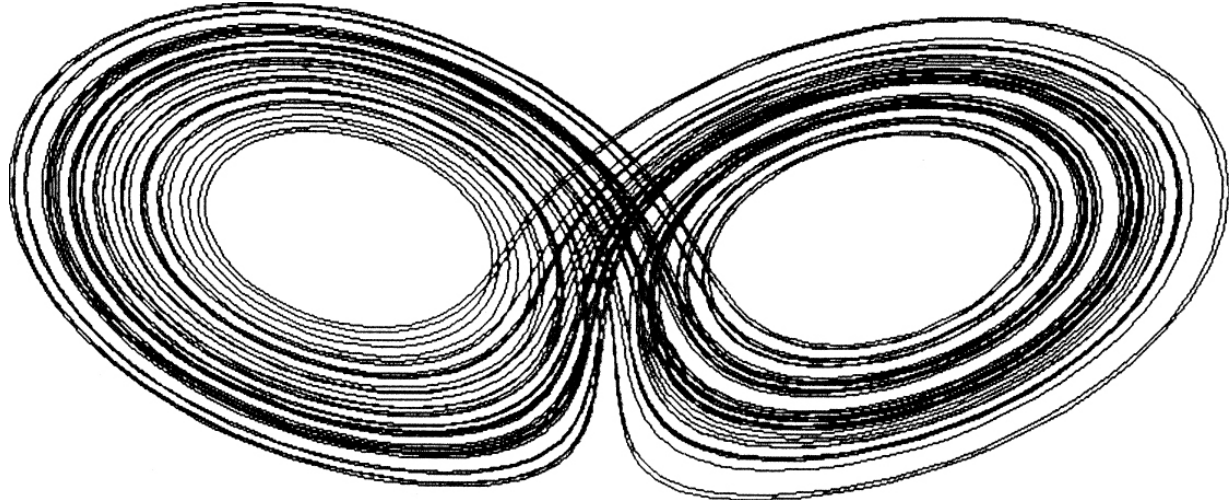


Figure 13.14 A view of the Lorenz attractor for $\sigma = 10, b = \frac{8}{3}, r = 28$. Note the spiralling round the two discs and the ‘jumps’ from one disc to the other.

The Lorenz attractor appears to be a fractal with numerical estimates suggesting a dimension of 2.06 when $\sigma = 10, b = \frac{8}{3}, r = 28$.

Other systems of differential equations also have fractal attractors.
The equations

$$\begin{aligned}\dot{x} &= -y - z \\ \dot{y} &= x + ay \\ \dot{z} &= b + z(x - c)\end{aligned}$$

were studied by Rössler. Fixing suitable b and c , the nature of the attractor changes as a is varied. When a is small, the attractor is a simple closed curve, but on increasing a , this splits into a double loop, then a quadruple loop, and so on. Thus, a type of period doubling takes place, and when a reaches a critical value, there is a fractal attractor in the form of a band ([Figure 13.15](#)). The band has a twist in it, rather like a Möbius strip.

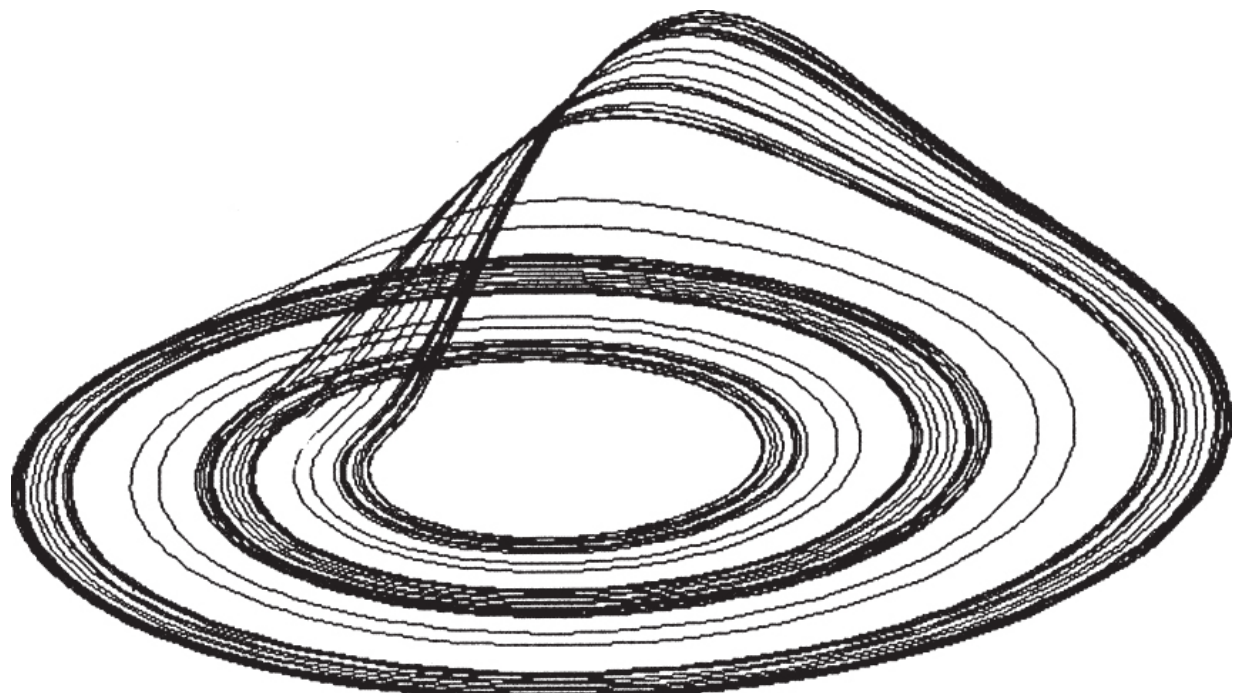


Figure 13.15 A view of the Rössler band attractor for $a = 0.173, b = 0.4, c = 8.5$. Note the banding, suggestive of a set that is locally the product of a Cantor set and a line segment.

To a large extent, each continuous dynamical system (or family of dynamical systems) must be studied individually; many differing types of behaviour can occur. Attractors of continuous systems are well suited to computer study, and mathematicians are frequently challenged to explain ‘strange’ attractors that are observed on computer screens.

*13.6 Small divisor theory

There are a number of important dynamical systems dependent on a parameter ω , which are, in some sense, stable, provided that ω is ‘not too close to a rational number’, in other words if ω is badly approximable in the sense of Section 1.3. By Jarník’s theorem 10.3, the well-approximable numbers form fractal sets, so the stable parameters lie in sets with fractal complement. The following simple example indicates how badly approximable parameters can result in stable systems.

Let C be the (surface of an) infinite cylinder of unit radius parameterised by $\{(\theta, y) : 0 \leq \theta < 2\pi, -\infty < y < \infty\}$. Fix $\omega \in \mathbb{R}$ and define a discrete dynamical system $f : C \rightarrow C$ by

$$f(\theta, y) = (\theta + 2\pi\omega \pmod{2\pi}, y). \quad \text{13.9}$$

Clearly, f just rotates points on the cylinder through an angle $2\pi\omega$, and the circles $y = \text{constant}$ are invariant under f . It is natural to ask if these invariant curves are stable—if the transformation (13.9) is perturbed slightly, will the cylinder still be covered by a family of invariant closed curves ([Figure 13.16](#))? The surprising thing is that this depends on the nature of the number ω : if ω is ‘sufficiently irrational’, then invariant curves remain.

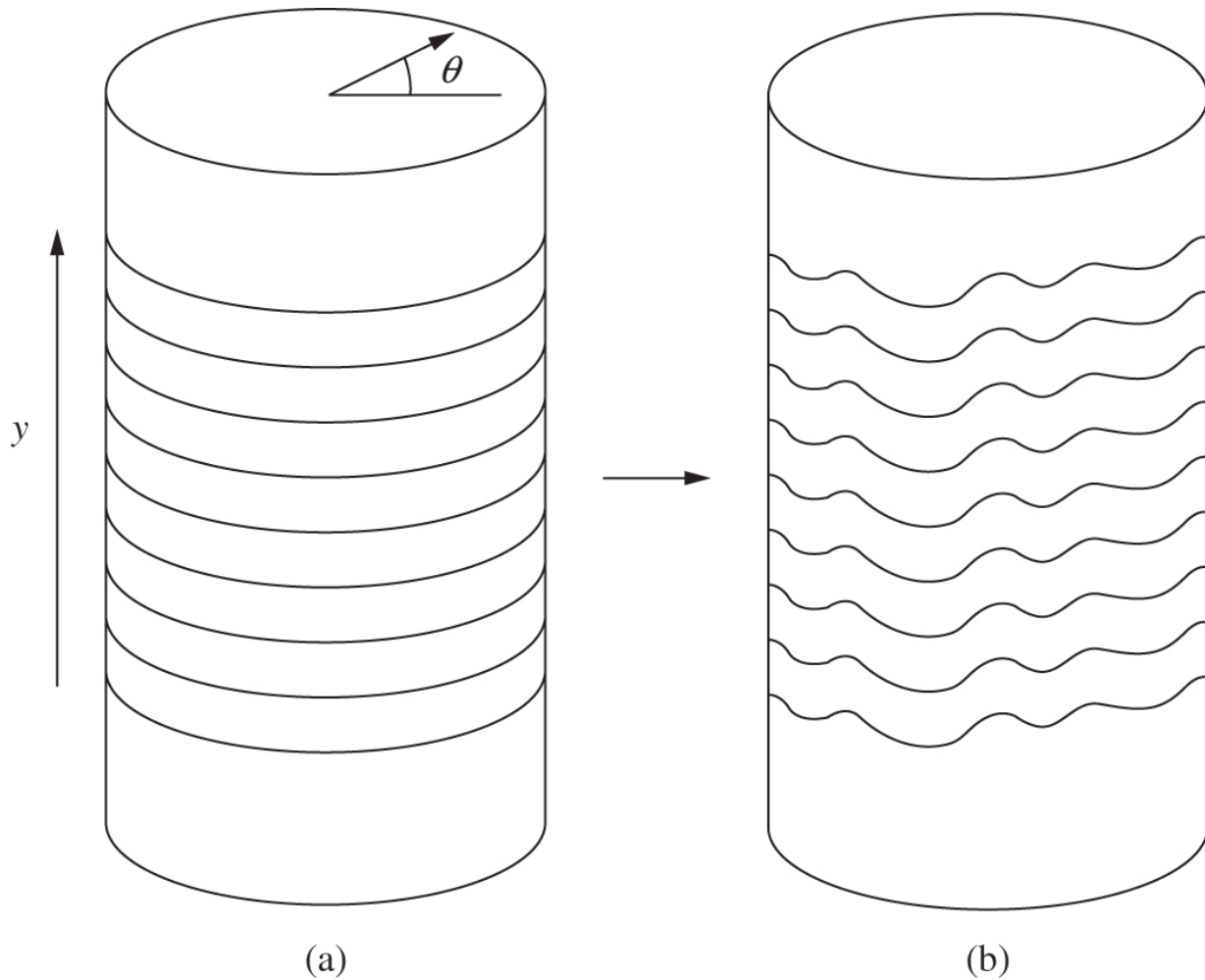


Figure 13.16 (a) Invariant circles for the mapping $f(\theta, y) = (\theta + 2\pi\omega(\text{mod } 2\pi), y)$. (b) If ω is not ‘too rational’, a small perturbation of the mapping to $f(\theta, y) = (\theta + 2\pi\omega(\text{mod } 2\pi), y + g(\theta))$ distorts the circles to a family of smooth invariant curves.

We modify transformation (13.9) to

$$f(\theta, y) = (\theta + 2\pi\omega(\text{mod } 2\pi), y + g(\theta)), \quad \text{13.10}$$

where g is a C^∞ function (i.e. has continuous derivatives of all orders). It is easy to show, using integration by parts, that a function is C^∞ if and only if its Fourier coefficients a_k converge to 0 faster than any power of k . Thus, if

$$g(\theta) = \sum_{-\infty}^{\infty} a_k e^{ik\theta}$$

is the Fourier series of g , then for every positive integer m , there is a constant c such that for $k \neq 0$

$$|a_k| \leq c|k|^{-m}.$$

Suppose that $y = y(\theta)$ is an invariant curve under (13.10), and suppose that y has Fourier series

$$y(\theta) = \sum_{-\infty}^{\infty} b_k e^{ik\theta}.$$

The point $(\theta + 2\pi\omega \pmod{2\pi}, y(\theta) + g(\theta))$ must lie on the curve whenever $(\theta, y(\theta))$ does; hence

$$y(\theta + 2\pi\omega \pmod{2\pi}) = y(\theta) + g(\theta)$$

or

$$\sum_{-\infty}^{\infty} b_k e^{ik(\theta+2\pi\omega)} = \sum_{-\infty}^{\infty} b_k e^{ik\theta} + \sum_{-\infty}^{\infty} a_k e^{ik\theta}.$$

Equating terms in $e^{ik\theta}$, we get that $a_0 = 0$ and b_0 is arbitrary, and

$$b_k = \frac{a_k}{e^{2\pi ik\omega} - 1} \quad (k \neq 0),$$

provided ω is irrational. Thus, the invariant curves are given by

$$y(\theta) = b_0 + \sum_{k \neq 0} \frac{a_k}{e^{2\pi ik\omega} - 1} e^{ik\theta}, \quad \text{13.11}$$

provided that this Fourier series converges to a continuous function. This will happen if the denominators $e^{2\pi ik\omega} - 1$ are not ‘too small too often’. Suppose that ω is not α -well-approximable for some $\alpha > 2$; see (10.4). Then, there is a constant c_1 such that

$$|e^{2\pi ik\omega} - 1| \geq \min_{m \in \mathbb{Z}} |k\omega - m| = \|k\omega\| \geq c_1 |k|^{1-\alpha}$$

for all $k \neq 0$, so

$$\begin{aligned} \left| \frac{a_k}{e^{2\pi i k \omega} - 1} \right| &\leq c_1^{-1} \frac{|a_k|}{|k|^{1-\alpha}} \\ &\leq c c_1^{-1} |k|^{-m-1+\alpha} \end{aligned}$$

for some constant c for each m . Thus, if g is a C^∞ function and ω is not α -well-approximable for some $\alpha > 2$, the function $y(\theta)$ given by (13.11) is C^∞ using standard properties on differentiation of series, so that f has a family of C^∞ invariant curves. We saw in Theorem 10.3 that the set of numbers that are α -well-approximable for all $\alpha > 2$ has dimension 0, so for ‘most’ ω , the invariant curves are stable.

The above example is a special case of a much more general class of transformations of the cylinder known as twist maps. Define

$f : C \rightarrow C$ by

$$f(\theta, y) = (\theta + 2\pi\omega(y)(\text{mod } 2\pi), y). \quad \text{13.12}$$

Again the circles with $y = c$, for c a constant, are invariant, but this time the angle of rotation $\omega(y)$ is allowed to vary smoothly with y . We perturb f to

$$f(\theta, y) = (\theta + 2\pi\omega(y) + \varepsilon h(\theta, y)(\text{mod } 2\pi), y + \varepsilon g(\theta, y)), \quad \text{13.13}$$

where h and g are smooth functions and ε is small, and ask if the invariant curves round C are preserved. Moser's twist theorem, a very deep result, roughly says that the invariant circles $y = c$ of (13.12), for which $\omega(y) = \omega$, will deform into differentiable closed invariant curves of (13.13) if ε is small enough, provided that $\|k\omega\| \geq c_1 |k|^{-3/2}$ for all $k \neq 0$ for some constant c_1 . Thus, the exceptional set of frequencies ω has dimension $\frac{4}{5}$ by Theorem 10.3.

Typically, C is filled by invariant curves corresponding to badly approximable ω where the motion is regular, and regions in between where the motion is chaotic. The chaotic regions grow as ε increases.

Perhaps the most important application of small divisor theory is to the stability of Hamiltonian systems. Consider a 4-dimensional space parametrised by $(\theta_1, \theta_2, j_1, j_2)$. A Hamiltonian function $H(\theta_1, \theta_2, j_1, j_2)$ determines a conservative (volume-preserving) dynamical system according to the differential equations

$$\dot{\theta}_1 = \frac{\partial H}{\partial j_1}, \quad \dot{\theta}_2 = \frac{\partial H}{\partial j_2}, \quad \dot{j}_1 = -\frac{\partial H}{\partial \theta_1}, \quad \dot{j}_2 = -\frac{\partial H}{\partial \theta_2}.$$

Thus, if $H(\theta_1, \theta_2, j_1, j_2) = H_0(j_1, j_2)$ is independent of θ_1, θ_2 , we get the solution

$$\theta_1 = \omega_1 t + c_1, \quad \theta_2 = \omega_2 t + c_2, \quad j_1 = c_3, \quad j_2 = c_4,$$

where ω_1 and ω_2 are angular frequencies (which may depend on j_1, j_2) and c_1, \dots, c_4 are constants. A trajectory of the system remains on the same 2-dimensional torus, $(j_1, j_2) = \text{constant}$, for all time; such tori are called invariant.

It is important to know whether such invariant tori are stable under small perturbations of the system. If the Hamiltonian is replaced by

$$H_0(j_1, j_2) + \varepsilon H_1(\theta_1, \theta_2, j_1, j_2),$$

where ε is small, do the trajectories of this new system stay on new invariant tori expressible as $(j'_1, j'_2) = \text{constant}$, after a suitable coordinate transformation $(\theta_1, \theta_2, j_1, j_2) \mapsto (\theta'_1, \theta'_2, j'_1, j'_2)$? In other words, do the invariant tori of the original system distort slightly to become invariant tori for the new system, or do they break up altogether? The celebrated Kolmogorov–Arnold–Moser (KAM) theorem gives an answer to this question—essentially a torus is stable under sufficiently small perturbations, provided that the frequency ratio ω_1/ω_2 is badly approximable by rationals; more precisely it is stable if for some $c > 0$ we have $|(\omega_1/\omega_2) - (p/q)| \geq c/q^{5/2}$ for all positive integers p, q . The set of numbers that fails to satisfy this condition is a fractal of dimension $\frac{4}{5}$ by Theorem 10.3, so in particular, almost all frequency ratios (in the sense of Lebesgue measure) have tori that

are stable under sufficiently small perturbations. (In fact, the condition can be weakened to $|(\omega_1/\omega_2) - (p/q)| \geq c/q^\alpha$ for any $\alpha > 2$.)

There is some astronomical evidence for small divisor theory. For example, the angular frequencies ω of asteroids tend to avoid values for which the ratio ω/ω_J is close to p/q , where q is a small integer and ω_J is the angular frequency of Jupiter, the main perturbing influence. On the assumptions that orbits in the solar system are stable (which, fortunately, seems to be the case) and that we can consider a pair of orbiting bodies in isolation (a considerable oversimplification), this avoidance of rational frequency ratios is predicted by KAM theory.

*13.7 Lyapunov exponents and entropies

So far we have looked at attractors of dynamical systems largely from a geometrical point of view. However, a dynamical system f provides a much richer structure than a purely geometric one. In this section, we outline some properties of f that often go hand in hand with fractal attractors.

The concept of an invariant measures is fundamental to dynamical systems. A measure μ on D is *invariant* for a mapping $f : D \rightarrow D$ if for every subset A of D we have

$$\mu(f^{-1}(A)) = \mu(A). \quad \text{13.14}$$

We will assume that μ has been normalised, so that $\mu(D) = 1$. Any attractor F supports at least one invariant measure: for fixed x in the basin of attraction of F and A a Borel set, write

$$\mu(A) = \lim_{m \rightarrow \infty} \frac{1}{m} \# \{k : 1 \leq k \leq m \text{ and } f^k(x) \in A\}, \quad \text{13.15}$$

giving the limiting proportion of the iterates that lie in A . It may be shown using ergodic theory that, under very general circumstances, this limit exists and is the same for μ -almost all points in the basin of attraction. It is then easily checked that μ defines a measure.

Furthermore, $f^k(x) \in A$ if and only if $f^{k-1}(x) \in f^{-1}(A)$, leading to (13.14). The measure (13.15) is concentrated on the set of points to which $f^k(x)$ comes arbitrarily close infinitely often, thus μ is supported by an attractor of f . The measure $\mu(A)$ reflects the proportion of the iterates that lie in A , and may be thought of as the distribution that is seen when a large number of iterates $f^k(x)$ are plotted on a computer screen. The intensity of the measure can vary widely across the attractor A ; this variation is often analysed using multifractal analysis (see Chapter 17). As far as the size of an attractor is concerned, it is often the dimension of the set occupied by the invariant measure μ that is relevant, rather than the entire

attractor. With this in mind, we define the *Hausdorff dimension of a measure μ* as

$$\dim_H \mu = \inf \{ \dim_H E : E \text{ is a Borel set with } \mu(E) > 0 \}. \quad \mathbf{13.16}$$

If μ is supported by F , then clearly $\dim_H \mu \leq \dim_H F$, but we may have strict inequality; see Exercise 13.10. However, if there are numbers $s > 0$ and $c > 0$ such that for every set U

$$\mu(U) \leq c|U|^s, \quad \mathbf{13.17}$$

then the Mass distribution principle 4.2 implies that for each set E with $0 < \mu(E)$, we have $\mathcal{H}^s(E) \geq \mu(E)/c > 0$, so that $\dim_H E \geq s$. Hence, if (13.17) holds then

$$\dim_H \mu \geq s. \quad \mathbf{13.18}$$

Once f is equipped with an invariant measure μ , several other dynamical constants may be defined. For simplicity, we assume that D is a domain in \mathbb{R}^2 and $f : D \rightarrow D$ is differentiable. The derivative $(f^k)'(x)$ is a linear mapping on \mathbb{R}^2 ; we write $a_k(x)$ and $b_k(x)$ for the lengths of the major and minor semi-axes of the ellipse $(f^k)'(x)(B)$, where B is the unit ball. Thus, the image under f^k of a small ball of radius r and centre x approximates to an ellipse with semi-axes of lengths $ra_k(x)$ and $rb_k(x)$. We define the *Lyapunov exponents* as the average logarithmic rate of growth with k of these semi-axes:

$$\lambda_1(x) = \lim_{k \rightarrow \infty} \frac{1}{k} \log a_k(x) \quad \lambda_2(x) = \lim_{k \rightarrow \infty} \frac{1}{k} \log b_k(x). \quad \mathbf{13.19}$$

Techniques from ergodic theory show that if μ is invariant for f , these exponents exist and have the same values λ_1, λ_2 for μ -almost all x . Hence, in a system with an invariant measure, we refer to λ_1 and λ_2 as *the Lyapunov exponents* of the system. The Lyapunov exponents represent the ‘average’ rates of expansion of f in the principal directions. If B is a disc of small radius r , then $f^k(B)$ will ‘typically’ be close to an ellipse with semi-axes of lengths $r e^{\lambda_1 k}$ and $r e^{\lambda_2 k}$; see Figure 13.17.

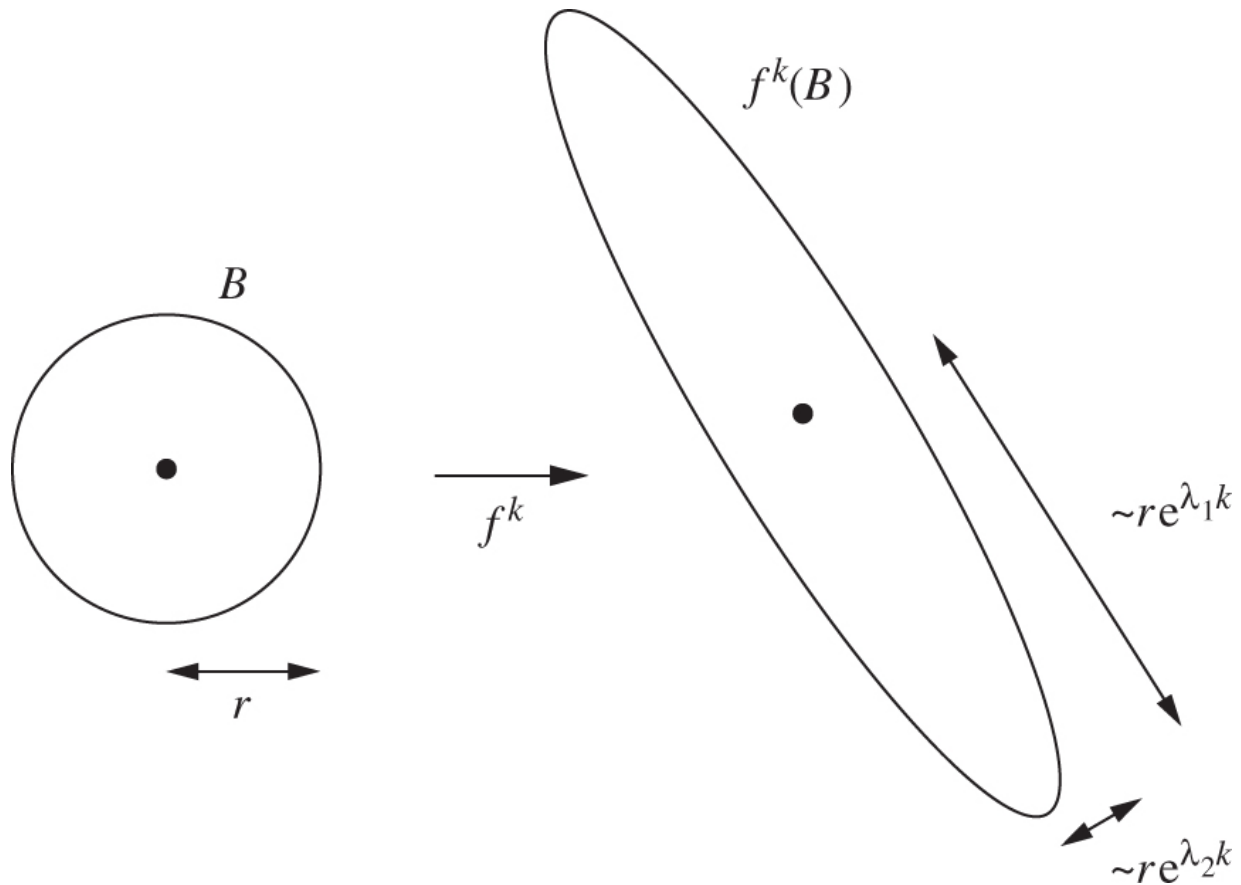


Figure 13.17 The definition of the Lyapunov exponents λ_1 and λ_2 .

A related dynamical idea is the entropy of a mapping $f : D \rightarrow D$. Write

$$V(x, \varepsilon, k) = \{y \in D : |f^i(x) - f^i(y)| < \varepsilon \text{ for } 0 \leq i \leq k\} \quad \text{13.20}$$

for the set of points with their first k iterates within ε of those of x . If μ is an invariant measure for f , we define the μ -entropy of f as

$$h_\mu(f) = \lim_{\varepsilon \rightarrow 0} \lim_{k \rightarrow \infty} \left(-\frac{1}{k} \log \mu(V(x, \varepsilon, k)) \right). \quad \text{13.21}$$

Under reasonable conditions, this limit exists and has a constant value for μ -almost all x . The entropy $h_\mu(f)$ reflects the rate at which nearby points spread out under iteration by f , or alternatively the amount of extra information about an orbit $\{f^k(x)\}_{k=1}^\infty$ that is gained from knowing the position of an additional point on the orbit.

The baker's transformation (13.4) provides a simple illustration of these ideas (the line of discontinuity makes little difference). There is a natural invariant mass distribution μ on the attractor F such that each of the 2^k strips of E_k has mass 2^{-k} , with this mass spread uniformly across the width of the E . Just as in Example 4.3, we get that $\mu(U) \leq c|U|^s$, where $s = 1 + \log 2 / (-\log \lambda)$, so by (13.17) and (13.18), $s \leq \dim_H \mu \leq \dim_H F = s$.

The Lyapunov exponents are also easily found. The derivative of (13.4) is $f'(x, y) = \begin{bmatrix} 2 & 0 \\ 0 & \lambda \end{bmatrix}$ (provided $x \neq \frac{1}{2}$), so $(f^k)'(x, y) = \begin{bmatrix} 2^k & 0 \\ 0 & \lambda^k \end{bmatrix}$ (except where $x = p/2^k$ for non-negative integers p and k). Hence, $a_k(x, y) = 2^k$ and $b_k(x, y) = \lambda^k$. By (13.19), $\lambda_1(x, y) = \log 2$ and $\lambda_2(x, y) = \log \lambda$ for μ -almost all (x, y) , so the Lyapunov exponents of the system are $\lambda_1 = \log 2$ and $\lambda_2 = \log \lambda$.

Since f^k stretches by a factor 2^k horizontally and contracts by a factor λ^k vertically, we get, using (13.20) and ignoring the 'cutting' effect of f , that, for $(x, y) \in F$, the set $V((x, y), \varepsilon, k)$ is approximately a rectangle with sides $2^{-k}\varepsilon$ and ε , which has μ -measure approximately $\varepsilon^s 2^{-k}$. Thus,

$$h_\mu(f) = \lim_{\varepsilon \rightarrow 0} \lim_{k \rightarrow \infty} \left(-\frac{1}{k} \log(\varepsilon^s 2^{-k}) \right) = \log 2.$$

The dimensions, Lyapunov exponents and entropies of an invariant measure of a dynamical system can be estimated computationally or experimentally and are often useful when comparing different systems. However, the very nature of these quantities suggests that they may not be completely independent of each other. One relationship that has been derived rigorously applies to a smooth bijective transformation f on a 2-dimensional surface. If μ is an invariant measure for f with Lyapunov exponents $\lambda_1 > 0 > \lambda_2$, then

$$\dim_H \mu = h_\mu(f) \left(\frac{1}{\lambda_1} - \frac{1}{\lambda_2} \right). \quad \textbf{13.22}$$

It is easily seen that the exponents calculated for the baker's transformation satisfy this formula.

The following relationship holds in many cases: if f is a plane transformation with attractor F and Lyapunov exponents $\lambda_1 > 0 > \lambda_2$, then

$$\dim_B F \leq 1 - (\lambda_1 / \lambda_2).$$

13.23

An argument to support this runs is as follows. Let $N_\delta(F)$ be the least number of discs of radius δ that can cover F . If $\{U_i\}$ are $N_\delta(F)$ such discs, then $f^k(F)$ is covered by the $N_\delta(F)$ sets $f^k(U_i)$, which are approximately elliptical with semi-axis lengths $\delta \exp(\lambda_1 k)$ and $\delta \exp(\lambda_2 k)$. These ellipses may be covered by approximately $\exp((\lambda_1 - \lambda_2)k)$ discs of radii $\delta \exp(\lambda_2 k)$. Hence,

$$N_{\delta \exp(\lambda_2 k)}(F) \leq \exp((\lambda_1 - \lambda_2)k) N_\delta(F)$$

so

$$\begin{aligned} \frac{\log N_{\delta \exp(\lambda_2 k)}(F)}{-\log(\delta \exp(\lambda_2 k))} &\leq \frac{\log(\exp((\lambda_1 - \lambda_2)k) N_\delta(F))}{-\log(\delta \exp(\lambda_2 k))} \\ &= \frac{(\lambda_1 - \lambda_2)k + \log N_\delta(F)}{-\lambda_2 k - \log \delta}. \end{aligned}$$

Letting $k \rightarrow \infty$ gives $\overline{\dim}_B F \leq 1 - (\lambda_1 / \lambda_2)$. This argument can often be justified, but it assumes that the Lyapunov exponents are constant across the domain D , which need not be the case.

The relationships between these and other dynamical parameters are complex, being closely interrelated with the chaotic properties of f and the fractal nature of the attractor.

The theory of multifractal measures has been introduced to analyse measures such as the invariant measures of dynamical systems. This is discussed in Chapter 17.

13.8 Notes and references

The literature on dynamical systems is vast. The classic books by Guckenheimer and Holmes (2002) and Hale and Kocak (2011) give an overview of the whole subject. Material more specific to topics in this chapter, including symbolic dynamics and the logistic map, may be found in the books by Katok and Hasselblatt (1996); Pesin (1997); Pesin and Climenhaga (2009); Brin and Stuck (2002); Devaney (2003), Peitgen, Jürgens and Saupe (2004) and Barreira and Valls (2012). The collections of papers edited by Bedford and Swift (1988) and Cvitanović (1989) highlight a variety of related aspects.

The horseshoe attractor was introduced in the fundamental paper by Smale (1967) and the Hénon attractor in Hénon and Pomeau (1976). The book by Sparrow (1982) contains a full account of the Lorenz equations.

The main theory and applications of small divisor theory are brought together in the collected papers on Hamiltonian dynamical systems, which are edited by MacKay and Meiss (1987). For results relating Lyapunov exponents to dimensions, see the papers by Young (1982); Frederickson, Kaplan, and Yorke (1983) and Barreira, Pesin and Schmeling (1999), as well as the collection edited by Mayer-Kress (2011) and the books by Pesin (1997) and Temam (2012).

Exercises

13.1 Find a fractal invariant set F for the ‘tent-like’ map $f : \mathbb{R} \rightarrow \mathbb{R}$ given by $f(x) = 2(1 - |2x - 1|)$. Show that F is a repeller for f and that f is chaotic on F . What is $\dim_H F$?

13.2 Let $f : \mathbb{R} \rightarrow \mathbb{R}$ be given by

$$f(x) = \begin{cases} 5x & (x \leq 1) \\ 10 - 5x & (1 < x < 2) \\ 5x - 10 & (x \geq 2). \end{cases}$$

Determine an IFS $S_1, S_2, S_3 : [0, 5] \rightarrow [0, 5]$ such that $f_i(x) = x$ for each i . Show that the attractor F of this IFS is a repeller for f , and determine the Hausdorff and box dimension of F .

13.3 Let $f_\lambda : [0, 1] \rightarrow \mathbb{R}$ be given by $f_\lambda(x) = \lambda \sin \pi x$. Show that for λ sufficiently large, f_λ has a repeller F , in the sense that if $x \notin F$, then $f_\lambda^k(x) \notin [0, 1]$ for some positive integer k . Find an IFS that has F as its attractor, and thus estimate $\dim_H F$ for large λ (see Section 13.2).

13.4 Investigate the iterates $f_\lambda^k(x)$ of x in $[0, 1]$ under the logistic mapping (13.2) for various values of λ and initial points x . Show that if the sequence of iterates converges, then it converges either to 0 or to $1 - 1/\lambda$. Show that if $\lambda = \frac{1}{2}$, then for all x in $(0, 1)$, the iterates converge to 0, but that if $\lambda = 2$, they converge to $\frac{1}{2}$. Show that if $\lambda = 4$, then there are infinitely many values of x in $(0, 1)$ such that $f_\lambda^k(x)$ converges to 0, infinitely many x in $(0, 1)$ for which $f_\lambda^k(x)$ converges to $\frac{3}{4}$, and infinitely many x in $(0, 1)$ for which $f_\lambda^k(x)$ does not converge. Use a programmable calculator or computer to investigate the behaviour of the orbits for other values of λ . Investigate other transformations listed at the end of Section 13.2 in a similar way.

13.5 In the cases $\lambda = 2$ and $\lambda = 4$, it is possible to obtain a simple formula for the iterates of the logistic map f_λ on $[0, 1]$. For a given $x = x_0$, we write $x_k = f_\lambda^k(x)$.

- Show that if $\lambda = 2$ and a is chosen so that $x = \frac{1}{2}(1 - \exp a)$, then the iterates are given by $x_k = \frac{1}{2}(1 - \exp(2^k a))$.
- Show that if $\lambda = 4$ and $0 \leq a < 1$ is chosen so that $x = \sin^2(\pi a)$, then $x_k = \sin^2(2^k \pi a)$. By writing $a = 0 \cdot a_1 a_2 \dots$ in binary form, show that f_4 has an unstable orbit of period p for all positive integers p and also has a dense orbit.

13.6 Consider the modified baker's transformation $f : E \rightarrow E$, where E is the unit square, given by

$$f(x, y) = \begin{cases} (2x, \lambda y) & (0 \leq x \leq \frac{1}{2}) \\ (2x - 1, \mu y + \frac{1}{2}) & (\frac{1}{2} < x \leq 1) \end{cases},$$

where $0 < \lambda, \mu < \frac{1}{2}$. Show that there is a set F that attracts all points of E , and find an expression for the Hausdorff dimension of F .

13.7 Consider the Hénon mapping (13.5) with $a = 1.4$ and $b = 0.3$. Show that the quadrilateral D with vertices $(1.32, 0.133), (-1.33, 0.42), (-1.06, -0.5)$ and $(1.245, -0.14)$ is mapped into itself by f . Use a computer to plot the iterates of a typical point in D .

13.8 With notation as in Section 13.4, consider the transformation f of the solid torus D given by

$$f(\phi, w) = \left(3\phi \pmod{2\pi}, aw + \frac{1}{2}\hat{\phi} \right),$$

where $0 < a < \frac{1}{10}$. Show that f has an attractor F of Hausdorff and box dimensions equal to $1 + \log 3 / -\log a$, and verify that f is chaotic on F .

13.9 Let $g : \mathbb{R} \rightarrow \mathbb{R}$ be a differentiable bounded function, and let $h : \mathbb{R}^2 \rightarrow \mathbb{R}^2$ be given by

$$h(t, x) = (\lambda t, \lambda^{2-s}(x - g(t)))$$

where $\lambda > 1$ and $0 < s < 2$. Show that $\text{graph } f$ is a repeller for h , where f is the function

$$f(t) = \sum_{k=0}^{\infty} \lambda^{(s-2)k} g(\lambda^k t).$$

Thus, functions of Weierstrass type (see (11.7)) can occur as invariant sets in dynamical systems.

13.10 Give an example of a mass distribution μ on $[0, 1]$ for which $\dim_H \mu < \dim_H F$, where F is the support of μ . (Hint: see Section 1.1.)

13.11 Consider the mapping $f : E \rightarrow E$, where E is the unit square, given by

$$f(x, y) = (x + y \pmod{1}, x + 2y \pmod{1}).$$

(This mapping has become known as Arnold's cat map.) Show that plane Lebesgue measure is invariant for f (i.e. f is area-preserving), and find the Lyapunov exponents of f .

13.12 Write a computer program that plots the orbits of a point x under iteration by a mapping of a region in the plane. Use it to study the attractors of the baker's transformation, the Hénon mapping and experiment with other functions.

13.13 Write a computer program to draw trajectories of the Lorenz equations (13.8). See how the trajectories change as σ, r and b are varied. Do a similar study for the Rössler equations.

Chapter 14

Iteration of complex functions—Julia sets and the Mandelbrot set

Julia sets provide a striking illustration of how a seemingly simple process can lead to highly intricate sets. Functions on the complex plane \mathbb{C} as simple as $f(z) = z^2 + c$, with c a constant, can give rise to fractals of an exotic appearance—look ahead to [Figure 14.7](#).

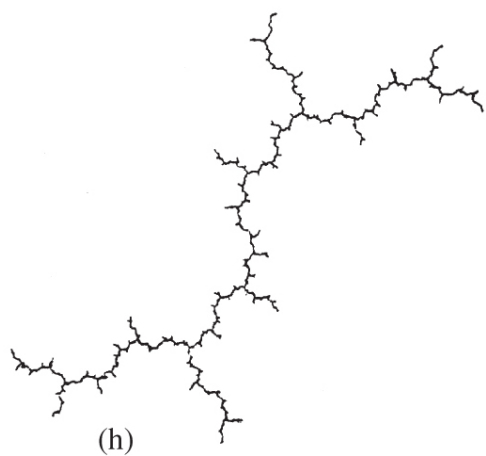
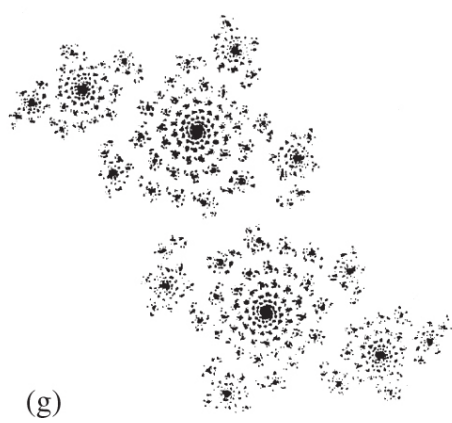
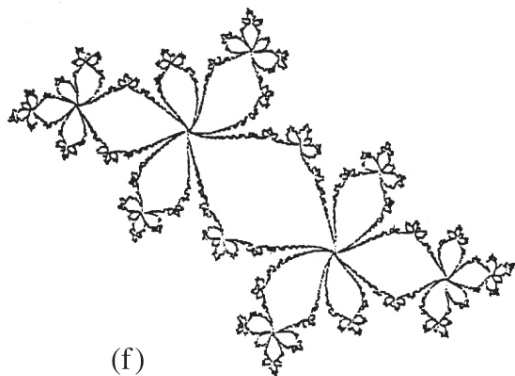
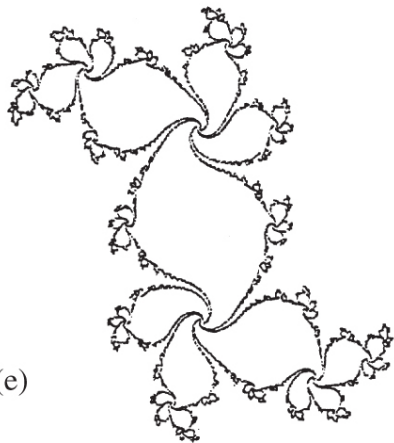
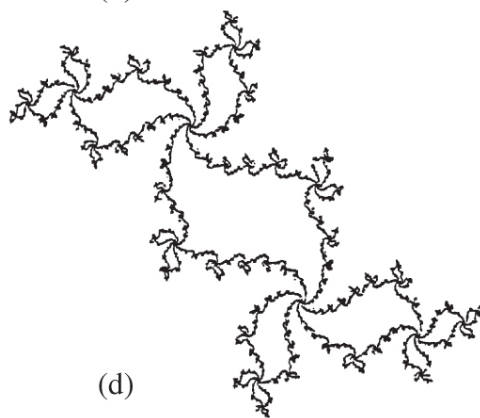
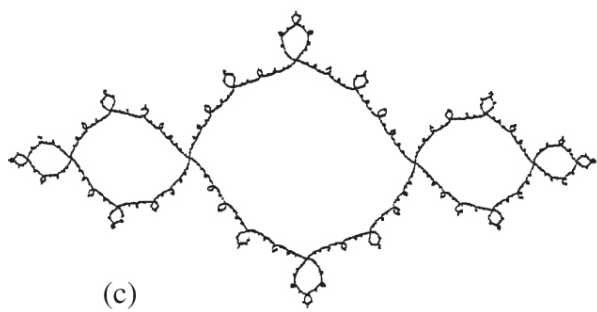
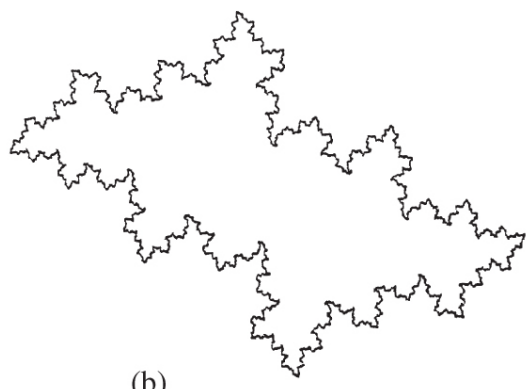
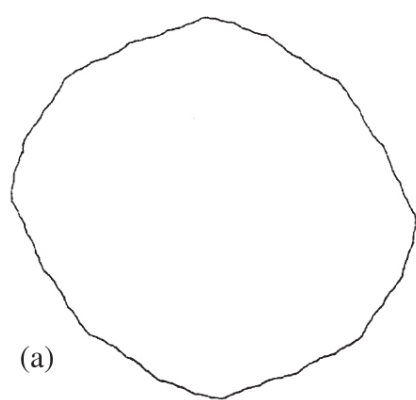


Figure 14.7 A selection of Julia sets of the quadratic function $f_c(z) = z^2 + c$. (a) $c = -0.1 + 0.1i$; f_c has an attractive fixed point, and J is a quasi-circle. (b) $c = -0.5 + 0.5i$; f_c has an attractive fixed point, and J is a quasi-circle. (c) $c = -1 + 0.05i$; f_c has an attractive period-2 orbit. (d) $c = -0.2 + 0.75i$; f_c has an attractive period-3 orbit. (e) $c = 0.25 + 0.52i$; f_c has an attractive period-4 orbit. (f) $c = -0.5 + 0.55i$; f_c has an attractive period-5 orbit. (g) $c = 0.66i$; f_c has no attractive orbits and J is totally disconnected. (h) $c = -i$; $f_c^2(0)$ is periodic and J is a dendrite.

Julia sets result from iteration of a function of a complex variable f ; in general, a Julia set is a dynamical repeller of the form discussed in the previous chapter. However, by specialising to functions that are analytic on the complex plane (i.e. differentiable in the sense that $f'(z) = \lim_{w \rightarrow 0} (f(z+w) - f(z))/w$ exists as a complex number, where $z, w \in \mathbb{C}$), we can use the powerful techniques of complex variable theory to obtain much more detailed information about the structure of these repelling sets. The celebrated Mandelbrot set then provides the key to understand the many different forms of Julia set that arise.

14.1 General theory of Julia sets

For convenience of exposition, throughout this chapter, we take $f : \mathbb{C} \rightarrow \mathbb{C}$ to be a polynomial of degree $n \geq 2$ with complex coefficients, $f(z) = a_n z^n + a_{n-1} z^{n-1} + \cdots + a_0$. Note that with minor modifications, the theory remains true if f is a rational function $f(z) = p(z)/q(z)$ (where p, q are polynomials) on the extended complex plane $\mathbb{C} \cup \{\infty\}$, and much of it holds if f is any meromorphic function (that is, a function that is analytic on \mathbb{C} except at isolated poles).

As usual we write f^k for the k -fold composition $f \circ \cdots \circ f$ of the function f , so that $f^k(z)$ is the k th iterate $f(f(\cdots(f(z))\cdots))$ of z .

Julia sets may be defined in terms of the behaviour of the iterates $f^k(z)$ for large k . First, we define the *filled-in Julia set* of the

polynomial f ,

$$K(f) = \{z \in \mathbb{C} : f^k(z) \not\rightarrow \infty\}.$$

The *Julia set* of f is the boundary of the filled-in Julia set, $J(f) = \partial K(f)$. (We write K for $K(f)$ and J for $J(f)$ when the function is clear.) Thus, $z \in J(f)$ if in every neighbourhood of z there are points w and v with $f^k(w) \rightarrow \infty$ and $f^k(v) \not\rightarrow \infty$.

The complement of the Julia set is called the *Fatou set* or *stable set* $F(f)$. This chapter investigates the geometry and structure of the Julia sets of polynomials; in particular, J is usually a fractal.

For the simplest example, let $f(z) = z^2$, so that $f^k(z) = z^{2^k}$. Clearly, $f^k(z) \rightarrow 0$ as $k \rightarrow \infty$ if $|z| < 1$ and $f^k(z) \rightarrow \infty$ if $|z| > 1$, but with $f^k(z)$ remaining on the circle $|z| = 1$ for all k if $|z| = 1$. Thus, the filled-in Julia set K is the unit disc $|z| \leq 1$, and the Julia set J is its boundary, the unit circle, $|z| = 1$. The Julia set J is the boundary between the sets of points that iterate to 0 and ∞ . Of course, in this special case, J is not a fractal.

Suppose that we modify this example slightly, taking $f(z) = z^2 + c$ where c is a small complex number. It is easy to see that we still have $f^k(z) \rightarrow w$ if z is small, where w is the fixed point of f close to 0, and that $f^k(z) \rightarrow \infty$ if z is large. Again, the Julia set is the boundary between these two types of behaviour, but it turns out that now J is a fractal curve; see [Figure 14.1](#).

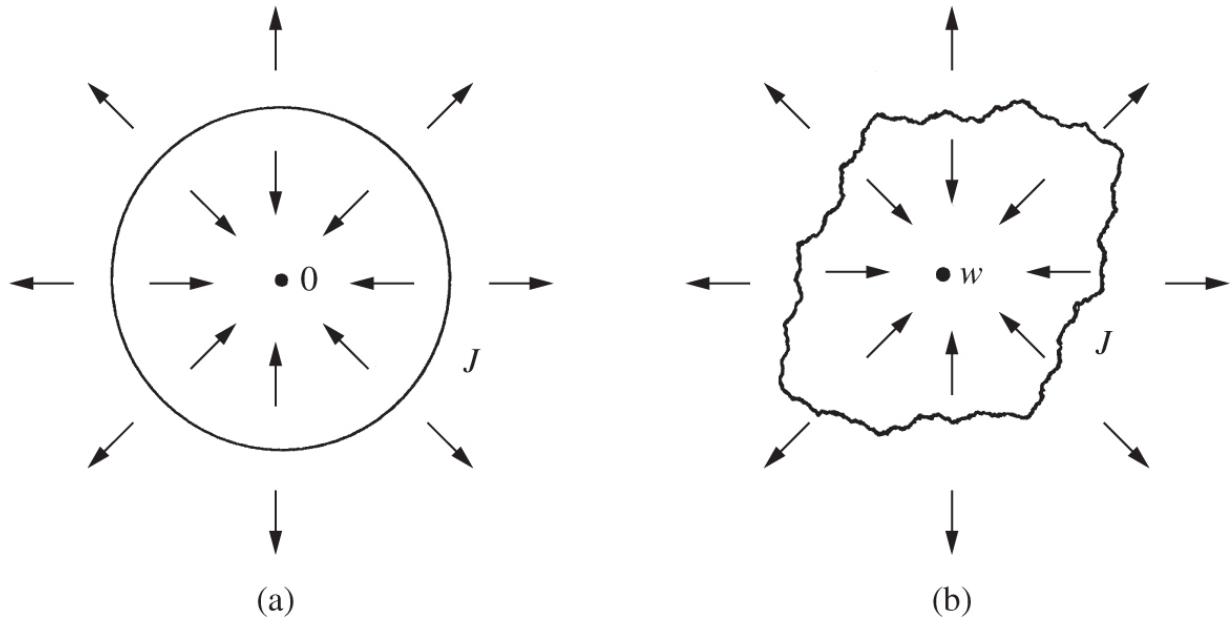


Figure 14.1 (a) The Julia set of $f(z) = z^2$ is the circle $|z| = 1$, with the iterates $f^k(z) \rightarrow 0$ if z is inside J , and $|f^k(z)| \rightarrow \infty$ if z is outside J . (b) If f is perturbed to the function $f(z) = z^2 + c$ for small c , this picture distorts slightly, with a curve J separating those points z for which $f^k(z)$ converges to the fixed point w of f near 0 from those points z with $|f^k(z)| \rightarrow \infty$. The curve J is now a fractal.

We shall need some terminology about fixed and periodic points of f . Recall that if $f(w) = w$, we call w a *fixed point* of f , and if $f^p(w) = w$ for some integer $p \geq 1$, we call w a *periodic point* of f ; the least such p is called the *period* of w . We call $w, f(w), \dots, f^p(w)$ a *period p orbit*. Let w be a periodic point of period p , with $(f^p)'(w) = \lambda$, where the prime denotes complex differentiation. The point w is called *attractive* if $0 \leq |\lambda| < 1$, in which case nearby points are attracted to the orbit under iteration by f , and *repelling* if $|\lambda| > 1$, in which case points close to the orbit move away. The study of sequences $f^k(z)$ for various initial z is known as *complex dynamics*. The position of z relative to the Julia set $J(f)$ is a key to this behaviour.

The following lemma is extremely useful in determining whether a sequence iterates to infinity, that is, whether points are outside the filled-in Julia set.

Lemma 14.1

Given a polynomial $f(z) = a_n z^n + a_{n-1} z^{n-1} + \cdots + a_0$ with $n \geq 2$ and $a_n \neq 0$, there exists a number r such that if $|z| \geq r$, then $|f(z)| \geq 2|z|$. In particular, if $|f^m(z)| \geq r$ for some $m \geq 0$, then $f^k(z) \rightarrow \infty$ as $k \rightarrow \infty$. Thus, either $f^k(z) \rightarrow \infty$ or the set $\{f^k(z) : k = 0, 1, 2, \dots\}$ is bounded.

Proof

We may choose r sufficiently large to ensure that if $|z| \geq r$, then $\frac{1}{2}|a_n||z|^n \geq 2|z|$ and $(|a_{n-1}||z|^{n-1} + \cdots + |a_1||z| + |a_0|) \leq \frac{1}{2}|a_n||z|^n$. Then, if $|z| \geq r$,

$$\begin{aligned}|f(z)| &\geq |a_n||z|^n - (|a_{n-1}||z|^{n-1} + \cdots + |a_1||z| + |a_0|) \\ &\geq \frac{1}{2}|a_n||z|^n \geq 2|z|.\end{aligned}$$

Furthermore, if $|f^m(z)| \geq r$ for some m , then applying this inductively, we get $|f^{m+k}(z)| \geq 2^m |f^k(z)| \geq r$, so $f^k(z) \rightarrow \infty$.

Some basic observations on the structure of the filled-in Julia set and the Julia set follow easily.

Proposition 14.2

Let $f(z)$ be a polynomial. Then, the filled-in Julia set $K(f)$ and the Julia set $J(f)$ are non-empty and compact, with $J(f) \subset K(f)$. Furthermore, $J(f)$ has an empty interior.

Proof

With r given by Lemma 14.1, it is immediate from the lemma that K is contained in the disc $B(0, r)$ and so is bounded, as is its boundary J .

If $z \notin K$, then $f^k(z) \rightarrow \infty$, so $|f^m(z)| > r$ for some integer m . By continuity of f^m , $|f^m(w)| > r$ for all w in a sufficiently small disc centred at z , so for such w , $f^k(w) \rightarrow \infty$ by Lemma 14.1, giving that $w \notin K$. Thus, the complement of K is open, so K is closed. As the boundary of K , the Julia set J is closed and contained in K . Thus, K and J are closed and bounded, and so are compact.

The equation $f(z) = z$ has at least one solution z_0 , say, so $f^k(z_0) = z_0$ for all k , so $z_0 \in K$ and K is non-empty. Let $z_1 \in \mathbb{C} \setminus K$. Then, the point $\lambda z_0 + (1 - \lambda)z_1$ on the line joining z_0 and z_1 will lie on the boundary of K for some $0 \leq \lambda \leq 1$; taking λ as the infimum value for which $\lambda z_0 + (1 - \lambda)z_1 \in K$ will do. Thus, $J = \partial K$ is non-empty.

Finally, if J has non-empty interior, there is a non-empty open set $U \subset J \subset K$, so U lies in the interior of K and has empty intersection with its boundary J , a contradiction.

Hardly surprisingly, $J(f)$ gets mapped onto itself by f and its inverse.

Proposition 14.3

The Julia set $J = J(f)$ off is forward and backward invariant under f , that is, $J = f(J) = f^{-1}(J)$.

Proof

Let $z \in J$. Then, $f^k(z) \not\rightarrow \infty$, and we may find $w_n \rightarrow z$ with $f^k(w_n) \rightarrow \infty$ as $k \rightarrow \infty$ for all n . Thus, $f^k(f(z)) \not\rightarrow \infty$ and $f^k(f(w_n)) \rightarrow \infty$, where by continuity of f , $f(w_n)$ can be chosen as close as we like to $f(z)$. Thus, $f(z) \in J$, so $f(J) \subset J$, which also implies $J \subset f^{-1}(f(J)) \subset f^{-1}(J)$.

Similarly, with z and w_n as above, if $f(z_0) = z$, then we may find $v_n \rightarrow z_0$ with $f(v_n) = w_n$ by the mapping properties of polynomials on \mathbb{C} . Hence, $f^k(z_0) = f^{k-1}(z) \not\rightarrow \infty$ and $f^k(v_n) = f^{k-1}(w_n) \rightarrow \infty$ as $k \rightarrow \infty$, so $z_0 \in J$. Thus, $f^{-1}(J) \subset J$ which implies $J = f(f^{-1}(J)) \subset f(J)$.

Proposition 14.4

$J(f^p) = J(f)$ for every positive integer p .

Proof

It follows from Lemma 14.1 that $f^k(z) \rightarrow \infty$ if and only if $(f^p)^k(z) = f^{kp}(z) \rightarrow \infty$. Thus, f and f^p have identical filled-in Julia sets and so identical Julia sets.

To develop the theory of Julia sets much further, we cannot avoid introducing some technical tools from complex variable theory, in particular, normal families of analytic functions and Montel's theorem.

**Readers who wish to omit fairly technical arguments on complex analytic functions should skip to Summary 14.12.*

Let U be an open subset of \mathbb{C} , and let $g_k : U \rightarrow \mathbb{C}$ ($k = 1, 2, \dots$) be a family of complex analytic functions (i.e. functions differentiable on

U in the complex sense). The family $\{g_k\}$ is said to be *normal on U* if every sequence of functions selected from $\{g_k\}$ has a subsequence that converges uniformly on every compact subset of U , either to a bounded analytic function or to ∞ . Notice that by standard complex variable theory, this means that the subsequence converges either to a finite analytic function or to ∞ on each connected component of U . In the former case, the derivatives of the subsequence must converge to the derivative of the limit function. The family $\{g_k\}$ is *normal at the point w of U* if there is some open subset V of U containing w such that $\{g_k\}$ is a normal family on V . Observe that this is equivalent to there being a neighbourhood V of w on which every sequence $\{g_k\}$ has a subsequence convergent to a bounded analytic function or to ∞ .

The key result which we will use repeatedly in our development of Julia sets is the remarkable theorem of Montel, which asserts that non-normal families of functions take virtually all complex values.

Montel's theorem 14.5

Let $\{g_k\}$ be a family of complex analytic functions on an open domain U . If $\{g_k\}$ is not a normal family, then for all $w \in \mathbb{C}$ with at most one exception we have $g_k(z) = w$ for some $z \in U$ and some k .

Proof

Consult the literature on complex function theory.

Montel's theorem quickly leads to the following characterisation of a Julia set.

Proposition 14.6

$$J(f) = \{z \in \mathbb{C} : \text{the family } \{f^k\} \text{ is not normal at } z\}.$$

[14.1](#)

Proof

If $z \in J$, then in every neighbourhood V of z , there are points w such that $f^k(w) \rightarrow \infty$, whilst $f^k(z)$ remains bounded. Thus, no subsequence of $\{f^k\}$ is uniformly convergent on V , so that $\{f^k\}$ is not normal at z .

Suppose that $z \notin J$. Either $z \in \text{int } K$, in which case, taking an open set V with $z \in V \subset \text{int } K$, we have $f^k(w) \in K$ for all $w \in V$ and all k , so by Montel's theorem 14.5, $\{f^k\}$ is normal at w . Otherwise, $z \in \mathbb{C} \setminus K$, so $|f^k(z)| > r$ for some k , where r is given by Lemma 14.1, so $|f^k(w)| > r$ for all w in some neighbourhood V of z , so by Lemma 14.1, $f^k(w) \rightarrow \infty$ uniformly on V , so again $\{f^k\}$ is normal at w .

The expression (14.1) is normally taken as the definition of the Julia set in more advanced work, since it is more widely applicable and lends itself to techniques from complex analysis. Then, the theory developed from Montel's theorem extends to a wide class of complex functions including rational functions and meromorphic functions. Note, however, that if $f : \mathbb{C} \cup \{\infty\} \rightarrow \mathbb{C} \cup \{\infty\}$ is a rational function, then J must be closed, but need not be bounded. Indeed, it is possible for J to be the whole complex plane; for example, if $f(z) = ((z - 2)/z)^2$.

The main aim now is to obtain a further characterisation of the Julia set $J(f)$ as the closure of the repelling periodic points of f . On the way, we encounter further interesting properties of Julia sets; for example, our next result tells that f is ‘mixing’ near $J(f)$, that is,

neighbourhoods of points of $J(f)$ are spread right across \mathbb{C} by iterates of f .

Lemma 14.7

Let f be a polynomial, let $w \in J(f)$, and let U be any neighbourhood of w . Then, for each $j = 1, 2, \dots$, the set $W \equiv \bigcup_{k=j}^{\infty} f^k(U)$ is the whole of \mathbb{C} , except possibly for a single point. Any such exceptional point is not in $J(f)$, and is independent of w and U .

Proof

By Proposition 14.6, the family $\{f^k\}_{k=j}^{\infty}$ is not normal at w , so the first part is immediate from Montel's theorem 14.5.

Suppose $v \notin W$. If $f(z) = v$, then, since $f(W) \subset W$, it follows that $z \notin W$. As $\mathbb{C} \setminus W$ consists of at most one point, then $z = v$. Hence, f is a polynomial of degree n such that the only solution of $f(z) - v = 0$ is v , which implies that $f(z) - v = c(z - v)^n$ for some constant c .

If z is sufficiently close to v , then $f^k(z) - v \rightarrow 0$ as $k \rightarrow \infty$, convergence being uniform on, say, $\{z : |z - v| < (2c)^{-1/(n-1)}\}$. Thus, $\{f^k\}$ is normal at v , so the exceptional point $v \notin J(f)$. Clearly, v only depends on the polynomial f . (In fact, if W omits a point v of \mathbb{C} , then $J(f)$ is the circle with centre v and radius $c^{-1/(n-1)}$.)

The following corollary is the basis for many computer pictures of Julia sets; see Section 14.3. Note that, for a polynomial f of degree n , the set $f^{-1}(z)$ contains n points, that is, the solutions of $f(w) = z$, except when this equation has multiple roots. Thus, the set $f^{-k}(z)$ is large, ‘typically’ containing n^k points.

Corollary 14.8

- a. *The following holds for all $z \in \mathbb{C}$ with at most one exception: if U is an open set that intersects $J(f)$ then $f^{-k}(z)$ intersects U for infinitely many values of k . If there is an exceptional point z , it cannot be in $J(f)$.*
- b. *If $z \in J(f)$, then $J(f)$ is the closure of $\bigcup_{k=1}^{\infty} f^{-k}(z)$.*

Proof

- a. Provided z is not the exceptional point of Lemma 14.7, $z \in f^k(U)$, and thus $f^{-k}(z)$ intersects U , for some k . Applying this repeatedly to such inverse iterates, we can obtain ever larger integers k for which this is the case.
- b. If $z \in J(f)$, then $f^{-k}(z) \subset J(f)$, by Proposition 14.3, so that $\bigcup_{k=1}^{\infty} f^{-k}(z)$ and, therefore, its closure is contained in the closed set $J(f)$. On the other hand, if $z \in J(f)$ and U is any open set that intersects $J(f)$, then $f^{-k}(z)$ intersects U for some k by part (a), so $J(f)$ is in the closure of $\bigcup_{k=1}^{\infty} f^{-k}(z)$.

Proposition 14.9

$J(f)$ is a perfect set (i.e. closed and with no isolated points) and is therefore uncountable.

Proof

Let $v \in J(f)$ and let U be an open neighbourhood of v . We must show that U contains other points of $J(f)$. We consider three cases separately.

- i. v is not a fixed or periodic point of f . By Corollary 14.8(b) and Proposition 14.3, U contains a point of $f^{-k}(v) \subset J(f)$ for some $k \geq 1$, and this point must be different from v .
- ii. $f(v) = v$. If $f(z) = v$ has no solution other than v , then, just as in the proof of Lemma 14.7, $v \notin J(f)$. Thus, there exists $w \neq v$ with $f(w) = v$. By Corollary 14.8(b), U contains a point u of $f^{-k}(w) = f^{-k-1}(v)$ for some $k \geq 1$. Any such u is in $J(f)$ by backward invariance and is distinct from v , since
$$f^k(v) = v \neq w = f^k(u).$$
- iii. $f^p(v) = v$ for some $p > 1$. By Proposition 14.4, $J(f) = J(f^p)$, so by applying (ii) to f^p , we see that U contains points of $J(f^p) = J(f)$ other than v .

Thus, $J(f)$ has no isolated points; since it is closed, it is perfect. Finally, every perfect set is uncountable; see Exercise 14.1.

We can now prove the main result of this section, that the Julia set $J(f)$ is the closure of the repelling periodic points of f .

Theorem 14.10

For a polynomial f , the Julia set $J(f)$ is the closure of the repelling periodic points of f .

Proof

Let w be a repelling periodic point of f of period p , so w is a repelling fixed point of $g = f^p$. Suppose that $\{g^k\}$ is normal at w , then w has an open neighbourhood V on which a subsequence $\{g^{k_i}\}$ converges to a finite analytic function g_0 (it cannot converge to ∞ since $g^k(w) = w$ for all k). By a standard result from complex analysis, the derivatives also converge, $(g^{k_i})'(z) \rightarrow g'_0(z)$, for $z \in V$. However, by the chain rule, $|(g^{k_i})'(w)| = |(g'(w))^{k_i}| \rightarrow \infty$ since w is a repelling fixed point and $|g'(w)| > 1$. This contradicts the finiteness of $g'_0(w)$, so $\{g^k\}$ cannot be normal at w . Thus, $w \in J(g) = J(f^p) = J(f)$ using Proposition 14.4. Since $J(f)$ is closed, it follows that the closure of the repelling periodic points is a subset of $J(f)$.

Let $E = \{w \in J(f) \text{ such that there exists } v \neq w \text{ with } f(v) = w \text{ and } f'(v) \neq 0\}$. Suppose that $w \in E$. Then, there is an open neighbourhood V of w on which we may find a local analytic inverse $f^{-1} : V \rightarrow \mathbb{C} \setminus W$, so that $f^{-1}(w) = v \neq w$ (just choose values of $f^{-1}(z)$ in a continuous manner). Define a family of analytic functions $\{h_k\}$ on V by

$$h_k(z) = \frac{(f^k(z) - z)}{(f^{-1}(z) - z)};$$

provided V is chosen to be a sufficiently small neighbourhood of w the denominator will be non-zero. Let U be any open neighbourhood of w with $U \subset V$. Since $w \in J(f)$, the family $\{f^k\}$ and thus, from the definition, the family $\{h_k\}$ is not normal on U . By Montel's theorem 14.5, $h_k(z)$ must take either the value 0 or 1 for some k and $z \in U$. In the first case, $f^k(z) = z$ for some $z \in U$; in the second case, $f^k(z) = f^{-1}(z)$, so $f^{k+1}(z) = z$ for some $z \in U$. Thus, U contains a periodic point of f , so w is in the closure of the repelling periodic points of f for all $w \in E$.

Since f is a polynomial, E contains all of $J(f)$ except for a finite number of points. Since $J(f)$ contains no isolated points, by

Proposition 14.9, $J(f) \subset \overline{E}$ is a subset of the closure of the repelling periodic points.

If w is an attractive fixed point of f , we write

$$A(w) = \{z \in \mathbb{C} : f^k(z) \rightarrow w \text{ as } k \rightarrow \infty\} \quad \mathbf{14.2}$$

for the *basin of attraction* of w . We define the basin of attraction of infinity, $A(\infty)$, in the same way. Since w is attractive, there is an open set V containing w in $A(w)$ (if $w = \infty$, we may take $\{z : |z| > r\}$, for sufficiently large r). This implies that $A(w)$ is open since if $f^k(z) \in V$ for some k , then $z \in f^{-k}(V)$, which is open.

The following characterisation of J as the boundary of any basin of attraction is extremely useful in determining Julia sets. Particularly significant is that, even though the domain of attraction may have many connected components, its boundary is the entire Julia set and not just part of it. Recall the notation ∂A for the boundary of the set A .

Lemma 14.11

Let w be an attractive fixed point of f . Then, $\partial A(w) = J(f)$. The same is true if $w = \infty$.

Proof

If $z \in J(f)$, then $f^k(z) \in J(f)$ for all k and so cannot converge to an attractive fixed point, and $z \notin A(w)$. However, if U is any neighbourhood of z , the set $f^k(U)$ contains points of $A(w)$ for some k by Lemma 14.7, so there are points arbitrarily close to z that iterate to w . Thus, $z \in \overline{A(w)}$ and so $z \in \partial A(w)$.

Suppose $z \in \partial A(w)$ but $z \notin J(f)$. Then, z has a connected open neighbourhood V on which $\{f^k\}$ has a subsequence convergent either to an analytic function or to ∞ . The subsequence converges to w on $V \cap A(w)$, which is open and non-empty, and therefore on V , since an analytic function is constant on a connected set if it is constant on any open subset. All points of V are mapped into $A(w)$ by iterates of f , so $V \subset A(w)$, contradicting that $z \in \partial A(w)$.

For an example of this lemma, recall the case $f(z) = z^2$. The Julia set is the unit circle, which is the boundary of both $A(0)$ and $A(\infty)$.

We summarise the main points of this section.

Summary 14.12

The Julia set $J(f)$ of the polynomial f is the boundary of the set of points $z \in \mathbb{C}$ such that $f^k(z) \rightarrow \infty$. It is an uncountable non-empty compact set containing no isolated points and is invariant under f and f^{-1} , with $J(f) = J(f^p)$ for each positive integer p . If $z \in J(f)$, then $J(f)$ is the closure of $\bigcup_{k=1}^{\infty} f^{-k}(z)$. The Julia set is the boundary of the basin of attraction of each attractive fixed point of f , including ∞ , and is the closure of the repelling periodic points of f .

Proof

This collects together the results of this section.

It is possible to discover a great deal more about the dynamics of f both on and off the Julia set. It may be shown that ' f ' acts chaotically on J' (see Chapter 13). Periodic points of f are dense in J but, on the other hand, J contains points z with iterates $f^k(z)$ that are dense in J . Moreover, f has 'sensitive dependence on initial conditions' on J ; thus, $|f^k(z) - f^k(w)|$ will be large for certain k regardless of how close $z, w \in J$ are, making accurate computation of iterates impossible.

14.2 Quadratic functions—the Mandelbrot set

We now specialise to quadratic functions on \mathbb{C} . We study Julia sets of polynomials of the form

$$f_c(z) = z^2 + c, \quad 14.3$$

where c is a complex constant. This is not as restrictive as it first appears: if $h(z) = \alpha z + \beta$ ($\alpha \neq 0$) then

$$h^{-1}(f_c(h(z))) = (\alpha^2 z^2 + 2\alpha\beta z + \beta^2 + c - \beta)/\alpha.$$

By choosing appropriate values of α, β and c , we can make this expression into any quadratic function f that we please. Then, $h^{-1} \circ f_c \circ h = f$, so $h^{-1} \circ f_c^k \circ h = f^k$ for all k . This means that the sequence of iterates $\{f^k(z)\}$ of a point z under f is just the image under h^{-1} of the sequence of iterates $\{f_c^k(h(z))\}$ of the point $h(z)$ under f_c . The mapping h transforms the dynamical picture of f to that of f_c in a linear manner. In particular, $f^k(z) \rightarrow \infty$ if and only if $f_c^k(z) \rightarrow \infty$; thus, the Julia set of f is the image under h^{-1} of the Julia set of f_c .

The transformation h is called a *conjugacy* between f and f_c . Any quadratic function is conjugate to f_c for some c , so, by studying the Julia sets of f_c for $c \in \mathbb{C}$, we effectively study the Julia sets of all quadratic polynomials. Since h is a similarity transformation, the Julia set of any quadratic polynomial is geometrically similar to that of f_c for some $c \in \mathbb{C}$.

It should be borne in mind throughout this section that $f_c^{-1}(z)$ takes two distinct values $\pm(z - c)^{1/2}$, called the two *branches* of $f_c^{-1}(z)$, except when $z = c$. Thus, if U is a small open set with $c \notin U$, then the pre-image $f_c^{-1}(U)$ has two parts, both of which are mapped bijectively and smoothly by f_c onto U .

We define the *Mandelbrot set* M to be the set of parameters c for which the Julia set of f_c is connected

$$M = \{c \in \mathbb{C} : J(f_c) \text{ is connected}\}.$$

14.4

At first, M appears to relate to one rather specific property of $J(f_c)$. In fact, as we shall see, M contains an enormous amount of information about the structure of Julia sets.

The definition (14.4) is awkward for computational purposes. We derive an equivalent definition that is much more useful for determining whether a parameter c lies in M and for investigating the extraordinarily intricate form of M ; see Figure 14.2: we show that $c \in M$ if and only if $f_c^k(0) \not\rightarrow \infty$.

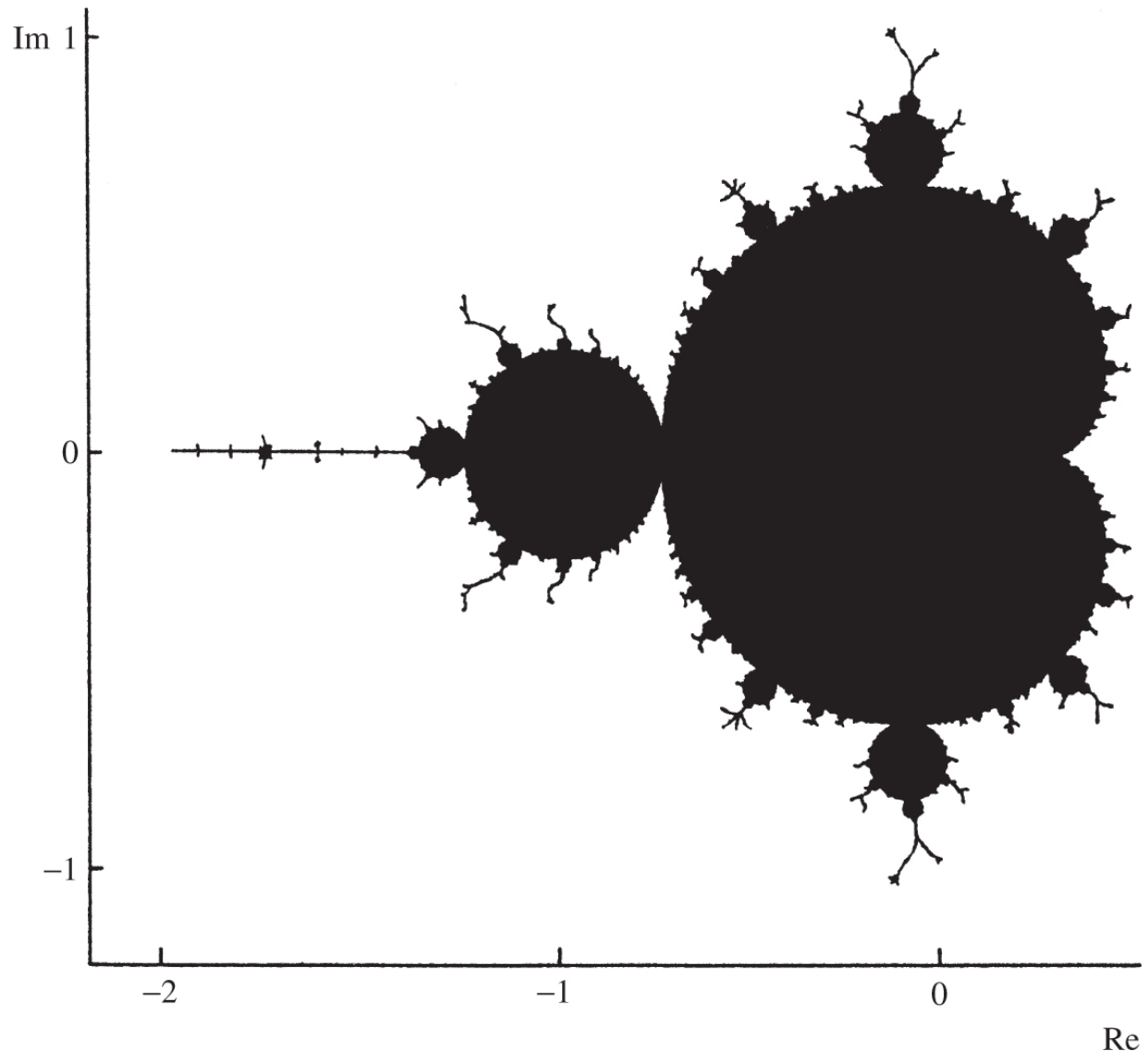


Figure 14.2 The Mandelbrot set M in the complex plane.

To do this, we first need to know a little about the effect of the transformation f_c on smooth curves. For brevity, we term a smooth (i.e. differentiable), closed, simple (i.e. non-self-intersecting) curve in the complex plane a *loop*. We refer to the parts of \mathbb{C} inside and outside such a curve as the *interior* and *exterior* of the loop.

Lemma 14.13

Let C be a loop in the complex plane.

- a. If c is inside C , then $f_c^{-1}(C)$ is a loop. Moreover, f_c maps the interior of $f_c^{-1}(C)$ onto the interior of C and the exterior of $f_c^{-1}(C)$ onto the exterior of C .
- b. If c is outside C , then $f_c^{-1}(C)$ comprises two disjoint loops, neither contained inside the other. Moreover f_c maps the interior of each loop of $f_c^{-1}(C)$ onto the interior of C and the region outside these two loops onto the exterior of C .

Proof

Note that $f_c^{-1}(z) = \pm(z - c)^{1/2}$ and $(f_c^{-1})'(z) = \pm\frac{1}{2}(z - c)^{-1/2}$, which is finite and non-zero if $z \neq c$. Hence, provided $c \notin C$, if we select one of the two branches of f_c^{-1} , the set $f_c^{-1}(C)$ is locally a smooth curve.

Assume that c does not lie on C . Choose an initial point w on C and let z_0 and $-z_0$ be the two values of $f_c^{-1}(w)$. Starting at w , as z moves around the curve C , the two values of $f_c^{-1}(z)$ vary continuously with z and trace out two ‘inverse image’ curves, C^+ and C^- , which are symmetrical with each other about the origin (i.e. $u \in C^+$ if and only if $-u \in C^-$). When z completes a circuit of C and returns to w , the inverse image curves C^+ and C^- end at the two values of $f_c^{-1}(w)$, that is, at z_0 and $-z_0$ in some order. There are two possibilities.

- a. The inverse image curve C^+ starts at z_0 and ends at $-z_0$ and C^- starts at $-z_0$ and ends at z_0 . Joining the two curves C^+ and C^- together at their end points gives a single loop, which comprises the whole of $f_c^{-1}(C)$. Since f_c is a continuous function that maps this loop $f_c^{-1}(C)$, and no other points, onto the loop C , the polynomial f_c must map the interior and exterior of $f_c^{-1}(C)$ onto the interior and exterior of C , respectively. As the two portions C^+ and C^- of $f_c^{-1}(C)$ are symmetric to each other with respect to 0 , the point 0 must lie inside $f_c^{-1}(C)$ and so $c = f_c(0)$ lies inside C .
- b. The inverse image curve C^+ starts at z_0 and ends at z_0 and C^- starts at $-z_0$ and ends at $-z_0$, that is, C^+ and C^- are both closed loops which are disjoint from each other and symmetric to each other about 0 . Then, f_c maps the interior of both of these loops onto the interior of C , and the region outside C^+ and C^- onto the exterior of C . The origin 0 cannot lie inside

either C^+ or C^- , otherwise it would have to be inside both, so $c = f_c(0)$ lies outside C .

In the context of the Lemma 14.13, we remark that if c lies on C , then $f_c^{-1}(C)$ is a ‘figure of eight’, that is a smooth closed curve with a single point of self-intersection.

We now prove the ‘fundamental theorem of the Mandelbrot set’, which characterises M in terms of iterates of f_c .

Theorem 14.14

For $c \in \mathbb{C}$, the Julia set $J(f_c)$ is connected if the sequence of iterates $\{f_c^k(0)\}_{k=1}^\infty$ is bounded and is totally disconnected otherwise. Thus:

$$M = \{c \in \mathbb{C} : J(f_c) \text{ is connected}\} \quad \mathbf{14.5}$$

$$= \{c \in \mathbb{C} : \{f_c^k(0)\}_{k=1}^\infty \text{ is bounded}\} \quad \mathbf{14.6}$$

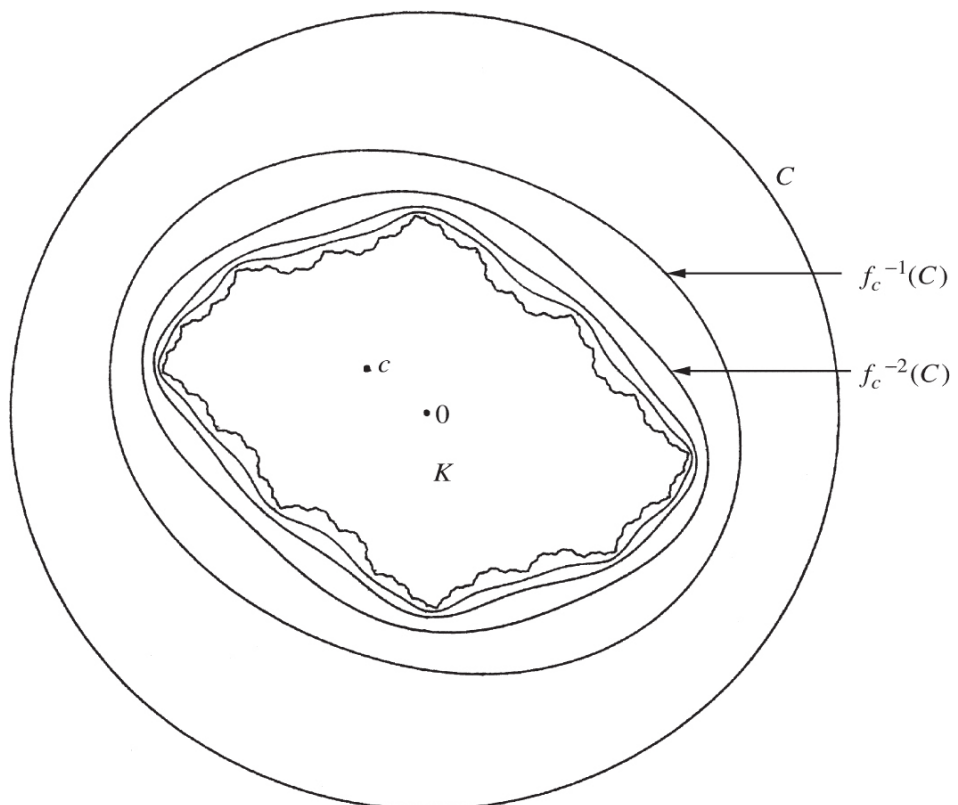
$$= \{c \in \mathbb{C} : f_c^k(0) \not\rightarrow \infty \text{ as } k \rightarrow \infty\}. \quad \mathbf{14.7}$$

Proof

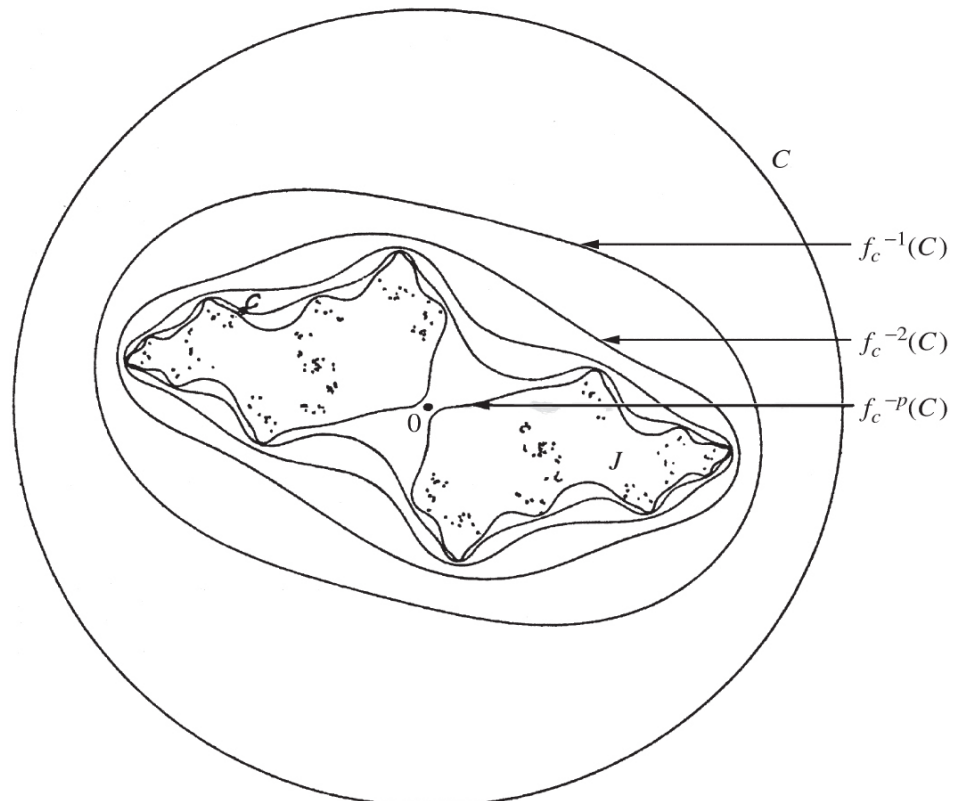
It is clear from Lemma 14.1 that $f_c^k(0) \not\rightarrow \infty$ if and only if $\{f_c^k(0)\}$ is bounded, so (14.6) and (14.7) are equal.

- a. We first show that if $\{f_c^k(0)\}_{k=1}^\infty$ is bounded, then $J(f_c)$ is connected. Let C be a large circle in \mathbb{C} such that all the points $\{f_c^k(0)\}$ lie inside C , such that $f_c^{-1}(C)$ is interior to C and such that points outside C are iterated to ∞ by f_c^k . We show that the sequence of loops $\{f_c^{-k}(C)\}_{k=0}^\infty$ ‘home in’ onto the Julia set. Since $c = f_c(0)$ is inside C , Lemma 14.13(a) gives that $f_c^{-1}(C)$ is a loop contained in the interior of C and also that c is inside $f_c^{-1}(C)$, for otherwise $f_c(c) = f_c^2(0)$ would be outside C . Applying Lemma 14.13(a) again, $f_c^{-2}(C)$ is a loop contained in the interior of $f_c^{-1}(C)$ with c inside $f_c^{-2}(C)$. Proceeding in this way, we see that $\{f_c^{-k}(C)\}$ consists of a sequence of loops, each in the interior of its predecessor ([Figure 14.3a](#)). Let K denote the closed set of points that are on or inside the loops $f_c^{-k}(C)$ for all k . If $z \in K$, then $f_c^k(z)$ lies inside C for all k , but if $z \notin K$, then z is outside one of the loops $f_c^{-k}(C)$ for some k , so $f_c^k(z)$ is outside C and $f_c^k(z) \rightarrow \infty$. Thus, K is the filled-in Julia set of f_c . But K is the intersection of a decreasing sequence of closed simply connected sets (i.e. sets that are connected and have connected complement), so, by a simple topological argument, K is simply connected and therefore has connected boundary. Thus, $J(f_c)$ is connected.
- b. Now suppose that $\{f_c^k(0)\}_{k=1}^\infty$ is unbounded; we show, using a fairly similar approach to (a), that $J(f_c)$ is not connected. Let C be a large circle such that $f_c^{-1}(C)$ is inside C , such that all points outside C iterate to ∞ , and such that none of the iterates $f_c^k(0)$ lie on C . Let p be the least integer such that $f_c^p(0)$ is outside C . Just as in the first part of the proof, we construct a series of loops $\{f_c^{-k}(C)\}$, each containing the next

in its interior ([Figure 14.3](#)b). However, the argument breaks down when we get to the loop $f_c^{1-p}(C)$ since $c = f(0)$ is outside the loop $f_c^{1-p}(C)$ and we have to apply Lemma 14.13(b) rather than Lemma 14.13(a). Thus, we get that $f_c^{-p}(C)$ consists of two disjoint loops inside the loop $f_c^{1-p}(C)$, with f_c mapping the interior of these loops onto the interior of $f_c^{1-p}(C)$. The Julia set $J(f_c)$ lies inside these loops since points outside iterate to infinity. Since $J(f_c)$ is invariant under f_c^{-1} , parts of it must be contained in each of these loops, so $J(f_c)$ is not connected. In fact, if we continue to apply Lemma 14.13(b), we see that the Julia set $J(f_c)$ lies inside a ‘Cantor-like’ hierarchy of pairs of disjoint loops within loops, so is totally disconnected.



(a)



(b)

Figure 14.3 Inverse iterates of a circle c under f_c , illustrating the two parts of the proof of Theorem 14.14: (a) $c = -0.3 + 0.3i$; (b) $c = -0.9 + 0.5i$.

The reason for considering the iterates of the origin in (14.6) and (14.7) is that the origin is the *critical point* of f_c for each c , that is, the point for which $f'_c(z) = 0$. The critical points are the points where f_c fails to be a local bijection—a property that was crucial in distinguishing the two cases in the proof of Theorem 14.14 and which is crucial in analysing the dynamics of any polynomial or meromorphic function.

The equivalent definition of M provided by (14.6) is the basis of computer pictures of the Mandelbrot set. Choose numbers $r > 2$ and k_0 of the order of, say, 100. For each c , compute successive terms of the sequence $\{f_c^k(0)\}$ until either $|f_c^k(0)| \geq r$, in which case $c \notin M$, noting Exercise 14.12, or $k = k_0$, in which case we deem c to be in M . Repeating this process for values of c across a region enables a picture of M to be drawn. Often colours are assigned to the complement of M depending on the first integer k for which $|f_c^k(0)| \geq r$.

Pictures of the Mandelbrot set (see Figure 14.2) suggest that it has a highly complicated form. It has certain obvious features: a main cardioid to which a series of prominent circular ‘buds’ are attached. Each of these buds is surrounded by further buds, and so on. However, this is not all. In addition, fine, branched ‘hairs’ grow outwards from the buds, and these hairs carry miniature copies of the entire Mandelbrot set along their length.

14.3 Julia sets of quadratic functions

In this section, we will see a little of how the structure of the Julia set $J(f_c)$ varies according to where the parameter c is the complex plane. In particular, the significance of the various parts of the Mandelbrot set will start to become apparent.

The attractive periodic points of f_c are crucial to the form of $J(f_c)$. It may be shown (see Exercise 14.17) that if $w \neq \infty$ is an attractive periodic point of a polynomial f , then there is a critical point z (a point with $f'(z) = 0$) such that $f^k(z)$ is attracted to the periodic orbit containing w . Since the only critical point of f_c is 0, f_c can have at most one attractive periodic orbit. Moreover, if $c \notin M$ then, by Theorem 14.14, $f_c^k(0) \rightarrow \infty$, so f_c can have no attractive periodic orbit. It is conjectured that the set of c for which f_c has an attractive periodic orbit fills the interior of M .

It is natural to categorise f_c by the period p of the (finite) attractive orbit, and indeed the values of c corresponding to different p may be identified as different regions of the Mandelbrot set M .

Firstly, suppose that c lies outside M , so f_c has no attractive periodic points. By definition, $J(f_c)$ is not connected and, as indicated in the second half of the proof of Theorem 14.14, $J(f_c)$ is totally disconnected. Indeed, this follows since $J(f_c)$ may be expressed as the disjoint union $J = S_1(J) \cup S_2(J)$, where S_1 and S_2 are the two branches of f_c^{-1} on J , so that J is the attractor of the IFS $\{S_1, S_2\}$, see (9.4) and the remarks after (9.8).

We look at this situation in more detail when c is large enough to allow some simplifications to be made.

Theorem 14.15

Suppose $|c| > \frac{1}{4}(5 + 2\sqrt{6}) = 2.475 \dots$. Then, $J(f_c)$ is totally disconnected, and is the attractor (in the sense of (9.4)) of the contractions given by the two branches of $f_c^{-1}(z) = \pm(z - c)^{1/2}$ for z near J . When $|c|$ is large

$$\dim_B J(f_c) = \dim_H J(f_c) \simeq \frac{2 \log 2}{\log 4|c|}.$$

Proof

With $f(z) = z^2 + c$, there are two possible values of $f^{-1}(z) = \pm(z - c)^{1/2}$, provided $z \neq c$. Let D be the disc $D = \{z : |z| \leq |2c|^{1/2}\}$. If $f(z) \in D$, then by the triangle inequality,

$$|z^2| \leq |z^2 + c| + |c| = |f(z)| + |c| \leq |2c|^{1/2} + |c| \leq 2|c|,$$

(since $|c| > 2$), so $|z| \leq |2c|^{1/2}$, giving $f^{-1}(D) \subset D$.

Note that, $f(z) \in D$ if and only if $|z^2 + c| \leq |2c|^{1/2}$, that is, if z^2 lies in the disc D_0 of centre $-c$ and radius $|2c|^{1/2}$. Since $0 \notin D_0$, the ‘square root’ of D_0 , that is, $\{z : z^2 \in D_0\} = f^{-1}(D)$, comprises two disjoint regions, D_1 and D_2 say, on opposite sides of some straight line through 0 , see [Figure 14.4](#). Thus, we may define mappings $S_1, S_2 : D \rightarrow D$ by

$$S_1(z) = (z - c)^{1/2} \in D_1, \quad S_2(z) = (z - c)^{1/2} \in D_2,$$

so that S_1 and S_2 are the two branches of the inverse of f on D .

For $i = 1, 2$,

$$|S_i(z_1) - S_i(z_2)| = |(z_1 - c)^{1/2} - (z_2 - c)^{1/2}| = \frac{|z_1 - z_2|}{|(z_1 - c)^{1/2} + (z_2 - c)^{1/2}|}.$$

Taking least and greatest values of this expression over $z_1, z_2 \in D$, that is, with $|z_1|, |z_2| \leq |2c|^{1/2}$,

$$\frac{1}{2}(|c| + |2c|^{1/2})^{-1/2} \leq \frac{|S_i(z_1) - S_i(z_2)|}{|z_1 - z_2|} \leq \frac{1}{2}(|c| - |2c|^{1/2})^{-1/2}. \quad \text{14.8}$$

The upper bound is less than 1 if $|c| > \frac{1}{4}(5 + 2\sqrt{6})$, in which case S_1 and S_2 are contractions on D . By Theorem 9.1, there is a unique non-empty compact attractor $F \subset D$ of the IFS $\{S_1, S_2\}$ satisfying

$$S_1(F) \cup S_2(F) = F. \quad \text{14.9}$$

Since $S_1(D)$ and $S_2(D)$ are disjoint, so are $S_1(F)$ and $S_2(F)$, so F is totally disconnected.

Of course, F is none other than the Julia set $J = J(f_c)$. One way to see this is to note that, since D contains at least one point z of J (for example, a repelling fixed point of f_c), we have

$J = \text{closure}(\bigcup_{k=1}^{\infty} f_c^{-k}(z)) \subset D$, since $f_c^{-k}(D) \subset D$. Using further results from Summary 14.12, J is a non-empty compact subset of D satisfying $J = f_c^{-1}(J)$ or, equivalently, $J = S_1(J) \cup S_2(J)$. Thus, $J = F$ by uniqueness of the IFS attractor satisfying (14.9).

Finally, to estimate the dimension of $J(f_c) = F$, we apply Propositions 9.6 and 9.7 with (14.8). Thus, lower and upper bounds for $\dim_H J(f_c)$ are given by the solutions of $2(\frac{1}{2}(|c| \pm |2c|^{1/2})^{-1/2})^s = 1$, that is, by $s = 2 \log 2 / \log 4(|c| \pm |2c|^{1/2})$, which gives the stated asymptotic estimate.

We next turn to the case where c is a small complex number. We know that if $c = 0$, then $J(f_c)$ is the unit circle. If c is small and z is small enough, then $f_c^k(z) \rightarrow w$ as $k \rightarrow \infty$, where w is the attractive fixed point $\frac{1}{2}(1 - \sqrt{1 - 4c})$ close to 0. On the other hand, $f_c^k(z) \rightarrow \infty$ if z is large. It is not unreasonable to expect the circle to ‘distort’ into a simple closed curve (i.e. having no points of self-intersection), separating these two types of behaviour as c moves away from 0.

In fact, this is the case provided that f_c retains an attractive fixed point, that is, if $|f'_c(z)| < 1$ at one of the roots of $f_c(z) = z$. Simple algebra shows that this happens if c lies inside the cardioid $z = \frac{1}{2}e^{i\theta} \left(1 - \frac{1}{2}e^{i\theta}\right)$ ($0 \leq \theta \leq 2\pi$); this is the main cardioid of the Mandelbrot set; see Exercise 14.15.

For convenience, we treat the case of $|c| < \frac{1}{4}$, but the proof is easily modified if f_c has any attractive fixed point.

Theorem 14.16

If $|c| < \frac{1}{4}$, then $J(f_c)$ is a simple closed curve.

Proof

Let C_0 be the curve $|z| = \frac{1}{2}$, which encloses both c and the attractive fixed point w of f_c . Then, by direct calculation, the inverse image $f_c^{-1}(C_0)$ is a loop C_1 surrounding C_0 . We may fill the annular region A_1 between C_0 and C_1 by a continuum of curves, which we call ‘trajectories’, which leave C_0 and reach C_1 perpendicularly; see [Figure 14.5](#)a. For each θ , let $\psi_1(\theta)$ be the point on C_1 at the end of the trajectory leaving C_0 at $\psi_0(\theta) = \frac{1}{2}e^{i\theta}$. The inverse image $f_c^{-1}(A_1)$ is an annular region A_2 with outer boundary the loop $C_2 = f_c^{-1}(C_1)$ and inner boundary C_1 , with f_c mapping A_2 onto A_1 in a two-to-one manner. The inverse image of the trajectories joining C_0 to C_1 provides a family of trajectories joining C_1 to C_2 . Let $\psi_2(\theta)$ be the point on C_2 at the end of the trajectory leaving C_1 at $\psi_1(\theta)$. We continue in this way to get a sequence of loops C_k , each surrounding its predecessor, and families of trajectories joining the points $\psi_k(\theta)$ on C_k to $\psi_{k+1}(\theta)$ on C_{k+1} for each k .

As $k \rightarrow \infty$, the curves C_k approach the boundary of the basin of attraction of w ; by Lemma 14.11, this boundary is just the Julia set $J(f_c)$. Since $|f'_c(z)| > \gamma$ outside C_1 for some $\gamma > 1$, it follows that f_c^{-1} is contracting near J . Thus, the length of the trajectory joining $\psi_k(\theta)$ to $\psi_{k+1}(\theta)$ converges to 0 at a geometric rate as $k \rightarrow \infty$. Consequently, $\psi_k(\theta)$ converges uniformly to a continuous function $\psi(\theta)$ as $k \rightarrow \infty$, and J is the closed curve given by $\psi(\theta)$ ($0 \leq \theta \leq 2\pi$).

It remains to show that ψ represents a simple curve. Suppose that $\psi(\theta_1) = \psi(\theta_2)$. Let D be the region bounded by C_0 and the two trajectories joining $\psi_0(\theta_1)$ and $\psi_0(\theta_2)$ to this common point. The boundary of D remains bounded under iterates of f_c , so by the maximum modulus theorem (that the modulus of an analytic function takes its maximum on the boundary point of a region) D remains bounded under iteration of f_c . Thus, D is a subset of

the filled-in Julia set, so the interior of D cannot contain any points of J . Thus, the situation of [Figure 14.5b](#) cannot occur, so that $\psi(\theta) = \psi(\theta_1) = \psi(\theta_2)$ for all θ between θ_1 and θ_2 . It follows that $\psi(\theta)$ has no point of self-intersection.

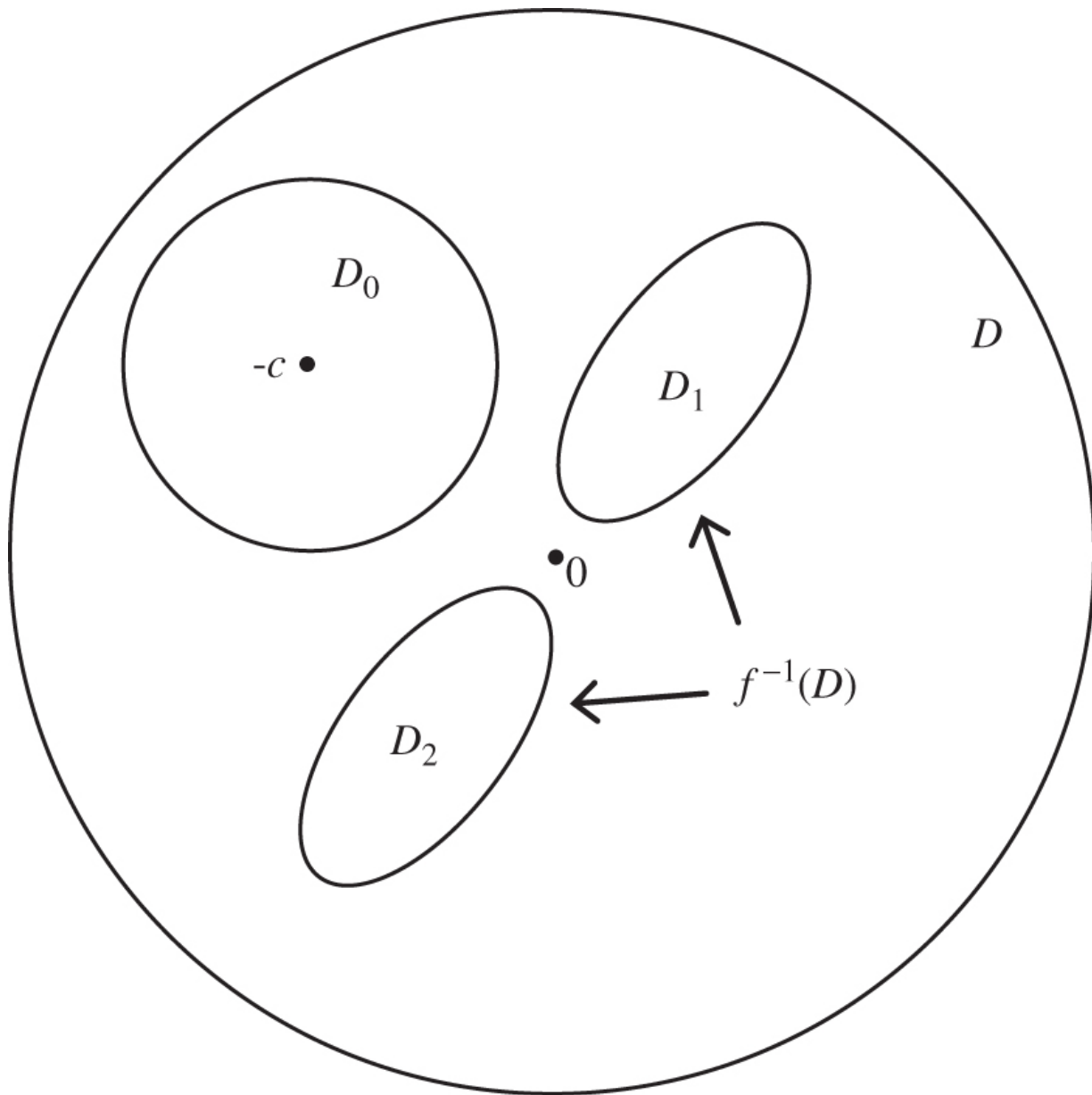


[**Figure 14.4.**](#) Proof of Theorem 14.15.

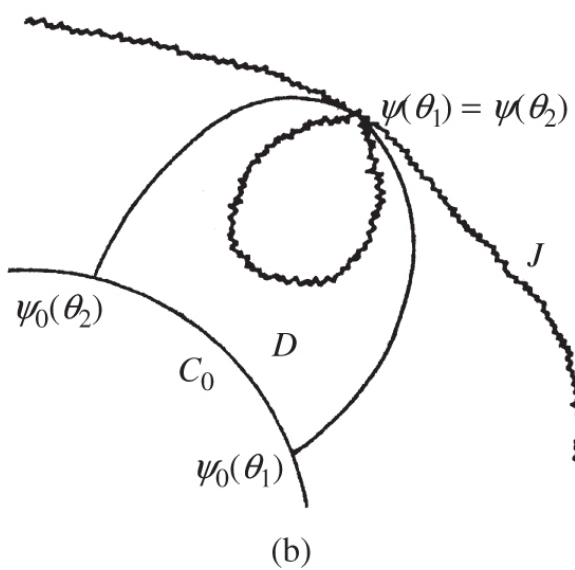
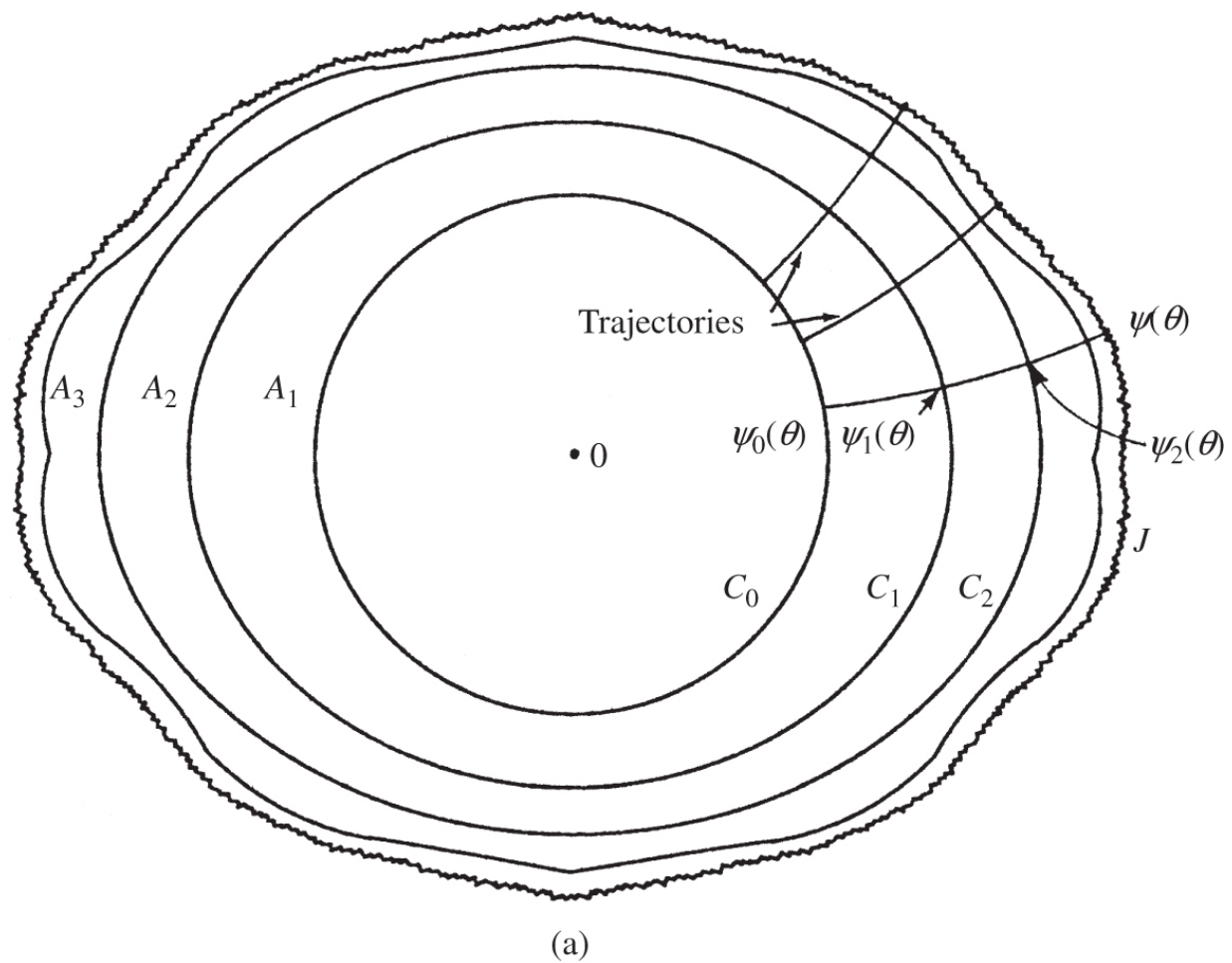


Figure 14.5 Proof of Theorem 14.16.

By an extension of this argument, if c is in the main cardioid of M , then $J(f_c)$ is a simple closed curve; such curves are sometimes referred to as quasi-circles. Of course, $J(f_c)$ will be a fractal curve if $|c| > 0$. It may be shown that, for small c , its dimension is given by

$$s = \dim_B J(f_c) = \dim_H J(f_c) = 1 + \frac{|c|^2}{4 \log 2} + \text{terms in } |c|^3 \text{ and higher powers.} \quad \text{14.10}$$

Moreover, $0 < \mathcal{H}^s(J) < \infty$, with $\dim_B J(f_c) = \dim_H J(f_c)$ given by a real analytic function of c .

The next case to consider is when f_c has an attractive periodic orbit of period 2. By a straightforward calculation, this occurs if $|c+1| < \frac{1}{4}$, that is if z lies in the prominent circular disc of M touching the left edge of the cardioid; see Exercise 14.16. Since f_c^2 is a polynomial of degree 4, f_c has two fixed points and two period-2 points. Let w_1 and w_2 be the points of the attractive period-2 orbit. It may be shown, as in the proof of Theorem 14.16, that the basin of attraction for w_i (i.e. $\{z : f_c^{2k}(z) \rightarrow w_i \text{ as } k \rightarrow \infty\}$) includes a region bounded by a simple closed curve C_i surrounding w_i , for $i = 1, 2$. By Lemma 14.11 and Proposition 14.4, $C_i = J(f_c^2) = J(f_c)$. The curves C_i are mapped onto themselves in a two-to-one fashion by f_c^2 , which implies that there is a fixed point of f_c^2 on each C_i . The period-2 points are strictly inside the C_i , so there is a fixed point of f_c on each C_i ; since the C_i are mapped onto each other by f_c , the only possibility is for C_1 and C_2 to touch at one of the fixed points of f_c . The inverse function f_c^{-1} is two-valued on C_1 . One of the inverse images is C_2 (which encloses w_2). However, the other branch of $f_c^{-1}(C_1)$ is a further simple closed curve enclosing the second value of $f_c^{-1}(w_1)$. We may continue to take inverse images in this way to find that $J(f_c)$ is made up of infinitely many simple closed curves, which enclose the pre-images of w_1 and w_2 of all orders and touch each other in pairs at ‘pinch points’—see [Figure 14.7c](#). Thus, we get fractal Julia sets that are topologically much more complicated than in the previous cases.

It is possible to use such ideas to analyse the case when f_c has an attractive periodic orbit of period $p > 2$. The immediate

neighbourhoods of the period- p points that are drawn into the attractive orbits are bounded by simple closed curves that touch each other at a common point. The Julia set consists of these fractal curves together with all their pre-images under f^k .

A variety of examples are shown in [Figures 14.6](#) and [14.7](#). The ‘buds’ on the Mandelbrot set corresponding to attractive orbits of period p are indicated in [Figure 14.8](#).

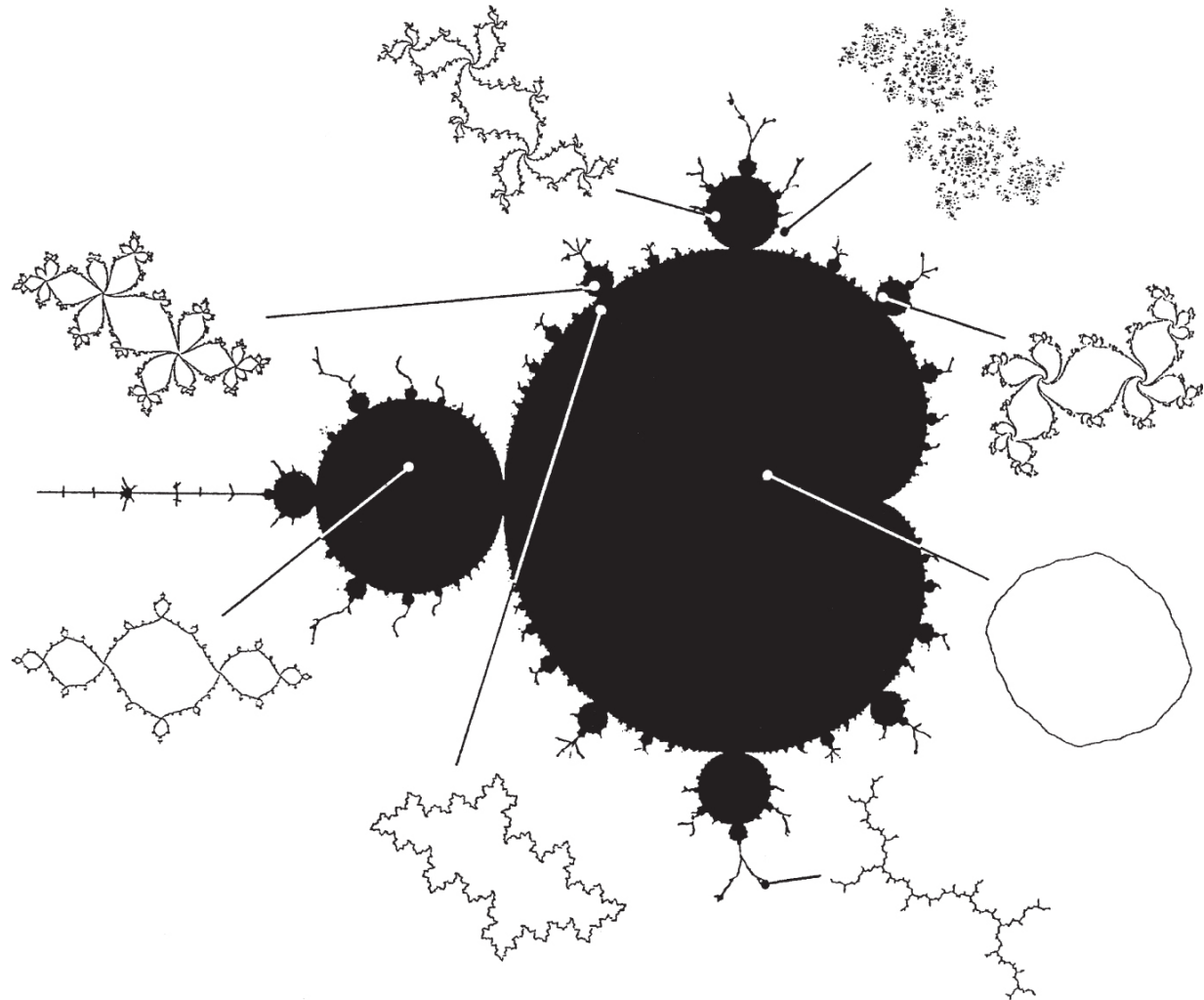


Figure 14.6 Julia sets $J(f_c)$ for c at various points in the Mandelbrot set. The Julia sets are displayed in more detail in [Figure 14.7](#).

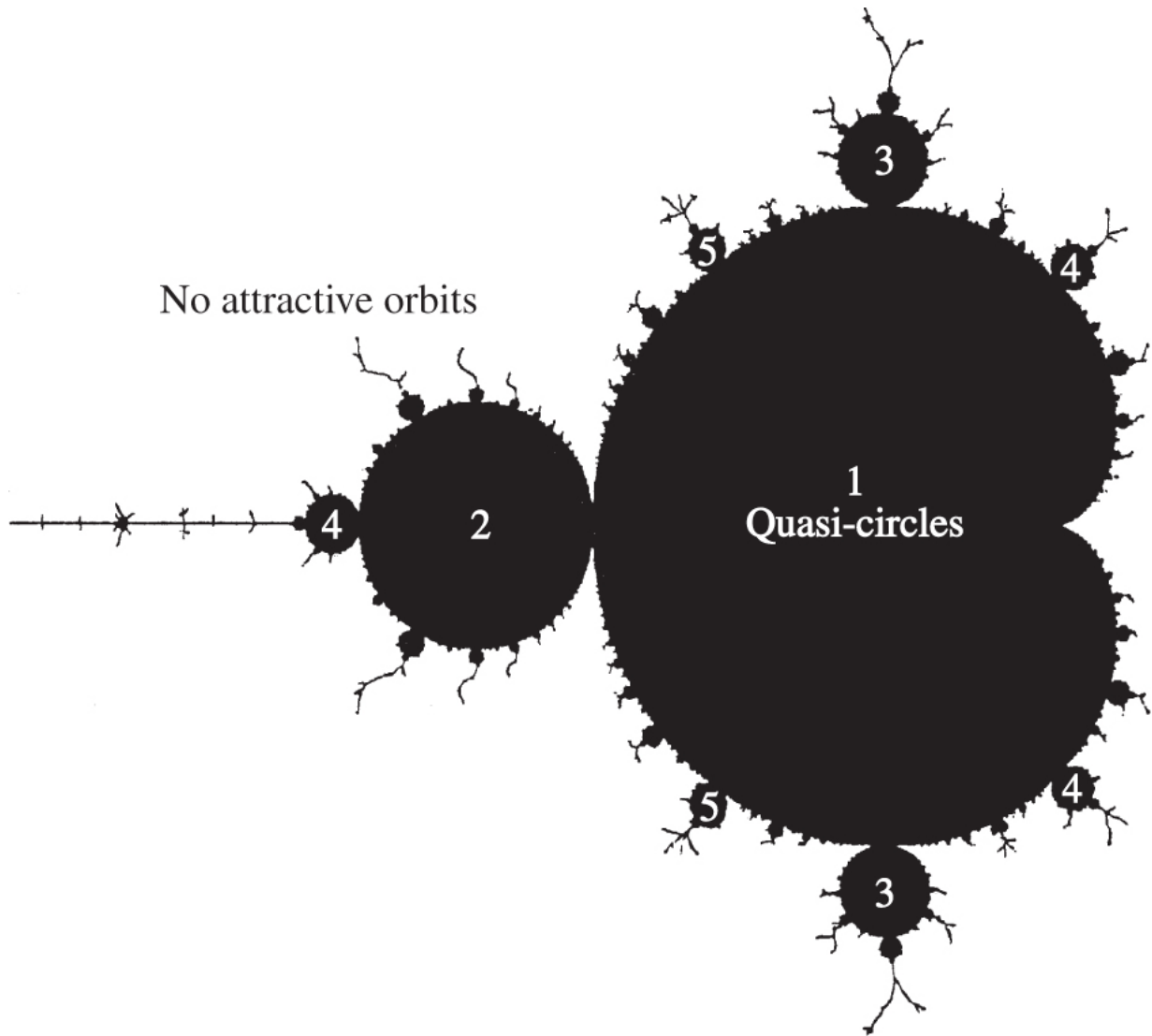


Figure 14.8 The periods of the attractive orbits of f_c for c in various parts of the Mandelbrot set M . If c is in the main cardioid, f_c has an attractive fixed point and the Julia set $J(f_c)$ is a quasi-circle. For c in the buds of M , f_c has an attractive orbit with the period p shown, with p regions inside the Julia set $J(f_c)$ meeting at each pinch point. Outside M , the function f_c has no attractive orbits and $J(f_c)$ is totally disconnected.

The Julia sets $J(f_c)$ that are most intricate, and are mathematically hardest to analyse are at the ‘exceptional’ values of c on the boundary of M . If c is on the boundary of the cardioid or a bud of M , then f_c has an indifferent periodic point (where $|f_c^{(p)}'(w)| = 1$). If c is at a ‘neck’ where a bud touches a parent region, then $J(f_c)$ includes a

series of ‘tendrils’ joining its boundary to the indifferent periodic points. For c elsewhere on the boundary of the cardioid, the Julia set may contain ‘Siegel discs’. The Julia set $J(f_c)$ consists of infinitely many curves bounding open regions, with f_c mapping each region into a ‘larger’ one, until the region containing the fixed point is reached. Inside this *Siegel disc*, f_c rotates points on invariant loops around the fixed point.

There are still further possibilities. If c is on one of the ‘hairs’ of M , then $J(f_c)$ may be a *dendrite*, that is, of tree-like form. This occurs if an iterate of the critical point o is periodic, that is, if $f_c^k(0) = f_c^{k+q}(0)$ for positive integers k and q .

We have mentioned that there are miniature copies of M located in the hairs of M . If c belongs to one of these, then $J(f_c)$ will be of dendrite form, but with small copies of the Julia set from the corresponding value of c in the main part of M inserted at the ‘vertices’ of the dendrite.

The Mandelbrot set is connected, but its intricacy is reflected by the fact that its boundary, although of zero area, has Hausdorff dimension 2.

A good way to explore the structure of Julia sets and, indeed, the Julia sets of other functions, is using a computer. There are two usual methods of drawing Julia sets based on the properties that we have discussed.

For the first method, we choose a repelling periodic point z . For suitable k , we may compute the set of inverse images $J_k = f^{-k}(z)$. By Corollary 14.8(b), these 2^k points are in J , and should fill J as k becomes large. A difficulty with picturing J in this way is that the points of J_k need not be uniformly distributed across J —they may tend to cluster in some parts of J and be sparse in other parts. Consequently, even with k quite large, parts of J can be missed altogether. (This tends to happen for f_c with c close to the boundary of M .) There are various ways of getting around this difficulty. For instance, with $J_0 = \{z\}$, instead of taking $J_k = f^{-1}(J_{k-1})$ for each k , we

can choose a subset J_k of $f^{-1}(J_{k-1})$ by ignoring all but one of the points in every ‘small’ cluster. This ensures that we are working with a reasonably well-distributed set of points of J at each step of the iteration, and also reduces the calculation involved.

A second method is to test individual points to see if they are close to the Julia set. Suppose, for example, that f has two or more attractive fixed points (now including ∞ if f is a polynomial). If z is a point of $J(f)$, then there are points arbitrarily close to z in the attractive basin of each attractive point by Lemma 14.11. To find J , we divide a region of C into a fine mesh. We examine the ultimate destination under iteration by f of the four corners of each mesh square. If two of the corners are attracted to different points, we deem the mesh square to contain a point of J . Often, the other squares, the ‘Fatou set’, are coloured according to which point the vertices of the square is attracted to, perhaps with different shading according to how close the k th iterates are to the attractive point for some fixed k .

Both of these methods can be awkward to use in certain cases. A knowledge of the underlying mathematics helps to overcome the difficulties that can occur.

14.4 Characterisation of quasi-circles by dimension

We saw in the previous section that, if c is in the main cardioid of the Mandelbrot set, then the Julia set of $f_c(z) = z^2 + c$ is a simple (i.e. non-self-intersecting) closed curve. By similar arguments, the Julia set of $f(z) = z^n + c$ is a simple closed curve for any integer $n \geq 2$, provided that c is small enough, and, indeed, the same is true for $f(z) = z^2 + g(z)$ for a wide variety of analytic functions g that are ‘sufficiently small’ near the origin. Thus, all these functions have Julia sets that are topologically the same—they are all homeomorphic to a circle. The surprising thing is that they are essentially the same as *fractals*, in other words are bi-Lipschitz

equivalent, if and only if they have the same Hausdorff dimension. Of course, if two sets have different dimensions, they cannot be bi-Lipschitz equivalent (Proposition 3.3(b)). However, in this particular situation, the converse is also true.

We term a set F a *quasi-self-similar circle* or *quasi-circle*, if the following conditions are satisfied:

- i. F is homeomorphic to a circle, that is, F is a simple closed curve,
- ii. $0 < \mathcal{H}^s(F) < \infty$, where $s = \dim_H F$,
- iii. there are constants $a, b, r > 0$ such that for any subset U of F with $|U| \leq r$, there is a mapping $\varphi : U \rightarrow F$ such that

$$a|x - y| \leq |U|\|\varphi(x) - \varphi(y)\| \leq b|x - y| \quad (x, y \in F).$$

14.11

The ‘quasi-self-similar’ condition (iii) says that arbitrarily small parts of F are ‘roughly similar’ to a large part of F .

The following theorem depends on using s -dimensional Hausdorff measure to measure the ‘distance’ round quasi-circles.

Theorem 14.17

Quasi-circles E and F are bi-Lipschitz equivalent if and only if $\dim_H E = \dim_H F$.

Sketch of proof

If there is a bi-Lipschitz mapping between E and F , then $\dim_H E = \dim_H F$ by Corollary 3.3(b).

Suppose that $\dim_H E = \dim_H F$. Let $E(x, y)$ be the ‘arc’ of E between points $x, y \in E$, taken in the clockwise sense, with a similar notation for arcs of F . Conditions (ii) and (iii) imply that $\mathcal{H}^s(E(x, y))$ is continuous in $x, y \in E$ and is positive if $x \neq y$. We claim that there are constants $c_1, c_2 > 0$ such that

$$c_1 \leq \frac{\mathcal{H}^s(E(x, y))}{|x - y|^s} \leq c_2 \quad \text{14.12}$$

whenever $E(x, y)$ is the ‘shorter’ arc between x and y , that is, $\mathcal{H}^s(E(x, y)) \leq \mathcal{H}^s(E(y, x))$. To see this, let $\varepsilon > 0$ be a sufficiently small number. If $|x - y| \geq \varepsilon$, then (14.12) is true by a continuity argument for suitable constants. If $|x - y| < \varepsilon$, then there is a mapping $\varphi : E(x, y) \rightarrow E$ satisfying (14.11) such that $|\varphi(x) - \varphi(y)| \geq \varepsilon$. Inequalities (14.11) and (3.7) imply that the ratio (14.12) changes by a bounded amount if x and y are replaced by $\varphi(x)$ and $\varphi(y)$, so (14.12) holds for suitable c_1 and c_2 for all $x, y \in E$.

Now choose base points $p \in E$ and $q \in F$. Set $\gamma = \mathcal{H}^s(E)/\mathcal{H}^s(F)$ and define $\psi : E \rightarrow F$ by taking $\psi(x)$ to be the point of F such that

$$\mathcal{H}^s(E(p, x)) = \gamma \mathcal{H}^s(F(q, \psi(x)))$$

(Figure 14.9). Then, ψ is a continuous bijection, and also

$$\mathcal{H}^s(E(x, y)) = \gamma \mathcal{H}^s(F(\psi(x), \psi(y))) \quad (x, y \in E).$$

Using (14.12) together with the corresponding inequalities for arcs of F , this gives

$$c_3 \leq \frac{|\psi(x) - \psi(y)|}{|x - y|} \leq c_4$$

if $x \neq y$, so that ψ is bi-Lipschitz, as required.

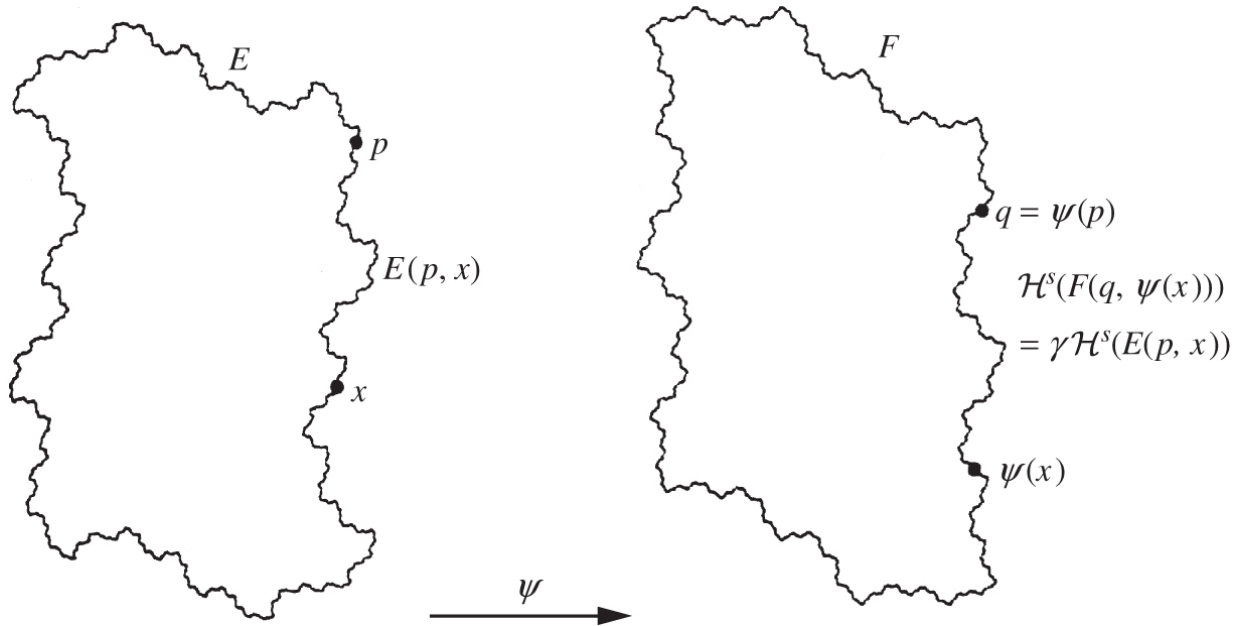


Figure 14.9. Setting up a bi-Lipschitz mapping ψ between two quasi-circles of Hausdorff dimension s .

Corollary 14.18

Suppose that the Julia sets J_1 and J_2 of the polynomials f_1 and f_2 are simple closed curves. Suppose that f_i is strictly repelling on J_i , (that is, $|f'_i(z)| > 1$ for $i = 1, 2$). Then, J_1 and J_2 are bi-Lipschitz equivalent if and only if $\dim_H J_1 = \dim_H J_2$.

Sketch of proof

It may be shown that if a polynomial f is strictly repelling on its Julia set J , then $0 < \mathcal{H}^s(J) < \infty$, where $s = \dim_H J$. Moreover, given a subset U of J , we may choose k , so that $f^k(U)$ has diameter comparable with that of J itself, and (14.11) holds, taking $\varphi = f^k$ (this reflects the quasi-self-similarity of J). Thus, J_1 and J_2 are quasi-circles to which Theorem 14.17 may be applied.

14.5 Newton's method for solving polynomial equations

Newton's method for finding roots of equations will be familiar to anyone who has done any numerical analysis. Let $p(x)$ be a function with continuous derivative. If $f(x) = x - p(x)/p'(x)$, then the iterates $f^k(x)$ converge to a solution of $p(x) = 0$, provided that $p'(x) \neq 0$ at the solution and that the initial value of x is chosen appropriately. Cayley suggested investigating the method in the complex plane, and in particular which initial points of \mathbb{C} iterate to which zero of p .

Let $p : \mathbb{C} \rightarrow \mathbb{C}$ be a polynomial with complex coefficients and form the rational function $f : \mathbb{C} \cup \{\infty\} \rightarrow \mathbb{C} \cup \{\infty\}$

$$f(z) = z - \frac{p(z)}{p'(z)}. \quad \text{14.13}$$

Then, the fixed points of f , given by $p(z)/p'(z) = 0$, are the zeros of p together with ∞ . Differentiating, we find that

$$f'(z) = \frac{p(z)p''(z)}{p'(z)^2}; \quad \text{14.14}$$

so a zero z of p is a *superattractive* fixed point of f , that is, $f'(z) = 0$, provided that $p'(z) \neq 0$. If $|z|$ is large, $f(z) \sim z(1 - 1/n)$, where n is the degree of p , so ∞ is a repelling point of f . As usual, we write

$$A(w) = \{z : f^k(z) \rightarrow w\}$$

14.15

for the basin of attraction of the zero w , that is, the set of initial points that converge to w under Newton iteration. Since the zeros are attractive, the basin $A(w)$ includes an open region containing w . We shall see, however, that $A(w)$ can be remarkably complicated further away from w .

The theory of Julia sets developed for polynomials in Section 14.1 is almost the same for a rational function, provided that the point ∞ is included in the natural way. The main differences are that if f is a rational function $J(f)$ need not be bounded (though it must be closed) and it is possible for $J(f)$ to have interior points, in which case $J(f) = \mathbb{C} \cup \{\infty\}$. However, Lemma 14.11 remains true, so that $J(f)$ is the boundary of $A(w)$ for each attractive fixed point w . Thus, $J(f)$ is likely to be important when analysing the domains of attraction of the roots in Newton's method.

A straightforward case is the quadratic polynomial

$$p(z) = z^2 - c \quad (c \neq 0)$$

with zeros $\pm \sqrt{c}$ (as before, more general quadratic polynomials can be reduced to this form by a conjugacy). Newton's formula (14.13) becomes

$$f(z) = (z^2 + c)/2z.$$

Thus,

$$f(z) \pm \sqrt{c} = (z \pm \sqrt{c})^2/2z,$$

so

$$\frac{f(z) + \sqrt{c}}{f(z) - \sqrt{c}} = \left(\frac{z + \sqrt{c}}{z - \sqrt{c}} \right)^2. \quad \text{14.16}$$

It follows that if $|z + \sqrt{c}|/|z - \sqrt{c}| < 1$, then $|f^k(z) + \sqrt{c}|/|f^k(z) - \sqrt{c}| \rightarrow 0$ so $f^k(z) \rightarrow -\sqrt{c}$ as $k \rightarrow \infty$, and similarly if $|z + \sqrt{c}|/|z - \sqrt{c}| > 1$, then

$f^k(z) \rightarrow \sqrt{c}$. The Julia set $J(f)$ is the line $|z + \sqrt{c}| = |z - \sqrt{c}|$, that is, the perpendicular bisector of $-\sqrt{c}$ and \sqrt{c} , and $A(-\sqrt{c})$ and $A(\sqrt{c})$ are the half-planes on either side. (Letting $h(z) = (z + \sqrt{c})/(z - \sqrt{c})$ in (14.16) gives $f(z) = h^{-1}(h(z))^2$, so that f is conjugate to, and therefore has similar dynamics to, the mapping $g(z) = z^2$.) In this case, the situation is very regular—any initial point is iterated by f to the nearest zero of p .

The quadratic example might lead us to hope that the domains of attraction under Newton iteration of the zeros of any polynomial are reasonably regular. However, for higher order polynomials, the situation is fundamentally different. Lemma 14.11, which is valid for rational functions, including Newton functions of polynomials, provides a hint that something very strange happens. If p has zeros z_1, \dots, z_n with $p'(z_i) \neq 0$, Lemma 14.11 tells us that the Julia set of f is the boundary of the domain of the attraction of *every* zero:

$$J(f) = \partial A(z_1) = \dots = \partial A(z_n).$$

A point on the boundary of any one of the domains of attraction must be on the boundary of all of them; since $J(f)$ is uncountable, there are a great many such multiple boundary points. An attempt to visualise three or more disjoint sets with this property will convince the reader that they must be very complicated indeed.

Let us look at a specific example. The cubic polynomial

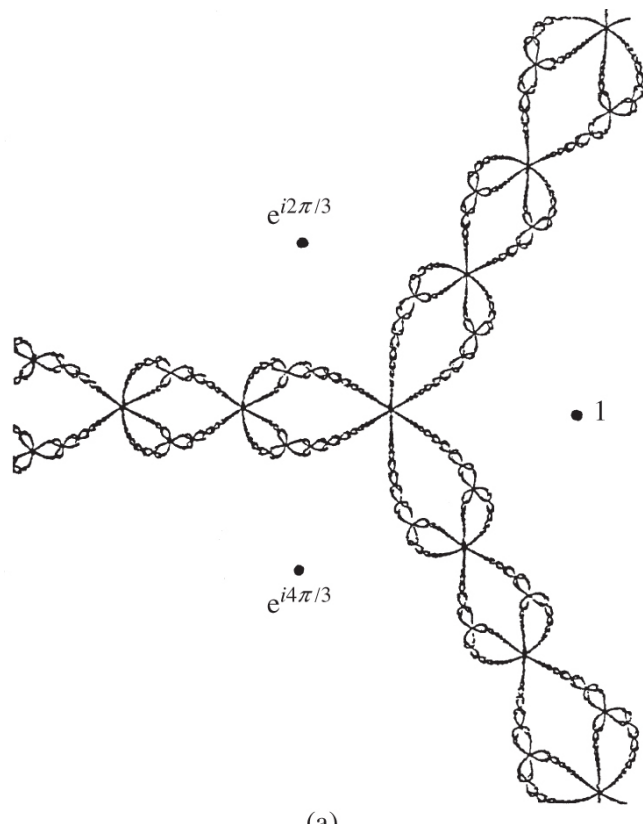
$$p(z) = z^3 - 1$$

has zeros $1, e^{i2\pi/3}, e^{i4\pi/3}$, and Newton function

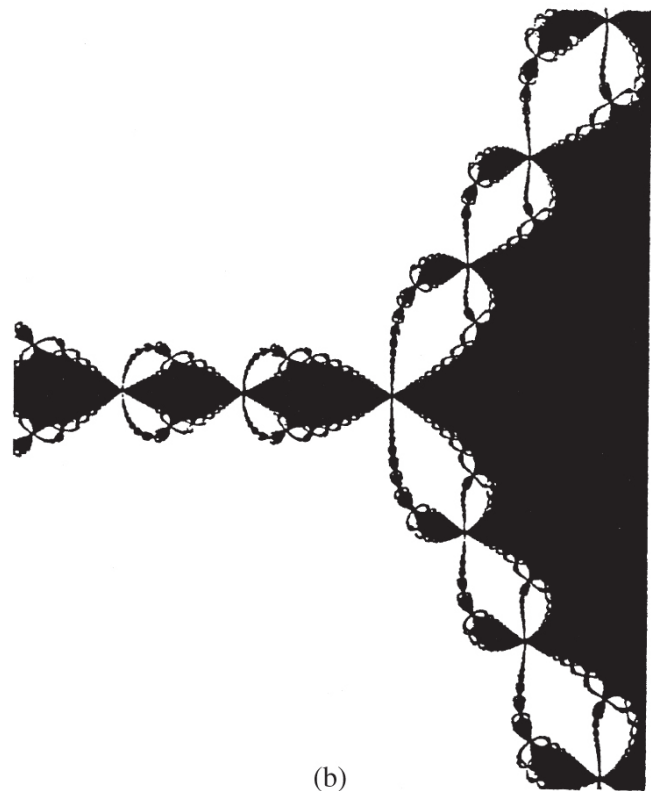
$$f(z) = \frac{2z^3 + 1}{3z^2}.$$

The transformation $\rho(z) = z e^{i2\pi/3}$ is a rotation of 120° about the origin. It is easily checked that $f(\rho(z)) = \rho(f(z))$; in other words, ρ is a conjugacy of f to itself. It follows that a rotation of 120° about the origin maps $A(w)$ onto $A(w e^{i2\pi/3})$ for each of the three zeros w , so that

the Julia set has threefold symmetry about the origin. (Of course, these symmetries would be expected from the symmetric disposition of the three zeros of p .) If z is real, then $f^k(z)$ remains real for all k , and, by elementary arguments, $f^k(z)$ converges to 1 except for countably many real z . Thus, $A(1)$ contains the real axis except for a countable number of points, and, by symmetry, $A(e^{i2\pi/3})$ and $A(e^{i4\pi/3})$ contain the lines through the origin making 120° and 240° to the real axis, again except for countably many points. We also know that each $A(w)$ contains an open region round w , that any point on the boundary of one of the $A(w)$ is on the boundary of all three, and that there are uncountably many such ‘triple points’. Most people require the insight of a computer drawing to resolve this almost paradoxical situation, see [Figure 14.10](#).



(a)



(b)

Figure 14.10 Newton's method for $p(z) = z^3 - 1$. The Julia set for the Newton function $f(z) = (2z^3 + 1)/3z^2$ is shown in (a), and the domain of attraction of the zero $z = 1$ is shown in black in (b).

The domain $A(1)$ is shown in black in [Figure 14.10b](#); note that the basins of attraction of the other two zeros, obtained by rotation of 120° and 240° , key into the picture in a natural way. The Julia set shown in [Figure 14.10a](#) is the boundary of the three basins and is made up of three ‘chains’ leading away from the origin. These fractal chains have a fine structure—arbitrarily close to each point of $J(f)$ is a ‘slightly distorted’ copy of the picture at the origin with six components of the $A(w)$ meeting at a point. This reflects Corollary 14.8(b), again valid for rational functions: $J(f)$ is the closure of $\bigcup_{k=1}^{\infty} f^{-k}(0)$, so that if z is in $J(f)$, then there is a point w arbitrarily close to z and an integer k such that $f^k(w) = 0$. But f^k is locally a conformal mapping, so that the local inverse $(f^k)^{-1}$ maps a neighbourhood of 0 to an ‘almost similar’ neighbourhood of w . The Julia set $J(f)$ exhibits quasi-self-similarity.

This, of course, is just the beginning. The domains of attraction of the zeros of other polynomials of degree 3 or more and, indeed, other analytic functions, may be investigated using a combination of theory and computer graphics. This leads to a wealth of sets of a highly intricate form which raise many intriguing mathematical questions.

In this chapter, we have touched on what is a complicated and fascinating area of mathematics in which fractals play a fundamental role. It is an area in which computer experiments often lead the way with mathematical theory then trying to explain what is observed. The variations are endless—we can investigate the Julia set of higher order polynomials and of other analytic functions such as $\exp z$, as well as invariant sets of non-analytic transformations of the plane. With the advent of high-quality colour computer graphics, these ideas have become the basis of much computer art. A single function of simple form can lead to highly

intricate yet regular pictures—often very beautiful, sometimes almost weird.

14.6 Notes and references

Much of the basic theory of iteration of complex functions was developed by Julia (1918) and Fatou (1919). For many years, the subject lay almost dormant, until computer graphics was sufficiently advanced to reveal the intricate form of Julia sets. The first pictures that indicated the complexity of the Julia sets and the Mandelbrot set appeared around 1980 in papers by Mandelbrot (1980) and Brooks and Matelski (1981). Nowadays, drawing Julia sets and the Mandelbrot set on computers has become a popular activity, with incredibly beautiful and intricate pictures easily produced.

The books by Peitgen and Richter (1986) and Peitgen, Jürgens and Saupe (2004) provide well-illustrated accounts of complex iteration. Other accounts of this area of complex dynamics include Blanchard (1984), McMullen (1994); Devaney (1995); Carleson and Gamelin (1996); Beardon (2000) and Milnor (2006). Theorem 14.14 is given by Brolin (1965). Collections of papers related to the Mandelbrot set include Mandelbrot's (2004) 'Selecta' and those edited by Tan (2000); Devaney and Keen (2006) and Schleicher (2009). Alexander (2011) gives a historical perspective on the area.

Considerable research has been done on the dynamics of other classes of complex functions such as transcendental meromorphic functions where the Julia sets may have exotic forms, see Morosawa et al. (2000) and the collection of papers edited by Rippon and Stallard (2008).

The formula (14.10) for the dimension of $J(f_c)$ is due to Ruelle (1982, 1983), and extensions have been obtained by Collet, Dobbertin and Moussa (1992) and Abenda, Moussa and Osbaldestin (1999). For details of the characterisation of quasi-circles by dimension, see Falconer and Marsh (1989). Fractals associated with Newton's

method are discussed in Curry, Garnett and Sullivan (1983); Peitgen, Saupe and von Haeseler (1984) and Peitgen and Richter (1986).

Exercises

Throughout these exercises, we write $f_c(z) = z^2 + c$.

14.1 Show that every perfect set E (i.e. every set that is closed and has no isolated points) is uncountable. (Hint: Construct a ‘Cantor-like’ set inside E .) Deduce that $J(f_c)$ is uncountable for all c .

14.2 Describe the Julia set of $f(z) = z^2 + 4z + 2$. (Hint: Write $z_1 = z + 2$.)

14.3 Let $f(z) = z^2 + 2iz + b$. By considering the mapping $h(z) = z + i$, show that the Julia set of f is connected if and only if $b + 1 + i \in M$.

14.4 Let $|c| \leq \frac{1}{4}$. Show that if $|z| \leq \frac{1}{2}$, then $|f_c(z)| \leq \frac{1}{2}$. Deduce that $B(0, \frac{1}{4}) \subset K(f_c)$. Also show that if $|z| \geq 2$ then $|f_c(z)| \geq \frac{3}{2}|z|$. Deduce that $K(f_c) \subset B(0, 2)$. What does this tell us about the location of $J(f_c)$?

14.5 Let $f(z) = z^2 - 2$. Find a repelling fixed point of f . Deduce from Corollary 14.8 that $J(f)$ is a subset of the real interval $[-2, 2]$. Use Theorem 14.14 to deduce that $J(f)$ is connected, and hence that it is the interval $[-2, 2]$.

14.6 Show that the Julia set $J(f_c)$ is symmetric about the origin (that is $z \in J(f_c)$ if and only if $-z \in J(f_c)$).

14.7 Show that if c is real with $c > \frac{1}{4}$ then $z \notin J(f_c)$ for all real numbers z . Deduce, using Exercise 14.6, that if $c > \frac{1}{4}$ then $J(f_c)$ is not connected, and so $c \notin M$.

14.8 Show that if c is a non-real number with $|c| < \frac{1}{4}$ and with $w = \frac{1}{2}(1 + (1 - 4c)^{-1/2})$ is the repelling fixed point of $f_c(z) = z^2 + c$ then $f'_c(w)$ is not real. Deduce that the simple closed curve that forms the Julia set $J(f_c)$ cannot have a tangent at w . Hence, deduce that the curve contains no differentiable arcs.

14.9 Show that if $|c| \leq \frac{1}{4}$ and $|z| \leq \frac{1}{2}$, then $|f_c(z)| \leq \frac{1}{2}$. Deduce that $B(0, \frac{1}{4}) \subset M$.

14.10 Show that if $|c+1| \leq \frac{1}{20}$ and $|z| \leq \frac{1}{10}$ then $|f_c(f_c(z))| \leq \frac{1}{10}$. Deduce that $B(-1, \frac{1}{20}) \subset M$.

14.11 Show that if $\epsilon > 0$ and if $|z| \geq \max(2 + \epsilon, |c|)$ then $|f_c(z)| \geq |z|(1 + \epsilon)$. Deduce that if $|c| > 2$, then $c \notin M$.

14.12 Use Exercise 14.11 to show that $M = \{c : |f_c^k(0)| > 2 \text{ for some } k\}$.

14.13 Show that if $|c| < 1$, then the Julia set of $f(z) = z^3 + 3z$ is a simple closed curve.

14.14 Obtain an estimate for the dimension of the Julia set of $f(z) = z^3 + c$ when $|c|$ is large.

14.15 Show that f_c has an attractive fixed point precisely when c lies inside the main cardioid of the Mandelbrot set given by

$$z = \frac{1}{2}e^{i\theta} \left(1 - \frac{1}{2}e^{i\theta}\right) \text{ for } 0 \leq \theta \leq 2\pi.$$

14.16 Show that $f_c^2(z) - z = (z^2 - z + c)(z^2 + z + c + 1)$. Deduce that f has an attractive period-2 point just when $|c+1| < \frac{1}{4}$ (the large disc in M).

14.17 Show that if w is an attractive fixed point of f_c , then the attractive basin $A(w)$ must contain the point c . (Hint: Show that otherwise there is an open neighbourhood of w on which the inverse iterates f^{-k} of f can be uniquely defined and form a normal family, which is impossible since w is a repelling fixed point of f^{-1} .) Deduce that f_c can have at most one attractive fixed point.

Generalise this to show that if w is an attractive fixed point of any polynomial f , then $A(w)$ contains a point $f(z)$ for some z with $f'(z) = 0$.

14.18 Let f be a quadratic polynomial. Show by applying Exercise 14.17 to f^p for positive integers p , that f can have at most one attractive periodic orbit.

14.19 Write a computer program to draw Julia sets of functions (see the end of Section 14.3). Try it out first on quadratic functions, then experiment with other polynomials and rational functions, and then other functions such as $\exp z$.

14.20 Use a computer to investigate the domains of attraction for the zeros of some other polynomials under Newton's method iteration; for example, for $p(z) = z^4 - 1$ or $p(z) = z^3 - z$.

Chapter 15

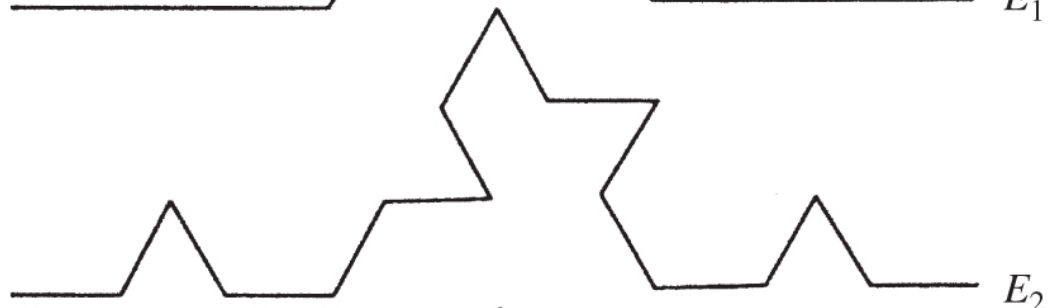
Random fractals

Many of the fractal constructions that have been encountered in this book have random analogues. For example, in the von Koch curve construction, each time we replace the middle third of an interval by the other two sides of an equilateral triangle, we might toss a coin to determine whether to position the new part ‘above’ or ‘below’ the removed segment. After a few steps, we get a rather irregular looking curve which nevertheless retains certain of the characteristics of the von Koch curve; see [Figure 15.1](#).

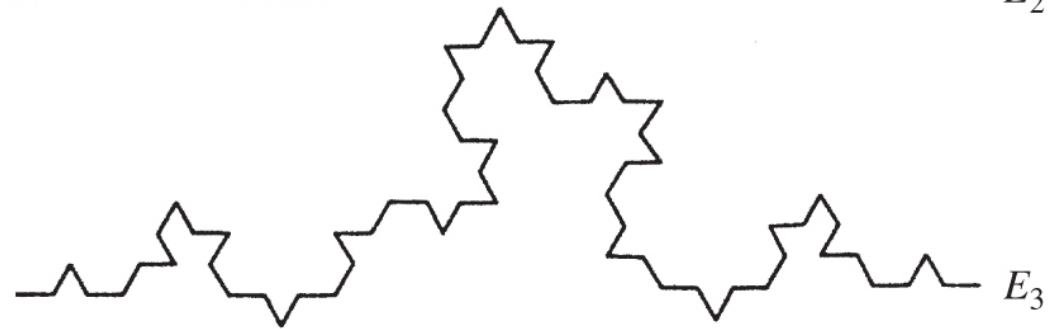
E_0



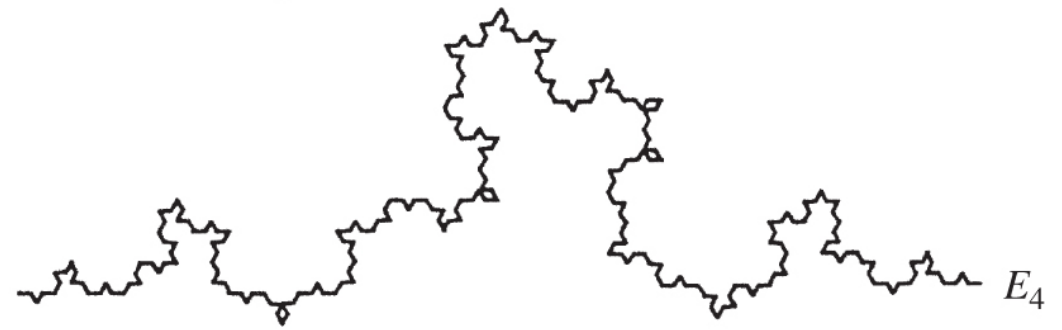
E_1



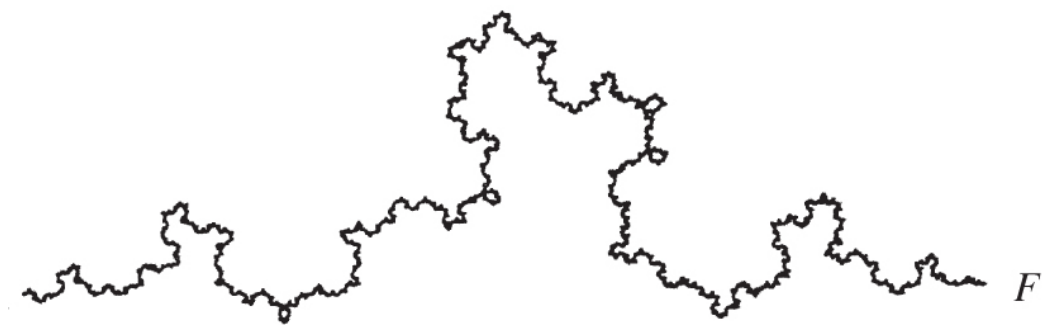
E_2



E_3



E_4



F

Figure 15.1 Construction of a ‘random von Koch curve’. At each step, a coin is tossed to determine on which side of the removed segment to place the new pair of segments.

The middle third Cantor set construction may be randomised in several ways. Each time we divide a segment into three parts we could, instead of always removing the middle segment, throw a die to decide which parts to remove (Figure 15.2a). Alternatively, we might choose the interval lengths at each stage of the construction at random, so that at the k th stage we are left with 2^k intervals of differing lengths, resulting in a rather irregular looking fractal (Figure 15.2b).

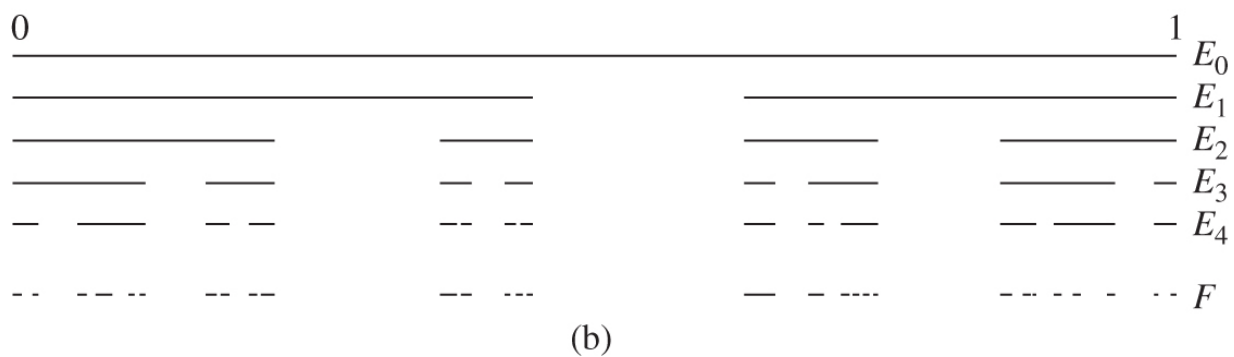
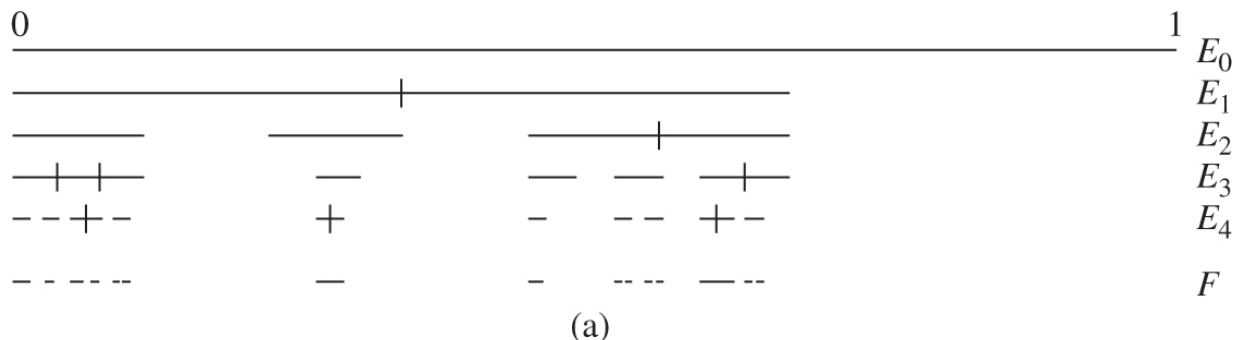


Figure 15.2 Two random versions of the Cantor set. In (a), each interval is divided into three equal parts from which some are selected at random. In (b), each interval is replaced by two sub-intervals of random lengths.

Whilst such ‘random fractals’ do not have the self-similarity of their non-random counterparts, their non-uniform appearance is often rather closer to natural phenomena such as coastlines,

topographical surfaces or cloud boundaries. Indeed, random fractal constructions are the basis of many impressive computer-drawn landscapes or skyscapes.

Most fractals discussed in this book involve a sequence of approximations E_k , each obtained from its predecessor by modification in increasingly fine detail, with a fractal F as a limiting set. A random fractal worthy of the name should display randomness at all scales, so it is appropriate to introduce a random element at each stage of the construction. By relating the size of the random variations to the scale, we can arrange for the fractal to be *statistically self-similar* in the sense that enlargements of small parts have the same statistical distribution as the whole set. This compares with (non-random) self-similar sets (see Chapter 9), where enlargements of small parts are identical to the whole.

In order to describe fractal constructions involving infinitely many random steps with precision, we need to use the language of probability theory, which is surveyed briefly in Section 1.4.

15.1 A random Cantor set

We analyse a basic statistically self-similar Cantor set, where the intervals at each stage of the construction are of random lengths. This analysis may be adapted to a large class of random fractals.

We construct a set $F = \bigcap_{k=1}^{\infty} E_k$, where $[0, 1] = E_0 \supset E_1 \supset \dots$ is a decreasing sequence of closed sets, with E_k a union of 2^k disjoint closed k th-level basic intervals. We assume that each k th-level interval I contains two $(k+1)$ th-level intervals I_L and I_R , abutting the left- and right-hand ends of I , respectively. The lengths of the intervals are random, and we impose statistical self-similarity by the requirement that the length ratios $|I_L|/|I|$ have independent and identical probability distribution for every basic interval I of the construction, and similarly for the ratios $|I_R|/|I|$. This ‘random Cantor set’ F is statistically self-similar, in that the distribution of

the set $F \cap I$ is the same as that of F , but scaled by a factor $|I|$, for each interval I in the construction.

We describe this random construction more precisely and in probabilistic terms. Let a, b be constants with $0 < a \leq b < \frac{1}{2}$. We let Ω denote the class of all decreasing sequences of sets

$[0, 1] = E_0 \supset E_1 \supset E_2 \supset \dots$ satisfying the following conditions. The set E_k comprises 2^k disjoint closed intervals I_{i_1, \dots, i_k} indexed by i_1, \dots, i_k , where $i_j = 1$ or 2 ($1 \leq j \leq k$); see [Figure 15.3](#). The interval I_{i_1, \dots, i_k} of E_k contains the two sub-intervals $I_{i_1, \dots, i_k, 1}$ and $I_{i_1, \dots, i_k, 2}$ of E_{k+1} , so that the left-hand ends of I_{i_1, \dots, i_k} and $I_{i_1, \dots, i_k, 1}$ coincide as do the right-hand ends of I_{i_1, \dots, i_k} and $I_{i_1, \dots, i_k, 2}$. We write $R_{i_1, \dots, i_k} = |I_{i_1, \dots, i_k}| / |I_{i_1, \dots, i_{k-1}}|$ for the ratio of the lengths of each sub-interval to its ‘parent’ interval, and suppose that $a \leq R_{i_1, \dots, i_k} \leq b$ for all i_1, \dots, i_k . We thus obtain a random Cantor set $F = \bigcap_{k=1}^{\infty} E_k$.

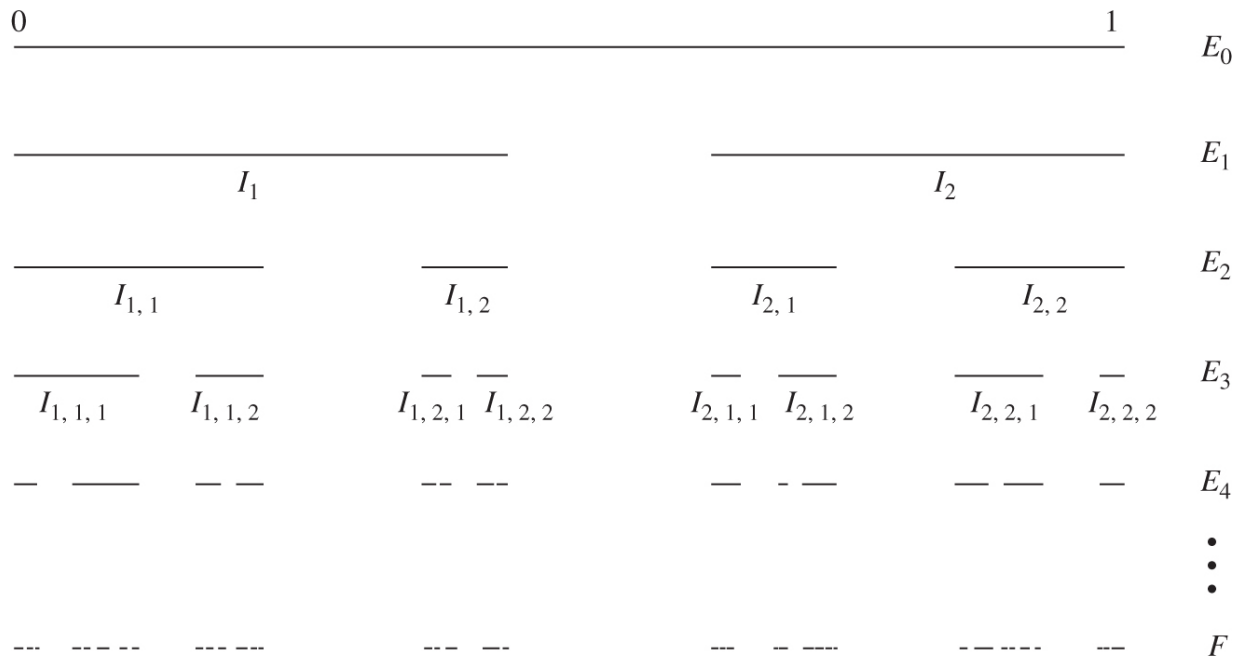


Figure 15.3 Construction of the random Cantor set analysed in Theorem 15.1. The length ratios $|I_{i_1, \dots, i_k, 1}| / |I_{i_1, \dots, i_k}|$ have the same statistical distribution for each i_1, \dots, i_k , as do the ratios $|I_{i_1, \dots, i_k, 2}| / |I_{i_1, \dots, i_k}|$.

We take Ω to be our sample space, and assume that a probability measure P is defined on a suitably large family \mathcal{F} of subsets of Ω , such that the ratios R_{i_1, \dots, i_k} are random variables. We impose statistical self-similarity on the construction by requiring $R_{i_1, \dots, i_k, 1}$ to have the same distribution as $R_1 = |I_1|$, and $R_{i_1, \dots, i_k, 2}$ to have the same distribution as $R_2 = |I_2|$ for every sequence i_1, \dots, i_k . We assume that the R_{i_1, \dots, i_k} are independent random variables, except that for each sequence i_1, \dots, i_k we do not require $R_{i_1, \dots, i_k, 1}$ and $R_{i_1, \dots, i_k, 2}$ to be independent. It may be shown that $\dim_H F$ is a random variable which may be expressed in terms of the R_{i_1, \dots, i_k} .

The following result is a random version of Theorem 9.3, indeed if the random ratios R_1 and R_2 are constant, then (15.1) reduces to the similarity dimension formula (9.14), that is, $r_1^s + r_2^s = 1$.

Theorem 15.1

With probability 1, the random Cantor set F described above has $\dim_H F = s$, where s is the solution of the expectation equation

$$E(R_1^s + R_2^s) = 1.$$

15.1

*Proof

It is easy to see that $\mathbb{E}(R_1^s + R_2^s)$ is continuous and strictly decreasing in s , and thus that (15.1) has a unique solution.

By slight abuse of notation, we write $I \in E_k$ to mean that the interval I is a k th-level interval I_{i_1, \dots, i_k} of E_k . For such an interval I , we write I_L and I_R for $I_{i_1, \dots, i_k, 1}$ and $I_{i_1, \dots, i_k, 2}$, respectively. We write $\mathbb{E}(X|\mathcal{F}_k)$ for the conditional expectation of a random variable X given a knowledge of the R_{i_1, \dots, i_j} for all sequences i_1, \dots, i_j with $j \leq k$. (Intuitively, we imagine that E_0, \dots, E_k have been constructed, and we are analysing what happens thereafter.) Let I_{i_1, \dots, i_k} be an interval of E_k . Then, for $s > 0$

$$\begin{aligned}\mathbb{E}(|I_{i_1, \dots, i_k, 1}|^s + |I_{i_1, \dots, i_k, 2}|^s) | \mathcal{F}_k) &= \mathbb{E}(R_{i_1, \dots, i_k, 1}^s + R_{i_1, \dots, i_k, 2}^s) | I_{i_1, \dots, i_k} |^s \\ &= \mathbb{E}(R_1^s + R_2^s) | I_{i_1, \dots, i_k} |^s\end{aligned}$$

as the ratios are identically distributed. Summing over all the intervals in E_k ,

$$\mathbb{E}\left(\sum_{I \in E_{k+1}} |I|^s \middle| \mathcal{F}_k\right) = \sum_{I \in E_k} |I|^s \mathbb{E}(R_1^s + R_2^s). \quad 15.2$$

It follows that the unconditional expectation satisfies

$$\mathbb{E}\left(\sum_{I \in E_{k+1}} |I|^s\right) = \mathbb{E}\left(\sum_{I \in E_k} |I|^s\right) \mathbb{E}(R_1^s + R_2^s). \quad 15.3$$

With s the solution of (15.1), (15.2) becomes

$$\mathbb{E}\left(\sum_{I \in E_{k+1}} |I|^s \middle| \mathcal{F}_k\right) = \sum_{I \in E_k} |I|^s. \quad 15.4$$

Readers familiar with probability theory will recognise (15.4) as saying that the sequence of random variables

$$X_k = \sum_{I \in E_k} |I|^s$$

15.5

is a martingale with respect to \mathcal{F}_k . Moreover, a routine calculation, see Exercise 15.7, shows that it is an L^2 -bounded martingale, that is, there is a number c such that $\mathbb{E}(X_k^2) \leq c$ for all k . The crucial fact for our purposes, which we ask other readers to take on trust, is that, in this situation, X_k converges with probability 1 as $k \rightarrow \infty$ to a random variable X such that $\mathbb{E}(X) = \mathbb{E}(X_0) = \mathbb{E}(1^s) = 1$. In particular, $0 \leq X < \infty$ with probability 1 and $X = 0$ with probability $q < 1$. But $X = 0$ if and only if $\sum_{I \in E_k \cap I_1} |I|^s$ and $\sum_{I \in E_k \cap I_2} |I|^s$ both converge to 0 as $k \rightarrow \infty$, where I_1 and I_2 are the intervals of E_1 , and this happens with probability q^2 , by virtue of the statistical self-similarity of the construction. Hence, $q = q^2$, so $q = 0$, and we conclude that $0 < X < \infty$ with probability 1. In particular, this implies that with probability 1, there are (random) numbers M_1, M_2 such that

$$0 < M_1 \leq X_k = \sum_{I \in E_k} |I|^s \leq M_2 < \infty$$

15.6

for all k . We have $|I| \leq 2^{-k}$ for all $I \in E_k$, so $\mathcal{H}_\delta^s(F) \leq \sum_{I \in E_k} |I|^s \leq M_2$ if $k \geq -\log \delta / \log 2$, giving $\mathcal{H}^s(F) \leq M_2$. Thus, $\dim_H F \leq s$ with probability 1.

We use the potential theoretic method of Section 1.3 to derive the almost sure lower bound for $\dim_H F$. To do this, we introduce a random mass distribution μ on the random set F . Let s satisfy (15.1). For $I \in E_k$, let $\mu(I)$ be the random variable

$$\mu(I) = \lim_{j \rightarrow \infty} \left\{ \sum |J|^s : J \in E_j \text{ and } J \subset I \right\}.$$

As with (15.5), this limit exists, and $0 < \mu(I) < \infty$ with probability 1. Furthermore, if $I \in E_k$,

$$\mathbb{E}(\mu(I)|\mathcal{F}_k) = |I|^s.$$

15.7

If $I \in E_k$, then $\mu(I) = \mu(I_L) + \mu(I_R)$, so μ is additive on the k th-level sets for all k , and so μ extends to a mass distribution with support contained in $\bigcap_{k=0}^{\infty} E_k = F$, see Proposition 1.7. (We ignore measure theoretic questions connected with the definition of μ .)

We fix $0 < t < s$ and estimate the expectation of the t -energy of μ . If $x, y \in F$, there is a greatest integer k such that x and y belong to a common k th-level interval; denote this interval by $x \wedge y$. If I is a k th-level interval, its $(k+1)$ th-level sub-intervals I_L and I_R are separated by a gap of at least $d|I|$, where $d = 1 - 2b$. Thus,

$$\begin{aligned} \iint_{x \wedge y = I} |x - y|^{-t} d\mu(x) d\mu(y) &= 2 \int_{x \in I_L} \int_{y \in I_R} |x - y|^{-t} d\mu(x) d\mu(y) \\ &\leq 2d^{-t} |I|^{-t} \mu(I_L) \mu(I_R). \end{aligned}$$

If $I \in E_k$,

$$\begin{aligned} \mathbb{E} \left(\iint_{x \wedge y = I} |x - y|^{-t} d\mu(x) d\mu(y) \middle| \mathcal{F}_{k+1} \right) \\ \leq 2d^{-t} |I|^{-t} \mathbb{E}(\mu(I_L) | \mathcal{F}_{k+1}) \mathbb{E}(\mu(I_R) | \mathcal{F}_{k+1}) \\ \leq 2d^{-t} |I|^{-t} |I_L|^s |I_R|^s \\ \leq 2d^{-t} |I|^{2s-t} \end{aligned}$$

using (15.7). Since the expectation does not depend on \mathcal{F}_k , using a variation of (1.21), this gives an inequality for the unconditional expectation

$$\mathbb{E} \left(\iint_{x \wedge y = I} |x - y|^{-t} d\mu(x) d\mu(y) \right) \leq 2d^{-t} \mathbb{E}(|I|^{2s-t}).$$

Summing over $I \in E_k$,

$$\mathbb{E} \left(\sum_{I \in E_k} \iint_{x \wedge y = I} |x - y|^{-t} d\mu(x) d\mu(y) \right) \leq 2d^{-t} \mathbb{E} \left(\sum_{I \in E_k} |I|^{2s-t} \right) = 2d^{-t} \lambda^k,$$

where $\lambda = \mathbb{E}(R_1^{2s-t} + R_2^{2s-t}) < 1$, using (15.3) repeatedly. Then,

$$\begin{aligned} \mathbb{E} \left(\int_F \int_F |x-y|^{-t} d\mu(x) d\mu(y) \right) &= \mathbb{E} \left(\sum_{k=0}^{\infty} \sum_{I \in E_k} \iint_{x \wedge y = I} |x-y|^{-t} d\mu(x) d\mu(y) \right) \\ &\leq 2d^{-t} \sum_{k=0}^{\infty} \lambda^k < \infty, \end{aligned}$$

so that the t -energy of μ is finite, with probability 1. As we have noted, $0 < \mu(F) = \mu([0,1]) < \infty$ with probability 1, so $\dim_H F \geq t$ by Theorem 4.13(a).

Note that the proof of Theorem 15.1 is typical of many random models, in that the key to both upper and lower estimates is the estimation of the moments $\mathbb{E} \left(\sum_{I \in E_k} |I|^t \right)$ for certain t .

This theorem and proof generalise in many directions. Each interval in E_k might give rise to a random number of intervals of random lengths in E_{k+1} . Of course, the construction generalises to \mathbb{R}^n , and the separation condition between different component intervals can be relaxed, provided some sort of ‘open set condition’ (see (9.12)) is satisfied. The following construction is a full random analogue of the sets discussed in Section 9.2.

Let V be an open subset of \mathbb{R}^n with closure \bar{V} , let $m \geq 2$ be an integer, and let $0 < b < 1$. We take Ω to be the class of all decreasing sequences $\bar{V} = E_0 \supset E_1 \supset E_2 \supset \dots$ of closed sets satisfying the following conditions. The set E_k is a union of the m^k closed sets $\bar{V}_{i_1, \dots, i_k}$ where $i_j = 1, \dots, m$ ($1 \leq j \leq k$) and V_{i_1, \dots, i_k} is either similar to V or is the empty set.

We assume that, for each i_1, \dots, i_k , the set V_{i_1, \dots, i_k} contains $V_{i_1, \dots, i_k, i}$ ($1 \leq i \leq m$) and that these sets are disjoint; this is essentially equivalent to the open set condition. If V_{i_1, \dots, i_k} is non-empty, we write $R_{i_1, \dots, i_k} = |V_{i_1, \dots, i_k}| / |V_{i_1, \dots, i_{k-1}}|$ for the similarity ratio between successive sets and we take $R_{i_1, \dots, i_k} = 0$ if V_{i_1, \dots, i_k} is the empty set. We define the random self-similar set $F = \bigcap_{k=0}^{\infty} E_k$.

Let \mathbb{P} be a probability measure on a family of subsets of Ω such that the R_{i_1, \dots, i_k} are random variables. Suppose that given $R_{i_1, \dots, i_k} > 0$, that is, given that V_{i_1, \dots, i_k} is non-empty, $R_{i_1, \dots, i_k, i}$ has identical distribution to R_i for each sequence i_1, \dots, i_k and for $1 \leq i \leq m$. We assume that the R_{i_1, \dots, i_k} are independent, except that, for each sequence i_1, \dots, i_k , the random variables $R_{i_1, \dots, i_k, 1}, \dots, R_{i_1, \dots, i_k, m}$ need not be independent. This defines a self-similar probability distribution on the constructions in Ω . We write N for the (random) number of the R_1, \dots, R_k that are positive, that is, the number of the sets V_1, \dots, V_k that are non-empty.

Theorem 15.2

The random set F described above has probability q of being empty, where $t = q$ is the smallest non-negative solution to the polynomial equation

$$f(t) \equiv \sum_{j=0}^m \mathbb{P}(N=j)t^j = t. \quad \text{15.8}$$

With probability $1 - q$, the set F has Hausdorff and box dimensions given by the solution s of

$$\mathbb{E} \left(\sum_{j=0}^m R_i^s \right) = 1. \quad \text{15.9}$$

*Note on proof

Basically, this is a combination of the probabilistic argument of Theorem 15.1 and the geometric argument of Theorem 9.3. Note that, if there is a positive probability that $N = 0$, then there is a positive probability that $E_1 = \emptyset$ and therefore that $F = \emptyset$. This ‘extinction’ occurs if each of the component sets in E_1 becomes extinct. By the statistical self-similarity of the process, if the probability of this happening is q , then $q = f(q)$. If q is any non-negative solution to this equation, then by induction,

$q \geq P(E_k = \emptyset)$ for all k : clearly this is that case when $k = 0$, and if this is satisfied for some k , then as f is increasing,

$q = f(q) \geq f(P(E_k = \emptyset)) = P(E_{k+1} = \emptyset)$. If $F = \emptyset$, then $E_k = \emptyset$ for some k , so $q \geq P(F = \emptyset)$, thus the probability of extinction is the least non-negative solution of $q = f(q)$

Observe that F has probability 0 of being empty, that is, $q = 0$, if and only if $N \geq 1$ with probability 1. It is also not hard to show that F is empty with probability 1, that is, $q = 1$, if and only if either $E(N) < 1$ or $E(N) = 1$ and $P(N = 1) < 1$. (These extinction probabilities are closely related to the theory of branching processes.)

Example 15.3 Random von Koch curve

Let R be a random variable with uniform distribution on the interval $(0, \frac{1}{3})$. Let E_0 be a unit line segment in \mathbb{R}^2 . We form E_1 by removing a proportion R from the middle of E_0 and replacing it by the other two sides of an equilateral triangle based on the removed interval. We repeat this for each of the four segments in E_1 independently and continue in this way to get a limiting curve F . Then, with probability 1, $\dim_H F = \dim_B F = 1.144\dots$.

Calculation

This is a special case of Theorem 15.2. The set V may be taken as the isosceles triangle based on E_0 and of height $\frac{1}{6}\sqrt{3}$. At each stage, a segment of length L is replaced by four segments of lengths $\frac{1}{2}(1-R)L, RL, RL$ and $\frac{1}{2}(1-R)L$, so we have $m = 4$ and $R_1 = R_4 = \frac{1}{2}(1-R)$ and $R_2 = R_3 = R$. Since R is uniformly distributed on $(0, \frac{1}{3})$, expression (15.9) becomes

$$1 = E \left(2 \left(\frac{1}{2}(1-R) \right)^s + 2R^s \right) = \int_0^{1/3} 3 \times 2 \left[\left(\frac{1}{2}(1-r) \right)^s + r^s \right] dr$$

or

$$s+1 = 12 \times 2^{-(s+1)} - 6 \times 3^{-(s+1)},$$

giving the dimension stated.

15.2 Fractal percolation

Fractals can have many different topological structures, they may be totally disconnected or they may be highly multiply connected. The statistically self-similar construction known as ‘fractal percolation’ exhibits a ‘phase transition’, where the topological structure changes dramatically as a parameter increases through a critical value.

Let p be a number with $0 < p < 1$. We divide the unit square E_0 into nine squares of side $\frac{1}{3}$ in the obvious way. We select a subset of these squares to form E_1 in such a way that each square has independent probability p of being selected. Similarly, each square of E_1 is divided into nine squares of side $\frac{1}{9}$, and each of these has independent probability p of being chosen to be a square of E_2 . We continue in this way, so that E_k is a random collection of k th-level

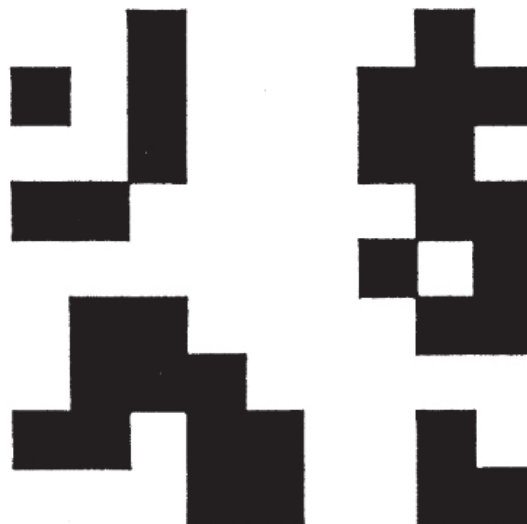
squares of side 3^{-k} . This procedure, which depends on the parameter p , defines a random fractal $F_p = \bigcap_{k=0}^{\infty} E_k$; see [Figures 15.4](#) and [15.5](#). (It is not difficult to describe this construction in precise probabilistic terms; for example, by taking the possible nested sequences of squares E_k as the sample space.) First we apply Theorem 15.2 to this random construction.



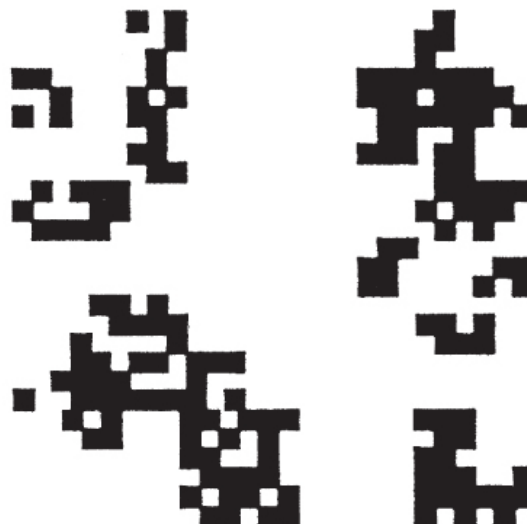
E_0



E_1

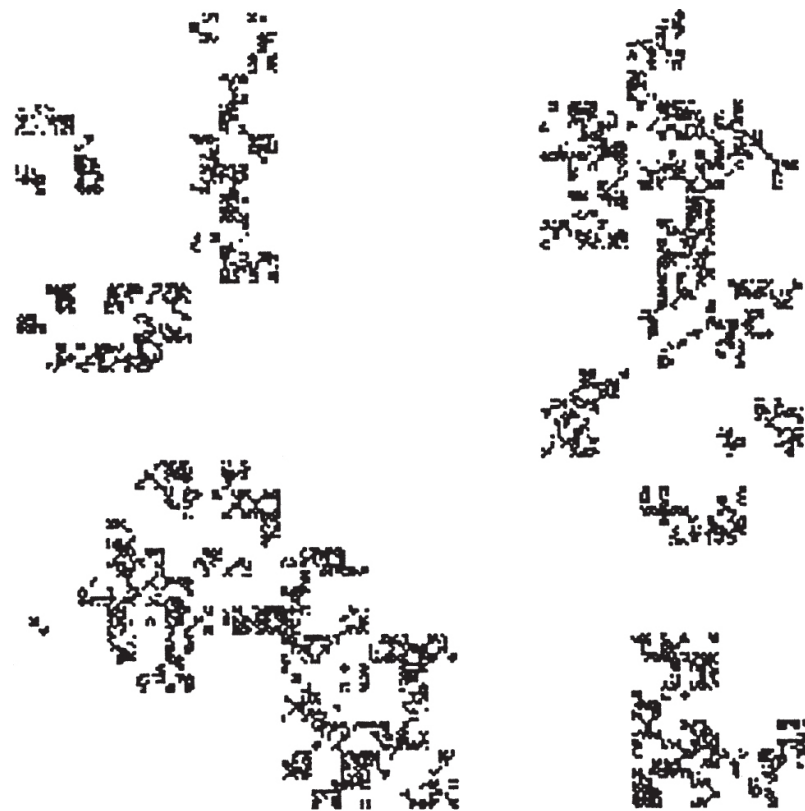


E_2

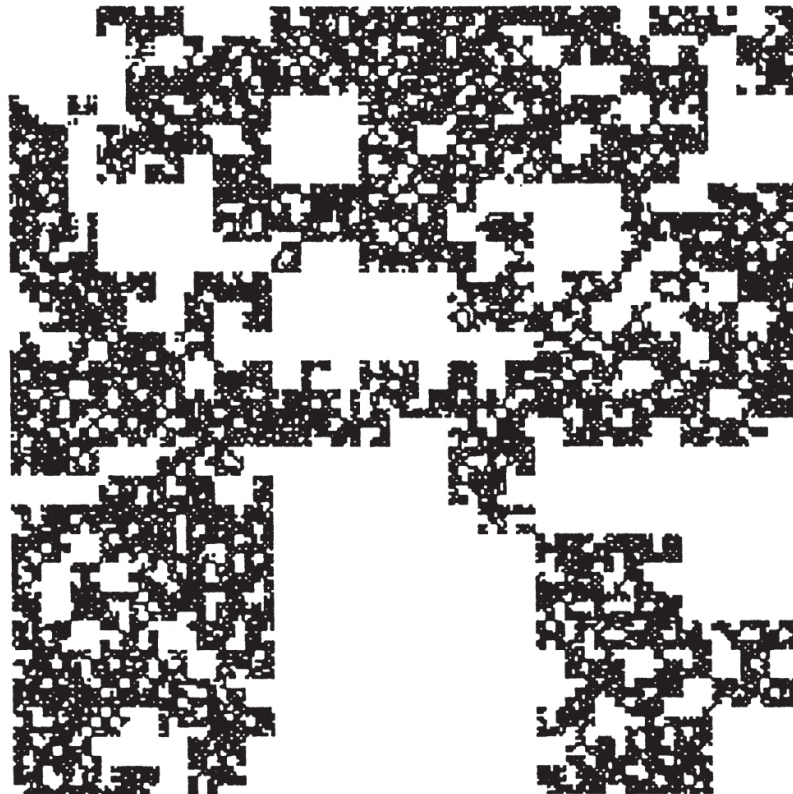


E_3

Figure 15.4. Steps in the construction of the random fractal discussed in Section 15.2 with $p = 0.6$. The fractal obtained is shown in [Figure 15.5a](#).



(a)



(b)

Figure 15.5 Random fractals realised by the percolation process discussed in Section 15.2 with (a) $p = 0.6$ and (b) $p = 0.8$.

Proposition 15.4

Given p , let $t = q$ be the least positive solution of the equation

$$t = (pt + 1 - p)^9.$$

Then F_p is empty with probability q . If $0 < p \leq \frac{1}{9}$, then $q = 1$. If $\frac{1}{9} < p < 1$, then $0 < q < 1$ and, with probability $1 - q$, $\dim_H F_p = \dim_B F_p = \log 9p / \log 3$.

Proof

Let N be the (random) number of squares in E_1 . Then,

$P(N = j) = \binom{9}{j} p^j (1-p)^{9-j}$, where $\binom{n}{r} = \frac{n!}{r!(n-r)!}$ denotes the

binomial coefficient, so the probability that $F_p = \emptyset$ is, using (15.8), the smallest positive solution of

$$t = \sum_{j=0}^9 \binom{9}{j} p^j (1-p)^{9-j} t^j = (pt + 1 - p)^9.$$

Each square of E_1 has side $\frac{1}{3}$, so (15.9) becomes

$$1 = E\left(\sum_{j=0}^N R_i^s\right) = E\left(\sum_{j=0}^N 3^{-s}\right) = 3^{-s} E(N) = 3^{-s} 9p$$

(each of the nine squares of side $\frac{1}{3}$ is selected with probability p , so the expected number chosen is $9p$). Thus, by Theorem 15.2, the almost sure dimension of F_p , given it is non-empty, is $\log 9p / \log 3$.

How does the qualitative nature of the random set F_p change as p increases from 0 to 1? We have noted that F_p is almost surely empty if $0 < p \leq \frac{1}{9}$. Also, if $\frac{1}{9} < p < \frac{1}{3}$, with probability 1 either $F_p = \emptyset$ or $\dim_H F_p = \log 9p / \log 3 < 1$, so, by Proposition 3.5, F_p is totally disconnected. At the other extreme, if p is close to 1, it is plausible that such a high proportion of the squares are retained at each stage of the construction that F_p will connect the left and right sides of the square E_0 ; when this happens we say that *percolation* occurs between the sides. We show that this is the case at least if p is very close to 1; the ridiculous bound 0.999 obtained below can certainly be reduced considerably.

Proposition 15.5

Suppose that $0.999 \leq p < 1$. Then, there is a positive probability (in fact bigger than 0.9999) that the random fractal F_p joins the left- and right-hand sides of E_0 .

*Proof

The proof depends on the observation that if I_1 and I_2 are abutting squares in E_k and both I_1 and I_2 contain either 8 or 9 subsquares of E_{k+1} , then there is a subsquare in I_1 and one in I_2 that abut, so that the squares of E_{k+1} in I_1 and I_2 form a connected unit.

We say that a square of E_k is *full* if it contains either eight or nine squares of E_{k+1} . We say that a square of E_k is *2-full* if it contains 8 or 9 full squares of E_{k+1} , and, inductively, that a square of E_k is *m-full* if it contains either eight or nine squares of E_{k+1} that are $(m-1)$ -full. By the above observation, if E_0 is *m*-full, then opposite sides of E_0 are joined by a sequence of abutting squares of E_m .

The square E_0 is *m*-full ($m \geq 1$) if either

- E_1 contains nine squares all of which are $(m-1)$ -full, or
- E_1 contains nine squares of which eight are $(m-1)$ -full, or
- E_1 contains eight squares all of which are $(m-1)$ -full.

Thus, if p_m is the probability that E_0 is *m*-full, we get, summing the probabilities of these three alternatives using (1.16), and using the self-similarity of the process,

$$\begin{aligned} p_m &= p^9 p_{m-1}^9 + p^9 9 p_{m-1}^8 (1 - p_{m-1}) + 9 p^8 (1 - p) p_{m-1}^8 \\ &= 9 p^8 p_{m-1}^8 - 8 p^9 p_{m-1}^9 \end{aligned} \quad \text{15.10}$$

if $m \geq 2$. Furthermore, $p_1 = p^9 + 9p^8(1-p) = 9p^8 - 8p^9$, so we have a discrete dynamical system defined by $p_m = f(p_{m-1})$ for $m \geq 1$, where $p_0 = 1$ and

$$f(t) = 9p^8 t^8 - 8p^9 t^9. \quad \text{15.11}$$

Suppose that $p = 0.999$. Then, (15.11) becomes

$$f(t) = 8.928\,251t^8 - 7.928\,287t^9$$

and a little calculation shows that $t_0 = 0.999\,961$ is a fixed point of f , which is stable in the sense that $0 < f(t) - t_0 \leq \frac{1}{2}(t - t_0)$ if $t_0 < t \leq 1$.

It follows that p_m is decreasing and converges to t_0 as $m \rightarrow \infty$, so there is a probability $t_0 > 0$ that E_0 is m -full for all m . When this happens, opposite sides of E_0 are joined by a sequence of squares in E_m for each m , so the intersection $F = \bigcap_{k=0}^{\infty} E_k$ joins opposite sides of E_0 . Thus, there is a positive probability of percolation occurring if $p = 0.999$, and consequently for larger values of p .

We have seen that if $0 < p < \frac{1}{3}$, then with probability 1, F_p is empty or totally disconnected. On the other hand, if $p > 0.999$, then there is a high probability of percolation. The next theorem states that one or other of these situations pertains for each value of p .

Theorem 15.16

There is a critical number p_c with $0.333 < p_c < 0.999$ such that if $0 < p < p_c$, then F_p is totally disconnected with probability 1, but if $p_c < p < 1$, then there is positive probability that F_p connects the left- and right-hand sides of E_0 .

Idea of proof

Suppose p is such that there is a positive probability of F_p not being totally disconnected. Then, there is positive probability of some two distinct points of F being joined by a path in F . This implies that there is a positive probability of the path passing through opposite sides of one of the squares in E_k for some k ; by virtue of the statistical self-similarity of the construction, there is a positive probability of a path crossing E_0 from left to right. Clearly, if F_p has probability 1 of being totally disconnected, the same is true of $F_{p'}$ if $p' < p$. Thus, the critical probability p_c is the supremum of those p such that F_p is totally disconnected and has the properties stated.

Experiment suggests that $0.7 < p_c < 0.8$.

The change in form of F_p as p increases through p_c is even more dramatic than Theorem 15.6 suggests. Let F'_p be a random set obtained by placing an independent random copy of F_p in every square of a grid of unit squares covering the plane. If $p < p_c$, then, almost surely, F'_p is totally disconnected. However, if $p \geq p_c$, then, with probability 1, F'_p has a single unbounded connected component. Thus, as p increases through p_c , there is a ‘phase transition’ as the isolated points of F'_p suddenly coalesce to form what is basically a single unit. The idea underlying this is that, if $p > p_c$, then if parts of F'_p lie in two different squares of the grid, there is a positive probability of them being joined by a path in F'_p . There are infinitely many such squares in an unbounded component of F'_p , so, if F'_p had two unbounded components, there would be probability 1 of them being joined.

15.3 Notes and references

Various extensions and generalisations of the random fractal construction discussed in Section 15.1 are given in Mandelbrot (1974, 1982); Kahane (1974); Peyrière (1974); Falconer (1986b); Mauldin and Williams (1986a); Graf (1987); Graf, Mauldin and Williams (1988); Olsen (1994); Kifer (1995); Hutchinson (2000); Hutchinson and Rüschendorf (2000) and Mörters (2010). ‘V-variable fractals’, which combine deterministic and random constructions in an novel way and are presented in Barnsley (2006) and Barnsley, Hutchinson and Stenflo (2008)

An interesting construction for fractals by random deletion was introduced by Mandelbrot (1972); see also Zähle (1984); Kahane (1993) and Falconer (1997). For other applications of probability to fractals, see Stoyan and Stoyan (1994).

The fractal percolation model was suggested by Mandelbrot (1974). Chayes, Chayes and Durrett (1988) analysed the phase transition in detail, and Dekking and Meester (1990) highlighted other phase transitions of the model. Chayes (1995) surveys fractal percolation and its generalisations. Some recent variants are given in Broman, van de Brug, and Camia (2012).

‘Discrete’ percolation, where points are selected at random from a large square mesh, is discussed in the books by Bollobás and Riordan (2006) and Grimmett (2010), with a more applied approach in Stauffer and Aharony (1994). There are many relationships between discrete and fractal percolation.

Exercises

15.1 Find the almost sure Hausdorff dimension of the random Cantor set constructed by removing the middle third of each interval with probability $\frac{1}{2}$ and the middle two-thirds of the interval with probability $\frac{1}{2}$ at each step of the construction.

15.2 Consider the following random version of the von Koch construction. We start with a unit segment. With probability $\frac{1}{2}$, we

replace the middle third of the segment by the other two sides of the (upwards pointing) equilateral triangle, and with probability $\frac{1}{2}$, we remove the middle third altogether. We repeat this procedure with the segments that remain, in the usual way. Show that, with probability 1, this random fractal has Hausdorff dimension 1.

15.3 Show that the random von Koch curve depicted in [Figure 15.1](#) *always* has Hausdorff dimension $s = \log 4 / \log 3$ and, indeed, is an s -set. (This is not typical of random constructions.)

15.4 Let $0 < p < 1$. We may randomise the construction of the Sierpiński triangle (Figure 0.3) by selecting each of the three equilateral subtriangles independently with probability p at each step. (Thus, we have a percolation process based on the Sierpiński gasket.) Show that if $p \leq \frac{2}{3}$ then the limiting set F is empty with probability 1, but if $\frac{2}{3} < p < 1$, then there is a positive probability that F is non-empty. Find an expression for this probability, and show that, given F is non-empty, $\dim_H F = \log 3p / \log 2$ with probability 1.

15.5 For the random Sierpiński gasket described in Exercise 15.4, show that F is totally disconnected with probability 1 for every $p < 1$. (We regard two triangles as being joined if they touch at a vertex.)

15.6 Consider the random Cantor set analysed in Theorem 15.1. With $\mathcal{H}_\infty^s(F)$ denoting the infimum of the sums in (3.1) over arbitrary coverings of F , show that

$$\mathcal{H}_\infty^s(F) = \min\{1, \mathcal{H}_\infty^s(F \cap I_1) + \mathcal{H}_\infty^s(F \cap I_2)\}$$

where s is the solution of (15.1). Use statistical self-similarity to deduce that, unless $P(R_1^s + R_2^s = 1) = 1$, then, almost surely, $\mathcal{H}_\infty^s(F) = 0$, and thus $\mathcal{H}^s(F) = 0$.

15.7 Show that the martingale X_k given by (15.5) is L^2 -bounded, that is, $E(X_k^2) \leq m$ for all k , for some number m . (Hint: Show that $E(X_{k+1}^2 | \mathcal{F}_k) \leq X_k^2 + a\gamma^k$, where $\gamma = E(R_1^{2s} + R_2^{2s}) < 1$ and a is a constant, and then take unconditional expectations.)

15.8 Consider the fractal percolation model F constructed with selection probability p , where $p_c < p < 1$. Show that with probability 1, either $F = \emptyset$ or F contains infinitely many non-trivial connected components. (Here, non-trivial means containing at least two distinct points.)

Chapter 16

Brownian motion and Brownian surfaces

In 1827, the botanist Robert Brown noticed that minute particles suspended in a liquid moved on highly irregular trails. This, and a similar phenomenon for smoke particles in air, was eventually explained as a result of molecular bombardment of the particles. Einstein published a mathematical study of this motion, which eventually led to Perrin's Nobel Prize-winning calculation of Avogadro's number.

In 1923, Wiener proposed a rigorous mathematical model that exhibited random behaviour similar to that observed in Brownian motion. The paths described by this 'Wiener process' in 3-dimensional space are so irregular as to have Hausdorff dimension equal to 2. This is a good example of a natural phenomenon with a fractal appearance that can be explained by a simple mathematical model.

A trail may be described by a function $f : \mathbb{R} \rightarrow \mathbb{R}^n$, where $f(t)$ is the position of a particle at time t . We can study f from two differing viewpoints. Either we can think of the *trail* or *image*

$f([t_1, t_2]) = \{f(t) : t_1 \leq t \leq t_2\}$ as a subset of \mathbb{R}^n with t regarded merely as a parameter, or we can consider the *graph* of f ,

$\text{graph } f = \{(t, f(t)) : t_1 \leq t \leq t_2\} \subset \mathbb{R}^{n+1}$, as a record of the variation of f with time. We investigate the form of Brownian trails and graphs which are, in general, fractals.

Brownian motion is a random phenomenon, and probability theory is central in its study. We first examine classical Brownian motion, and then consider some variants that have been used to model a wide variety of phenomena, including polymer chains, stock market prices and topographical surfaces.

16.1 Brownian motion in \mathbb{R}

We introduce Brownian motion on the real line as a limit of a random walk or ‘drunkard’s walk’, and extend the definition to the higher dimensional cases in the next section.

A random walker on a straight road (which we identify with a point on the real line \mathbb{R}) takes a step of length δ at time intervals of τ , moving forwards or backwards with equal probability $\frac{1}{2}$ with the direction of the steps all independent. Let $X_\tau(t)$ denote the position of the walker at time t . Then, given the position $X_\tau(k\tau)$ at time $k\tau$, the position $X_\tau((k+1)\tau)$ at time $(k+1)\tau$ is equally likely to be $X_\tau(k\tau) + \delta$ or $X_\tau(k\tau) - \delta$. Assuming that the walker starts at the origin at time 0, then for $t > 0$, the position at time t is described by the random variable

$$X_\tau(t) = \delta(Y_1 + \cdots + Y_{[t/\tau]}),$$

where Y_1, Y_2, \dots are independent random variables, each taking the value of $+1$ with probability $\frac{1}{2}$ and -1 with probability $\frac{1}{2}$. Here, $[t/\tau]$ denotes the largest integer less than or equal to t/τ . We normalise the step length by setting $\delta = \sqrt{\tau}$ so that

$$X_\tau(t) = \sqrt{\tau}(Y_1 + \cdots + Y_{[t/\tau]}). \quad \text{16.1}$$

Then the mean and variance of the walker’s position at time t are

$$\mathbb{E}(X_\tau(t)) = \sqrt{\tau}(\mathbb{E}(Y_1) + \cdots + \mathbb{E}(Y_{[t/\tau]})) = 0$$

and

$$\text{var}(X_\tau(t)) = \tau(\text{var}(Y_1) + \cdots + \text{var}(Y_{[t/\tau]})) = \tau[t/\tau] \sim t$$

if t is large compared with τ . Thus, over a large number of random walks the average position at time t is 0 and the typical distance of the walker from the origin will be around \sqrt{t} , the standard deviation of $X_\tau(t)$. Moreover, the central limit theorem (see (1.26)) tells us that

the random variable $X_\tau(t)$ is approximately normally distributed with mean 0 and variance close to τ . In the same way, if t and h are fixed and τ is sufficiently small, then the increment $X_\tau(t+h) - X_\tau(t)$ is approximately normal with mean 0 and variance h . We also note that, if $0 \leq t_1 \leq t_2 \leq \dots \leq t_{2m}$, then the increments

$X_\tau(t_2) - X_\tau(t_1), X_\tau(t_4) - X_\tau(t_3), \dots, X_\tau(t_{2m}) - X_\tau(t_{2m-1})$ are independent random variables. We define Brownian motion with the limit of the random walk $X_\tau(t)$ as $\tau \rightarrow 0$ in mind.

Let $(\Omega, \mathcal{F}, \mathbb{P})$ be a probability space. We will call X a *random process* or *random function* from $[0, \infty)$ to \mathbb{R} if $X(t)$ is a random variable for each t with $0 \leq t < \infty$. Sometimes, we consider random functions on a finite interval $[t_1, t_2]$ instead, but the ideas are very similar. (In the formal definition of a random process, there is an additional measurability condition, which need not concern us here.) We think of X as defining a *sample function* $t \mapsto X(\omega, t)$ for each point ω in the sample space Ω . The points of Ω parametrise the functions $X : [0, \infty) \rightarrow \mathbb{R}$, so \mathbb{P} may be regarded as a probability measure on this class of functions. We will be particularly interested in the fractal nature of typical sample functions.

We define *Brownian motion* or the *Wiener process* to be a random process X such that:

(BM)

- i. with probability 1, $X(0) = 0$ (i.e. the process starts at the origin), and $X(t)$ is a continuous function of t ;
- ii. for all $t \geq 0$ and $h > 0$, the increment $X(t+h) - X(t)$ is normally distributed with mean 0 and variance h ; thus,

$$\mathbb{P}(X(t+h) - X(t) \leq x) = \frac{1}{\sqrt{2\pi h}} \int_{-\infty}^x \exp\left(-\frac{u^2}{2h}\right) du; \quad \text{16.2}$$

- iii. if $0 \leq t_1 \leq t_2 \leq \dots \leq t_{2m}$, the increments $X(t_2) - X(t_1), X(t_4) - X(t_3), \dots, X(t_{2m}) - X(t_{2m-1})$ are independent.

Note that it is immediate from (i) and (ii) that $X(t)$ is itself normally distributed with mean 0 and variance t for each t . Observe that the increments of X are *stationary*, that is, the distribution of $X(t+h) - X(t)$ is independent of t .

The first question that arises is whether there actually is a random function satisfying the conditions (BM). It requires some effort to show that Brownian motion does exist, and we do not do so here. The proof uses the special properties of the normal distribution. For example, given that $X(t_2) - X(t_1)$ and $X(t_3) - X(t_2)$ are independent and normal with means 0 and variances $t_2 - t_1$ and $t_3 - t_2$, respectively, the sum $X(t_3) - X(t_1)$ is necessarily normal with mean 0 and variance $t_3 - t_1$; see (1.24) *et seq.* This is essential for the definition (BM) to be self-consistent. However, it should at least seem plausible that a continuous process $X(t)$ satisfying (BM) exists, if only as a limit of the random walks $X_\tau(t)$ as $\tau \rightarrow 0$.

Instead of proving existence, we mention three methods of simulating Brownian sample functions on a computer. Each method can, in fact, be used as a basis for existence proofs. The first method uses the random walk approximation (16.1). Values of 1 or -1 are assigned by ‘coin tossing’ to Y_i for $1 \leq i \leq m$, where m is large, and $X_\tau(t)$ is plotted when t is an integer multiple of τ . If τ is large compared with τ , then this gives a good approximation to a Brownian sample function.

The ‘random midpoint displacement’ method may also be used to obtain a sample function $X : [0, 1] \rightarrow \mathbb{R}$. We define the values of $X(k2^{-j})$, where $0 \leq k \leq 2^j$ by induction on j . We set $X(0) = 0$ and choose $X(1)$ at random from a normal distribution with mean 0 and variance 1. Next we select $X(\frac{1}{2})$ from a normal distribution with mean $\frac{1}{2}(X(0) + X(1))$ and variance $\frac{1}{2}$. At the next step, $X(\frac{1}{4})$ and $X(\frac{3}{4})$ are chosen, and so on. At the j th stage, the values $X(k2^{-j})$ for odd k are chosen independently from a normal distribution with mean $\frac{1}{2}(X((k-1)2^{-j}) + X((k+1)2^{-j}))$ and variance 2^{-j} . This procedure determines $X(t)$ at all binary points $t = k2^{-j}$. Assuming that X is continuous, then X is completely determined. It may be shown,

using properties of normal distributions, that the functions thus generated have a distribution satisfying (BM).

Brownian motion on $[0, \pi]$ has a Fourier series representation

$$X(t) = \frac{1}{\sqrt{\pi}} C_0 t + \sqrt{\frac{2}{\pi}} \sum_{k=1}^{\infty} C_k \frac{\sin kt}{k},$$

where the C_k have independent normal distributions of mean 0 and variance 1. The series converges almost surely, though rather slowly. Choosing the C_k at random and curtailing the series gives an approximation to a sample function.

The graph of a Brownian sample function is shown in [Figure 16.1](#).

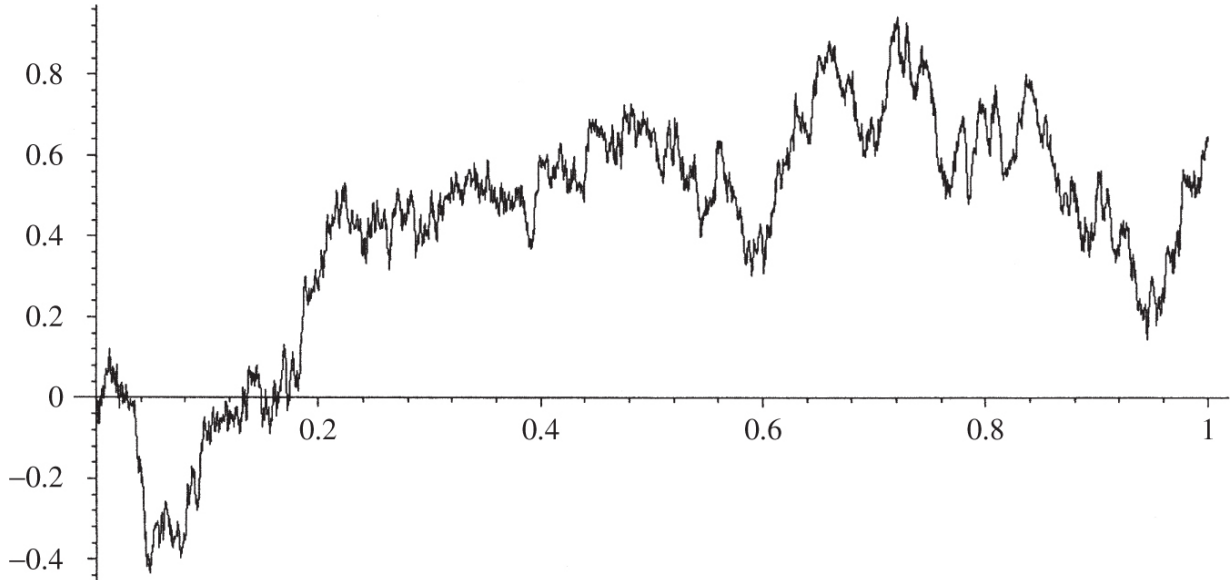


Figure 16.1 Graph of a realisation of Brownian motion.

If $\gamma > 0$, replacing h by γh and x by $\gamma^{1/2}x$ does not alter the value of the right-hand side of [\(16.2\)](#) on substituting $u = \gamma^{1/2}u_1$ in the integral. Thus,

$$\mathbb{P}(X(\gamma(t+h)) - X(\gamma t) \leq \gamma^{1/2}x) = \mathbb{P}(X(t+h) - X(t) \leq x) \quad \text{16.3}$$

for all x . It follows that $X(t)$ and $\gamma^{-1/2}X(\gamma t)$ have the same distribution. Changing the temporal scale by a factor γ and the spatial scale by a factor $\gamma^{1/2}$ gives a process with the same statistical distribution as

the original, so we term Brownian motion $X(t)$ and its graph *statistically self-affine*. But we call Brownian trails *statistically self-similar*, in that, the spatial distribution of the trails $\{X(t) : 0 \leq t \leq T\}$ and $\{X(t) : 0 \leq t \leq \gamma T\}$ are indistinguishable except for a scale factor of $\gamma^{1/2}$.

A fundamental property of Brownian motion is that, with probability 1, the sample functions satisfy a Hölder condition of exponent λ for all $0 < \lambda < \frac{1}{2}$, in particular, for λ arbitrarily close to $\frac{1}{2}$.

Proposition 16.1

Suppose $0 < \lambda < \frac{1}{2}$. With probability 1, the Brownian sample function $X : [0, 1] \rightarrow \mathbb{R}$ satisfies

$$|X(t+h) - X(t)| \leq b|h|^\lambda \quad (|h| < H_0) \quad \text{16.4}$$

for some (random) $H_0 > 0$, where b depends only on λ . Equivalently, there is a random constant B such that

$$|X(t+h) - X(t)| \leq B|h|^\lambda \quad (t, t+h \in [0, 1]). \quad \text{16.5}$$

Proof

For $h > 0$ we have, by (16.2),

$$\begin{aligned}
 \mathbb{P}(|X(t+h) - X(t)| > h^\lambda) &= \frac{2}{\sqrt{2\pi h}} \int_{h^{\lambda-1/2}}^{\infty} \exp\left(\frac{-u^2}{2h}\right) du \\
 &= c_1 \int_{h^{\lambda-1/2}}^{\infty} \exp\left(\frac{-w^2}{2}\right) dw \\
 &\leq c_2 \int_{h^{\lambda-1/2}}^{\infty} \exp(-w) dw \\
 &= c_2 \exp(-h^{\lambda-1/2}) \\
 &\leq c_3 h^2
 \end{aligned} \tag{16.6}$$

after a substitution $w = uh^{-1/2}$ and some estimates, including $\exp(-x) \leq \text{const } x^{-\alpha}$ for each $\alpha > 0$, where c_1, c_2 and c_3 do not depend on h or t (though c_3 depends on λ). Taking $[t, t+h]$ as the binary intervals $[(m-1)2^{-j}, m2^{-j}]$, we have for each positive integer k ,

$$\begin{aligned}
 \mathbb{P}(|X((m-1)2^{-j}) - X(m2^{-j})| > 2^{-j\lambda} \text{ for some } j \geq k \text{ and } 1 \leq m \leq 2^j) \\
 &\leq c_3 \sum_{j=k}^{\infty} 2^j 2^{-2j} \\
 &= c_3 2^{-k+1}.
 \end{aligned}$$

Thus, with probability 1, there is an integer K such that

$$|X((m-1)2^{-j}) - X(m2^{-j})| \leq 2^{-j\lambda} \tag{16.7}$$

for all $j > K$ and $1 \leq m \leq 2^j$. If $h < H_0 \equiv 2^{-K}$, the interval $[t, t+h]$ may, except possibly for the end points, be expressed as a countable union of contiguous binary intervals of the form $[(m-1)2^{-j}, m2^{-j}]$ with $2^{-j} \leq h$ and with no more than two intervals of any one length. (Take all the binary intervals in $[t, t+h]$ not contained in any other such intervals.) Then, using the continuity of X , if k is the least integer with $2^{-k} \leq h$,

$$|X(t) - X(t+h)| \leq 2 \sum_{j=k}^{\infty} 2^{-j\lambda} = \frac{2^{-k\lambda} 2}{(1-2^{-\lambda})} \leq \frac{2h^\lambda}{(1-2^{-\lambda})}.$$

Since $X(t)$ is almost surely continuous and therefore bounded on $[0, 1]$, the inequality in (16.4) holds for some (different) value of b for $H_0 \leq |h| \leq 1$, so (16.5) follows for all $0 \leq t, t+h \leq 1$ for some random B .

With more delicate estimates, (16.4) may be improved to give that, with probability 1, a Brownian sample function satisfies

$$|X(t+h) - X(t)| \leq B|h \log(1/h)|^{1/2} \quad (t, t+h \in [0, 1])$$

for some (random) B . Thus, on the one hand, the increments of Brownian motion over intervals of length h are essentially no bigger than of order $h^{1/2}$, but on the other hand, the variance of the increments equals $h^{1/2}$, so they are frequently of this sort of size.

The Hölder estimate (16.4) enables us to show the important property that the dimension of the graph of Brownian motion is exactly $1\frac{1}{2}$ almost surely.

Theorem 16.2

With probability 1, the graph of a Brownian sample function $X : [0, 1] \rightarrow \mathbb{R}$ has Hausdorff and box dimension $1\frac{1}{2}$.

Proof

From the Hölder condition (16.4) and Corollary 11.2(a), it follows that, with probability 1, graph X has Hausdorff dimension and upper box dimension at most $2 - \lambda$ for every $\lambda < \frac{1}{2}$, so has dimensions at most $1\frac{1}{2}$.

For the lower bound, we estimate negative powers of the distance between two points $(t, X(t))$ and $(t + h, X(t + h))$ on the graph of X to enable us to use the potential theoretic method. We define

$$p(x) \equiv \mathbb{P}(|X(t + h) - X(t)| \leq x) = ch^{-1/2} \int_0^x \exp\left(\frac{-u^2}{2h}\right) du,$$

for a constant c , this estimate coming from (16.2). Then, for $1 < s < 2$,

$$\begin{aligned} \mathbb{E}((|X(t + h) - X(t)|^2 + h^2)^{-s/2}) &= \int_0^\infty (x^2 + h^2)^{-s/2} dp(x) \\ &= ch^{-1/2} \int_0^\infty (x^2 + h^2)^{-s/2} \exp\left(\frac{-x^2}{2h}\right) dx \\ &\leq ch^{-1/2} \int_0^\infty (x^2 + h^2)^{-s/2} dx \\ &\leq ch^{-1/2} \int_0^h h^{-s} dx + ch^{-1/2} \int_h^\infty x^{-s} dx \\ &\leq c_1 h^{1/2-s}, \end{aligned}$$

where c_1 does not depend on h , on splitting the range of integration and estimating the integrand in two ways. We may lift Lebesgue measure \mathcal{L} from the t -axis to get a mass distribution μ_f on the graph of a function f given by

$$\mu_f(A) = \mathcal{L}\{t : 0 \leq t \leq 1 \text{ and } (t, f(t)) \in A\}.$$

Using Pythagoras' Theorem to give the distance between two points on $\text{graph } f$,

$$\begin{aligned} & \mathbb{E} \left(\iint |x - y|^{-s} d\mu_X(x) d\mu_X(y) \right) \\ &= \int_0^1 \int_0^1 \mathbb{E}((|X(t) - X(u)|^2 + |t - u|^2)^{-s/2}) dt du \\ &\leq \int_0^1 \int_0^1 c_1 |t - u|^{1/2-s} dt du \\ &< \infty \end{aligned}$$

if $s < 1\frac{1}{2}$. Thus, $\mu_X(\text{graph } f) = 1$ and μ_X has finite s -energy with probability 1, so Theorem 4.13(a) gives $\dim_{\text{H}} \text{graph } X \geq 1\frac{1}{2}$.

In fact, Brownian graphs have dimension logarithmically smaller than $1\frac{1}{2}$: with probability 1, the graph of X over the range $[0, 1]$ has positive finite measure with respect to the gauge function $h(t) = t^{3/2} \log \log(1/t)$; see Section 1.6.

Since, with probability 1, the graph of X over any interval has dimension $1\frac{1}{2}$, it is immediate that Brownian functions, though continuous, do not have a continuous derivative in any interval. Indeed, it may be shown that, with probability 1, a Brownian function is nowhere differentiable.

The sets of times at which a Brownian sample function takes particular values are often of interest. If $f : [0, 1] \rightarrow \mathbb{R}$ is a function, we define the *level sets* $f^{-1}(c) = \{t : f(t) = c\}$ for each $c \in \mathbb{R}$. The level sets are, essentially, the intersections of the graph of f with lines parallel to the t -axis.

Proposition 16.3

With probability 1, a Brownian sample function $X : [0, 1] \rightarrow \mathbb{R}$ has $\dim_H X^{-1}(c) \leq \frac{1}{2}$ for almost all c (in the sense of 1-dimensional Lebesgue measure). Moreover, for any given c , $\dim_H X^{-1}(c) = \frac{1}{2}$ with positive probability.

Note on proof

With probability 1, we have $\dim_H X^{-1}(c) = \dim_H((\text{graph } X) \cap L_c)$ for almost all c , where L_c is the line $y = c$; otherwise Corollary 7.10 would imply that $\dim_H \text{graph } X > 1 \frac{1}{2}$, contradicting Theorem 16.2.

It is harder to show that $\dim_H X^{-1}(c) = \frac{1}{2}$ with positive probability. One possible approach is along the lines of that indicated for the proof of Theorem 8.3.

16.2 Brownian motion in \mathbb{R}^n

It is easy to extend the definition of Brownian motion from \mathbb{R} to \mathbb{R}^n : we just define Brownian motion on \mathbb{R}^n so that the coordinate components are independent 1-dimensional Brownian motions.

Thus, $X : [0, \infty) \rightarrow \mathbb{R}^n$, given by $X(t) = (X_1(t), \dots, X_n(t))$, is an n -dimensional Brownian motion on a suitable probability space if the random processes X_i are independent 1-dimensional Brownian motions for each i . It follows from the properties of 1-dimensional Brownian motion and Pythagoras' theorem that the increments $X(t+h) - X(t)$ of n -dimensional Brownian motion have (vector) mean 0 and their lengths $|X(t+h) - X(t)|$ have variance nh .

We term a path $X[0, a]$ followed by Brownian motion in \mathbb{R}^n a *Brownian trail*; see [Figure 16.2](#).

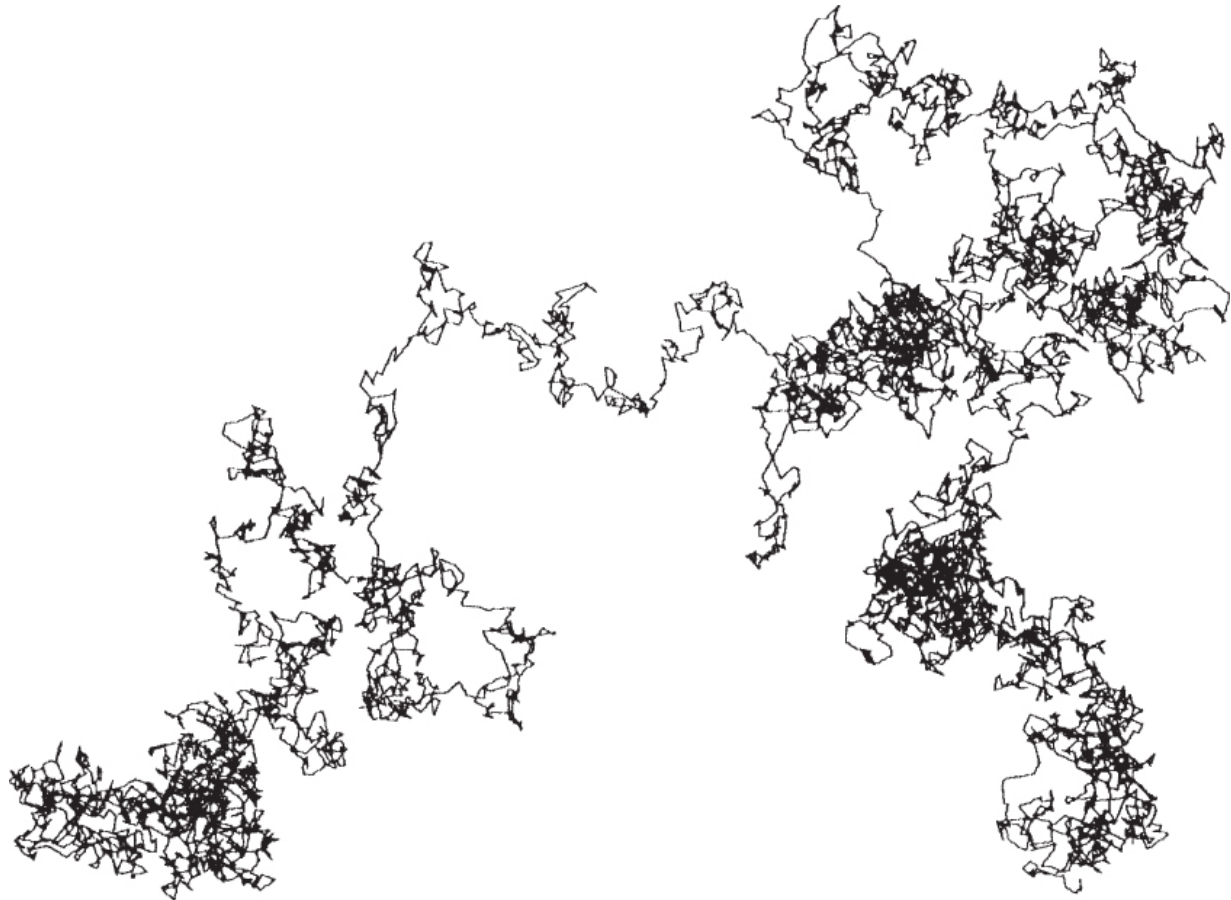


[Figure 16.2](#) A simulation of a Brownian trail in \mathbb{R}^2 .

By definition, the projection of $X(t)$ onto each of the coordinate axes is a 1-dimensional Brownian motion. However, the coordinate axes are not special in this respect: n -dimensional Brownian motion is *isotropic*; that is, has the same characteristics in every direction. To see this, consider, for convenience, the case of 2-dimensional Brownian motion $X(t) = (X_1(t), X_2(t))$. The projection of $X(t)$ onto the line L_θ at angle θ through the origin is $X_1(t)\cos\theta + X_2(t)\sin\theta$. For $t \geq 0$ and $h > 0$, the random variables $X_1(t+h) - X_1(t)$ and $X_2(t+h) - X_2(t)$ are independent and normally distributed with means 0 and variances h . Thus, the increments of the projection onto L_θ , given by

$$(X_1(t+h) - X_1(t))\cos\theta + (X_2(t+h) - X_2(t))\sin\theta,$$

are normally distributed with mean 0 and variance $h \cos^2\theta + h \sin^2\theta = h$; see the remarks after (1.24). Similarly, the increments of the projection are independent, so the projection of $X(t)$ onto L_θ is 1-dimensional Brownian motion, for all angles θ .

For $\gamma > 0$, applying (16.3) to each coordinate of $X(t)$ gives

$$\mathbb{P}(X_i(\gamma(t+h)) - X_i(\gamma t) \leq \gamma^{1/2}x_i) = \mathbb{P}(X_i(t+h) - X_i(t) \leq x_i)$$

for all x_i . For n -dimensional Brownian motion, just as in the 1-dimensional case, $X(t)$ and $\gamma^{-1/2}X(\gamma t)$ have the same distribution, so the process is statistically self-affine. The trails $\{X(t) : 0 \leq t \leq T\}$ and $\{X(t) : 0 \leq t \leq \gamma T\}$ scaled by a factor $\gamma^{1/2}$ have the same distribution in n -dimensional space, so the Brownian trails are statistically self-similar.

As in the 1-dimensional case, sample functions of n -dimensional Brownian motion satisfy a Hölder condition of exponent λ for all $0 < \lambda < \frac{1}{2}$.

Proposition 16.4

Suppose $0 < \lambda < \frac{1}{2}$. With probability 1, the Brownian sample function $X : [0, 1] \rightarrow \mathbb{R}^n$ satisfies

$$|X(t+h) - X(t)| \leq B|h|^\lambda \quad (t, t+h \in [0, 1]). \tag{16.8}$$

for some random constant B .

Proof

With $X(t) = (X_1(t), \dots, X_n(t))$, applying (16.5) to each coordinate gives random constants B_1, \dots, B_n such that $|X_i(t+h) - X_i(t)| \leq B_i|h|^\lambda$ for all $t, t+h \in [0, 1]$ for each i . Inequality (16.8) follows with $B = (\sum_{i=1}^n B_i^2)^{1/2}$ using Pythagoras' theorem.

To study the properties of Brownian trails, we need to know the spatial distribution of n -dimensional Brownian and its increments. With n -dimensional Brownian motion in coordinate form $X(t) = (X_1(t), \dots, X_n(t))$, the increments $X_i(t+h) - X_i(t)$ have independent normal distribution for each i , so, for intervals $[a_i, b_i]$,

$$\mathbb{P}(X_i(t+h) - X_i(t) \in [a_i, b_i]) = \frac{1}{\sqrt{2\pi h}} \int_{a_i}^{b_i} \exp\left(-\frac{x_i^2}{2h}\right) dx_i,$$

by (16.2). Hence, if E is the coordinate parallelepiped $[a_1, b_1] \times \dots \times [a_n, b_n]$

$$\begin{aligned} \mathbb{P}(X(t+h) - X(t) \in E) &= \prod_{i=1}^n \left(\frac{1}{\sqrt{2\pi h}} \int_{a_i}^{b_i} \exp\left(-\frac{x_i^2}{2h}\right) dx_i \right) \\ &= \frac{1}{(2\pi h)^{n/2}} \int_E \exp\left(-\frac{|x|^2}{2h}\right) dx, \end{aligned} \tag{16.9}$$

where $x = (x_1, \dots, x_n)$. By approximating sets by unions of such parallelepipeds, it follows that (16.9) holds for any Borel set E . In particular, taking E as the ball $B(0, \rho)$ and converting into polar coordinates,

$$\mathbb{P}(|X(t+h) - X(t)| \leq \rho) = ch^{-n/2} \int_{r=0}^{\rho} r^{n-1} \exp\left(-\frac{r^2}{2h}\right) dr, \tag{16.10}$$

where $c = (2\pi)^{-n/2} a_n$ with a_n the $(n-1)$ -dimensional area of the surface of $B(0, 1)$.

We use (16.10) to find the dimension of Brownian trails in n -dimensional space.

Theorem 16.5

With probability 1, a Brownian trail in $\mathbb{R}^n (n \geq 2)$ has Hausdorff dimension and box dimension 2.

Proof

For every $0 < \lambda < \frac{1}{2}$, the function $X : [0, 1] \rightarrow \mathbb{R}^n$ satisfies a Hölder condition (16.8) with probability 1, so by Proposition 3.3, $\dim_H X([0, 1]) \leq (1/\lambda) \dim_H [0, 1] = 1/\lambda$, with a similar inequality for box dimensions. Thus, almost surely, Brownian trails have dimension at most 2.

For the lower bound, we use the potential theoretic method. Take $1 < s < 2$. For given t and h , let $p(\rho)$ denote the expression in (16.10). Taking the expectation, it follows that

$$\begin{aligned} \mathbb{E}(|X(t+h) - X(t)|^{-s}) &= \int_0^\infty r^{-s} dp(r) \\ &= ch^{-n/2} \int_0^\infty r^{-s+n-1} \exp\left(\frac{-r^2}{2h}\right) dr \\ &= \frac{1}{2} ch^{-s/2} \int_0^\infty w^{(n-s-2)/2} \exp\left(\frac{-w}{2}\right) dw \\ &= c_1 h^{-s/2} \end{aligned} \tag{16.11}$$

after substituting $w = r^2/h$, where c_1 is independent of h and t . Then,

$$\begin{aligned} \mathbb{E}\left(\int_0^1 \int_0^1 |X(t) - X(u)|^{-s} dt du\right) &= \int_0^1 \int_0^1 \mathbb{E}(|X(t) - X(u)|^{-s}) dt du \\ &= \int_0^1 \int_0^1 c_1 |t-u|^{-s/2} dt du \\ &< \infty \end{aligned} \tag{16.12}$$

since $s < 2$. There is a natural way of defining a mass distribution μ_X on a trail X , with the mass of a set equal to the time the trail spends in the set, that is, $\mu_X(A) = \mathcal{L}\{t : 0 \leq t \leq 1 \text{ and } X(t) \in A\}$, where \mathcal{L} is Lebesgue measure. Then, $\int g(x) d\mu_X(x) = \int_0^1 g(X(t)) dt$ for any function g , so (16.12) becomes

$$\mathbb{E} \left(\iint |x-y|^{-s} d\mu_X(x) d\mu_X(y) \right) < \infty.$$

Hence, if $s < 2$, then $\iint |x-y|^{-s} d\mu_X(x) d\mu_X(y) < \infty$ with probability 1, where μ_X is a mass distribution on $X([0, 1])$, so $\dim_H X([0, 1]) \geq s$ by Theorem 4.13(a).

In fact, with probability 1, Brownian trails in $\mathbb{R}^n (n \geq 2)$ have 2-dimensional Hausdorff measure 0. More delicate arguments involving the finer definitions of dimension given in Section 1.7 show that, with probability 1, the trails $X([0, 1])$ have positive finite measure with respect to the gauge function $\frac{h(t)}{t^2 \log(1/t) \log \log(1/t)}$, if $n = 2$, and with respect to $h(t) = t^2 \log \log(1/t)$, if $n \geq 3$. In this sense, Brownian trails have a dimension that is ‘logarithmically smaller’ than 2.

An obvious qualitative question about Brownian trails is how ‘tangled’ they are, and in particular whether they are simple curves or whether they are self-intersecting. Given a function f , we say that x is a point of *multiplicity* k if $f(t) = x$ for k distinct values of t . Dimensional methods may be used to determine whether Brownian functions have multiple points.

Theorem 16.6

With probability 1, a Brownian sample function $X : [0, \infty) \rightarrow \mathbb{R}^n$ has multiple points as follows:

$n = 2$: there are points of multiplicity k for every positive integer k ;

$n = 3$: there are double points but no triple points;

$n \geq 4$: there are no multiple points.

Idea of proof

One approach is to use the intersection theorems of Chapter 8. For the case $n = 3$, suppose that $\dim_H(X([0, 1]) \cap X([2, 3])) < 1$ with probability 1. Using isotropy and scaling of Brownian motion, it is not difficult to see that this implies that

$\dim_H(X([0, 1]) \cap \sigma(X([2, 3]))) < 1$ with probability 1 for any similarity transformation σ . It follows that, with probability 1, $\dim_H(X([0, 1]) \cap \sigma(X([2, 3]))) < 1$ for almost all similarities σ . Since, by Theorem 16.5, $\dim_H X([0, 1]) = \dim_H X([2, 3]) = 2$ with probability 1, this contradicts Theorem 8.3(a), and we conclude that

$\dim_H(X([0, 1]) \cap X([2, 3])) = 1$ with positive probability p , say. Using the statistical self-similarity of $X(t)$, it follows that

$\dim_H(X([t, t + \delta]) \cap X([t + 2\delta, t + 3\delta])) = 1$ with probability p for every t and δ , so, since the increments are independent, the set of double points has Hausdorff dimension 1, and in particular is non-empty, with probability 1.

Similar techniques may be used to prove the other statements.

The *exterior frontier* of a planar Brownian trail is the boundary of the unbounded component of the complement of the trail, that is, the points on the trail that are accessible from afar. A further indication of the complexity of planar Brownian motion is that, although the trail has dimension 2, its exterior frontier has Hausdorff dimension only $\frac{4}{3}$, implying that much of the trail lies within tiny loops. The proof of this remarkable property was central in the development of a new area of mathematics known as conformal invariance.

16.3 Fractional Brownian motion

Brownian motion, although of central theoretical importance, is often too restrictive. The graph of a Brownian sample function has dimension $1\frac{1}{2}$ almost surely, but random functions with graphs of other dimensions are required for a variety of modelling purposes.

Brownian motion is the unique probability distribution on functions, which has independent increments that are stationary and of finite variance with mean 0. To obtain sample functions with different characteristics, it is necessary to relax one or more of these conditions.

We will discuss two of the main variations. *Fractional Brownian motion* has stationary increments that are normally distributed but no longer independent. *Lévy processes*, which will be considered in Section 16.5, dispense with the Gaussian condition and this can lead to discontinuous functions. For simplicity, we just discuss these processes in the 1-dimensional case; analogous processes may be defined taking values in n -dimensional space.

A process $X(t)$ defined on some interval is called a *Gaussian process* if for $0 \leq t_1 \leq t_2 \leq \dots \leq t_m$ and scalars $\lambda_1, \dots, \lambda_m$, the random variable $\lambda_1 X(t_1) + \dots + \lambda_m X(t_m)$ has normal distribution (we say that the vector $(X(t_1), \dots, X(t_m))$ is *multivariate normal*). Of course, Brownian motion is a Gaussian process.

Fractional Brownian motion of index- α ($0 < \alpha < 1$) is defined to be a Gaussian process $X : [0, \infty) \rightarrow \mathbb{R}$ on some probability space such that:

(FBM)

- i. with probability 1, $X(t)$ is continuous and $X(0) = 0$;
- ii. for every $t \geq 0$ and $h > 0$ the increment $X(t+h) - X(t)$ has normal distribution with mean zero and variance $h^{2\alpha}$, so that

$$\mathbb{P}(X(t+h) - X(t) \leq x) = \frac{1}{h^\alpha \sqrt{2\pi}} \int_{-\infty}^x \exp\left(\frac{-u^2}{2h^{2\alpha}}\right) du. \quad \text{16.13}$$

It may be shown that for all $0 < \alpha < 1$, a process satisfying (FBM) exists. [Figure 16.3](#) shows sample graphs of fractional Brownian motion for various α . Index- $\frac{1}{2}$ fractional Brownian motion is just standard Brownian motion. As for Brownian motion, ([16.13](#)) implies that these processes are self-affine, that is, the scaled processes $\gamma^{-\alpha}X(\gamma t)$ have the same statistical distribution as $X(t)$ for $\gamma > 0$.

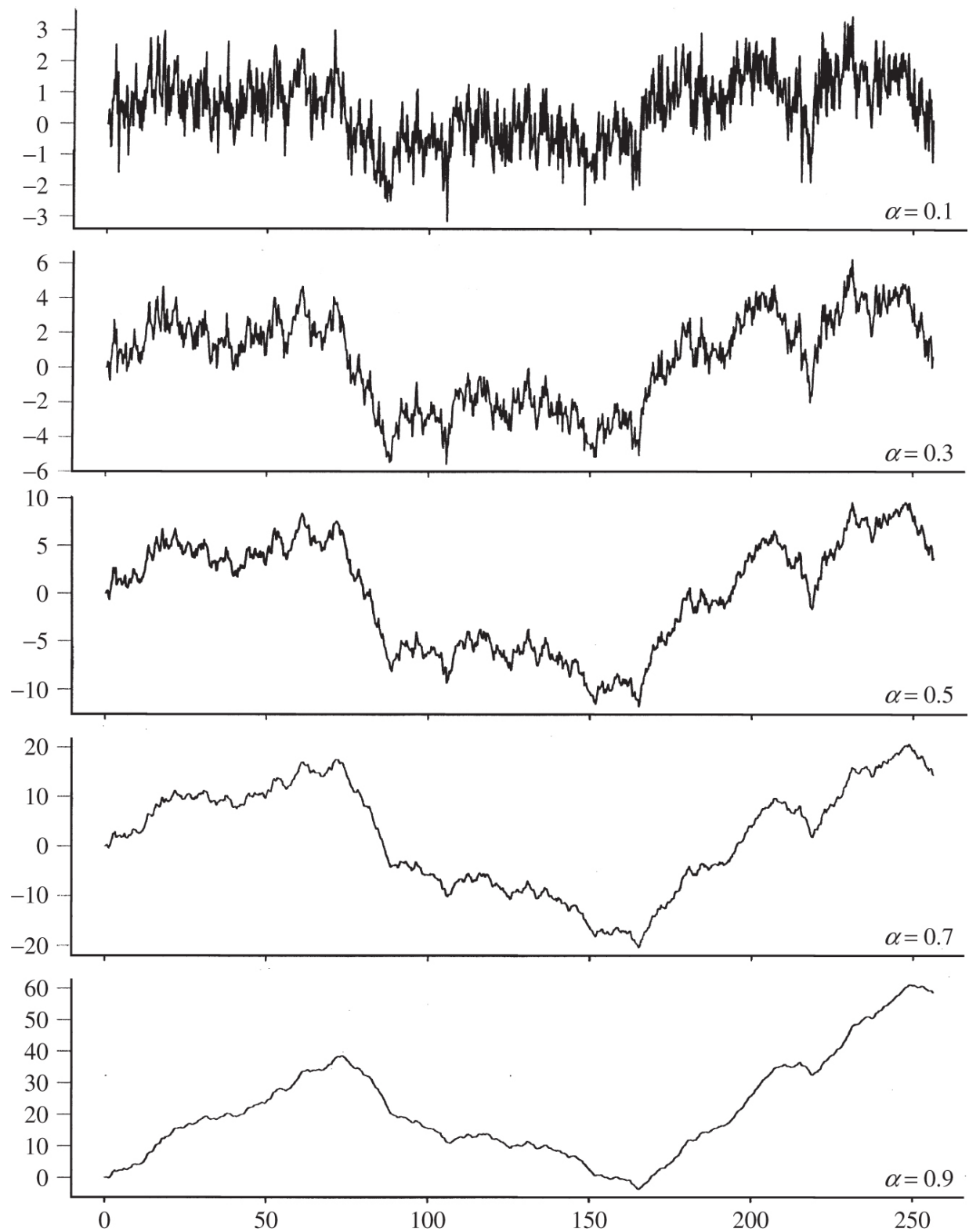


Figure 16.3 Realisations of index- α fractional Brownian for $\alpha = 0.1, 0.3, 0.5, 0.7, 0.9$.

It is implicit in the above definition that the increments $X(t+h) - X(t)$ are stationary, that is, they have probability distribution independent of t . However, the distribution of functions specified by (FBM) cannot have independent increments except in the Brownian case of $\alpha = \frac{1}{2}$. By conditions (i) and (ii), $E(X(t)^2) = t^{2\alpha}$ and

$$E((X(t+h) - X(t))^2) = h^{2\alpha}$$

from which

$$E(X(t)X(t+h)) = \frac{1}{2}[t^{2\alpha} + (t+h)^{2\alpha} - h^{2\alpha}]$$

so that

$$E(X(t)(X(t+h) - X(t))) = \frac{1}{2}[(t+h)^{2\alpha} - t^{2\alpha} - h^{2\alpha}] \quad \mathbf{16.14}$$

which is non-zero if $\alpha \neq \frac{1}{2}$. Hence, $E((X(t) - X(0))(X(t+h) - X(t)))$ is positive or negative according to whether $\alpha > \frac{1}{2}$ or $\alpha < \frac{1}{2}$. Thus, the increments are not independent—if $\alpha > \frac{1}{2}$, then $X(t) - X(0)$ and $X(t+h) - X(t)$ tend to be of the same sign, so that $X(t)$ tends to increase in the future if it has had an increasing history. Similarly, if $\alpha < \frac{1}{2}$, then $X(t) - X(0)$ and $X(t+h) - X(t)$ tend to be of opposite sign.

Index- α fractional Brownian motion satisfies a Hölder condition for all exponents less than α .

Proposition 16.7

Let $X : [0, 1] \rightarrow \mathbb{R}$ be a sample function of index- α fractional Brownian motion. If $0 < \lambda < \alpha$, then with probability 1, there is a random constant B such that

$$|X(t+h) - X(t)| \leq B|h|^\lambda \quad (t, t+h \in [0, 1]). \quad \mathbf{16.15}$$

Note on proof

Provided that $\lambda < \frac{1}{2}$, the proof goes through as in Proposition 16.1, using (16.13) instead of (16.2). However, if $\alpha > \lambda \geq \frac{1}{2}$, this leads to an estimate $c_2 h^{1/2-\lambda}$ in place of (16.6), which is no longer useful for small h , so rather more sophisticated techniques from probability theory are required to demonstrate the Hölder condition (16.15).

The almost sure dimension of fractional Brownian graphs may be determined in a similar way to the strict Brownian case.

Theorem 16.8

With probability 1, the graph of an index- α Brownian sample function $X : [0, 1] \rightarrow \mathbb{R}$ has Hausdorff and box dimensions $2 - \alpha$.

Proof

Corollary 11.2(a) together with the Hölder condition (16.15) shows that the dimension is almost surely at most $2 - \alpha$. The lower bound is obtained as in Theorem 16.2 using the probability distribution (16.13).

The autocorrelation theory discussed in Section 1.2 may be applied to fractional Brownian functions. It is convenient to assume that X is defined for all time, that is, $X : (-\infty, \infty) \rightarrow \mathbb{R}$. This requires only trivial modification to the definition (FBM). Since the variance $E(|X(t + h) - X(t)|^2)$ tends to infinity with h , we have

$$\lim_{T \rightarrow \infty} \mathbb{E} \left(\frac{1}{2T} \int_{-T}^T X(t)^2 dt \right) = \infty,$$

so the sample functions tend to have an infinite mean square. Nevertheless, for fixed T ,

$$\mathbb{E} \left(\frac{1}{2T} \int_{-T}^T (X(t+h) - X(t))^2 dt \right) = \frac{1}{2T} \int_{-T}^T \mathbb{E}(X(t+h) - X(t))^2 dt = h^{2\alpha}$$

It may be deduced that ‘on an average’, the sample functions satisfy

$$\frac{1}{2T} \int_{-T}^T (X(t+h) - X(t))^2 dt \simeq ch^{2\alpha}$$

and, according to (11.18) and (11.19), this does indeed correspond to a graph of dimension $2 - \alpha$. Taking this parallel further, we might expect $X(t)$ to have a power spectrum (11.15) approximately $1/\omega^{1+2\alpha}$.

Simulation of fractional Brownian motion is much more awkward than Brownian motion because the increments are not independent. However, with modern computing power, exact simulation is possible. To get a realisation of index- α fractional Brownian motion X at points t_1, \dots, t_k , we recall that the covariances of X are given by the covariance matrix A with entries

$$A_{ij} = \mathbb{E}(X(t_i)X(t_j)) = \frac{1}{2}(|t_i|^{2\alpha} + |t_j|^{2\alpha} - |t_i - t_j|^{2\alpha}).$$

Then, if M is a matrix such that $MM^T = A$, where T denotes transpose, and $V = (V_1, \dots, V_k)^T$ is a column vector of independent random variables with normal distribution of mean 0 and variance 1, $X \equiv X(t_i) = MV$ has the distribution of index- α fractional Brownian motion at the points t_i . To see this we check the covariances, using matrix notation:

$$\begin{aligned} \mathbb{E}(X(t_i)X(t_j)) &= \mathbb{E}(XX^T) = \mathbb{E}(MV(MV)^T) \\ &= \mathbb{E}(M V V^T M^T) = M \mathbb{E}(V V^T) M^T = M I M^T = A. \end{aligned}$$

Thus, by drawing a sequence of independent normally distributed random numbers for the V_i , the vector $X = MV$ gives a realisation of

index- α fractional Brownian motion at the points t_i . Finding a matrix M such that A has ‘Choleski decomposition’ $A = MM^T$ is computationally intensive if k is large, but there are sophisticated numerical approaches to facilitate this.

An alternative method of constructing random functions with characteristics similar to index- α Brownian functions is to randomise the Weierstrass function (11.4). Let

$$X(t) = \sum_{k=1}^{\infty} C_k \lambda^{-\alpha k} \sin(\lambda^k t + A_k), \quad \text{16.16}$$

where $\lambda > 1$ and where the C_k are independent random variables with the normal distribution of mean 0 and variance 1, and the random ‘phases’ A_k are independent with uniform distribution on $[0, 2\pi]$. Clearly, $E(X(t+h) - X(t)) = 0$ for all t and h . Using the formula for the difference of two sines,

$$\begin{aligned} E(X(t+h) - X(t))^2 &= E\left(\sum_{k=1}^{\infty} C_k \lambda^{-\alpha k} 2 \sin\left(\frac{1}{2}\lambda^k h\right) \cos\left(\lambda^k \left(t + \frac{1}{2}h\right) + A_k\right)\right)^2 \\ &= 2 \sum_{k=1}^{\infty} \lambda^{-2\alpha k} \sin^2\left(\frac{1}{2}\lambda^k h\right) \end{aligned}$$

using that $E(C_k C_j) = 1$ or 0 according as to whether $k = j$ or not, and that the mean of $\cos^2(t+A_k)$ is $\frac{1}{2}$. Choosing N so that $\lambda^{-(N+1)} \leq h < \lambda^{-N}$ gives

$$\begin{aligned} E(X(t+h) - X(t))^2 &\simeq \frac{1}{2} \sum_{k=1}^N \lambda^{-2\alpha k} \lambda^{2k} h^2 + 2 \sum_{k=N+1}^{\infty} \lambda^{-2\alpha k} \\ &\simeq c \lambda^{-2\alpha N} \\ &\simeq c h^{2\alpha} \end{aligned}$$

in the sense that $0 < c_1 \leq E(X(t+h) - X(t))^2/h^{2\alpha} \leq c_2 < \infty$ for $h < 1$. Thus, (16.16) has certain statistical characteristics resembling index- α fractional Brownian motion and provides a usable method for drawing random graphs of various dimensions. Such functions are

often used in fractal modelling. A value of $\alpha = 0.8$, corresponding to a graph of dimension 1.2, is about right for a ‘mountain skyline’.

As might be expected, the level sets of index- α Brownian sample functions are typically of dimension $1 - \alpha$. Proposition 16.3 generalises to give that, with probability 1, $\dim_H X^{-1}(c) \leq 1 - \alpha$ for almost all c , and that, for given c , $\dim_H X^{-1}(c) = 1 - \alpha$ with positive probability.

A further generalisation of fractional Brownian motion is *multifractional Brownian motion*, which looks and behaves like index- $\alpha(t)$ fractional Brownian motion close to t , where $\alpha : [0, \infty) \rightarrow (0, 1)$ is a given continuous function.

16.4 Fractional Brownian surfaces

Brownian surfaces have been used very effectively in creating computer-generated landscapes. We replace the time variable t by coordinates (x, y) , so the random variable $X(x, y)$ may be thought of as the height of a surface at the point (x, y) .

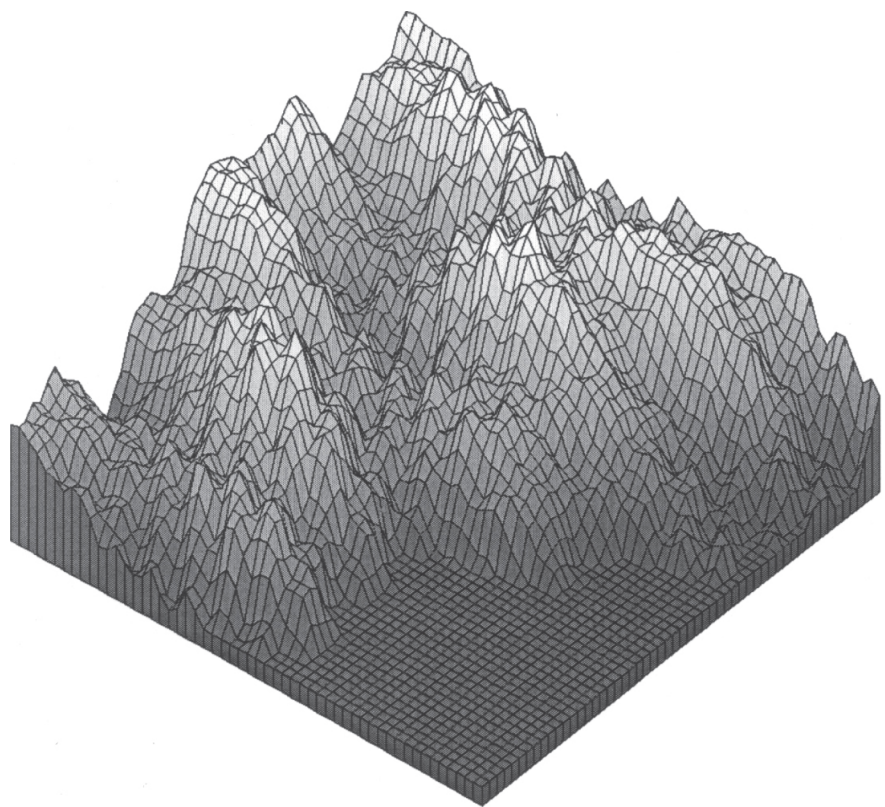
For $0 < \alpha < 1$, we define an *index- α fractional Brownian function* $X : \mathbb{R}^2 \rightarrow \mathbb{R}$ to be a Gaussian random function such that:

- i. with probability 1, $X(0, 0) = 0$ and $X(x, y)$ is a continuous function of (x, y) ;
- ii. for $(x, y), (h, k) \in \mathbb{R}^2$, the height increments $X(x + h, y + k) - X(x, y)$ are normally distributed with mean zero and variance $(h^2 + k^2)^\alpha = |(h, k)|^{2\alpha}$; thus,

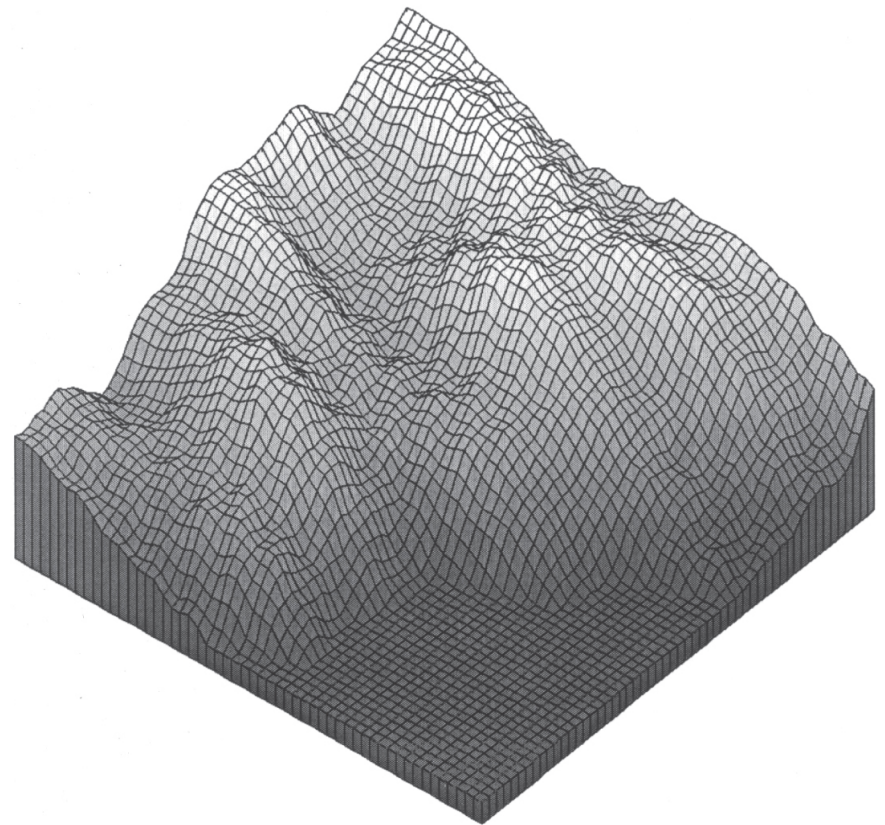
$$\begin{aligned} \mathsf{P}(X(x + h, y + k) - X(x, y) \leq z) \quad &\text{16.17} \\ &= \frac{1}{(h^2 + k^2)^{\alpha/2} \sqrt{2\pi}} \int_{-\infty}^z \exp\left(\frac{-r^2}{2(h^2 + k^2)^\alpha}\right) dr. \end{aligned}$$

Some effort is required to demonstrate the existence of a process satisfying these conditions. The correlations between the random variables $X(x, y)$ at different points are quite involved.

We term $\{(x, y, X(x, y)) : (x, y) \in \mathbb{R}^2\}$ an *index- α fractional Brownian surface*. Some sample surfaces are depicted in [Figure 16.4](#).



(a)



(b)

Figure 16.4 Index- α fractional Brownian surfaces: (a) $\alpha = 0.5$, dimension = 2.5; (b) $\alpha = 0.8$, dimension = 2.2.

Comparing (16.17) with the distribution (16.13), we see that the graph obtained by intersecting $X(x, y)$ with any vertical plane is that of a 1-dimensional index- α Brownian function (after adding a constant to ensure $X(0) = 0$). We can often gain information about surfaces by considering such vertical sections.

Theorem 16.9

With probability 1, an index- α Brownian sample surface has Hausdorff and box dimensions equal to $3 - \alpha$.

Proof

Using similar methods to Propositions 16.1 and 16.7, it may be shown that if $\lambda < \alpha$, then, with probability 1, an index- α Brownian function $X : [0, 1] \times [0, 1] \rightarrow \mathbb{R}$ satisfies a Hölder condition

$$|X(x+h, y+k) - X(x, y)| \leq B(h^2 + k^2)^{\lambda/2} = B|(h, k)|^\lambda,$$

where B is a random constant. The analogue of Corollary 11.2(a) for a function of two variables (see Exercise 11.9) then gives $3 - \lambda$ as an upper bound for the upper box dimension of the surface.

If we fix x_0 , then $X(x_0, y) - X(x_0, 0)$ is an index- α Brownian function on $[0, 1]$, so by Theorem 16.8 $X(x_0, y)$ has graph of Hausdorff dimension $2 - \alpha$ with probability 1. Thus, with probability 1, the graph of $X(x_0, y)$ has dimension $2 - \alpha$ for almost all $0 \leq x_0 \leq 1$. But these graphs are just parallel sections of the surface given by X , so by the obvious analogue of Corollary 7.10 in \mathbb{R}^3 , the surface has Hausdorff dimension at least $(2 - \alpha) + 1 = 3 - \alpha$.

The level sets $X^{-1}(c) = \{(x, y) : X(x, y) = c\}$ are the contours of the random surface. Proposition 16.3 extends to index- α surfaces. It may be shown that, with probability 1, $\dim_H X^{-1}(c) \leq 2 - \alpha$ for almost all c (in the sense of 1-dimensional measure), and that $\dim_H X^{-1}(c) = 2 - \alpha$ with positive probability. Thus, the contours of index- α surfaces ‘typically’ have dimension $2 - \alpha$.

The problems of generating sample surfaces for index- α Brownian functions are considerable, and we do not go into details here. However, we remark that an analogue of (16.16) for index- α surfaces is

$$X(x, y) = \sum_{k=1}^{\infty} C_k \lambda^{-\alpha k} \sin(\lambda^k(x \cos B_k + y \sin B_k) + A_k),$$

where the C_k are independent with normal distribution of mean zero and variance 1, and the A_k and B_k are independent with uniform distribution on $[0, 2\pi]$. Such functions provide one possible approach to computer generation of random surfaces.

16.5 Lévy stable processes

Lévy stable processes provide an alternative and important variant of Brownian motion. A *Lévy process* is a random function $X : [0, \infty) \rightarrow \mathbb{R}$ with stationary independent increments, that is:

(LP)

- i. with probability 1, $X(0) = 0$ and $X(t)$ is right continuous and has left limits at every point t , that is, $\lim_{u \searrow t} f(u) = t$ and $\lim_{u \nearrow t} f(u)$ exists;
- ii. the increments are stationary, that is, $X(t+h) - X(t)$ has the same distribution as $X(h) - X(0)$ for all $t, h > 0$;
- iii. if $0 \leq t_1 \leq t_2 \leq \dots \leq t_{2m}$, the increments $\frac{X(t_2) - X(t_1)}{\dots}, \frac{X(t_4) - X(t_3)}{\dots}, \dots, \frac{X(t_{2m}) - X(t_{2m-1})}{\dots}$ are independent.
- A Lévy process is *stable* or α -*stable* for some $\alpha > 0$ if a self-affinity condition holds:
- iv. $\gamma^{-1/\alpha} X(\gamma t)$ and $X(t)$ have the same distribution for all $\gamma > 0$, and is *symmetric* if
- v. $X(t)$ and $-X(t)$ have the same distribution.

Except in very special cases such as Brownian motion, Lévy processes have increments with infinite variance and are discontinuous with probability 1. It is not, in general, feasible to specify the probability distribution of stable processes directly. Fourier transforms or characteristic functions are usually used to

define such distributions, and analysis of the dimensions of graphs and trails of stable processes requires Fourier transform methods.

The probability distribution of a random variable Y may be specified by its *characteristic function*, that is, the Fourier transform $E(\exp(iuY))$ for $u \in \mathbb{R}$. To define a stable process, we take a suitable function $\psi : \mathbb{R} \rightarrow \mathbb{R}$ and require that the increments $X(t+h) - X(t)$ satisfy

$$E(\exp(iu(X(t+h) - X(t)))) = \exp(-h\psi(u)) \quad \text{16.18}$$

with $X(t_2) - X(t_1), \dots, X(t_{2m}) - X(t_{2m-1})$ independent if $0 \leq t_1 \leq t_2 \leq \dots \leq t_{2m}$. Clearly the increments are stationary. This definition is, at least, consistent in the following sense. If $t_1 < t_2 < t_3$, then, taking expectations and using independence,

$$\begin{aligned} E(\exp(iu(X(t_3) - X(t_1)))) &= E(\exp iu((X(t_3) - X(t_2)) + (X(t_2) - X(t_1)))) \\ &= E(\exp iu(X(t_3) - X(t_2)))E(\exp iu(X(t_2) - X(t_1))) \\ &= \exp(-(t_3 - t_2)\psi(u))\exp(-(t_2 - t_1)\psi(u)) \\ &= \exp(-(t_3 - t_1)\psi(u)). \end{aligned}$$

It may be shown that, for suitable ψ , stable processes do exist.

Taking $\psi(u) = c|u|^\alpha$ with $0 < \alpha \leq 2$ gives the *stable symmetric process of index- α* . Then, replacing h by γh and u by $\gamma^{-1/\alpha}u$ leaves the right-hand side of (16.18) unaltered, and it follows that $\gamma^{-1/\alpha}X(\gamma t)$ has the same statistical distribution as $X(t)$, so such processes are symmetric and self-affine. The case $\alpha = 2$ is standard Brownian motion.

Theorem 16.10

With probability 1, the graph of the stable symmetric process of index- α , where $1 < \alpha \leq 2$, has Hausdorff and box dimension $2 - 1/\alpha$.

Partial proof

We show that $\dim_H \text{graph } X \leq \overline{\dim}_B \text{graph } X \leq 2 - 1/\alpha$. Write $R_f[t_1, t_2] = \sup\{|f(t) - f(u)| : t_1 \leq t, u \leq t_2\}$ for the maximum range of a function f over the interval $[t_1, t_2]$. By virtue of the self-affinity and stationarity of the process X , for all t and $0 < \delta < 1$

$$\mathbb{E}(R_X[t, t + \delta]) = \delta^{1/\alpha} \mathbb{E}(R_X[0, 1]).$$

If N_δ squares of the δ -coordinate mesh are intersected by $\text{graph } X$ (note that N_δ is random), it follows from a variant of Proposition 11.1 that

$$\begin{aligned}\mathbb{E}(N_\delta) &\leq 2m + \delta^{-1} \sum_{i=0}^{m-1} \mathbb{E}(R_X[i\delta, (i+1)\delta]) \\ &= 2m + m\delta^{-1} \delta^{1/\alpha} \mathbb{E}(R_X[0, 1]),\end{aligned}$$

where m is the least integer greater than or equal to $1/\delta$, so $m \leq 2/\delta$. It may be shown, and is at least plausible, that $\mathbb{E}(R_X[0, 1]) < \infty$ if $1 < \alpha \leq 2$, so there is a constant c such that $\mathbb{E}(N_\delta \delta^\beta) \leq c$ for all small δ , where $\beta = 2 - 1/\alpha$. Then, $\mathbb{E}(N_\delta \delta^{\beta+\varepsilon}) \leq c \delta^\varepsilon$ if $\varepsilon > 0$, so that

$$\mathbb{E}\left(\sum_{k=1}^{\infty} N_{2^{-k}} (2^{-k})^{\beta+\varepsilon}\right) \leq c \sum_{k=1}^{\infty} (2^{-k})^\varepsilon < \infty.$$

It follows that, with probability 1, $\sum_{k=1}^{\infty} N_{2^{-k}} (2^{-k})^{\beta+\varepsilon} < \infty$, so $N_{2^{-k}} (2^{-k})^{\beta+\varepsilon} \rightarrow 0$ as $k \rightarrow \infty$, giving $\overline{\dim}_B \text{graph } X \leq \beta + \varepsilon$ for all $\varepsilon > 0$ using Proposition 4.1, as required.

If $0 < \alpha < 1$, then almost surely $\dim_H \text{graph } X = 1$, the smallest dimension possible for the graph of any function on $[0, 1]$. This reflects the fact that the sample functions consist of ‘jumps’, with infinitely many jumps in every positive time interval, though many

such jumps are very small. The image of X , that is, $\{X(t) : 0 \leq t \leq 1\}$, has dimension α with probability 1, which is indicative of the distribution of the jumps. It may be shown that the probability of there being k jumps of absolute value at least a in the interval $[t, t+h]$ is $(ha^{-\alpha})^k \exp(-ha^{-\alpha})/k!$, corresponding to a Poisson distribution of mean $ha^{-\alpha}$.

If $1 < \alpha < 2$, the stable symmetric process combines a ‘continuous’ component and a ‘jump’ component.

The ideas in this chapter may be extended in many directions and combined in many ways. Fractional Brownian motion and stable processes may be defined from \mathbb{R}^n to \mathbb{R}^m for any n, m and there are many other variations. Questions of level sets, multiple points, intersections with fixed sets, the images $X(F)$ for various fractals F , and so on arise in all these situations. Analysis of such problems often requires sophisticated probabilistic techniques alongside a variety of geometrical arguments.

16.6 Notes and references

Brownian motion is constructed rigorously in the books by Rogers and Williams (2000); Mörters and Peres (2010); Lawler (2010) and Billingsley (2012).

Fractional Brownian motion was introduced by Mandelbrot and Van Ness (1968); see the papers in Mandelbrot (2002). There are many books on fractional Brownian functions and surfaces: Kahane (1993) and Adler (2009) include dimensional aspects, Samorodnitsky and Taqqu (1994) and Embrechts and Maejima (2002) emphasise self-similarity and Biagini, Hu, and Øksendal (2008) and Nourdin (2012) concentrate on stochastic calculus. For conformal invariance and the Brownian frontier, see Lawler (2008) and references therein. Multifractional Brownian motion was introduced in Peltier and Lévy Véhel (1995); Ayache and Lévy Véhel (1999) and Ayache, Cohen and Lévy Véhel (2000); see Ayache, Shieh and Xiao (2011) for some recent work and further references.

Stable processes were introduced by Lévy (1948); see Samorodnitsky and Taqqu (1994); Bertoin (1996), Rogers and Williams (2000) and Mandelbrot (2002). Falconer and Lévy Véhel (2009) introduced multifractional multistable motion. There is a vast literature on dimensional properties of these processes; see the surveys by Taylor (1973b, 1986); Khoshnevisan (2009) and Xiao (2013) and references therein. Lowen and Teich (2005) consider a variety of other fractal-based random processes.

Computer simulation of Brownian-type paths and surfaces is not always straightforward. For various approaches, see Voss (1985); Peitgen and Saupe (2011); Falconer and Lévy Véhel (2000) and Embrechts and Maejima (2002).

Exercises

16.1 Use the statistical self-similarity of Brownian motion to show that, with probability 1, a Brownian trail in \mathbb{R}^3 has box dimension of at most 2.

16.2 Let $X : [0, \infty) \rightarrow \mathbb{R}^3$ be Brownian motion. Show that, with probability 1, the image $X(F)$ of the middle third Cantor set F has Hausdorff dimension at most $\log 4 / \log 3$. (Harder: show that it is almost surely equal to $\log 4 / \log 3$.) What is the analogous result for index- α fractional Brownian motion?

16.3 Let $X : [0, \infty) \rightarrow \mathbb{R}^3$ be Brownian motion, and let F be a compact subset of \mathbb{R}^3 . Use Theorem 8.3 to show that if $\dim_H F > 1$, then there is a positive probability of the Brownian trail $X(t)$ hitting F .

16.4 Let $X(t)$ be Brownian motion and c a constant. Show that the graph of the process $X(t) + ct$ has dimension $1\frac{1}{2}$ with probability 1. (This process is called Brownian motion with drift.)

16.5 Show that, with probability 1, the Brownian sample function $X : [0, \infty) \rightarrow \mathbb{R}$ is not monotonic on any interval $[t, u]$.

16.6 Let $X(t)$ be Brownian motion. Show that with probability 1, $X(t) = 0$ for some $t > 0$. Use self-affinity to show that with probability 1, for each $a > 0$, $X(t) = 0$ for some t with $0 < t < a$, and thus $X(t) = 0$ for infinitely many t with $0 < t < a$.

16.7 Let $X(t)$ be Brownian motion. Show that for $q > 0$, $\mathbb{E}(|X(t+h) - X(t)|^q) = c|h|^q$, where c depends only on q .

16.8 Show that, if $\lambda > \alpha$, then with probability 1, the Hölder inequality ([16.15](#)) fails for almost all t .

16.9 Take $\frac{1}{2} \leq \alpha_1 \leq \alpha_2 < 1$ and let $X_1(t)$ and $X_2(t)$ be independent fractional Brownian functions from $[0, 1]$ to \mathbb{R} of indices α_1 and α_2 , respectively. Show that, with probability 1, the path in \mathbb{R}^2 given by $\{(X_1(t), X_2(t)) : 0 \leq t \leq 1\}$ has Hausdorff and box dimensions of $(1 + \alpha_2 - \alpha_1)/\alpha_2$.

16.10 Verify that for index- α fractional Brownian motion the covariance $\mathbb{E}((X(t) - X(0))(X(t+h) - X(t))) = \frac{1}{2}[(t+h)^{2\alpha} - t^{2\alpha} - h^{2\alpha}]$. Show that

this is positive if $\frac{1}{2} < \alpha < 1$ and negative if $0 < \alpha < \frac{1}{2}$. What does this tell us about the sample functions?

Chapter 17

Multifractal measures

A mass distribution μ may be spread over a region in such a way that the concentration of mass is highly irregular. In particular, the set of points where the local mass concentration obeys an index- α power law, say $\mu(B(x, r)) \simeq r^\alpha$ for small r , may determine a different fractal for different values of α . Thus, a whole range of fractals may arise from a single measure, and we may examine the structure of these fractals and their inter-relationship. A measure μ with such a rich structure is called a *multifractal measure* or just a *multifractal*. As with fractals, a precise definition of ‘multifractal’ tends to be avoided.

Multifractal measures have been observed in many physical situations, for example, in fluid turbulence, rainfall distribution, mass distribution across the universe, viscous fingering, neural networks, share prices and in many other phenomena.

An important class of multifractal occurs in dynamical systems (see Section 13.7). If $f : D \rightarrow D$ is a mapping on a domain D , we can define a ‘residence measure’ by

$$\mu(A) = \lim_{m \rightarrow \infty} \frac{1}{m} \# \{k : 1 \leq k \leq m \text{ and } f^k(x) \in A\}$$

for subsets A of D , where $x \in D$ is some initial point. Assuming the limit exists, $\mu(A)$ represents the proportion of time that the iterates of x spend in A . We have seen that the support of μ is often an attractor of f and may be a fractal. However, the non-uniformity of μ across the attractor may highlight further dynamical structure that can be recorded and analysed using multifractal theory.

Many ideas related to fractals have counterparts in multifractals, for example, projection of multifractal measures onto a line or plane may be considered in an analogous manner to the projection of

fractals, although the calculations can be considerably more awkward.

There are two basic approaches to multifractal analysis: *fine theory*, where we examine the structure and dimensions of the fractals defined by local properties of the measure, and *coarse theory*, where we consider the irregularities of distribution of the measure over an r -mesh for small r and then take a limit as $r \rightarrow 0$. In many ways, fine multifractal analysis parallels finding the Hausdorff dimension of sets, whilst coarse theory is related to box-counting dimension. The coarse approach is usually more practicable when it comes to analysing physical examples or computer experiments, but the fine theory may be more convenient for mathematical analysis. There are many parallels between the fine and the coarse approaches, and for many measures, both the approaches lead to the same ‘multifractal spectra’.

We outline coarse and fine multifractal theories and then consider the special case of self-similar measures in more detail, both to illustrate the theory and to demonstrate central ideas such as Legendre transformation.

Throughout our discussion, we refer to the following example of a self-similar multifractal measure on a Cantor set. Just as the middle third Cantor set illustrates many features of fractal mathematics, this basic self-similar measure supported by the Cantor set has features typical of a large class of multifractal measures.

Example 17.1

Let $p_1, p_2 > 0$ be given, with $p_1 + p_2 = 1$. We construct a measure μ on the middle third Cantor set $F = \bigcap_{k=0}^{\infty} E_k$ by repeated subdivision. (Here, E_k comprises the 2^k k th level intervals of length 3^{-k} in the usual Cantor set construction; see [Figure 0.1](#).) Assign the left interval of E_1 mass p_1 and the right interval mass p_2 . Divide the mass on each interval of E_1 between its two subintervals in E_2 in the ratio $p_1 : p_2$. Continue in this way, so that the mass on each interval of E_k is divided in ratio $p_1 : p_2$ between its two subintervals in E_{k+1} . This defines a mass distribution on F (see [Proposition 1.7](#)).

It is easily seen that if I is a k th level interval of E_k , then $\mu(I) = p_1^r p_2^{k-r}$ where, in constructing I , a left-hand interval is taken r times and a right-hand interval $k-r$ times. If $p_1 \neq p_2$ and k is large, the masses of the k th level intervals will vary considerably (see [Figure 17.1](#)), and this is a manifestation of multifractality.



Figure 17.1 Construction of the self-similar measure described in Example 17.1. The mass on each interval of E_k in the construction of the Cantor set, indicated by the area of the rectangle, is divided in the ratio $p_1 : p_2$ (in this case, $\frac{1}{3} : \frac{2}{3}$) between its two subintervals in E_{k+1} . Continuing this process yields a self-similar measure on the Cantor set.

17.1 Coarse multifractal analysis

Coarse multifractal analysis of a measure μ on \mathbb{R}^n with $0 < \mu(\mathbb{R}^n) < \infty$ is akin to box-counting dimension, in that we count the number of mesh cubes C for which $\mu(C)$ is roughly r^α . (Recall that the r -mesh cubes in \mathbb{R}^n are the cubes of the form

$[m_1 r, (m_1 + 1)r] \times \cdots \times [m_n r, (m_n + 1)r]$ where m_1, \dots, m_n are integers.) For μ a finite measure on \mathbb{R}^n and $\alpha \geq 0$, we write

$$N_r(\alpha) = \#\{r\text{-mesh cubes } C \text{ with } \mu(C) \geq r^\alpha\} \quad \underline{\text{17.1}}$$

and define the *coarse multifractal spectrum* or *coarse singularity spectrum* of μ as

$$f_C(\alpha) = \lim_{\epsilon \rightarrow 0} \lim_{r \rightarrow 0} \frac{\log^+(N_r(\alpha + \epsilon) - N_r(\alpha - \epsilon))}{-\log r} \quad \underline{\text{17.2}}$$

if the double limit exists. (We write $\log^+ x \equiv \max\{0, \log x\}$, which ensures $f_C(\alpha) \geq 0$.) Definition (17.2) implies that if $\eta > 0$, and $\epsilon > 0$ is small enough, then

$$r^{-f_C(\alpha)+\eta} \leq N_r(\alpha + \epsilon) - N_r(\alpha - \epsilon) \leq r^{-f_C(\alpha)-\eta} \quad \underline{\text{17.3}}$$

for all sufficiently small r . Roughly speaking $-f_C(\alpha)$ is the power law exponent for the number of r -mesh cubes C such that $\mu(C) \simeq r^\alpha$. Note that $f_C(\alpha)$ is *not* the box dimension of the set of x such that $\mu(C(x, r)) \simeq r^\alpha$ as $r \rightarrow 0$ where $C(x, r)$ is the r -mesh cube containing x ; the coarse spectrum provides a global overview of the fluctuations of μ at scale r but gives no information about the limiting behaviour of μ at any point.

To allow for the possibility of the limit (17.2) not existing, we define the *lower* and the *upper coarse multifractal spectra* of μ by

$$f_{\text{C}}(\alpha) = \lim_{\epsilon \rightarrow 0} \lim_{r \rightarrow 0} \frac{\log^+(N_r(\alpha + \epsilon) - N_r(\alpha - \epsilon))}{-\log r} \quad 17.4$$

and

$$\bar{f}_{\text{C}}(\alpha) = \lim_{\epsilon \rightarrow 0} \lim_{r \rightarrow 0} \frac{\log^+(N_r(\alpha + \epsilon) - N_r(\alpha - \epsilon))}{-\log r} \quad 17.5$$

for $\alpha \geq 0$.

It is usually awkward to calculate the coarse multifractal spectrum f_{C} directly.

Continuation of Example 17.1

In this example, the set E_k is made up of 2^k intervals of length 3^{-k} , and for each r , a number $\binom{k}{r}$ of these have mass $p_1^r p_2^{k-r}$,

where $\binom{k}{r}$ is the usual binomial coefficient. Thus, assuming without loss of generality that $0 < p_1 < \frac{1}{2}$, we have

$$N_{3^{-k}}(\alpha) = \sum_{r=0}^m \binom{k}{r},$$

where m is the largest integer such that

$$p_1^m p_2^{k-m} \geq 3^{-k\alpha}, \quad \text{that is,} \quad m \simeq \frac{k(\log p_2 + \alpha \log 3)}{\log p_2 - \log p_1}.$$

It is now possible, but tedious, to estimate $N_{3^{-k}}(\alpha)$ and thus examine its power law exponent. However, we shortly encounter a better approach.

Next, we introduce moment sums: for $q \in \mathbb{R}$ and $r > 0$, the q th power moment sum of μ is given by

$$M_r(q) = \sum_{\mathcal{M}_r} \mu(C)^q, \quad \text{17.6}$$

where the sum is over the set \mathcal{M}_r of r -mesh cubes C for which $\mu(C) > 0$. (There is a problem of stability for negative q : if a cube C just clips the edge of $\text{spt } \mu$, then $\mu(C)^q$ can be very large. There are ways around this difficulty, for example, by restricting the sums to cubes with a central portion intersecting $\text{spt } \mu$, but we do not pursue this here.) We identify the power law behaviour of $M_r(q)$ by defining

$$\beta(q) = \lim_{r \rightarrow 0} \frac{\log M_r(q)}{-\log r}, \quad \text{17.7}$$

assuming this limit exists.

It is hardly surprising that these moment sums are related to the $N_r(\alpha)$. Using (17.1), it follows that if $q \geq 0$ and $\alpha \geq 0$,

$$M_r(q) = \sum_{\mathcal{M}_r} \mu(C)^q \geq r^{q\alpha} N_r(\alpha), \quad \text{17.8}$$

and if $q < 0$,

$$M_r(q) = \sum_{\mathcal{M}_r} \mu(C)^q \geq r^{q\alpha} \# \{r\text{-mesh cubes with } 0 < \mu(C) \leq r^\alpha\}. \quad \text{17.9}$$

These inequalities lead to a useful relationship between $f_C(\alpha)$ and $\beta(q)$ in terms of Legendre transformation. The *Legendre transform* f_L of β is defined for $\alpha \geq 0$ by

$$f_L(\alpha) = \inf_{-\infty < q < \infty} \{\beta(q) + \alpha q\}, \quad \text{17.10}$$

provided this is finite. There is a useful geometrical interpretation of the Legendre transform. For those α for which the graph of β has under it a tangent L_α of slope $-\alpha$, the Legendre transform of β is given by the value of the intercept of L_α with the vertical axis (see [Figure 17.2](#)).

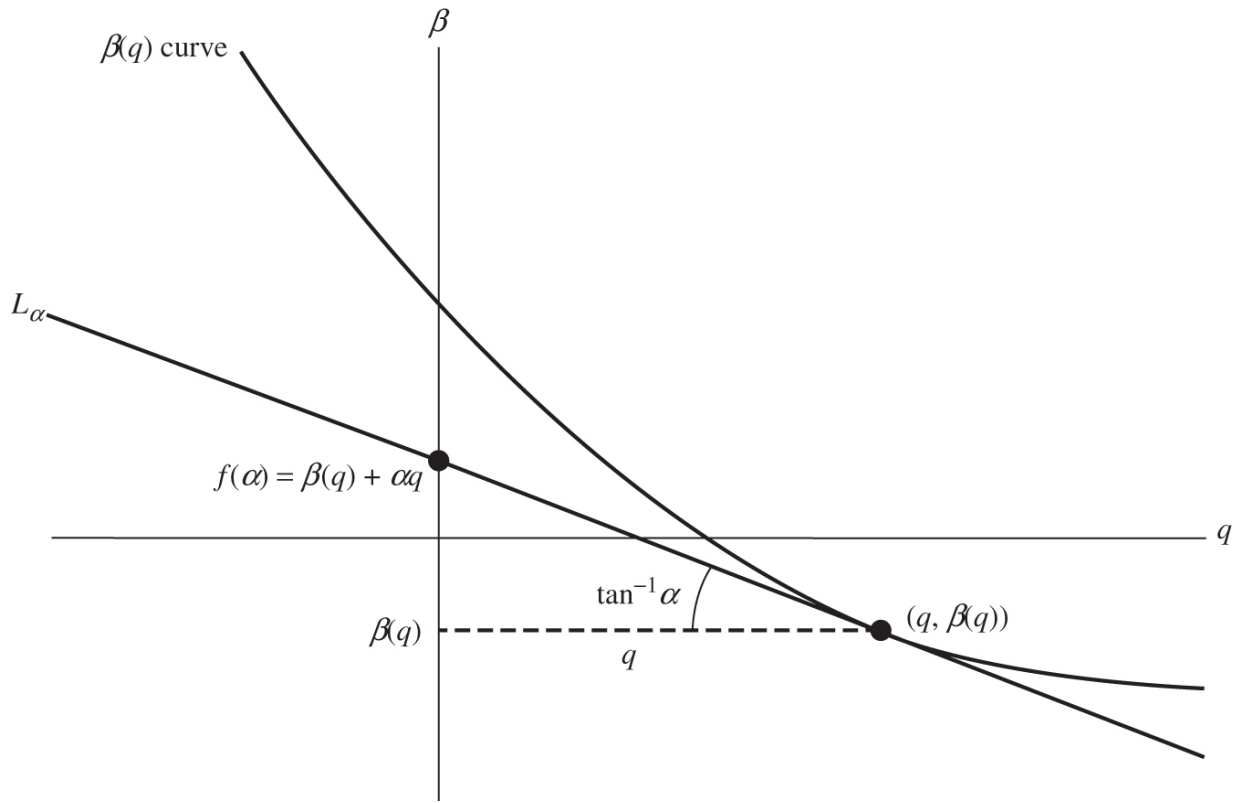


Figure 17.2 The Legendre transform of $\beta(q)$ is $f(\alpha)$, the intersection of the tangent L_α of slope $-\alpha$ with the β -axis.

It is easy to see that the coarse spectrum is bounded above by the Legendre transform of β .

Proposition 17.2

Let μ be a finite measure on \mathbb{R}^n , and assume that the limit in (17.7) exists. Then for all $\alpha \geq 0$,

$$f_{-C}(\alpha) \leq \bar{f}_C(\alpha) \leq f_L(\alpha), \quad 17.11$$

where f_L is the Legendre transform of β .

Proof

First take $q \geq 0$. Then given $\epsilon > 0$, (17.8) and (17.5) imply that

$$M_r(q) \geq r^{q(\alpha+\epsilon)} N_r(\alpha + \epsilon) \geq r^{q(\alpha+\epsilon)} r^{-\bar{f}_C(\alpha)+\epsilon} \quad \mathbf{17.12}$$

for arbitrarily small values of r . It follows using (17.7) that

$$-\beta(q) \leq q(\alpha + \epsilon) - \bar{f}_C(\alpha) + \epsilon,$$

so $\bar{f}_C(\alpha) \leq \beta(q) + \alpha q$ by taking ϵ arbitrarily small. This inequality also holds when $q < 0$ by a parallel argument, using (17.9) with α replaced by $\alpha - \epsilon$.

The Legendre transform f_L of β given by (17.10) is termed the *Legendre spectrum* of μ . There are many measures for which the Legendre spectrum equals the coarse multifractal spectrum, that is, for which equality occurs in (17.11).

Continuation of Example 17.1

Recalling that in this example $\binom{k}{r}$ of the k th level intervals of lengths 3^{-k} have mass $p_1^r p_2^{k-r}$, we get

$$M_{3^{-k}}(q) = \sum_{r=0}^k \binom{k}{r} p_1^{qr} p_2^{q(k-r)} = (p_1^q + p_2^q)^k.$$

Hence,

$$\beta(q) = \lim_{r \rightarrow 0} \frac{\log M_r(q)}{-\log r} = \lim_{k \rightarrow \infty} \frac{\log M_{3^{-k}}(q)}{-\log 3^{-k}} = \frac{\log(p_1^q + p_2^q)}{\log 3}. \quad \text{17.13}$$

(It is easy to see that it is enough to let r tend to 0 through the values 3^{-k} , compare (2.10).)

The Legendre spectrum of μ comes from taking the Legendre transform of β , that is, by minimising $\beta(q) + \alpha q$ over $q \in \mathbb{R}$. Elementary calculus gives that the minimum occurs when q satisfies

$$\alpha = -\frac{p_1^q \log p_1 + p_2^q \log p_2}{(p_1^q + p_2^q) \log 3}.$$

The Legendre spectrum is this minimum value, which is given in terms of the parameter q by

$$f_L(\alpha) = \frac{\log(p_1^q + p_2^q)}{\log 3} - \frac{q(p_1^q \log p_1 + p_2^q \log p_2)}{(p_1^q + p_2^q) \log 3}. \quad \text{17.14}$$

The graph of $f_L(\alpha)$ when $p_1 = \frac{1}{3}, p_2 = \frac{2}{3}$ is displayed in [Figure 17.3](#). As we shall see in Section 17.3, $f_L(\alpha) = f_C(\alpha)$, that is, the Legendre spectrum coincides with the coarse multifractal spectrum.

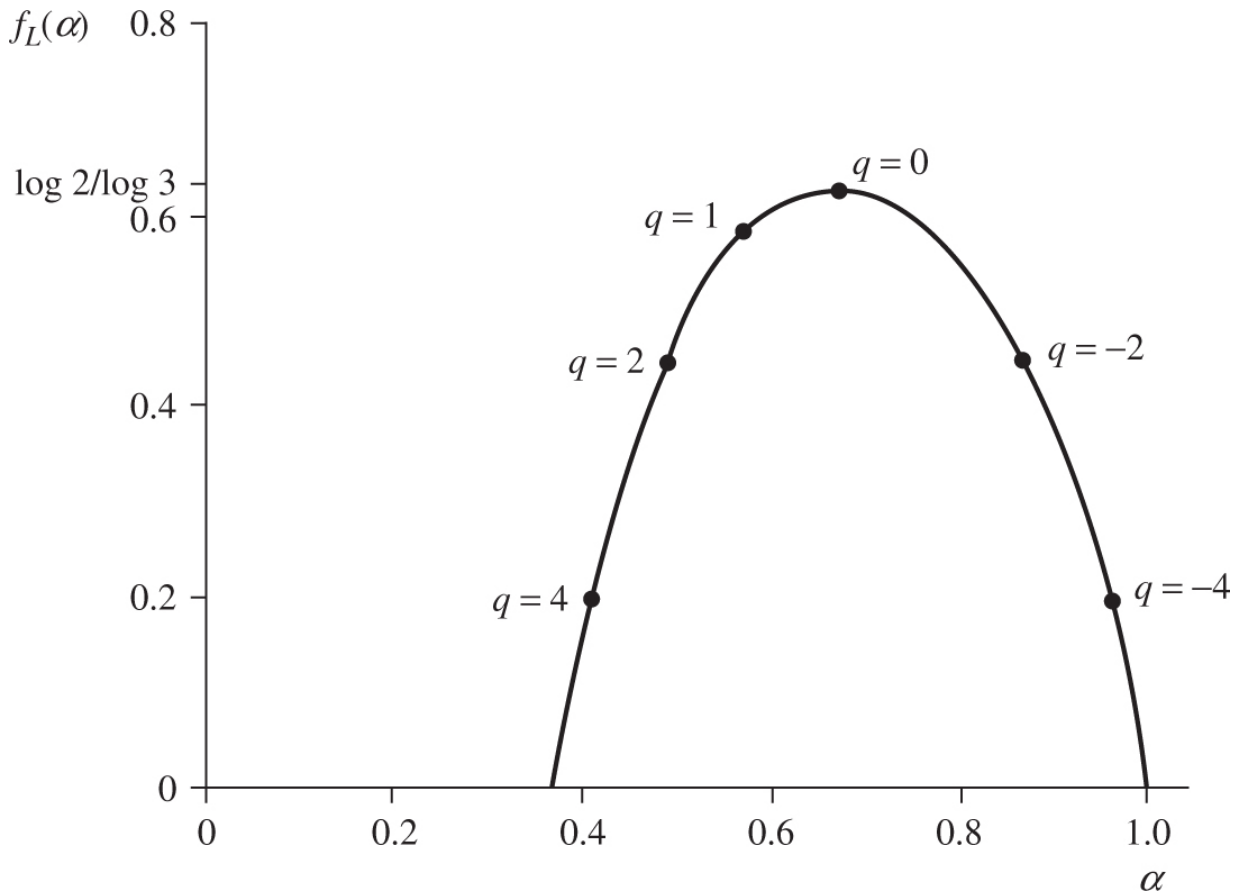


Figure 17.3 The multifractal spectrum of Example 17.1 with $p_1 = \frac{1}{3}$, $p_2 = \frac{2}{3}$.

In practical situations, multifractal spectra are often awkward to estimate and work with. One might hope to compute the coarse spectrum f_C by ‘box-counting’. For instance, if μ is a residence measure on the attractor of a dynamical system in the plane, a count of the proportion of the iterates of an initial point that lie in each r -mesh square C might be used to estimate the number of squares for which $\alpha_i \leq \log \mu(C)/\log r < \alpha_{i+1}$, where $0 \leq \alpha_1 < \dots < \alpha_k$. Examining this ‘histogram’ for various r enables the power law behaviour of $N_r(\alpha + \epsilon) - N_r(\alpha - \epsilon)$ to be studied and $f(\alpha)$ to be estimated. However, this *histogram method* tends to be computationally slow and awkward.

In general, it is more satisfactory to use the *method of moments* for experimental determination of a multifractal spectrum. Thus, for a

range of q , the moment sums (17.6) are estimated for various small r and the power law behaviour examined to estimate $\beta(q)$ using (17.7). Legendre transformation of β gives a Legendre spectrum of μ , and this is often taken to be the coarse spectrum. The method of moments is usually more numerically manageable than the histogram method.

17.2 Fine multifractal analysis

Fine multifractal analysis looks directly at the fractals determined by the local intensity of a measure. Let μ be a measure on \mathbb{R}^n with $0 < \mu(\mathbb{R}^n) < \infty$. We define the *local dimension* or *Hölder exponent* of μ at x by

$$\dim_{\text{loc}} \mu(x) = \lim_{r \rightarrow 0} \frac{\log \mu(B(x, r))}{\log r}, \quad 17.15$$

provided this limit exists. (More generally, one can work with upper and lower local limits leading to upper and lower local dimensions, but we do not pursue this here.) We study the sets of points $x \in \mathbb{R}^n$ where the local dimension takes particular values. For $\alpha \geq 0$, we define

$$\begin{aligned} F_\alpha &= \{x \in \mathbb{R}^n : \dim_{\text{loc}} \mu(x) = \alpha\} \\ &= \left\{ x \in \mathbb{R}^n : \lim_{r \rightarrow 0} \frac{\log \mu(B(x, r))}{\log r} = \alpha \right\}. \end{aligned} \quad 17.16$$

Thus, F_α comprises those points where the local dimension exists and equals α .

In fine multifractal analysis, we aim to find the dimensions of F_α over a range of α . In most examples of interest, F_α is dense in the support of μ so $\underline{\dim}_B F_\alpha = \underline{\dim}_B \bar{F}_\alpha = \underline{\dim}_B (\text{spt } \mu)$ and similarly for upper box dimensions, by Proposition 2.6, so box-counting dimensions are of little use in discriminating between the F_α . Thus, we concentrate on the *fine (Hausdorff) multifractal spectrum* or *singularity spectrum* of μ defined by

$$f_H(\alpha) = \dim_H F_\alpha.$$

17.17

Clearly, $0 \leq f_H(\alpha) \leq \dim_H(\text{spt } \mu)$ for all $\alpha \geq 0$, and it follows from Proposition 4.9(b) that

$$0 \leq f_H(\alpha) \leq \alpha.$$

17.18

Continuation of Example 17.1

We may code the points x of the Cantor set F as (i_1, i_2, \dots) in the usual way, with $i_k = 1$ if x is in the left sub-interval at the k th stage of the Cantor set construction and $i_k = 2$ if x is in the right sub-interval. Then, writing $n_j(x|_k), j = 1, 2$, for the number of occurrences of j in the first k terms of the sequence coding x , we have $\mu(B(x, 3^{-k})) = p_1^{n_1(x|_k)} p_2^{n_2(x|_k)}$, so that

$$\frac{\log \mu(B(x, 3^{-k}))}{\log 3^{-k}} = \frac{-1}{\log 3} \left(\frac{n_1(x|_k)}{k} \log p_1 + \frac{n_2(x|_k)}{k} \log p_2 \right).$$

Thus, if $n_j(x|_k)/k \rightarrow \alpha_j, j = 1, 2$, then $x \in F_\alpha$ where

$\alpha = -(\alpha_1 \log p_1 + \alpha_2 \log p_2) / \log 3$. In this instance, we could now calculate $f_H(\alpha) = \dim_H F_\alpha$ as in Proposition 10.1, and this gives a parametric expression equivalent to (17.14). We defer a formal calculation until the next section, where it will be done in a more general context.

Just as the Hausdorff dimension of a set is never more than its box dimension, there is a basic inequality between the fine and coarse spectra.

Lemma 17.3

Let μ be a finite measure on \mathbb{R}^n . Then

$$f_H(\alpha) \leq f_{-C}(\alpha) \leq \bar{f}_C(\alpha)$$

17.19.

for all $\alpha \geq 0$.

Proof

The right-hand inequality of (17.19) is obvious. We prove the left-hand inequality in the case where μ is a measure on \mathbb{R} ; the proof is similar for $n \geq 2$ except that measures of balls and cubes have to be compared instead of measures of intervals.

For fixed $\alpha \geq 0$, write for brevity $f \equiv f_H(\alpha) = \dim_H F_\alpha$; we may assume $f > 0$. Given $0 < \epsilon < f$, then $\mathcal{H}^{f-\epsilon}(F_\alpha) = \infty$. Using (17.16) and Egoroff's theorem, there is a set $F_\alpha^0 \subset F_\alpha$ with $\mathcal{H}^{f-\epsilon}(F_\alpha^0) > 1$ and a number $c_0 > 0$ such that

$$3r^{\alpha+\epsilon} \leq \mu(B(x, r)) < 2^{\epsilon-\alpha} r^{\alpha-\epsilon} \quad \text{17.20}$$

for all $x \in F_\alpha^0$ and all $0 < r \leq c_0$. We may choose δ with $0 < \delta \leq \frac{1}{2}c_0$ such that $\mathcal{H}_\delta^{f-\epsilon}(F_\alpha^0) \geq 1$.

For each $r \leq \delta$, we consider r -mesh intervals (of the form $[mr, (m+1)r]$ with $m \in \mathbb{Z}$) that intersect F_α^0 . Such an interval I contains a point x of F_α^0 , with

$$B(x, r) \subset I \cup I_L \cup I_R \subset B(x, 2r),$$

where I_L and I_R are the r -mesh intervals immediately to the left and right of I . By (17.20)

$$3r^{\alpha+\epsilon} \leq \mu(B(x, r)) \leq \mu(I \cup I_L \cup I_R) \leq \mu(B(x, 2r)) < r^{\alpha-\epsilon},$$

so that

$$r^{\alpha+\epsilon} \leq \mu(I_0) < r^{\alpha-\epsilon}, \quad \text{17.21}$$

where I_0 is one of I , I_L and I_R . From the definition of $\mathcal{H}_\delta^{f-\epsilon}$, there are at least $r^{\epsilon-f} \mathcal{H}_\delta^{f-\epsilon}(F_\alpha^0) \geq r^{\epsilon-f}$ distinct r -mesh intervals that intersect F_α^0 , so there are at least $\frac{1}{3}r^{\epsilon-f}$ distinct r -mesh intervals I_0 that satisfy (17.21) (note that two intervals I separated by $2r$ or

more give rise to different intervals I_0). We conclude that for

$$r \leq \delta$$

$$N_r(\alpha + \epsilon) - N_r(\alpha - \epsilon) \geq \frac{1}{3} r^{\epsilon - f},$$

so from (17.4), $f_C(\alpha) \geq f - \epsilon$; as this is true for all positive ϵ , we conclude $f_C(\alpha) \geq f = f_H(\alpha)$.

Just as many fractals we have encountered have equal box and Hausdorff dimensions, many common multifractal measures have equal coarse and fine spectra, that is, equality in (17.19). In Section 17.3, we shall show that this is the case for self-similar measures.

By setting up Hausdorff-type measures tailored for multifractal purposes, it is possible to define a quantity $\beta(q)$ playing a similar role in the fine theory to that of (17.7) in the coarse theory. The Legendre transform of this $\beta(q)$ gives an upper bound for the fine multifractal spectrum and again in many cases gives the actual value.

17.3 Self-similar multifractals

In this section, we calculate the fine multifractal spectrum of a self-similar measure on \mathbb{R} , of which Example 17.1 is a specific case. Not only are self-similar measures important in their own right but also the methods to be described adapt to many other classes of measures.

We consider a self-similar measure μ supported on a self-similar subset F of \mathbb{R} . Let $S_1, \dots, S_m : \mathbb{R} \rightarrow \mathbb{R}$ be contracting similarities with ratios r_1, \dots, r_m . As in Chapter 9, the iterated function system $\{S_1, \dots, S_m\}$ has a (unique non-empty compact) attractor $F \subset \mathbb{R}$. We assume that a strong separation condition holds, that is, there is a closed interval I such that $S_i(I) \subset I$ for all i , and $S_i(I) \cap S_j(I) = \emptyset$ whenever $i \neq j$.

As in Chapter 9, we index the intervals in the natural construction of F by the finite sequences $\mathcal{I}_k = \{(i_1, \dots, i_k) : 1 \leq i \leq m\}$, writing $\mathbf{i} = (i_1, \dots, i_k)$ for a typical sequence of \mathcal{I}_k . Thus,

$$I_{\mathbf{i}} = I_{i_1, \dots, i_k} = S_{i_1} \circ \dots \circ S_{i_k}(I). \quad \text{17.22}$$

For convenience, we assume that $|I| = 1$, so for $\mathbf{i} = (i_1, i_2, \dots, i_k) \in \mathcal{I}_k$, we have

$$|I_{\mathbf{i}}| = r_{\mathbf{i}} \equiv r_{i_1} r_{i_2} \cdots r_{i_k}. \quad \text{17.23}$$

We define a self-similar measure μ with support F by repeated subdivision. Let p_1, \dots, p_m be ‘probabilities’ or ‘mass ratios’, that is, $p_i > 0$ for all i and $\sum_{i=1}^m p_i = 1$. Repeatedly dividing the mass on intervals I_{i_1, \dots, i_k} between subintervals $I_{i_1, \dots, i_k, 1}, \dots, I_{i_1, \dots, i_k, m}$ in the ratios $p_1 : \dots : p_m$ defines a measure μ on F (see Proposition 1.7). Thus,

$$\mu(I_{i_1, i_2, \dots, i_k}) = p_{\mathbf{i}} \equiv p_{i_1} p_{i_2} \cdots p_{i_k}. \quad \text{17.24}$$

It is easy to see that μ is a *self-similar measure*, in the sense that

$$\mu(A) = \sum_{i=1}^m p_i \mu(S_i^{-1}(A)) \quad \text{17.25}$$

for all sets A , with $\mu(F) = 1$.

Next, given a real number q , we define $\beta = \beta(q)$ as the positive number satisfying

$$\sum_{i=1}^m p_i^q r_i^{\beta(q)} = 1; \quad \text{17.26}$$

such a number $\beta(q)$ exists and is unique since $0 < r_i, p_i < 1$. Moreover, $\beta : \mathbb{R} \rightarrow \mathbb{R}$ is a decreasing function with

$$\lim_{q \rightarrow -\infty} \beta(q) = \infty \quad \text{and} \quad \lim_{q \rightarrow \infty} \beta(q) = -\infty. \quad \text{17.27}$$

Differentiating (17.26) implicitly with respect to q gives

$$0 = \sum_{i=1}^m p_i^q r_i^{\beta(q)} \left(\log p_i + \frac{d\beta}{dq} \log r_i \right), \quad \underline{17.28}$$

and differentiating again gives

$$0 = \sum_{i=1}^m p_i^q r_i^{\beta(q)} \left(\frac{d^2\beta}{dq^2} \log r_i + \left(\log p_i + \frac{d\beta}{dq} \log r_i \right)^2 \right).$$

Thus, $d^2\beta/dq^2 \geq 0$, so β is convex in q . Provided $\log p_i / \log r_i$ is not the same for all $i = 1, \dots, m$, then $d^2\beta/dq^2 > 0$ and β is strictly convex; we assume henceforth that this holds to avoid degenerate cases.

We will show that the fine (Hausdorff) multifractal spectrum, $f_H(\alpha) = \dim F_\alpha$, is the Legendre transform of β , where we now write f for the *Legendre transform* of β , defined by

$$f(\alpha) = \inf_{-\infty < q < \infty} \{ \beta(q) + \alpha q \}, \quad \underline{17.29}$$

provided this is finite. Since $\beta : \mathbb{R} \rightarrow \mathbb{R}$ is a convex function, there is a range of α , say $\alpha \in [\alpha_{\min}, \alpha_{\max}]$ for which the graph of β has a line of support L_α of slope $-\alpha$, and for such α , this support line is unique (thus, $-\alpha_{\min}$ and $-\alpha_{\max}$ are the slopes of the asymptotes of the graph of β). Then the Legendre transform of β is $f : [\alpha_{\min}, \alpha_{\max}] \rightarrow \mathbb{R}$ given by the value of the intercept of L_α with the vertical axis (again see [Figure 17.2](#)). It is clear that f is continuous in α .

Since β is strictly convex, for a given α , the infimum in [\(17.29\)](#) is attained at a unique $q = q(\alpha)$. Equating the derivative of $\beta(q) + \alpha q$ to 0, this occurs when

$$\alpha = -\frac{d\beta}{dq} \quad \underline{17.30}$$

so that

$$f(\alpha) = \alpha q + \beta(q) = -q \frac{d\beta}{dq} + \beta(q). \quad \underline{17.31}$$

Note that if any one of $q \in \mathbb{R}$, $\beta \in \mathbb{R}$ and $\alpha \in (\alpha_{\min}, \alpha_{\max})$ is given, the other two and f are determined by (17.26), (17.30) and (17.31). Using (17.30) and rearranging (17.28) gives

$$\alpha = \frac{\sum_{i=1}^m p_i^q r_i^\beta \log p_i}{\sum_{i=1}^m p_i^q r_i^\beta \log r_i}. \quad \mathbf{17.32}$$

On inspecting this expression, we see that

$$\alpha_{\min} = \min_{1 \leq i \leq m} \log p_i / \log r_i \quad \text{and} \quad \alpha_{\max} = \max_{1 \leq i \leq m} \log p_i / \log r_i, \quad \mathbf{17.33}$$

which correspond to q approaching ∞ and $-\infty$, respectively.

Provided that the numbers $\{\log p_i / \log r_i\}_{i=1}^m$ are all different, $f(\alpha_{\min}) = f(\alpha_{\max}) = 0$ (see Exercise 17.8).

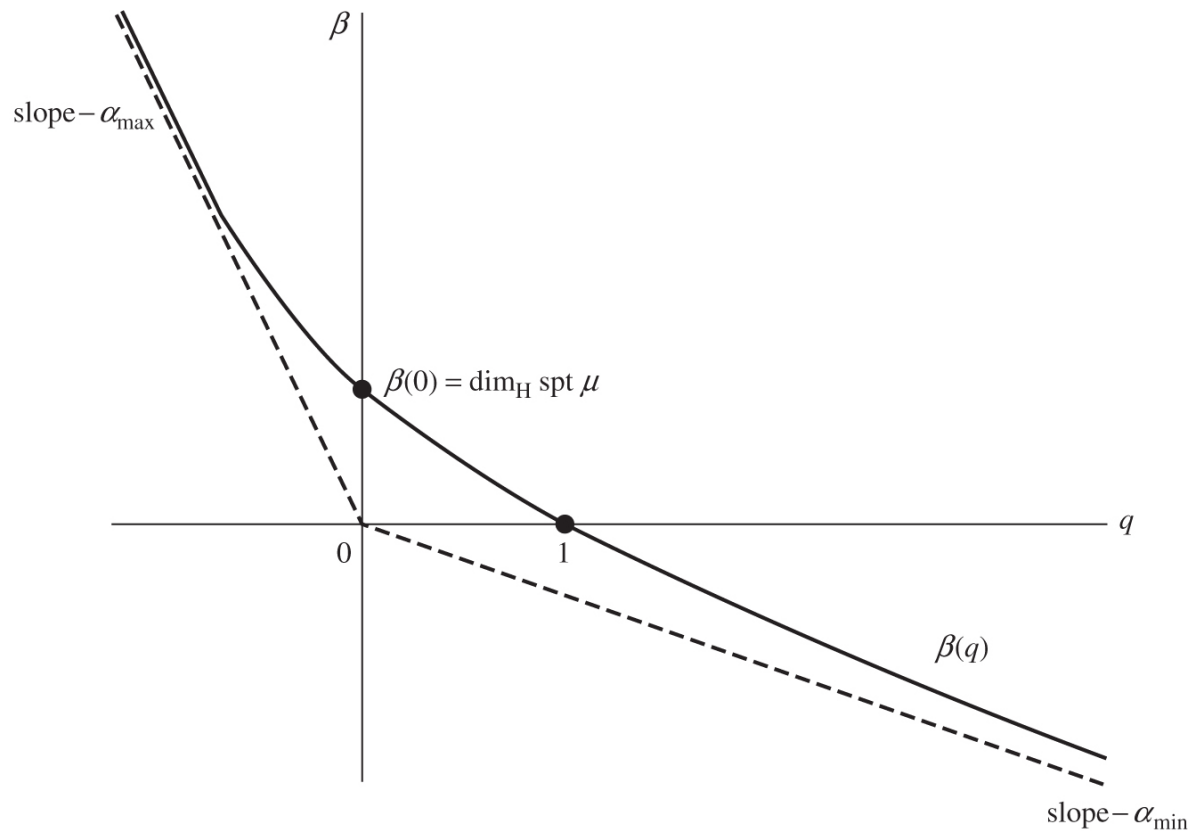
Differentiating (17.31) with respect to α and using (17.30),

$$\frac{df}{d\alpha} = \alpha \frac{dq}{d\alpha} + q + \frac{d\beta}{dq} \frac{dq}{d\alpha} = q. \quad \mathbf{17.34}$$

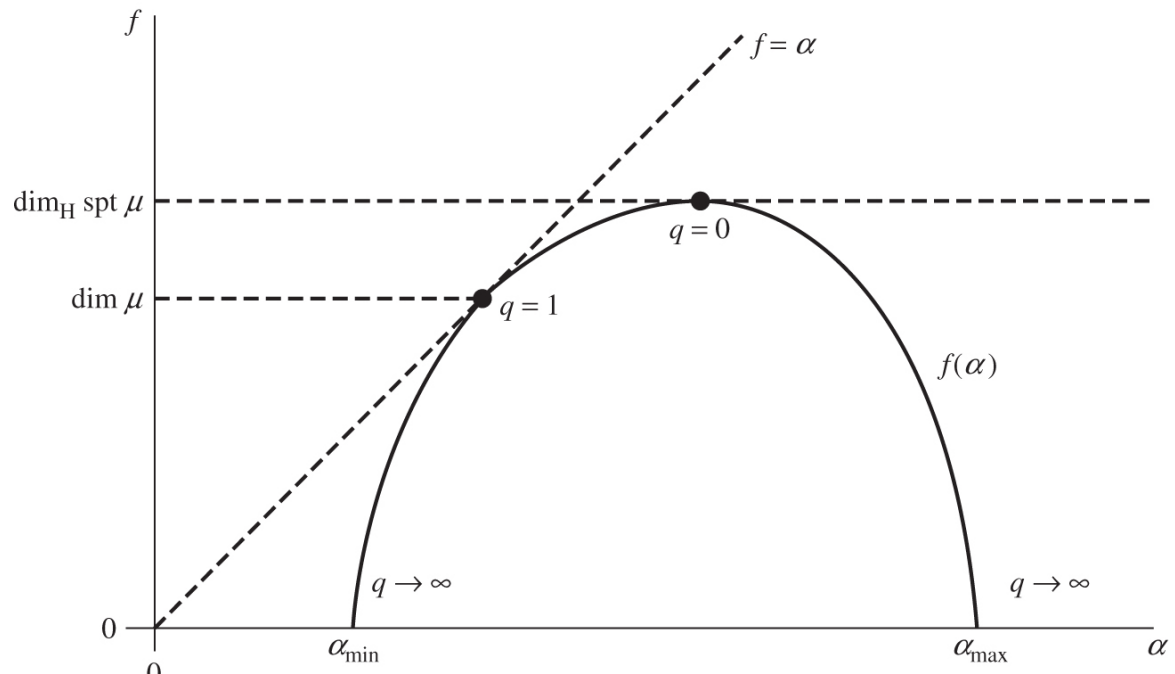
Since q decreases as α increases, it follows that f is a concave function of α .

Some values of q are of special interest (see Figure 17.4). If $q = 0$, then $\beta(q) = \dim_H F = \dim_H(\text{spt } \mu)$, comparing (17.26) and the dimension formula for self-similar sets (9.14). Moreover, by (17.34), $q = 0$ corresponds to the maximum of $f(\alpha)$, hence

$$\dim_H F = \dim_H(\text{spt } \mu) = \max_{\alpha} f(\alpha).$$



(a)



(b)

Figure 17.4 Form of the multifractal functions for a typical self-similar measure. (a) The $\beta(q)$ curve; (b) the ‘multifractal spectrum’ $f(\alpha) = \dim_H F_\alpha$, which is the Legendre transform of $\beta(q)$.

When $q = 1$, (17.26) implies $\beta(q) = 0$ so $f(\alpha) = \alpha$ by (17.31). Moreover, $df(\alpha)/d\alpha = q = 1$, so that the $f(\alpha)$ curve lies under the line $f = \alpha$ and touches it just at the point corresponding to $q = 1$. It will follow later that $\alpha(1) = f(\alpha(1)) = \dim_H \mu$, where

$$\dim_H \mu = \inf \{ \dim_H E : E \text{ is a Borel set with } \mu(E) > 0 \} \quad 17.35$$

is the *Hausdorff dimension of the measure μ* . Thus, the dimension of μ is the dimension of a set on which a significant part of μ is concentrated.

We can now state the main result on the fine multifractal spectrum of a self-similar measure, that the Hausdorff multifractal spectrum is given by the Legendre transform (17.29) of $\beta(q)$ given by (17.26).

Theorem 17.4

Let μ be a self-similar measure as above and let

$$F_\alpha = \{x \in \mathbb{R}^n : \dim_{\text{loc}} \mu(x) = \alpha\}.$$

If $\alpha \notin [\alpha_{\min}, \alpha_{\max}]$, then $F_\alpha = \emptyset$, and if $\alpha \in [\alpha_{\min}, \alpha_{\max}]$, then

$$f_H(\alpha) \equiv \dim_H F_\alpha = f(\alpha), \quad 17.36$$

where f is the Legendre transform of $\beta(q)$.

We first give a simple partial proof and then a slightly more involved full proof of this theorem.

As is usual in this sort of work, it is convenient to redefine F_α in terms of the component intervals I_i rather than the balls $B(x, r)$. For $x \in \text{spt } \mu$, we write $I_k(x)$ for the k th level set I_{i_1, \dots, i_k} that contains x . We

shall go back and forth between the set $I_k(x)$ and the ball $B(x, r)$ where $|I_k(x)|$ is comparable with r .

Lemma 17.5

For all $x \in F$,

$$\dim_{\text{loc}} \mu(x) \equiv \lim_{r \rightarrow 0} \frac{\log \mu(B(x, r))}{\log r} = \lim_{k \rightarrow \infty} \frac{\log \mu(I_k(x))}{\log |I_k(x)|}, \quad \text{17.37}$$

with either both or neither of these limits existing. In particular,

$$F_\alpha = \left\{ x \in F : \lim_{k \rightarrow \infty} \frac{\log \mu(I_k(x))}{\log |I_k(x)|} = \alpha \right\}. \quad \text{17.38}$$

Proof

Let $b = \min_{1 \leq i \leq m} |I_i|$, and let d be the minimum gap between the intervals I_1, \dots, I_m . Let $x \in F$, let $0 < r < 1$ and let k be the integer such that

$$|I_k(x)| \leq r < |I_{k-1}(x)| \leq b^{-1} |I_k(x)|.$$

Then $I_k(x) \subset B(x, r)$ and $B(x, dr) \cap E \subset I_k(x)$ since the gap between $I_k(x)$ and any other k th level interval is at least $d|I_{k-1}(x)| > dr$. Then

$$\mu(B(x, dr)) \leq \mu(I_k(x)) \leq \mu(B(x, r)).$$

Hence,

$$\begin{aligned} \frac{\log \mu(B(x, dr))}{\log(dr) - \log d} &= \frac{\log \mu(B(x, dr))}{\log r} \leq \frac{\log \mu(I_k(x))}{\log |I_k(x)|} \leq \frac{\log \mu(B(x, r))}{\log br} \\ &= \frac{\log \mu(B(x, r))}{\log b + \log r}. \end{aligned}$$

Letting $r \rightarrow 0$, that is, $k \rightarrow \infty$, gives the result.

We now give a direct proof of the upper bound $\dim_H F_\alpha \leq f(\alpha)$; this is included as it uses the idea of summing over a restricted class on intervals, a technique that is used frequently in multifractal theory.

Partial proof of Theorem 17.8

We shall show that $\dim_H F_\alpha \leq \beta(q) + q\alpha$ for $q > 0$. The case of $q \leq 0$ is similar but with sign changes (see Exercise 17.13) and taking all values of q together gives $\dim_H F_\alpha \leq f(\alpha)$.

Take $\epsilon > 0$. Let \mathcal{Q}_k denote those k th level sequences $\mathbf{i} = (i_1, \dots, i_k) \in \mathcal{I}_k$ such that

$$|I_{\mathbf{i}}|^{\alpha+\epsilon} \leq \mu(I_{\mathbf{i}}). \quad \text{17.39}$$

Then

$$\begin{aligned} \sum_{\mathbf{i} \in \mathcal{Q}_k} |I_{\mathbf{i}}|^{\beta+q(\alpha+\epsilon)} &\leq \sum_{\mathbf{i} \in \mathcal{Q}_k} |I_{\mathbf{i}}|^\beta \mu(I_{\mathbf{i}})^q \\ &\leq \sum_{\mathbf{i} \in \mathcal{I}_k} |I_{\mathbf{i}}|^\beta \mu(I_{\mathbf{i}})^q \\ &= \sum_{i_1, \dots, i_k} (r_{i_1} r_{i_2} \dots r_{i_k})^\beta (p_{i_1} p_{i_2} \dots p_{i_k})^q \\ &= \left(\sum_{i=1}^m p_i^q r_i^\beta \right)^k = 1, \end{aligned} \quad \text{17.40}$$

using a multinomial expansion and (17.26).

For each integer K , write

$$F^K = \{x \in F : \mu(I_k(x)) \geq |I_k(x)|^{\alpha+\epsilon} \text{ for all } k \geq K\}.$$

Then, for all $k \geq K$, the set $F^K \subset \bigcup_{\mathbf{i} \in \mathcal{Q}_k} I_{\mathbf{i}}$ by (17.39), so by (17.40), $\mathcal{H}_{c^k}^{\beta+q(\alpha+\epsilon)}(F^K) \leq 1$, since for a k th level interval, $|I_{\mathbf{i}}| \leq c^k$ where $c = \max_{1 \leq i \leq m} r_i$. Letting $k \rightarrow \infty$ gives $\mathcal{H}^{\beta+q(\alpha+\epsilon)}(F^K) \leq 1$, so that $\dim_H F^K \leq \beta + q(\alpha + \epsilon)$. But $F_\alpha \subset \bigcup_{K=1}^\infty F^K$ by (17.38), since if $\log \mu(I_k(x)) / \log |I_k(x)| \rightarrow \alpha$ then $\mu(I_k(x)) \geq |I_k(x)|^{\alpha+\epsilon}$ for all k sufficiently large. Thus, $\dim_H F_\alpha \leq \beta + q(\alpha + \epsilon)$ for all $\epsilon > 0$, giving $\dim_H F_\alpha \leq \beta + q\alpha$.

*The rest of this section may be omitted.

We now embark on a full proof of Theorem 17.4. Writing

$$\Phi(q, \beta) = \sum_{i=1}^m p_i^q r_i^\beta \quad (q, \beta \in \mathbb{R}), \quad \underline{\text{17.41}}$$

$\beta(q)$ is defined by $\Phi(q, \beta(q)) = 1$ (see (17.26)). We require the following estimate of Φ near $(q, \beta(q))$.

Lemma 17.6

For all $\epsilon > 0$,

$$\Phi(q + \delta, \beta(q) + (-\alpha + \epsilon)\delta) < 1 \quad \underline{\text{17.42}}$$

and

$$\Phi(q - \delta, \beta(q) + (\alpha + \epsilon)\delta) < 1 \quad \underline{\text{17.43}}$$

for all sufficiently small $\delta > 0$.

Proof

Recalling that $d\beta/dq = -\alpha$, expansion about q gives

$$\beta(q + \delta) = \beta(q) - \alpha\delta + O(\delta^2) < \beta(q) + (-\alpha + \epsilon)\delta$$

if δ is small enough. Since $\Phi(q + \delta, \beta(q + \delta)) = 1$ and Φ is decreasing in its second argument, (17.42) follows. Inequality (17.43) is derived in a similar way.

To prove Theorem 17.4, for each α , we concentrate a measure v on F_α and examine the power law behaviour of $v(B(x, r))$ as $r \rightarrow 0$, so that we can use Proposition 4.9 to find the dimension of F_α . Given $q \in \mathbb{R}$ and $\beta = \beta(q)$, (17.26) enables us to define a probability measure v on $\text{spt } \mu$ by repeated subdivision such that

$$v(I_{i_1, \dots, i_k}) = (p_{i_1} p_{i_2} \cdots p_{i_k})^q (r_{i_1} r_{i_2} \cdots r_{i_k})^\beta, \quad \text{17.44}$$

for each (i_1, \dots, i_k) , and extending this to a measure on F in the usual way. Together with (17.23) and (17.24), this gives three ways of quantifying the I_i :

$$|I_i| = r_i, \quad \mu(I_i) = p_i, \quad v(I_i) = p_i^q r_i^\beta \quad \text{17.45}$$

for all $i = (i_1, \dots, i_k)$.

The following proposition contains the crux of the multifractal spectrum calculation.

Proposition 17.7

With q, β, α and f as above, and with v determined by (17.44),

- a. $v(F_\alpha) = 1$,
- b. for all $x \in F_\alpha$, we have $\log v(B(x, r)) / \log r \rightarrow f(\alpha)$ as $r \rightarrow 0$.

Proof

Let $\epsilon > 0$ be given. Then for all $\delta > 0$,

$$\begin{aligned}
\nu\{x : \mu(I_k(x)) \geq |I_k(x)|^{\alpha-\epsilon}\} &= \nu\{x : 1 \leq \mu(I_k(x))^\delta |I_k(x)|^{(\epsilon-\alpha)\delta}\} \\
&\leq \int \mu(I_k(x))^\delta |I_k(x)|^{(\epsilon-\alpha)\delta} d\nu(x) \\
&= \sum_{i \in I_k} \mu(I_i)^\delta |I_i|^{(\epsilon-\alpha)\delta} \nu(I_i) \\
&= \sum_{i \in I_k} p_i^{q+\delta} r_i^{\beta+(\epsilon-\alpha)\delta} \\
&= \left(\sum_{i=1}^m p_i^{q+\delta} r_i^{\beta+(\epsilon-\alpha)\delta} \right)^k \\
&= [\Phi(q + \delta, \beta + (\epsilon - \alpha)\delta)]^k,
\end{aligned}$$

where Φ is given by (17.41), using (17.45) and a multinomial expansion. Choosing δ small enough and using (17.42) gives that

$$\nu\{x : \mu(I_k(x)) \geq |I_k(x)|^{\alpha-\epsilon}\} \leq \gamma^k \quad \text{17.46}$$

for some $\gamma < 1$ independent of k . Thus,

$$\nu\{x : \mu(I_k(x)) \geq |I_k(x)|^{\alpha-\epsilon} \text{ for some } k \geq K\} \leq \sum_{k=K}^{\infty} \gamma^k \leq \gamma^K / (1 - \gamma).$$

It follows that for ν -almost all x , we have

$$\lim_{k \rightarrow \infty} \frac{\log \mu(I_k(x))}{\log |I_k(x)|} \geq \alpha - \epsilon.$$

This is true for all $\epsilon > 0$, so we get the left-hand inequality of

$$\alpha \leq \liminf_{k \rightarrow \infty} \frac{\log \mu(I_k(x))}{\log |I_k(x)|} \leq \overline{\lim}_{k \rightarrow \infty} \frac{\log \mu(I_k(x))}{\log |I_k(x)|} \leq \alpha.$$

The right-hand inequality follows in the same way, using (17.43) in estimating $\nu\{x : \mu(I_k(x)) \leq |I_k(x)|^{\alpha+\epsilon}\}$. From (17.37), we conclude that for ν -almost all x ,

$$\dim_{\text{loc}} \mu(x) = \lim_{k \rightarrow \infty} \frac{\log \mu(I_k(x))}{\log |I_k(x)|} = \alpha$$

and it follows that $\nu(F_\alpha) = \nu(F) = 1$.

For (b), note that from (17.45),

$$\frac{\log \nu(I_k(x))}{\log |I_k(x)|} = q \frac{\log \mu(I_k(x))}{\log |I_k(x)|} + \beta \frac{\log |I_k(x)|}{\log |I_k(x)|}, \quad 17.47$$

so for all $x \in F_\alpha$,

$$\frac{\log \nu(I_k(x))}{\log |I_k(x)|} \rightarrow q\alpha + \beta = f \quad 17.48$$

as $k \rightarrow \infty$, using (17.31). Part (b) follows, applying (17.37) to ν .

Our main Theorem 17.4 on the multifractal spectrum of self-similar measures now follows easily.

Proof of Theorem 17.4

From (17.45),

$$\frac{\log \mu(I_i)}{\log |I_i|} = \frac{\sum_{j=1}^k \log p_{i_j}}{\sum_{j=1}^k \log r_{i_j}},$$

where $\mathbf{i} = (i_1, \dots, i_k)$, so by (17.33), $\log \mu(I_i)/\log |I_i| \in [\alpha_{\min}, \alpha_{\max}]$ for all \mathbf{i} . Thus, the only possible limit points of $\log \mu(I_i)/\log |I_i|$, and so by (17.37) of $\log B(x, r)/\log r$, are in $[\alpha_{\min}, \alpha_{\max}]$. In particular, $F_\alpha = \emptyset$ if $\alpha \notin [\alpha_{\min}, \alpha_{\max}]$.

If $\alpha \in (\alpha_{\min}, \alpha_{\max})$, then by Proposition 17.7, there exists a measure v concentrated on F_α with $\lim_{r \rightarrow 0} \log v(B(x, r))/\log r = f(\alpha)$ for all $x \in F_\alpha$, so (17.36) follows from Proposition 4.9. For the cases $\alpha = \alpha_{\min}$ and $\alpha = \alpha_{\max}$, see Exercise 17.14.

Thus, for a self-similar measure, the dimension of F_α may be calculated by taking the Legendre transform of $\beta(q)$ given by (17.26).

The dimensions of $\text{spt}\mu$ and of the measure μ (see (17.35)) may easily be found from the multifractal spectrum.

Proposition 17.8

Let μ be a self-similar measure as above. Regarding $\alpha = \alpha(q)$ as a function of q ,

- $f(\alpha)$ takes its maximum when $\alpha = \alpha(0)$, with $f(\alpha(0)) = \dim_H \text{spt}\mu$.
- $f(\alpha(1)) = \alpha(1) = \dim_H \mu$.

Proof

Part (a) and that $f(\alpha(1)) = \alpha(1)$ were noted as a consequence of (17.34). For the dimension of the measure μ , if $q = 1$, then $\beta = 0$ from (17.26), so by (17.44), the measure ν is identical to μ . By Proposition 17.7, $\mu(F_{\alpha(1)}) = 1$ and $\dim_{\text{loc}} \mu(x) = f(\alpha(1))$ for all $x \in F_{\alpha(1)}$, so by Proposition 4.9, $\dim_H E = f(\alpha(1))$ for all E with $\mu(E) > 0$. Thus, (b) follows from the definition of the dimension of a measure (17.35).

Next, we show that the coarse spectrum of a self-similar measure is also equal to $f(\alpha)$, the Legendre transform of β .

Proposition 17.9

Let μ be a self-similar measure on \mathbb{R} as above. Then

$$f_C(\alpha) = \bar{f}_C(\alpha) = f_H(\alpha) = f(\alpha) \quad \text{17.49}$$

for all $\alpha = \alpha(q)$ for which $q \geq 0$.

Proof

We first note that by Theorem 17.4 and Lemma 17.3, we have $f(\alpha) = f_H(\alpha) \leq f_C(\alpha) \leq \bar{f}_C(\alpha)$, where the coarse spectra are given by (17.4) and (17.5).

To prove the opposite inequality, let d be the minimum separation of I_i and I_j for $i \neq j$, and write $a = 2/d$. Given $r < a^{-1}$, let \mathcal{Q} be the set of all sequences $\mathbf{i} = (i_1, \dots, i_k) \in \mathcal{I}_k$ such that $|I_{i_1, \dots, i_k}| \leq ar$ but $|I_{i_1, \dots, i_{k-1}}| > ar$. Then

$$abr < |I_{\mathbf{i}}| = r_{\mathbf{i}} \leq ar \quad \text{17.50}$$

if $\mathbf{i} \in \mathcal{Q}$, where $b = \min_{1 \leq i \leq m} r_i$. We note that each point of F lies in exactly one set $I_{\mathbf{i}}$ with $\mathbf{i} \in \mathcal{Q}$ and also that for distinct $\mathbf{i}, \mathbf{j} \in \mathcal{Q}$ the sets $I_{\mathbf{i}}$ and $I_{\mathbf{j}}$ have separation at least $dar = 2r$.

Suppose $q > 0$ and let β, α and f be the corresponding values given by (17.26), (17.30) and (17.31). Then

$$\begin{aligned} \#\{\mathbf{i} \in \mathcal{Q} : \mu(I_{\mathbf{i}}) \geq a^{-\alpha} |I_{\mathbf{i}}|^{\alpha}\} &= \#\{\mathbf{i} \in \mathcal{Q} : 1 \leq (a^{\alpha} |I_{\mathbf{i}}|^{-\alpha} \mu(I_{\mathbf{i}}))^q\} \\ &= \#\{\mathbf{i} \in \mathcal{Q} : 1 \leq a^{\alpha q} p_{\mathbf{i}}^q r_{\mathbf{i}}^{-\alpha q}\} \\ &\leq a^{\alpha q} \sum_{\mathbf{i} \in \mathcal{Q}} p_{\mathbf{i}}^q r_{\mathbf{i}}^{-\alpha q} \\ &= a^{\alpha q} \sum_{\mathbf{i} \in \mathcal{Q}} p_{\mathbf{i}}^q r_{\mathbf{i}}^{\beta} r_{\mathbf{i}}^{-\beta - \alpha q} \\ &\leq a^{\alpha q} (abr)^{-\beta - \alpha q} \sum_{\mathbf{i} \in \mathcal{Q}} p_{\mathbf{i}}^q r_{\mathbf{i}}^{\beta} \\ &\leq a^{\alpha q} (ab)^{-f} r^{-f}, \end{aligned}$$

using (17.50), (17.31) and that $\sum_{\mathbf{i} \in \mathcal{Q}} p_{\mathbf{i}}^q r_{\mathbf{i}}^{\beta} = 1$, an identity that follows by repeated substitution of $\sum_{i=1}^m p_{\mathbf{i}, i}^q r_{\mathbf{i}, i}^{\beta} = p_{\mathbf{i}}^q r_{\mathbf{i}}^{\beta}$ in itself. Every r -mesh interval intersects at most one of the sets $I_{\mathbf{i}}$ for $\mathbf{i} \in \mathcal{Q}$. With $N_r(\alpha)$ as in (17.1)

$$\begin{aligned}
N_r(\alpha) &= \#\{r\text{-mesh intervals } C : \mu(C) \geq r^\alpha\} \\
&\leq \#\{\mathbf{i} \in \mathcal{Q} : \mu(I_{\mathbf{i}}) \geq r^{-\alpha} |I_{\mathbf{i}}|^\alpha\} \\
&\leq a^{\alpha q} (ab)^{-f(\alpha)} r^{-f(\alpha)},
\end{aligned}$$

It follows that there is a number c such that for sufficiently small ϵ and r

$$N_r(\alpha + \epsilon) - N_r(\alpha - \epsilon) \leq N_r(\alpha + \epsilon) \leq cr^{-f(\alpha+\epsilon)},$$

so, by (17.5), $\bar{f}_C(\alpha) \leq f(\alpha + \epsilon)$ for all $\epsilon > 0$; since f is continuous

$$\frac{\bar{f}_C(\alpha)}{f(\alpha)} \leq 1.$$

The coarse spectrum, as we have defined it, is not well-enough behaved to give equality in (17.49) for α corresponding to $q < 0$.

Continuation of Example 17.1

Proposition 17.9 allows us to complete our analysis of this example. With $\beta(q) = \log(p_1^q + p_2^q)/\log 3$, the coarse and fine multifractal spectra of μ are equal to the Legendre transform $f(\alpha)$ of $\beta(q)$, that is, $f_C(\alpha) = f_H(\alpha) = f(\alpha)$ for $\alpha \in [\alpha_{\min}, \alpha_{\max}]$, where $\alpha_{\min} = \min_{i=1,2} \log p_i / -\log 3$ and $\alpha_{\max} = \max_{i=1,2} \log p_i / -\log 3$. As before, this leads to the parametric expression for f given in (17.14).

These methods generalise to many further multifractal measures. In particular, the derivation of the multifractal spectrum for self-similar measures extends to self-similar measures on \mathbb{R}^n without difficulty, and the separation condition on the intervals $S_i(I)$ can be weakened to the open set condition.

17.4 Notes and references

The literature on multifractals is vast and we mention a small selection of the many references where further details may be

found.

The idea of studying measures from a fractal viewpoint is implicit in Mandelbrot's essay (1982), see also Mandelbrot (1974). Legendre transformation was introduced into multifractal analysis in Frisch and Parisi (1985) and Halsey et al. (1986). Treatments of the subject at a fairly basic level are given by Evertsz and Mandelbrot (1992); Falconer (1997); Feder (1988); McCauley (1993) and Schroeder (2009). Mandelbrot's 'Selecta' Mandelbrot (1999) includes reprints of many papers, as well as a wide-ranging survey and a comprehensive bibliography on multifractals. A survey by Olsen (2000) considers their geometrical properties such as projections and intersections. The book by Harte (2001) gives a substantial treatment of the theory with many references and, in particular, addresses statistical estimation of spectra. Mörters (2009) presents some novel applications of multifractals to stochastic processes.

Measure theoretic approaches to multifractal theory, including the use of measures of Hausdorff type and relationships between different types of spectra, are given by Brown, Michon and Peyrière (1992); Olsen (1995) and Pesin (1997).

Here are a very few references to the wide range of classes of multifractal measures that have been analysed. Cawley and Mauldin (1992) consider self-similar measures, and Edgar and Mauldin (1992) develop this to graph-directed measure constructions. Self-similar multifractals with infinitely many similarities are addressed by Mandelbrot and Riedi (1995) and Mauldin and Urbański (1996). Random self-similar measures are considered by Mandelbrot (1974) and Kahane and Peyrière (1976) and random graph-directed constructions by Olsen (1994). Self-conformal measures are investigated by Patzschke (1997) and Rams and Lévy Vehel (2007) and vector-valued multifractals by Falconer and O'Neil (1996). Olsen (1998); Falconer (2010) and Barral and Feng (2013) consider various types of self-affine measures, and Olsen and Fraser (2011) examine random self-affine multifractals. Many authors, including McCauley (1993); Pesin (1997) and Barreira (2008), address multifractals that arise naturally in dynamical systems.

Multifractal methods have also been applied to analyse the local irregularities of fractal functions and processes, see Jaffard (1997); Riedi (2002) and Jin (2011).

There are many other interesting aspects of multifractal behaviour, such as the interpretation of negative dimensions, see Mandelbrot (1991).

Exercises

17.1 Find the Legendre transform of $\beta(q) = e^{-q}$.

17.2 Let μ_1, μ_2 be finite measures on \mathbb{R}^n with disjoint supports, and define $\nu = \mu_1 + \mu_2$. Show that $f_H^\nu(\alpha) = \max\{f_H^1(\alpha), f_H^2(\alpha)\}$ where f_H^1, f_H^2 and f_H are the Hausdorff spectra of ν, μ_1 and μ_2 . Deduce that $f_H(\alpha)$ need not be concave over the range of α for which it does not vanish.

17.3 Let μ be a finite measure on \mathbb{R}^n and let $g : \mathbb{R}^n \rightarrow \mathbb{R}^n$ be a bi-Lipschitz function. Define the image measure ν on \mathbb{R}^n by $\nu(A) = \mu(g^{-1}(A))$. Show that the local dimensions $\dim_{loc}\mu(x)$ and

$\dim_{\text{loc}} \nu(g(x))$ are equal when either exists. Hence, show that $f_H(\alpha)$ given by (17.17) is the same for both ν and μ .

17.4 Let μ be a self-similar measure supported by the ‘middle half’ Cantor set, so $r_1 = r_2 = \frac{1}{4}$, with the mass repeatedly divided between the left and right parts in the ratio $p_1 : p_2$, where $p_1 + p_2 = 1$ and $p_1 < p_2$. Show that $\beta(q) = \log(p_1^q + p_2^q)/\log 4$, and hence find α and f in terms of the parameter q .

17.5 Let μ be the measure on the middle half Cantor set of Exercise 17.4. For $q \geq 0$, estimate the moment sums (17.6). [Hint: consider the case where $r = 4^{-k}$ first.] Hence, show that $\beta(q)$ given by (17.7) coincides with that stated in Exercise 17.4.

17.6 Let μ be a self-similar measure constructed by repeated subdivision of the support in the ratios $r_1 = \frac{1}{2}$ and $r_2 = \frac{1}{4}$ and of the measure in ratios p_1 and p_2 . Obtain an explicit formula for $\beta(q)$.

17.7 Let μ be the measure of Example 17.1, with β given by (17.13). Show that $\beta(q) - \beta(-q) = q \log(p_1 p_2)/\log 3$. Hence, show the multifractal spectrum $f(\alpha)$ given by the Legendre transform (17.10) is symmetrical about $\alpha = -\log(p_1 p_2)/2 \log 3$, that is,

$$f(\alpha) = f(-\log(p_1 p_2)/\log 3 - \alpha).$$

17.8 Let μ be the measure of Example 17.1, with $0 < p_1 < p_2 < 1$ and β given by (17.13). Show that for large q , $\beta(q) = q \log p_2 / \log 3 + o(1)$, and obtain a similar expression for q large negative. (Here, $o(1)$ means a function of q that tends to 0 as $q \rightarrow \infty$.) Deduce that the asymptotes of the graph of $\beta(q)$ pass through the origin, that $\alpha_{\min} = -\log p_2 / \log 3$, $\alpha_{\max} = -\log p_1 / \log 3$ and that $f(\alpha_{\min}) = f(\alpha_{\max}) = 0$.

17.9 For the self-similar measures discussed in Section 17.3, show that $d^2f/d\alpha^2 < 0$ for $\alpha_{\min} < \alpha < \alpha_{\max}$; thus, the $f(\alpha)$ curve is strictly concave.

17.10 With β defined by (17.26), show that $\beta(q) \leq 1 - q$ if $0 < q \leq 1$ and $\beta(q) \geq 1 - q$ if $q \geq 1$. (Hint: recall Hölder's inequality:

$$\sum_{i=1}^m a_i b_i \leq (\sum_{i=1}^m a_i^p)^{1/p} (\sum_{i=1}^m b_i^{p'})^{1/p'},$$
 where $1 < p < \infty$ and $1/p + 1/p' = 1$.)

17.11 Let μ be a finite measure on \mathbb{R}^2 , and let proj denote projection onto a given line L . Define the projection of μ onto L by $(\text{proj } \mu)(A) = \mu\{x \in \mathbb{R}^2 : \text{proj } x \in A\}$ for $A \subset L$. For $x \in \mathbb{R}^2$, show that

$$\overline{\lim}_{r \rightarrow 0} \log((\text{proj } \mu)(B_L(\text{proj } x, r))) / \log r \leq \overline{\lim}_{r \rightarrow 0} \log \mu(B(x, r)) / \log r$$

where $B_L(y, r)$ is the interval within L of centre y and length $2r$.

17.12 Adapt the ‘Partial proof of Theorem 17.4’ to show that $\dim_H F_\alpha \leq \beta(q) + q\alpha$ for the case of α corresponding to $q < 0$. (Hint: consider $\sum |I|^{\beta+q(\alpha-\epsilon)}$ for intervals I with $\mu(I) \leq |I|^{\alpha-\epsilon}$.)

17.13 Extend the ‘Partial proof of Theorem 17.4’ to show that for α corresponding to $q > 0$,

$$\dim_H \{x \in F : \varliminf_{k \rightarrow \infty} \log \mu(I_k(x)) / \log |I_k(x)| \leq \alpha\} \leq f(\alpha).$$

17.14 Prove (17.36) when $\alpha = \alpha_{\min}$. (Hint: take α close to α_{\min} , and note that Proposition 17.7 remains true with (b) replaced by ‘for all x such that $\log \mu(B(x, r)) / \log r \leq \alpha$, we have $\lim_{r \rightarrow 0} \log \nu(B(x, r)) / \log r \leq f(\alpha)$ ’.)

Chapter 18

Physical applications

Cloud boundaries, mountain skylines, coastlines, forked lightning and so on: these, and many other natural objects have a form much better described in fractal terms than by the straight lines and smooth curves of classical geometry. Fractal mathematics ought, therefore, to be well suited to modelling and making predictions about such phenomena.

There are, however, considerable difficulties in applying the mathematics of fractal geometry to real-life examples. We might estimate the box dimension of, say, the coastline of Britain by counting the number N_δ of mesh squares of side δ intersected by the coastline. For a range of δ between 20 m and 200 km, the graph of $\log N_\delta$ against $-\log \delta$ is closely matched by a straight line of slope about 1.2. Thus, the power law $N_\delta \simeq \text{constant} \times \delta^{-1.2}$ is valid for such δ and it makes sense to say that the coastline has dimension 1.2 over this range of scales. However, as δ gets smaller, this power law first becomes inaccurate and then meaningless. Similarly, with other physical examples, estimates of dimension using boxes of side δ inevitably break down well before a molecular scale is reached.

The theory of fractals studied in Part I of this book depends on taking limits as $\delta \rightarrow 0$, which cannot be achieved in reality. There are no true fractals in nature—but for that matter, neither are there the inextensible strings and frictionless pulleys often assumed in applied mathematics!

Nevertheless, it should be possible to apply the mathematical theory of ‘exact’ fractals to the ‘approximate’ fractals of nature, and this has been achieved convincingly in many situations. This is analogous to the well-established use of classical geometry in science—for example, regarding the earth as spherical provides a good enough

approximation for many calculations involving its distant gravitational effects.

Perhaps the most convincing example of a physical phenomenon with a fractal model is that of Brownian motion (see Chapter 16). The underlying physical assumption that a particle subject to random molecular bombardment moves with increments distributed according to a normal distribution leads to the theoretical conclusion that the particle trail has dimension 2. This can be checked experimentally using box-counting methods. The motion can also be simulated on a computer by plotting a trail formed by a large number of small random increments. The dimension of such computer realisations can also be estimated by box counting. Brownian motion, which may be observed in reality or on a computer, has a fractal form predicted by a theoretical model. Even so, Brownian paths fail to have a fractal form on a very fine scale, since infinite energy would be required for a particle to follow a nowhere-differentiable path of dimension 2.

The study of fractals in nature thus proceeds on three fronts: experiment, simulation and theory. Physical objects are observed and measured, dimensions, and perhaps multifractal spectra, are estimated over an appropriate range of scales, and their dependence on various parameters noted. Theoretical techniques, such as assuming the Projection theorem 6.1 to estimate the dimension of an object from a photograph, are sometimes used here. Of course, for a dimension to have any significance, repeating an experiment must lead to the same value.

Whilst a dimension may have some interest purely as a physical constant, it is much more satisfying if fractal properties can be explained in physical terms. Therefore, the next stage is to devise some sort of mechanism to explain the natural phenomena. Computational simulation then permits evaluation of various models by comparing qualitative and quantitative features of the simulation and the reality. Computational methods are always approximate; this can actually be an advantage when modelling

natural rather than exact fractals in that very fine scale effects will be neglected.

It is desirable to have a theoretical model that is mathematically manageable, with basic physical characteristics, such as the dimension, derivable from a mathematical argument. The model should account for the dependence of these characteristics on the various parameters and, ideally, be predictive as well as descriptive. Fractal phenomena in nature are often rather complicated to describe, and various assumptions and approximations may be required in setting up and analysing a mathematical model. Of course, the ability to do this in a way that preserves the physical content is the mark of a good theoretical scientist! Sometimes, differential equations may describe a physical situation, and fractal attractors can often result (see Section 13.5). On the other hand, analysis of differential equations where the boundary or domain is fractal can present problems of an entirely different nature.

There is a vast literature devoted to examining fractal phenomena in these ways; often agreement of dimension between experiment, simulation and theory is surprisingly good. Moreover, analysis of dimension has been used effectively to isolate the dominant features underlying certain physical processes. Nevertheless, there is still a long way to go. Questions such as ‘Why do projections of clouds have perimeters of dimension 1.35 over a very wide range of scales?’, ‘How does the dimension of the surface of a metal affect the physical properties such as radiation of heat or the coefficient of friction?’ and ‘What are the geological processes that lead to a landscape of dimension 2.2?’ should be answered in the framework of fractal modelling.

For most experimental purposes, box-counting dimension has to be used. With N_δ defined by one of the Equivalent definitions 3.1, the box dimension of an object is usually found by estimating the gradient of a graph of $\log N_\delta$ against $-\log \delta$ over a range of scales where the counts can be done and where the object behaves like a fractal.

Sometimes, other quantities are more useful or convenient to measure than dimension. For example, in the case of a time-dependent signal, the autocorrelation function (see Section 1.2) might be measured, with (11.20) providing an indication of the dimension.

We examine in more detail some examples from science and nature where a fractal approach can aid understanding of physical processes.

18.1 Fractal fingering

Many natural objects grow in an apparently fractal form, with branches repeatedly splitting and begetting smaller side branches. When viewed at appropriate scales, certain trees, root systems and plants (in particular, more primitive ones such as lichens, mosses and seaweeds) appear as fractals. Forked patterns of lightning or other electrical discharges and the ‘viscous fingering’ that occurs when water is injected into a viscous liquid such as oil also have a branched fractal form. During electrolysis of copper sulphate solution, the copper deposit at the cathode grows in a fractal pattern.

The biological laws that govern plant growth are far too complex to be used as a basis for a mathematical model. However, other phenomena may be modelled by relatively simple growth laws, and we examine some of these.

A simple experiment demonstrates fractal growth by electrolysis of copper sulphate (CuSO_4) (see [Figure 18.1](#)). The bottom of a circular dish is covered with a little copper sulphate solution. A copper cathode is suspended in the centre of the dish and a strip of copper is curved around the edge of the dish to form an anode. If a potential of a few volts is applied between the electrodes, then after a few minutes, a deposit of copper starts to form around the cathode. After half an hour or so, the copper deposit will have

extended into repeatedly branching fractal fingers several inches long.

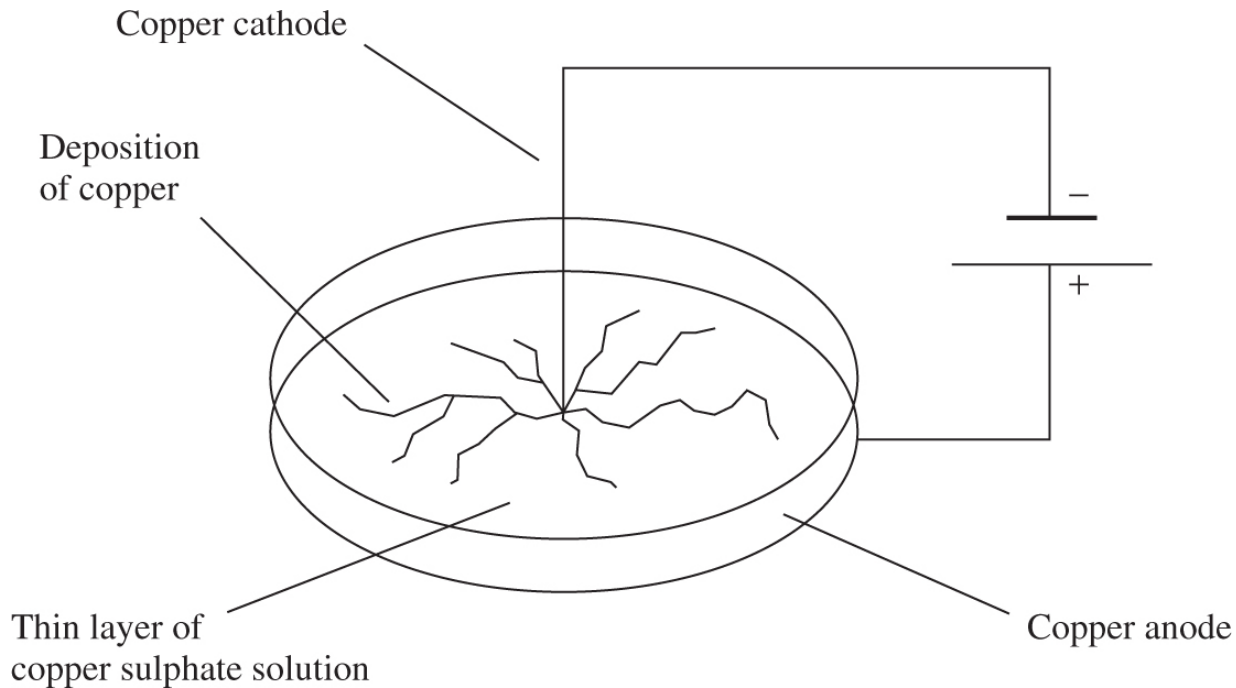


Figure 18.1 Electrolysis of copper sulphate leads to fractal-like deposits of copper growing outwards from the cathode.

The mechanism for this electrolysis is as follows. In solution, the copper sulphate splits into copper Cu^{2+} ions and sulphate SO_4^{2-} ions which drift around in a random manner. When the voltage is applied, the copper ions that hit the cathode receive two electrons and are deposited as copper. Copper ions that hit any copper already present are also deposited as copper, so the residue grows outwards from the cathode. Assuming that the copper ions move in a sufficiently random manner, for example, following Brownian paths (see Chapter 16), ions are more likely to hit the exposed finger ends than the more central parts of the deposition which tend to be ‘protected’ by subsequent growth. Thus, it is at least plausible that growth of the copper deposit will be in thin branching fingers rather than in a solid ‘block’ around the cathode.

In this experiment, the Cu^{2+} ions follow a Brownian path with a drift towards the cathode as a result of the electric field between the

cathode and the anode. Enriching the sulphate in the solution, for example, by addition of sodium sulphate, screens the copper ions from the electric field. Fractal deposits still occur, but this situation is more convenient for mathematical modelling since the Cu^{2+} ions may be assumed to follow Brownian paths. A similar process occurs in electrolysis of zinc sulphate (ZnSO_4) with a zinc anode and carbon cathode, with fingers of zinc growing out from the cathode.

The *diffusion-limited aggregation* (DLA) model provides a convincing simulation of the growth. The model is based on a lattice of small squares. An initial square is shaded to represent the cathode, and a large circle is drawn centred on this square. A particle is released from a random point on the perimeter of the circle and allowed to follow a Brownian path until it either leaves the circle or reaches a square neighbouring a shaded one, in which case that square is also shaded. As this process is repeated for a large number of times, a connected set of squares grows outward from the initial one. It is computationally more convenient to let the particle follow a random walk (which gives an approximation to a Brownian path), so when the particle is released, it moves, left, right, up or down, each direction with probability $\frac{1}{4}$, to a neighbouring square, continuing until it leaves the circle or occupies a square next to a shaded one (see [Figure 18.2](#)). (There are ways of shortening the computation required; for example, if the particle is k squares away from the shaded part, the particle might as well move k steps at once.)

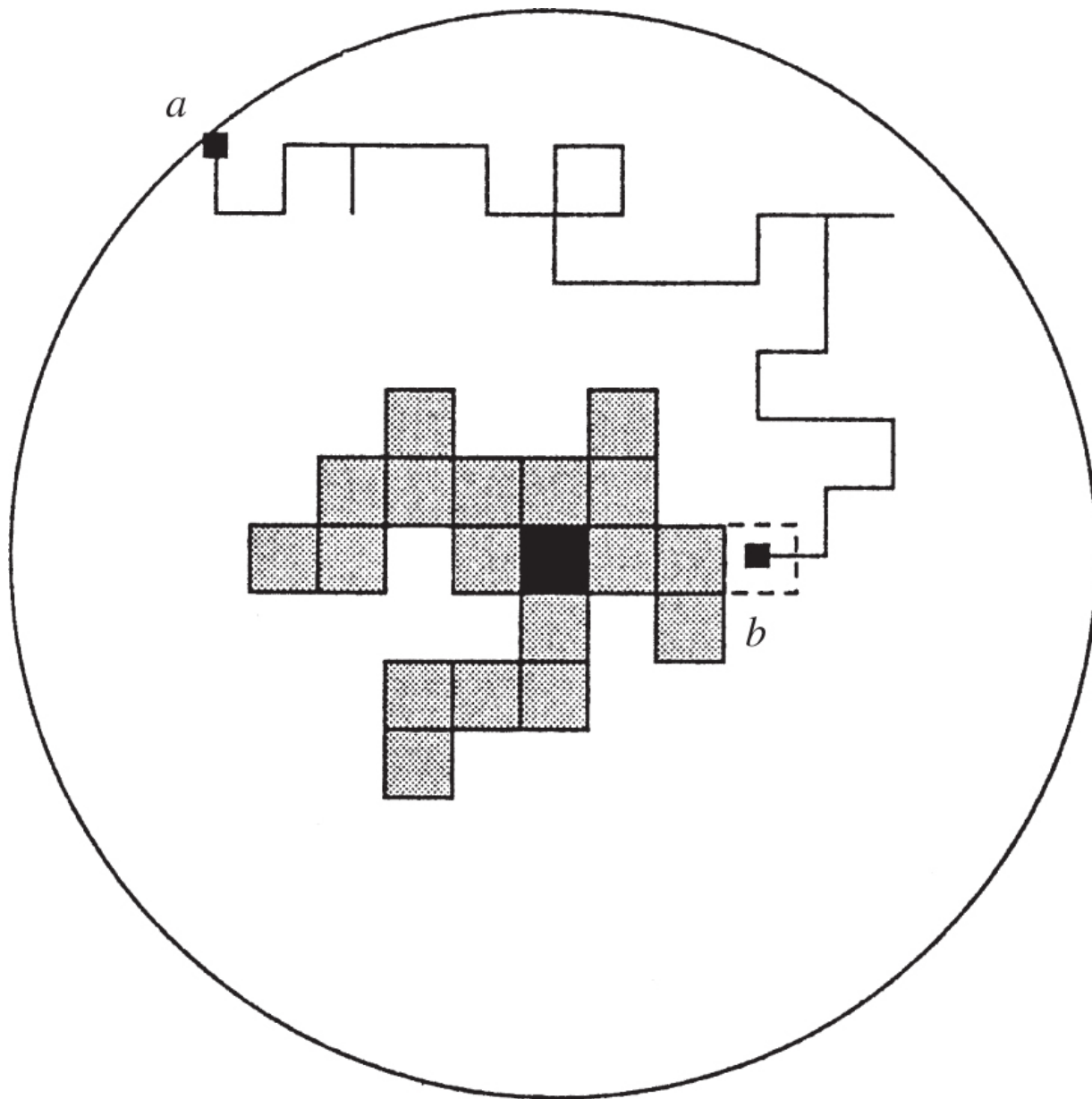


Figure 18.2 The diffusion-limited aggregation (DLA) model. A particle is released from a random point *a* on the circle and performs a random walk until it either leaves the circle or reaches a square *b* next to one that has already been shaded, in which case this square is also shaded.

Running the model for, say, 10 000 shaded squares gives a highly branched picture ([Figure 18.3](#)) that resembles the patterns in the electrolysis experiment. Main branches radiate from the initial point and bifurcate as they grow, giving rise to subsidiary side

branches, all tending to grow outwards. It is natural to use box-counting methods to estimate the dimension of these structures on scales larger than a square side, and there is a remarkably close agreement between the electrolysis experiment and the simulation with a consistent dimension of about 1.70, and 2.43 for the analogous growth process in 3-dimensional space.

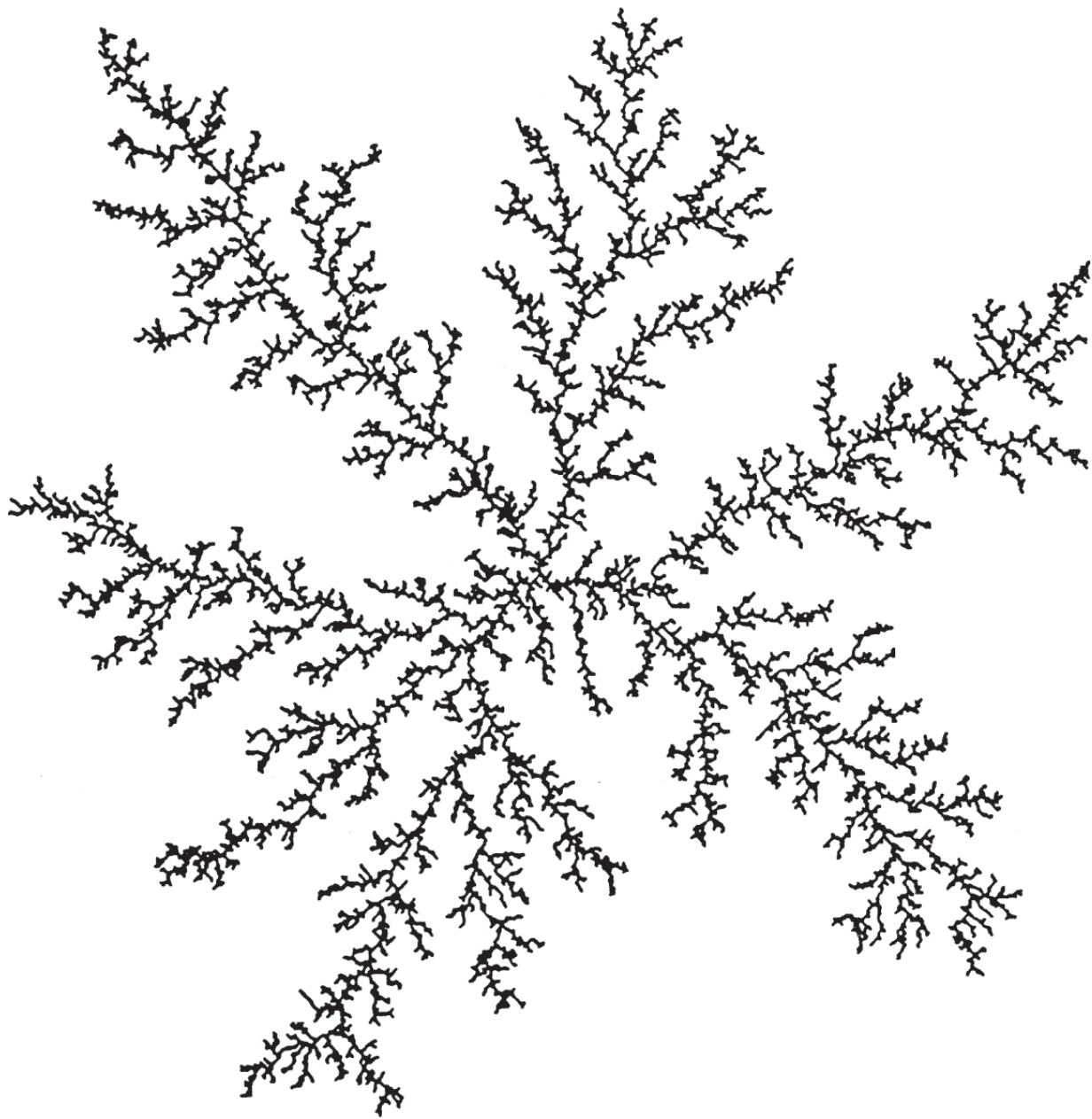


Figure 18.3 A computer realisation of diffusion-limited aggregation. The square was divided into a 700×700 mesh from which 16 000 squares were selected using the method described.

The DLA model may be thought of as a representation of a succession of ions released from a distance one after another. Whilst this provides a good model for the form of the deposit, it gives little idea of its development with time, which depends on a large number of ions in simultaneous random motion that adhere

to the copper deposit on meeting it. Therefore, a ‘continuous’ version of this ‘discrete’ model is useful. Suppose that the large number of copper ions in the solution have density $u(x, t)$ at point x and time t , so that the number of ions in a very small disc of area δx and centre x is $u(x, t)\delta x$. Assuming that the ions follow independent Brownian paths, the ions that are in this small disc at time t will have spread out at time $t + h$ to have density at point x' given by the 2-dimensional normal distribution

$$\delta u(x', t + h) = \frac{1}{2\pi h} \exp\left(-\frac{(x - x')^2}{2h}\right) u(x, t) \delta x$$

(see (16.9)) and so

$$u(x', t + h) = \frac{1}{2\pi h} \int \exp\left(-\frac{(x - x')^2}{2h}\right) u(x, t) dx,$$

where integration is across the fluid region. This assumes that h is small relative to the distance of x' from the deposit and the boundary, so that the effect of the introduction or removal of ions can be neglected. Differentiating under the integral sign with respect to x' and h gives

$$\frac{\partial u}{\partial t} = \frac{1}{2} \nabla^2 u \quad \text{18.1}$$

as the differential equation governing the change of the ion density in the solution. This is the well-known diffusion equation or heat equation in two dimensions.

We need to specify the boundary conditions for this differential equation. At the outer boundary, say a circle of radius r_0 , ions are supplied at a constant rate, so

$$u = u_0 \quad \text{on} \quad |x| = r_0. \quad \text{18.2}$$

Denote the boundary of the copper deposit at time t by F_t . Sufficiently close to this boundary, virtually all the ions lose their charge, so

$$u = 0$$

18.3

on F_t . Since the discharged ions are deposited as metallic copper, the rate of advance v of the boundary F_t is in a direction n normal to F_t , equal in magnitude to the derivative of the concentration in a direction n normal to F_t . Thus, for a constant k ,

$$v_n = kn \cdot \nabla u$$

18.4

on F_t . (We are assuming that F_t is actually smooth on a very small scale.)

Provided that the growth remains a long way from the outer electrode, the diffusion rate is, to a good approximation, time independent, so (18.1) may be replaced by Laplace's equation

$$\nabla^2 u = 0.$$

18.5

Solving this with boundary conditions (18.2) and (18.3) allows the rate of growth of the deposit to be found, using (18.4).

These equations alone are too idealised to provide an accurate model. First, to prevent the equation being unstable with respect to surface irregularities, a short scale ‘cutoff’ for the equations is required. This is provided in the square-lattice DLA model—if a particle gets close enough, it sticks to the aggregate. Second, our derivation of the differential equations assumed a continuously varying particle density, rather than a large number of discrete particles. It is the random variation in motion of these individual particles that creates the irregularities that are amplified into the branching fingers. Thus, (18.4) needs to be modified to include a random perturbation

$$v_n = kn \cdot \nabla u + p,$$

18.6

where p may be thought of as a ‘noise’ term. Both of these features are present in the square-lattice DLA model, which is consequently more suitable for simulation of the growth form than direct numerical attempts to solve the differential equations.

One interpretation of the square-lattice DLA model is as providing a spatial solution of equations (18.2)-(18.5) subject to a small random perturbation of the boundary F_t . Surprisingly, the same differential equations and boundary conditions describe several rather different physical phenomena. The DLA model may, therefore, be expected to apply to some degree in these different cases.

The growth of viscous fingers in a fluid is an example. Suppose two glass plates are fixed a small distance apart (perhaps 0.5 mm) and the region in between is filled with a viscous liquid such as an oil. (This apparatus is called a Hele-Shaw cell.) If a low-viscosity liquid such as water is injected through a small hole in one of the plates, then, under certain conditions, the water spreads out into the oil in thin highly branched fingers. The patterns resemble closely the deposits of copper in the electrolysis experiment.

Lubrication theory tells us that in this situation, the velocity of flow v of the oil is proportional to the pressure gradient.

$$v = -c \nabla p, \quad \underline{18.7}$$

where $p(x)$ is the pressure at a point x in the oil. The oil is assumed incompressible, so the velocity has zero divergence $\nabla \cdot v = 0$, giving

$$\nabla^2 p = 0$$

throughout the oil. If the viscosity of the water is negligible compared with that of the oil, then the pressure throughout the water is effectively constant. Thus, we have the boundary conditions

$$p(x) = p_0$$

at the fluid interface and

$$p(x) = 0$$

at a large distance r_0 from the point of injection. Thus, the pressure difference $u(x) = p_0 - p(x)$ satisfies the differential equation (18.5) and boundary conditions (18.2) and (18.3) of the electrolysis example.

Furthermore, at the fluid interface, the pressure gradient in the oil is normal to the boundary (since the pressure is constant on the boundary), so (18.4) gives the rate of advance of the boundary, $v_n = -kn \cdot \nabla p$, with short-range cutoff provided by surface tension effects. The pressure is analogous to the ion density in the electrolysis example and the irregularities in the interface are amplified to give the fingering effect.

A very similar situation pertains for fluid flow through a porous medium—(18.7) is Darcy's law governing such flow. Fractal fingering can also occur in this situation.

Electrical discharge in a gas provides a further example. The electrostatic potential u satisfies Laplace's equation $\nabla^2 u = 0$ away from the ionised region of discharge. The ionised path conducts well enough to be regarded as being at constant potential, so u satisfies the same boundary conditions as in the viscous fingering example. The (questionable) assumption that the rate of breakdown is proportional to the electric field gives (18.4). This is another example with similar differential equations for which the square-mesh DLA model provides a realistic picture.

Under suitable experimental conditions, the growth patterns in electrolysis, viscous fingering and electrical discharge have a dimension of about 1.7 when estimated over a suitable range of scales. This coincides with the value obtained from computer studies of square-mesh DLA and the universality of this dimension is striking.

18.2 Singularities of electrostatic and gravitational potentials

The electrostatic (or Coulomb) potential at a point x due to a charge distribution μ and the gravitational (or Newtonian) potential due to a mass distribution μ in \mathbb{R}^3 are given, to within a constant multiplier, by

$$\phi(x) = \int \frac{d\mu(y)}{|x-y|}.$$

[18.8](#)

We show that the dimension of the singularity set of the potential, that is, the set of x for which $\phi(x) = \infty$, cannot be too large.

Proposition 18.1

Let μ be a mass distribution of bounded support on \mathbb{R}^3 . Suppose that the potential (18.8) has singularity set $F = \{x : \phi(x) = \infty\}$. Then $\dim_H F \leq 1$.

Proof

Let $s > 1$, $x \in \mathbb{R}^3$ and write $m(r) = \mu(B(x, r))$ for $r > 0$. Suppose that there are numbers $a > 0, c > 0$ such that $m(r) \leq cr^s$ for all $0 < r \leq a$. Then

$$\begin{aligned}\phi(x) &= \int_{|x-y|\leq a} \frac{d\mu(y)}{|x-y|} + \int_{|x-y|>a} \frac{d\mu(y)}{|x-y|} \\ &\leq \int_{r=0}^a \frac{dm(r)}{r} + \int_{|x-y|>a} \frac{d\mu(y)}{a} \\ &\leq [r^{-1}m(r)]_0^a + \int_0^a r^{-2}m(r)dr + a^{-1}\mu(\mathbb{R}^3) \\ &\leq [cr^{s-1}]_0^a + \int_0^a cr^{s-2}dr + a^{-1}\mu(\mathbb{R}^3) \\ &\leq c(1 + (s-1)^{-1})a^{s-1} + a^{-1}\mu(\mathbb{R}^3) < \infty,\end{aligned}$$

after integrating by parts. So, if $x \in F$, we must have that $\overline{\lim}_{r \rightarrow \infty} (\mu(B(x, r))/r^s) \geq c$ for all $c > 0$. It follows from Proposition 4.9(b) that $\mathcal{H}^s(F) = 0$ for $s > 1$, as required.

Often μ is expressible in terms of a ‘density function’ f , so that $\mu(A) = \int_A f(x)dx$ for Borel sets A , and (18.8) becomes

$$\phi(x) = \int \frac{f(y)}{|x-y|} dy. \quad \underline{\text{18.9}}$$

Given conditions on f , for example, if $\int |f(x)|^p dx < \infty$ for some $p > 1$, similar methods can be used to place further bounds on the dimension of the singularity set (see Exercise 18.5).

It is easily verified that if f is a sufficiently smooth function, then (18.9) is the solution of Poisson's equation

$$\nabla^2 \phi = -4\pi f$$

satisfying $\phi(x) \rightarrow 0$ as $|x| \rightarrow \infty$. For a general integrable function f , the potential ϕ need not be differentiable. Nevertheless, (18.9) may be regarded as a *weak solution* of Poisson's equation in a sense that can be made precise using the theory of distributions.

By expressing weak solutions as singular integrals, this technique extends to give bounds for the dimension of the singularity sets for other partial differential equations.

18.3 Fluid dynamics and turbulence

Despite many years of intense study, turbulence in fluids is still not fully understood. Slowly moving fluids tend to flow in a smooth unbroken manner, which is described accurately by the Navier–Stokes equations—the fundamental differential equations of fluid dynamics. Such smooth flow is termed *laminar*. At higher speeds, the flow often becomes *turbulent*, with the fluid particles following convoluted paths of rapidly varying velocity with eddies and irregularities at all scales. Readers will no doubt be familiar with the change from laminar to turbulent flow as a tap is turned from low to full. Although the exact form of turbulent flow is irregular and unpredictable, its overall features are consistently present.

There is no uniformly accepted definition of turbulent flow—this has the advantage that it can reasonably be identified with any convenient ‘singular feature’ of a flow description. We consider a

model in which turbulence is manifested by a significant local generation of heat due to viscosity, that is, ‘fluid friction’, at points of intense activity.

At reasonably small scales, turbulence may be regarded as isotropic, that is, direction independent. Our intuitive understanding of isotropic turbulence stems largely from the qualitative approach of Kolmogorov rather than from an analysis of differential equations. Kolmogorov's model is based on the idea that kinetic energy is introduced into a fluid on a large scale, such as by stirring. However, kinetic energy can only be dissipated (in the form of heat) on very small scales where the effect of viscosity becomes important. At intermediate scales dissipation can be neglected. If there are circulating eddies on all scales, then energy is transferred by the motion of the fluid through a sequence of eddies of decreasing size, until it reaches the small eddies at which dissipation occurs. If, as Kolmogorov assumed, the fluid region is filled by eddies of all scales, then dissipation of energy as heat should occur uniformly throughout the fluid.

Let $\varepsilon(x)$ be the rate of dissipation per unit volume at the point x , so that the heat generated in a small volume δV around x in time δt is $\varepsilon(x)\delta V\delta t$. Then, on the assumption of uniform dissipation,

$$\varepsilon(x) = \bar{\varepsilon} \quad \text{for all } x \text{ in } D,$$

where $\bar{\varepsilon}$ is the rate of input of energy into the fluid region D , which is assumed to have unit volume.

Although such ‘homogeneous’ turbulence is appealing in its simplicity, it is not supported by experimental observations. Measurements using a hot-wire anemometer show that in a turbulent fluid, the rate of dissipation differs greatly in different parts of the fluid. This is the phenomenon of intermittency. Dissipation is high in some regions and very low in others, whereas the Kolmogorov model requires it to be constant. This variation can be quantified using correlation functions. For a small vector h , the

correlation of dissipation rates between points distance h apart is given by

$$\langle \varepsilon(x)\varepsilon(x+h) \rangle,$$

18.10

where angle brackets denote the average over all x in D . If dissipation were constant, we would have $\langle \varepsilon(x)\varepsilon(x+h) \rangle = \bar{\varepsilon}^2$. However, experiment indicates that

$$\langle \varepsilon(x)\varepsilon(x+h) \rangle \simeq \bar{\varepsilon}^2 |h|^{-d}$$

18.11

for a value of d between 0.4 and 0.5.

The Kolmogorov model can be modified to explain the intermittency by assuming that, instead of the eddies at each scale filling space, the eddies fill a successively smaller proportion of space as their size decreases. Kinetic energy is introduced into the largest eddy and passed through eddies of decreasing size until it is dissipated at the smallest scale. Now, however, the energy and dissipation are concentrated on a small part of the fluid. The cascade of eddies may be visualised as the first k stages E_i of the construction of a self-similar fractal F (see Chapter 9) where k is quite large, with dissipation occurring across the k th stage E_k . For convenience, we assume that each k th level basic set of E_i is replaced by a constant number of sets of equal size to form E_{i+1} .

If A is a subset of D , we define $\mu(A) = \int_A \varepsilon(x) dx$ as the total rate of dissipation of energy in the set A , thus, $\mu(D) = \bar{\varepsilon}$, the rate of energy input. Then μ has the properties of a mass distribution on D . Moreover, if we assume that the rate of dissipation in each component of E_i is divided equally between the equal-sized subcomponents in E_{i+1} , we have, as a simple consequence of $F = \bigcap_{i=1}^{\infty} E_i$ being self-similar of Hausdorff or box dimension s , that

$$c_1 \bar{\varepsilon} r^s \leq \mu(B(x, r)) \leq c_2 \bar{\varepsilon} r^s$$

if $x \in F$ and $0 < r < r_0$, where c_1 and c_2 are positive constants (see Exercise 9.11). These inequalities hold not only for $x \in F$ as the size

of the dissipation eddies tends to 0 but also for x in the physical approximation E_k , provided that r is larger than the dissipation scale. Then

$$\begin{aligned}\int_{|h|\leq r} \langle \varepsilon(x)\varepsilon(x+h) \rangle dh &= \int_{x \in D} \int_{|h|\leq r} \varepsilon(x)\varepsilon(x+h) dh dx \\ &= \int_{x \in D} \varepsilon(x)\mu(B(x, r)) dx \\ &= \int_{x \in E_k} \varepsilon(x)\mu(B(x, r)) dx\end{aligned}$$

since dissipation is concentrated on E_k , so

$$c_1 \bar{\varepsilon}^2 r^s \leq \int_{|h|\leq r} \langle \varepsilon(x)\varepsilon(x+h) \rangle dh \leq c_2 \bar{\varepsilon}^2 r^s. \quad \text{18.12}$$

This may be achieved if the correlation satisfies a power law

$$\langle \varepsilon(x)\varepsilon(x+h) \rangle \simeq \bar{\varepsilon}^2 |h|^{s-3}$$

for then the integral in (18.12) becomes

$$4\pi \int_{t=0}^r \bar{\varepsilon}^2 t^{s-3} t^2 dt = \frac{4\pi \bar{\varepsilon}^2 r^s}{s}.$$

Comparison with (18.11) suggests that $s = 3 - d$, so the hypothesis of ‘fractally homogeneous turbulence’, that dissipation is concentrated on an approximate fractal of dimension between 2.5 and 2.6, is consistent with experimental results.

It is natural to seek theoretical reasons for the turbulent region to have a fractal form. One possible explanation is in terms of the vortex tubes in the fluid. According to Kelvin's circulation theorem, such tubes are preserved throughout the motion, at least in the approximation of inviscid flow. However, the vortex tubes are stretched by the fluid motion and become long and thin. Repeated folding is necessary to accommodate this length, so the tubes might

assume an approximate fractal form not unlike the horseshoe example in [Figure 13.5](#).

The behaviour of a (viscous) fluid should be predicted by the Navier–Stokes equation

$$\frac{\partial \mathbf{u}}{\partial t} + (\mathbf{u} \cdot \nabla) \mathbf{u} - \nu \nabla^2 \mathbf{u} + \nabla p = \mathbf{f}, \quad \text{18.13}$$

where \mathbf{u} is the velocity, p is the pressure, ν is the viscosity and \mathbf{f} is the applied force density. Deducing the existence of fractal regions of activity from the Navier–Stokes equation is far from easy.

Nevertheless, the method indicated in Section 18.2 may be generalised beyond recognition to demonstrate rigorously that, for example, the set on which a solution $\mathbf{u}(x, t)$ of (18.13) fails to be bounded for all t has dimension at most $2\frac{1}{2}$. Thus, it is possible to show from the equations of fluid flow that certain types of ‘intense activity’ must be concentrated on sets of small dimension.

18.4 Fractal antennas

A remarkable application of fractals is their use as antennas in high-frequency radio and in particular, in mobile telephones. There are two advantages of using fractals. First, the ‘space-filling’ nature of some fractals, such as variations on the von Koch curve, allows a high response fractal antenna to be fitted into a relatively small space. Second, depending on their geometry, antennas can be multiband with resonant frequencies reflecting the self-similarities of the fractal or alternatively can have frequency independent response, for example, in the case of certain random fractal antennas.

Electrodynamics, and in particular the behaviour of radio waves, is governed by Maxwell’s equations. Assume a time dependence of the electromagnetic quantities proportional to $e^{i\omega t}$, where ω is the frequency, so that the electric field at the point x is $e^{i\omega t}\mathbf{E}(x)$ and the

magnetic field is $e^{i\omega t}\mathbf{H}(x)$. Then Maxwell's 'curl' equations in a vacuum reduce to

$$\nabla \times \mathbf{E} = -i\omega\mu\mathbf{H}$$

$$\nabla \times \mathbf{H} = i\omega\epsilon\mathbf{E},$$

where ϵ is the permittivity and μ the permeability of space. It is immediate that these equations are invariant under the pair of transformations

$$x \mapsto \lambda x \quad \text{and} \quad \omega \mapsto \omega/\lambda,$$

for every (positive or negative) scalar λ , with both sides of the equations multiplied by $1/\lambda$ under the transformations.

If the antenna has a similar form when scaled by a factor λ , the boundary conditions for Maxwell's equations are similar under this scaling, so the radiation properties might be expected to behave in a similar manner when the frequency is scaled by $1/\lambda$, that is, when the wavelength is scaled by λ .

This is borne out in the *Sierpiński dipole*, a practical instance of a fractal antenna (see [Figure 18.4](#)). In one realisation, two Sierpiński triangles are etched on a printed circuit board, vertex to vertex (a fractal 'bow-tie'), with the vertices fed by a two-wire transmission line from a transmitter or receiver. The fundamental frequency of the antenna corresponds to a wavelength comparable to the overall diameter of the Sierpiński triangle. Sharp peaks are observed in the antenna response at $1, \frac{1}{2}, \frac{1}{4}, \frac{1}{8}$ and $\frac{1}{16}$ times this wavelength, these ratios corresponding to the fundamental similarity ratios of the triangle, bearing out the above argument. At each of these resonances, the current density is concentrated on the pair of similar copies of the Sierpiński triangle nearest to the feed point and at the appropriate scale. Varying the construction parameters of the Sierpiński triangle leads to antennas with other sequences of bands.

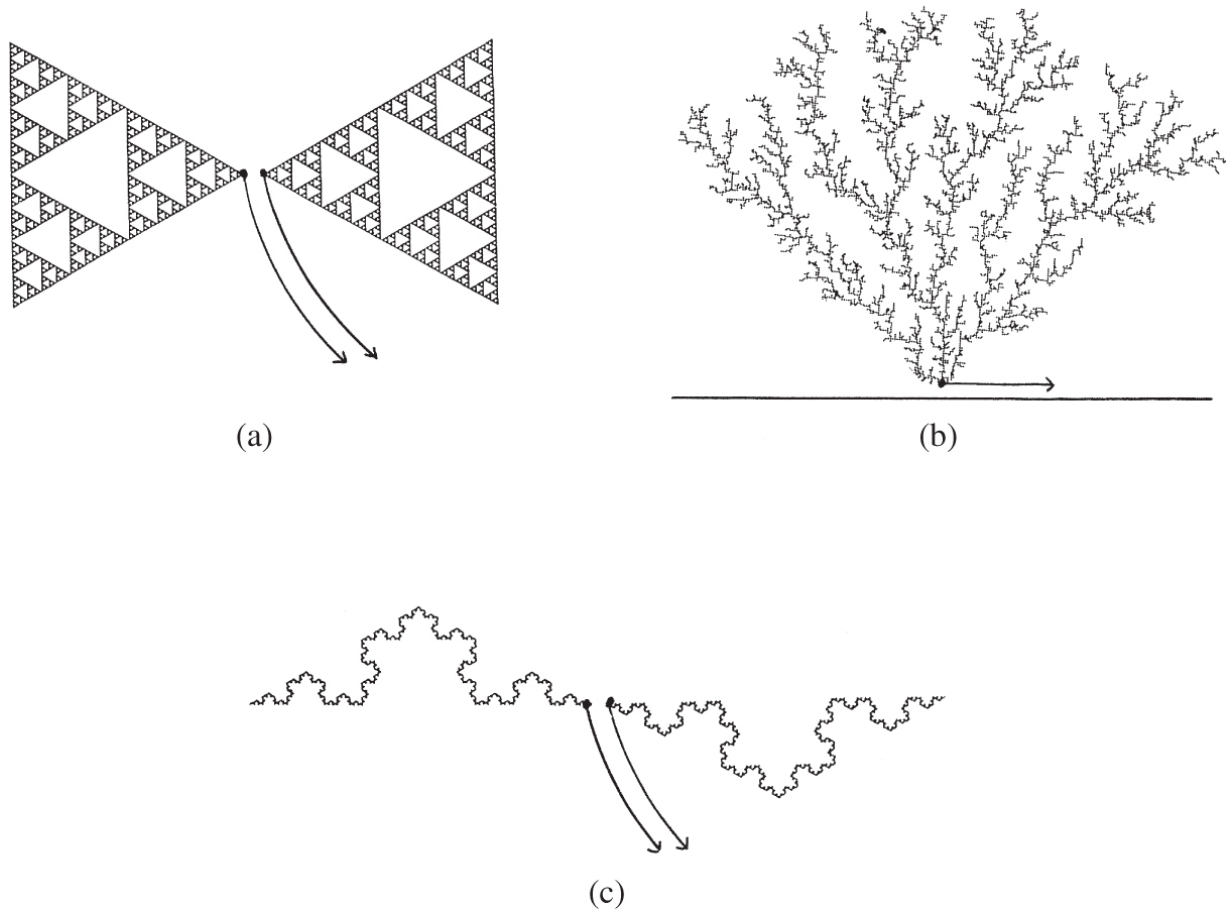


Figure 18.4 Fractal antennas showing feed lines. (a) Sierpiński dipole, (b) random tree antenna and (c) von Koch dipole.

Random fractals can be used to construct antennas suitable for a continuous range of frequencies. For example, tree antennas, which are statistical self-similar at all scales (such as those generated by electrochemical deposition of the form of [Figure 18.3](#)), give a relatively constant response across a range of frequencies. These compare well with traditional antennas designed for a continuous frequency band.

18.5 Fractals in finance

Examination of graphs of share prices, exchange rates, and so on, suggests some sort of self-affine scaling, that is, for a number $0 < \alpha < 1$, if $X(t)$ is the share price at time t , then the increment

$X(\gamma t) - X(\gamma t_0)$ has similar overall form to the increment $\gamma^\alpha(X(t) - X(t_0))$ for a range of $t > t_0$ and $\gamma > 0$. This suggests that a statistically self-affine process or even a deterministic self-affine function might be appropriate for modelling prices. Moreover, the self-affinity assumption has many consequences for features of the process modelled.

Because of its central place in stochastic processes, Brownian motion (see Section 16.1) is the most natural statistically self-affine model to try. Together with its variants, it is the basis for many financial models.

Let X be Brownian motion on $[0, \infty)$; we might think of a realisation of $X(t)$ as the price, or perhaps the logarithm of the price, of some stock at time t . A crucial feature of Brownian motion is the martingale or independent increment property: given the process up to time t , the expected value of $X(t+h)$ is just $X(t)$, for all $h > 0$, reflecting that the future value of the stock is unpredictable, with a profit as likely as a loss.

If we now take X to be index- α fractional Brownian motion (Section 16.3), the increments are no longer independent but are correlated, that is, $E((X(t) - X(0))(X(t+h) - X(t))) > 0$ or < 0 , according to whether $\alpha > \frac{1}{2}$ or $\alpha < \frac{1}{2}$. Moreover, if $\alpha > \frac{1}{2}$, the process has *long range dependence*, that is, for fixed small h , the covariances of the increments

$$\begin{aligned} E((X(h) - X(0))(X(t+h) - X(t))) &= \frac{1}{2}[(t+h)^{2\alpha} + (t-h)^{2\alpha} - 2t^{2\alpha}] \\ &\simeq \alpha(2\alpha-1)t^{2\alpha-2}h^2 \end{aligned}$$

decrease slowly with t in the sense that

$\sum_{k=0}^{\infty} E((X(h) - X(0))(X(k+h) - X(k))) \sim \sum_{k=0}^{\infty} k^{2\alpha-2}$ diverges. An interpretation might be that if, for some $\alpha > \frac{1}{2}$, index- α fractional Brownian motion provides a reasonable model of prices, then we may make inference on the future behaviour of share prices by studying past variations.

Many further variants are possible, for example, taking $cX(t) + at$ where X is index- α fractional Brownian motion and a and c are positive constants adds a ‘drift’ to the process, with an underlying upward trend of rate a . Statistical methods may be used to estimate values of α, a and c that fit most closely observed financial data over a period.

At first sight, realisations of Brownian motion appear qualitatively similar to share prices or exchange rates, but a more careful examination shows marked differences (see [Figure 18.5a](#) and c). Brownian motion does not exhibit the sudden jumps and periods of intense activity, or ‘volatility’, observed in prices. This is exemplified by considering increments: for fixed small $h > 0$, the increment $X(t+h) - X(t)$ regarded as a function of t appears as a ‘noise’ of fairly constant amplitude if X is Brownian motion ([Figure 18.6a](#)), whereas for stock prices, it has very marked sharp peaks and dips rising above the ambient noise level, corresponding to price jumps ([Figure 18.6c](#)).

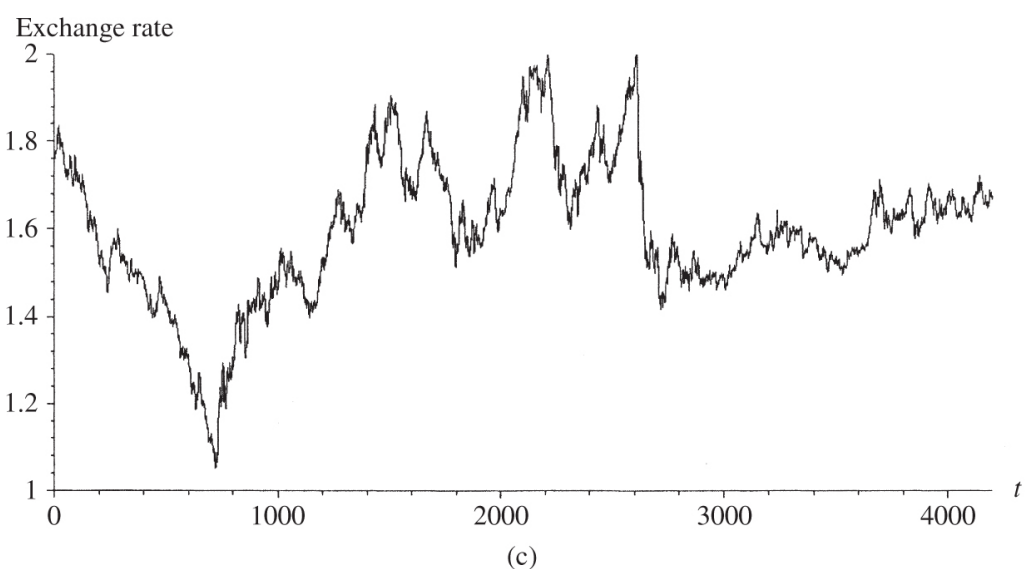
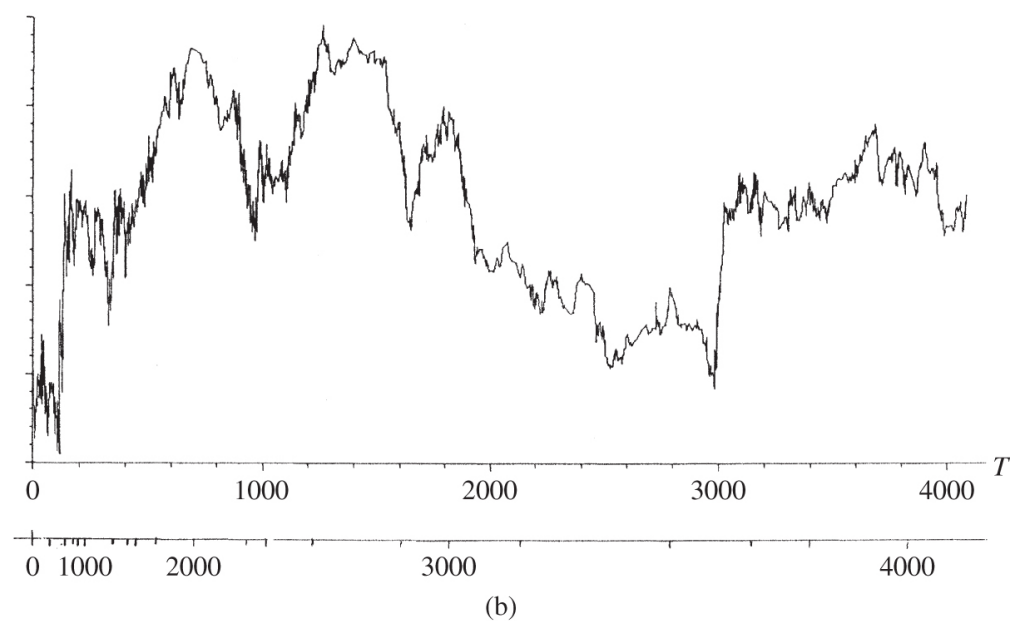
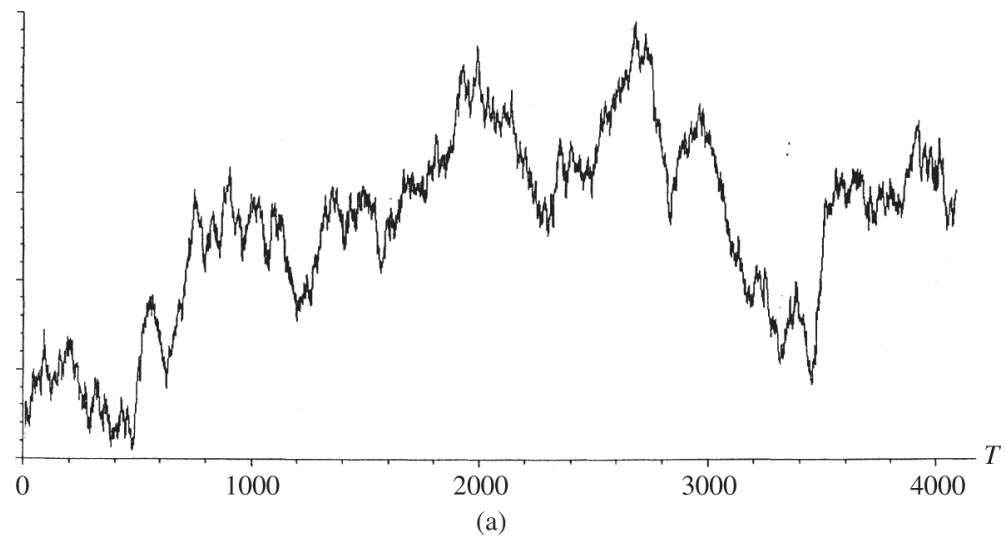
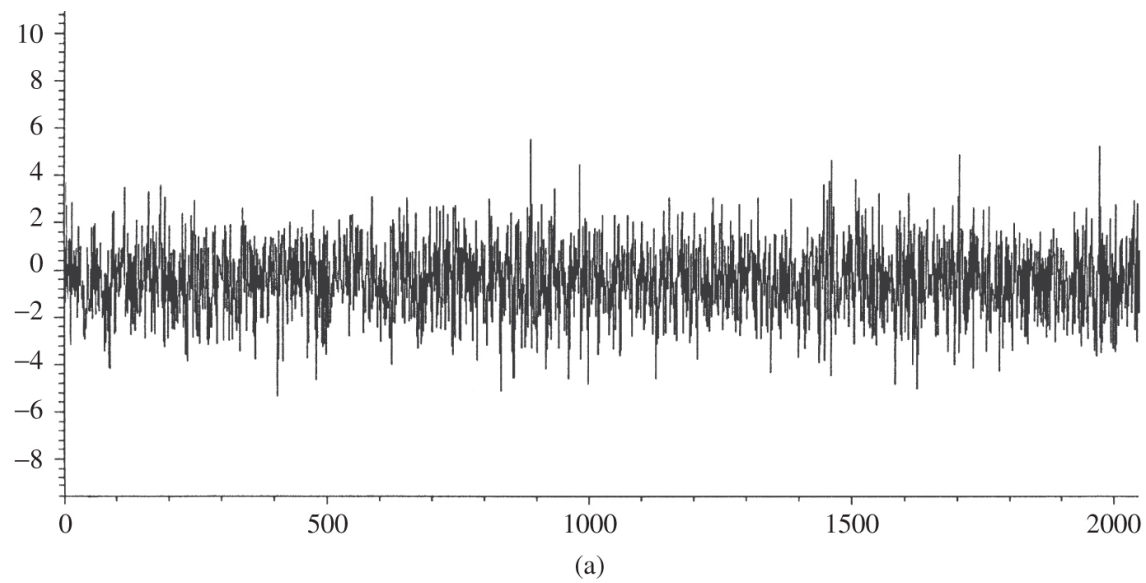
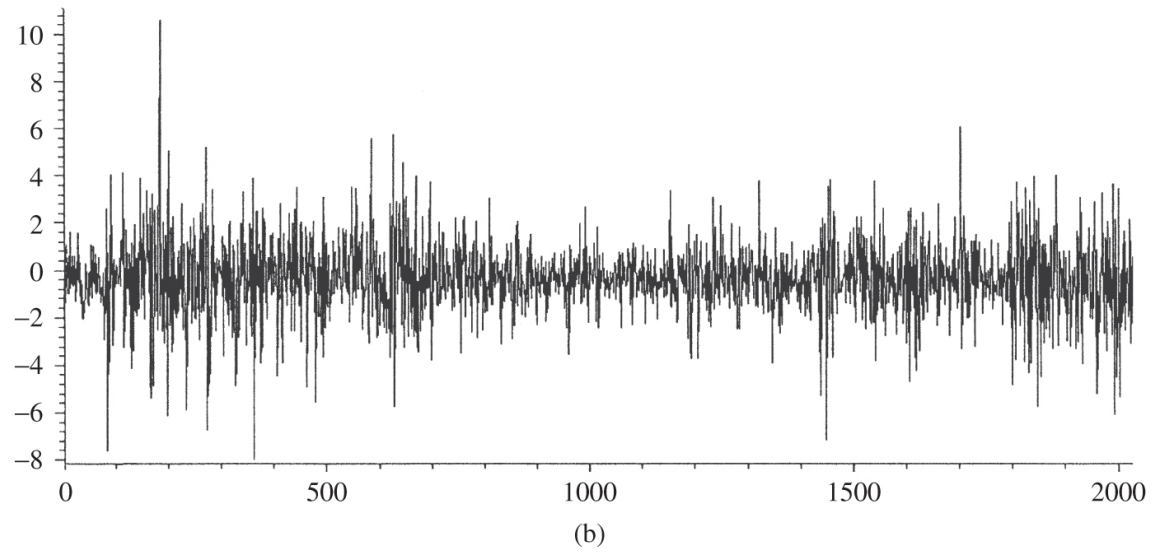


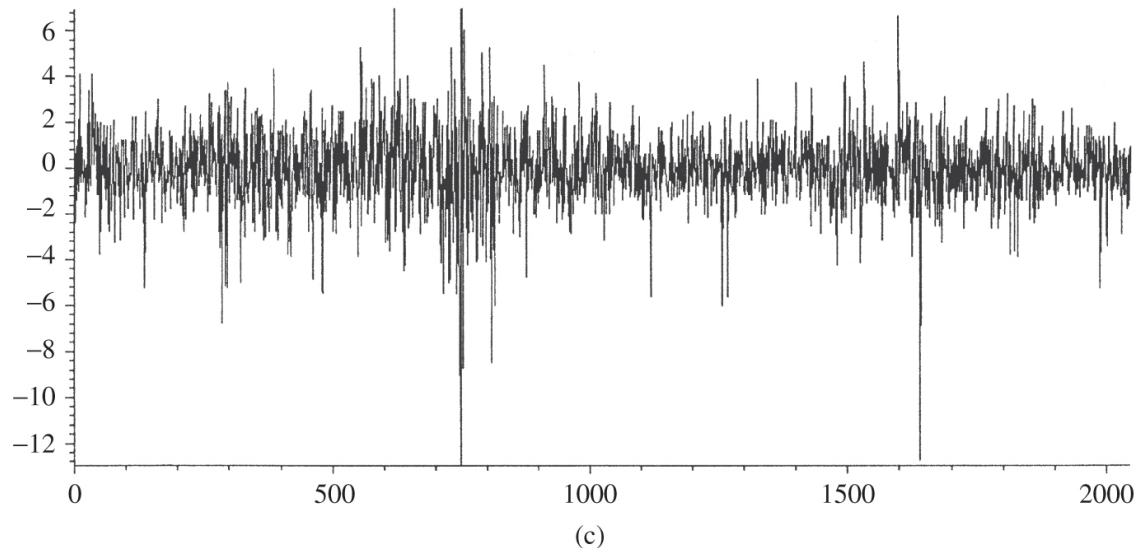
Figure 18.5 (a) A realisation of Brownian motion; (b) the same realisation with respect to ‘trading time’ T , given by a multifractal ‘warp’ of real time t ; (c) daily dollar/pound exchange rates over 11 years. The combination of periods of low volatility interspersed with periods of high activity is more reminiscent of (b) than that of (a).



(a)



(b)



(c)

Figure 18.6 (a) Increments of Brownian motion; (b) increments of Brownian motion ‘warped’ by multifractal time; (c) real data: increments of a stock price over period of $5\frac{1}{2}$ years. The character of (c) is closer to (b) than to (a).

One way this might arise is if X has a multifractal structure as a function, that is, with a relatively small set of times t where the local fluctuations are exceptionally large. This may be made precise in terms of the dimensions of the sets

$$E_a = \left\{ t : \lim_{h \rightarrow 0} \frac{\log |X(t+h) - X(t)|}{\log |h|} = a \right\};$$

thus, E_a comprises those t at which the Hölder exponent of X is a , an analogue of (17.16) for functions. There are several ways of modelling these more extreme fluctuations. A self-affine curve (Section 1.1) with a ‘generator’ that has several different gradients, has fluctuating Hölder exponents and can yield graphs with many of the features of share prices.

A more sophisticated approach uses *multifractal time*. The underlying idea is that prices follow Brownian or fractional Brownian motion, but with respect to rescaled or ‘warped’ time called *trading time* $T(t)$. Thus, when the market is volatile a short period in real time t is stretched to a long period of trading time T , whilst at inactive periods, a long t period corresponds to a short T period ([Figures 18.5b](#) and [18.6b](#)).

Let μ be a measure on \mathbb{R}^+ , typically a multifractal measure. For $t \geq 0$, we define the trading time $T(t) = \mu[0, t] = \int_0^t d\mu$. Writing B^α for index- α Brownian motion, we set $X(t) = B^\alpha(T(t))$. Given T , then $X(t)$ is a zero mean Gaussian process with variance of increments given by

$$\begin{aligned} \mathbb{E}(X(t+h) - X(t))^2 &= \mathbb{E}(B^\alpha(T(t+h)) - B^\alpha(T(t)))^2 \\ &= |T(t+h) - T(t)|^{2\alpha} = \mu[t, t+h]^{2\alpha} \sim |h|^{2\gamma\alpha} \end{aligned} \tag{18.14}$$

if $t \in F_\gamma$, where

$$F_\gamma = \left\{ t : \lim_{h \rightarrow 0} \frac{\log \mu[t, t+h]}{\log h} = \gamma \right\}$$

is the set of times where μ has a local dimension γ . Thus, the volatility of x at t depends on the local dimension of μ at t , and so the distribution of times of high and low activity in the share prices depends on the multifractal structure of μ . If we develop the model to make μ a random multifractal measure, the trading time T becomes a random process, so that the times of high and low activity are random.

Statistical methods may be applied to real price data to estimate α and the multifractal spectrum required for μ , which may be related to the ‘multifractal spectrum of x ’ given by $\dim_H E_\alpha$.

Fractality is a crucial feature in mathematical modelling of finance. Here, we have just indicated some of the simplest models; more sophisticated techniques include describing financial activity by stochastic differential equations, which may have solutions of a fractal form.

18.6 Notes and references

The literature on applications of fractals is enormous. Amongst the books with an emphasis on applications are those by Feder (1988); Takayasu (1990); Hastings and Sugihara (1993); Crilly, Earnshaw and Jones (2011); Gouyet (1996) and Meakin (2011). General conference proceedings include those edited by Pietronero and Tosatti (1986); Pietronero (1989); Aharony and Feder (1990); Fleischmann, Tildesley and Ball (1992), as well the proceedings of a series of interdisciplinary conferences edited by Peitgen, Henriquez and Pendo (1991); Novak (1994, 1995, 1998, 2000, 2002, 2004, 2006) and Novak and Dewey (1997).

For fractal growth and DLA, refer to Stanley and Ostrowsky (1988); Feder (1988); Vicsek (1991); Meakin (2011) and ben-Avraham and Havlin (2005). Surface growth is discussed by Barabási and Stanely (1995).

For an introduction to the ideas of turbulence, see Manneville (2010). The homogeneous model of Kolmogorov (1941) was adapted to the fractally homogeneous model by Mandelbrot (1974); see also Frisch (1995). The survey by Sreenivasan (1991) and the collection of papers by Temam (1976) cover fractal aspects of turbulence. The books by Temam (1983, 2012) discuss the dimension of sets related to solutions of the Navier–Stokes and other differential equations.

There are papers on fractal antennas by Hohlfeld and Cohen (1999); Jaggard (2011) and Puente et al. (2011).

There is considerable interest in setting up and solving partial differential equations such as the heat equation on fractal domains. The books by Kigami (2001) and Strichartz (2006) provide good entries into this area.

Fractals in finance are covered in the books by Peters (1994); Mandelbrot and Hudson (2008) and Kobeissi (2012) and in Mandelbrot's (1997) 'Selecta' and the many references therein. Multifractal time is presented in Mandelbrot (1997) and Riedi (2002).

Many books have been written about applications of fractals beyond those outlined in this chapter. For geosciences, see Scholz and Mandelbrot (1989); Turcotte (1997) and Dimri (2005); for fractal river basins, see Rodríguez-Iturbe and Rinaldo (2001) and for applications to rainfall, see Lovejoy and Schertzer (2013).

Applications to chemistry are given in Rothschild (1998), to astronomy in Heck and Perdang (1991), to internet traffic in Feldmann, Gilbert and Willinger (1998) and to music in Madden (2007). Molecular biophysics is treated in Dewey (1997), biology in Iannaccone and Khokha (1996) and Prusinkiewicz and Kaandorp (2012), physiology and medicine in West (2013) and ecology in Seuront (2009).

Many applications to engineering are presented in the proceedings edited by Lévy Véhel and Lutton (2010); Lévy Véhel, Lutton and Tricot (2011) and Dekking *et al.* (2011).

Exercises

18.1 Suppose that the DLA square-lattice model is run for a large number of very small squares. Suppose that the set obtained is an approximate fractal of dimension s . What power law would you expect the number of shaded squares within distance r of the initial square to obey? Assuming that during the process squares tend to be added to parts of the set further away from the initial square, how would you expect the ‘radius’ of the growth after k squares have been added to depend on k ?

18.2 Let $m(t)$ be the mass of copper that has been deposited and $r(t)$ be the ‘radius’ of the copper deposit after time t in the electrolysis experiment described in Section 18.1. It may be shown that the current flowing, and thus, by Faraday’s law, the rate of mass deposition, is proportional to $r(t)$. On the assumption that the growth forms an approximate fractal of dimension s , so that $m(t) \sim cr(t)^s$, give an argument to suggest that $r(t) \sim c_1 t^{1/(s-1)}$.

18.3 Verify that $u(x, t)$ in the DLA model satisfies the partial differential equation (18.1).

18.4 Verify that the potential in (18.9) satisfies Poisson’s equation if, say, f is a twice continuously differentiable function with $f(x) = 0$ for all sufficiently large x .

18.5 Show that if $f(x) = 0$ for all sufficiently large x and $\int |f(x)|^2 dx < \infty$, then the singularity set of ϕ , given by (18.9), is empty.

18.6 Show that the argument leading to (18.12) can be adapted to the case when, say, D is the unit cube in \mathbb{R}^3 and F is the product of the Cantor dust of Figure 0.4 and a unit line segment L .
(Dissipation is assumed to occur on the set $E_k \times L$, where E_k is the k th stage in the construction of the Cantor dust for some large k .)

18.7 For a fractal antenna made from a wire in the shape of a von Koch curve, if the fundamental frequency is ω , what are the higher resonant frequencies?

18.8 Generalise (18.14) to show that $E(|X(t+h) - X(t)|^q) \sim |h|^{q\gamma}$ for $t \in F_\gamma$ (see Exercise 16.7).

References

- Abenda S., Moussa P. and Osbaldestin A. H. (1999) Multifractal dimensions and thermodynamical description of nearly-circular Julia sets, *Nonlinearity*, **12**, 19–40.
- Abry P., Gonçalves P. and Lévy Véhel J. (Eds.) (2009) *Digital Signal and Image Processing Series*, John Wiley & Sons, Inc., Hoboken, NJ.
- Addison P. S. (1997) *Fractals and Chaos—An Illustrated Course*, Taylor & Francis, Abingdon.
- Adler R. J. (2009) *The Geometry of Random Fields*, Society for Industrial and Applied Mathematics, Philadelphia, PA.
- Aharony A. and Feder J. (1990) *Fractals in Physics*, North-Holland, Amsterdam.
- Al-Akaidi M. (2004) *Fractal Speech Processing*, Cambridge University Press, Cambridge.
- Alexander R. J. (2011) *Early Days in Complex Dynamics: A History of Complex Dynamics in One Variable During 1906–1942*, American Mathematical Society, Providence, RI.
- Anderson R. D. and Klee V. L. (1952) Convex functions and upper semi-continuous functions, *Duke Math. J.*, **19**, 349–357.
- Apostol T. M. (1974) *Mathematical Analysis*, 2nd ed., Addison-Wesley, Reading, MA.
- Ayache A., Cohen S. and Lévy Véhel J. (2000) The covariance structure of multifractional Brownian motion, with application to long range dependence, in ICASSP, June 2000.
- Ayache A. and Lévy Véhel J. (1999) Generalized multifractional Brownian motion: Definition and preliminary results. in *Fractals: Theory and Applications in Engineering*, 17–32. Springer, London.
- Ayache A., Shieh N.-R. and Xiao Y. (2011) Multiparameter multifractional Brownian motion: Local nondeterminism and joint continuity of the local times, *Ann. Inst. H. Poincar Probab. Statist.*, **47**, 1029–1054.

- BakerA. (2012) *A Comprehensive Course in Number Theory*, Cambridge University Press, Cambridge.
- Baker A. and Schmidt W. M. (1970) Diophantine approximation and Hausdorff dimension, *Proc. Lond. Math. Soc.* (3), **21**, 1–11.
- Bandt C., Graf S. and Zähle M. (Eds.) (1995) *Fractal Geometry and Stochastics. Progress in Probability*, **37**, Birkhauser, Basel.
- Bandt C., Graf S. and Zähle M. (Eds.) (2000) *Fractal Geometry and Stochastics, II. Progress in Probability*, **46**, Birkhauser, Basel.
- Bandt C., Mörters S. and Zähle M. (Eds.) (2009) *Fractal Geometry and Stochastics, IV Progress in Probability*, **61**, Birkhauser, Basel.
- Bandt C., Mosco S. and Zähle M. (Eds.) (2004) *Fractal Geometry and Stochastics, III. Progress in Probability*, **57**, Birkhauser, Basel.
- Barabási A.-L. and Stanley H. E. (1995) *Fractal Concepts in Surface Growth*, Cambridge University Press, Cambridge.
- Barnsley M. F. (2006) *Superfractals*, Cambridge University Press, Cambridge.
- Barnsley M. F. (2012) *Fractals Everywhere*, 3rd ed., Dover Publications, New York.
- Barnsley M. F. and Hurd L. P. (1993) *Fractal Image Compression*, A. K. Peters, Wellesley, MA.
- Barnsley M. F., Hutchinson J. E. and Stenflo Ö. (2008) V-variable fractals: Fractals with partial self similarity, *Adv. Math.*, **218**, 2051–2088.
- Barral J. and Feng D.-J. (2013) Multifractal formalism for almost all self-affine measures, *Commun. Math. Phys.*, **318**, 473–504.
- Barral J. and Seuret S. (Eds.) (2010) *Recent Developments in Fractals and Related Fields*, Birkhauser, Basel.
- Barral J. and Seuret S. (Eds.) (2013) *Further Developments in Fractals and Related Fields*, Birkhauser, Basel.
- Barreira L. (2008) *Dimension and Recurrence in Hyperbolic Dynamics*, Springer, New York.
- Barreira L. (2011) *Thermodynamic Formalism and Applications to Dimension Theory*, Springer, New York.
- Barreira L. (2012) *Ergodic Theory, Hyperbolic Dynamics and Dimension Theory*, Springer, New York.

- Barreira L., Pesin Y. and Schmeling J. (1999) Dimension and product structure of hyperbolic measures, *Ann. Math.*, **149**, 755–783.
- Barreira L. and Valls C. (2012) *Dynamical Systems: An Introduction*, Springer, New York.
- Bartholdi L., Grigorchuk R. and Nekrashevych V. (2002) From fractal groups to fractal sets. in *Fractals in Graz 2001*, 25–118, Birkhäuser, Basel.
- Baumann G. (2005) *Mathematica for Theoretical Physics: Electrodynamics, Quantum Mechanics, General Relativity, and Fractals*, 2nd ed., Springer, New York.
- Beardon A. F. (1965) On the Hausdorff dimension of general Cantor sets, *Proc. Camb. Philos. Soc.*, **61**, 679–694.
- Beardon A. F. (2000) *Iteration of Rational Functions*, Springer, New York.
- Bedford T. J. (1989) The box dimension of self-affine graphs and repellers, *Nonlinearity*, **2**, 53–71.
- Bedford T. J. and Swift J. (Eds.) (1988) *New Directions in Dynamical Systems*, Cambridge University Press, Cambridge.
- ben-Avraham D. and Havlin S. (2005) *Diffusion and Reactions in Fractals and Disordered Systems*, pbk., Cambridge University Press, Cambridge.
- Bernik V. I. and Dodson M. M. (2000) *Metric Diophantine Approximation on Manifolds*, Cambridge University Press, Cambridge.
- Berry M. V. and Lewis Z. V. (1980) On the Weierstrass–Mandelbrot fractal function, *Proc. R. Soc. Lond., A*, **370**, 459–484.
- Bertoin J. (1996) *Lévy Processes*, Cambridge University Press, Cambridge.
- Besicovitch A. S. (1928) On the fundamental geometrical properties of linearly measurable plane sets of points, *Math. Ann.*, **98**, 422–464.
- Besicovitch A. S. (1934) Sets of fractional dimensions IV: On rational approximation to real numbers, *J. Lond. Math. Soc.*, **9**, 126–131.

- Besicovitch A. S. (1938) On the fundamental geometric properties of linearly measurable plane sets of points II, *Math. Ann.*, **115**, 296–329.
- Besicovitch A. S. (1939) On the fundamental geometric properties of linearly measurable plane sets of points III, *Math. Ann.*, **116**, 349–357.
- Besicovitch A. S. (1952) On existence of subsets of finite measure of sets of infinite measure, *Indag. Math.*, **14**, 339–344.
- Besicovitch A. S. (1963) The Kakeya problem, *Am. Math. Monthly*, **70**, 697–706.
- Besicovitch A. S. (1964) On fundamental geometric properties of plane line sets, *J. Lond. Math. Soc.*, **39**, 441–448.
- Besicovitch A. S. and Moran P. A. P. (1945) The measure of product and cylinder sets, *J. Lond. Math. Soc.*, **20**, 110–120.
- Besicovitch A. S. and Taylor S. J. (1954) On the complementary intervals of a linear closed set of zero Lebesgue measure, *J. Lond. Math. Soc.*, **29**, 449–459.
- Besicovitch A. S. and Ursell H. D. (1937) Sets of fractional dimensions, V: On dimensional numbers of some continuous curves, *J. Lond. Math. Soc.*, **12**, 18–25.
- Biagini F., Hu Y., Øksendal B. and Zhang T. (2008) *Stochastic Calculus for Fractional Brownian Motion and Applications*, Springer-Verlag, New York.
- Billingsley P. (1978) *Ergodic Theory and Information*, Krieger, New York.
- Billingsley P. (2012) *Probability and Measure*, Anniversary ed., John Wiley & Sons, Inc., New York.
- Blanchard P. (1984) Complex analytic dynamics on the Riemann sphere, *Bull. Am. Math. Soc.*, **11**, 85–141.
- Bollobás B. and Riordan O. (2006) *Percolation*, Cambridge University Press, Cambridge.
- Bouligand G. (1928) Ensembles impropre et nombre dimensionnel, *Bull. Sci. Math.*, **II-52**, 320–334, 361–376.
- Brin M. and Stuck G. (2002) *Introduction to Dynamical Systems*, Cambridge University Press, Cambridge.

- Brolin H. (1965) Invariant sets under iteration of rational functions, *Ark. Math.*, **6**, 103–144.
- Broman E. I., van de Brug T., Camia F., Joosten M. and Meester R. (2012) Fat fractal percolation and k -fractal percolation, *Lat. Am. J. Probab. Math. Stat.*, **9**, 279–301.
- Brooks R. and Matelski J. P. (1981) The dynamics of 2-generator subgroups of $\text{PSL}(2, \mathbb{C})$. in *Riemann Surfaces and Related Topics: Proceedings of the 1978 Stony Brook Conference*, 65–71, Princeton University Press, Princeton, NJ.
- Brown G., Michon G. and Peyrière J. (1992) On the multifractal analysis of measures, *J. Stat. Phys.*, **66**, 775–790.
- Bugeaud Y. (2012) *Distribution Modulo One and Diophantine Approximation*, Cambridge University Press, Cambridge.
- Bugeaud Y. (2013) Hausdorff dimension and Diophantine approximation. in *Further Developments in Fractals and Related Fields*, 35–45, Birkhauser, Basel.
- Bugeaud Y., Dal'bo F. and Druțu C. (2009) *Dynamical Systems and Diophantine Approximation*, Séminaires et Congrès, **19**, Société Mathématique de France, Paris.
- Capinski M. and Kopp T. W. (2007) *Measure, Integral and Probability*, 2nd ed., Springer-Verlag, New York.
- Carathéodory C. (1914) *Über das lineare Mass von Punktmengen – eine Verallgemeinerung des Längenbegriffs*, Nach. Ges. Wiss. Göttingen, 406–426.
- Carleson A. (1998) *Selected Problems on Exceptional Sets*, Van Nostrand, Princeton, NJ.
- Carleson L. and Gamelin T. W. (1996) *Complex Dynamics*, Springer-Verlag, New York.
- Cawley R. and Mauldin R. D. (1992) Multifractal decomposition of Moran fractals, *Adv. Math.*, **92**, 196–236.
- Chayes L. (1995) Aspects of the fractal percolation process, in *Fractal Geometry and Stochastics, Progress in Probability*, **37**, 113–143. Birkhauser, Basel.
- Chayes J. T., Chayes L. and Durrett R. (1988) Connectivity of Mandelbrot's percolation process, *Probab. Theor. Related Fields*, **77**, 307–324.

- Collet P., Dobbertin R. and Moussa P. (1992) Multifractal analysis of nearly circular Julia set and thermodynamical formalism, *Ann. Inst. H. Poincaré Phys. Théor.*, **56**, 91–122.
- Crilly A. J., Earnshaw R. A. and Jones H. (Eds.) (2011) *Fractals and Chaos*, pbk., Springer-Verlag, Berlin.
- Csörnyei M. (2001) On planar sets with prescribed packing dimensions of line sections, *Math. Proc. Cambridge Philos. Soc.*, **130**, 523–539.
- Cunningham F. (1974) Three Kakeya problems, *Am. Math. Monthly*, **81**, 589–592.
- Curry J., Garnett L. and Sullivan D. (1983) On the iteration of rational functions: Computer experiments with Newton's method, *Commun. Math. Phys.*, **91**, 267–277.
- Cutler C. D. (1995) Strong and weak duality principles for fractal dimension in Euclidean space, *Math. Proc. Cambridge Philos. Soc.*, **118**, 393–410.
- Cvitanović P. (Ed.) (1989) *Universality in Chaos*, 2nd ed., Adam Hilger, Bristol.
- Dalla L. and Larman D. G. (1980) Convex bodies with almost all k -dimensional sections polytopes, *Math. Proc. Camb. Philos. Soc.*, **88**, 395–401.
- David G. (1999) Analytic capacity, Caldern-Zygmund operators, and rectifiability, *Publ. Mat.* **43**, 3–25.
- David G. and Semmes S. (1997) *Fractured Fractals and Broken Dreams: Self-similar Geometry through Metric and Measure*, Clarendon Press, Oxford.
- Davies R. O. (1952) On accessibility of plane sets and differentiation of functions of two real variables, *Proc. Camb. Philos. Soc.*, **48**, 215–232.
- Dekking F., Lévy Véhel J., Lutton E. and Tricot C. (Eds.) (2011) *Fractals: Theory and Applications in Engineering*, pbk., Springer-Verlag, London.
- Dekking F. M. and Meester R. W. J. (1990) On the structure of Mandelbrot's percolation process and other random Cantor sets, *J. Stat. Phys.* **58**, 1109–1126.

- Devaney R. L. (1995) *Complex Dynamical Systems: The Mathematics Behind the Mandelbrot and Julia Sets*, American Mathematical Society, Providence, RI.
- Devaney R. L. (2003) *Introduction to Chaotic Dynamic Systems*, Westview Press, Boulder, CO.
- Devaney R. L. and Keen L. (2006) *Complex Dynamics: Twenty-Five Years After the Appearance of the Mandelbrot Set*, American Mathematical Society, Providence, RI.
- Dewey T. G. (1997) *Fractals in Molecular Biophysics*, Oxford University Press, New York.
- Dimri T. G. (2005) *Fractal Behaviour of the Earth System*, Springer, New York.
- Dodson M. M., Rynne B. P. and Vickers J. A. G. (1990) Diophantine approximation and a lower bound for Hausdorff dimension, *Mathematika*, **37**, 59–73.
- Dudziak J. (2010) *Vitushkin's Conjecture for Removable Sets*, Springer, New York.
- Edgar G. A. (1993) *Classics on Fractals*, Addison-Wesley, Menlo Park, CA.
- Edgar G. A. (1998) *Integral, Probability, and Fractal Measures*, Springer-Verlag, New York.
- Edgar G. A. (2008) *Measure, Topology, and Fractal Geometry*, Springer, New York.
- Edgar G. A. and Mauldin R. D. (1992) Multifractal decompositions of digraph recursive fractals. *Proc. Lond. Math. Soc.* (3), **65**, 604–628.
- Edgar G. A. and Miller C. (2003) Borel subrings of the reals, *Proc. Am. Math. Soc.*, **131**, 1121–1129.
- Eggleston H. G. (1952) Sets of fractional dimension which occur in some problems of number theory, *Proc. Lond. Math. Soc.* (2), **54**, 42–93.
- Ellenberg J. S., Oberlin R. F. and Tao T. (2010) The Kakeya set and maximal conjectures for algebraic varieties over finite fields, *Mathematika*, **56**, 1–25.
- Embrechts P. and Maejima M. (2002) *Selfsimilar Processes*, Princeton University Press, Princeton, NJ.

- Erdoğan M. B. (2006) On Falconer's distance set conjecture, *Rev. Mat. Iberoamericana*, **22**, 649–662.
- Erdős P. and Volkmann B. (1966) Additive Gruppen mit vorgegebener Hausdorffscher Dimension, *J. Reine Rngew. Math.*, **221**, 203–208.
- Evertsz C. J. G. and Mandelbrot B. B. (1992) Multifractal measures. Appendix B. in *Chaos and Fractals* (Peitgen H.-O., Jürgens H. and Saupe D.), Springer-Verlag, New York.
- Evertsz C. J. G., Peitgen H.-O. and Voss R. F. (Eds.) (1995) *Fractal Geometry and Analysis: Papers from the Symposium in Honor of Benoit Mandelbrot*, World Scientific, River Edge, NJ.
- Falconer K. J. (1982) Hausdorff dimension and the exceptional set of projections, *Mathematika*, **29**, 109–115.
- Falconer K. J. (1985a) *The Geometry of Fractal Sets*, Cambridge University Press, Cambridge.
- Falconer K. J. (1985b) Classes of sets with large intersection, *Mathematika*, **32**, 191–205.
- Falconer K. J. (1985c) The Hausdorff dimension of distance sets, *Mathematika*, **32**, 206–212.
- Falconer K. J. (1986a) Sets with prescribed projections and Nikodym sets, *Proc. Lond. Math. Soc.* (3), **53**, 48–64.
- Falconer K. J. (1986b) Random fractals, *Math. Proc. Camb. Philos. Soc.*, **100**, 559–582.
- Falconer K. J. (1988) The Hausdorff dimension of self-affine fractals, *Math. Proc. Camb. Philos. Soc.*, **103**, 339–350.
- Falconer K. J. (1994) Sets with large intersection properties. *J. Lond. Math. Soc.* 2, **49**, 267–280.
- Falconer K. J. (1997) *Techniques in Fractal Geometry*, John Wiley & Sons, Ltd, Chichester.
- Falconer K. J. (2010) Generalised dimensions of measures on almost self-affine sets. *Nonlinearity*, **23**, 1047–1069.
- Falconer K. J. (2013) *Fractals—A Very Short Introduction*, Oxford University Press, Oxford.
- Falconer K. J. (2013) Dimensions of self-affine sets: A Survey. in *Further Developments in Fractals and Related Fields*, 115–133, Birkhauser, Basel.

- Falconer K. J. and Howroyd J. D. (1997) Packing dimensions of projections and dimension profiles, *Math. Proc. Camb. Philos. Soc.*, **121**, 269–286.
- Falconer K. J., Järvenpää M. and Mattila P. (1999) Examples illustrating the instability of packing dimensions of sections, *Real Anal. Exchange*, **25**, 629–640.
- Falconer K. J. and Lévy Véhel J. (2000) Horizons of fractional Brownian surfaces. *Proc. R. Soc. Lond. A*, **456**, 2153–2178.
- Falconer K. J. and Lévy Véhel J. (2009) Multifractional, multistable, and other processes with prescribed local form. *J. Theoret. Probab.*, **22**, 375–401.
- Falconer K. J. and Marsh D. T. (1989) Classification of quasi-circles by Hausdorff dimension, *Nonlinearity*, **2**, 489–493.
- Falconer K. J. and O’Neil T. C. (1996) Vector-valued multifractal measures, *Proc. R. Soc. Lond. A*, **452**, 1–26.
- Farag H. (2002) On the $\frac{1}{2}$ -problem of Besicovitch: Quasi-arcs do not contain sharp saw-teeth, *Rev. Mat. Iberoamericana*, **18**, 17–40.
- Fatou P. (1919) Sur les équations fonctionnelles, *Bull. Soc. Math. France*, **47**, 161–271.
- Feder J. (1988) *Fractals*, Plenum Press, New York.
- Federer H. (1947) The (φ, k) rectifiable subsets of n -space, *Trans. Am. Math. Soc.*, **62**, 114–192.
- Federer H. (1996) *Geometric Measure Theory*, Springer, New York.
- Feldmann A., Gilbert A. C. and Willinger W. (1998) Data networks as cascades: Investigating the multifractal nature of Internet WAN traffic. in *Proceedings ACM/SIGCOMM ’98, Vancouver, BC*, 25–38, ACM, New York.
- Fisher G. (2011) *Fractal Image Compression: Theory and Applications*, pbk., Springer-Verlag, New York.
- Fleischmann M., Tildesley D. J. and Ball R. C. (Eds.) (1992) *Fractals in the Natural Sciences*, Princeton University Press, Princeton, NJ.
- Frame M. L. and Mandelbrot B. B. (2002) *Fractals, Graphics and Mathematical Education*, Mathematical Association of America, Washington, DC.

- Frederickson P., Kaplan J., Yorke E. and Yorke J. (1983) The Lyapunov dimension of strange attractors, *J. Differ. Equations*, **49**, 185–207.
- Frisch U. (1995) *Turbulence: The Legacy of A. N. Kolmogorov*, Cambridge University Press, Cambridge.
- Frisch U. and Parisi G. (1985) Fully developed turbulence and intermittency. in *Turbulence and Predictability of Geophysical Flows and Climate Dynamics* (Ghil M., Benzi R. and Parisi G. Eds.), 84–88, North-Holland, Amsterdam.
- Frostman O. (1935) Potential d'équilibre et capacité des ensembles avec quelques applications à la théorie des fonctions, *Meddel. Lunds Univ. Math. Sem.*, **3**, 1–118.
- Furstenberg H. (2008) Ergodic fractal measures and dimension conservation, *Ergodic Theory Dynam. Syst.*, **28**, 405–422.
- Gouyet J.-F. (1996) *Physics and Fractal Structures*, Springer-Verlag, New York.
- Grabner P. and Woess W. (Eds.) (2003) *Fractals in Graz 2001*, Birkhauser, Basel.
- Graf S. (1987) Statistically self-similar fractals, *Prob. Theor. Related Fields*, **74**, 357–392.
- Graf S., Mauldin R. D. and Williams S. C. (1988) The exact Hausdorff dimension in random recursive constructions, *Mem. Am. Math. Soc.*, no. 381, **71**, 1–121.
- Grimmett G. R. (2010) *Percolation*, 2nd ed. pbk., Springer, New York.
- Grimmett G. R. and Stirzaker D. R. (2001) *Probability and Random Processes*, 3rd ed., Oxford University Press, Oxford.
- Gruber P. M. (2007) *Convex and Discrete Geometry*, Springer, New York.
- Guckenheimer J. and Holmes P. (2002) *Nonlinear Oscillations, Dynamical Systems and Bifurcations of Vector Fields*, Springer, New York.
- Hale J. K. and Koçak H. (2011) *Dynamics and Bifurcations*, Springer-Verlag, New York.
- Halsey T. C., Jensen M. H., Kadanoff L. P., Procaccia I. and Shraiman B. I. (1986) Fractal measures and their singularities: The

- characterization of strange sets, *Phys. Rev. A* (3) **33**, 1141–1151.
- Hardy G. H. and Wright E. M. (2008) *An Introduction to the Theory of Numbers*, 6th ed., Cambridge University Press, Cambridge.
- Harte D. (2001) *Multifractals, Theory and Applications*, Chapman & Hall/CRC, Boca Raton, FL.
- Hastings H. M. and Sugihara G. (1993) *Fractals. A User's Guide for the Natural Sciences*, Oxford University Press, New York.
- Hausdorff F. (1919) Dimension und äusseres Mass, *Math. Ann.*, **79**, 157–179.
- Hayman W. K. and Kennedy P. B. (1976) *Subharmonic Functions, Volume 1*, Academic Press, New York.
- Heck A. and Perdang J. M. (Eds.) (1991) *Applying Fractals in Astronomy*, Springer-Verlag, Berlin.
- Hénon M. and Pomeau Y. (1976) Two strange attractors with a simple structure. in *Turbulence and the Navier–Stokes Equations (Lecture Notes in Mathematics, 565)*, (Temam R. Ed.), 29–68, Springer, New York.
- Hensley D. (1996) A polynomial time algorithm for the Hausdorff dimension of continued fraction Cantor sets, *J. Number Theory*, **58**, 9–45.
- Hochman M. and Shmerkin P. (2012) Local entropy averages and projections of fractal measures, *Ann. Math.*, **175**, 1001–1059.
- Hoggar S. G. (1993) *Mathematics for Computer Graphics*, Cambridge University Press, Cambridge.
- Hohlfeld R. G. and Cohen N. (1999) Self-similarity and the geometric requirements for frequency independence in antennae, *Fractals*, **7**, 79–84.
- Howie J. M. (2001) *Real Analysis*, Springer, New York.
- Howroyd J. D. (1996) On Hausdorff and packing dimensions of product spaces, *Math. Proc. Camb. Philos. Soc.*, **119**, 715–727.
- Howroyd J. D. (2001) Box and packing dimensions of projections and dimension profiles, *Math. Proc. Cambridge Philos. Soc.*, **130**, 135–160.
- Hunt B. R. (1998) The Hausdorff dimension of graphs of Weierstrass functions, *Proc. Am. Math. Soc.*, **126**, 791–800.

- Hutchinson J. E. (1981) Fractals and self-similarity, *Indiana Univ. Math. J.*, **30**, 713–747.
- Hutchinson J. E. (2000) Selfsimilar fractals and selfsimilar random fractals. in *Fractal Geometry and Stochastics II*, 109–123, Birkhauser, Basel.
- Hutchinson J. E. and Rüschorf L. (2000) Random fractals and probability metrics, *Adv. Appl. Probab.* **32**, 925–947.
- Iannaccone P. M. and Khokha M. (1996) *Fractal Geometry in Biological Systems*, CRC Press, Baton Rouge, LA.
- Jaffard S. (1997) Multifractal formalism for functions I, II, *SIAM J. Math. Anal.*, **28**, 944–970, 971–998.
- Jaggard D. L. (2011) Fractal electrodynamics: From super antennas to superlattices. in *Fractals in Engineering: From Theory to Industrial Applications*, pbk., 204–221, Springer-Verlag, New York.
- Jarník V. (1931) Über die simultanen diophantischen Approximationen, *Math. Zeit.*, **33**, 505–543.
- Järvenpää E. (2010) Dimensions and porosities. in *Recent Developments in Fractals and Related Fields*, Birkhauser, Basel, 35–43.
- Järvenpää E., Järvenpää M. and Mauldin R. D. (2002) Deterministic and random aspects of porosities, *Discret. Contin. Dyn. Syst.*, **8**, 121–136.
- Jenkinson O. and Pollicott M. (2001) Computing the dimension of dynamically defined sets: E2 and bounded continued fractions, *Ergod. Theory & Dyn. Syst.*, **21**, 511–532.
- Jin X. (2011) The graph and range singularity spectra of b -adic independent cascade functions, *Adv. Math.*, **226**, 4987–5017.
- Jones P. W. and Murai T. (1988) Positive analytic capacity but zero Buffon needle probability, *Pac. J. Math.*, **133**, 99–114.
- Joyce H. and Preiss D. (1995) On the existence of subsets of finite positive packing measure, *Mathematika*, **42**, 15–24.
- Julia G. (1918) Sur l'itération des fonctions rationnelles, *J. Math. Pure Appl.*, Ser. 7, **4**, 47–245.
- Kahane J.-P. (1974) Sur le modèle de turbulence de Benoit Mandelbrot, *C. R. Acad. Sci. Paris*, **278A**, 621–623.

- Kahane J.-P. (1986) Sur la dimensions des intersections. in *Aspects of Mathematics and its Applications* (Barroso J. A. Ed.), 419–430, North-Holland, Amsterdam.
- Kahane J.-P. (1993) *Some Random Series of Functions*, 2nd ed. pbk., Cambridge University Press, Cambridge.
- Kahane J.-P. and Peyrière J. (1976) Sur certaines martingales de Benoit Mandelbrot, *Adv. Math.* **22**, 131–145.
- Katok A. and Hasselblatt B. (1996) *Introduction to the Modern Theory of Dynamical Systems*, pbk., Cambridge University Press, Cambridge.
- Katz N. and Tao T. (2000) Recent progress on the Kakeya conjecture, *Publicacions Matemàtiques*, in Proceedings of the 6th International Conference on Harmonic Analysis and P.D.E.s, Barcelona, 161–180.
- Kaufman R. (1968) On the Hausdorff dimension of projections, *Mathematika*, **15**, 153–155.
- Kaufman R. (1981) On the theorem of Jarník and Besicovitch, *Acta Arith.*, **39**, 265–267.
- Khoshnevisan Y. (2009) From fractals and probability to Lévy processes and stochastic PDEs. in *Fractal Geometry and Stochastics, IV Progress in Probability*, **61**, 111–141, Birkhauser, Basel.
- Kifer Y. (1995) Fractals via random iterated function systems and random geometric constructions. in *Fractal Geometry and Stochastics*, 145–164, Birkhauser, Basel.
- Kigami J. (2001) *Analysis on Fractals*, Cambridge University Press, Cambridge.
- Kobeissi Y. H. (2012) *Multifractal Financial Markets: An Alternative Approach to Asset and Risk Management*, Springer, New York.
- Kolmogorov A. N. (1941) Local structure of turbulence in an incompressible liquid for very large Reynolds numbers, *C. R. Acad. Sci. USSR*, **30**, 299–303.
- Lapidus M. L. and van Frankenhuyzen M. (Eds.) (2004) *Fractal Geometry and Applications: A Jubilee of Benoit Mandelbrot*, American Mathematical Society, Providence, RI.

- Lapidus M. L. and van Frankenhuysen M. (2012) *Fractal Geometry and Number Theory. Complex Dimensions of Fractal Strings and Zeros of Zeta Functions*, pbk., Birkhauser, Boston, MA.
- Lawler G. F. (2008) *Conformally Invariant Processes in the Plane*, American Mathematical Society, Providence, RI.
- Lawler G. F. (2010) *Random Walk and the Heat Equation*, American Mathematical Society, Providence, RI.
- Lesmoir-Gordon N., Rood W. B. and Edney R. (2000) *Introducing Fractals: A Graphic Guide*, Icon Books, London.
- Lévy P. (1948) *Processus Stochastiques et Mouvement Brownian*, 2nd ed., 1965, Gauthier-Villars, Paris.
- Lévy Véhel J. and Lutton E. (2010) *Fractals in Engineering: New Trends in Theory and Applications*, pbk., Springer-Verlag, New York.
- Lévy Véhel J., Lutton E. and Tricot C. (2011) *Fractals in Engineering: From Theory to Industrial Applications*, pbk., Springer-Verlag, New York.
- Lovejoy S. and Schertzer D. (2013) *The Weather and Climate: Emergent Laws and Multifractal Cascades*, Cambridge University Press, Cambridge.
- Lowen S. B. and Teich M. C. (2005) *Fractal-based Point Processes*, John Wiley & Sons, Inc., Hoboken, NJ.
- MacKay R. S. and Meiss J. D. (Eds.) (1987) *Hamiltonian Dynamical Systems*, Adam Hilger, Bristol.
- McCauley J. L. (1993) *Chaos, Dynamics and Fractals*, Cambridge University Press, Cambridge.
- McMullen C. (1984) The Hausdorff dimension of general Sierpiński carpets, *Nagoya Math. J.*, **96**, 1–9.
- McMullen C. T. (1994) *Complex Dynamics and Renormalization*, Princeton University Press, Princeton, NJ.
- Madden C. (2007) *Fractals in Music: Introductory Mathematics for Musical Analysis*, 2nd ed., High Art Press, Salt Lake City, UT.
- Mandelbrot B. B. (1972) Renewal sets and random cutouts, *Z. Warsch Verw. Geb.*, **22**, 145–157.
- Mandelbrot B. B. (1974) Intermittent turbulence in self-similar cascades: Divergence of high moments and dimension of the carrier,

- J. Fluid Mech.*, **62**, 331–358.
- Mandelbrot B. B. (1977) *Fractals: Form, Chance and Dimension*, Freeman, San Francisco, CA.
- Mandelbrot B. B. (1980) Fractal aspects of the iteration of $z \rightarrow \lambda z(1 - z)$ for complex λ, z , *Ann. N. Y. Acad. Sci.*, **357**, 249–259.
- Mandelbrot B. B. (1982) *The Fractal Geometry of Nature*, Freeman, San Francisco, CA.
- Mandelbrot B. B. (1991) Random multifractals: Negative dimensions and the resulting limitations of the thermodynamic formalism, *Proc. R. Soc. Lond.*, **A434**, 79–88.
- Mandelbrot B. B. (1995) Measures of fractal lacunarity: Minkowski content and alternatives. in *Fractal Geometry and Stochastics*, 15–42, Birkhauser, Basel.
- Mandelbrot B. B. (1997) *Fractals and Scaling in Finance: Discontinuity, Concentration, Risk*, Springer-Verlag, New York.
- Mandelbrot B. B. (1999) *Multifractals and 1/f Noise: Wild Self-affinity in Physics*, Springer-Verlag, New York.
- Mandelbrot B. B. (2002) *Gaussian Self-affinity and Fractals. Globality, the Earth, 1/f Noise, and R/S*, Springer-Verlag, New York.
- Mandelbrot B. B. (2004) *Fractals and Chaos: The Mandelbrot Set and Beyond*, Springer-Verlag, New York.
- Mandelbrot B. B. (2012) *The Fractalist: Memoir of a Scientific Maverick*, Pantheon, New York.
- Mandelbrot B. B. and Hudson R. L. (2008) *The (Mis)Behaviour of Markets: A Fractal View of Risk, Ruin and Reward*, Springer-Verlag, New York.
- Mandelbrot B. B. and Riedi R. (1995) Multifractal formalism for infinite multinomial measures, *Adv. Appl. Math.*, **16**, 132–150.
- Mandelbrot B. B. and Van Ness J. W. (1968) Fractional Brownian motions, fractional noises and applications, *SIAM Rev.*, **10**, 422–437.
- Manneville P. (2010) *Instabilities, Chaos and Turbulence*, 2nd ed., Imperial College Press, London.
- Marstrand J. M. (1954a) Some fundamental geometrical properties of plane sets of fractional dimensions, *Proc. Lond. Math. Soc.* (3), **4**, 257–302.

- Marstrand J. M. (1954b) The dimension of Cartesian product sets, *Proc. Camb. Philos. Soc.*, **50**, 198–202.
- Massopust P. R. (1995) *Fractal Functions, Fractal Surfaces, and Wavelets*, Academic Press, San Diego, CA.
- Massopust P. R. (2010) *Interpolation and Approximation with Splines and Fractals*, Oxford University Press, New York.
- Mattila P. (1975a) Hausdorff m regular and rectifiable sets in n -space, *Trans. Am. Math. Soc.*, **205**, 263–274.
- Mattila P. (1975b) Hausdorff dimension, orthogonal projections and intersections with planes, *Ann. Acad. Sci. Fennicae, A* **1**, 227–244.
- Mattila P. (1984) Hausdorff dimension and capacities of intersections of sets in n -space, *Acta Math.*, **152**, 77–105.
- Mattila P. (1985) On the Hausdorff dimension and capacities of intersections, *Mathematika*, **32**, 213–217.
- Mattila P. (1986) Smooth maps, null-sets for integral geometric measures and analytic capacity, *Ann. Math.*, **123**, 303–309.
- Mattila P. (1988) Distribution of sets and measures along planes, *J. Lond. Math. Soc. 2*, **38**, 125–132.
- Mattila P. (1999) *Geometry of Sets and Measures in Euclidean Spaces*, pbk., Cambridge University Press, Cambridge.
- Mauldin R. D. and Urbański M. (1996) Dimensions and measures in infinite iterated function systems, *Proc. Lond. Math. Soc. (3)*, **73**, 105–154.
- Mauldin R. D. and Urbański M. (1999) Conformal iterated function systems with applications to the geometry of continued fractions, *Trans. Am. Math. Soc.*, **351**, 4995–5025.
- Mauldin R. D. and Urbański M. (2003) *Graph Directed Markov Systems: Geometry and Dynamics of Limit Sets*, Cambridge University Press, Cambridge.
- Mauldin R. D. and Williams S. C. (1986a) Random recursive constructions: Asymptotic geometric and topological properties, *Trans. Am. Math. Soc.*, **295**, 325–346.
- Mauldin R. D. and Williams S. C. (1986b) On the Hausdorff dimension of some graphs, *Trans. Am. Math. Soc.*, **298**, 793–803.
- Mauldin R. D. and Williams S. C. (1988) Hausdorff dimension in graph directed constructions, *Trans. Am. Math. Soc.*, **309**, 811–829.

- Mayer-Kress G. (Ed.) (2011) *Dimensions and Entropies in Chaotic Dynamical Systems*, pbk., Springer-Verlag, Berlin.
- Meakin P. (2011) *Fractals, Scaling and Growth Far from Equilibrium*, Cambridge University Press, Cambridge.
- Milnor J. (2006) *Dynamics in One Complex Variable, Introductory Lectures*, 3rd ed., Princeton University Press, Princeton, NJ.
- Moran P. A. P. (1946) Additive functions of intervals and Hausdorff measure, *Proc. Camb. Philos. Soc.*, **42**, 15–23.
- Morgan F. (2008) *Geometric Measure Theory. A Beginner's Guide*, 4th ed., Academic Press, San Diego, CA.
- Morosawa S., Nishimura Y., Taniguchi M. and Ueda T. (2000) *Holomorphic Dynamics*, Cambridge University Press, Cambridge.
- Mörters P. (2009) Why study multifractal spectra? in *Trends in Stochastic Analysis*, London Mathematical Society Lecture Note Series, **353**, 99–120, Cambridge University Press, Cambridge.
- Mörters P. (2010) Random fractals. in *New Perspectives in Stochastic Geometry*, Progress in Probability, **46**, 275–305, Oxford University Press, Oxford.
- Mörters P. and Peres Y. (2010) *Brownian Motion*, Cambridge University Press, Cambridge.
- Nourdin P. (2012) *Selected Aspects of Fractional Brownian Motion*, Springer-Verlag, New York.
- Novak M. M. (Ed.) (1994) *Fractals in the Natural and Applied Sciences*, North Holland, Amsterdam.
- Novak M. M. (Ed.) (1995) *Fractal Reviews in the Natural and Applied Sciences*, Chapman and Hall, London.
- Novak M. M. (Ed.) (1998) *Fractals and Beyond*, World Scientific, Singapore.
- Novak M. M. (Ed.) (2000) *Paradigms of Complexity*, World Scientific, Singapore.
- Novak M. M. (Ed.) (2002) *Emergent Nature*, World Scientific, Singapore.
- Novak M. M. (Ed.) (2004) *Thinking in Patterns*, World Scientific, Singapore.
- Novak M. M. (Ed.) (2006) *Complexus Mundi*, World Scientific, Singapore.

- Novak M. M. and Dewey T. G.(Eds.) (1997) *Fractal Frontiers*, World Scientific, Singapore.
- Olsen L. (1994) *Random Geometrically Graph Directed Self-similar Multifractals*, Longman, Harlow.
- Olsen L. (1995) A multifractal formalism, *Adv. Math.*, **116**, 82–196.
- Olsen L. (1998) Self-affine multifractal Sierpinski sponges in \mathbb{R}^d , *Pac. J. Math.*, **116**, 143–199.
- Olsen L. (2000) Multifractal geometry. in *Fractal Geometry and Stochastics, II*, Progress in Probability, **46**, 3–37, Birkhauser, Basel.
- Olsen L. and Fraser J. M. (2011) Multifractal spectra of random self-affine multifractal Sierpiński sponges in \mathbb{R}^d , *Indiana Univ. Math. J.*, **60**, 937–984.
- Patzschke N. (1997) Self-conformal multifractal measures, *Adv. Appl. Math.* **19**, 486–513.
- Peitgen H.-O., Henriques J. M. and Penedo L. F. (Eds.) (1991) *Fractals in the Fundamental and Applied Sciences*, North Holland, Amsterdam.
- Peitgen H.-O., Jürgens H. and Saupe D. (2004) *Chaos and Fractals*, 2nd ed., Springer, New York.
- Peitgen H.-O. and Richter P. H. (1986) *The Beauty of Fractals*, Springer, Berlin.
- Peitgen H.-O. and Saupe D. (Eds.) (2011) *The Science of Fractal Images*, reprint, Springer, New York.
- Peitgen H.-O., Saupe D. and von Haeseler F. (1984) Cayley's problem and Julia sets, *Math. Intelligencer*, **6**, 11–20.
- Peltier R. F. and Lévy Vehel J. (1995) Multifractal Brownian motion: Definition and preliminary results, INRIA Report, 2645, INRIA, Paris.
- Peres Y. and Schlag B. (2000) Smoothness of projections, Bernoulli convolutions, and the dimension of exceptions, *Duke Math. J.* **102**, 193–251.
- Peres Y. and Solomyak B. (2000) Problems on self-similar sets and self-affine sets: An update. in *Fractal Geometry and Stochastics II*, Progress in Probability, **46**, 95–106, Birkhauser, Basel.
- Pesin Y. (1997), *Dimension Theory in Dynamical Systems*, University of Chicago Press, Chicago.

- Pesin Y. and Climenhaga V. (2009) *Lectures on Fractal Geometry and Dynamical Systems*, American Mathematical Society, Providence, RI.
- Peters E. E. (1994) *Fractal Market Analysis: Applying Chaos Theory to Investment and Economics*, John Wiley & Sons, Inc., New York.
- Peyrière J. (1974) Turbulence et dimension de Hausdorff, *C. R. Acad. Sci. Paris*, **278A**, 567–569.
- Peyrière J. (1977) Calculs de dimensions de Hausdorff, *Duke Math. J.*, **44**, 591–601.
- Pickover C. A. (Ed.) (2012) *Chaos and Fractals. A Computer Graphical Journey*, Elsevier, Amsterdam.
- Pietronero L. (Ed.) (1989) *Fractals*, Plenum Press, New York.
- Pietronero L. and Tosatti E. (Eds.) (1986) *Fractals in Physics*, North-Holland, Amsterdam.
- Pontrjagin L. and Schnirelman L. (1932) Sur une propriété métrique de la dimension, *Ann. Math.*, **33**, 156–162.
- Preiss D. (1987) Geometry of measures in \mathbb{R}^n : Distribution, rectifiability and densities, *Ann. Math.*, **125**, 537–641.
- Preiss D. and Tiser J. (1992) On Besicovitch's $\frac{1}{2}$ -problem, *J. Lond. Math. Soc.* **2**, **45**, 279–287.
- Prusinkiewicz P. and Kaandorp J. A. (2012) *Fractal Modelling: Growth and Form in Biology*, pbk., Springer-Verlag, Berlin.
- Przytycki F. and Urbański M. (2010) *Conformal Fractals: Ergodic Theory Methods*, Cambridge University Press, Cambridge.
- Puente C., Romeu J., Rous R. and Cardama A. (2011) Multiband fractal antennas and arrays. in *Fractals in Engineering: From Theory to Industrial Applications*, pbk., 221–236, Springer-Verlag, New York.
- Rams D. and Lévy Vehel J. (2007) Results on the dimension spectrum for self-conformal measures, *Nonlinearity*, **20**, 965–973.
- Riedi R. (2002) Multifractal processes. in *Long Range Dependence: Theory and Applications*, 625–715, Birkhauser, Basel.
- Rippon P. J. and Stallard G. M. (2008) *Transcendental Dynamics and Complex Analysis*, Cambridge University Press, Cambridge.

- Rodríguez-Iturbe I. and Rinaldo A. (2001) *Fractal River Basins*, pbk., Cambridge University Press, Cambridge.
- Rogers C. A. (1988) Dimension prints, *Mathematika*, **35**, 1–27.
- Rogers C. A. (1998) *Hausdorff Measures*, 2nd ed., Cambridge University Press, Cambridge.
- Rogers L. C. G. and Williams D. (2000) *Diffusions, Markov Processes and Martingales, Volume 1: Foundations*, 2nd ed., Cambridge University Press, Cambridge.
- Rothschild C. A. (1998) *Fractals in Chemistry*, Wiley-Blackwell, Hoboken, NJ.
- Rudin W. (1976) *Principles of Mathematical Analysis*, 3rd ed., McGraw-Hill, New York.
- Ruelle D. (1982) Repellers for real analytic maps, *Ergod. Theory Dyn. Syst.*, **2**, 99–108.
- Ruelle D. (1983) Bowen's formula for the Hausdorff dimension of self-similar sets. in *Scaling and Self-similarity in Physics, Progress in Physics*, **7**, Birkhauser, Boston, MA.
- Rynne B. P. (1992) Regular and ubiquitous systems, and M_∞^s -dense sequences, *Mathematika* **39**, 234–243.
- Salli A. (1991) On the Minkowski dimension of strongly porous fractal sets in \mathbb{R}^n , *Proc. Lond. Math. Soc.* **3**, **62**, 353–372.
- Samorodnitsky G. and Taqqu M. S. (1994) *Stable Non-Gaussian Random Processes*, Chapman & Hall/CRC, Boca Raton, FL.
- Santaló L. A. (2004) *Integral Geometry and Geometric Probability*, 2nd ed., Cambridge University Press, Cambridge.
- Schleicher D. (Ed.) (2009) *Complex Dynamics: Families and Friends*, A. K. Peters, Natick, MA.
- Schmidt W. M. (1980) *Diophantine Approximation, Lecture Notes in Mathematics*, **785**, Springer, Berlin.
- Schneider R. (1993) Convex surfaces, curvature and surface area measures. in *Handbook of Convex Geometry, Vol. A*, 273–299, North-Holland, Amsterdam.
- Scholz C. H. and Mandelbrot B. B. (Eds.) (1989) *Fractals in Geophysics*, Birkhauser, Boston, MA.
- Schroeder M. (2009) *Fractals, Chaos, Power Laws*, Dover, New York.

- Semmes S. (2000) *Some Novel Types of Fractal Geometry*, Oxford University Press, Oxford.
- Seuront L. (2009) *Fractals and Multifractals in Ecology and Aquatic Science*, CRC Press, Boca Raton, FL.
- Shmerkin P. (2011) Porosity, dimension, and local entropies: A survey, *Rev. Unión Mat. Argentina*, **52**, 81–103.
- Smale S. (1967) Differentiable dynamical systems, *Bull. Am. Math. Soc.*, **73**, 747–817.
- Solomyak B. (1998) Measure and dimension for some fractal families, *Math. Proc. Camb. Philos. Soc.*, **124**, 531–546.
- Sparrow C. (1982) *The Lorenz Equations: Bifurcations, Chaos, and Strange Attractors*, Springer, New York.
- Sprott J. C. (2003) *Chaos and Time-Series Analysis*, Oxford University Press, Oxford.
- Sreenivasan K. R. (1991) Fractals and Multifractals in Fluid Turbulence, *Annu. Rev. Fluid Mech.*, **23**, 539–600.
- Stanley H. E. and Ostrowsky N. (Eds.) (1988) *Random Fluctuations and Pattern Growth*, Springer, New York.
- Stauffer D. and Aharony A. (1994) *Introduction to Percolation Theory*, 2nd ed. pbk., CRC Press, London.
- Stein E. M. (1993) *Harmonic Analysis: Real-variable Methods, Orthogonality, and Oscillatory Integrals*, Princeton University Press, Princeton, NJ.
- Stoyan D. and Stoyan H. (1994) *Fractals, Random Shapes and Point Fields*, John Wiley & Sons, Ltd, Chichester.
- Strichartz R. S. (2006) *Differential Equations on Fractals. A Tutorial*, Princeton University Press, Princeton, RI.
- Takayasu H. (1990) *Fractals in the Physical Sciences*, Wiley-Blackwell, Hoboken, NJ.
- Tan L. (Ed.) (2000) *The Mandelbrot Set, Theme and Variations, London Mathematical Society Lecture Notes*, **274**, Cambridge University Press, Cambridge.
- Tao T. (2011). *An Introduction to Measure Theory*, American Mathematical Society, Providence, RI.
- Taylor S. J. (1961) On the connection between Hausdorff measures and generalized capacities, *Proc. Camb. Philos. Soc.*, **57**, 524–531.

- Taylor S. J. (1973a). *Introduction to Measure and Integration*, Cambridge University Press, Cambridge.
- Taylor S. J. (1973b) Sample path properties of processes with stationary independent increments. in *Stochastic Analysis* (Kendall D. G. and Harding E. F. Eds.), 387–414. John Wiley & Sons, Inc., New York.
- Taylor S. J. (1986) The measure theory of random fractals, *Math. Proc. Camb. Philos. Soc.*, **100**, 383–406.
- Temam R. (Ed.) (1976) *Turbulence and the Navier–Stokes Equations*, Lecture Notes in Mathematics, **565**, Springer, New York.
- Temam R. (1983) *Navier–Stokes Equations and Non-linear Functional Analysis*, Society for Industrial and Applied Mathematics, Philadelphia, PA.
- Temam R. (2012) *Infinite-dimensional Dynamical Systems in Mechanics and Physics*, pbk., Springer-Verlag, New York.
- Tricot C. (1982) Two definitions of fractional dimension, *Math. Proc. Camb. Philos. Soc.*, **91**, 54–74.
- Tricot C. (2011) *Curves and Fractal Dimension*, pbk. reprint, Springer-Verlag, New York.
- Turcotte D. L. (1997) *Fractals and Chaos in Geology and Geophysics*, Cambridge University Press, Cambridge.
- Urbanski C. (1990) The Hausdorff dimension of the graphs of continuous self-affine functions, *Proc. Am. Math. Soc.*, **108**, 921–930.
- Vicsek T. (1991) *Fractal Growth Phenomena*, 2nd ed., World Scientific, Singapore.
- Voss R. F. (1985) Random fractal forgeries. in *Fundamental Algorithms in Computer Graphics* (Earnshaw R. A. Eds.), 805–835. Springer, Berlin.
- Vretblad A. (2005) *Fourier Analysis and its Applications*, Springer, New York.
- Webster R. (1994) *Convexity*, Oxford University Press, Oxford.
- West B. J. (2013) *Fractal Physiology and Chaos in Medicine*, 2nd ed., World Scientific, Singapore.
- Wolff T. (1999) Recent work connected with the Kakeya problem. in *Prospects in Mathematics* (Rossi H. Ed.), 129–162, American

Mathematical Society, Providence, RI.

Xiao Y. (2013) Recent developments on fractal properties of Gaussian random fields. in *Further Developments in Fractals and Related Fields*, 255–285, Birkhauser, Basel.

Young L.-S. (1982) Dimension, entropies and Lyapunov exponents, *Ergod. Theory Dyn. Syst.*, **2**, 109–124.

Zähle U. (1984) Random fractals generated by random cutouts, *Math. Nachr.*, **116**, 27–52.

Index

abscissa of convergence
affine transformation
affinity
almost all
almost everywhere
almost surely
analytic function
antennas
area
scaling of
Arnold's cat map
astronomical evidence, for small divisors
attractive orbit
attractive point
attractor
 in continuous dynamical system
 in discrete dynamical system
autocorrelation
autocorrelation function
average
Avogadro's number

Baire's category theorem
baker's transformation
ball
Banach's contraction mapping theorem
basic interval
basin of attraction
Besicovitch construction
Besicovitch set
bifurcation diagram
bijection
bi-Lipschitz equivalence
bi-Lipschitz function
binary interval
Borel set
 and intersections
 measure on
 and products
 and projections
 and subrings
 and subsets of finite measure
boundary
bounded set
bounded variation
box counting

box(-counting) dimension

Brownian motion

fractional Brownian motion

fractional Brownian surface

and growth

and Hausdorff dimension

Lévy stable process

limitations

modified

problems

properties

ways of calculating

branch of complex function

branching process

Brown, Robert

Brownian graph

Brownian motion

Fourier series representation

fractional

multiperiodic

n -dimensional

Brownian sample function

graph

index- α fractional

multiple points

Brownian surface, fractional

Brownian trail

Cantor dust

calculation of Hausdorff dimension

Cantor product

Cantor set

as attractor

dimension of

middle- λ

middle third

non-linear

random

uniform

see also main entry: [middle third Cantor set](#)

Cantor target

(s -)capacity

capacity dimension

Cartesian product

cat map

category, second

Cauchy sequence

central limit theorem

chaos

chaotic attractor

chaotic repeller
characteristic function
Choleski decomposition
class \mathcal{C}^s
closed ball
closed interval
closed set
closure
cloud boundaries
coarse multifractal spectrum
lower
upper
coastline
codomain
collage theorem
compact set
complement of a set
complementary intervals
complete metric
complex dimensions
complex dynamics
composition of functions
computer drawings
conditional expectation
conditional probability

conformal mapping

congruence

direct

conjugacy

connected component

connected set

content

Minkowski

s -dimensional

continued fraction

examples

continued fraction expansion

continuity equation

continuous dynamical systems

continuous function

continuously differentiable function

contours

contracting similarity

contraction

contraction mapping theorem

convergence

pointwise

of sequence

uniform

convex function

convex surface
convolution theorem
coordinate cube
copper sulphate, electrolysis of
correlation
countable set
countable stability
 of dimension print
 of Hausdorff dimension
counting measure
covariance matrix
cover of a set

see also [delta-/ \$\Delta\$ -cover](#)

covering lemma
critical point
cross section
cube
cubic polynomial, Newton's method for
curve
fractal
Jordan
rectifiable
curve-free set
curve-like set

Darcy's law
data compression
decomposition of 1-sets
delta-/ Δ -cover
delta-/ Δ -mesh or grid
delta-/ Δ -neighbourhood or parallel body
dendrite
dense set
density
lower
upper
density function
derivative
diameter of subset
difference of sets
differentiability
continuous
diffusion equation
diffusion limited aggregation (DLA) model
digital sundial

dimension

alternative definitions
of attractors and repellers
box(-counting)
calculation of
of Cantor set
capacity
characterization of quasi-circles by
divider
entropy
experimental estimation of
finer definitions
Fourier
of graphs of functions
Hausdorff
Hausdorff– Besicovitch
Hausdorff dimension of a measure
information
of intersections
local
lower box(-counting)
of a measure
metric
Minkowski(– Bouligand)
modified box-counting

one-sided
packing
of products
of projections
of random sets
of self-affine sets
of self-similar sets
similarity
topological
upper box(-counting)
of von Koch curve
of (α -)well approximable number
dimension function
dimension print
examples
dimensionally homogeneous set
Diophantine approximation
direct congruence
Dirichlet's theorem
discrete dynamical system
disjoint binary intervals
disjoint collection of sets
distance set

distribution

Gaussian

multidimensional normal

normal

uniform

distribution of digits

divider dimension

domain

double sector

duality method

dynamical systems

continuous

discrete

dynamics, complex

eddies

Egoroff's theorem

Einstein

electrical discharge in gas

electrolysis

electrostatic potential

(s-)energy

entropy

entropy dimension

ergodic theory

Euclidean distance or metric

Euclidean space

event

independence of

event space

exchange rate variation

expectation

conditional

expectation equation

experiment (probabilistic)

experimental approach to fractals

exterior, of loop

extinction probability

Fatou set

Feigenbaum constant

figure of eight

filled-in Julia set

finance

fine (Hausdorff) multifractal spectrum

fine multifractal analysis

first return map

fixed point

fluid dynamics

forked lightning

Fourier dimension
Fourier series
Fourier transform
 methods using
fractal, definition
fractal curve
fractal group
fractal growth
fractal interpolation
fractal percolation
fractal string
fractally homogeneous turbulence
fractional Brownian motion
fractional Brownian surface
fractions, continued
Frostman's lemma
full square
function
 continuous
 convex
functional analysis

G -delta ($G\Delta$) set
gauge function
Gaussian distribution

Gaussian process
general construction
generator
examples
geometric invariance
geometric measure theory
graphs of functions
gravitational potential
group
Grigorchuk
fractal
of fractional dimension
group of transformations
growth

Hamiltonian
Hamiltonian systems, stability of
Hamilton's equations
Hausdorff– Besicovitch dimension

Hausdorff dimension
and box(-counting) dimension
Brownian motion
calculating
equivalent definitions
fractional Brownian motion
fractional Brownian surface
Lévy stable process
of a measure
and packing dimension
and projections
properties
of self-affine set
Hausdorff distance
Hausdorff measure
and packing measure
and product rule
and quasi-circle
Hausdorff metric
heat equation
Hele– Shaw cell
Hénon attractor/map
heuristic calculation(s)
histogram method, for multifractal spectrum
Hölder condition

Hölder exponent
Hölder's inequality
homeomorphism
homogeneous turbulence
horseshoe map

image
image encoding
in general
independence
 of events
 of random variables
independent increment
index- α fractional Brownian motion
index- α fractional Brownian surface
infimum
information dimension
injection
integral
integral geometry
interior
 of loop
intermittency
interpolation
intersection formulae

intersection

large

interval

interval density

invariance

geometric

Lipschitz

invariant curves

invariant measure

invariant set

invariant tori

inverse function

inverse image

irregular point

irregular set

isolated point, as attractor

isometry

isotropic

isotropic turbulence

iterated construction

iterated function system (IFS)

attractor for

and repellers

variations

iterated Venetian blind construction

iteration

Jarník's theorem

Jordan curve

Julia set

Kakeya problem

Koch curve, see [von Koch curve](#)

Kolmogorov– Arnold– Moser (KAM) theorem

Kolmogorov entropy

Kolmogorov model of turbulence

lacunarity

laminar flow

landscapes

Laplace's equation

lattice

law of averages

Lebesgue density theorem

Lebesgue measure

n -dimensional

Legendre spectrum

Legendre transform

length

scaling of

level set

level- k interval

level- k set

Lévy process

Lévy stable process

Liapounov exponents

limit

lower

of sequence

upper

lim sup sets

line segment

uniform mass distribution

line set

linear transformation

Lipschitz equivalence

Lipschitz function

Lipschitz invariance

local dimension

local product

local structure of fractals

logarithmic density

logarithms

logistic map

long range dependence

loop

closed

Lorenz attractor

Lorenz equations

lower box(-counting) dimension

lower coarse multifractal spectrum

lower density

lower limit

lubrication theory

Mandelbrot, Benoit

Mandelbrot set

mapping

Markov partition

martingale

mass distribution

construction by repeated subdivision

and distribution of digits

mass distribution

and product rule

uniform, on line segment

mass distribution principle

maximum modulus theorem

maximum range

Maxwell's equations

mean

mean-value theorem

measure

counting

Hausdorff

Hausdorff dimension of

invariant

Lebesgue

multifractal

n -dimensional Lebesgue

net

packing

probability

restriction of

on a set

self-similar

sigma-/ Σ -finite

tangent

meromorphic function

mesh cube

method of moments, for multifractal spectrum

metric dimension

middle- λ Cantor set

middle third Cantor set

box(-counting) dimension

construction of

features

generalizations of

Hausdorff dimension

in intersections

porosity

product

and repellers

and self-similarity

tangents

Minkowski content

Minkowski(-Bouligand) dimension

modified box(-counting) dimension

lower

upper

and packing dimension

modified von Koch curve

moment sum

monotonicity

of box(-counting) dimension

of dimension print

of Hausdorff dimension

of packing dimension

Montel's theorem

Moser's twist theorem

mountain skyline

multifractal

coarse analysis

fine analysis

self-similar

multifractal spectrum

multifractal time

multifractional Brownian motion

multiple points

multivariate normal variable(s)

natural fractals

natural logarithms

Navier– Stokes equations

nearest point mapping

neighbourhood

see also [delta-/ \$\Delta\$ -neighbourhood](#)

net measure

neural networks

Newton's method

non-lattice

non-linear Cantor set

non-removable set

non-singular transformation

normal distribution

normal family

at a point

normal numbers

number theory

often

one-sided dimension

one-to-one correspondence

one-to-one function

onto function

open ball

open interval

open set

open set condition

orbit

orthogonal projection

packing dimension

and modified upper box dimension

packing measure

and Hausdorff measure

parallel body

Parseval's theorem

partial quotient
percolation
perfect set
period
period doubling
period- p orbit
period- p point
Perrin
phase transition
physical applications
pinch point
plane cross section
plant growth
Poincaré– Bendixson theorem
Poincaré section
point mass
pointwise convergence
Poisson's equation
pole
 simple
polynomials, Newton's method for
population dynamics
porosity
 and Hausdorff dimension

porous

uniformly

porous medium, flow through

(s-)potential

potential theoretic methods

power spectrum

Prandtl number

pre-fractal(s)

pre-image

probability

conditional

probability density function

probability measure

probability space

probability theory

product, Cartesian

product formula

projection

of arbitrary sets

of arbitrary sets of integral dimension

of s-sets of integral dimension

Pythagoras's theorem

quadratic functions

quadratic polynomial, Newton's method for

quasi-circle

radio antennas

rainfall distribution

random Cantor set

random fractal

random function

random mid-point displacement method

random process

random variable

independence of

simple

random von Koch curve

random walk

range, maximum

ratio of contraction

rational function

rectifiable curve

tangent

reflection

regular point

regular set

tangent

removable set

repeller

repelling point
closure of
reservoir level variations
residence measure
residue
restriction of a measure
rigid motion
ring of fractional dimension
Rössler band
rotation

sample function
sample space
scalar multiple
scaling property
sections, parallel
sector, double
self-affine curve
construction of
self-affine set
as attractor
self-similar fractal, with two different similarity ratios
self-similar measure
construction of
multifractal spectrum

self-similar multifractals

self-similar set

similarity dimension

see also [middle third Cantor set](#); [Sierpiński gasket](#); [von Koch curve](#)

sensitive dependence on initial conditions

s -set

0-set

1-set

tangent to

set theory

share prices

Siegel disc

Sierpiński dipole

Sierpiński triangle or gasket

sigma-/ Σ -finite measure

similarity

similarity dimension

simple closed curve

simple function

simple random variable

simulation

singular value

singular value function

singularity set

singularity spectrum

small divisor theory
smooth manifold / set
snowflake curve
solenoid
solution curves
stability
countable
stable point
stable process
stable set
stable symmetric process
stationary increments
statistically self-affine set
statistically self-similar set
stock market prices
strange attractor
stretching and folding or cutting transformations
strong law of large numbers
subgroup
submanifold
submultiplicative sequence
subring
subset of finite measure
sundial, digital
superattractive point

support of a measure

supremum

surface, convex

surjection

symbolic dynamics

tangent

tangent measure

tendril

tends to

tends to infinity

tent map

thermal convection

topological dimension

torus

totally disconnected set

trading time

trail

trajectories

transformation

effects on a set

group of

linear

stretching and folding or cutting

translations

tree antenna

trial

triangle inequality

tube formula

turbulence

fractally homogeneous

homogeneous

isotropic

turbulent flow

twist map

ubiquity theorem

uncountable set

uniform Cantor set

uniform convergence

uniform distribution

uniformly porous

union of sets

unstable point

upper box(-counting) dimension

upper coarse multifractal spectrum

upper density of s -set

upper limit

variance

vector sum of sets
‘Venetian blind’ construction, iterated
viscous fingering
Vitushkin's conjecture
volume
von Koch curve
 construction of
 dimension of
 modified
 random
 as self-similar set
von Koch dipole
von Koch snowflake
vortex tubes

weak solution
weather prediction
Weierstrass function
 random
(α -)well approximable number
Wiener process

zeta function
 singularity of

WILEY END USER LICENSE AGREEMENT

Go to www.wiley.com/go/eula to access Wiley's ebook EULA.

Contents

[Cover](#)

[Preface to the first edition](#)

[Preface to the second edition](#)

[Preface to the third edition](#)

[Course suggestions](#)

[Introduction](#)

[Notes and references](#)

[Part I: Foundations](#)

[Chapter 1: Mathematical background](#)

[1.1 Basic set theory](#)

[1.2 Functions and limits](#)

[1.3 Measures and mass distributions](#)

[1.4 Notes on probability theory](#)

[1.5 Notes and references](#)

[Exercises](#)

[Chapter 2: Box-counting dimension](#)

[2.1 Box-counting dimensions](#)

[2.2 Properties and problems of box-counting dimension](#)

[*2.3 Modified box-counting dimensions](#)

[2.4 Some other definitions of dimension](#)

[2.5 Notes and references](#)

[Exercises](#)

[Chapter 3: Hausdorff and packing measures and dimensions](#)

[3.1 Hausdorff measure](#)

[3.2 Hausdorff dimension](#)

[3.3 Calculation of Hausdorff dimension—simple examples](#)

[3.4 Equivalent definitions of Hausdorff dimension](#)

[*3.5 Packing measure and dimensions](#)

[*3.6 Finer definitions of dimension](#)

[*3.7 Dimension prints](#)

[*3.8 Porosity](#)

[3.9 Notes and references](#)

[Exercises](#)

[Chapter 4: Techniques for calculating dimensions](#)

[4.1 Basic methods](#)

[4.2 Subsets of finite measure](#)

[4.3 Potential theoretic methods](#)

[*4.4 Fourier transform methods](#)

[4.5 Notes and references](#)

[Exercises](#)

[Chapter 5: Local structure of fractals](#)

[5.1 Densities](#)

[5.2 Structure of 1-sets](#)

[5.3 Tangents to \$s\$ -sets](#)

[5.4 Notes and references](#)

[Exercises](#)

[Chapter 6: Projections of fractals](#)

[6.1 Projections of arbitrary sets](#)

[6.2 Projections of \$s\$ -sets of integral dimension](#)

[6.3 Projections of arbitrary sets of integral dimension](#)

[6.4 Notes and references](#)

[Exercises](#)

[Chapter 7: Products of fractals](#)

[7.1 Product formulae](#)

[7.2 Notes and references](#)

[Exercises](#)

[Chapter 8: Intersections of fractals](#)

[8.1 Intersection formulae for fractals](#)

[8.2 Sets with large intersection](#)

[*8.3 Notes and references](#)

[Exercises](#)

[Part II: Applications and Examples](#)

[Chapter 9: Iterated function systems—self-similar and self-affine sets](#)

[9.1 Iterated function systems](#)

[9.2 Dimensions of self-similar sets](#)

[9.3 Some variations](#)

[9.4 Self-affine sets](#)

[9.5 Applications to encoding images](#)

[*9.6 Zeta functions and complex dimensions](#)

[9.7 Notes and references](#)

[Exercises](#)

[Chapter 10: Examples from number theory](#)

[10.1 Distribution of digits of numbers](#)

[10.2 Continued fractions](#)

[10.3 Diophantine approximation](#)

[10.4 Notes and references](#)

[Exercises](#)

[Chapter 11: Graphs of functions](#)

[11.1 Dimensions of graphs](#)

[*11.2 Autocorrelation of fractal functions](#)

[11.3 Notes and references](#)

[Exercises](#)

[Chapter 12: Examples from pure mathematics](#)

[12.1 Duality and the Kakeya problem](#)

[12.2 Vitushkin's conjecture](#)

[12.3 Convex functions](#)

[12.4 Fractal groups and rings](#)

[12.5 Notes and references](#)

[Exercises](#)

[Chapter 13: Dynamical systems](#)

[13.1 Repellers and iterated function systems](#)

[13.2 The logistic map](#)

[13.3 Stretching and folding transformations](#)

[13.4 The solenoid](#)

[13.5 Continuous dynamical systems](#)

[*13.6 Small divisor theory](#)

[*13.7 Lyapunov exponents and entropies](#)

[13.8 Notes and references](#)

[Exercises](#)

[Chapter 14: Iteration of complex functions—Julia sets and the Mandelbrot set](#)

[14.1 General theory of Julia sets](#)

[14.2 Quadratic functions—the Mandelbrot set](#)

[14.3 Julia sets of quadratic functions](#)

[14.4 Characterisation of quasi-circles by dimension](#)

[14.5 Newton's method for solving polynomial equations](#)

[14.6 Notes and references](#)

[Exercises](#)

Chapter 15: Random fractals

15.1 A random Cantor set

15.2 Fractal percolation

15.3 Notes and references

Exercises

Chapter 16: Brownian motion and Brownian surfaces

16.1 Brownian motion in \mathbb{R}

16.2 Brownian motion in \mathbb{R}^n

16.3 Fractional Brownian motion

16.4 Fractional Brownian surfaces

16.5 Lévy stable processes

16.6 Notes and references

Exercises

Chapter 17: Multifractal measures

17.1 Coarse multifractal analysis

17.2 Fine multifractal analysis

17.3 Self-similar multifractals

17.4 Notes and references

Exercises

Chapter 18: Physical applications

18.1 Fractal fingering

18.2 Singularities of electrostatic and gravitational potentials

18.3 Fluid dynamics and turbulence

18.4 Fractal antennas

18.5 Fractals in finance

18.6 Notes and references

Exercises

[References](#)

[Index](#)

[End User License Agreement](#)

List of Illustrations

[Figure 0.1](#)

[Figure 0.2](#)

[Figure 0.3](#)

[Figure 0.4](#)

[Figure 0.5](#)

[Figure 0.6](#)

[Figure 0.7](#)

[Figure 0.8](#)

[Figure 0.9](#)

[Figure 1.1](#)

[Figure 1.2](#)

[Figure 1.3](#)

[Figure 1.4](#)

[Figure 1.5](#)

[Figure 2.1](#)

[Figure 3.1](#)

[Figure 3.2](#)

[Figure 3.3](#)

[Figure 3.4](#)

[Figure 3.5](#)

[Figure 4.1](#)

[Figure 4.2](#)

[Figure 5.1](#)

[Figure 5.2](#)

[Figure 5.3](#)

[Figure 5.4](#)

[Figure 5.5](#)

[Figure 6.1](#)

[Figure 6.2](#)

[Figure 6.3](#)

[Figure 6.4](#)

[Figure 7.1](#)

[Figure 7.2](#)

[Figure 7.3](#)

[Figure 7.4](#)

[Figure 8.1](#)

[Figure 9.1](#)

[Figure 9.2](#)

[Figure 9.3](#)

[Figure 9.4](#)

[Figure 9.5](#)

[Figure 9.6](#)

[Figure 9.7](#)

[Figure 9.8](#)

[Figure 9.9](#)

[Figure 9.11](#)

[Figure 9.10](#)

[Figure 9.12](#)

[Figure 9.13](#)

[Figure 9.14](#)

[Figure 11.1](#)

[Figure 11.2](#)

[Figure 11.3](#)

[Figure 11.4](#)

[Figure 11.5](#)

[Figure 12.1](#)

[Figure 12.2](#)

[Figure 12.3](#)

[Figure 13.1](#)

[Figure 13.2](#)

[Figure 13.3](#)

[Figure 13.4](#)

[Figure 13.5](#)

[Figure 13.6](#)

[Figure 13.7](#)

[Figure 13.8](#)

[Figure 13.9](#)

[Figure 13.10](#)

[Figure 13.11](#)

[Figure 13.12](#)

[Figure 13.13](#)

[Figure 13.14.](#)

[Figure 13.15](#)

[Figure 13.16](#)

[Figure 13.17](#)

[Figure 14.2](#)

[Figure 14.3](#)

[Figure 14.4.](#)

[Figure 14.5](#)

[Figure 14.6](#)

[Figure 14.7.](#)

[Figure 14.1](#)

[Figure 14.8](#)

[Figure 14.9.](#)

[Figure 14.10](#)

[Figure 15.1](#)

[Figure 15.2](#)

[Figure 15.3](#)

[Figure 15.4.](#)

[Figure 15.5](#)

[Figure 16.1](#)

[Figure 16.2](#)

[Figure 16.3](#)

[Figure 16.4.](#)

[Figure 17.1](#)

[Figure 17.2](#)

[Figure 17.3](#)

[Figure 17.4](#)

[Figure 18.1](#)

[Figure 18.2](#)

[Figure 18.3](#)

[Figure 18.4](#)

[Figure 18.5](#)

[Figure 18.6](#)

Fractal Geometry

Mathematical Foundations and Applications

Third Edition

Kenneth Falconer

WILEY *Andrews, UK*

This edition first published 2014

© 2014 John Wiley & Sons, Ltd

Registered office

John Wiley & Sons Ltd, The Atrium, Southern Gate, Chichester, West Sussex, PO19 8SQ,
United Kingdom

For details of our global editorial offices, for customer services and for information about
how to apply for permission to reuse the copyright material in this book please see our
website at www.wiley.com.

The right of the author to be identified as the author of this work has been asserted in
accordance with the Copyright, Designs and Patents Act 1988.

All rights reserved. No part of this publication may be reproduced, stored in a retrieval
system, or transmitted, in any form or by any means, electronic, mechanical, photocopying,
recording or otherwise, except as permitted by the UK Copyright, Designs and Patents Act
1988, without the prior permission of the publisher.

Wiley also publishes its books in a variety of electronic formats. Some content that appears
in print may not be available in electronic books.

Designations used by companies to distinguish their products are often claimed as
trademarks. All brand names and product names used in this book are trade names, service
marks, trademarks or registered trademarks of their respective owners. The publisher is not
associated with any product or vendor mentioned in this book.

Limit of Liability/Disclaimer of Warranty: While the publisher and author have used their
best efforts in preparing this book, they make no representations or warranties with respect
to the accuracy or completeness of the contents of this book and specifically disclaim any
implied warranties of merchantability or fitness for a particular purpose. It is sold on the
understanding that the publisher is not engaged in rendering professional services and
neither the publisher nor the author shall be liable for damages arising herefrom. If
professional advice or other expert assistance is required, the services of a competent
professional should be sought.

Library of Congress Cataloging-in-Publication Data applied for.

A catalogue record for this book is available from the British Library.

ISBN: 978-1-119-94239-9